CARDE TECH. LETTER N-47-18

Copy No. 21

THIRD PROGRESS REPORT

on

CF-105 WEAPON SYSTEM ASSESSMENT

by

J. T. Macfarlane and C.J. Wilson

CANADIAN ARMAMENT RESEARCH AND DEVELOPMENT ESTABLISHMENT

Valcartier, Quebec.

April, 1957.

CANADIAN ARMAMENT RESEARCH AND DEVELOPMENT ESTABLISHMENT
DEFENCE RESEARCH BOARD

Technical Letter No. N-47-18 Date 1 April, 1957 Copy No. [redacted]

Author J.T. Macfarlane Approved by E.L. Smith Sheet Title of 470

58-15397
#311535

PROJECT
CF-105 ASSESSMENT

THIRD PROGRESS REPORT

Period 1 Nov 56 to 31 March 57

Compiled by

J.T. Macfarlane &
C.J. Wilson.

Classification / Designation Changed to / Remplacée par Unclassified now Unlimited
By Authority of Sur l'Autorisation de DREV DRP Serial #744/86 1109/99
Date 1986 Signature Bambrey
Appointment Fonction CRAD HQ DRP Unit Unité DRDIM 3-2

Enclosure (1) to CNO Serial 004955 P92

Chief Superintendent

65117005-01

SUMMARY

This technical letter is a progress report on work being done at C.A.R.D.E. in connection with the CF-105 Weapon System Assessment, recording work done in the period November 56/March 57.

Results obtained in the past quarter are presented in appendices, along with description of methods used, and in a few cases limited discussion of the results. A reader wishing to analyse the results should use them in conjunction with those published in the preceding progress report, issued as CARDE Technical Letter N-47-12.

Plans for work in the coming quarter and in the ensuing year are included.

TABLE OF CONTENTS

Page No.

THIRD PROGRESS REPORT

on

CF 105 WEAPON SYSTEM ASSESSMENT

1. INTRODUCTION

The engagement of high speed targets by supersonic interceptors armed with air-to-air missiles introduces a variety of new problems which cannot be assessed by extrapolation of data arising from experience with conventionally armed subsonic aircraft.

For this reason, CARDE has been requested by the RCAF to carry out an evaluation study of the effectiveness of a supersonic interceptor weapon system based on the AVRO CF-105 aircraft armed with Sparrow II or Sparrow III air-to-air missiles.

The primary objectives of the study as stated by the RCAF are:

(i) To evaluate the combat effectiveness of the system with different types of armament, beginning with the Sparrow series, for probable bomber threats including the Bison, Badger and Bear.

(ii) To investigate the effect of variation in fire control parameters such as A.I. radar range and look angle.

(iii) To establish the minimum acceptable level of aerodynamic performance and to investigate the effect of possible design changes in the aircraft and engine parameters, insofar as these changes affect combat performance.

(iv) To determine the effect of variations in G.C.I. placement accuracy.

(v) To explore possible tactics and suggest optimum modes of attack.

In order to arrive at an accurate assessment of the overall combat effectiveness of this weapon system, the many inter-dependent sub-systems of which it is composed require analysis, first individually and then collectively, so that the relative importance of the principal parameters can be established. Naturally, an exploratory study of this nature is quite involved and certainly time-consuming, if it is to be sufficiently exhaustive to achieve the above-stated objectives. Further, the task is rendered difficult in that very little primary information is available on which to base investigations, as it is evident that the establishment of such data is perhaps the primary object of the study.

The general approach then has been to adopt a range of parameters which should encompass final characteristics, then to conduct an analysis based on these and thus establish their validity and importance in the particular

sub-system, as well as their influence on the effectiveness of the system as a whole. In this way overall effectiveness can be established as a function of the parameters of individual sub-systems and optimum design values indicated.

Although this method is elongated and somewhat tedious, an important compensatory feature lies in the fact that the most critical areas requiring further study are highlighted.

2. PROGRESS OF STUDY

CARDE Technical Letter N-47-3, May 1956, gives a review of the general interceptor-weapon problem with particular reference to the proposed CF-105 system, and sets out in some detail a proposal for the prosecution of studies to attain the objectives enumerated by the RCAF. A directive to initiate the CF-105 Weapon System Assessment Study was received on May 29, 1956, and work has continued since. Progress of the work has been described in progress reports, CARDE Technical Letters N-47-8 and N-47-12, issued in August and November of 1956. As the study has progressed, alterations have been made in the original program plan, occasioned mainly by delays in procurement of additional computing facilities, and delay in provision of manpower.

As originally planned the Assessment Study was to be of one year's duration, from April 1st 1956 to April 1st 1957. In effect active work began on the project only in June 1956. Recently continuation of the

study for a further year has been approved, to permit more intensive investigations of certain subjects. A programme for this second year's work is appended to this report.

3. EFFORT ALLOTTED TO THE STUDY

3.1 Manpower Allocation

The work is being carried out by specialist sections within the Wings of CARDE, under the co-ordination and direction of the Systems Group which is generally responsible for the task.

During the period under review, a total of 18 professional personnel have been engaged in the program. The degree of participation was as follows:

	Full Time	Part Time
Systems Group	3	2
"B" Wing	1	2
"G" Wing	13	4
TOTAL	17	8

3.2 Computing Facilities

Difficulties with REAC equipment mentioned in the previous progress report have now been overcome and the enlarged CARDE REAC facility was in use on the placement problem during the period.

It is expected that work will continue at approximately the same level of effort during the next quarter.

4. GENERAL REVIEW OF PROBLEM

As we have already stressed in the original program plan for the assessment, and in progress reports, interceptor system effectiveness is necessarily described in terms of probability. It has been proposed that the overall effectiveness P_e of the system may be written as

$$P_e = P_d \cdot P_p \cdot P_s \cdot P_k \cdot R \cdot P_j$$

where

P_d = probability of detecting the threat,

P_p = probability of successful positioning of the interceptor,

P_s = probability of survival of the aircraft until missile launch,

P_k = lethality or kill probability of the weapons system ,

R = reliability of the system.

(This is separated out only to underline its importance: it is apparent that a reliability factor could instead be used to modify each of the other component probabilities.)

P_j = degradation of the system due to E.C.M.

A system effectiveness study must therefore, to be complete, provide numerical values, or ranges of values, for each of these factors.

To date, work on the study has been concentrated on computations of Placement Probability P_p for a supersonic interceptor attacking a supersonic target. This has been selected as the central point of the study, as being the factor that is most affected by variations in performance of the aircraft and the AI radar. Some work has been done towards obtaining values for P_k, P_j and P_s. The problem of ground environment and therefore the determination

of P_d has been entirely neglected at CARDE; it had been hoped that an independent ground environment study would provide a value or values for this element. Determination of a value for R has not yet been attempted.

5. ACTIVITIES Nov 1956/March 1957

5.1 Information Sources

The much awaited general tour of U.S. establishments by a group of CARDE personnel engaged in the study took place during December 1956. A summary of the itinerary and general results of the visit is given in Appendix 'T'. The party was well received at all the places visited and was able to compare the progress of the CARDE study with that of similar or related studies going on in the U.S.A. One unfortunate circumstance was that only one member of the party was cleared for a one day visit to the RCA Airborne Systems Laboratory in Waltham, so that little information was obtained from that source.

Liaison arrangements between CARDE and AVRO Aircraft Limited in Toronto have continued to function smoothly.

Liaison with the RCA group in Waltham has been rather weak. The one-day visit by one Systems Group member from CARDE served as an introduction to RCA's work. During February two members of the RCA staff who are assigned to the CF 105 project made a two-day visit to CARDE. RCA progress reports on their work are being procured as rapidly as possible.

In connection with lethality studies, a member of the Systems Group made a visit to Canadair to discuss the structure of modern aircraft, with useful results.

5.2 The Placement Problem

A large amount of work on the placement problem was done on various parts of the placement problem during the period under review. In most cases the results are presented as graphs of placement probability vs. AI acquisition range. The different problems in this field which are reported on are summarized in the following paragraphs. A consolidated table listing all the placement probability graphs which are published in this report will be found on pages 21 and 22.

5.2.1 Constant Speed Interceptor in Two Dimensions

Placement charts for evading supersonic targets, and a constant speed interceptor, were prepared at CARDE by the Analysis Group in "G" Wing, for one target speed and various values of interceptor performance capability. These results are given in Appendix 'B'.

5.2.2 Further Work for Constant Interceptor Speed

Some placement charts for other sets of parameters were prepared by Computing Devices of Canada under contract. These were reduced to probability form at CARDE and the results are given in Appendix 'C'. These results are for evading supersonic targets, at two different speeds, and a constant speed interceptor.

5.2.3 Non-Evading Target and Decelerating Interceptor

Appendix 'D' describes a graphical method which has been developed for drawing placement charts for a decelerating interceptor and a non-manoeuvring target. Results in the form of placement probabilities are published for two target speeds and two initial interceptor speeds, and for two different sets of CF-105 aerodynamic estimates.

5.2.4 Evading Target and Decelerating Interceptor

Methods for simulating the interceptor aerodynamics on the REAC have already been described in previous progress reports on this study. This two dimensional simulation was operated for some time at CARDE using one set of aerodynamic characteristics. The results are published in Appendix 'E'. Simultaneously a second set of aerodynamics has been inserted into a similar simulation at Computing Devices of Canada Limited, under contract. The placement charts were reduced at CARDE to the form of probabilities of successful placement. These results are given in Appendix 'F'.

5.2.5 Three Dimensional Work

The three dimensional simulation which was proposed and described in previous progress reports in this series has been set in operation, and checked out. Preliminary results only are available, and these have not yet been reduced. Several placement charts for

non-coaltitude climbing attacks are however published in this report, to illustrate the problem. (Appendix 'G').

5.2.6 Look Angle Limits

One of the AI parameters which affects placement probabilities is the Look Angle Limit. Tactical methods of reducing deterioration of placement chance by this limit have been investigated, and are studied in Appendix 'K'.

5.2.7 Placement Probabilities with Unguided Rockets

A brief study of placement probabilities with the CF-105 using unguided long range rockets was made, in particular to determine effect of reduction in magnetion power below the specified megawatt value. This investigation is described in Appendix 'M'.

5.3 Other Simulation Results

The REAC interception simulation has been used for other work than the drawing of placement charts. A brief study of dog-leg evasion of subsonic targets has been made and is described in Appendix 'L'. Here the CF-105 is assumed to be operated in the subsonic speed range, and a placement barrier in terms of engagement time is drawn.

A brief study of the time required for interception in supersonic attacks has been made, to determine the range of cases where this time may be too short for decision making on the part of the CF 105 pilot/navigator crew. This is reported in Appendix 'H'. A study of post-launch fighter manoeuvres is given in Appendix 'J'.

Some effects of launch zone variations on the placement chart are studied in Appendix 'A'.

5.4 Fire Control Studies

The effort of the small group working on the Fire Control problem was centred on study of the RCAF Specification for the CF 105 electronic system and the RCA proposal on which the Astra I design is based. Discussion of these two documents is given in Appendix 'P'.

5.5 IR Studies

Work on I.R. has also been restricted to evaluation of R.C.A. work, and a discussion of this is given in Appendix 'Q'.

5.6 Lethality Studies

Construction of the engagement simulator and models for use with it has been completed. Work on the simulation of warhead bursts has not yet started pending the allotment of personnel to this work. A preliminary study of the vulnerability of the targets to be considered, for the warheads being investigated, has been made and is reported in Appendix 'N'.

5.7 E.C.M.

The Defence Research Telecommunications Establishment has been investigating the effects of certain postulated electronic counter measures on the Astra I AI. A preliminary draft of their analysis has been received and is

as Appendix 'R' of this report. These results are subject to revision if any changes in assumptions appear to be warranted.

Very little was learned during the recent U.S. visit of techniques of injecting E.C.M. studies into systems evaluations. The Systems Group is continuing to study this matter.

Work on the use of range finding manoeuvres has been continued within the Systems Group. The method proposed in Appendix 'G' of the previous progress report in this series is being evaluated. The equations have been programmed for the ALWAC Digital Computer at CARDE and results should be obtained in the next quarter. These results when available should furnish information on the feasibility of range finding manoeuvres, and should enable CARDE to specify a useful type of manoeuvre for this purpose.

6. PRESENT INDICATIONS

Although the results obtained thus far in the study have not yet been exhaustively analysed, some general observations and conclusions are given here.

6.1 Subsonic Targets

To the present, supersonic targets have been studied almost exclusively in the CARDE study. This is a consequence of the emphasis which is placed on the probability of placement. For the subsonic

target, where the CF-105 has a distinct speed advantage when required, it can be assumed that the placement chance P_p is effectively 1, and evaluation will then be in terms of the other component probabilities. In work leading to values for these other factors, the subsonic target will not be neglected. In lethality work it is proposed to study a typical subsonic target and a typical supersonic target. The other major field where the subsonic and supersonic bombers will provide different results is in computation of P_d the detection probability, and in operational studies where attrition of a bomber force by a defence squadron is to be calculated. Operational studies of this type have been assumed to be outside of CARDE's terms of reference in this assessment.

6.2 Target Evasion

Realistic target evasion has a large effect on values of placement probability; a Mach 2 target can turn and run away from a CF-105. There is a large dependence between the effect of evasion and the evasion tactics assumed. In most cases CARDE has assumed an intelligent enemy and results are given for this most pessimistic case. The assumption of the bomber's freedom to evade may not be justified in all operational situations; on the other hand the advantage for the bomber of using evasive manoeuvre is so great that some sacrifice of raid effectiveness may be accepted by the bomber force in order to improve its survival chance by permitting such manoeuvres. These considerations on evasion philosophy are again beyond the scope of CARDE's study. Results will in general be presented for evading as well as for straight-flying targets.

6.3 Missiles

Work in this quarter again pointed out the relative unimportance of the missile parameters in determining placement probability. Variations of missile characteristics which have been studied have been small, however, merely to point out any inaccuracies in the placement results due to possible errors in missile launch zone or kinematic assumptions. Use of a second generation very long range missile has not been studied.

6.4 Aircraft Performance

The presently accepted value of the load factor limit for a constant speed turn for the CF-105 is 1.63 g at M 1.5 at 50,000 feet. This corresponds to a lateral turn capability of 1.3 g's. The results for placement probability at this level of performance may be obtained from the results which have been published to date, both in this report and the preceding progress report. A brief analysis is given here.

6.4.1 Constant Speed Manoeuvre

This paragraph summarizes the values of AI performance and ground environment accuracy necessary for acceptable placement probability in constant speed manoeuvres with this turn capability. A value of 85% has been taken as an acceptable level of placement chance. Plots of acceptable values of the two parameters: AI acquisition range and σ of ground environment accuracy are drawn in Figs. 1 and 2 for several cases to show typical results.

[redacted]

Figure 1a

85% Isoprobs for 1.63 g performance level.
NON-MANOEUVRING MACH 2 TARGET

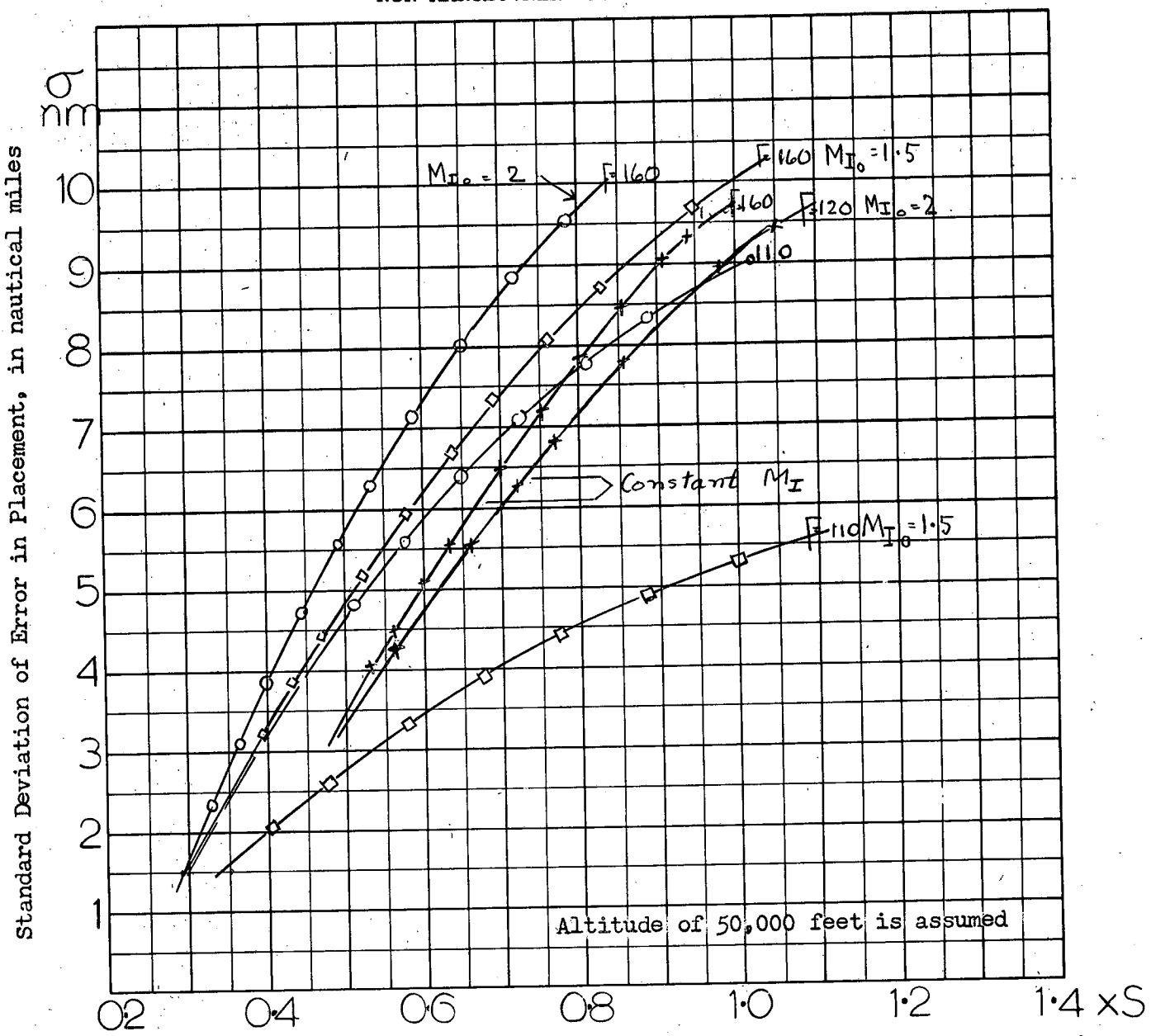

Drawn for the CARDE "Delta" AI Acquisition Contour, for which S = 34 n.m. range on the nose. The area below each curve represents acceptable values of σ and AI range.

—o—o—o— Interceptor manoeuvring to the buffet limit, initial Mach No. 2 (AVRO Performance)

—□—□—□— Interceptor manoeuvring to the buffet limit, initial Mach No. 1.5

—×—×—×— Interceptor making constant speed power-limited manoeuvre at M.No. 1.5

Results are shown for two values of Course Difference Γ.

The 1.63g load factor represents lateral manoeuvre 1.3g.

Figure 1b

85% Isoprobs for 1.63g performance level.
MANOEUVRING MACH 2 TARGET

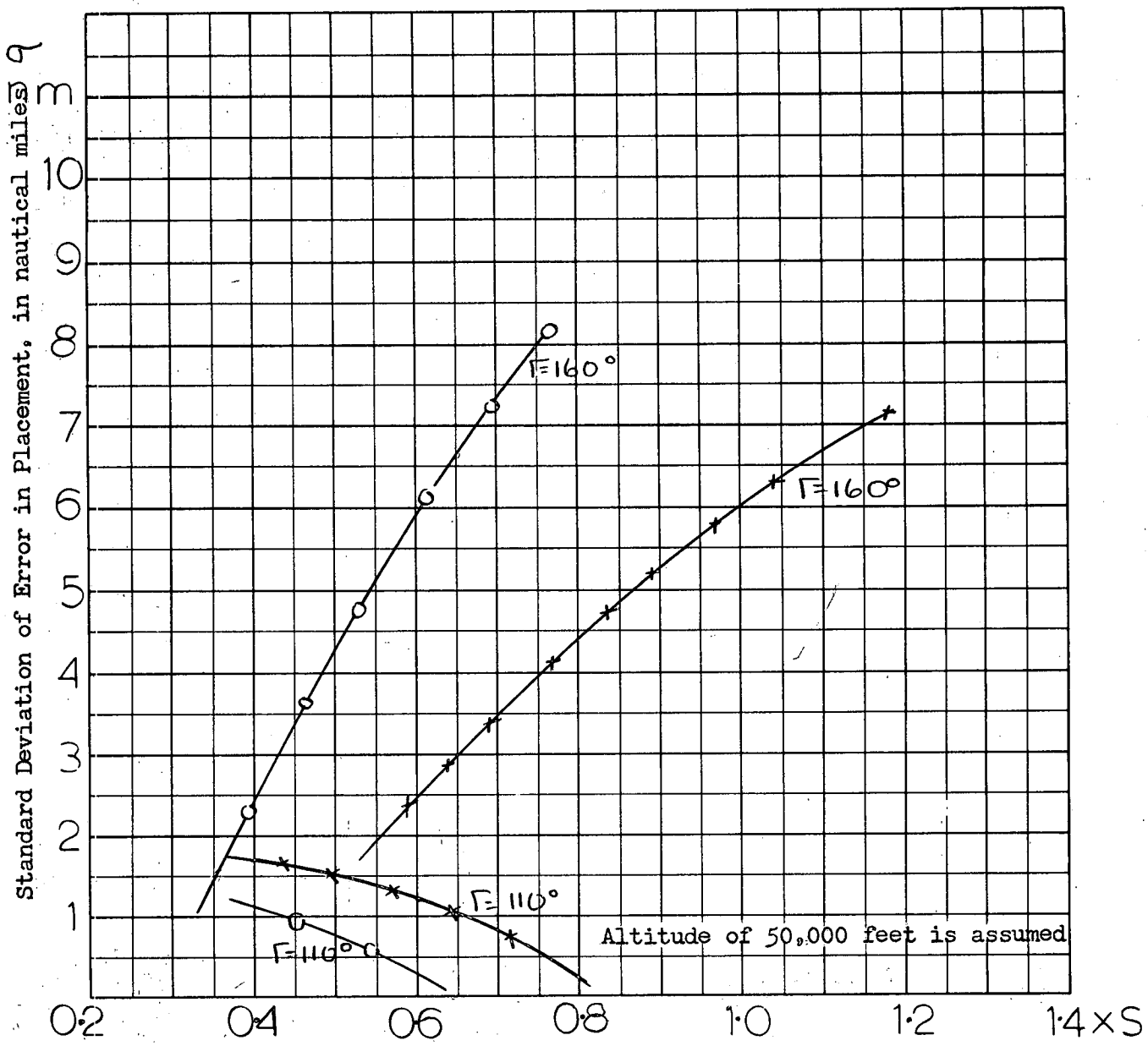

Drawn for the CARDE "Delta" AI Acquisition Contour, for which S = 34 n.m. range on the nose. The area below each curve represents acceptable values of σ and AI range.

—o—o—o— Interceptor manoeuvre to the buffet limit, initial Mach No. 1.8 (AVRO Performance)

—×—×—×— Interceptor making constant speed power-limited manoeuvre at Mach No. 1.5

Results for two values of Course Difference Γ are shown.
The 1.63g load factor represents lateral manoeuvre 1.3g.
Target manoeuvre Load factor 1.12 g
[Lateral g's .5]

Figure 2a

85% Isoprobs for 1.63g performance level.

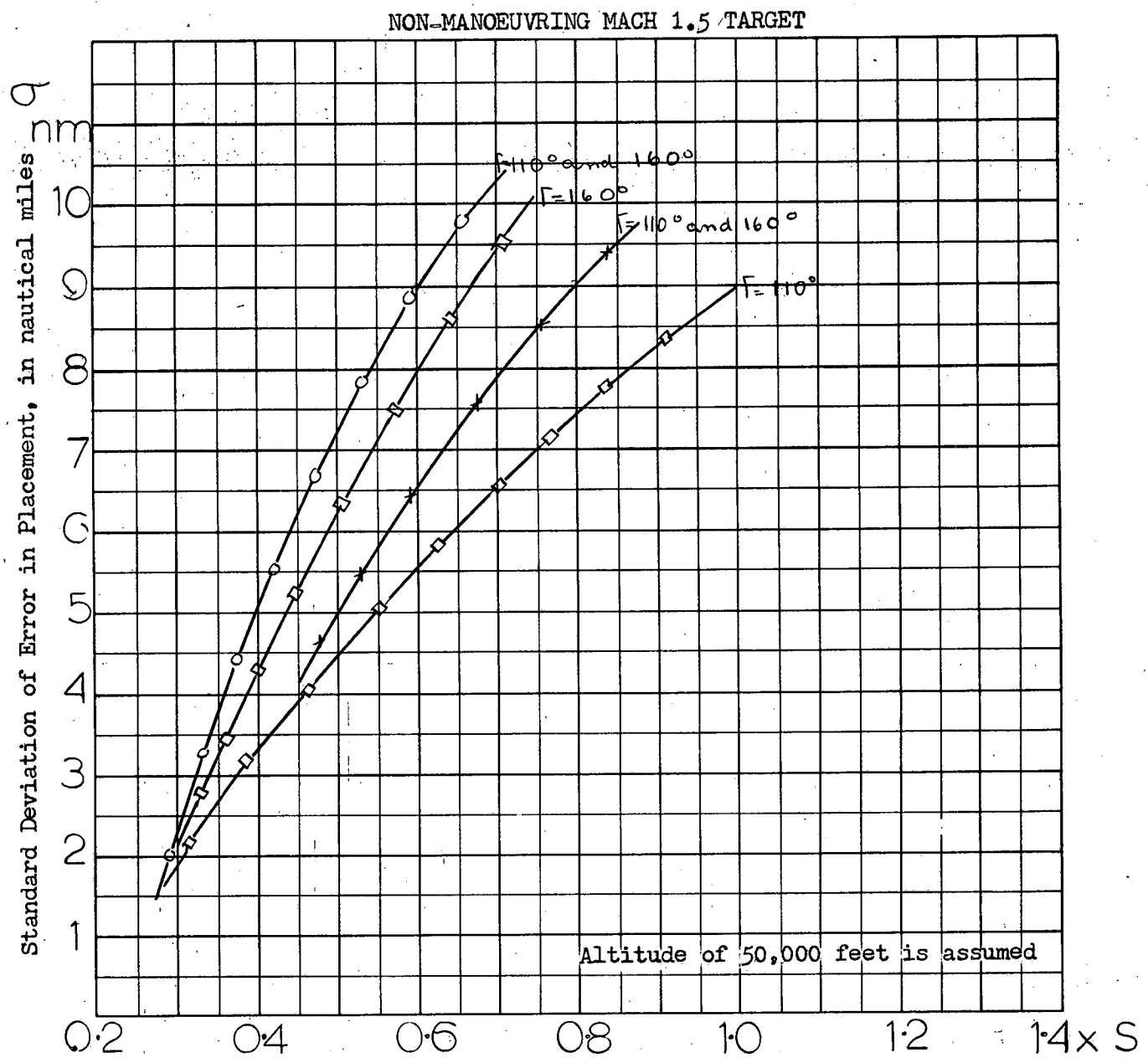

Drawn for the CARDE "Delta" AI Acquisition Contour, for which S = 34 n.m. on the nose. The area below each curve represents acceptable values of σ and AI range.

—o—o—o— Interceptor manoeuvring to the buffet limit, initial Mach No. 2

—□—□—□— Interceptor manoeuvring to the buffet limit, initial Mach No. 1.5 (AVRO Performance)

—×—×—×— Interceptor making constant speed power-limited manoeuvre at M.No. 1.5

Results are shown for two values of Course Difference Γ.
The 1.63g load factor represents lateral manoeuvre 1.3g.

Figure 2b

85% Isoprobs for 1.63g performance level

MANOEUVRING MACH 1.5 TARGET

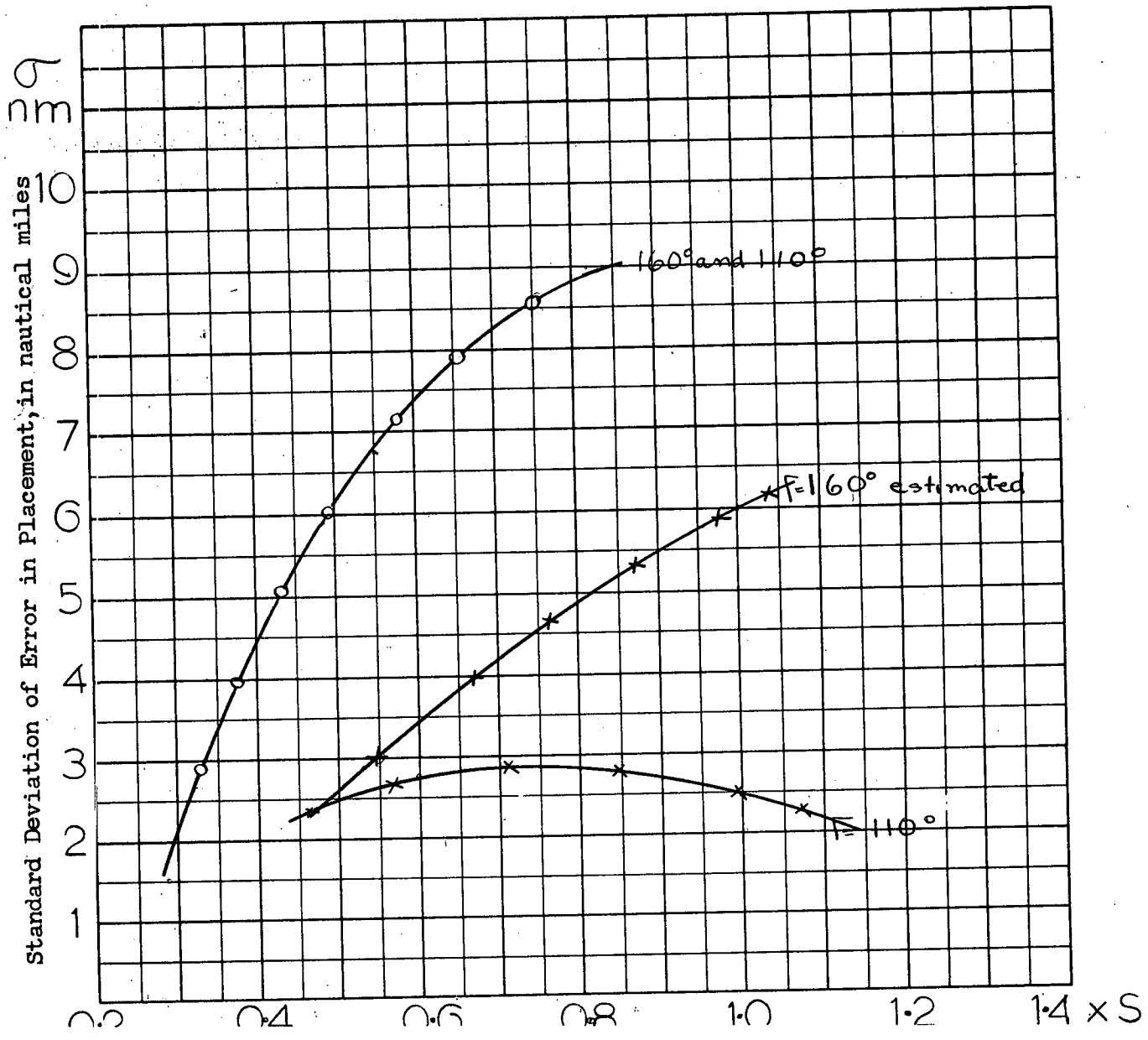

6.4.2 Decelerating Fighter Manoeuvre

Plots of acceptable σ and AI acquisition range values for the decelerating fighter case for the two aerodynamic estimates have been plotted on the same sheets, at the risk of confusing the reader. It is immediately evident that a fighter manoeuvring to the buffet limit to obtain sharper turn radius is sometimes slightly better but sometimes much worse than one making a lower load factor constant speed manoeuvre. Another conclusion on the basis of these graphs is that attacks on a more forward course difference (160°) are more often successful than beam attacks [course difference (110°)].

6.4.3 Ground Environment

A conclusion that may be drawn regarding ground environment accuracy is that good accuracy is required if the interception of a target which will manoeuvre upon engagement is required. The numerical answer given in this case is sensitive to AI acquisition range, which is in turn dependent on target echoing area assumed. The graphs of Figures 1 and 2 above are drawn for an optimistic specification range of 34 miles head-on (so called "Delta" target in this study). CARDE prefers to make a more complete analysis of the available results before giving even an approximate value for required GCI accuracy.

7. FUTURE PROGRAM

7.1 Immediate Plans

The principal activities in the coming quarter will be

(a) Exhaustive analysis of the results obtained to date, leading to publication of a summary report of the first year's work on the CF-105 Assessment in May 1957.

(b) Preparation of results in a form suitable for oral presentation to interested parties in DRB and RCAF Headquarters. It is planned that this will be held at the beginning of May.

(c) Continuation of the three-dimensional simulation placement studies.

(d) Continuation of the lethality studies.

(e) Fire Control studies in combination with the three dimensional interception simulation.

(f) Continued work on E.C.M.

7.2 Second Year of the Study

A program plan for the second year's work on the CF-105 Assessment Study has been prepared and is given in Appendix 'S'.

8. DISTRIBUTION

Recipient	Copy No.
Chief Supt. CARDE	1
D/Chief Supt. "	2
A/Chief Supt. "	3
Supt. A Wing "	4
B "	5
C "	6
D "	7
E "	8
F "	9
G "	10
Librarian CARDE	11
Document Library CARDE	12-15
Systems Group "	16-18
DRB HQ: Ch.of Establish'ts	19
Ch.Scientist	20
DWR	21-22
D Eng R	23
D Phys R	24
DSIS for circulation	25-27
Director/N.A.E.	28
S/ORG	29
S/DRTE	30-31
DRM, London	32-33
DRM, Washington	34-35
DRB Liaison Officer, Lincoln Lab MIT.	36
RCAF, HQ: ATTN COR/DSE	37-38
ATTN S/L Peek, 2630 A Bldg.	39-41
ATTN C ArmE	42-44
ATTN SACAS	45
ATTN TSO, RCA, Camden, N.J.	46-47*
RCA Airborne Systems Lab., Waltham, Mass., ATTN Mr. Daelhousen	48-49*

Recipient	Copy No.
Contributors:	
C.J. Wilson	50
L. Shepherd	51
J. Cummins	52
For Information	
Dr. G.V. Bull	53
Spares	54-75

---

* Copies 46-47 and 48-49 are to be addressed S/L G. Peek, DSE, for distribution to:- TSO, RCA, Camden, N.J.
- RCA Airborne Systems Lab., Waltham, Mass. Attn.Mr. Daelhousen.

PLACEMENT PROBABILITY GRAPHS

The following table lists the graphs of placement probabilities which are published in this report.

Notes. A.I. Radar Range is expressed as a fraction of the specification value, S. Two typical contours of acquisition range are used. The CARDE "Delta" pattern implies a range of 34 nm. on the nose; the CARDE Straight Wing, a range of 21.5 nm. on the nose.

Ground Environment placement accuracy is described by the standard deviation, σ, in the error of placement, measured perpendicular to the interceptor track.

Target evasion is described in lateral g's. Corresponding values of lateral acceleration and load factor g's are:

Lateral g's:	.25	.4	.5	.75
Load factor:	1.05	1.08	1.12	1.25

App.	Case	Delta Target Figure	Page	Straight Wing Figure	Page
'B'	Constant Speed Interceptor, Evading Target. M_T = 2.0, M_I = 1.5, H = 50K, n_T = .5 lateral g's, 4 values of Γ, 3 values of interceptor g's.	D1-12	41	S1-12	53
'C'	Constant Speed Interceptor, Evading Target. Evasion starting at fixed range.				
	M_T = 1.5, M_I = 1.5, H = 50K, n_T = .4 lateral g's, 4 values of Γ, 3 values of interceptor g's.	D3-18	68	S3-18	100
	M_T = 2.0, M_I = 1.5, H = 50K, n_T = .5 lateral g's, 4 values of Γ, 3 values of interceptor g's.	D19-34	84	S19-34	128
'D'	Non-evading Target and Decelerating Interceptor. NAE Performance Estimates.				
	M_T = 1.5, M_{I_o} = 1.5, H = 50K, 4 values of Γ.	5-8	151		
	M_T = 1.5, M_{I_o} = 2.0, H = 50K, 4 values of Γ.	9-12	155		
	M_T = 2.0, M_{I_o} = 1.5, H = 50K, 4 values of Γ.	13-16	159		
	M_T = 2.0, M_{I_o} = 2.0, H = 50 K, 4 values of Γ.	17-20	163		

App.	Case	Delta Target Figure	Delta Target Page	Straight Wing Figure	Straight Wing Page
'D'	Cont'd.. AVRO Performance Estimates				
	$M_T = 1.5, M_{I_o} = 1.5$, H = 50K, 4 values of Γ.	21-24	167		
	$M_T = 1.5, M_{I_o} = 2.0$, H = 50K, 4 values of Γ.	25-28	171		
	$M_T = 2.0, M_{I_o} = 1.5$, H = 50K, 4 values of Γ.	29-32	175		
	$M_T = 2.0, M_{I_o} = 2.0$, H = 50K, 4 values of Γ.	33-36	179		
	$M_T = 2.0, M_{I_o} = 1.5$, H = 40K, 4 values of Γ.	37-40	183		
	$M_T = 2.0, M_{I_o} = 2.0$, H = 60K, 4 values of Γ.	41-44	187		
'E'	Evading Target and Decelerating Interceptor. NAE 28% CofG Pessimistic Estimates. Evasion starting at acquisition.				
	$M_T = 1.5, M_{I_o} = 1.5$, H = 50K, $n_T = .75$, 30° & 60° off course evasion limits, 4 values of Γ.	D1-4	201	S1-4	229
	$M_T = 2.0, M_{I_o} = 1.8$, H = 50K, $n_T = .25$, $\Gamma = 110°$ only.	D5	205	S5	233
	$M_T = 2.0, M_{I_o} = 1.8$, H = 50K, $n_T = .5$, 4 values of Γ, several values of interceptor g limit.	D6-9	206	S6-9	234
	$M_T = 2.0, M_{I_o} = 1.8$, H = 50K, $n_T = .75$, 30° & 60° off course evasion limits, 4 values of Γ.	D10-13	217	S10-13	245
	$M_T = 2.0, M_{I_o} = 1.8$, H = 55K, $n_T = .5$, 4 values of Γ.	D14-17	225	S14-17	253
	Plots of Probability vs Target Change of Course. $M_T = 2.0, M_I = 1.8$, H = 50K, $n_T = .75$ Three values of Γ and AI Range.	D18-26	257	S18-26	266
'F'	Evading Target and Decelerating Interceptor. Final AVRO Estimates of CF 105 Performance. No evasion beyond 150,000 ft. range.				
	$M_T = 2.0, M_{I_o} = 1.5$, H = 50K, $n_T = .5$, Several values of Interceptor g-limit, 5 values of Γ.	D1-5	279	S1-5	319
	$M_T = 2.0, M_{I_o} = 1.8$, H = 50K, $n_T = .5$, 3 values of Γ. 2 values of Interceptor g-limit.	D6-8	290	S6-8	330
	$M_T = 2.0, M_{I_o} = 1.8$, H = 50K, $n_T = .5$, 4 values of Γ. Buffet limit for interceptor.	D9-12	298	S9-12	338
	$M_T = 2.0, M_{I_o} = 1.8$, H = 60K, $n_T = .5$, 4 values of Γ. Buffet Limit	D13-16	302	S13-16	342
	$M_T = 2.0, M_{I_o} = 2$, H = 50K, $n_T = .5$, 5 values of Γ. 3 values of Interceptor g-limit.	D17-21	306	S17-21	346

APPENDIX 'A'

A Survey of Launch Zones and their Effect on Placement Probability

by Lloyd Shepherd

1. Introduction

Before work on the 2-dimensional placement study could begin, it was necessary to have launch zone information for the missile. Since insufficient launch zone information was available for the missiles in the Sparrow family, a hypothetical missile similar to Sparrow II was simulated by CARDE in a preliminary REAC study. (Ref.1.) The results from this study were used to construct the launch zones for the REAC work. For some phases of the 2-D study some further assumptions and simplifications were necessary. It is the object of this appendix to survey what has been done and to show what effect these assumptions and simplifications have on the values obtained for placement probability.

2. Launch Zones

The hypothetical missile studied by CARDE was a simplified version of Sparrow II. This study produced curves of launch range and allowable heading error for different target aspects. The maximum range launch contour was modified at front aspects by a missile seeker range which was taken to be 50,000 ft. on the target nose. Figure 1 shows the process. The minimum range contour is arbitrarily chosen as that for some allowable heading error, which may be 0°, 5° or 10°. The maximum range contour is due to aerodynamic range (flight time, oil supply, closing rate) except in nose aspects where the seeker lock-on contour governs. The launch zones which have been used for the REAC trajectory work were published in Reference 4. (Appendix K, pp 700-1).

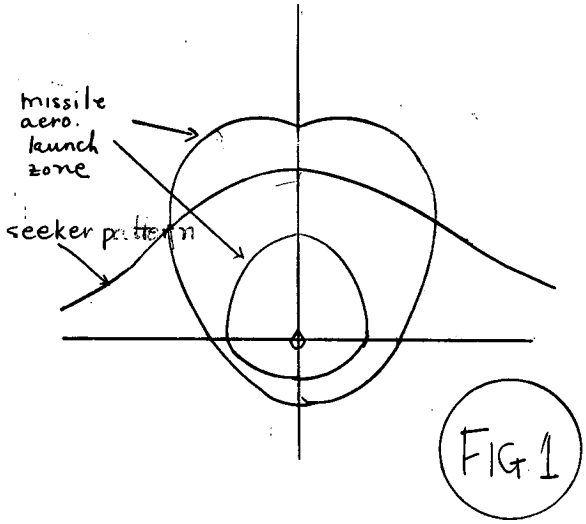

FIG 1

2.1 Early in the REAC analysis it had been proposed to adopt the lead collision navigation method described in Hughes Aircraft Company TM 339.(Ref.2). It became evident however that the lead collision navigation provided for missile launch on a circle only, and thus was not too suitable for an irregular launch contour or a zone with depth. A lead pursuit course on the

other hand provides for the proper lead angle at all times. The mode of attack which was finally adopted was lead collision to a point outside the launch zone and lead pursuit for the remainder of the attack.

2.2 For some of the paper-and-pencil work (compare Appendix D) it was not convenient to handle the conversion to lead pursuit so the pure lead collision attack was adopted and an F-circle was taken as the launch contour. The adoption of an F-circle for a launch zone assumes an average missile velocity and a constant time of missile flight. The launch circle which is chosen must lie within the allowable zone.

3. The Effect of Launch Zone Variation on the Placement Zone

3.1 Because of the uncertainty of the actual characteristics of the Sparrow missile family and the simplifications which were made, it is necessary to know how changes in launch zone assumptions will affect the placement probability values. The effect of missile launch zone on placement probability is best analysed by considering the components of the placement zone. In the 2-D work the placement zone has been bounded by barriers designated as (i) look angle, (ii) fallback, (iii) manoeuvre.

3.2 Look-angle Barrier

The look angle barrier is due to the navigation computer instructing the interceptor to turn until the target is no longer illuminated by the AI radar. This barrier is independent of any launch zone or missile considered in the 2-D placement study, being affected by interceptor and target speeds, the look angle limit, and the fire-control computer.

3.3 Fallback Barrier

The fallback barrier gives the limit of the placement zone for which the fighter is just able to approach to the missile maximum range launch contour. This applies only in cases of fighter speed disadvantage. If evasion begins when the fighter is at long range, this barrier is close to or crosses the ideal approach line. For this reason there is often a decrease in placement probability at long AI acquisition ranges and small changes in the position of this barrier have marked effects on the placement probability.

3.3.1 Universal Fallback Barrier

For the purpose of understanding the fallback barrier and its dependence on launch zones, it is convenient to define the universal fallback barrier as the theoretical limit to the placement zone. This barrier for the manoeuvring target cases corresponds to the straight line fallback barrier which can be drawn for the straight flying target case. (Ref.3, Appendix M). A construction is used which assumes constant fighter and target velocities, constant rate of target evasion, and that the fighter flies in a straight line to the actual collision point. This construction is independent of fighter aerodynamics and neglects the curvature of the lead collision course against a manoeuvring target.

It is assumed that the missile maximum range launch contour can be expressed in the lead collision equations as a length of F-pole, due to the equation

$$V_M T_f = V_F T_f + F,$$

or

$$F = \Delta V_M T_f.$$

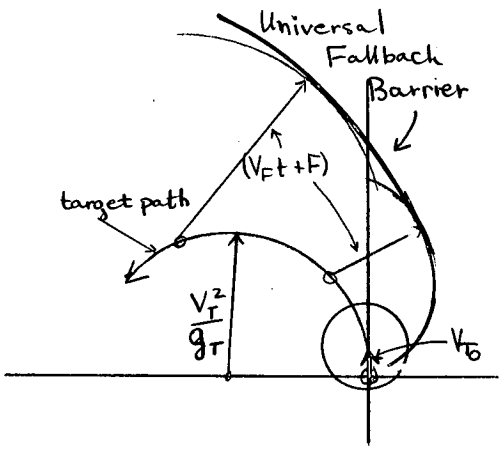

FIG 2

If a launch zone variation is expressed as a variation in $\Delta V_M T_f$, the universal fallback barrier construction readily gives the extent of the change in the fallback barrier.

The construction of the universal fallback barrier is illustrated in Figure 2. The future path of the target can be drawn knowing the speed and rate of evasion. From a point on this path corresponding to an interception t seconds from now, a circle of radius $V_F t + F$ can be drawn. For a successful attack terminating at this point the fighter must now be within this circle. Drawing a series of such circles will form a barrier which will be called the universal fallback barrier.

3.3.2 Results

Figures 3, 4 and 5 show the effects on placement probability due to variations in the launch zone expressed as changes in the value of $\Delta V_M T_f$. The curves cover a much wider range of values than would normally be expected. These curves illustrate the drop in placement at long AI ranges because the target evasion places the fallback barrier close to the ideal approach line. It is in these cases where the barrier lies close to the ideal approach line that the variations in $\Delta V_M T_f$ have a large effect on the placement probability. It is true that these may be unrealistic cases since target evasion may not begin at such extreme ranges.

The values of course difference quoted for these results have meaning only in the placement of the ideal approach line. It should also be noted that the actual fallback barrier is not as far out as is indicated by this construction. This construction is then optimistic and the actual variations for a given set of parameters will have a more pronounced effect on the probability than is indicated by the curves of Figures 3, 4, and 5.

3.4 Manoeuvre Barrier

The launch zone and variations in the launch zone have their greatest effect on the manoeuvre barrier. From REAC work it is noted that the actual displacement of the barrier is small; however at close ranges the placement zone is narrow and small displacements in the barrier make large variations in the placement probability.

A special REAC study was made to determine the effect of launch zones on placement probability for the constant speed fighter case. Characteristics were assumed for a hypothetical missile similar to Sparrow II and a series of F-circles were used as launch zones. (See Fig.6.).

3.4.1 Effect of Launch Range

Figures 7, 8, 9 and 10 show the effect on placement probability of launching the missile from different F-circles. These curves could be used in determining the effect of a variation in the missile seeker range or the effect of an increased permissible time of missile flight.

3.4.2 Effect of Heading Error Allowance

The order of variation of probability in the manoeuvre region due to a change in the allowable heading error for the constant speed case is shown in Figs. 11, 12 and 13. Additional curves showing the effect of heading error have been published in Appendix K of Ref. 4.

4. Conclusions

From the study some insight has been gained into the manner in which variations in the launch zone affect placement probability. It has shown that moderate changes in the launch zone would have only small effects on the placement zone and the placement probability. If the actual missile characteristics are vastly different from the ones assumed for the missile of this study, larger variations in the placement probability can be expected. The amount by which the placement probabilities vary due to launch zone variation is sharply dependent on the value of AI acquisition range used. Probabilities computed for the medium values of AI performance (specification or .85 specification values) are little affected both for non-evading and evading targets. The placement probability values for poor AI performance are affected by variations in heading error allowance and launch range for both evading and non-evading targets: placement probability increases as heading error allowance increases and as launch range decreases. When high AI performance is assumed (better than specification value), changes in launch zone affect the probability values for evading targets, while those for non-evading targets are unaffected.

5. References

1. CARDE Technical Letter No. N-47-2 "Launch Zones for a Hypothetical Constant-Bearing Missile" by J.T. Macfarlane.

2. Hughes Aircraft Company, Technical Memorandum 339. "A General Description of the Universal Computer".

3. CARDE Technical Memorandum No. 119/55. "A Study to Determine the Effectiveness of the CF-100 Mk. 4B Armed with Sparrow II Missiles against a Type 37 Bomber" by S.Z. Mack.

4. CARDE Technical Letter # N-47-12. "Second Quarterly Report on CF-105 Weapon System Assessment" by Systems Group.

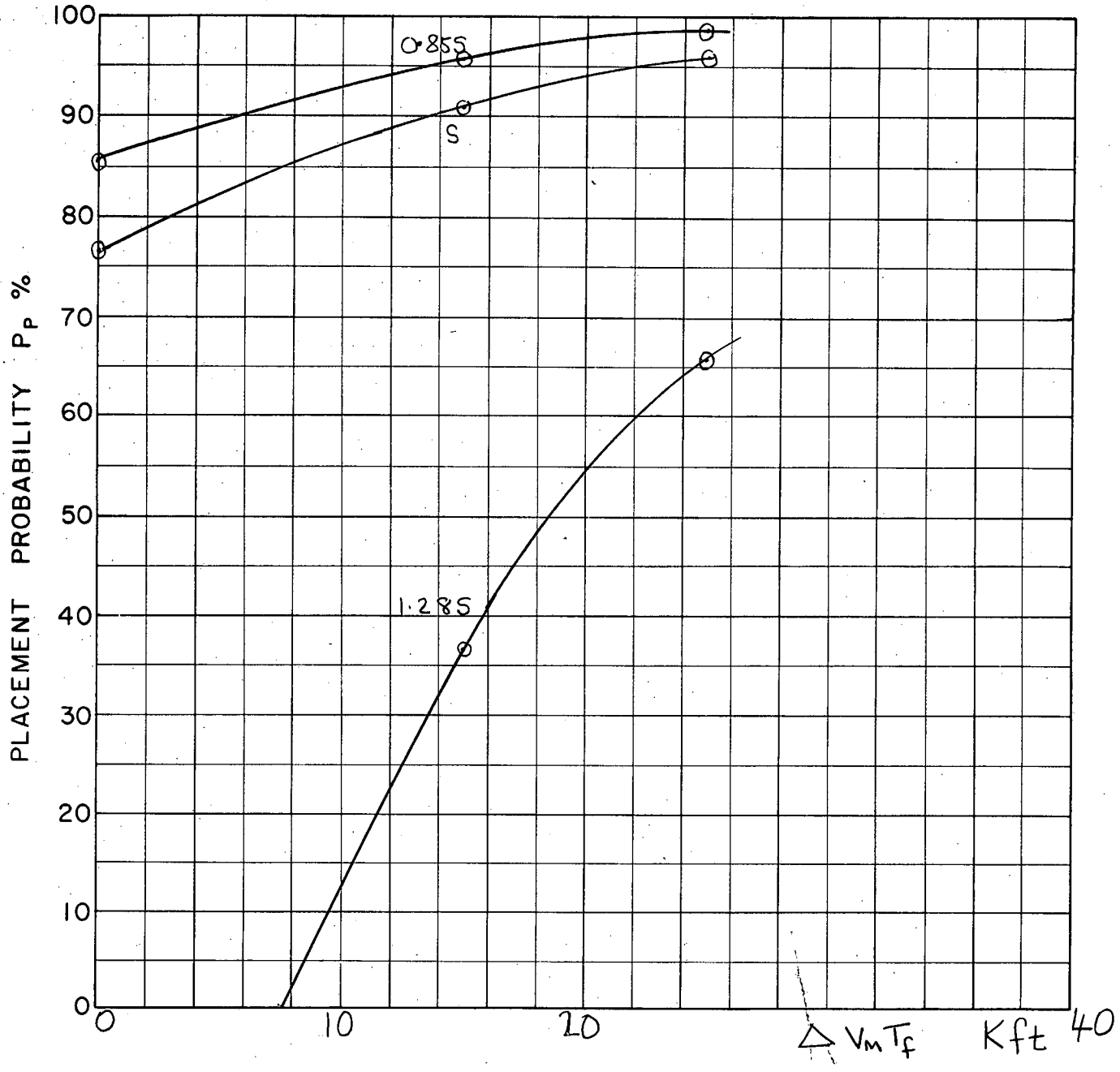

FIG 3 A

COURSE DIFFERENCE: 180°
TARGET EVASION: 0.75 lateral g's
TARGET MACH NO.: 2.0
INTERCEPTOR LATERAL G's: -
INTERCEPTOR MACH NO.: 1.5
σ OF G.C.I. ACCURACY: 4.75
A.I. DETECTION RANGE AS FRACTION OF SPECIFICATION RANGE, S: 3 values
A.I. DETECTION RANGE CONTOUR: Delta
ALTITUDE: -

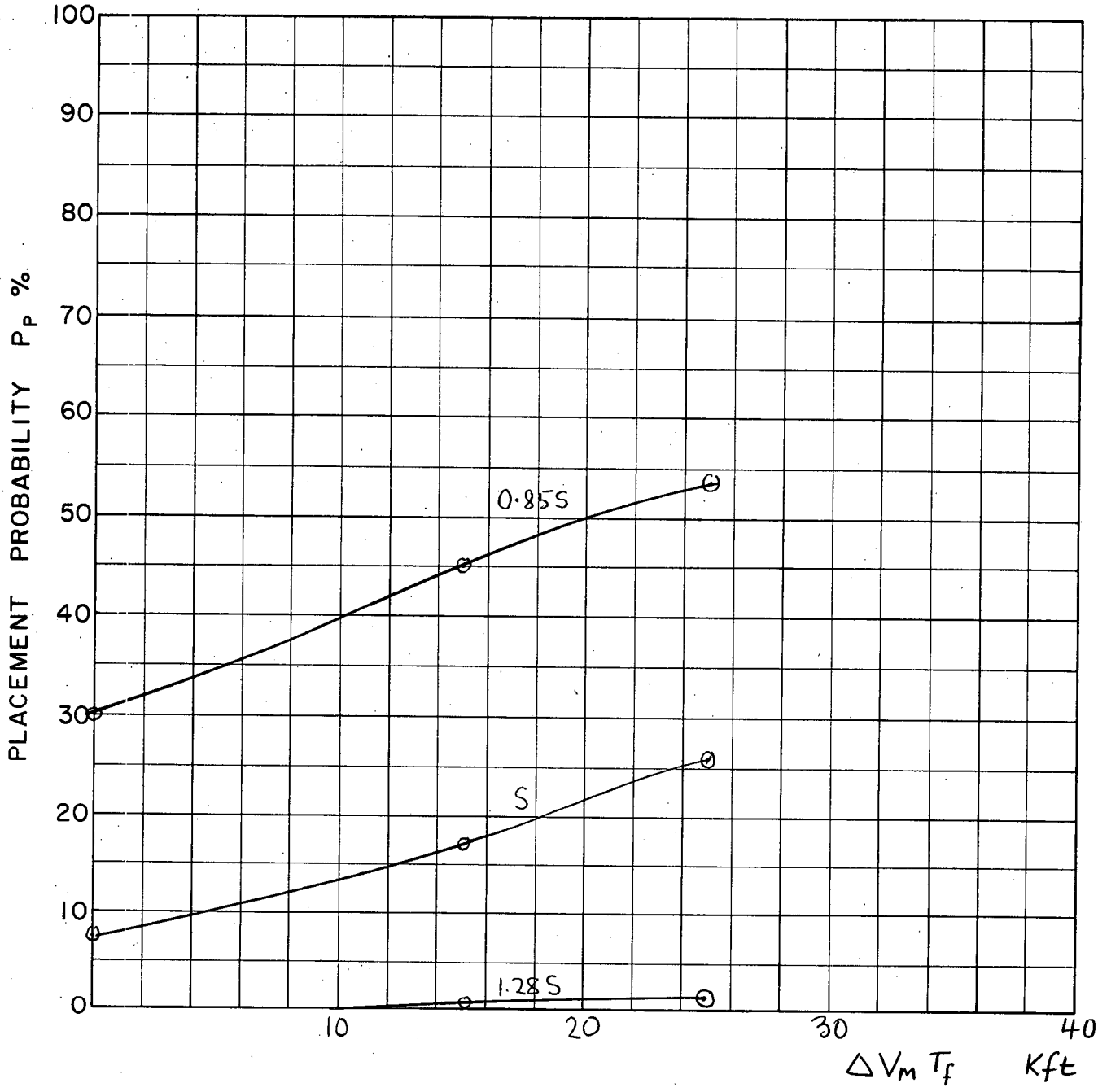

COURSE DIFFERENCE: 135°
TARGET EVASION: 0.75
TARGET MACH NO.: 2.0
INTERCEPTOR LATERAL G's: -
INTERCEPTOR MACH NO.: 1.5
σ OF G.C.I. ACCURACY: 4.75 n.m.
A.I. DETECTION RANGE AS FRACTION OF SPECIFICATION RANGE, S: 3 values
A.I. DETECTION RANGE CONTOUR: Delta
ALTITUDE: -

FIG. 4 A

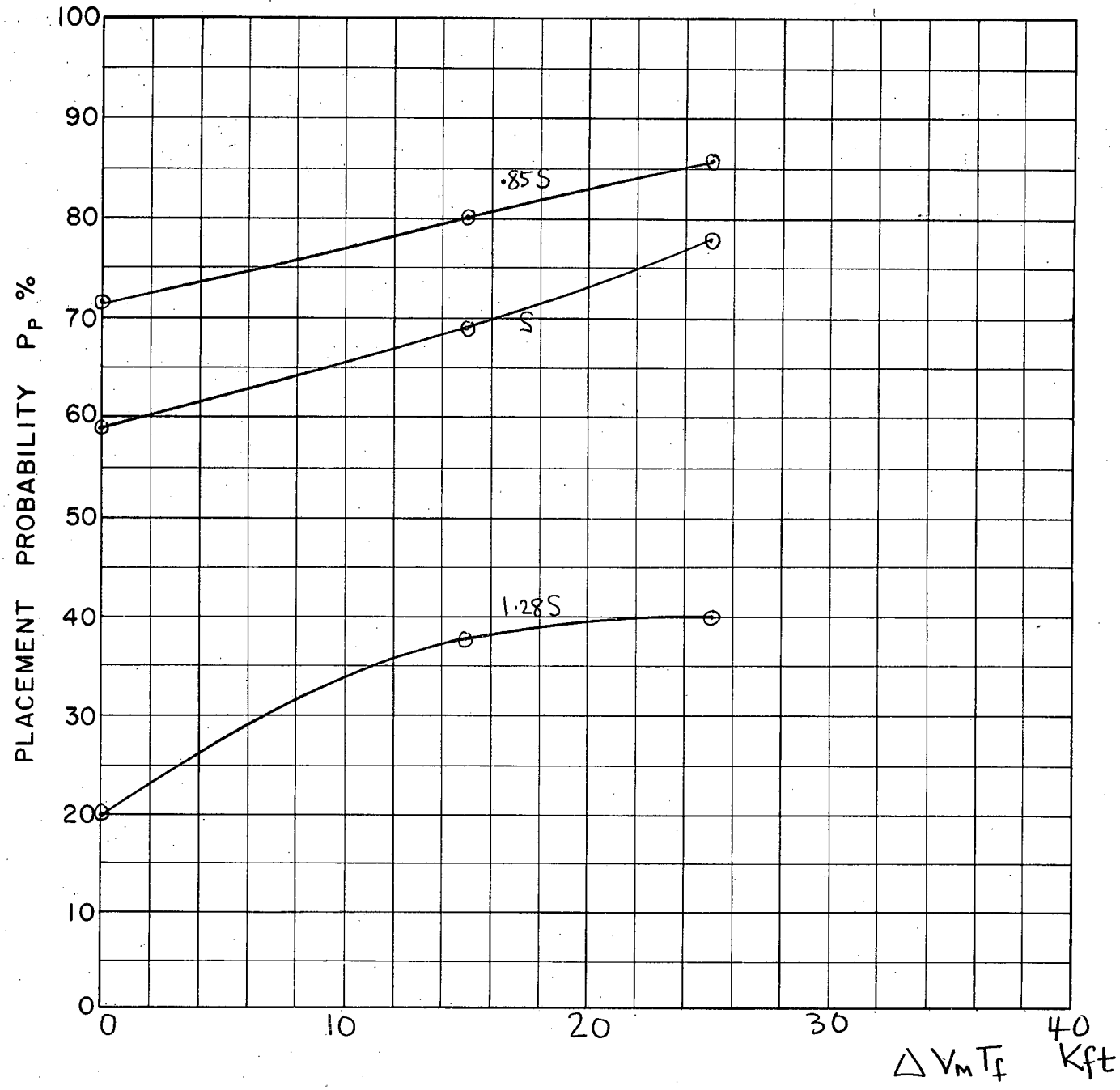

COURSE DIFFERENCE: 135°
TARGET EVASION: 0.5
TARGET MACH NO.: 2.0
INTERCEPTOR LATERAL G's: -
INTERCEPTOR MACH NO.: 1.5
σ OF G.C.I. ACCURACY: 4.75 n.m.
A.I. DETECTION RANGE AS FRACTION OF SPECIFICATION RANGE, S: 3 values
A.I. DETECTION RANGE CONTOUR: Delta
ALTITUDE: -

FIG. 5 A

COMPOSITE LAUNCH ZONE

$M_T = 2.0$ $M_F = 1.5$

$V_M = 1200$ ft/sec (boost)

$\dot{V}_M = 40'/sec^2$ (glide)

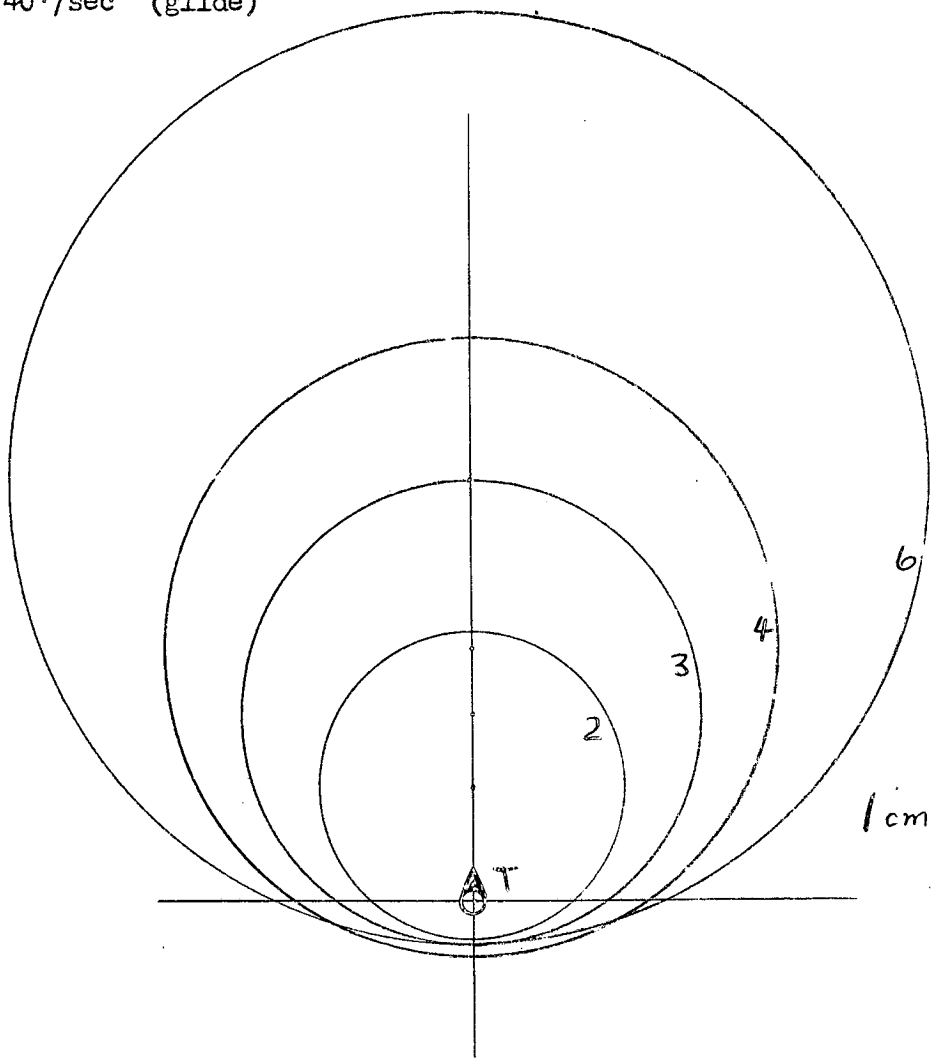

1 cm = 10,000 ft

	$V_M t_f$	t_f secs	$\bar{M}_m$	$V_T t_f$ feet	F
2	20,000	8.3	2.47	16,100	7,930
3	30,000	12.7	2.43	24,500	11,500
4	40,000	17.3	2.38	33,600	15,000
6	60,000	28.2	2.20	54,100	18,900

FIG 6 A

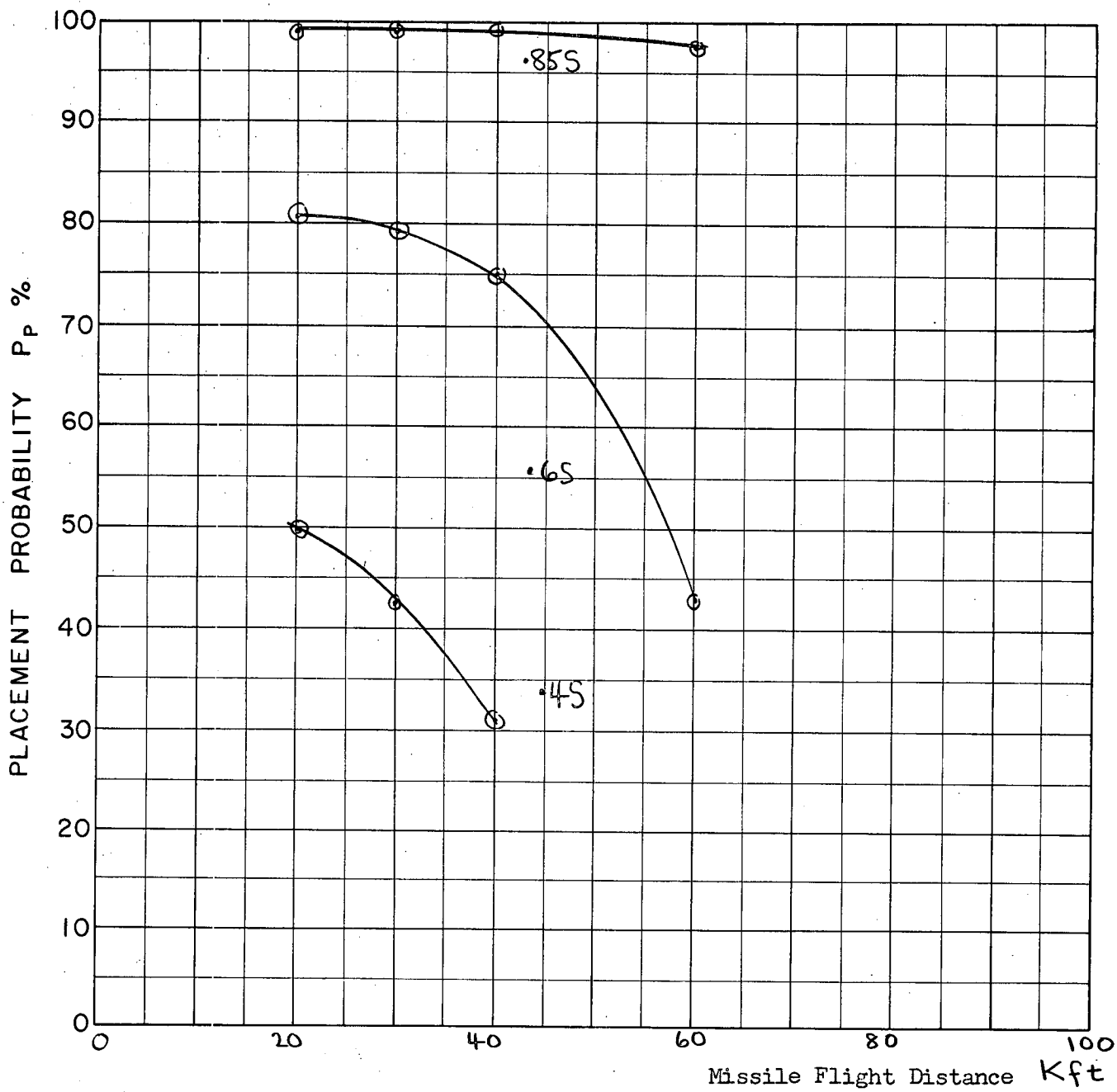

$\epsilon = \pm 15^{\circ}$

$F = 15{,}000$

COURSE DIFFERENCE: 180°
TARGET EVASION: 0
TARGET MACH NO.: 2.0
INTERCEPTOR LATERAL G's: 1.6
INTERCEPTOR MACH NO.: 1.5
σ OF G.C.I. ACCURACY: 4.75 n.m.
A.I. DETECTION RANGE AS FRACTION OF SPECIFICATION RANGE, S: 3 values
A.I. DETECTION RANGE CONTOUR: Delta
ALTITUDE: -

FIG. 7 A

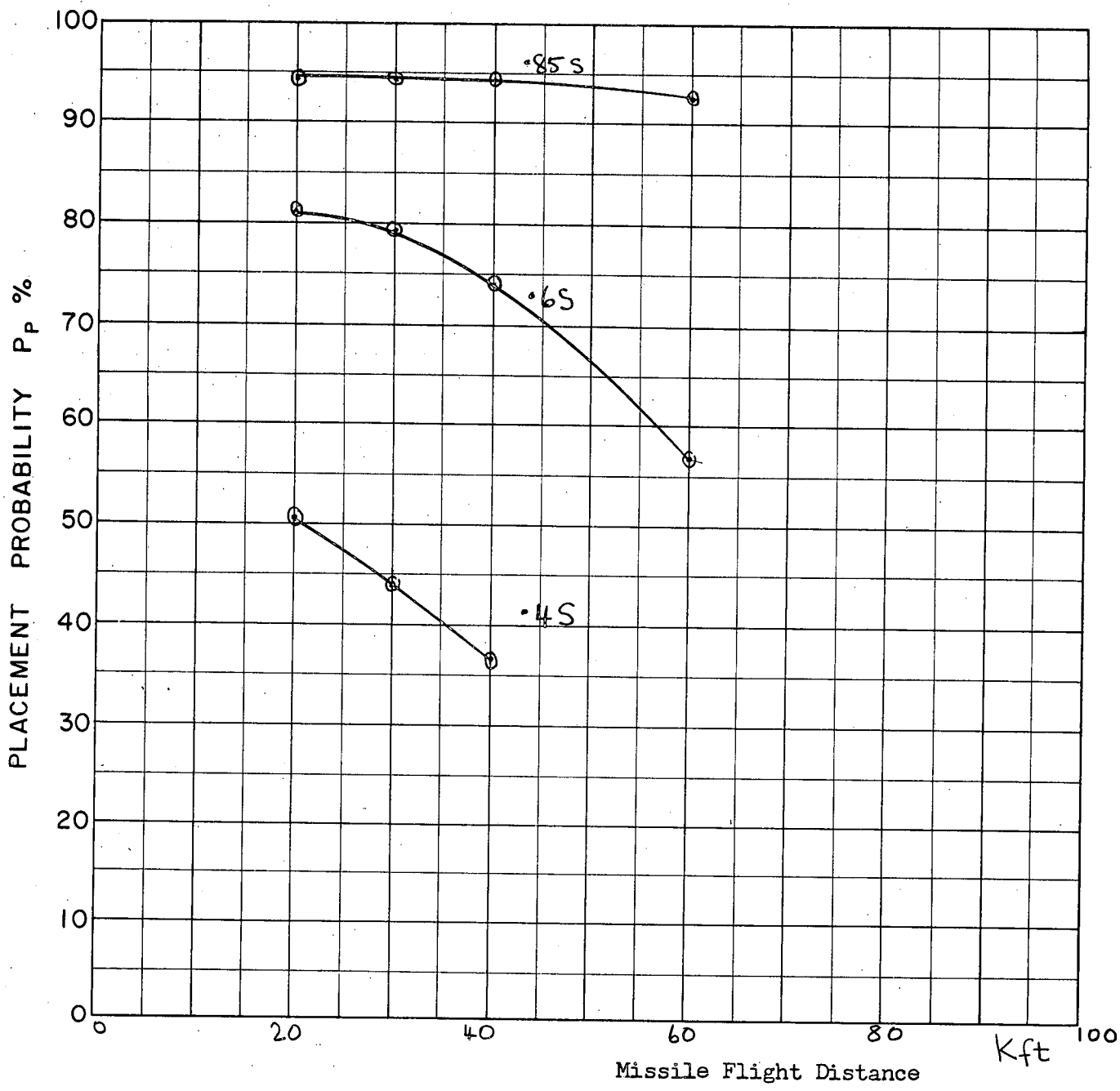

$\epsilon = \pm 15^\circ$
F = 15,000'

FIG 8
A

COURSE DIFFERENCE: 110°
TARGET EVASION: 0
TARGET MACH NO.: 2.0
INTERCEPTOR LATERAL G's: 1.6
INTERCEPTOR MACH NO.: 1.5
σ OF G.C.I. ACCURACY: 4.75 n.m.
A.I. DETECTION RANGE AS FRACTION OF SPECIFICATION RANGE, S: 3 values
A.I. DETECTION RANGE CONTOUR: Delta
ALTITUDE: -

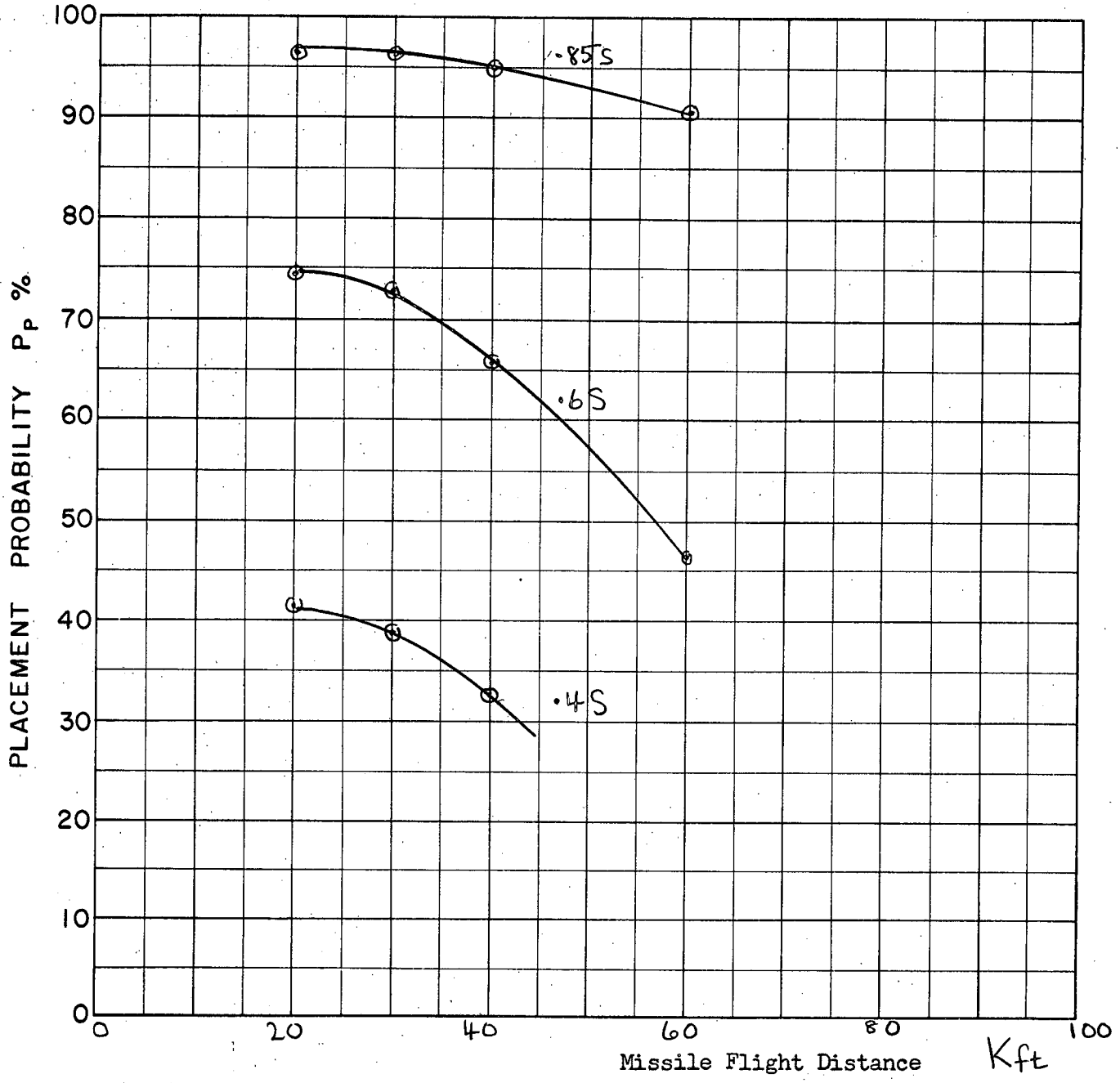

$\epsilon = \pm 15°$
$F = 15{,}000'$

FIG. 9 A

COURSE DIFFERENCE: 180°
TARGET EVASION: 0.5
TARGET MACH NO.: 2.0
INTERCEPTOR LATERAL G's: 1.6
INTERCEPTOR MACH NO.: 1.5
σ OF G.C.I. ACCURACY: 4.75 n.m.
A.I. DETECTION RANGE AS FRACTION OF SPECIFICATION RANGE, S: 3 values
A.I. DETECTION RANGE CONTOUR: Delta
ALTITUDE: -

Pessimistic Zone ($\pm$ evasion)

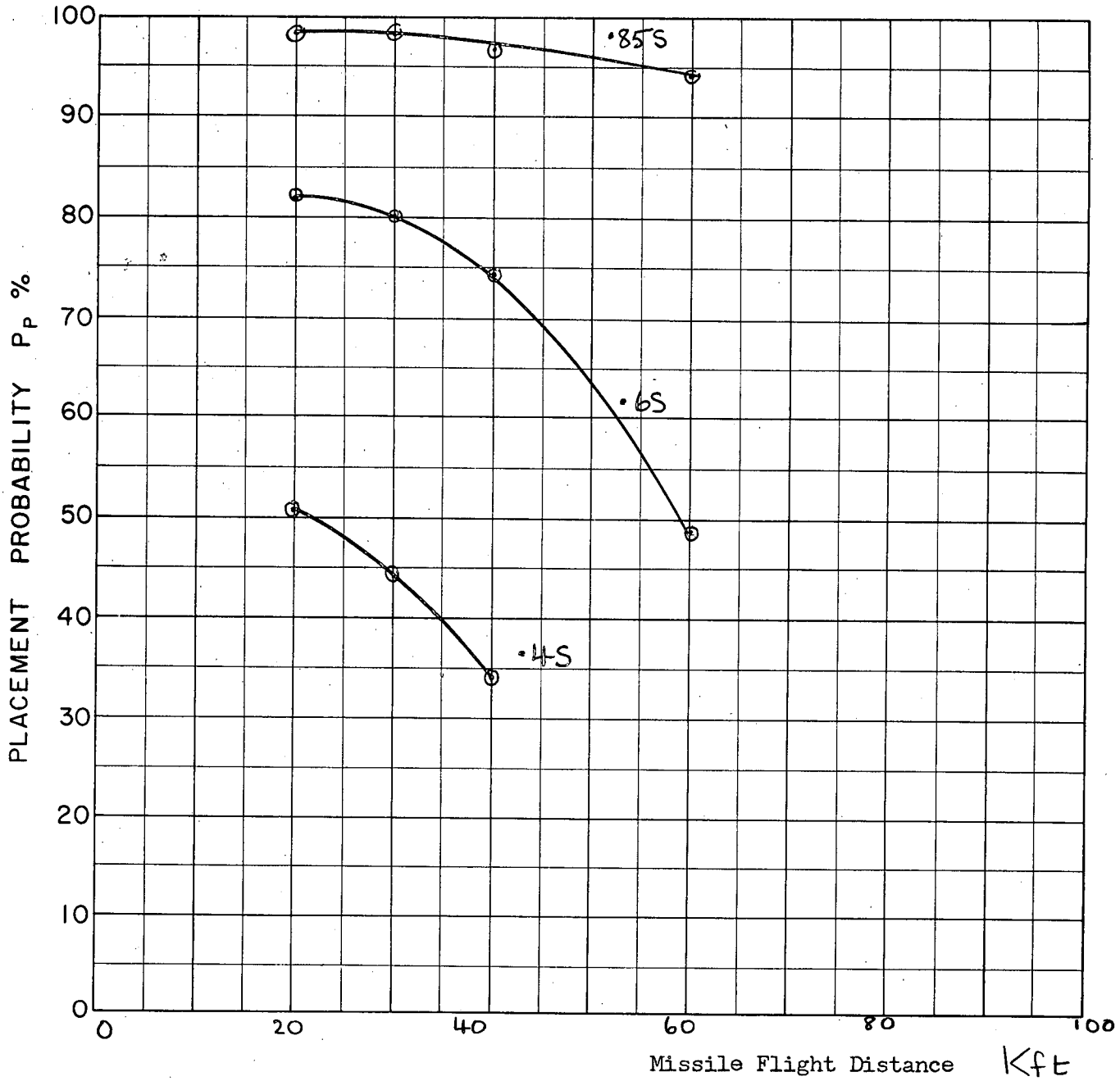

$\epsilon = \pm 15^\circ$
F = 15,000'

FIG 10 A

COURSE DIFFERENCE: 180°
TARGET EVASION: 0.5
TARGET MACH NO.: 2.0
INTERCEPTOR LATERAL G's: 1.6
INTERCEPTOR MACH NO.: 1.5
σ OF G.C.I. ACCURACY: 4.75 n.m.
A.I. DETECTION RANGE AS FRACTION OF SPECIFICATION RANGE, S: 3 values
A.I. DETECTION RANGE CONTOUR: Delta
ALTITUDE: -

Evasion one way only.

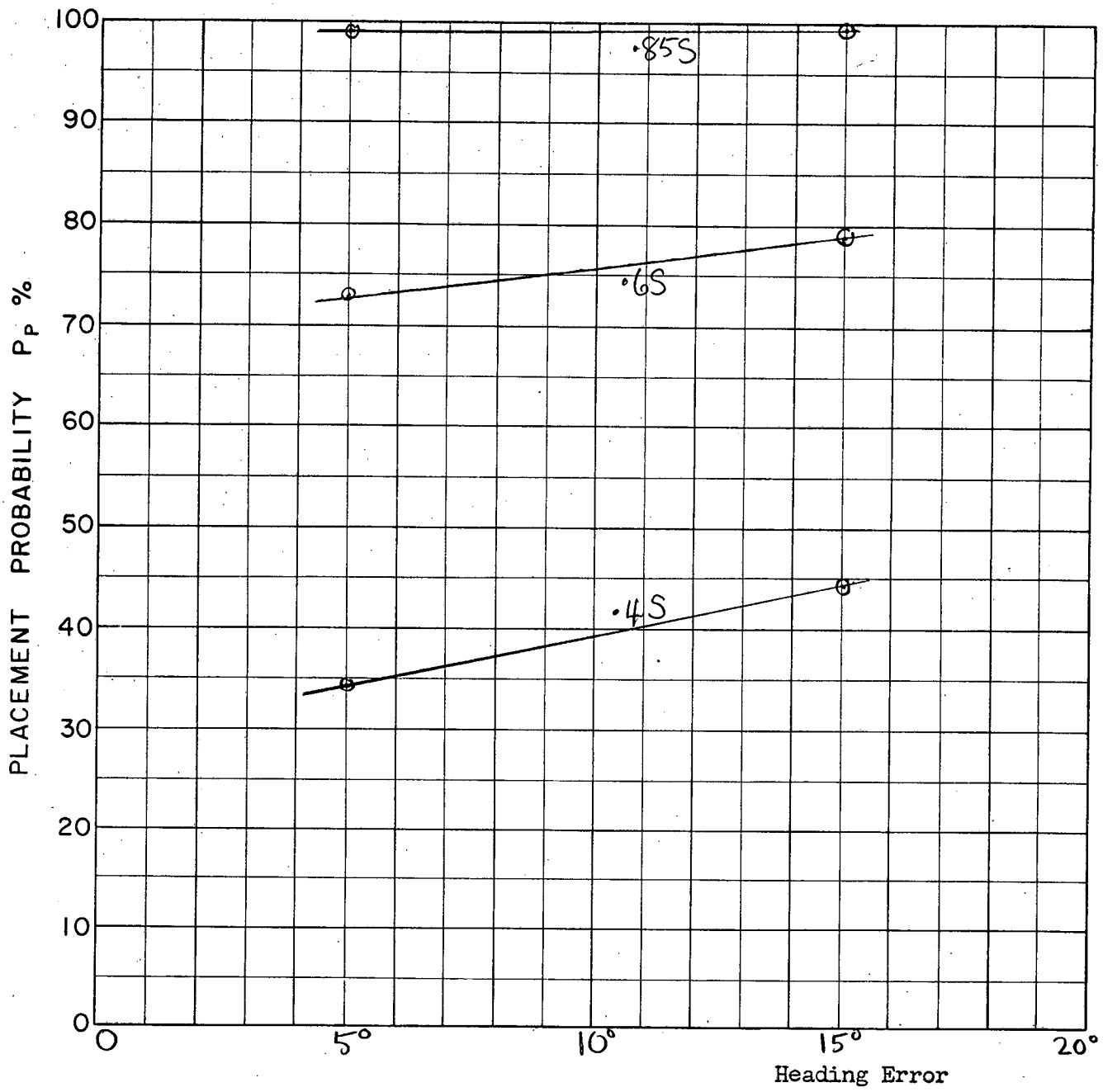

COURSE DIFFERENCE: 180°
TARGET EVASION: 0
TARGET MACH NO.: 2.0
INTERCEPTOR LATERAL G's: 1.6
INTERCEPTOR MACH NO.: 1.5
σ OF G.C.I. ACCURACY: 4.75
A.I. DETECTION RANGE AS FRACTION OF SPECIFICATION RANGE, S: 3 values
A.I. DETECTION RANGE CONTOUR: Delta
ALTITUDE: -

F = 11,500'

FIG 11 A

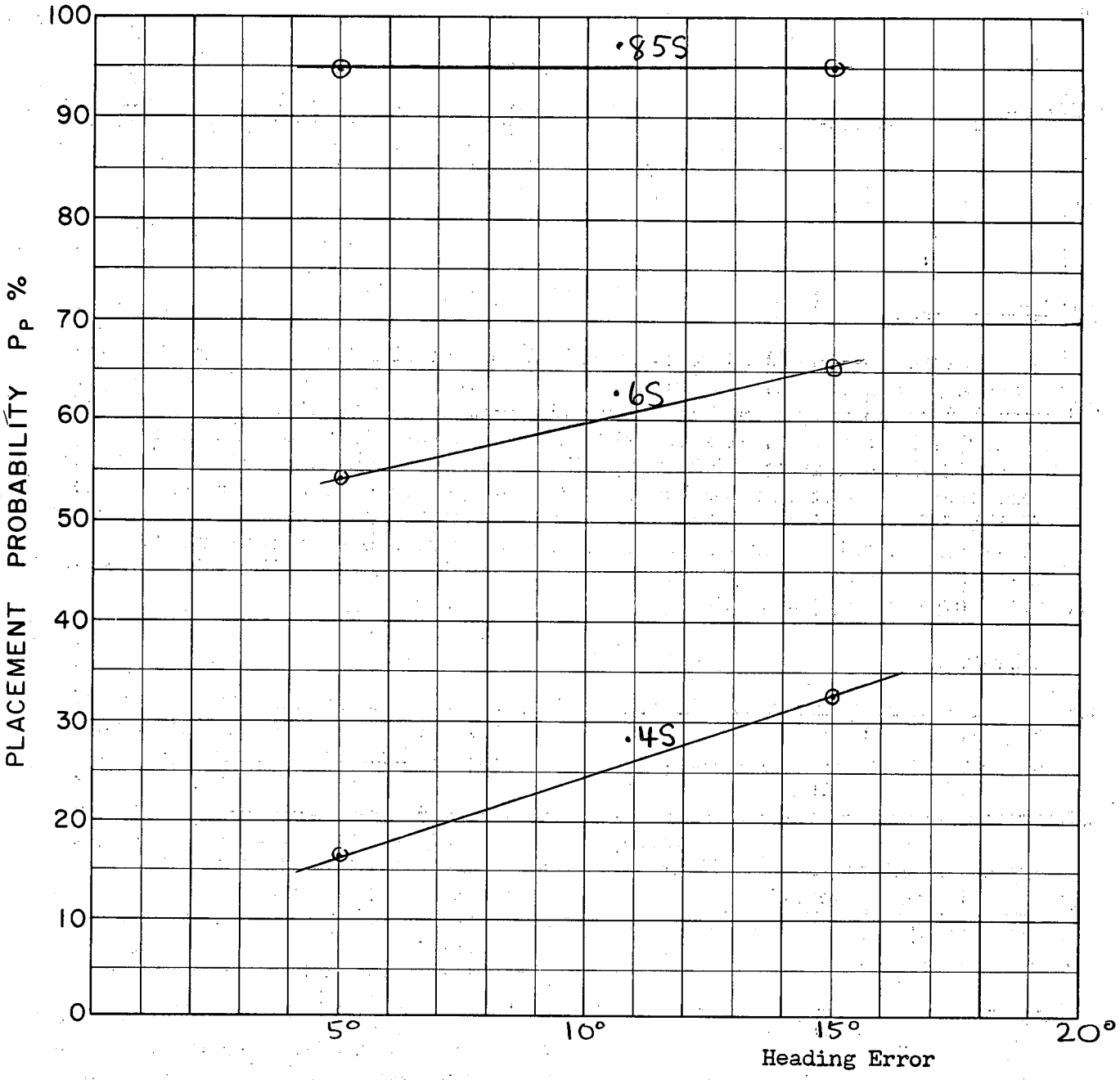

F = 11,500'

FIG 12 A

COURSE DIFFERENCE: 180°
TARGET EVASION: 0.5
TARGET MACH NO.: 2.0
INTERCEPTOR LATERAL G's: 1.6
INTERCEPTOR MACH NO.: 1.5
σ OF G.C.I. ACCURACY: 4.75 n.m.
A.I. DETECTION RANGE AS FRACTION OF SPECIFICATION RANGE, S: 3 values
A.I. DETECTION RANGE CONTOUR: Delta
ALTITUDE: -

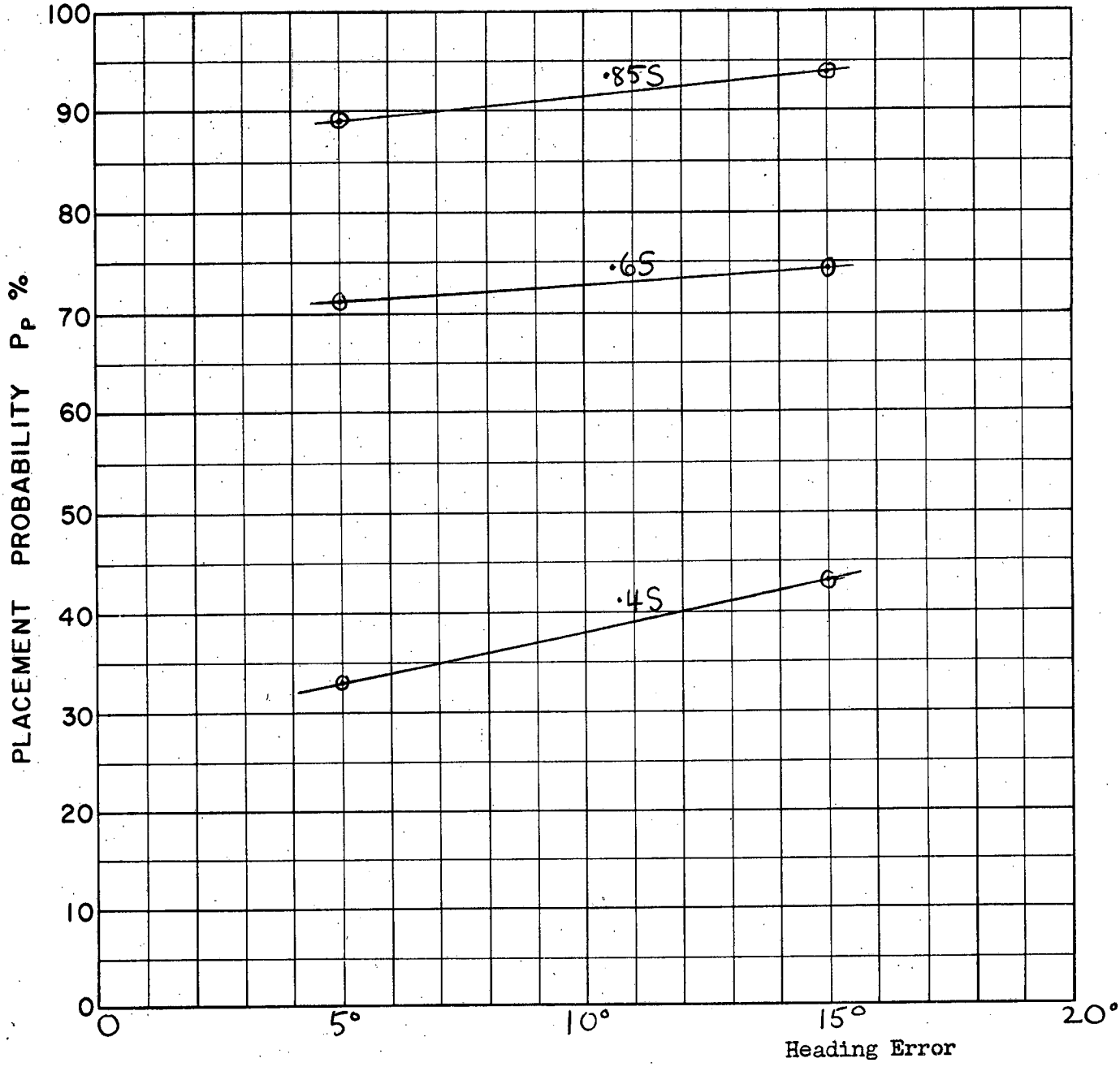

F = 11,500'

FIG 13 A

COURSE DIFFERENCE: 110°
TARGET EVASION: 0
TARGET MACH NO.: 2.0
INTERCEPTOR LATERAL G's: 1.6
INTERCEPTOR MACH NO.: 1.5
σ OF G.C.I. ACCURACY: 4.75
A.I. DETECTION RANGE AS FRACTION OF SPECIFICATION RANGE, S: 3 values
A.I. DETECTION RANGE CONTOUR: Delta
ALTITUDE: -

APPENDIX 'B'

Placement Probability for a Constant Speed Interceptor (Part 1)

by L. Shepherd
&
J. Cummins

1. Introduction

This appendix contains the probability curves obtained from REAC work by the Analysis Group which have not yet been published. The description of the problem and the method of solution are given in Reference 2. An introductory discussion and the first published probability curves are given in Reference 1.

The curves given here are for a supersonic manoeuvring target with a speed advantage. The target is assumed to be turning with a constant 0.5 lateral g acceleration continuously from the time of fighter lock on. The navigation adopted was lead collision followed by lead pursuit at the theoretical maximum range launch zone or F-circle.

The values of parameters used in this work include:

$M_T = 2.0$

$M_I = 1.5$

H = 50,000 ft.

F = 25,000 ft.

Target lateral g's = 0.5 (Load factor 1.12)

Interceptor lateral g's = 0.85, 1.60, 3.0 (Load factor 1.33, 1.89, 3.2)

Initial course differences 110°, 135°, 160°, 180°

Look angle limit = 66°

The launch zone is shown in Figure 1 of Appendix 'C' of this report.

The placement zone was considered to be the zone common to the zones for evasion in the clockwise and counterclockwise directions. This is then a pessimistic placement zone.

The placement charts were reduced in terms of AI detection range for both the Delta and Straight wing targets. (See Appendix E of Reference 1).

2. Notes on Constant Speed Placement Probability Curves

The curves contained in this appendix are for a Mach 2 target evading at 0.5 lateral g's from the time of fighter lock-on. In Appendix 'C' the conditions are repeated with the evasion beginning at lock-on or 150,000 feet, whichever is least. The effect of evasion is to swing the limits of the placement zone toward the ideal approach line with a consequent drop in placement probability, especially at long AI ranges. This effect is not as pronounced when the target does not begin evading until the interceptor is at a range of 150,000 feet. In Appendix 'C', the case of the Mach 1.5 target evading at 0.4 lateral g's displays the same characteristics as the other cases, however to a lesser extent.

To obtain an indication of the trends in this work, the points corresponding to the specification radar acquisition range and a GCI accuracy of 3 n.m. were studied with the following results:

i) The placement probability drops rapidly with course difference below 160°. At a course difference of 110° the pessimistic placement zone is extremely small.

ii) There is no indication that the increased radar look angle of 75° has any advantage at all AI ranges over the radar with only 66° look angle. In the curves studied there was no change in probability greater than 5%.

iii) For these constant speed cases at the specification AI range there is an increase in probability with a fighter pulling 1.6 lateral g's over one pulling 0.85 lateral g's, however there is virtually no improvement in probability by pulling lateral g's in excess of 1.6. (1.89 load factor).

The Analysis Group would like to express their thanks to the 'G' Wing Data Reduction Group for their assistance in this work.

3. References

1. CARDE Technical Letter N-47-12, "Second Quarterly Report on CF-105 Weapon System Assessment", by Baker, Mitchell & Macfarlane.

2. CARDE Technical Letter N-47-14, "A Method of Solution using the REAC for the 2-Dimensional Constant Fighter Speed Case", by 'G' Wing Analysis Group.

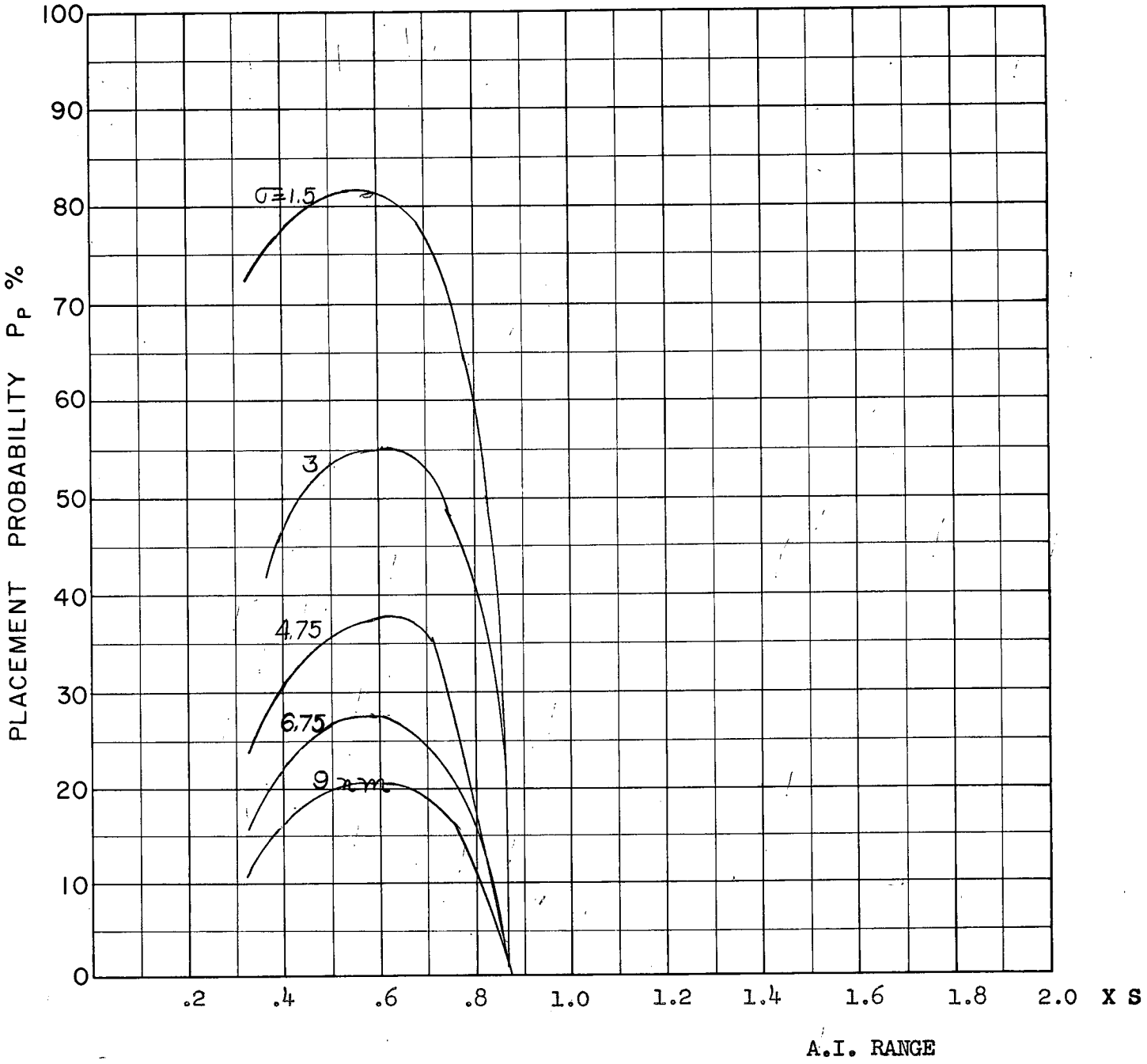

COURSE DIFFERENCE: 110°
TARGET EVASION: 0.5
TARGET MACH NO.: 2.0
INTERCEPTOR LATERAL G's: 0.85
INTERCEPTOR MACH NO.: 1.5
σ OF G.C.I. ACCURACY: 5 Values
A.I. DETECTION RANGE AS FRACTION OF SPECIFICATION RANGE, S: ABSCISSA
A.I. DETECTION RANGE CONTOUR: Delta
ALTITUDE: 50 K

D 1
B

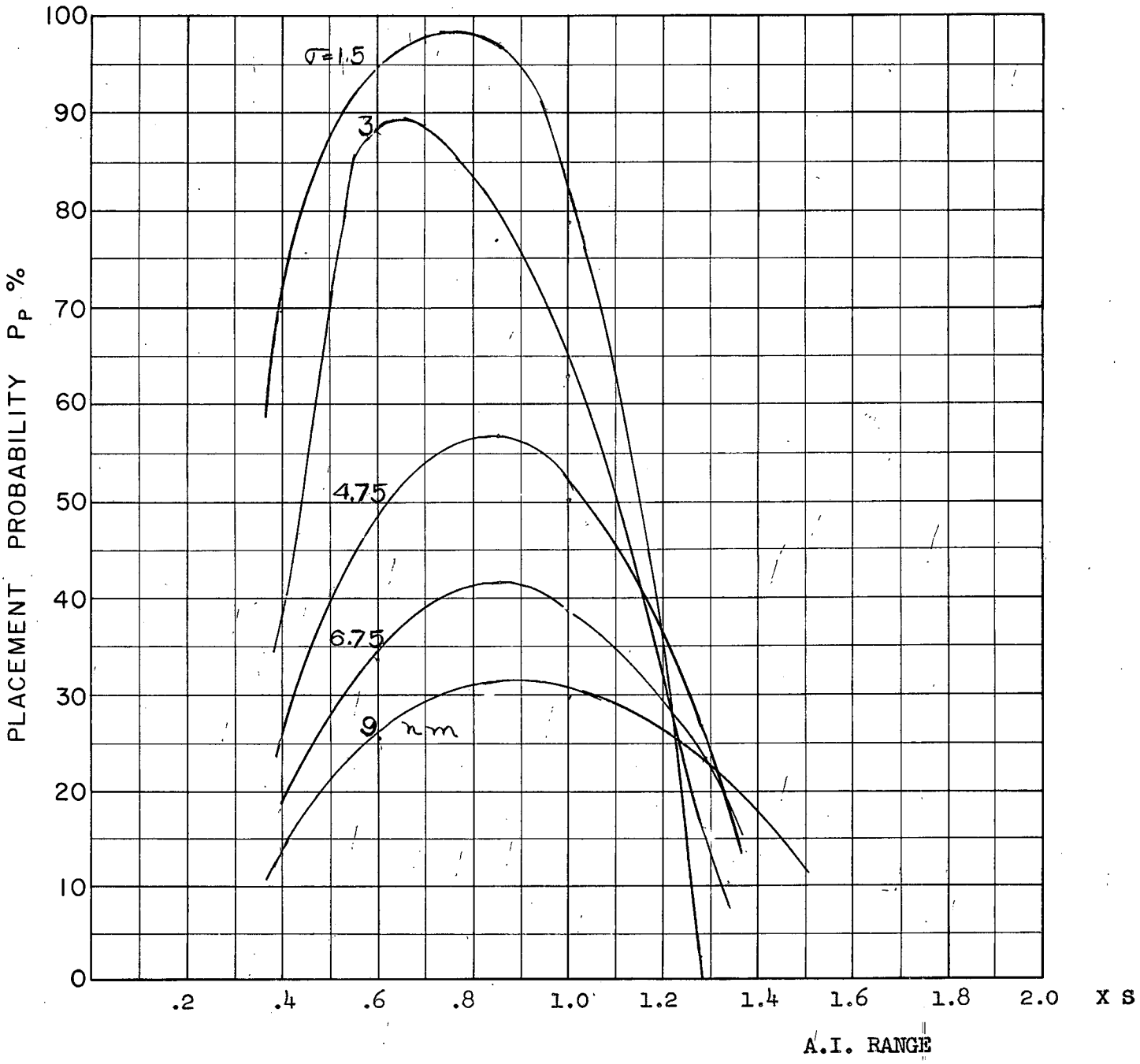

COURSE DIFFERENCE: 135°
TARGET EVASION: 0.5
TARGET MACH NO.: 2.0
INTERCEPTOR LATERAL G's: 0.85
INTERCEPTOR MACH NO.: 1.5
σ OF G.C.I. ACCURACY: 5 Values
A.I. DETECTION RANGE AS FRACTION OF SPECIFICATION RANGE, S: ABSCISSA
A.I. DETECTION RANGE CONTOUR: Delta
ALTITUDE: 50 K

D-2
B

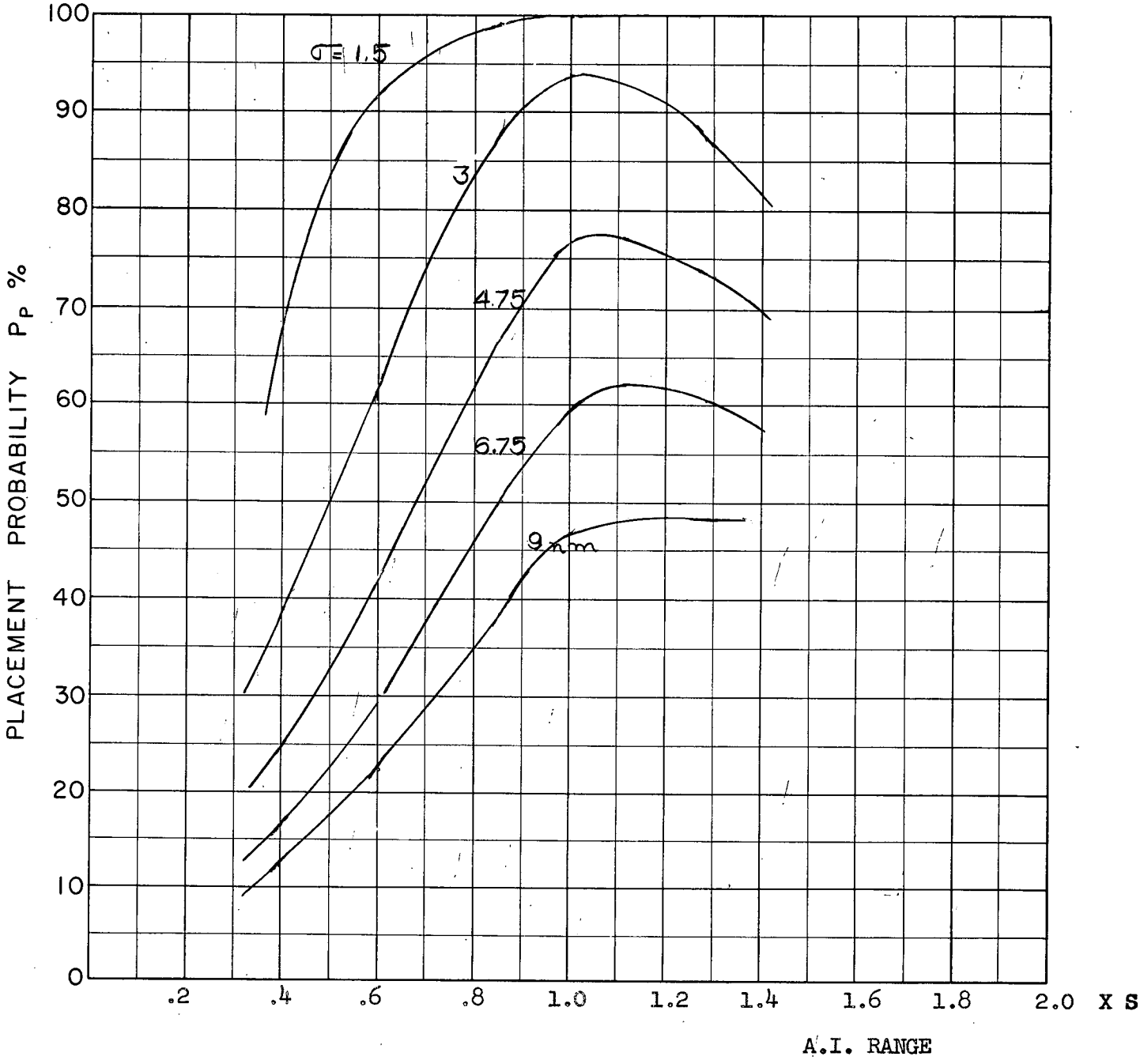

COURSE DIFFERENCE: 160°
TARGET EVASION: 0.5
TARGET MACH NO.: 2.0
INTERCEPTOR LATERAL G's: 0.85
INTERCEPTOR MACH NO.: 1.5
σ OF G.C.I. ACCURACY: 5 Values
A.I. DETECTION RANGE AS FRACTION OF SPECIFICATION RANGE, S: ABSCISSA
A.I. DETECTION RANGE CONTOUR: Delta
ALTITUDE: 50 K

D 3
B

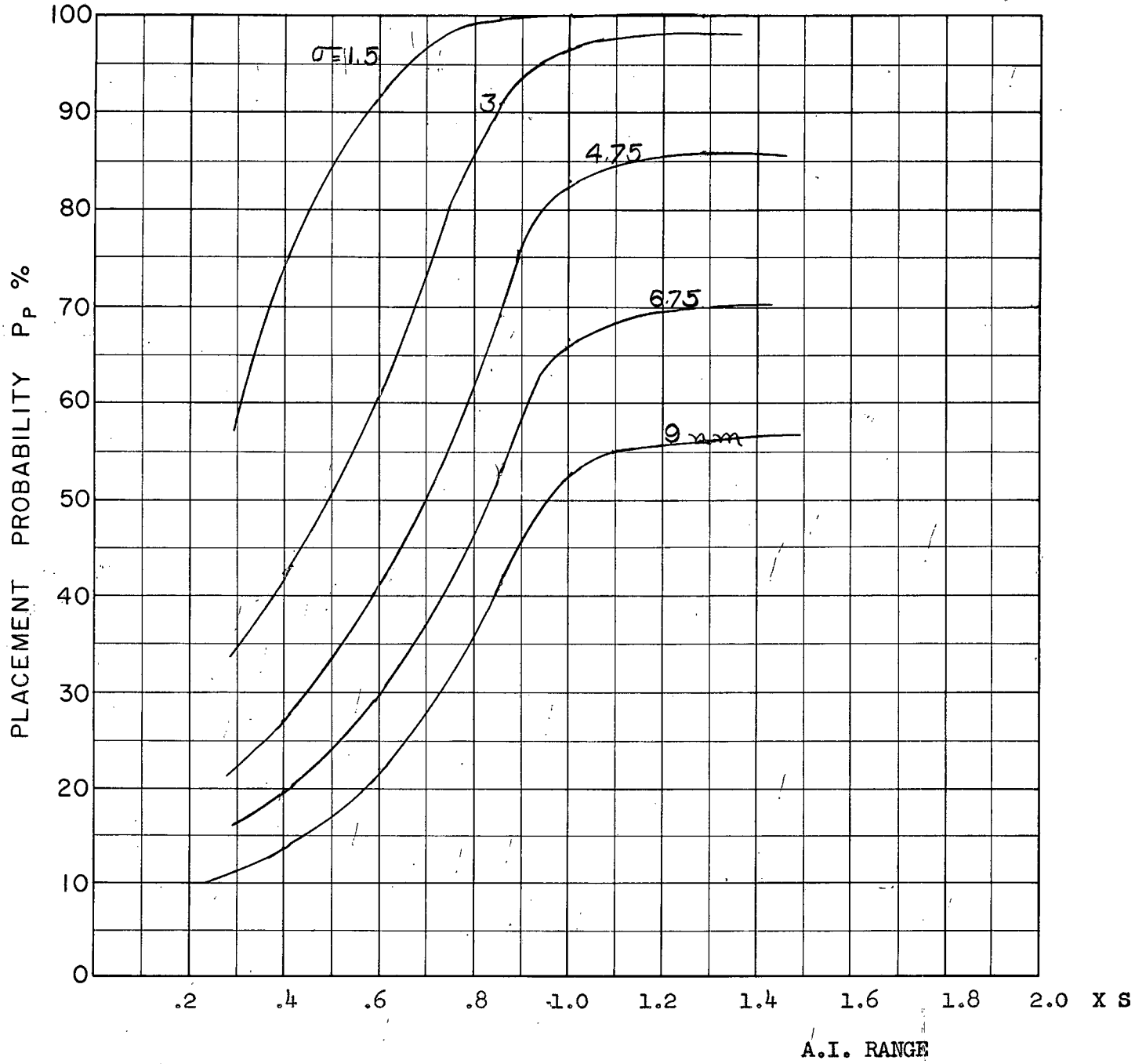

COURSE DIFFERENCE: 180°
TARGET EVASION: 0.5
TARGET MACH NO.: 2.0
INTERCEPTOR LATERAL G's: 0.85
INTERCEPTOR MACH NO.: 1.5
σ OF G.C.I. ACCURACY: 5 Values
A.I. DETECTION RANGE AS FRACTION OF SPECIFICATION RANGE, S: ABSCISSA
A.I. DETECTION RANGE CONTOUR: Delta
ALTITUDE: 50 K

D·4
B

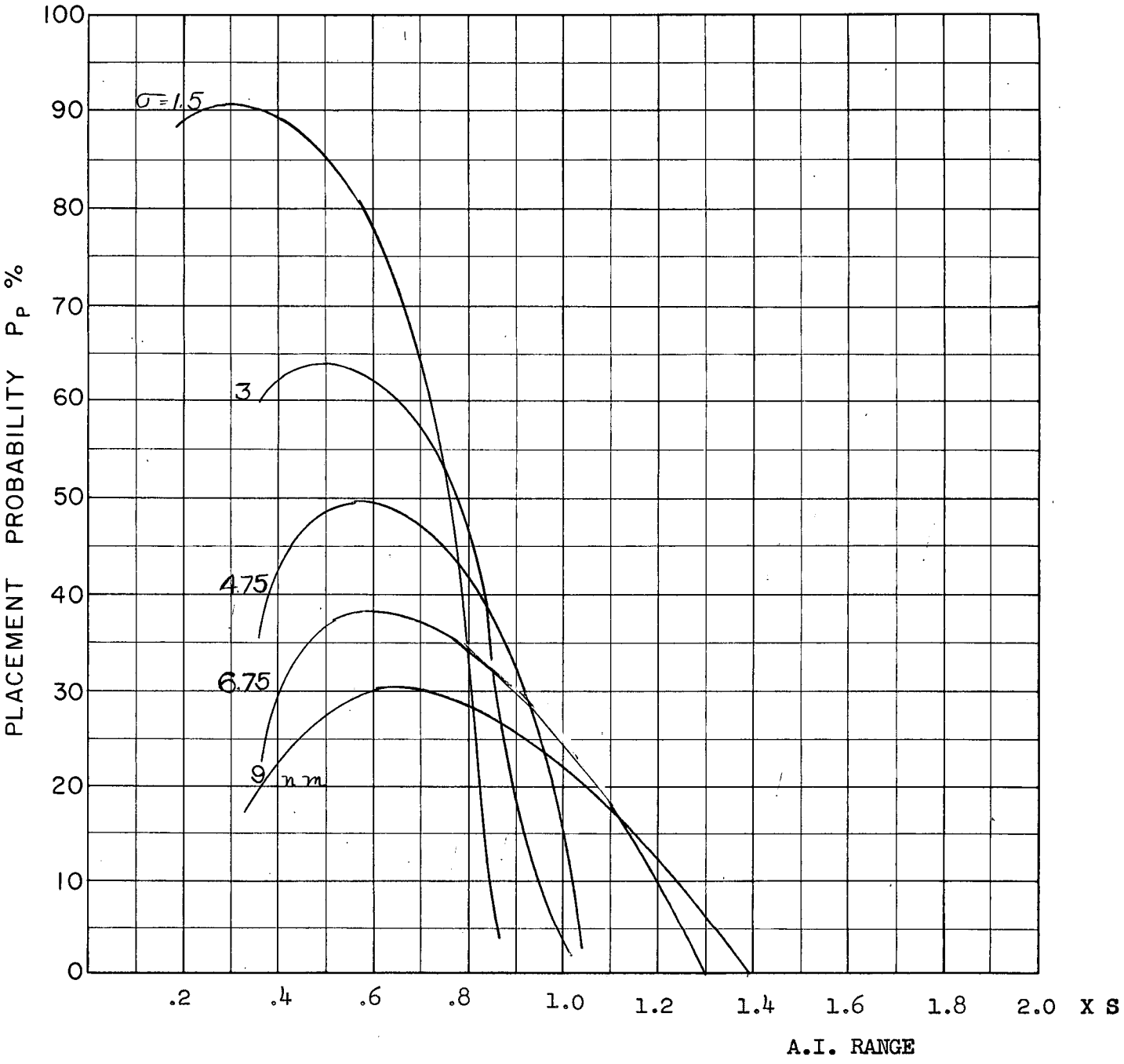

COURSE DIFFERENCE: 110°
TARGET EVASION: 0.5
TARGET MACH NO.: 2.0
INTERCEPTOR LATERAL G's: 1.6
INTERCEPTOR MACH NO.: 1.5
σ OF G.C.I. ACCURACY: 5 Values
A.I. DETECTION RANGE AS FRACTION OF SPECIFICATION RANGE, S: ABSCISSA
A.I. DETECTION RANGE CONTOUR: Delta
ALTITUDE: 50 K

D.5
B

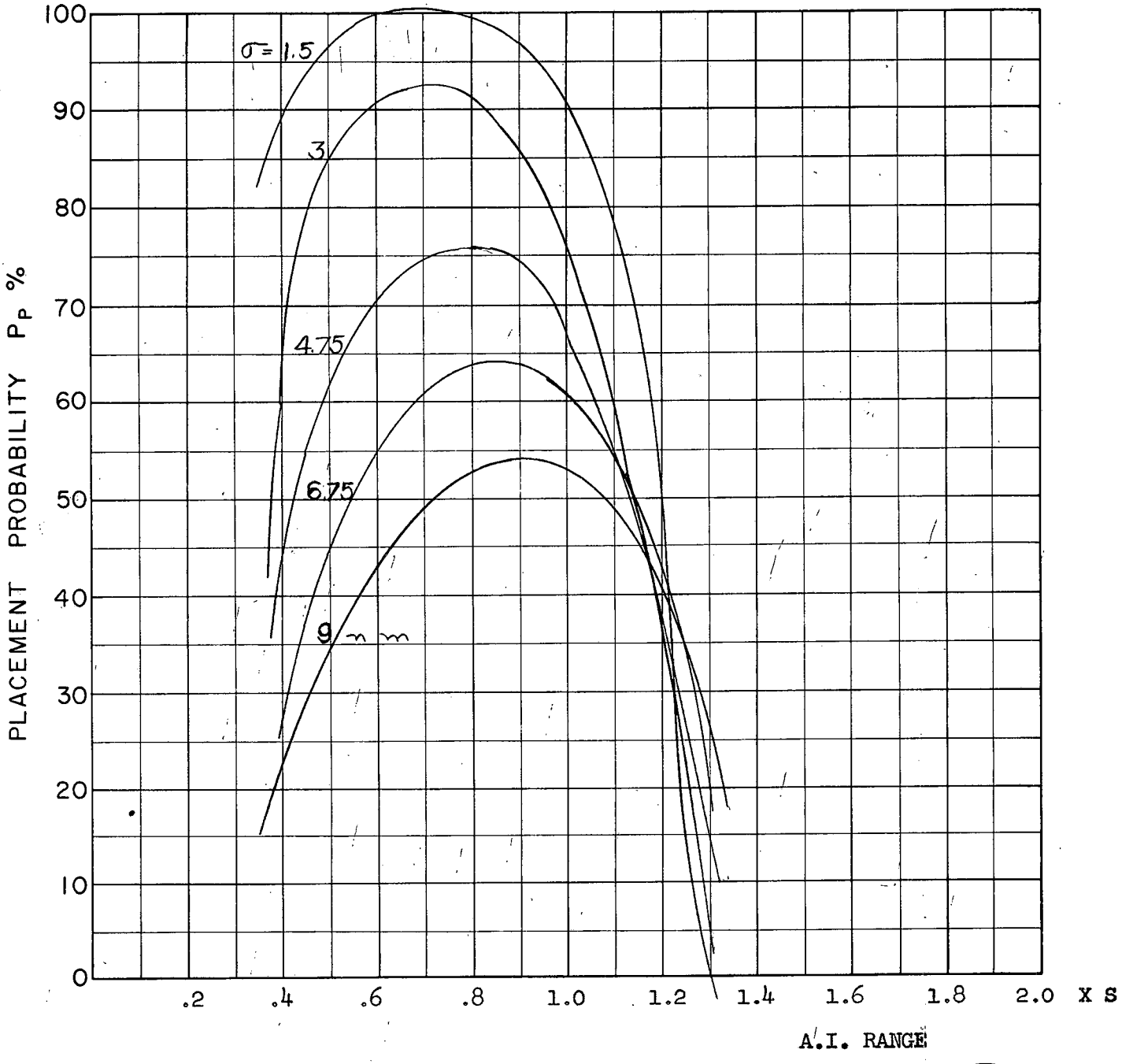

COURSE DIFFERENCE: 135°
TARGET EVASION: 0.5
TARGET MACH NO.: 2.0
INTERCEPTOR LATERAL G's: 1.6
INTERCEPTOR MACH NO.: 1.5
σ OF G.C.I. ACCURACY: 5 Values
A.I. DETECTION RANGE AS FRACTION OF SPECIFICATION RANGE, S: ABSCISSA
A.I. DETECTION RANGE CONTOUR: Delta
ALTITUDE: 50 K

D.6
B

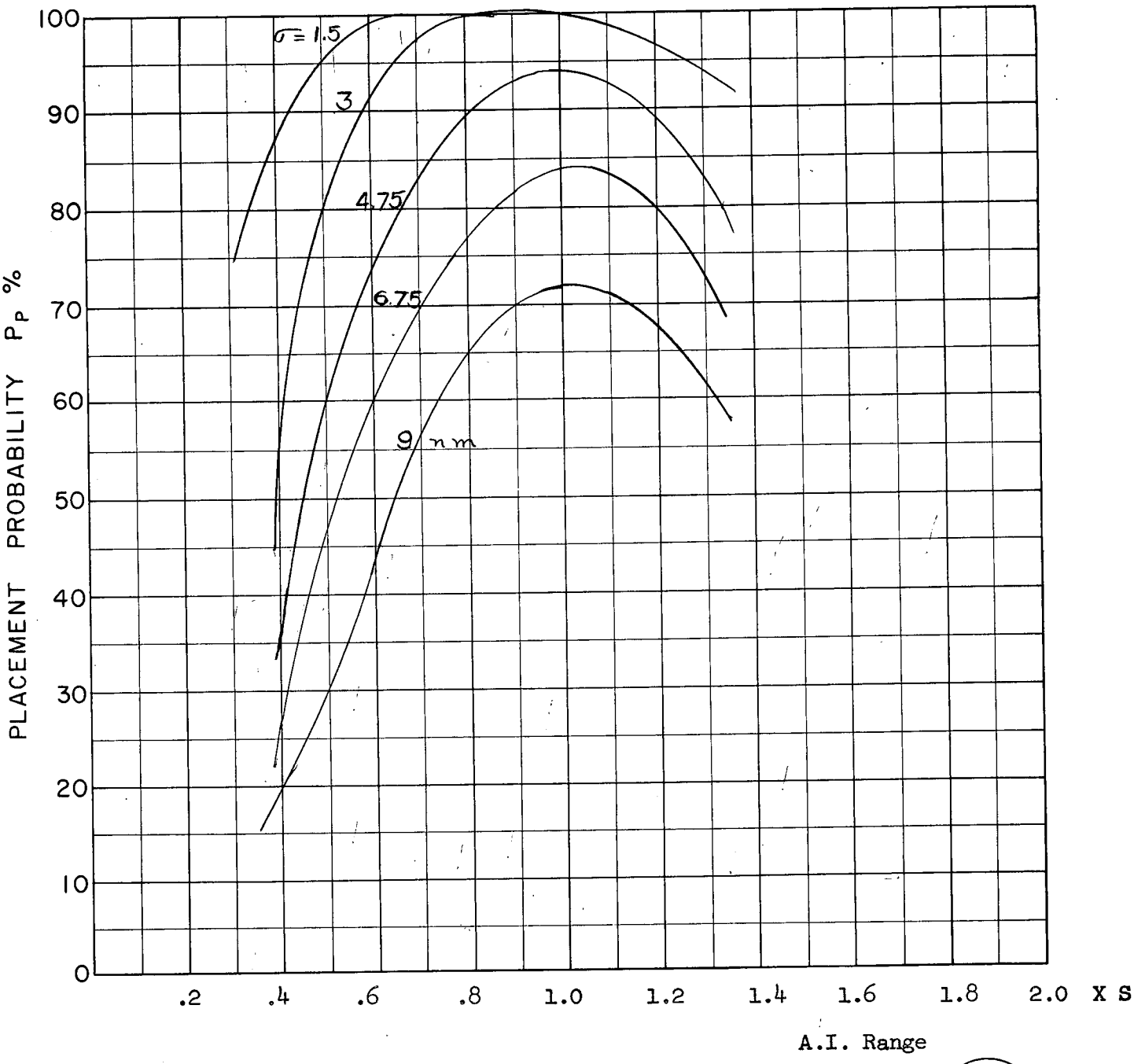

COURSE DIFFERENCE: 160°
TARGET EVASION: 0.5
TARGET MACH NO.: 2.0
INTERCEPTOR LATERAL G's: 1.6
INTERCEPTOR MACH NO.: 1.5
σ OF G.C.I. ACCURACY: 5 Values
A.I. DETECTION RANGE AS FRACTION OF SPECIFICATION RANGE, S: ABSCISSA
A.I. DETECTION RANGE CONTOUR: Delta
ALTITUDE: 50 K

D.7
B

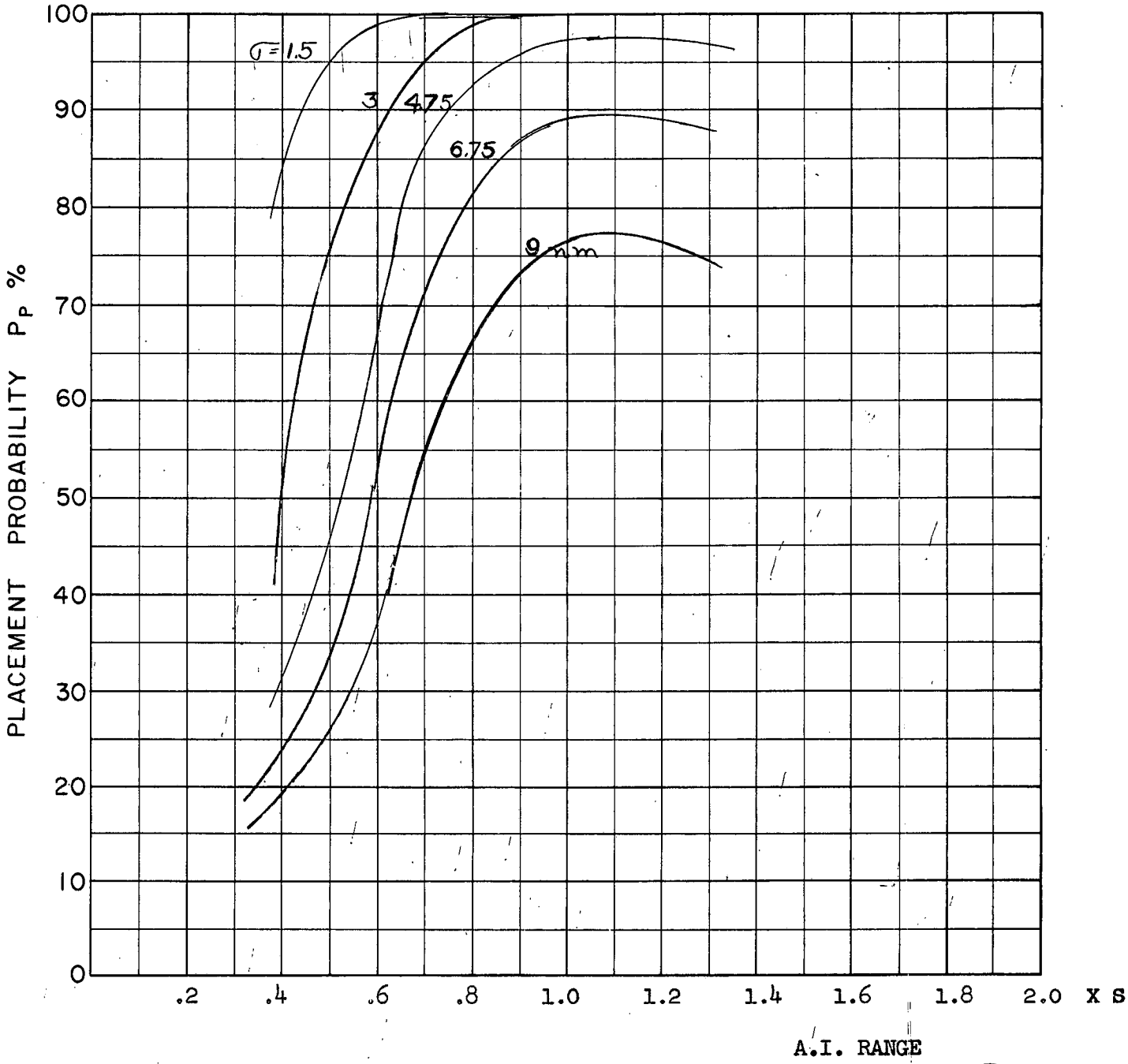

COURSE DIFFERENCE: 180°
TARGET EVASION: 0.5
TARGET MACH NO.: 2.0
INTERCEPTOR LATERAL G's: 1.6
INTERCEPTOR MACH NO.: 1.5
σ OF G.C.I. ACCURACY: 5 Values
A.I. DETECTION RANGE AS FRACTION OF SPECIFICATION RANGE, S ABSCISSA
A.I. DETECTION RANGE CONTOUR: Delta
ALTITUDE: 50 K

D.8
B

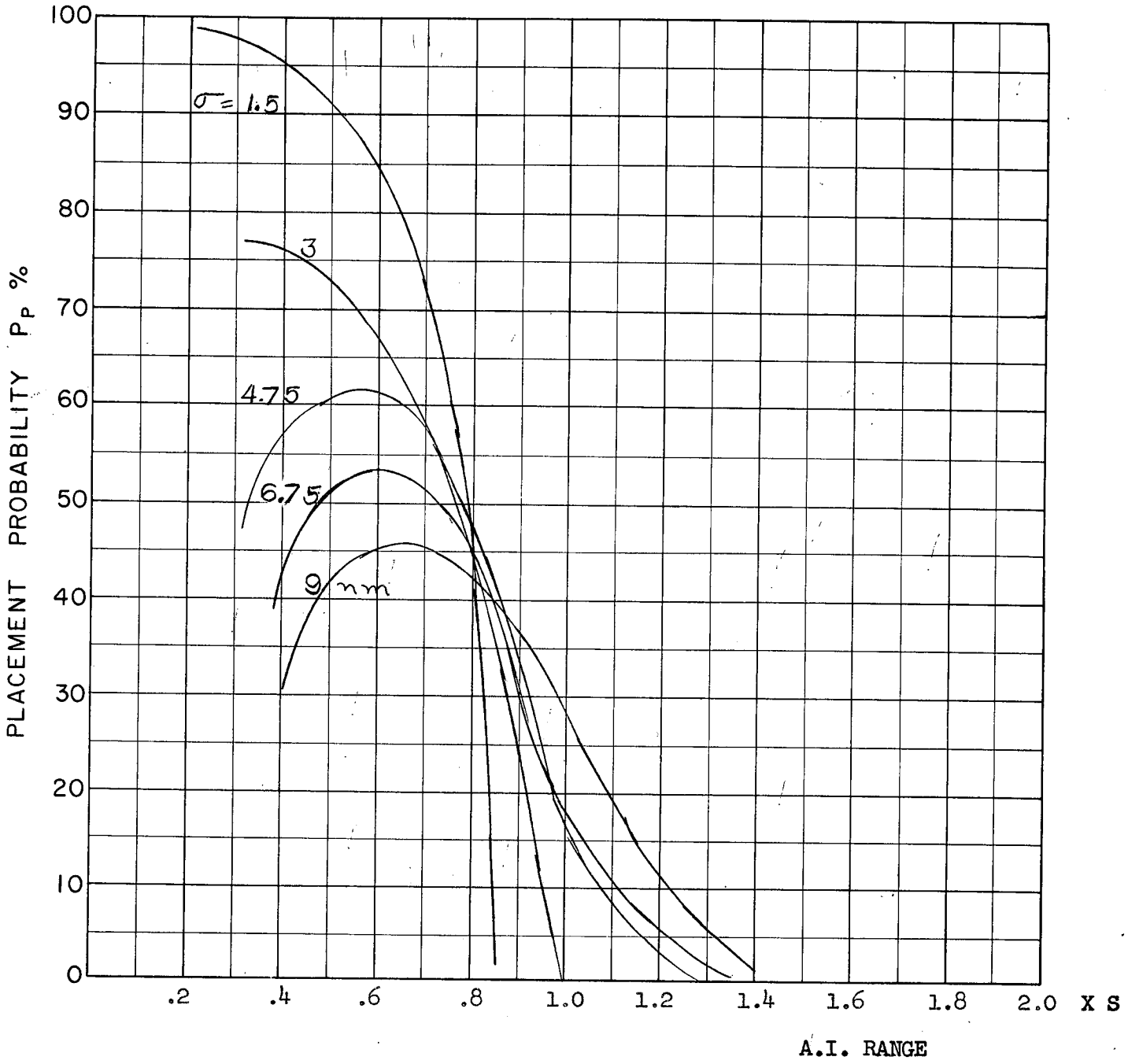

COURSE DIFFERENCE: 110°
TARGET EVASION: 0.5
TARGET MACH NO.: 2.0
INTERCEPTOR LATERAL G's: 3.0
INTERCEPTOR MACH NO.: 1.5
σ OF G.C.I. ACCURACY: 5 Values
A.I. DETECTION RANGE AS FRACTION OF SPECIFICATION RANGE, S: ABSCISSA
A.I. DETECTION RANGE CONTOUR: Delta
ALTITUDE: 50 K

D.9
B

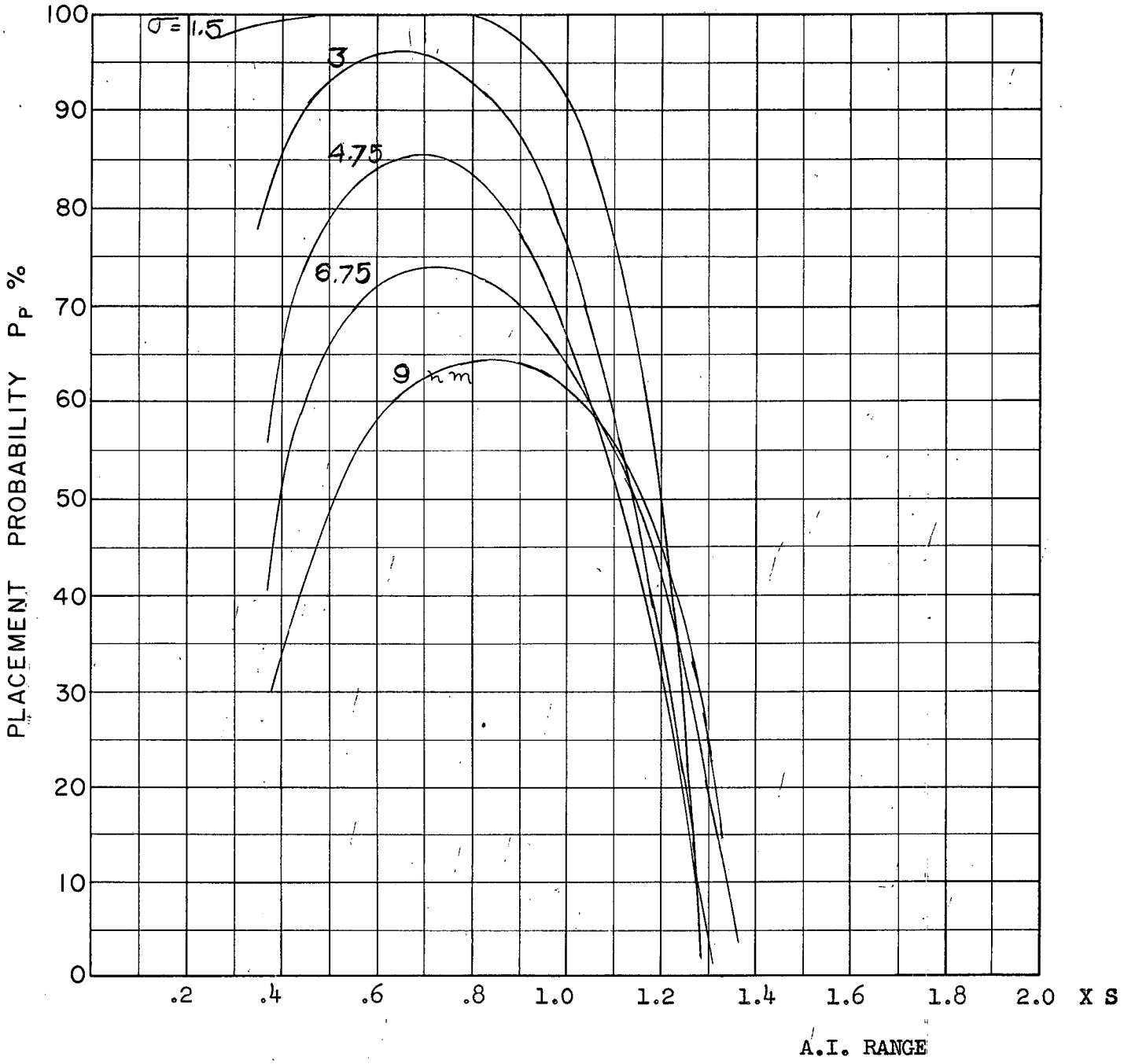

COURSE DIFFERENCE: 135°
TARGET EVASION: 0.5
TARGET MACH NO.: 2.0
INTERCEPTOR LATERAL G's: 3.0
INTERCEPTOR MACH NO.: 1.5
σ OF G.C.I. ACCURACY: 5 Values
A.I. DETECTION RANGE AS FRACTION OF SPECIFICATION RANGE, S: ABSCISSA
A.I. DETECTION RANGE CONTOUR: Delta
ALTITUDE: 50 K

D-10
B

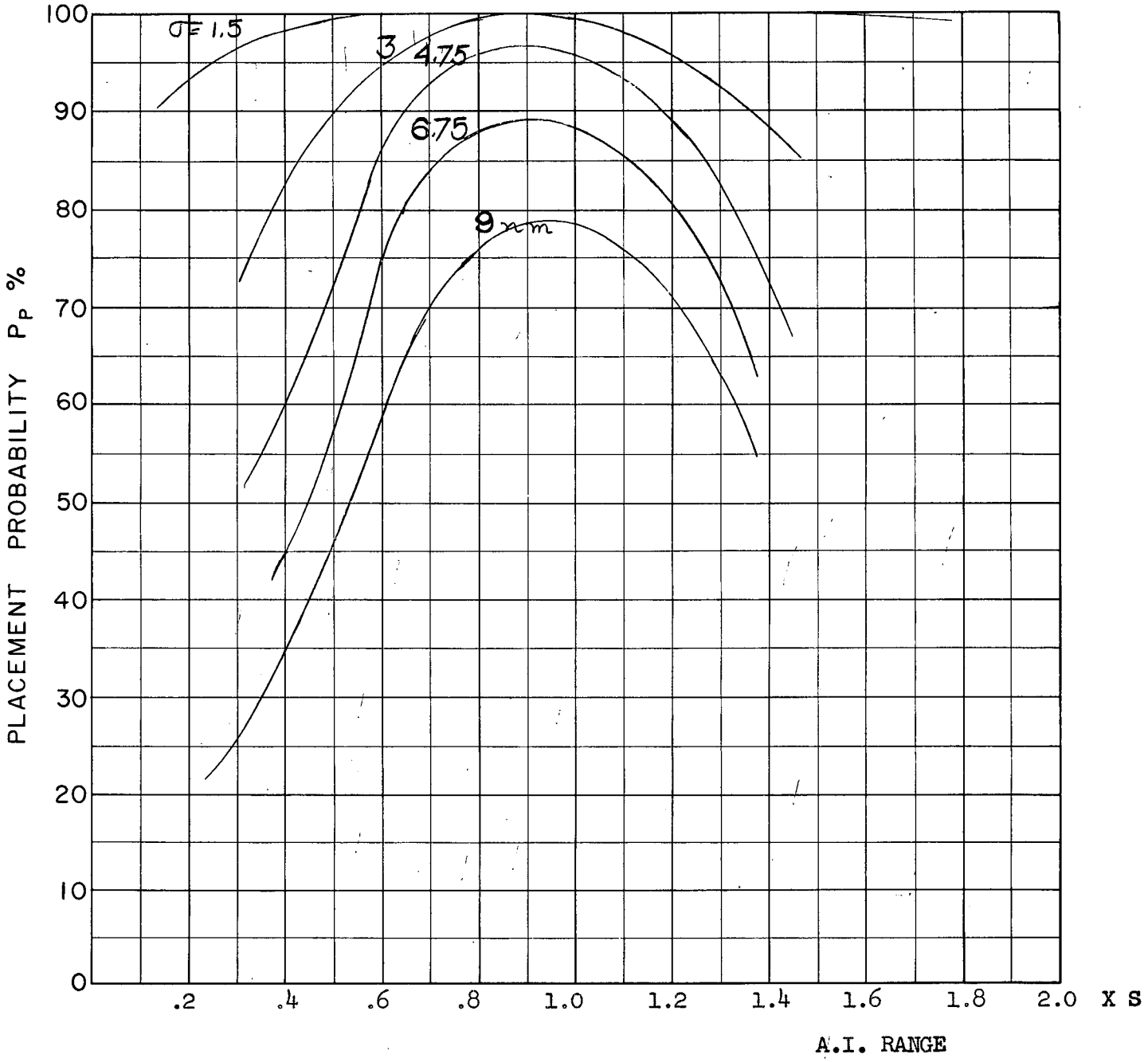

COURSE DIFFERENCE: 160°
TARGET EVASION: 0.5
TARGET MACH NO.: 2.0
INTERCEPTOR LATERAL G's: 3.0
INTERCEPTOR MACH NO.: 1.5
σ OF G.C.I. ACCURACY: 5 Values
A.I. DETECTION RANGE AS FRACTION OF SPECIFICATION RANGE, S: ABSCISSA
A.I. DETECTION RANGE CONTOUR: Delta
ALTITUDE: 50 K

D11
B

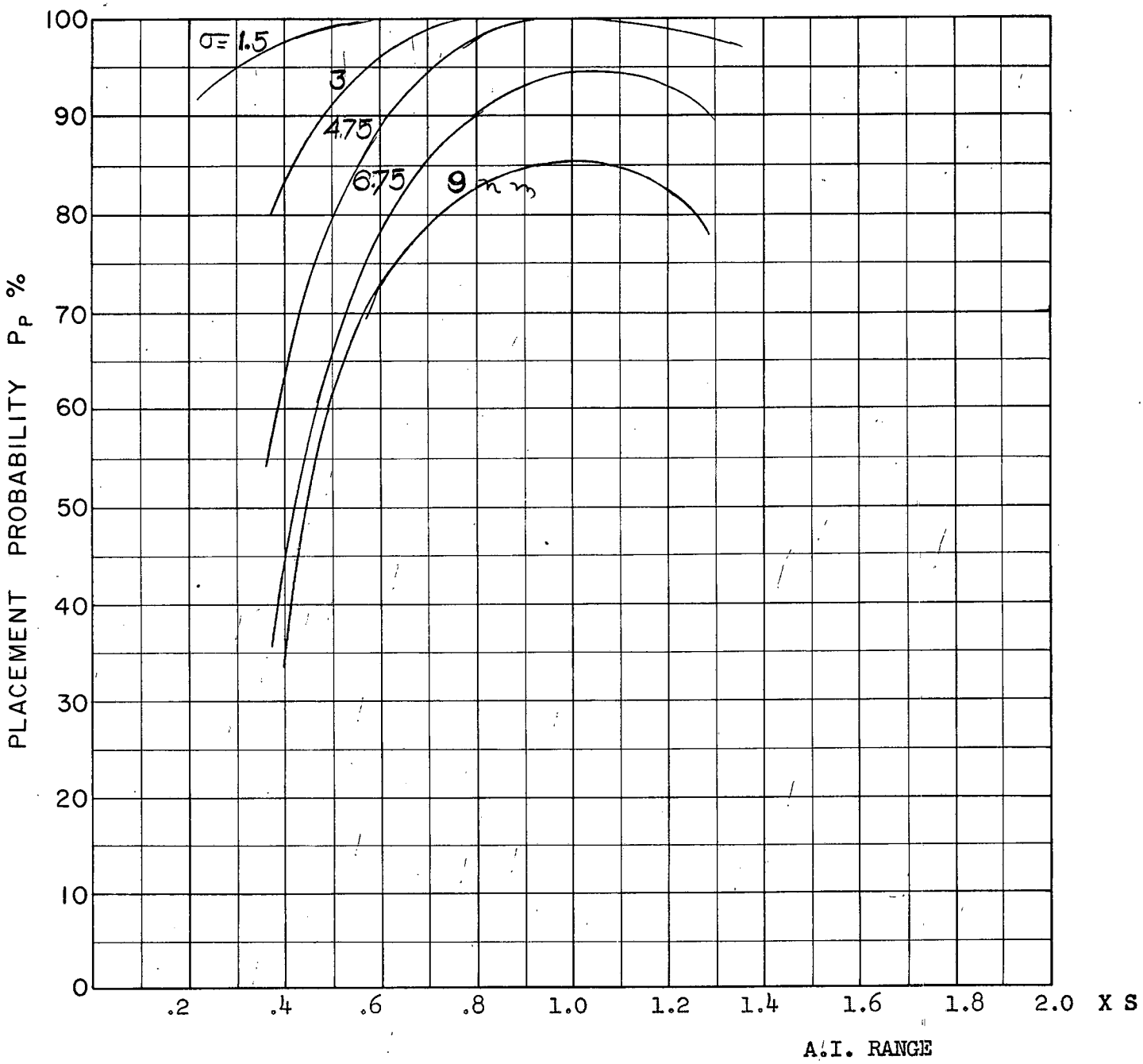

COURSE DIFFERENCE: 180°
TARGET EVASION: 0.5
TARGET MACH NO.: 2.0
INTERCEPTOR LATERAL G's: 3.0
INTERCEPTOR MACH NO.: 1.5
σ OF G.C.I. ACCURACY: 5 Values
A.I. DETECTION RANGE AS FRACTION OF SPECIFICATION RANGE, S: ABSCISSA
A.I. DETECTION RANGE CONTOUR: Delta
ALTITUDE: 50 K

D12
B

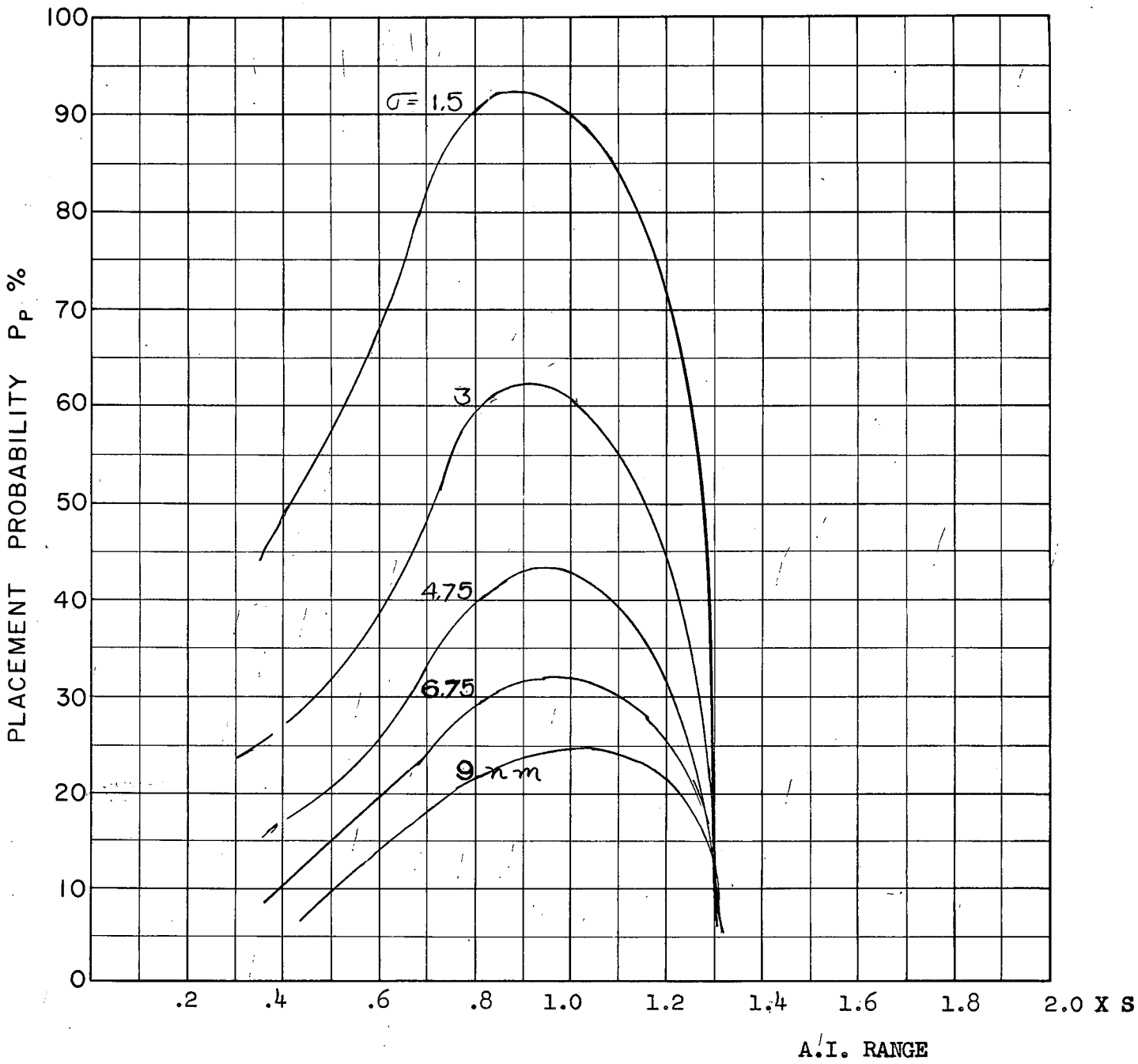

COURSE DIFFERENCE: 110°
TARGET EVASION: 0.5
TARGET MACH NO.: 2.0
INTERCEPTOR LATERAL G's: 0.85
INTERCEPTOR MACH NO.: 1.5
σ OF G.C.I. ACCURACY: 5 Values
A.I. DETECTION RANGE AS FRACTION OF SPECIFICATION RANGE, S: ABSCISSA
A.I. DETECTION RANGE CONTOUR: Straight
ALTITUDE: 50 K

S1
B

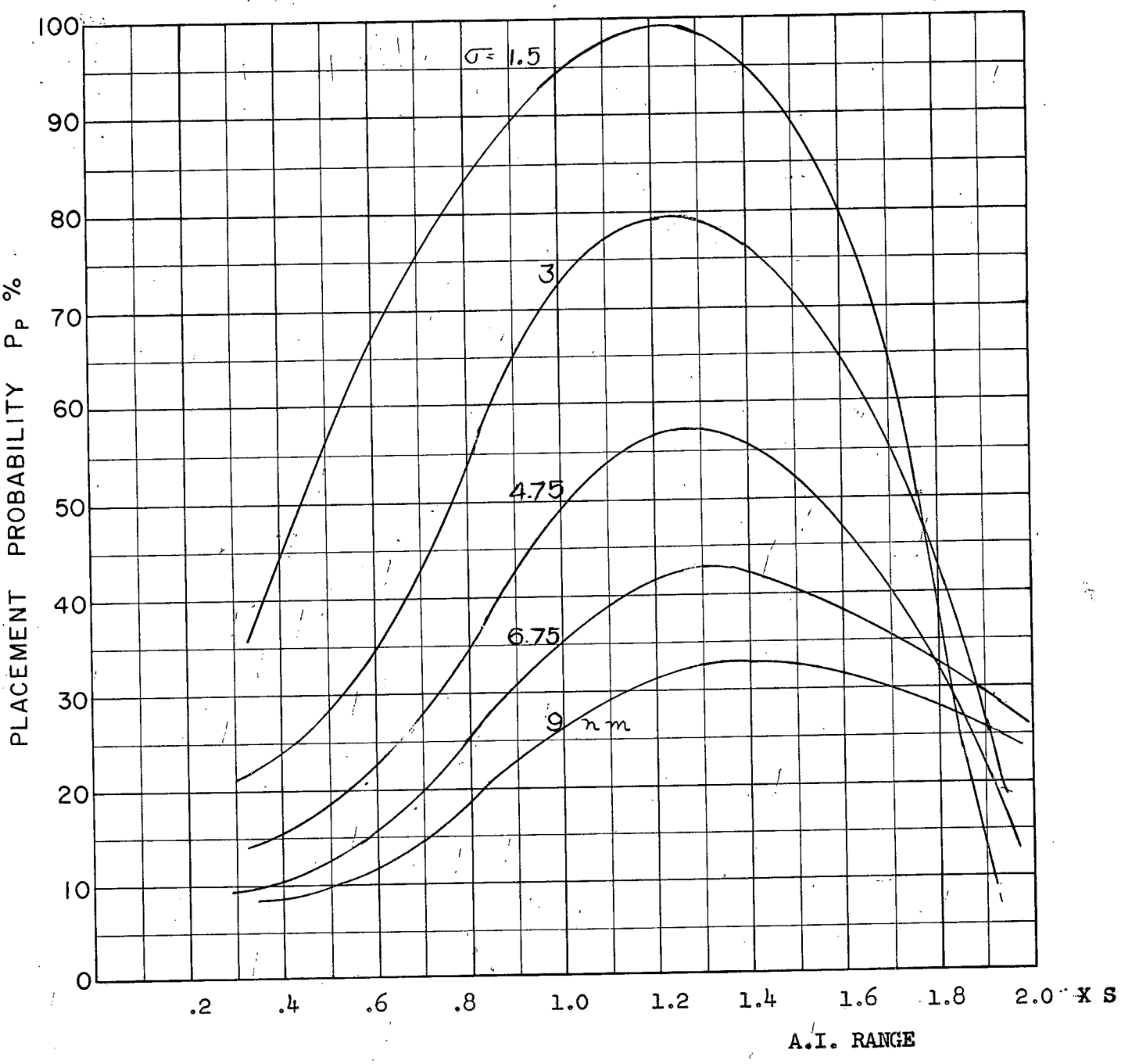

COURSE DIFFERENCE: 135°
TARGET EVASION: 0.5
TARGET MACH NO.: 2.0
INTERCEPTOR LATERAL G's: 0.85
INTERCEPTOR MACH NO.: 1.5
σ OF G.C.I. ACCURACY: 5 Values
A.I. DETECTION RANGE AS FRACTION OF SPECIFICATION RANGE, S: ABSCISSA
A.I. DETECTION RANGE CONTOUR: Straight
ALTITUDE: 50 K

S-2
B

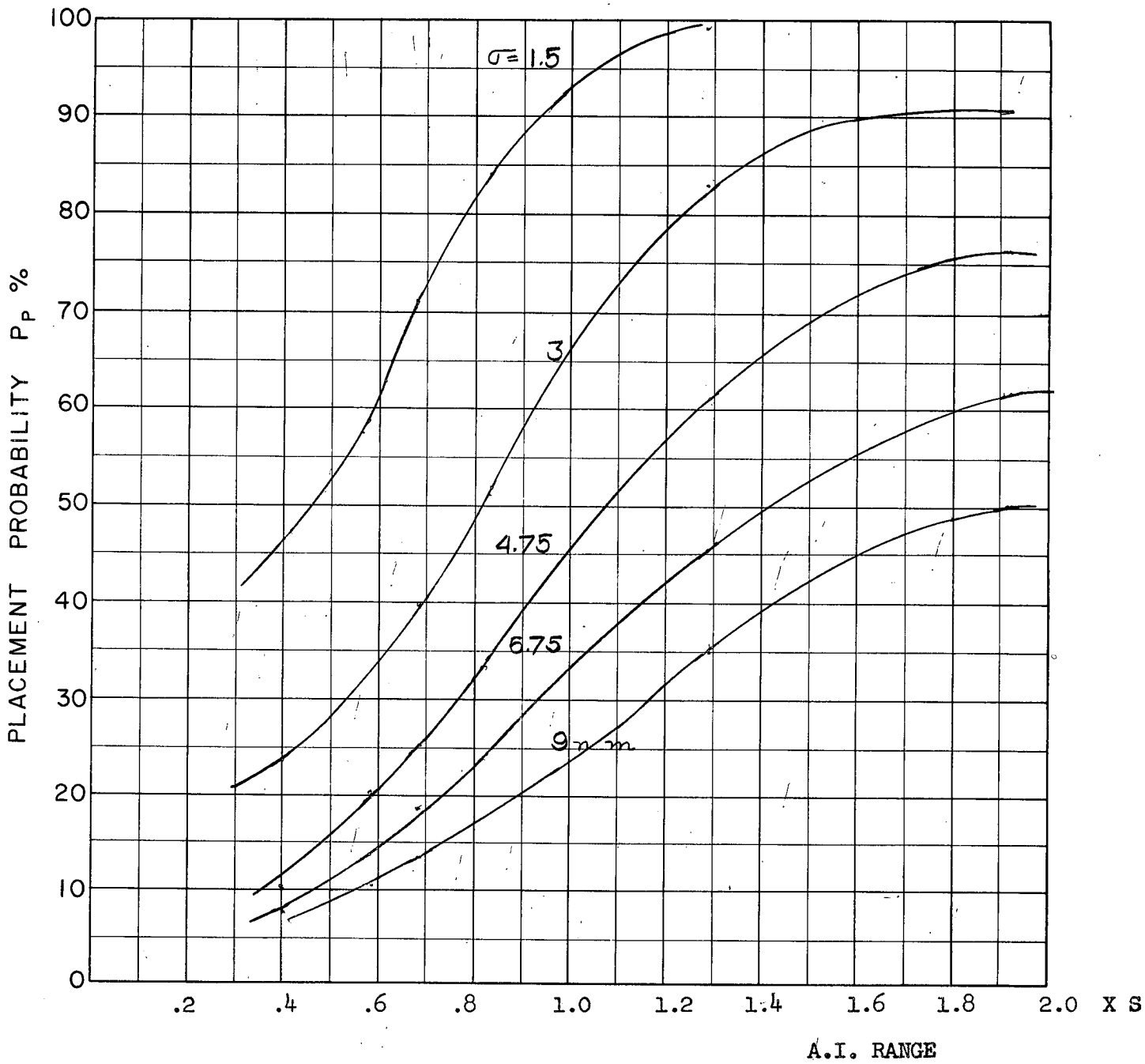

COURSE DIFFERENCE: 160°
TARGET EVASION: 0.5
TARGET MACH NO.: 2.0
INTERCEPTOR LATERAL G's: 0.85
INTERCEPTOR MACH NO.: 1.5
σ OF G.C.I. ACCURACY: 5 Values
A.I. DETECTION RANGE AS FRACTION OF SPECIFICATION RANGE, S: ABSCISSA
A.I. DETECTION RANGE CONTOUR: Straight
ALTITUDE: 50 K

S 3
B

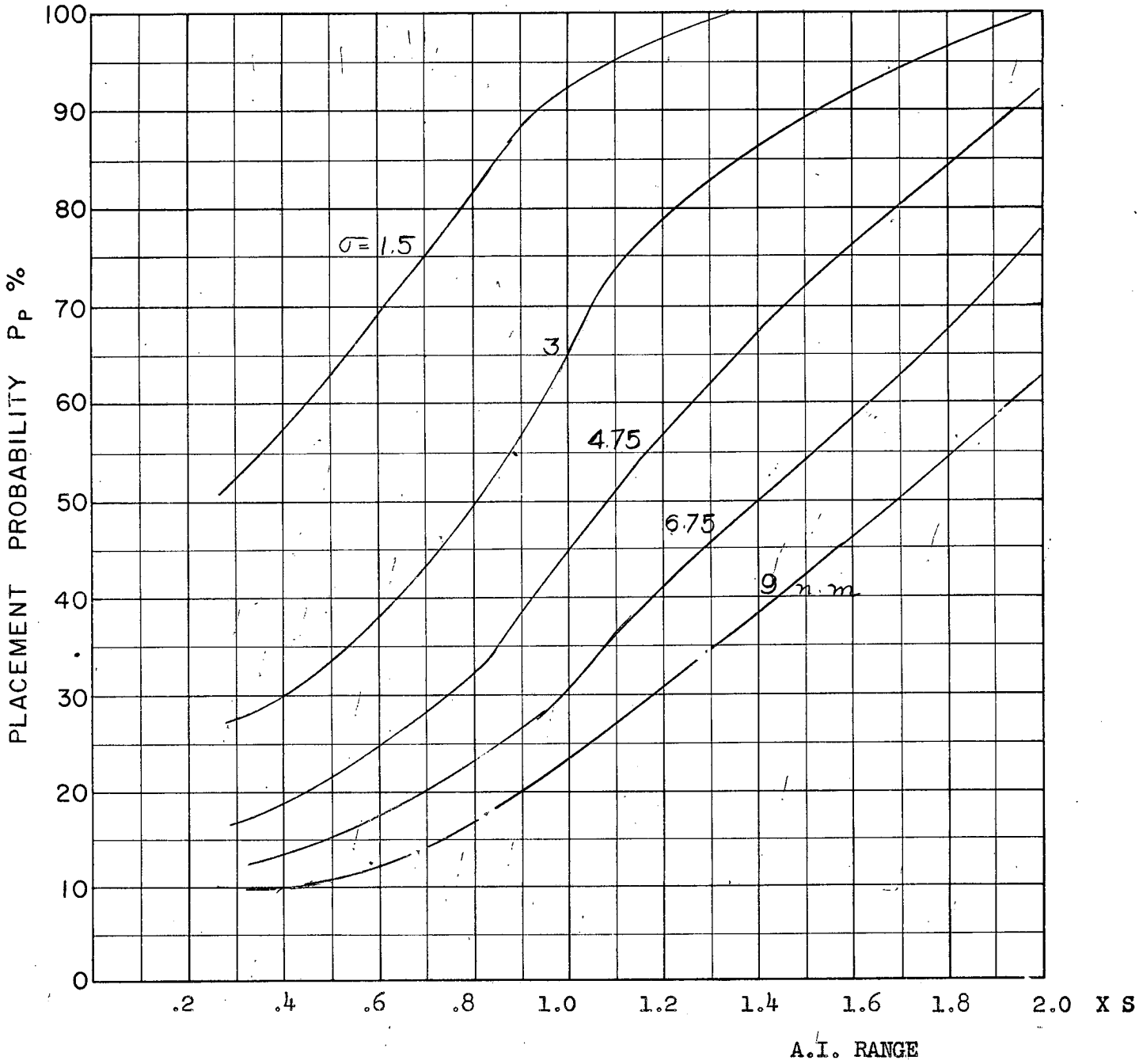

COURSE DIFFERENCE: 180°
TARGET EVASION: 0.5
TARGET MACH NO.: 2.00
INTERCEPTOR LATERAL G's: 0.85
INTERCEPTOR MACH NO.: 1.50
σ OF G.C.I. ACCURACY: 5 Values
A.I. DETECTION RANGE AS FRACTION OF SPECIFICATION RANGE, S: ABSCISSA
A.I. DETECTION RANGE CONTOUR: Straight
ALTITUDE: 50 K

S.4
B

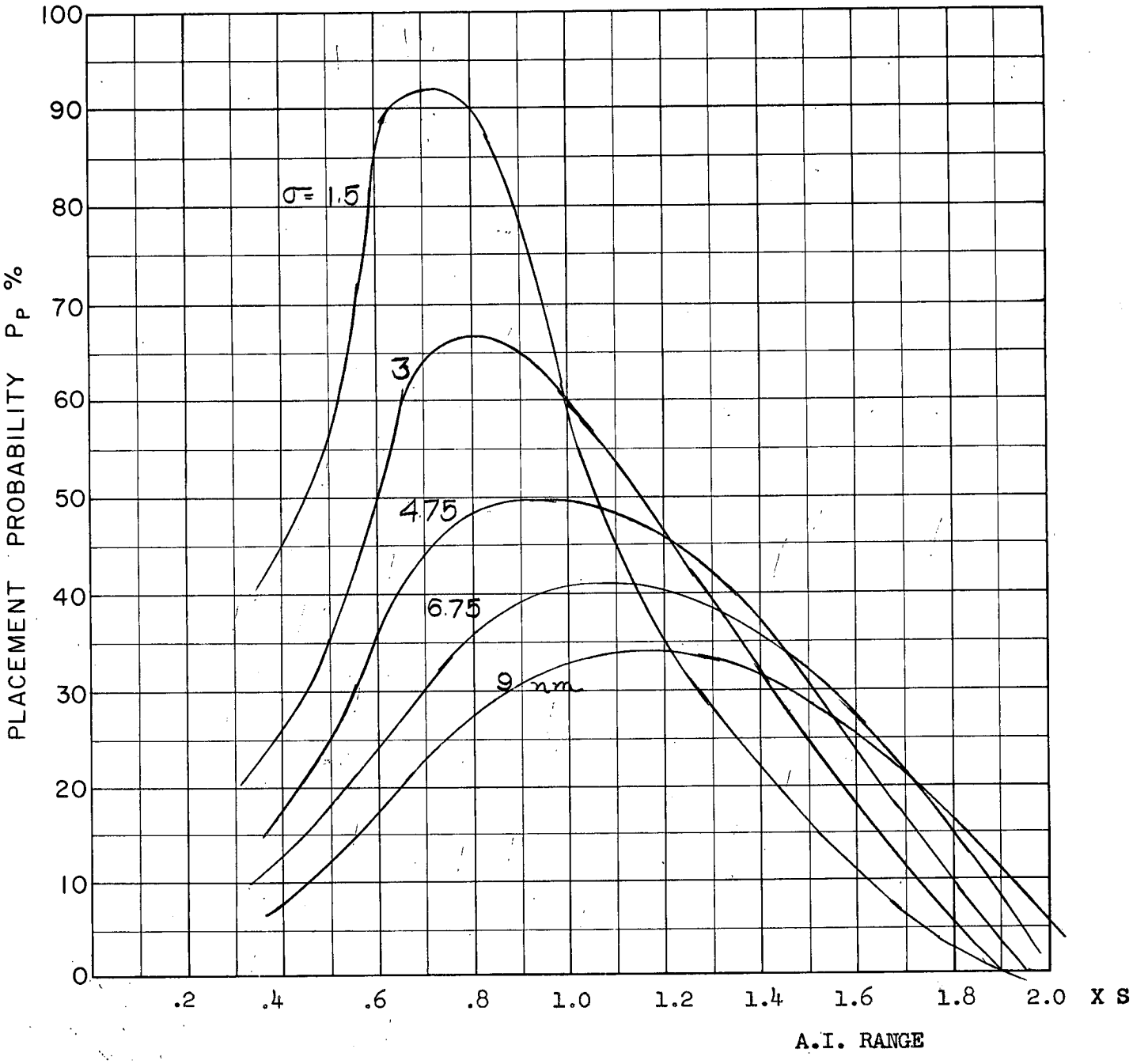

COURSE DIFFERENCE: 110°
TARGET EVASION: 0.5
TARGET MACH NO.: 2.0
INTERCEPTOR LATERAL G's: 1.6
INTERCEPTOR MACH NO.: 1.5
σ OF G.C.I. ACCURACY: 5 Values
A.I. DETECTION RANGE AS FRACTION OF SPECIFICATION RANGE, S: ABSCISSA
A.I. DETECTION RANGE CONTOUR: Straight
ALTITUDE: 50 K

S-5
B

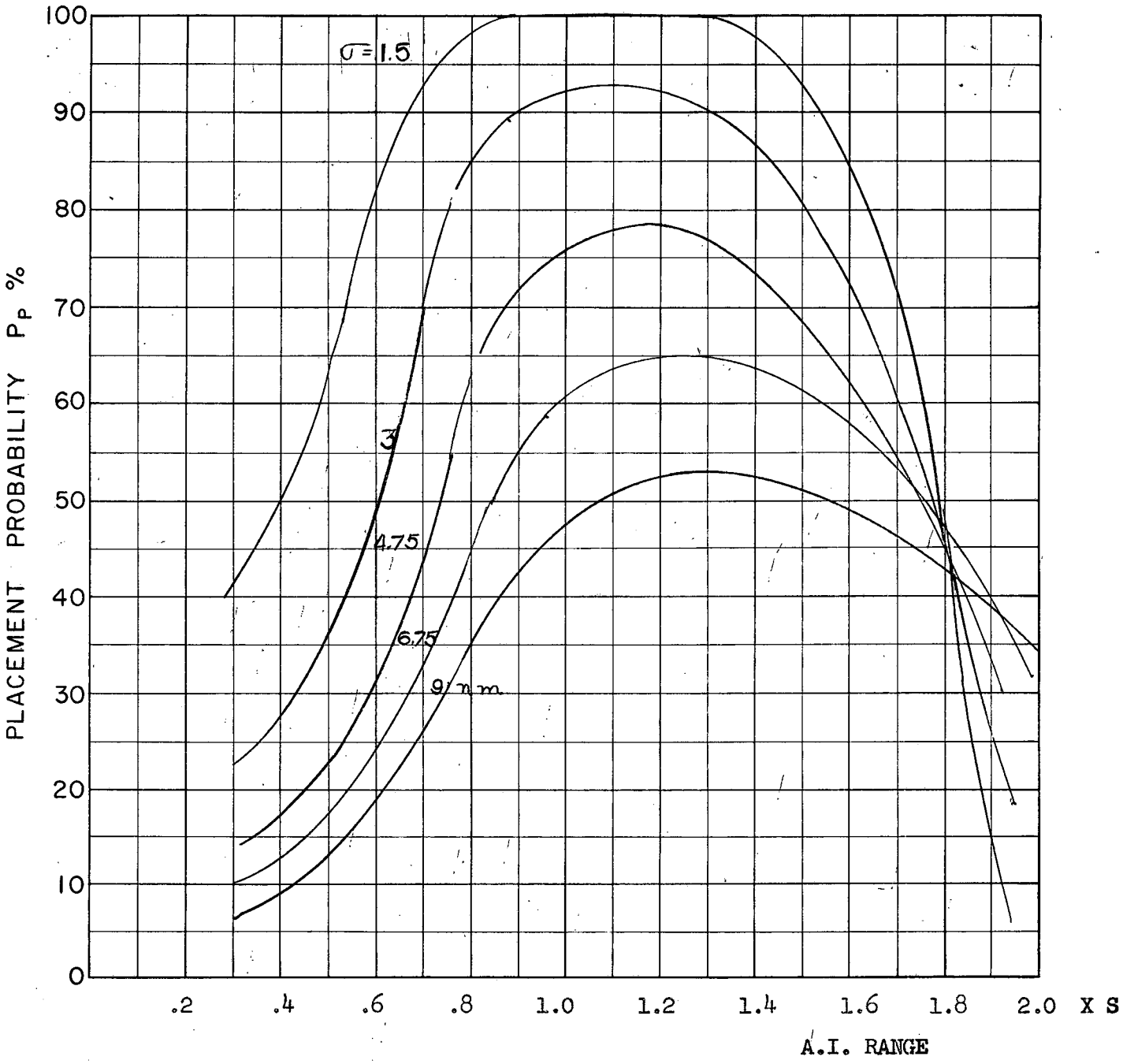

COURSE DIFFERENCE: 135°
TARGET EVASION: 0.5
TARGET MACH NO.: 2.0
INTERCEPTOR LATERAL G's: 1.6
INTERCEPTOR MACH NO.: 1.5
σ OF G.C.I. ACCURACY: 5 Values
A.I. DETECTION RANGE AS FRACTION OF SPECIFICATION RANGE, S: ABSCISSA
A.I. DETECTION RANGE CONTOUR: Straight
ALTITUDE: 50 K

S 6
B

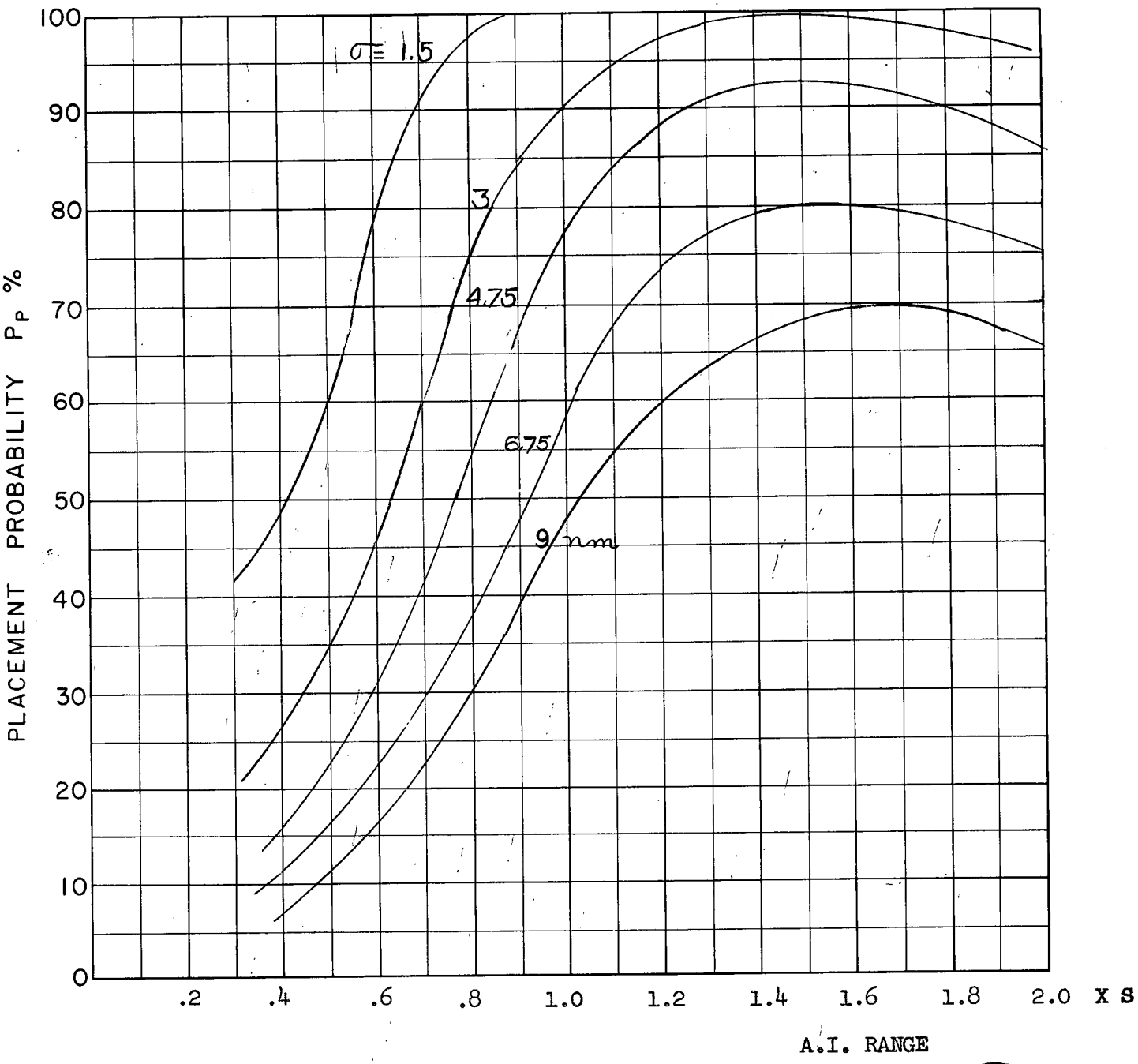

COURSE DIFFERENCE: 160°
TARGET EVASION: 0.5
TARGET MACH NO.: 2.0
INTERCEPTOR LATERAL G's: 1.6
INTERCEPTOR MACH NO.: 1.8
σ OF G.C.I. ACCURACY: 5 Values
A.I. DETECTION RANGE AS FRACTION OF SPECIFICATION RANGE, S: ABSCISSA
A.I. DETECTION RANGE CONTOUR: Straight
ALTITUDE: 50 K

S 7
B

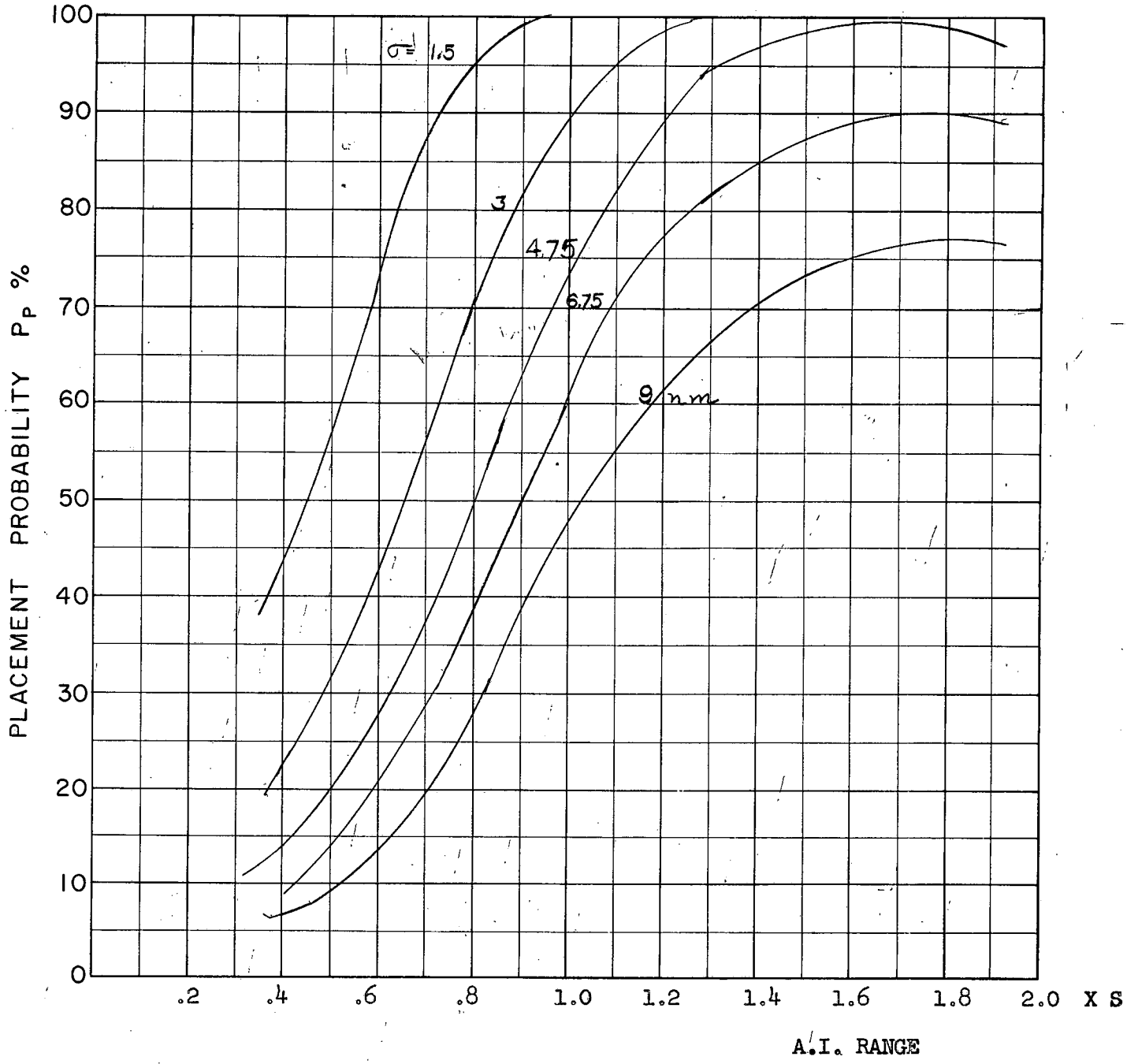

COURSE DIFFERENCE: 180°
TARGET EVASION: 0.5
TARGET MACH NO.: 2.0
INTERCEPTOR LATERAL G's: 1.6
INTERCEPTOR MACH NO.: 1.5
σ OF G.C.I. ACCURACY: 5 Values
A.I. DETECTION RANGE AS FRACTION OF SPECIFICATION RANGE, S: ABSCISSA
A.I. DETECTION RANGE CONTOUR: Straight
ALTITUDE: 50 K

S 8
B

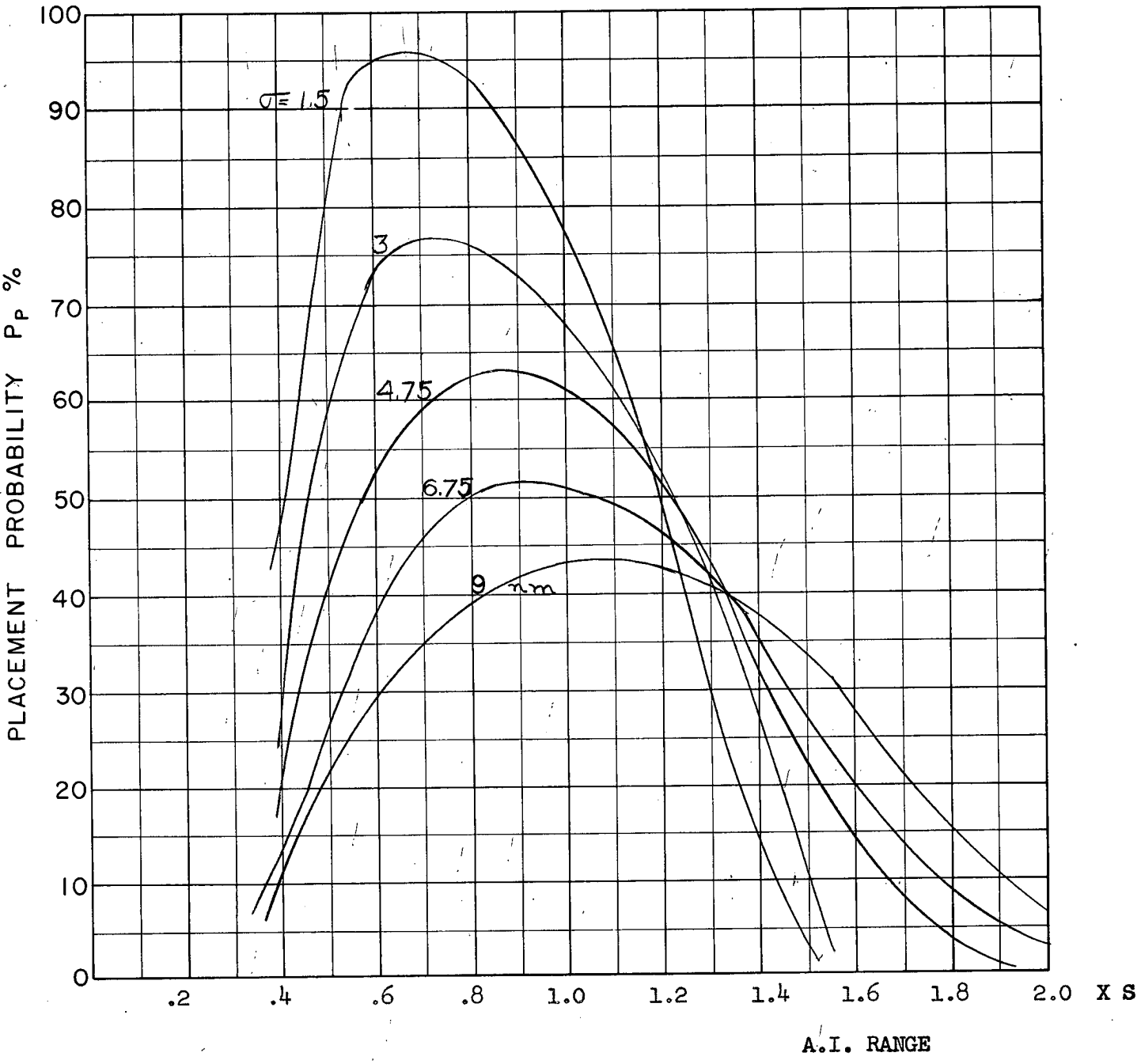

COURSE DIFFERENCE: 110°
TARGET EVASION: 0.5
TARGET MACH NO.: 2.0
INTERCEPTOR LATERAL G's: 3.0
INTERCEPTOR MACH NO.: 1.5
σ OF G.C.I. ACCURACY: 5 Values
A.I. DETECTION RANGE AS FRACTION OF SPECIFICATION RANGE, S: ABSCISSA
A.I. DETECTION RANGE CONTOUR: Straight
ALTITUDE: 50 K

S 9 B

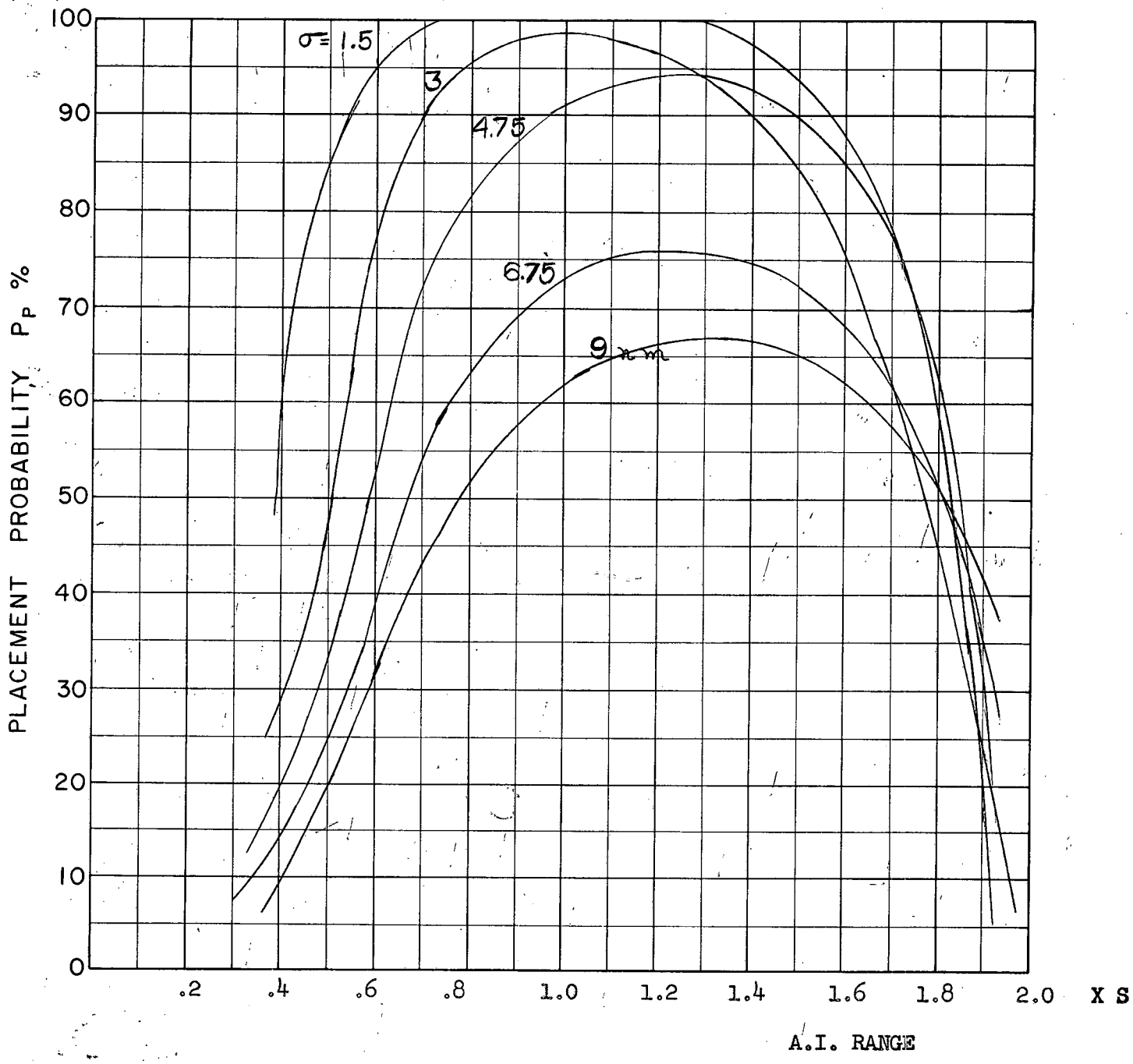

COURSE DIFFERENCE: 135°
TARGET EVASION: 0.5
TARGET MACH NO.: 2.0
INTERCEPTOR LATERAL G's: 3.0
INTERCEPTOR MACH NO.: 1.5
σ OF G.C.I. ACCURACY: 5 Values
A.I. DETECTION RANGE AS FRACTION OF SPECIFICATION RANGE, S: ABSCISSA
A.I. DETECTION RANGE CONTOUR: Straight
ALTITUDE: 50 K

S-10
B

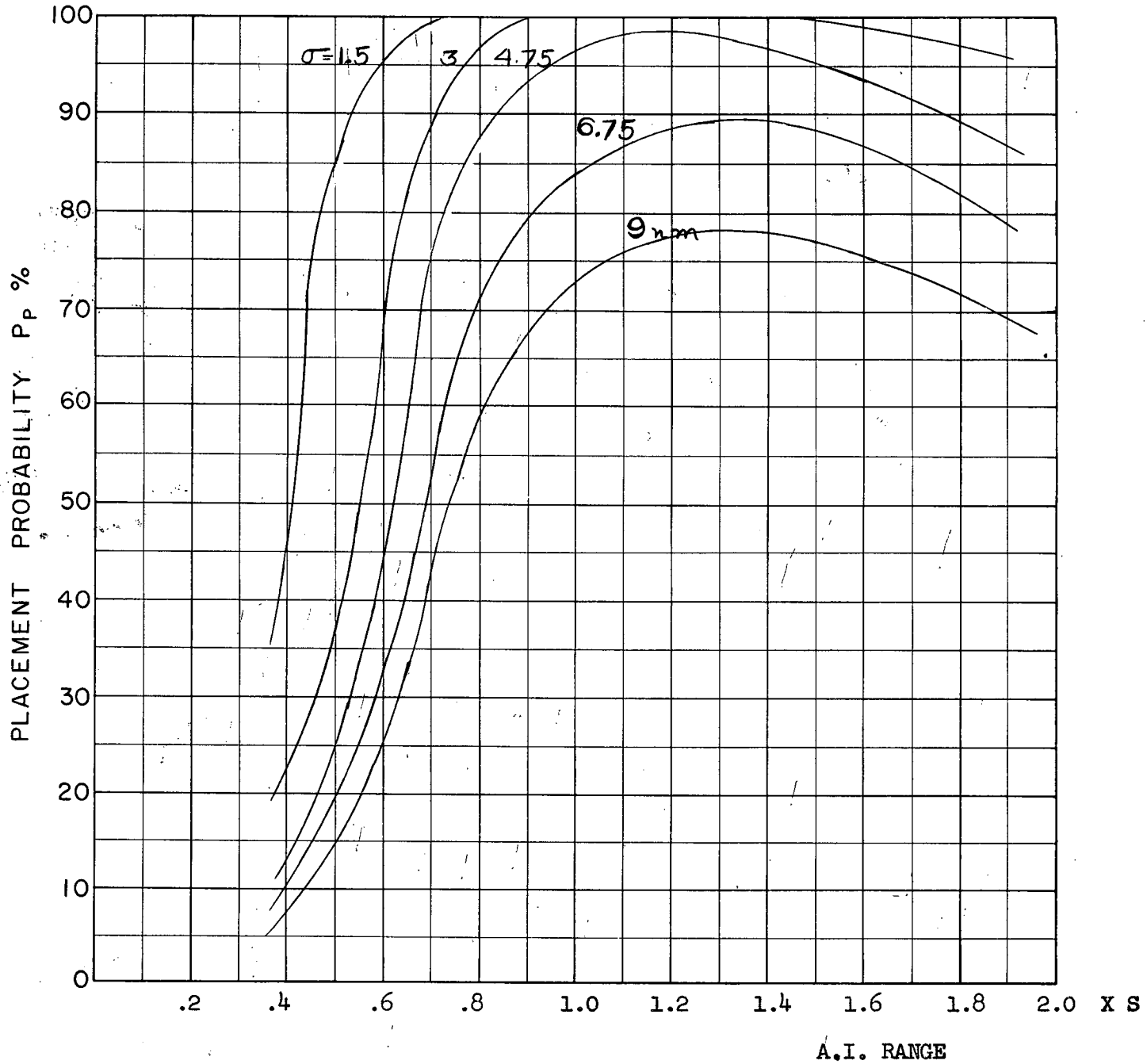

COURSE DIFFERENCE: 160°
TARGET EVASION: 0.5
TARGET MACH NO.: 2.0
INTERCEPTOR LATERAL G's: 3.0
INTERCEPTOR MACH NO.: 1.5
σ OF G.C.I. ACCURACY: 5 Values
A.I. DETECTION RANGE AS FRACTION OF SPECIFICATION RANGE, S: ABSCISSA
A.I. DETECTION RANGE CONTOUR: Straight
ALTITUDE: 50 K

S 11
B

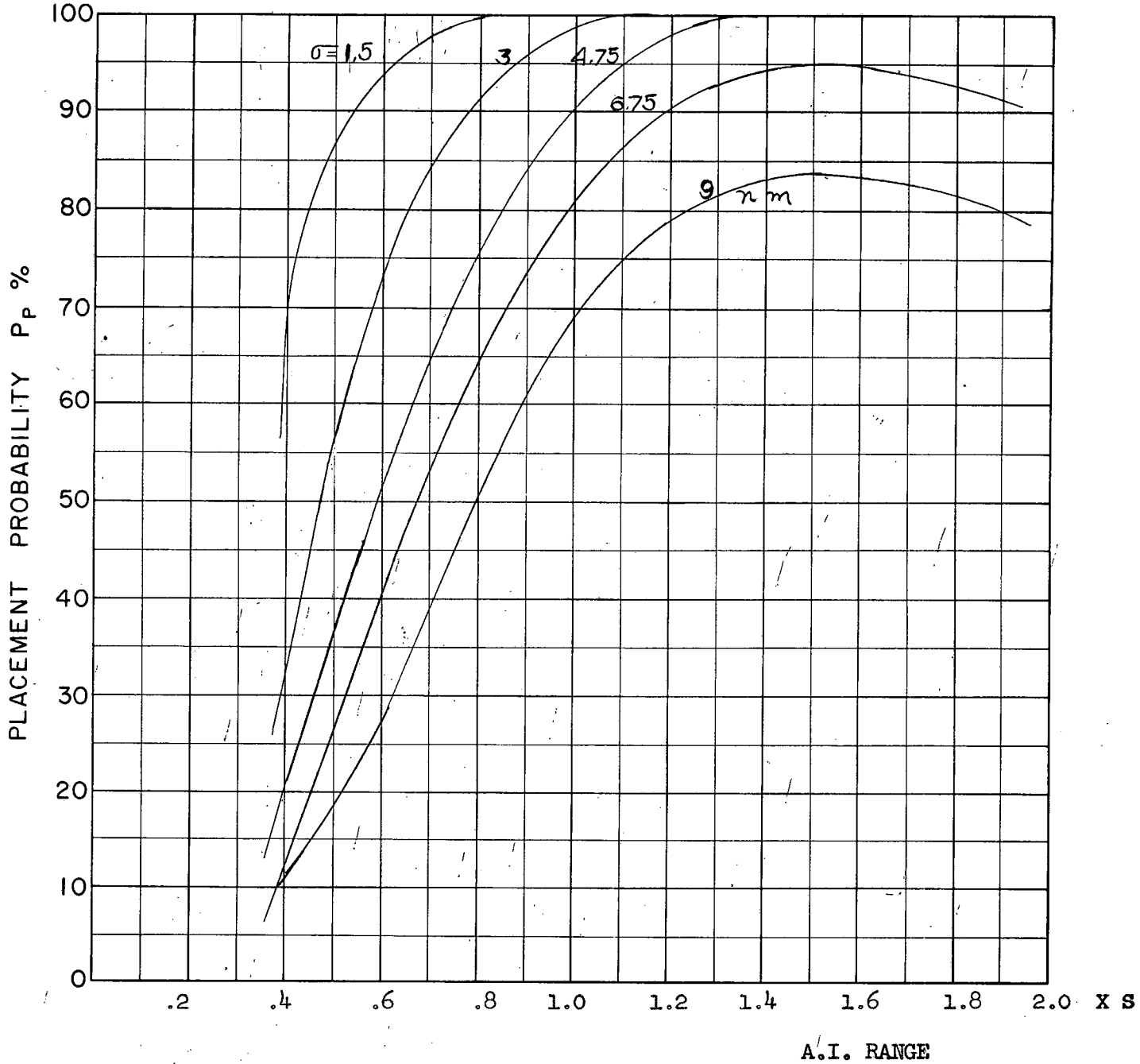

COURSE DIFFERENCE: 180°
TARGET EVASION: 0.5
TARGET MACH NO.: 2.0
INTERCEPTOR LATERAL G's: 3.0
INTERCEPTOR MACH NO.: 1.5
σ OF G.C.I. ACCURACY: 5 Values
A.I. DETECTION RANGE AS FRACTION OF SPECIFICATION RANGE, S ABSCISSA
A.I. DETECTION RANGE CONTOUR: Straight
ALTITUDE: 50 K

S12
B

APPENDIX 'C'

Placement Probability for a Constant Speed Interceptor (Part 2)

by L. Sheppherd

In order to ease the work load on the REAC facilities at CARDE, some of the two dimensional placement analysis was done under contract by Computing Devices of Canada. The equations and parameter values were supplied by CARDE so that the results would fit in with the work done here. Data processing was done by the Analysis and Data Reduction Groups of 'G' Wing, CARDE.

The same lead collision geometry as that used at CARDE was specified. The equations used have been published in Section 4 of Reference 1. The launch zones used for the two sets of parameters considered are given in Figures 1 and 2.

Target evasion was considered in a different fashion than in the CARDE work. The target was assumed to begin manoeuvring when the interceptor approached to a range of 150,000 feet. If interceptor AI lock-on occurred at some lesser range than the target manoeuvring began immediately on lock-on.

Initial course difference values of 110°, 135°, 160° and 180° were used for all cases.

Two sets of parameters were used:

(a) $M_T = 2.0$

$M_I = 1.5$

$H_T = 50{,}000$ feet

Target evasion 0.5 g lateral (load factor 1.12)

Interceptor Turn Capability 3.0g 1.6g 0.85g lateral (load factor 3.2g 1.89g 1.33g)

(b) $M_T = 1.5$

$M_I = 1.5$

$H_T = 50{,}000$ feet

Target Evasion = 0.4g lateral (load factor 1.09)

Interceptor Turn Capability 3.0g 1.6g 0.85g lateral
(load factor 3.2g 1.89g 1.33g)

Look angle limit of 66° was used; the cases where interceptor capability was 1.6g were repeated for a look angle of 75°.

The placement charts were reduced to curves of probability vs. AI range for both Delta and Straight Wing targets. The pessimistic zone common to those for both evasion towards and evasion away was used. The graphs are given in the following figures.

Reference 1. CARDE Technical Letter N-47-14, "Methods of Solution Using the REAC for the 2-Dimensional Constant Speed Fighter Case".

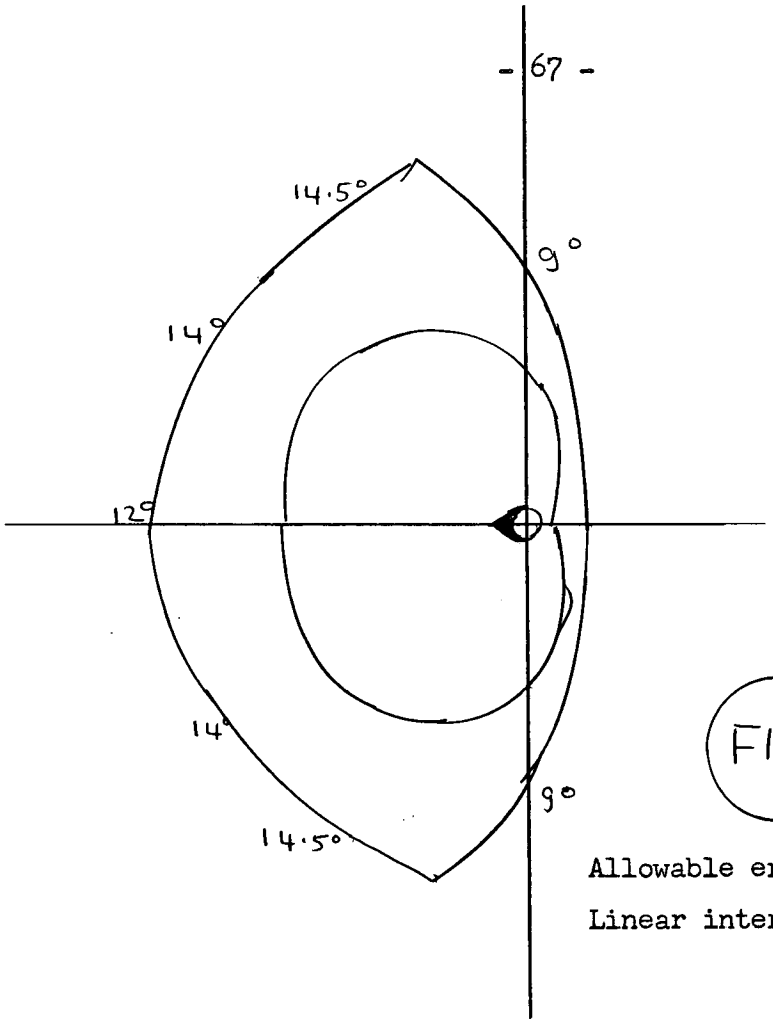

M_T = 2.0
M_I = 1.5
H = 50,000 ft.
g_T = 0.5
$\overline{M}_m$ = 2.8
F = 25,000

FIG 1

Allowable error at minimum range 5°.
Linear interpolation to be used.

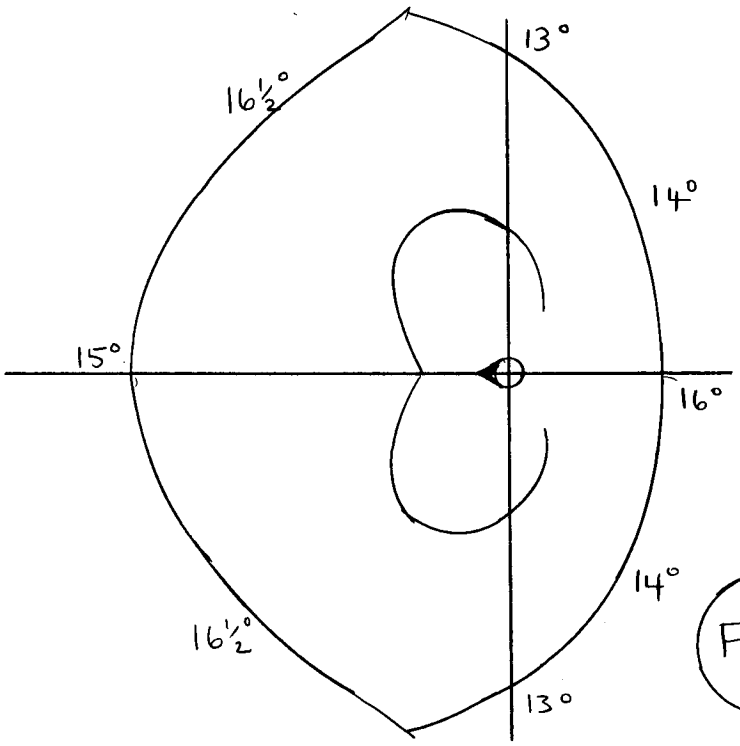

M_T = 1.5
M_I = 1.5
g_T = 0.4
H = 50,000 ft.
F = 22,500 ft.
$\overline{M}_m$ = 2.9

FIG 2

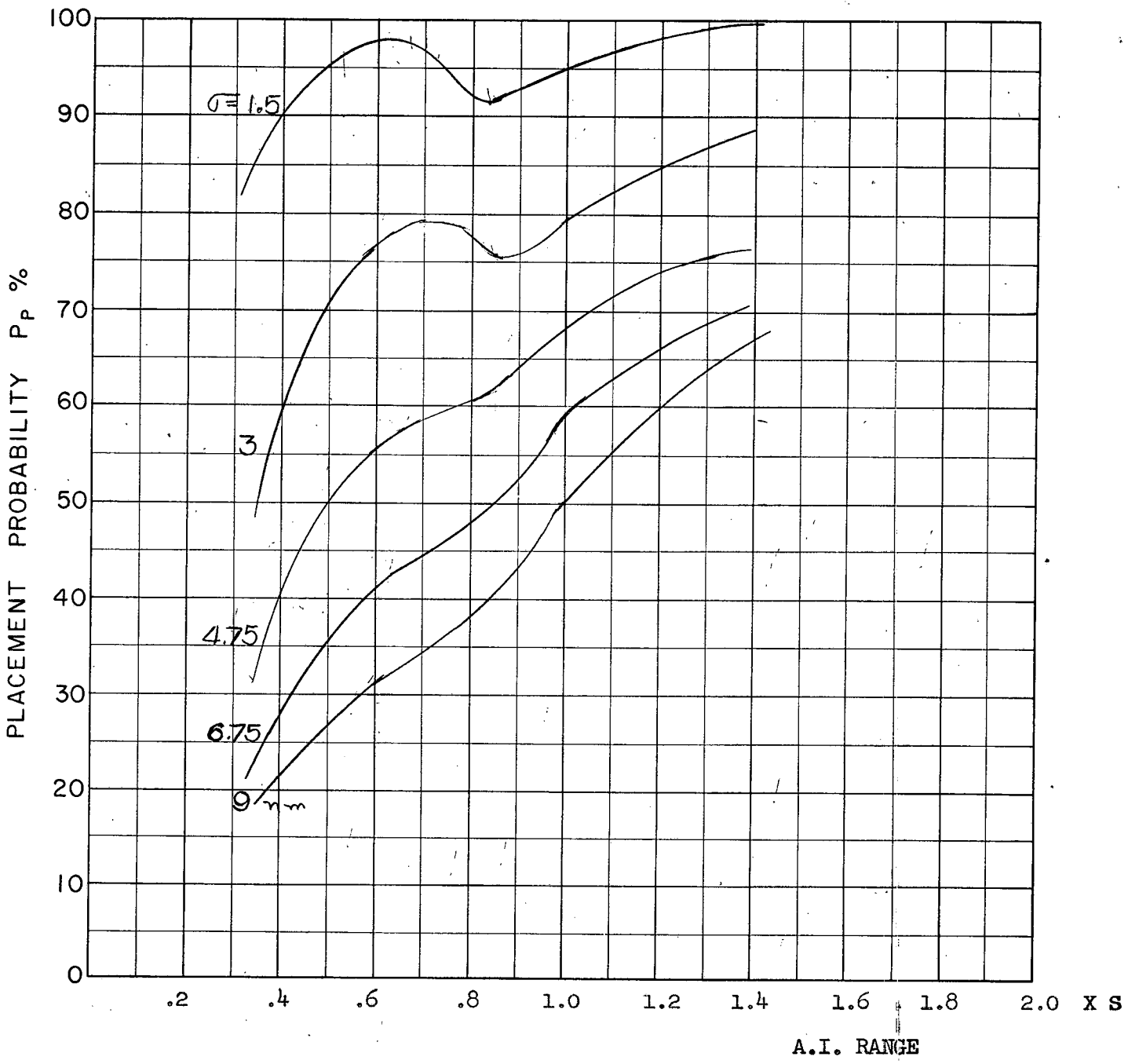

COURSE DIFFERENCE: 110°
TARGET EVASION: 0.4
TARGET MACH NO.: 1.5
INTERCEPTOR LATERAL G's: 0.85
INTERCEPTOR MACH NO.: 1.5
σ OF G.C.I. ACCURACY: 5 Values
A.I. DETECTION RANGE AS FRACTION OF SPECIFICATION RANGE, S: ABSCISSA
A.I. DETECTION RANGE CONTOUR: Delta
ALTITUDE: 50 K

D-3 C

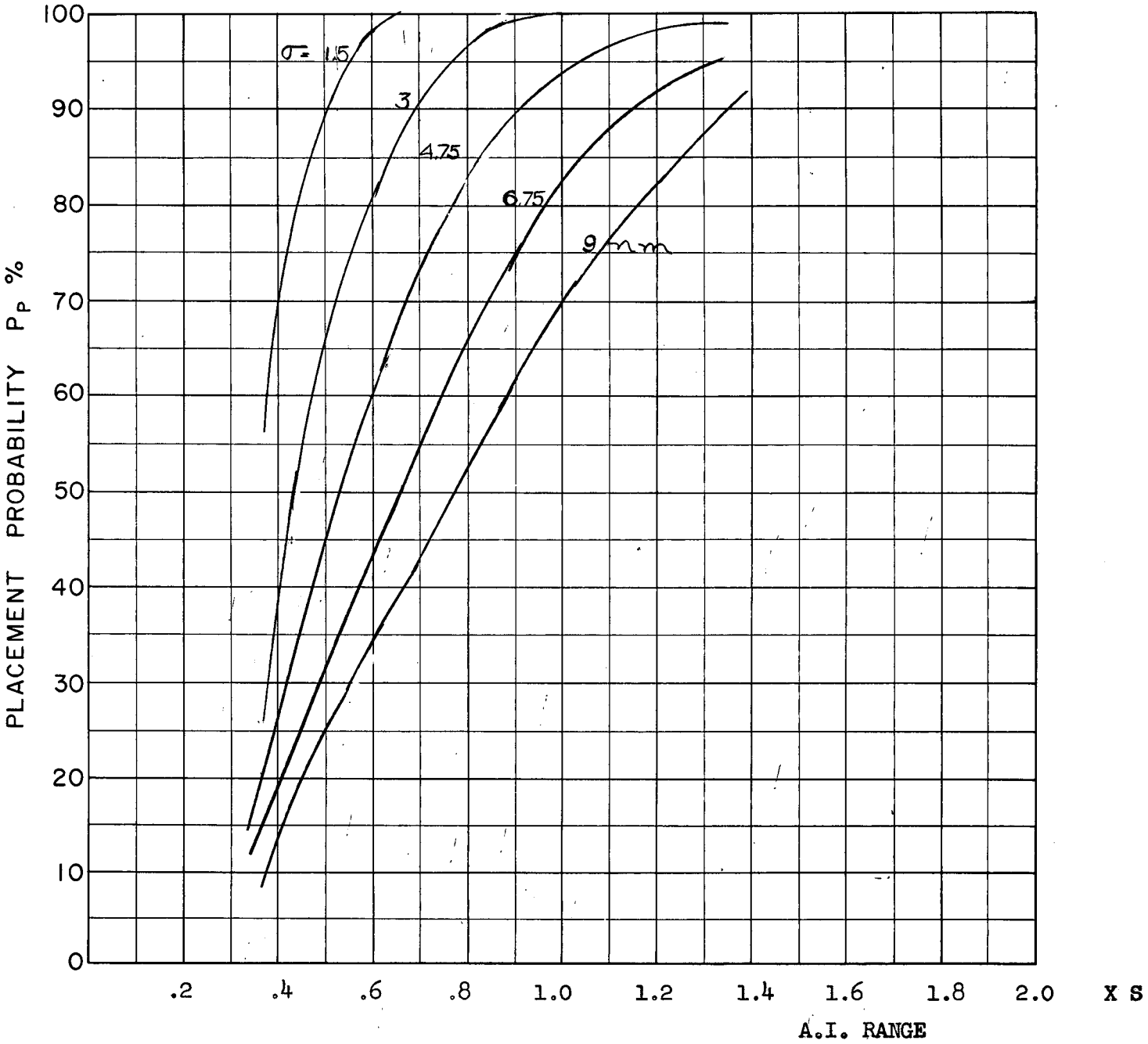

COURSE DIFFERENCE: 135°
TARGET EVASION: 0.4
TARGET MACH NO.: 1.5
INTERCEPTOR LATERAL G's: 0.85
INTERCEPTOR MACH NO.: 1.5
σ OF G.C.I. ACCURACY: 5 Values
A.I. DETECTION RANGE AS FRACTION OF SPECIFICATION RANGE, S: ABSCISSA
A.I. DETECTION RANGE CONTOUR: Delta
ALTITUDE: 50 K

D.4
c

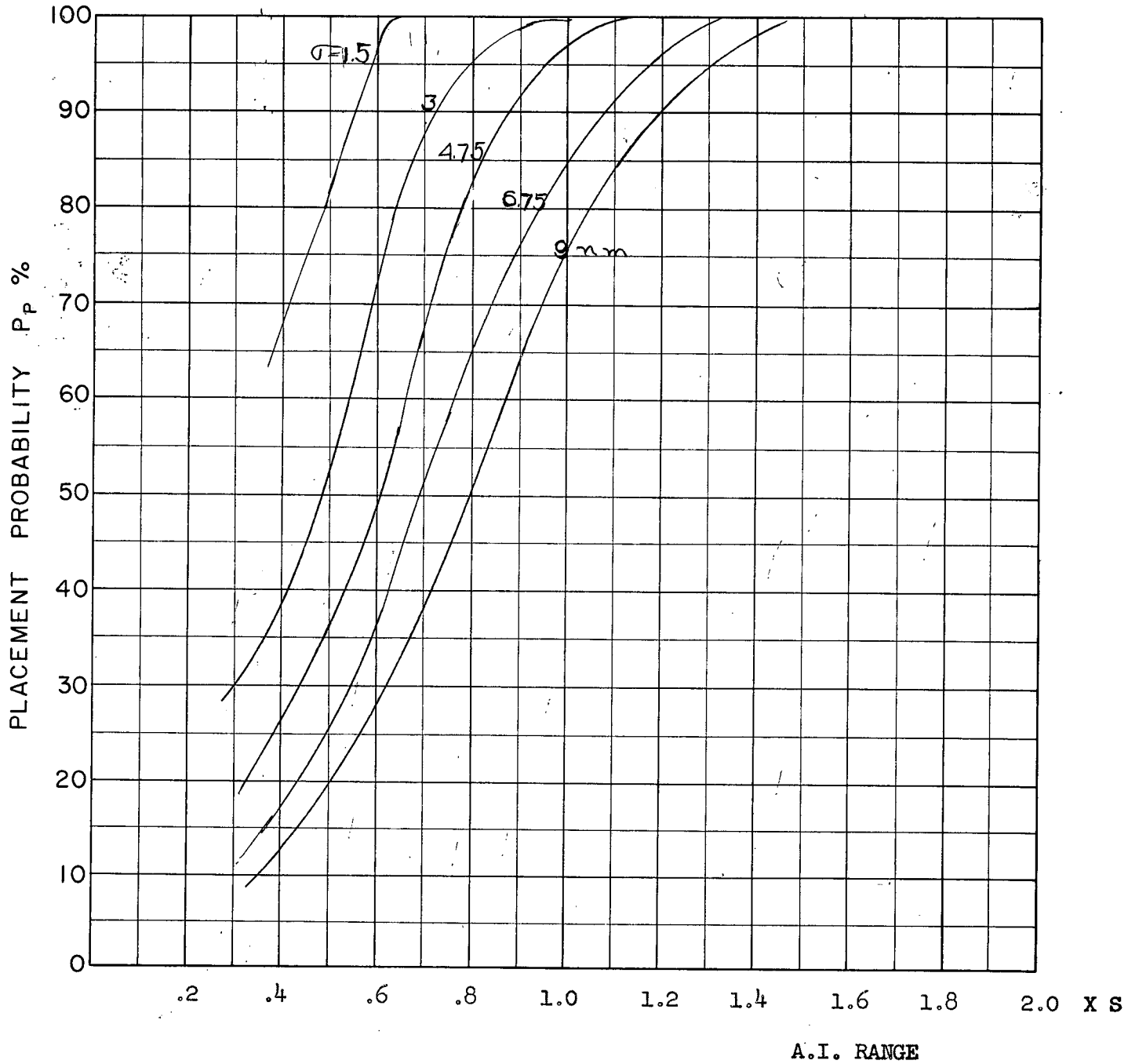

COURSE DIFFERENCE: 160°
TARGET EVASION: 0.4
TARGET MACH NO.: 1.5
INTERCEPTOR LATERAL G's: 0.85
INTERCEPTOR MACH NO.: 1.5
σ OF G.C.I. ACCURACY: 5 Values
A.I. DETECTION RANGE AS FRACTION OF SPECIFICATION RANGE, S: ABSCISSA
A.I. DETECTION RANGE CONTOUR: Delta
ALTITUDE: 50 K

D5
c

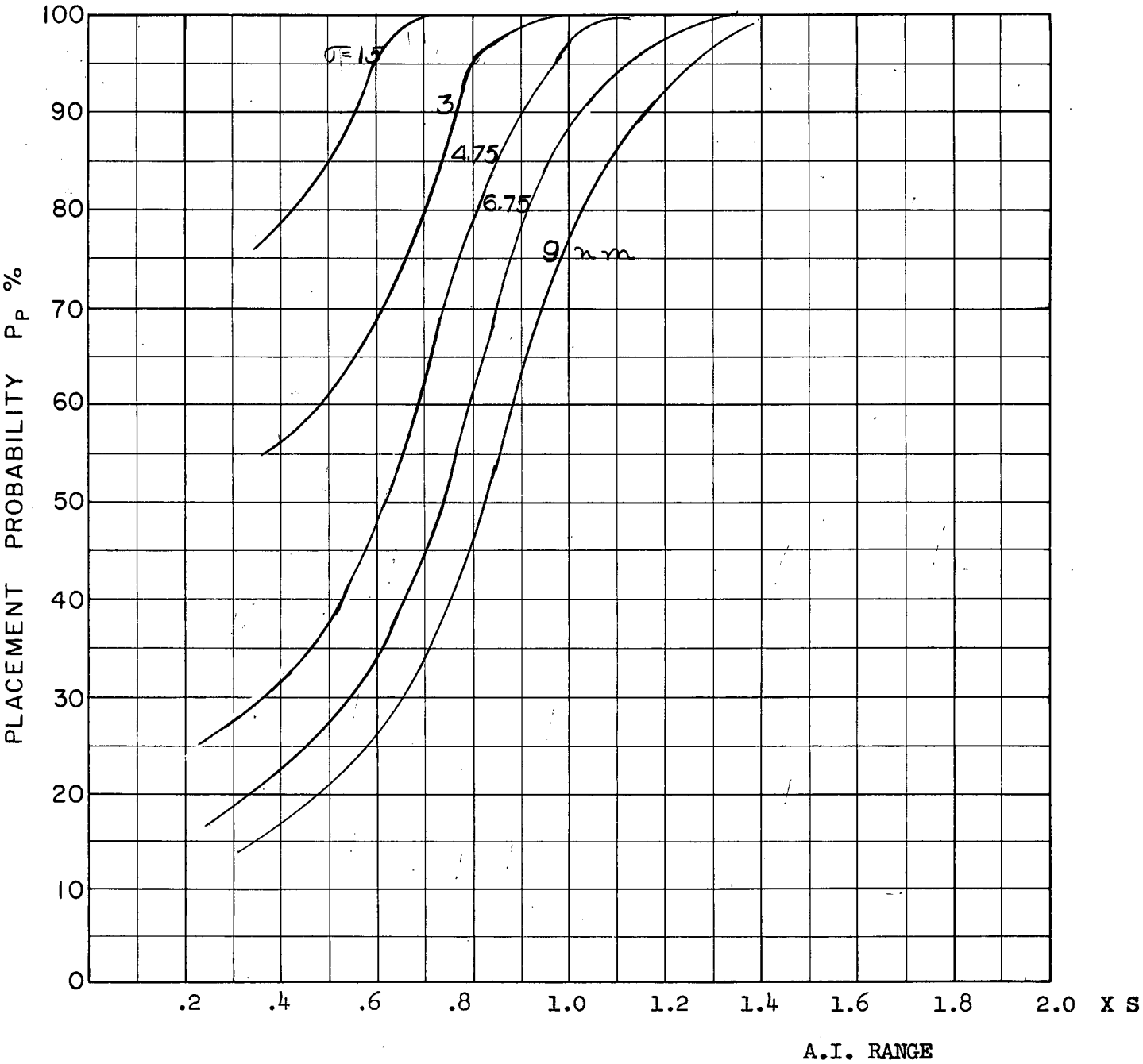

COURSE DIFFERENCE: 180°
TARGET EVASION: 0.4
TARGET MACH NO.: 1.5
INTERCEPTOR LATERAL G's: 0.85
INTERCEPTOR MACH NO.: 1.5
σ OF G.C.I. ACCURACY: 5 Values
A.I. DETECTION RANGE AS FRACTION OF SPECIFICATION RANGE, S: ABSCISSA
A.I. DETECTION RANGE CONTOUR: Delta
ALTITUDE: 50 K

D.6
C

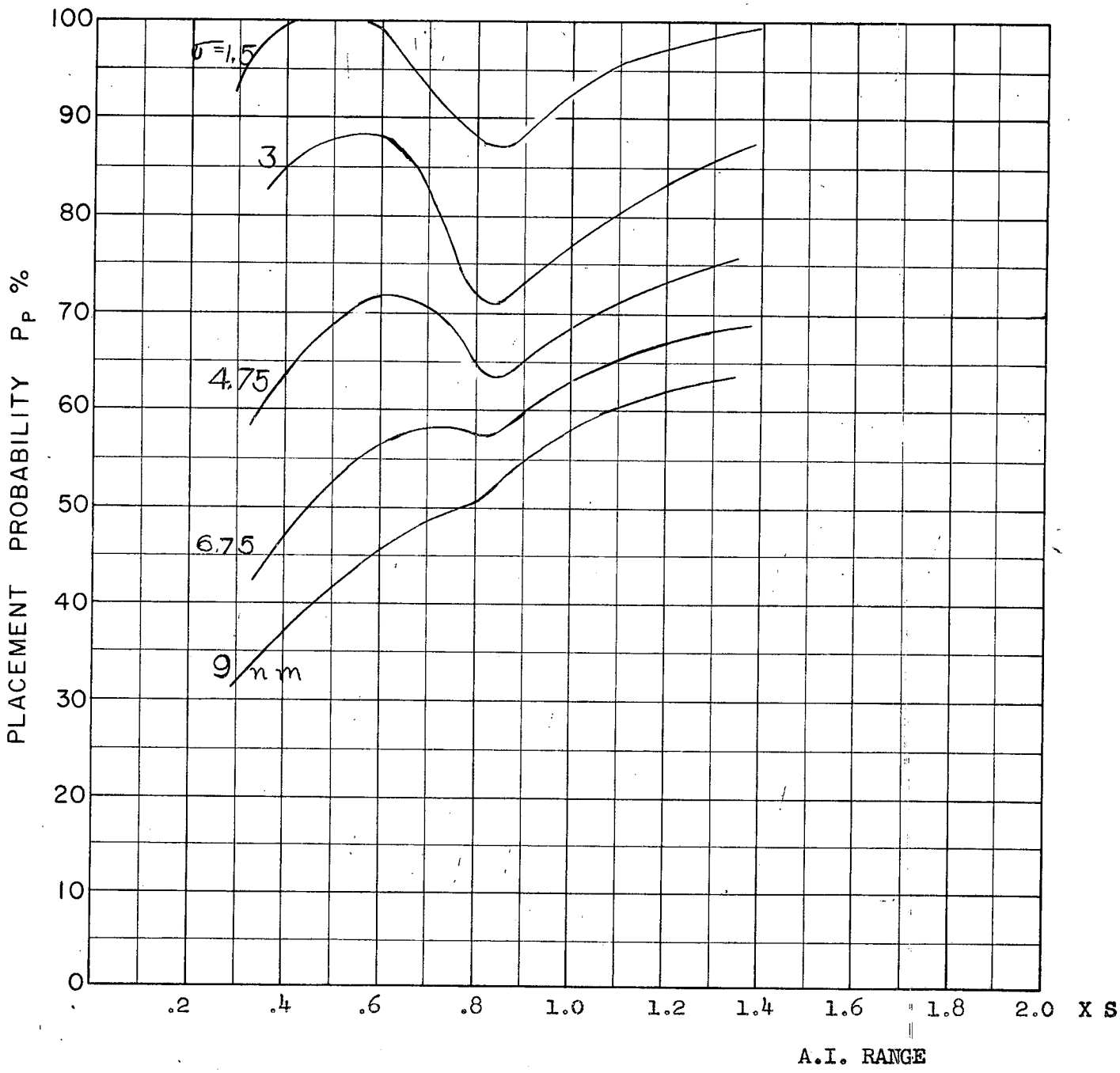

COURSE DIFFERENCE: 110°
TARGET EVASION: 0.4
TARGET MACH NO.: 1.5
INTERCEPTOR LATERAL G's: 1.6
INTERCEPTOR MACH NO.: 1.5
σ OF G.C.I. ACCURACY: 5 Values
A.I. DETECTION RANGE AS FRACTION OF SPECIFICATION RANGE, S: ABSCISSA
A.I. DETECTION RANGE CONTOUR: Delta
ALTITUDE: 50 K

D.7
c

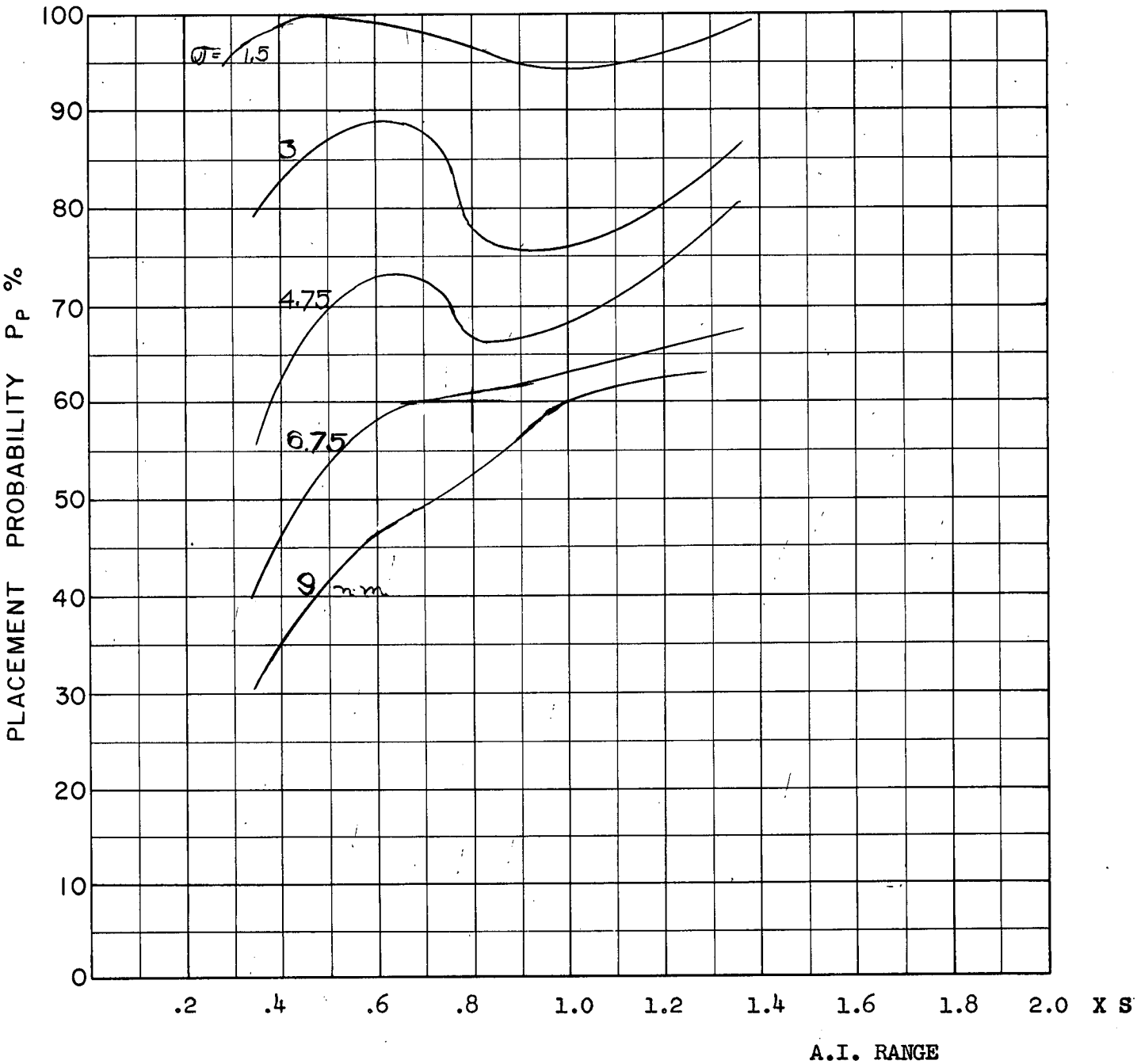

COURSE DIFFERENCE: 110°
TARGET EVASION: 0.4
TARGET MACH NO.: 1.5
INTERCEPTOR LATERAL G's: 1.6
INTERCEPTOR MACH NO.: 1.5
σ OF G.C.I. ACCURACY: 5 Values
A.I. DETECTION RANGE AS FRACTION OF SPECIFICATION RANGE, S: ABSCISSA
A.I. DETECTION RANGE CONTOUR: Delta
ALTITUDE: 50 K
LOOK ANGLE LIMIT = 75°

D.8 c

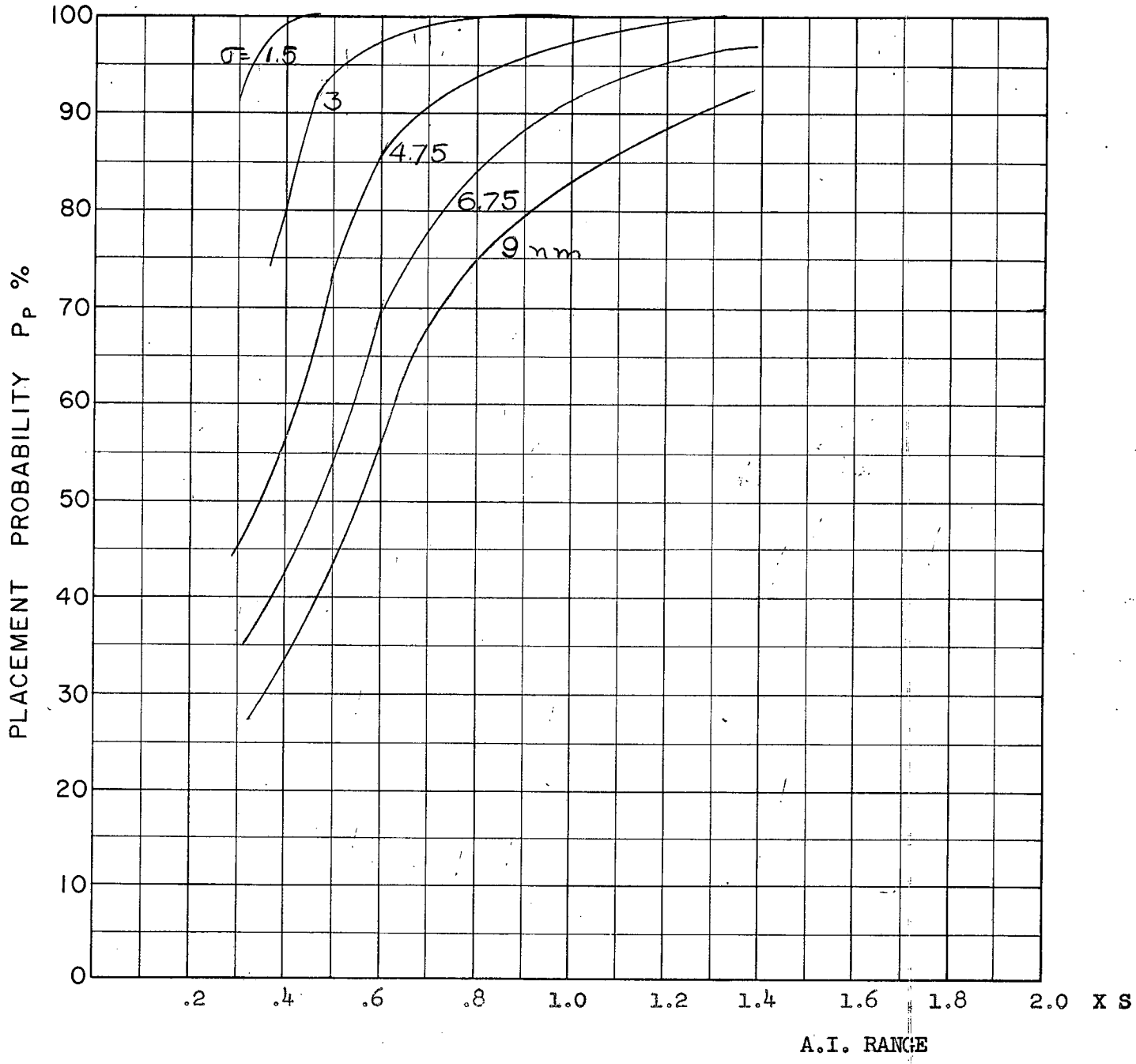

COURSE DIFFERENCE: 135°
TARGET EVASION: 0.4
TARGET MACH NO.: 1.5
INTERCEPTOR LATERAL G's: 1.6
INTERCEPTOR MACH NO.: 1.5
σ OF G.C.I. ACCURACY: 5 Values
A.I. DETECTION RANGE AS FRACTION OF SPECIFICATION RANGE, S: ABSCISSA
A.I. DETECTION RANGE CONTOUR: Delta
ALTITUDE: 50 K

D.9 C

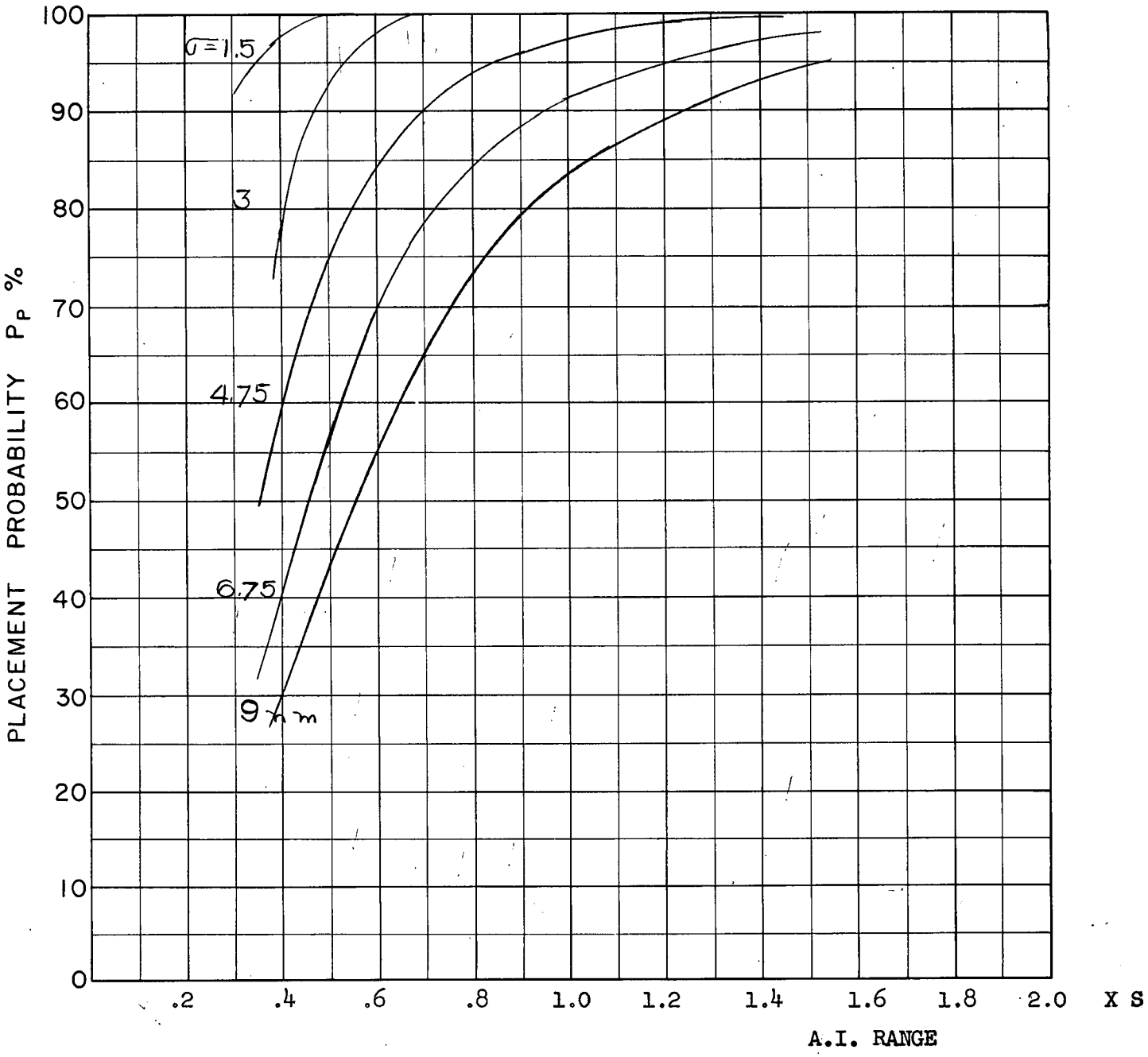

COURSE DIFFERENCE: 135°
TARGET EVASION: 0.4
TARGET MACH NO.: 1.5
INTERCEPTOR LATERAL G's: 1.6
INTERCEPTOR MACH NO.: 1.5
σ OF G.C.I. ACCURACY: 5 Values
A.I. DETECTION RANGE AS FRACTION OF SPECIFICATION RANGE, S: ABSCISSA
A.I. DETECTION RANGE CONTOUR: Delta
ALTITUDE: 50 K
LOOK ANGLE LIMIT = 75°

D10
C

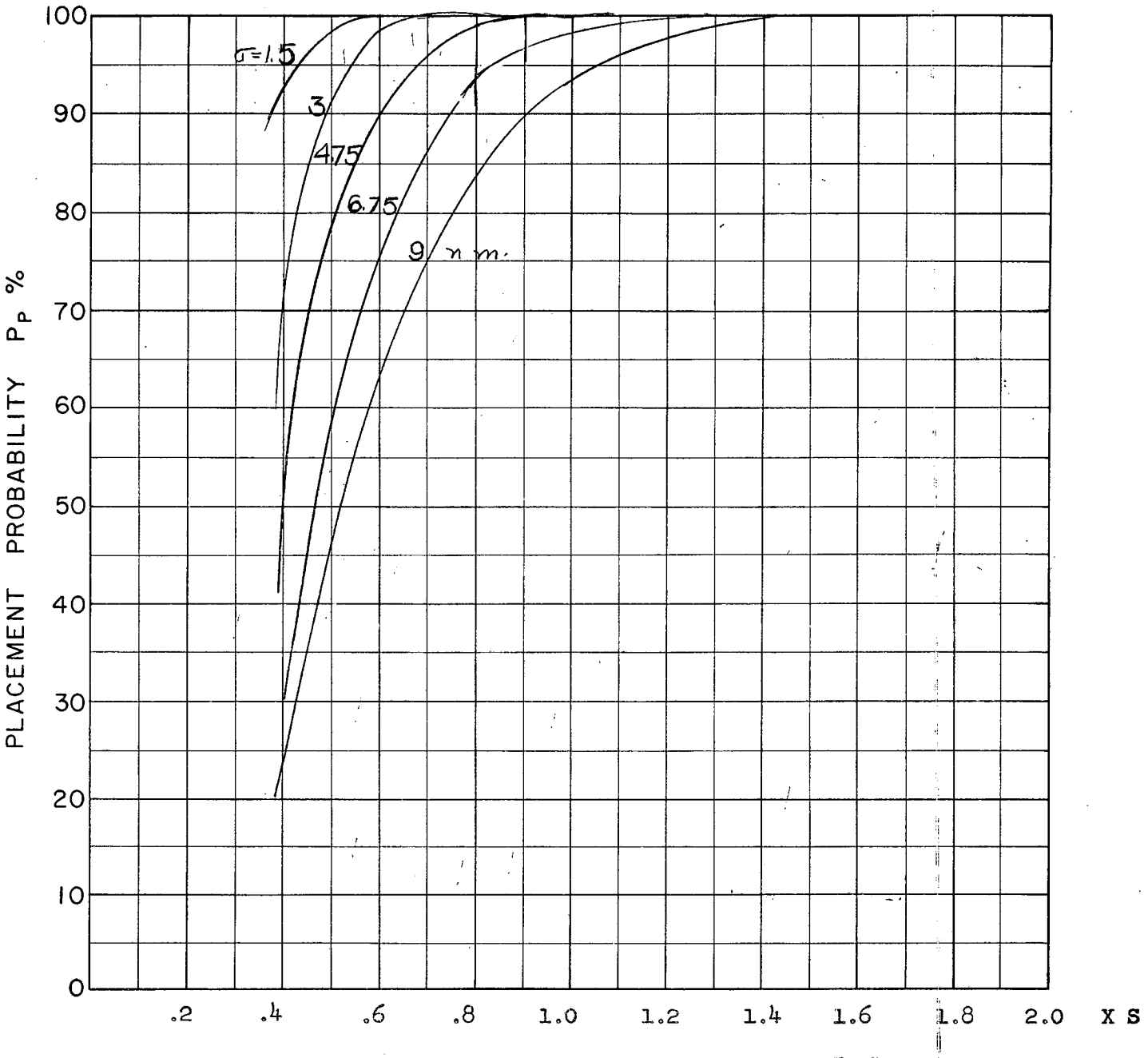

COURSE DIFFERENCE: 160°
TARGET EVASION: 0.4
TARGET MACH NO.: 1.5
INTERCEPTOR LATERAL G's: 1.6
INTERCEPTOR MACH NO.: 1.5
σ OF G.C.I. ACCURACY: 5 Values
A.I. DETECTION RANGE AS FRACTION OF SPECIFICATION RANGE, S: ABSCISSA
A.I. DETECTION RANGE CONTOUR: Delta
ALTITUDE: 50 K

D11
C

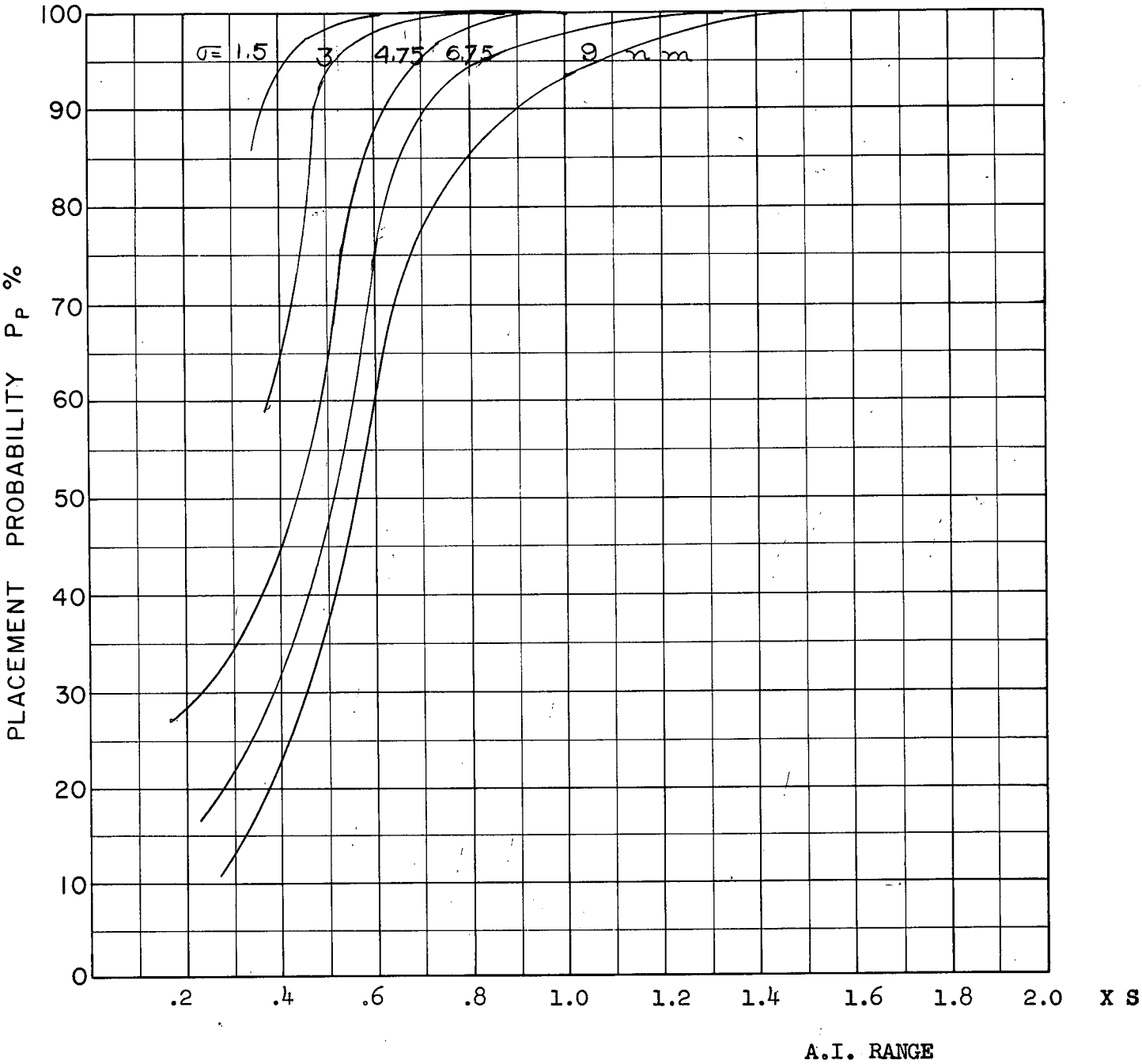

COURSE DIFFERENCE: 160°
TARGET EVASION: 0.4
TARGET MACH NO.: 1.5
INTERCEPTOR LATERAL G's: 1.6
INTERCEPTOR MACH NO.: 1.5
σ OF G.C.I. ACCURACY: 5 Values
A.I. DETECTION RANGE AS FRACTION OF SPECIFICATION RANGE, S: ABSCISSA
A.I. DETECTION RANGE CONTOUR: Delta
ALTITUDE: 50 K
LOOK ANGLE LIMIT = 75°

D12
C

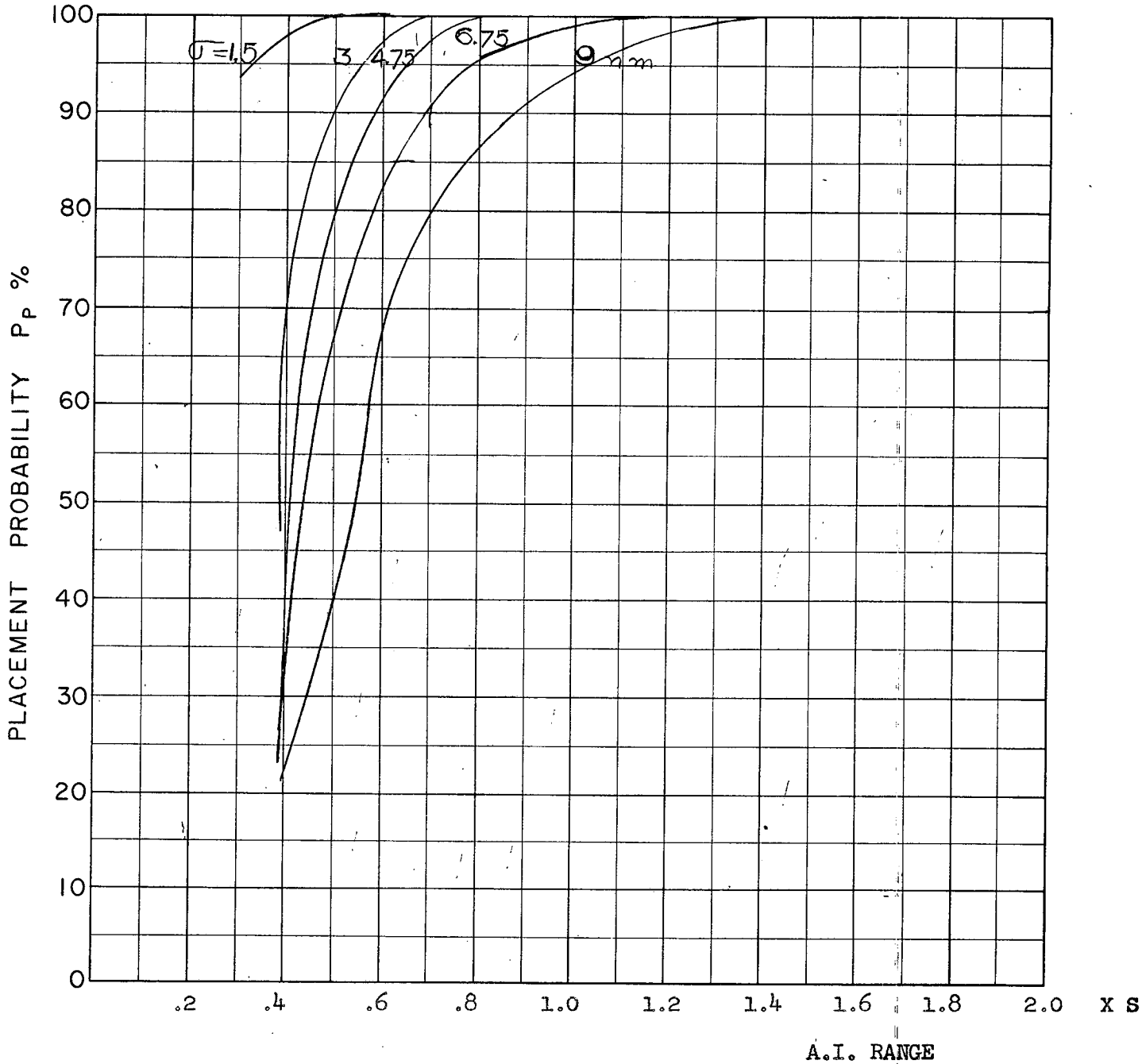

COURSE DIFFERENCE: 180°
TARGET EVASION: 0.4
TARGET MACH NO.: 1.5
INTERCEPTOR LATERAL G's: 1.6
INTERCEPTOR MACH NO.: 1.5
σ OF G.C.I. ACCURACY: 5 Values
A.I. DETECTION RANGE AS FRACTION OF SPECIFICATION RANGE, S: ABSCISSA
A.I. DETECTION RANGE CONTOUR: Delta
ALTITUDE: 50 K

D13
C

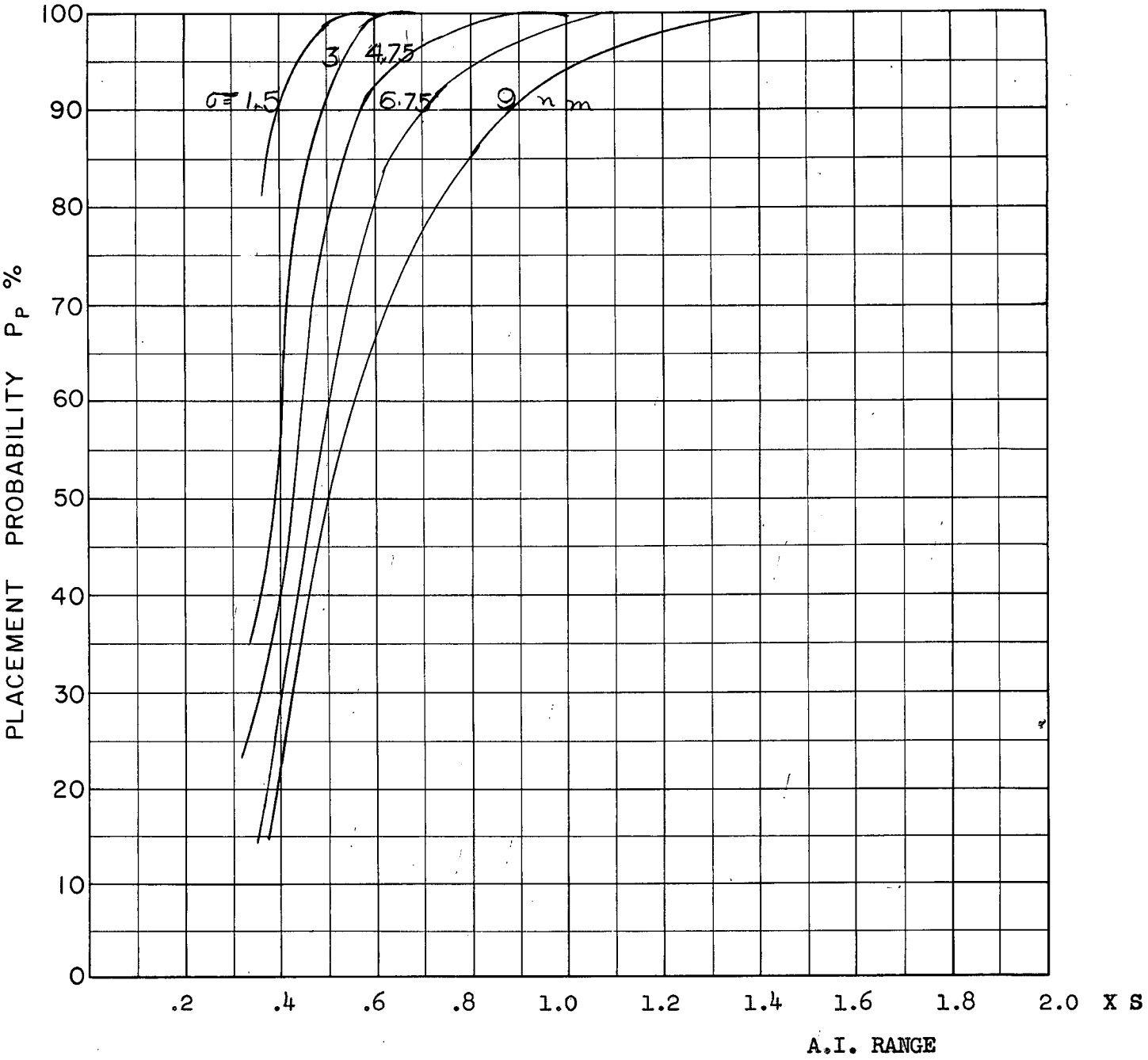

COURSE DIFFERENCE: 180°
TARGET EVASION: 0.4
TARGET MACH NO.: 1.5
INTERCEPTOR LATERAL G's: 1.6
INTERCEPTOR MACH NO.: 1.5
σ OF G.C.I. ACCURACY: 5 Values
A.I. DETECTION RANGE AS FRACTION OF SPECIFICATION RANGE, S: ABSCISSA
A.I. DETECTION RANGE CONTOUR: Delta
ALTITUDE: 50 K
LOOK ANGLE LIMIT = 75°

D14 c

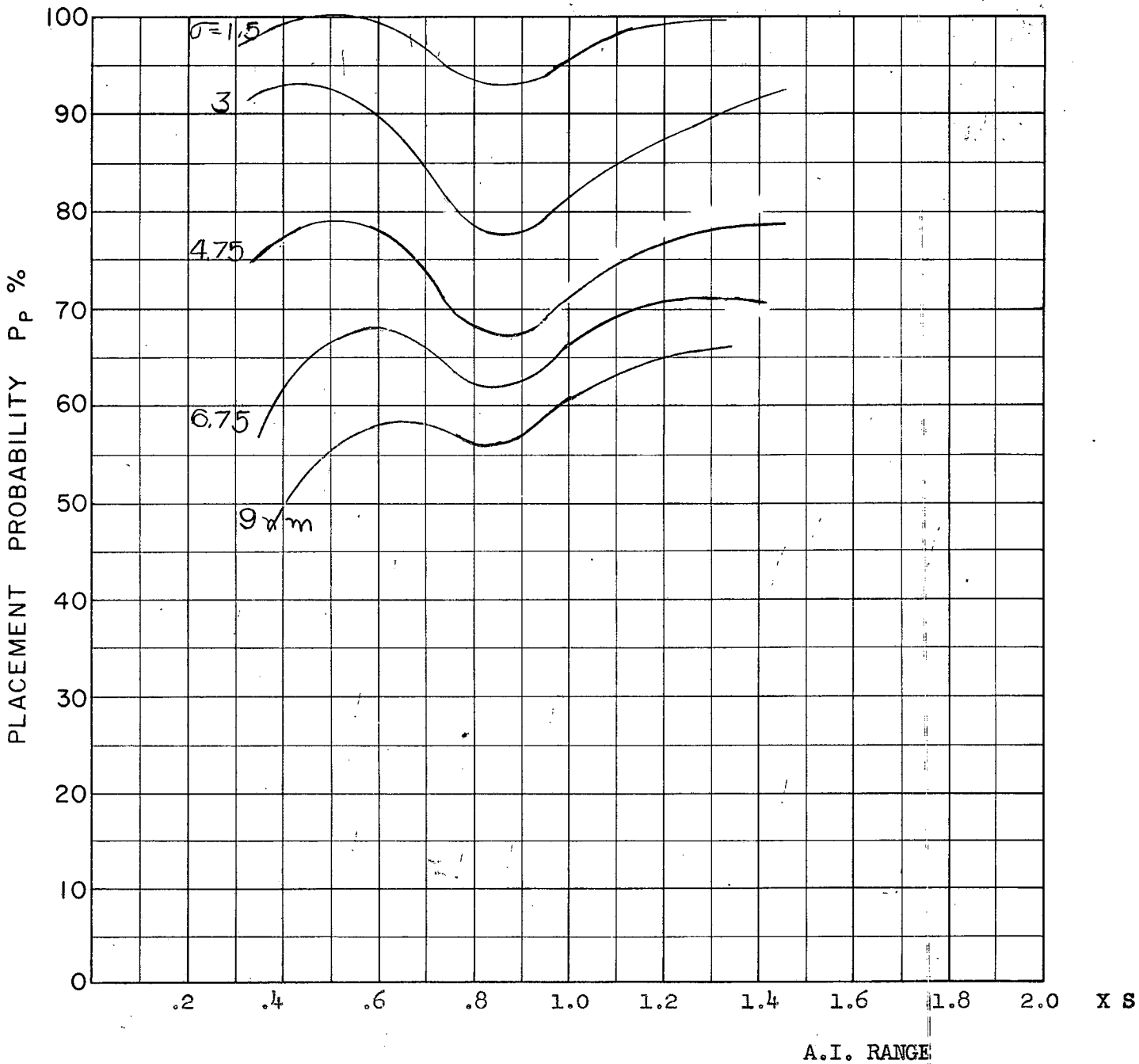

COURSE DIFFERENCE: 110°
TARGET EVASION: 0.4
TARGET MACH NO.: 1.5
INTERCEPTOR LATERAL G's: 3.0
INTERCEPTOR MACH NO.: 1.5
σ OF G.C.I. ACCURACY: 5 Values
A.I. DETECTION RANGE AS FRACTION OF SPECIFICATION RANGE, S: ABISCISSA
A.I. DETECTION RANGE CONTOUR: Delta
ALTITUDE: 50 K

D15
C

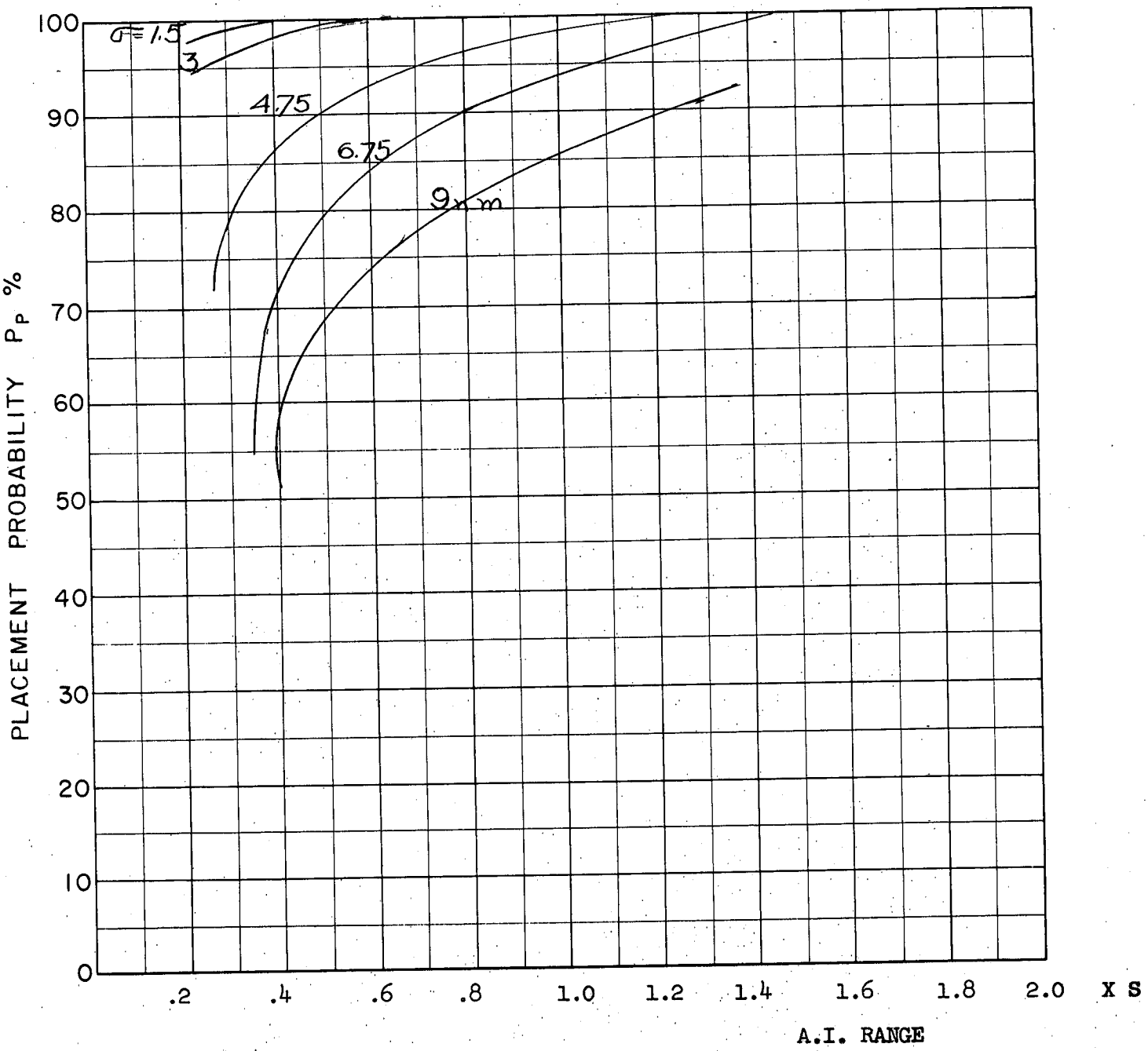

COURSE DIFFERENCE: 135°
TARGET EVASION: 0.4
TARGET MACH NO.: 1.5
INTERCEPTOR LATERAL G's: 3.0
INTERCEPTOR MACH NO.: 1.5
σ OF G.C.I. ACCURACY: 5 Values
A.I. DETECTION RANGE AS FRACTION OF SPECIFICATION RANGE, S: ABSCISSA
A.I. DETECTION RANGE CONTOUR: Delta
ALTITUDE: 50 K

D16
C

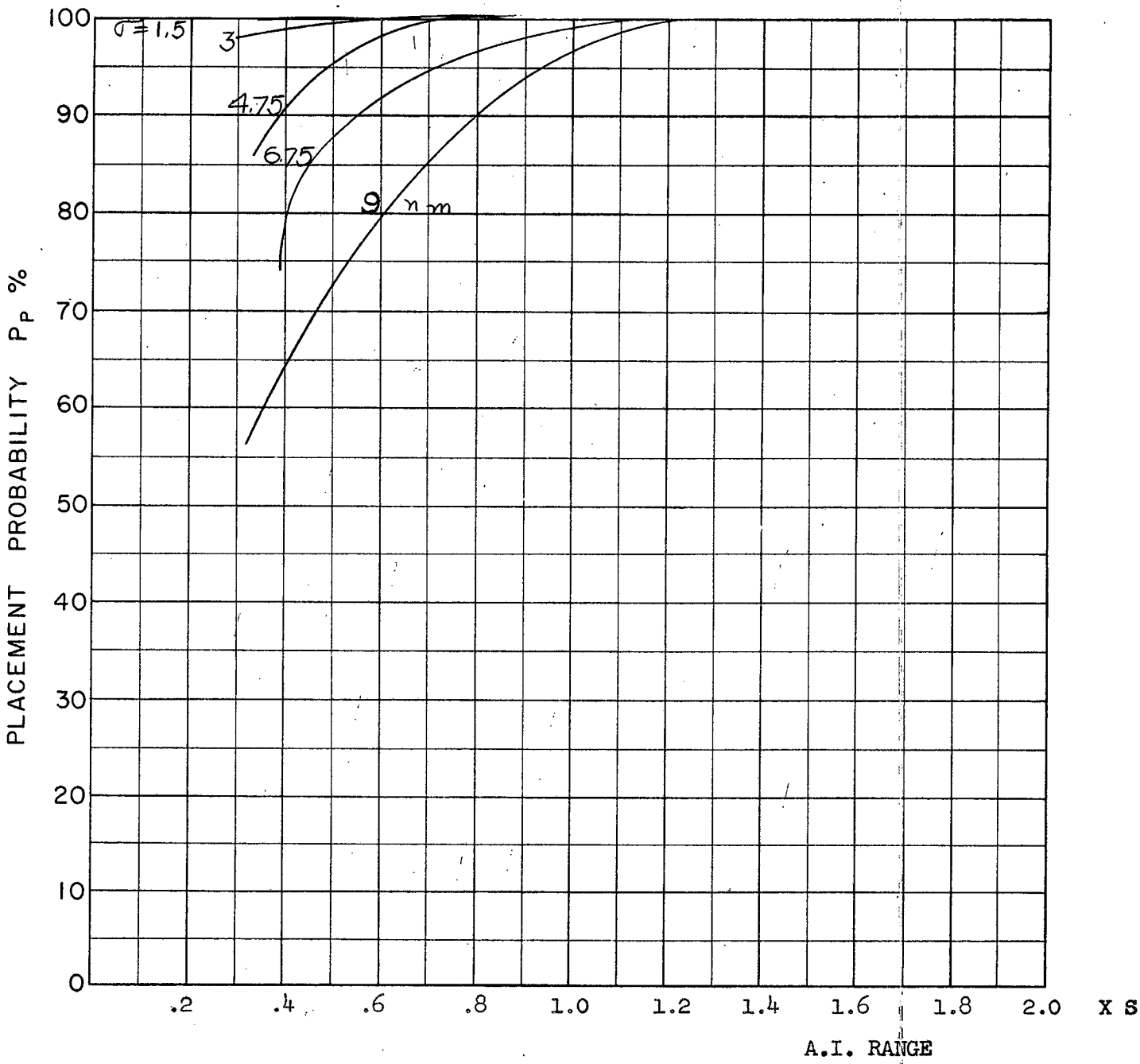

COURSE DIFFERENCE: 160°
TARGET EVASION: 0.4
TARGET MACH NO.: 2.0
INTERCEPTOR LATERAL G's: 3.0
INTERCEPTOR MACH NO.: 1.5
σ OF G.C.I. ACCURACY: 5 Values
A.I. DETECTION RANGE AS FRACTION OF SPECIFICATION RANGE, S : ABSCISSA
A.I. DETECTION RANGE CONTOUR: Delta
ALTITUDE: 50 K

D.17
C

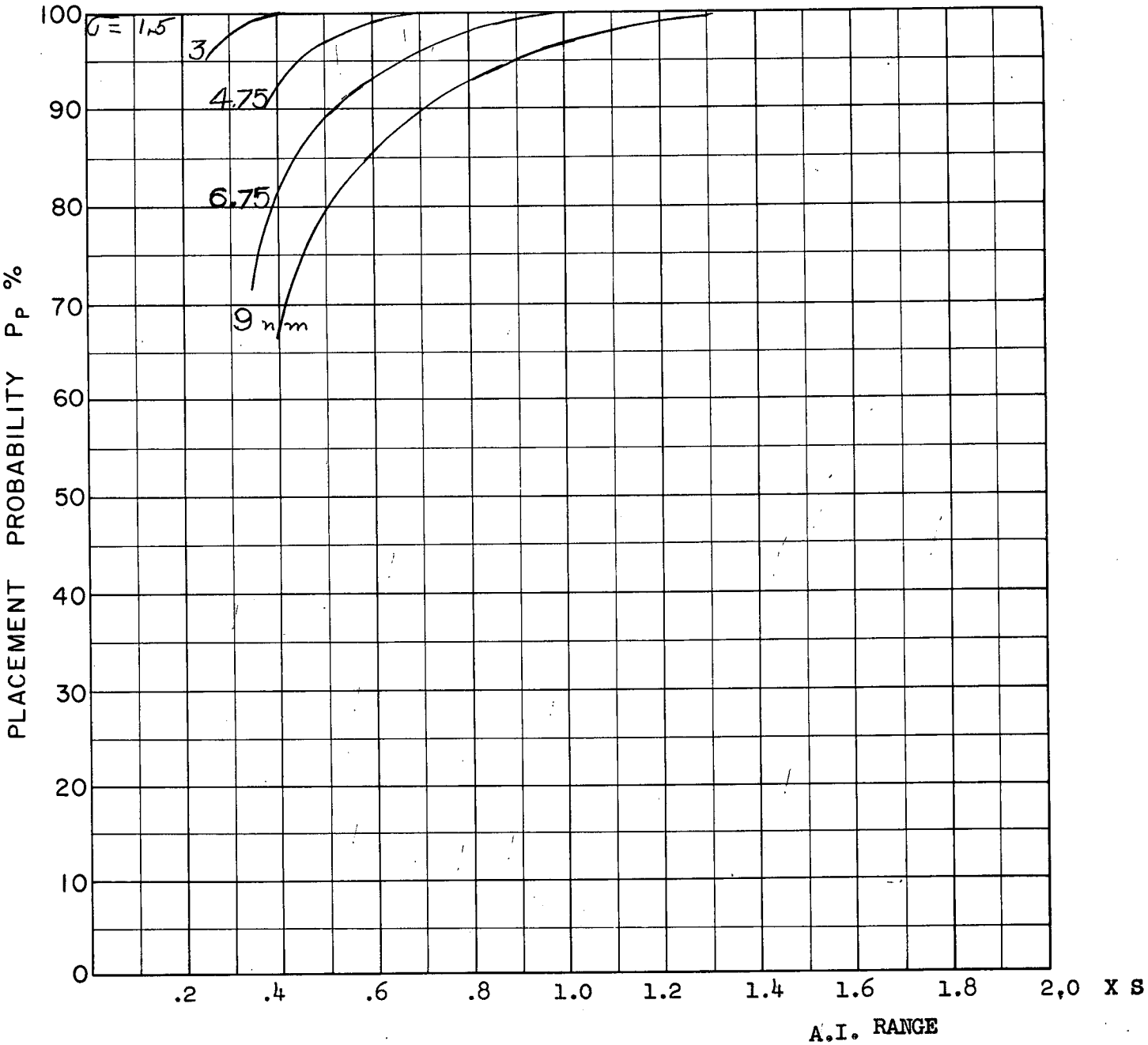

COURSE DIFFERENCE: 180°
TARGET EVASION: 0.4
TARGET MACH NO.: 1.5
INTERCEPTOR LATERAL G's: 3.0
INTERCEPTOR MACH NO.: 1.5
σ OF G.C.I. ACCURACY: 5 Values
A.I. DETECTION RANGE AS FRACTION OF SPECIFICATION RANGE, S: ABSCISSA
A.I. DETECTION RANGE CONTOUR: Delta
ALTITUDE: 50 K

D18
C

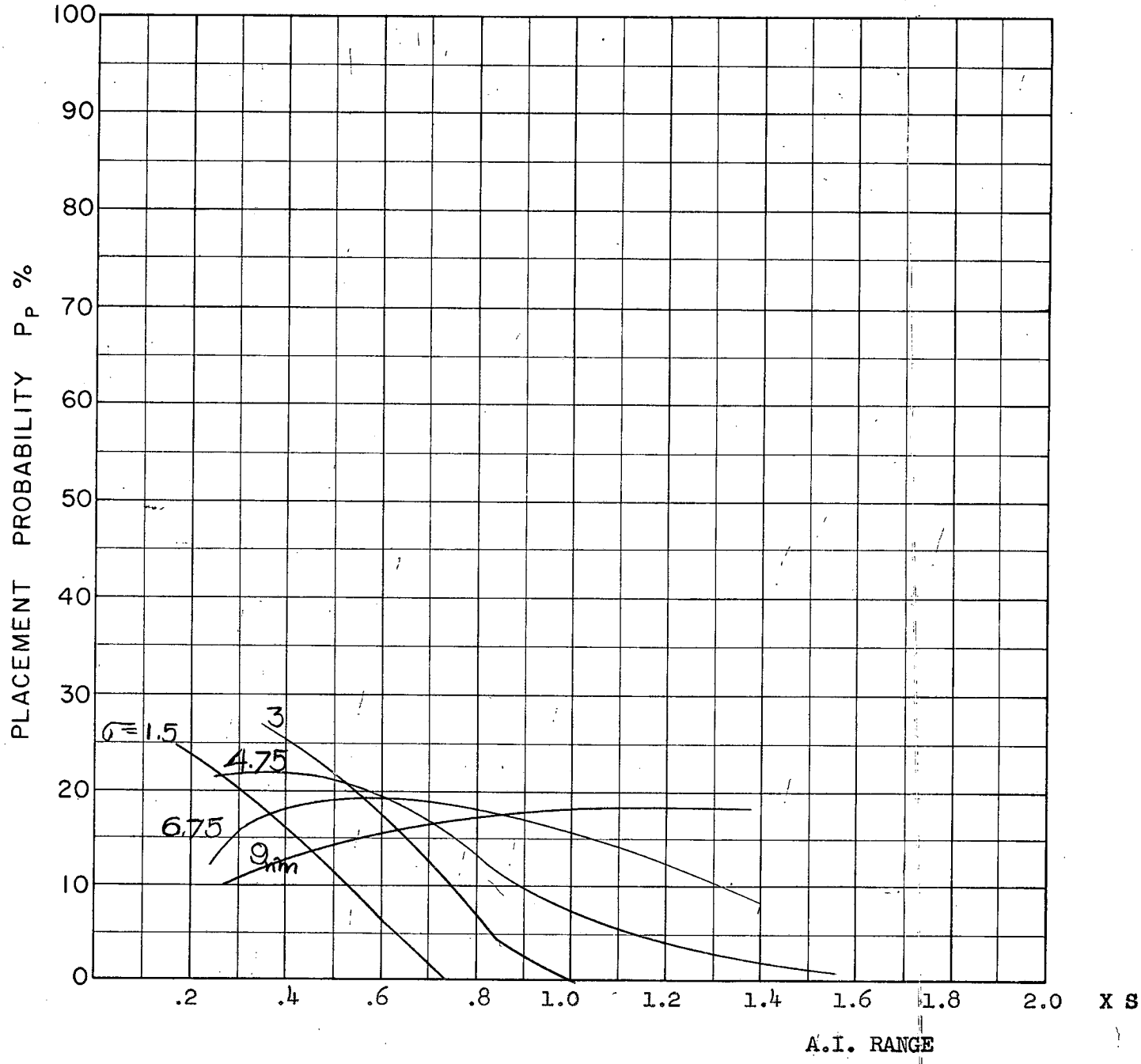

COURSE DIFFERENCE: 110°
TARGET EVASION: 0.5
TARGET MACH NO.: 2.0
INTERCEPTOR LATERAL G's: .85
INTERCEPTOR MACH NO.: 1.5
σ OF G.C.I. ACCURACY: 5 Values
A.I. DETECTION RANGE AS FRACTION OF SPECIFICATION RANGE, S: ABSCISSA
A.I. DETECTION RANGE CONTOUR: Delta
ALTITUDE: 50 K

D.19
C

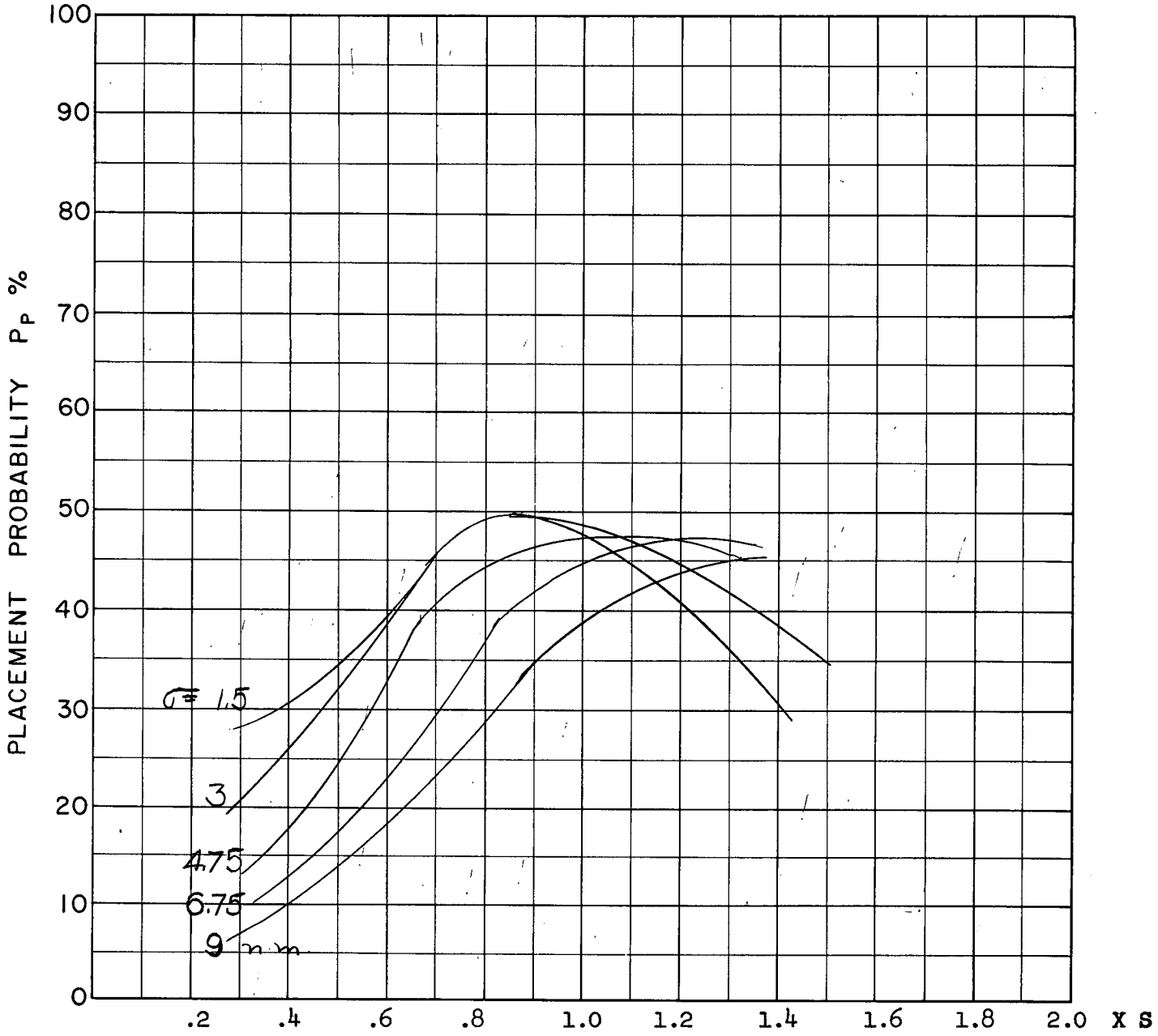

COURSE DIFFERENCE: 135°
TARGET EVASION: 0.5
TARGET MACH NO.: 2.0
INTERCEPTOR LATERAL G's: .85
INTERCEPTOR MACH NO.: 1.5
σ OF G.C.I. ACCURACY: 5 Values
A.I. DETECTION RANGE AS FRACTION OF SPECIFICATION RANGE, S: ABSCISSA
A.I. DETECTION RANGE CONTOUR: Delta
ALTITUDE: 50 K

D 2.0
C'

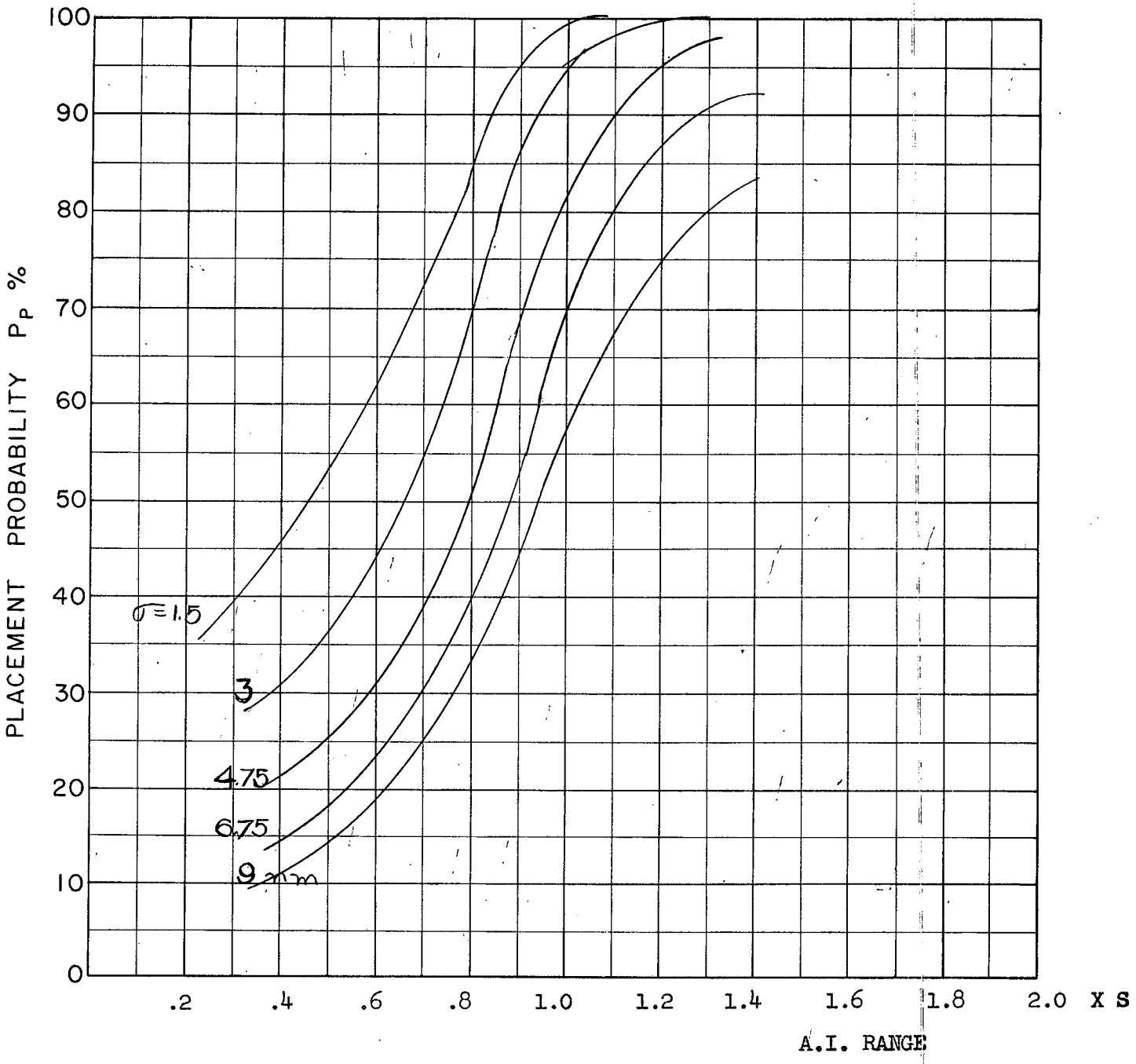

COURSE DIFFERENCE: 160°
TARGET EVASION: 0.5
TARGET MACH NO.: 2.0
INTERCEPTOR LATERAL G's: 0.85
INTERCEPTOR MACH NO.: 1.5
σ OF G.C.I. ACCURACY: 5 Values
A.I. DETECTION RANGE AS FRACTION OF SPECIFICATION RANGE, S: ABSCISSA
A.I. DETECTION RANGE CONTOUR: Delta
ALTITUDE: 50 K

D-21
C

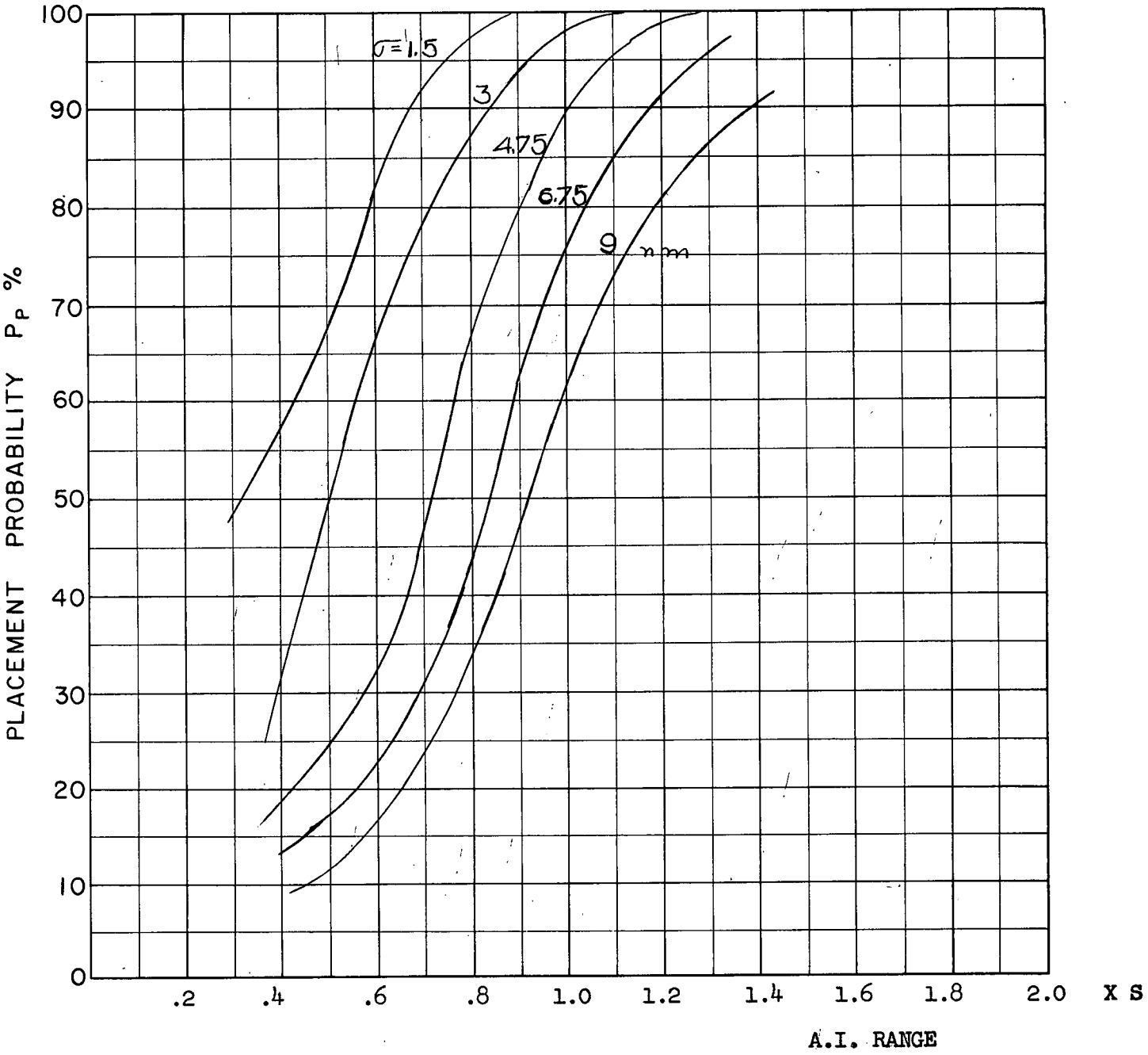

COURSE DIFFERENCE: 180°
TARGET EVASION: 0.5
TARGET MACH NO.: 2.0
INTERCEPTOR LATERAL G's: 0.85
INTERCEPTOR MACH NO.: 1.5
σ OF G.C.I. ACCURACY: 5 Values
A.I. DETECTION RANGE AS FRACTION OF SPECIFICATION RANGE, S: ABSCISSA
A.I. DETECTION RANGE CONTOUR: Delta
ALTITUDE: 50 K

D 22
C

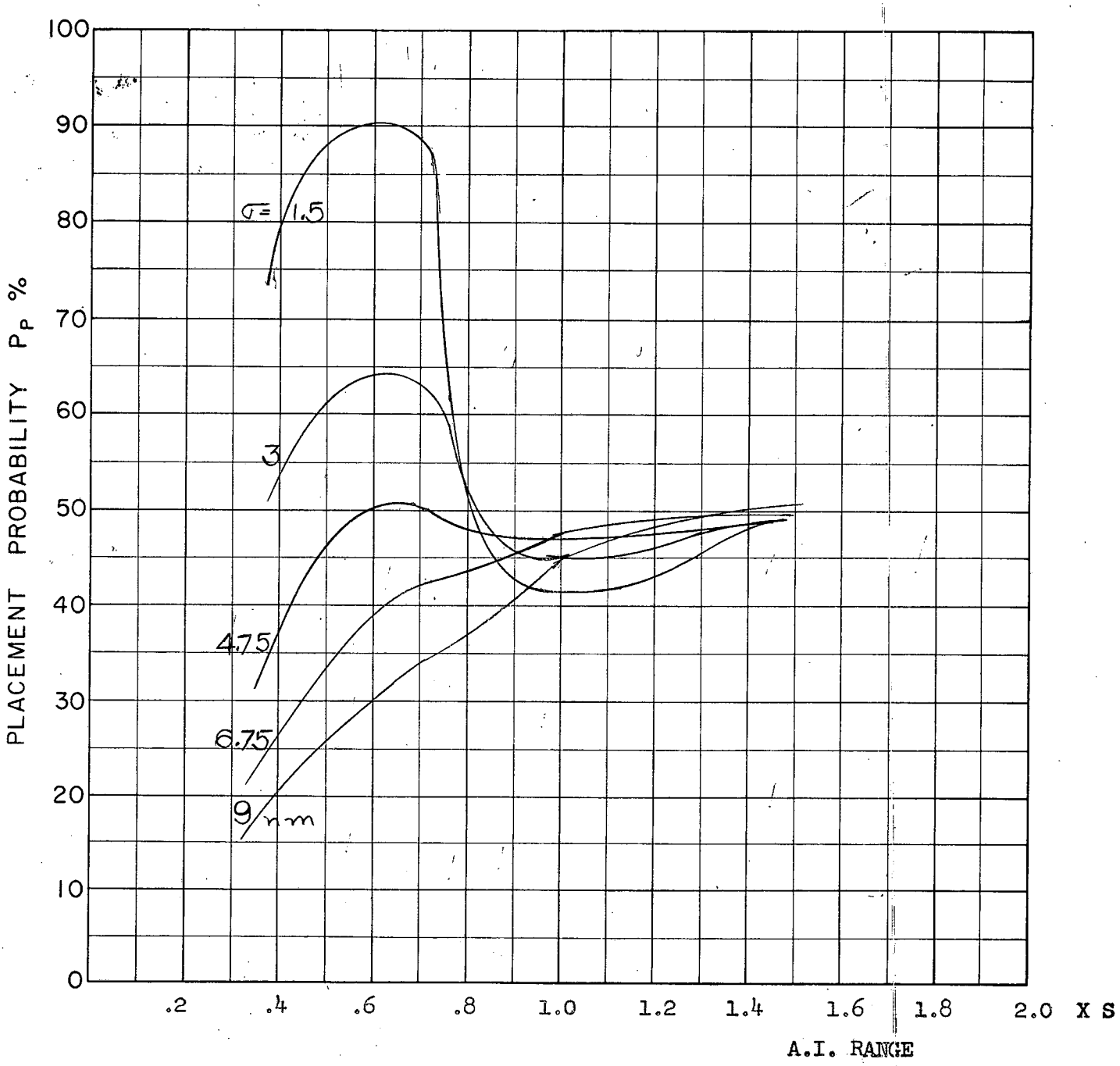

COURSE DIFFERENCE: 110°
TARGET EVASION: 0.5
TARGET MACH NO.: 2.0
INTERCEPTOR LATERAL G's: 1.6
INTERCEPTOR MACH NO.: 1.5
σ OF G.C.I. ACCURACY: 5 Values
A.I. DETECTION RANGE AS FRACTION OF SPECIFICATION RANGE, S: ABSCISSA
A.I. DETECTION RANGE CONTOUR: Delta
ALTITUDE: 50 K

D 23
C

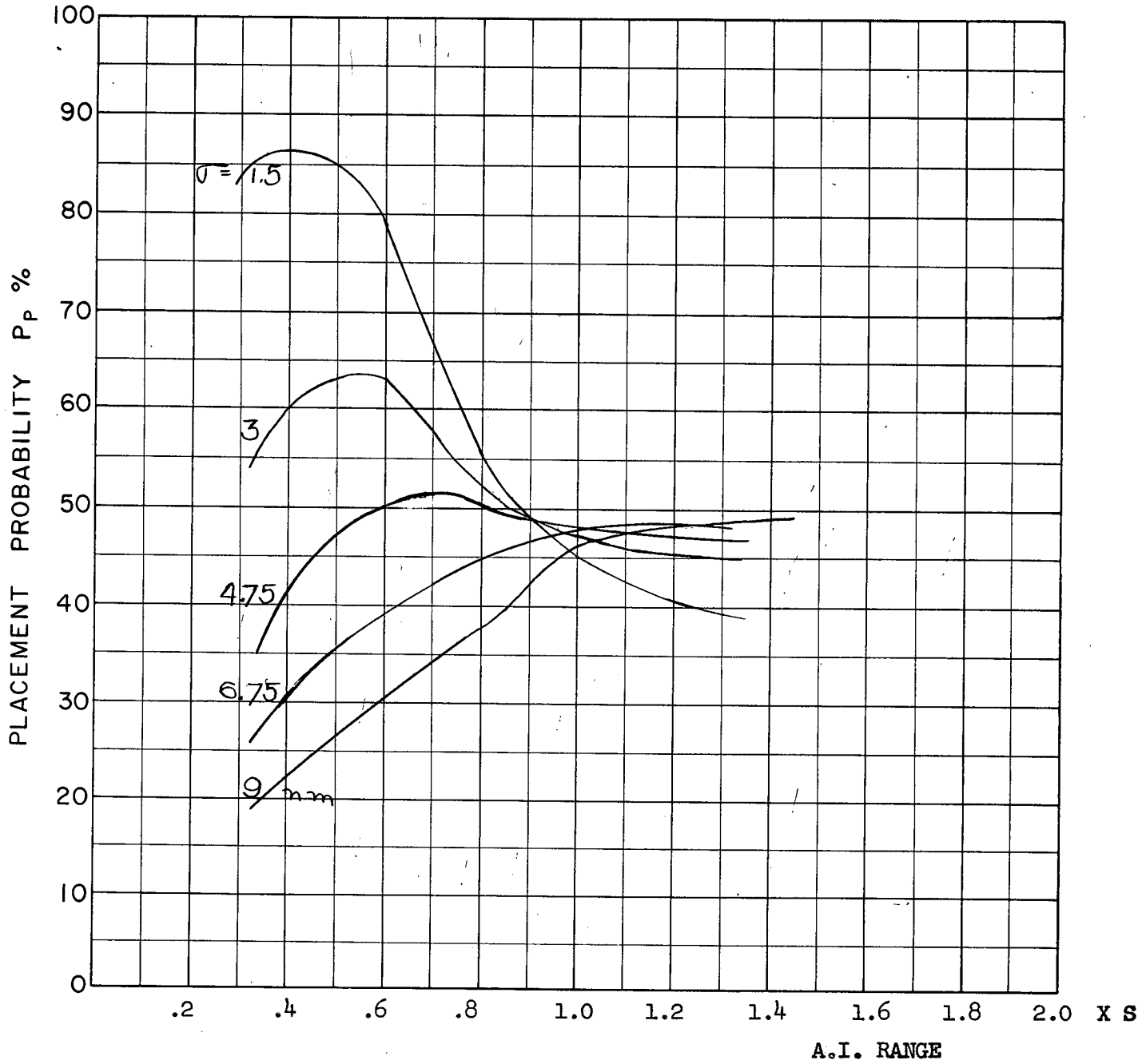

COURSE DIFFERENCE: 110°
TARGET EVASION: 0.5
TARGET MACH NO.: 2.0
INTERCEPTOR LATERAL G's: 1.6
INTERCEPTOR MACH NO.: 1.5
σ OF G.C.I. ACCURACY: 5 Values
A.I. DETECTION RANGE AS FRACTION OF SPECIFICATION RANGE, S: ABSCISSA
A.I. DETECTION RANGE CONTOUR: Delta
ALTITUDE: 50 K
LOOK ANGLE LIMIT = 75°

D24
C

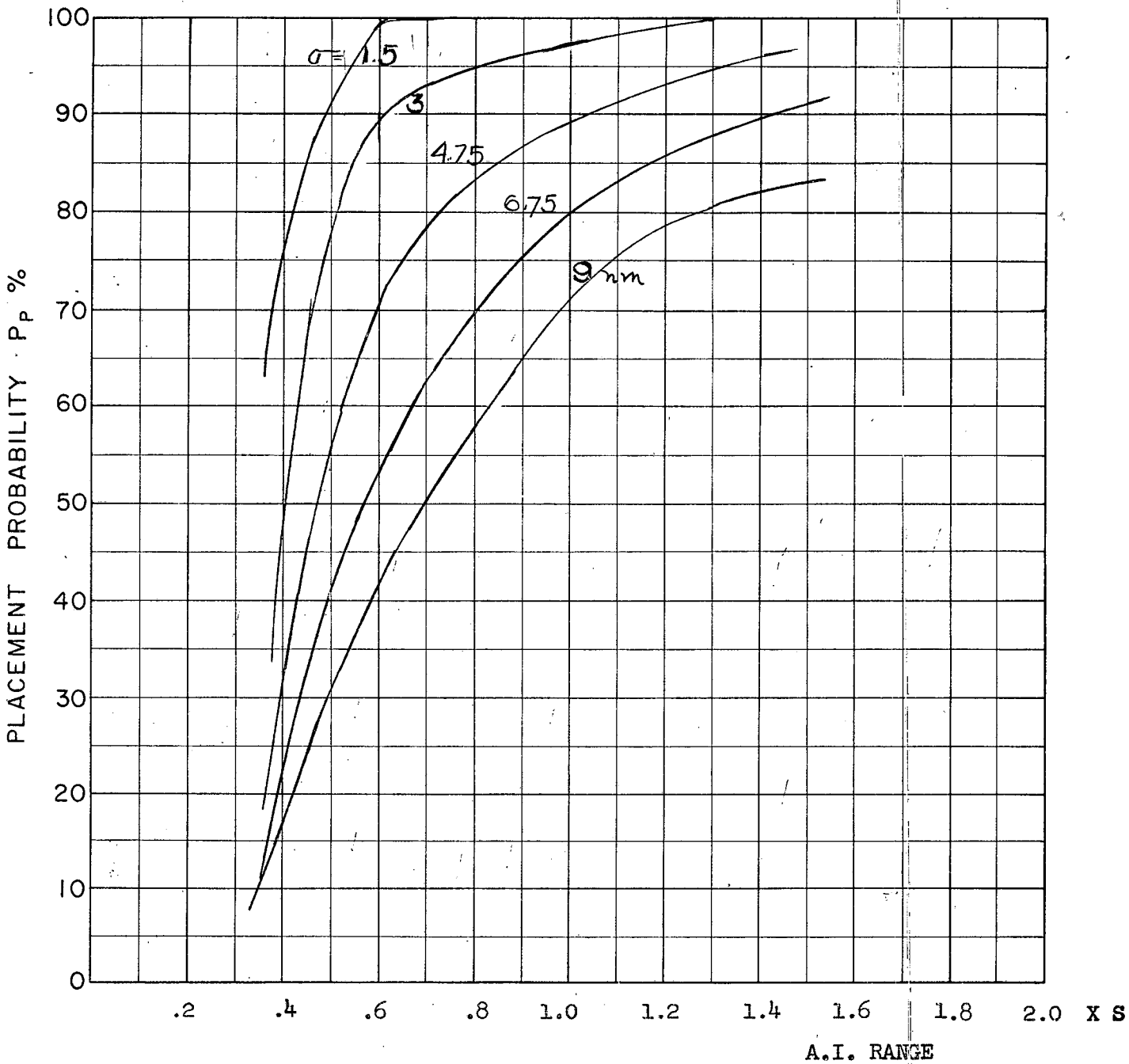

COURSE DIFFERENCE: 135°
TARGET EVASION: 0.5
TARGET MACH NO.: 2.0
INTERCEPTOR LATERAL G's: 1.6
INTERCEPTOR MACH NO.: 1.5
σ OF G.C.I. ACCURACY: 5 Values
A.I. DETECTION RANGE AS FRACTION OF SPECIFICATION RANGE, S: ABSCISSA
A.I. DETECTION RANGE CONTOUR: Delta
ALTITUDE: 50 K

D25
C

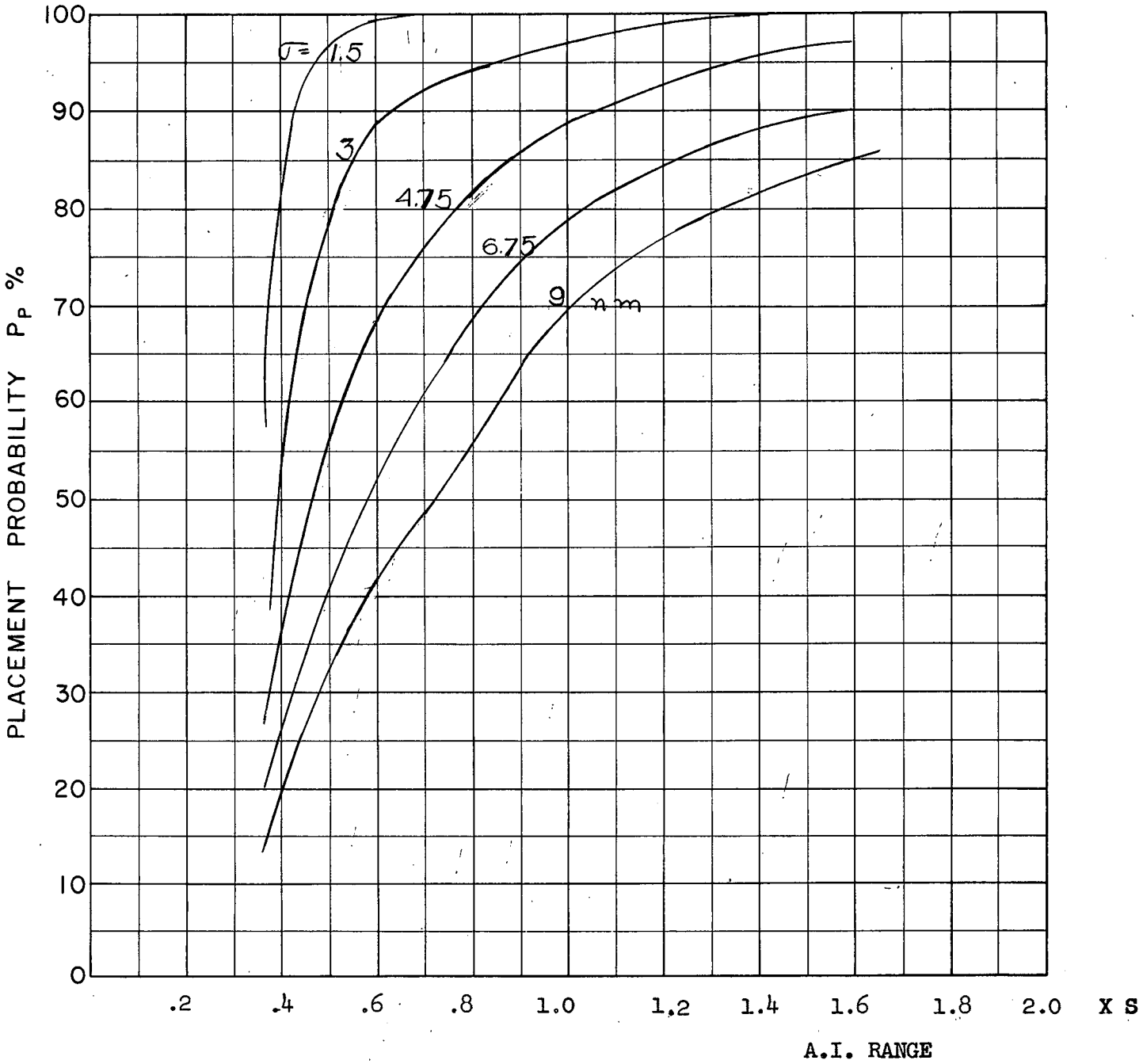

COURSE DIFFERENCE: 135°
TARGET EVASION: 0.5
TARGET MACH NO.: 2.0
INTERCEPTOR LATERAL G's: 1.6
INTERCEPTOR MACH NO.: 1.5
σ OF G.C.I. ACCURACY: 5 Values
A.I. DETECTION RANGE AS FRACTION OF SPECIFICATION RANGE, S: ABSCISSA
A.I. DETECTION RANGE CONTOUR: Delta
ALTITUDE: 50 K
Look Angle limit = 75°

D26
C

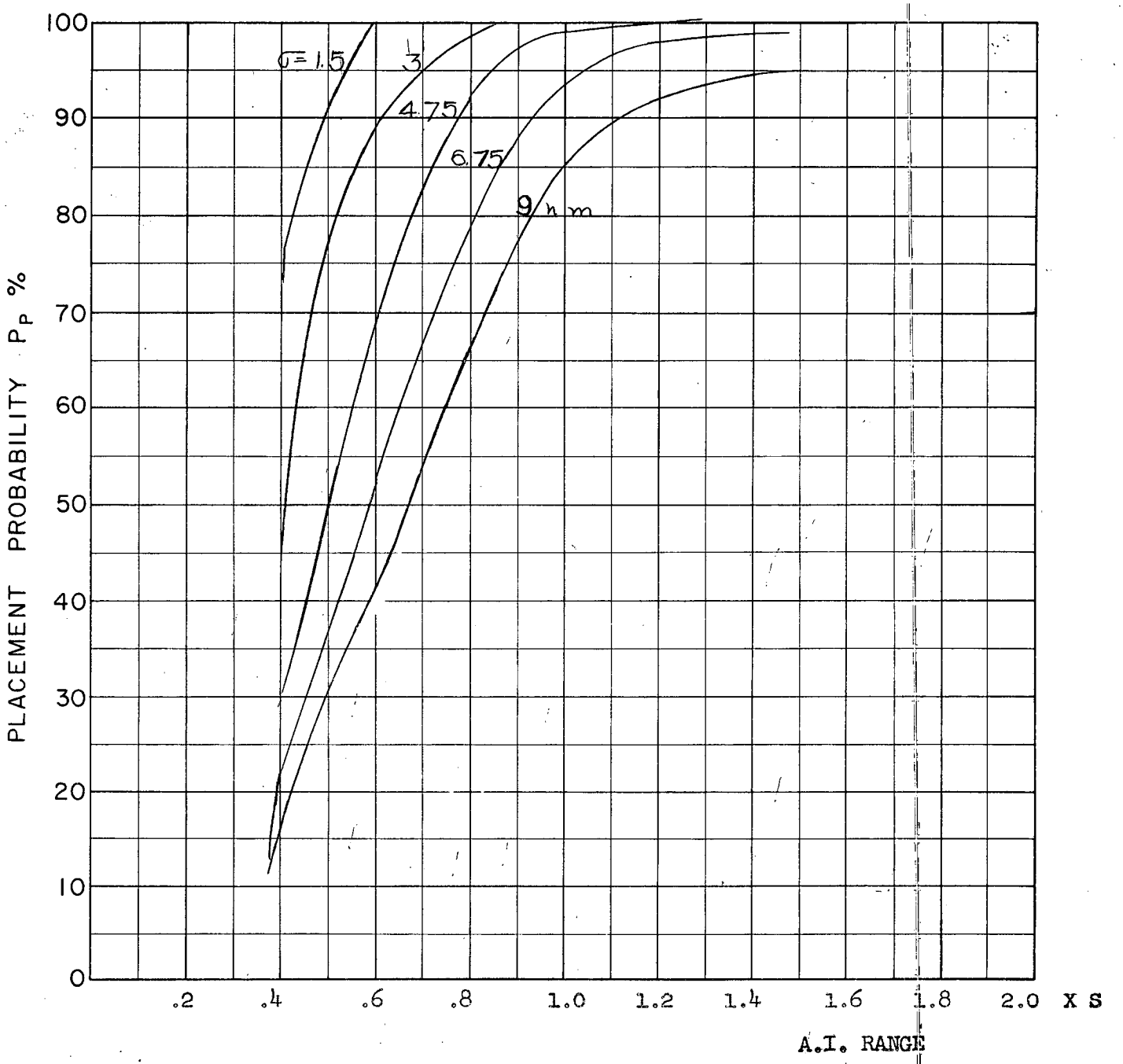

COURSE DIFFERENCE: 160°
TARGET EVASION: 0.5
TARGET MACH NO.: 2.0
INTERCEPTOR LATERAL G's: 1.6
INTERCEPTOR MACH NO.: 1.5
σ OF G.C.I. ACCURACY: 5 $V_a$lues
A.I. DETECTION RANGE AS FRACTION OF SPECIFICATION RANGE, S: ABSCISSA
A.I. DETECTION RANGE CONTOUR: Delta
ALTITUDE: 50 K

D27
C

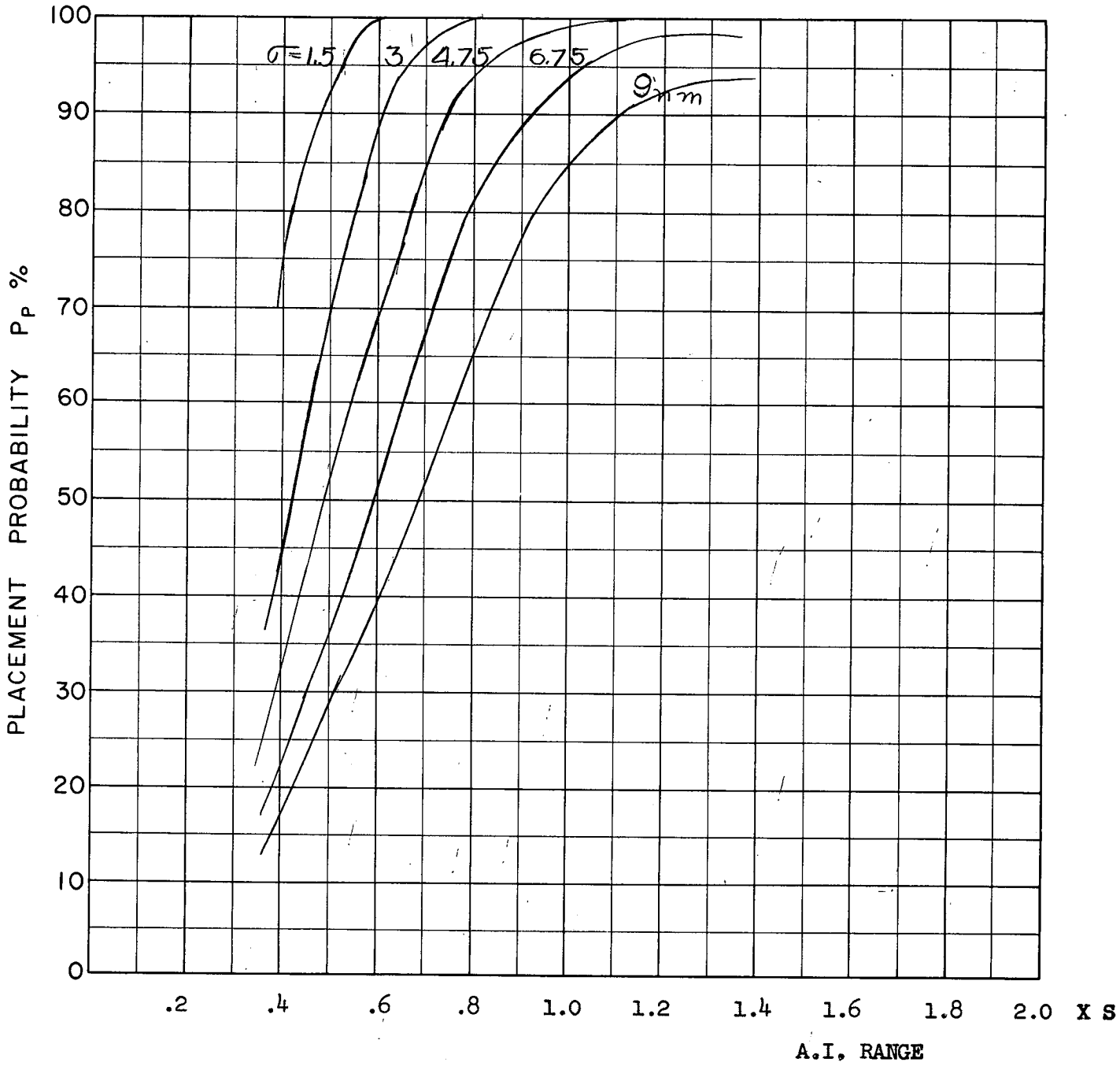

COURSE DIFFERENCE: 160°
TARGET EVASION: 0.5
TARGET MACH NO.: 2.0
INTERCEPTOR LATERAL G's: 1.6
INTERCEPTOR MACH NO.: 1.5
σ OF G.C.I. ACCURACY: 5 Values
A.I. DETECTION RANGE AS FRACTION OF SPECIFICATION RANGE, S: ABSCISSA
A.I. DETECTION RANGE CONTOUR: Delta
ALTITUDE: 50 K
LOOK ANGLE LIMIT = 75°

D28
C

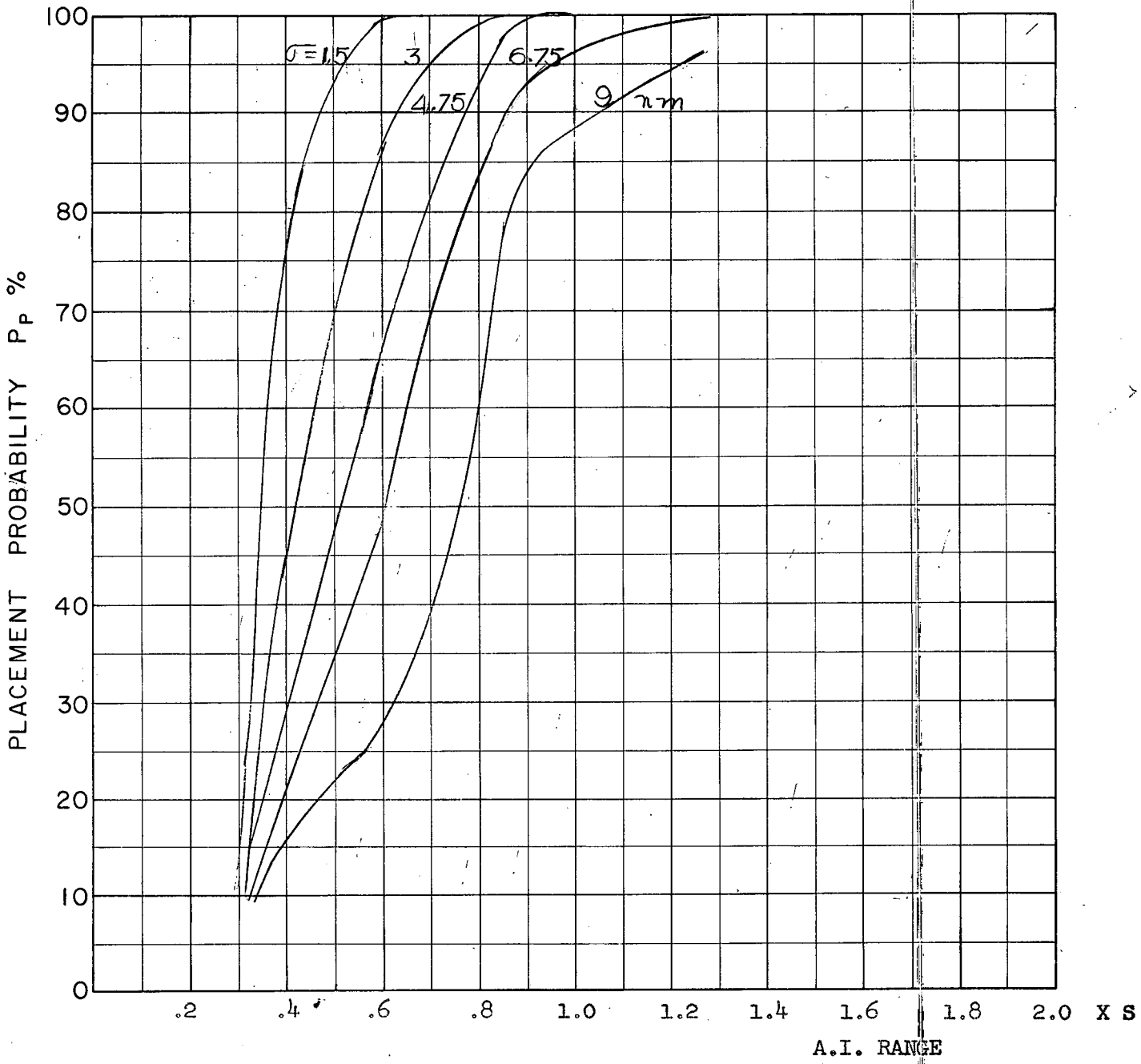

COURSE DIFFERENCE: 180°
TARGET EVASION: 0.5
TARGET MACH NO.: 2.0
INTERCEPTOR LATERAL G's: 1.6
INTERCEPTOR MACH NO.: 1.5
σ OF G.C.I. ACCURACY: 5 Values
A.I. DETECTION RANGE AS FRACTION OF SPECIFICATION RANGE, S: ABSCISSA
A.I. DETECTION RANGE CONTOUR: Delta
ALTITUDE: 50 K

D29
C

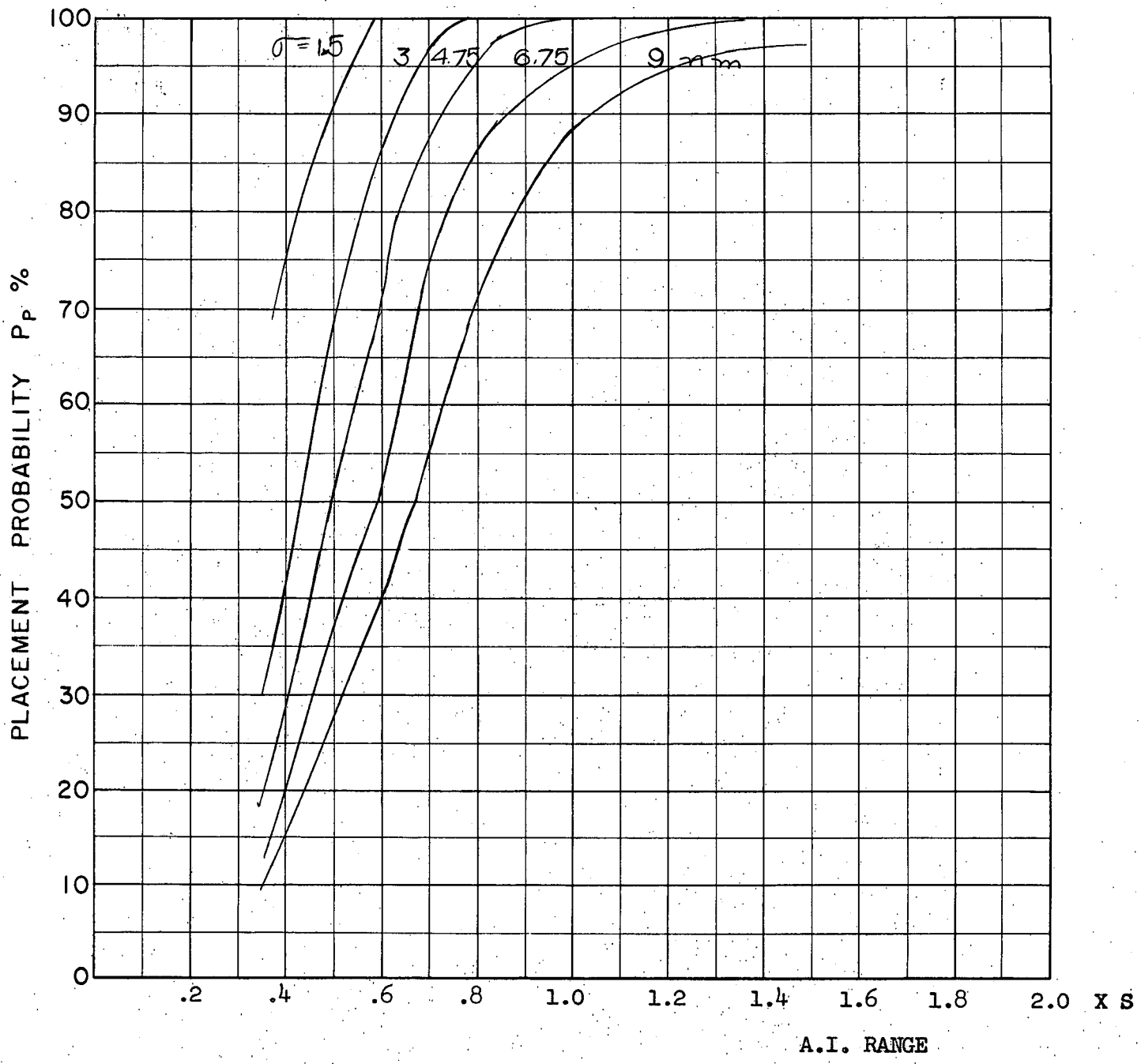

COURSE DIFFERENCE: 180°
TARGET EVASION: 0.5
TARGET MACH NO.: 2.0
INTERCEPTOR LATERAL G's: 1.6
INTERCEPTOR MACH NO.: 1.5
σ OF G.C.I. ACCURACY: 5 Values
A.I. DETECTION RANGE AS FRACTION OF SPECIFICATION RANGE, S: ABSCISSA
A.I. DETECTION RANGE CONTOUR: Delta
ALTITUDE: 50 K
LOOK ANGLE LIMIT = 75°

D 30
C

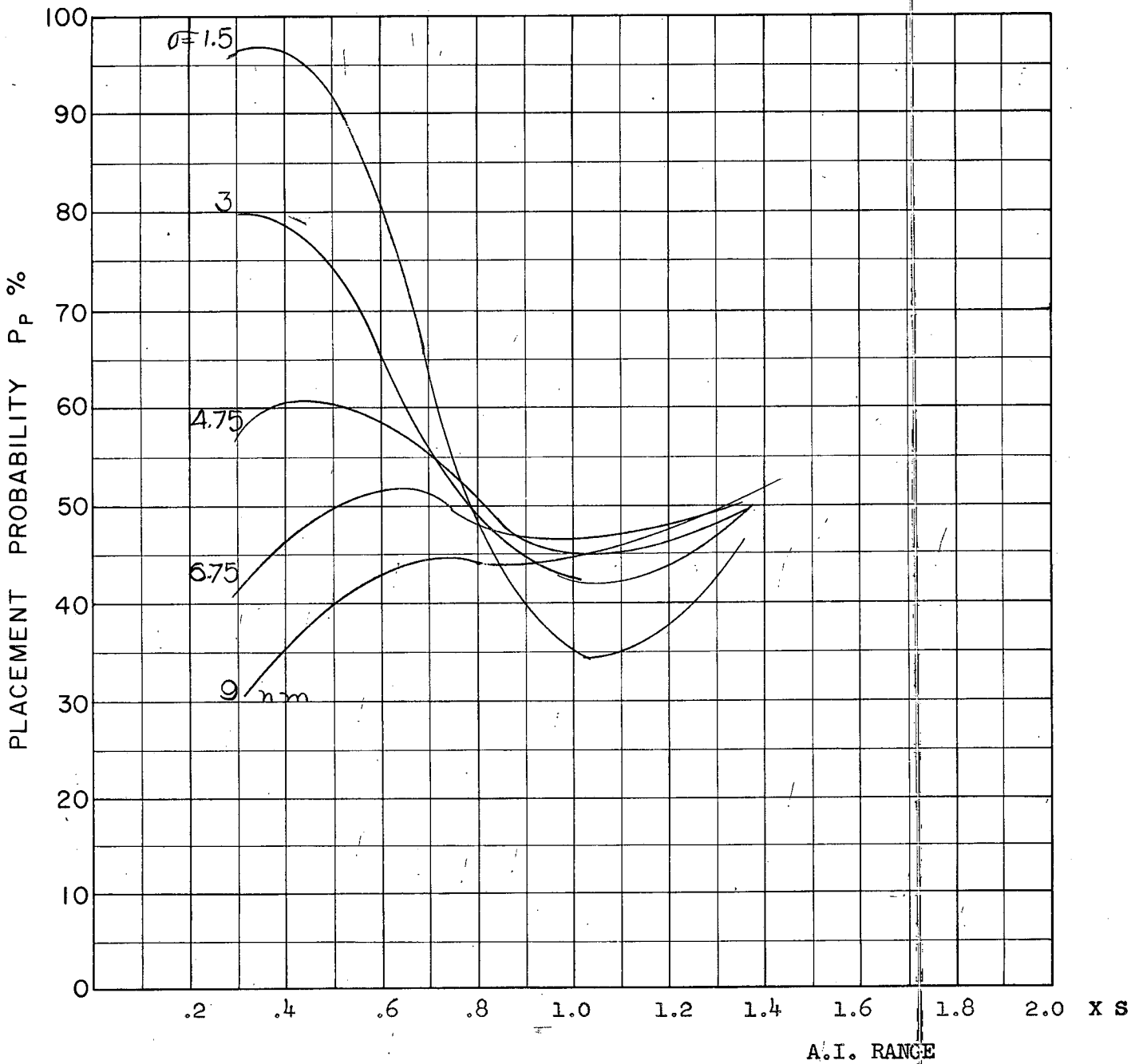

COURSE DIFFERENCE: 110°
TARGET EVASION: 0.5
TARGET MACH NO.: 2.0
INTERCEPTOR LATERAL G's: 3.0
INTERCEPTOR MACH NO.: 1.5
σ OF G.C.I. ACCURACY: 5 Values
A.I. DETECTION RANGE AS FRACTION OF SPECIFICATION RANGE, S: ABSCISSA
A.I. DETECTION RANGE CONTOUR: Delta
ALTITUDE: 50 K

D31
c

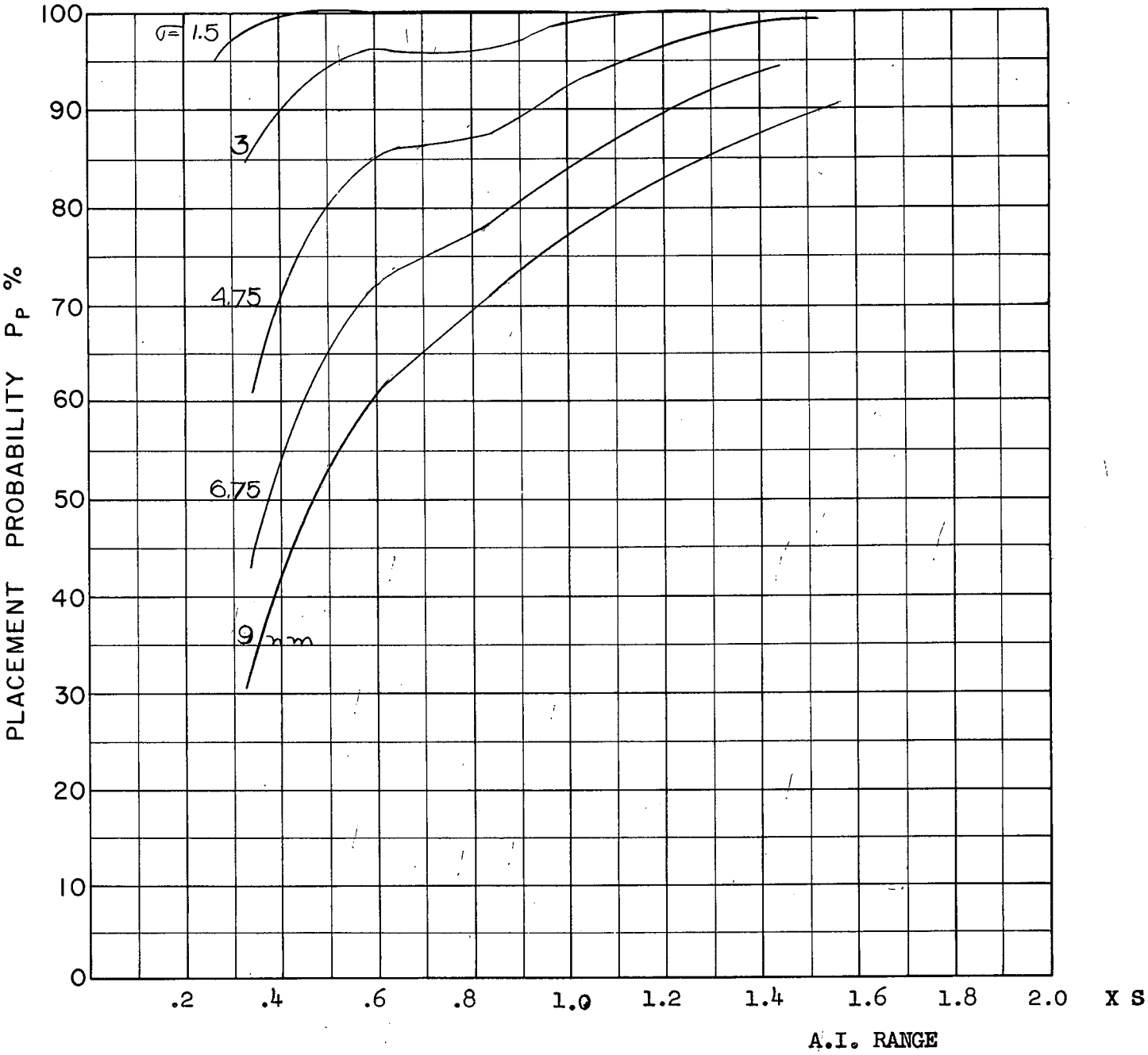

COURSE DIFFERENCE: 135°
TARGET EVASION: 0.5
TARGET MACH NO.: 2.0
INTERCEPTOR LATERAL G's: 3.0
INTERCEPTOR MACH NO.: 1.5
σ OF G.C.I. ACCURACY: 5 Values
A.I. DETECTION RANGE AS FRACTION OF SPECIFICATION RANGE, S : ABSCISSA
A.I. DETECTION RANGE CONTOUR : Delta
ALTITUDE : 50 K

D32
c

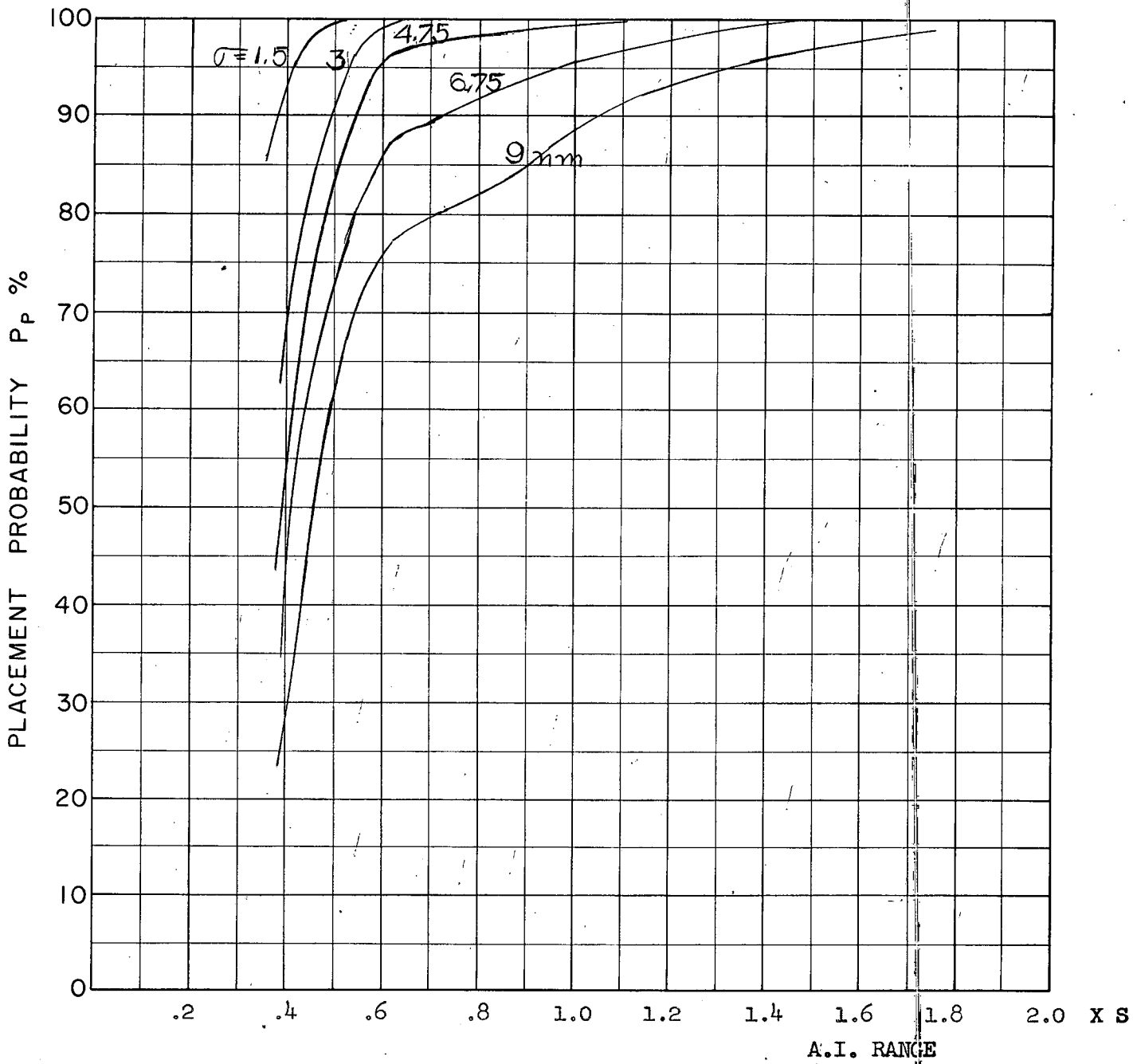

COURSE DIFFERENCE: 160°
TARGET EVASION: 0.5
TARGET MACH NO.: 2.0
INTERCEPTOR LATERAL G's: 3.0
INTERCEPTOR MACH NO.: 2.0
σ OF G.C.I. ACCURACY: 5 Values
A.I. DETECTION RANGE AS FRACTION OF SPECIFICATION RANGE, S: ABSCISSA
A.I. DETECTION RANGE CONTOUR: Delta
ALTITUDE: 50 K

D33

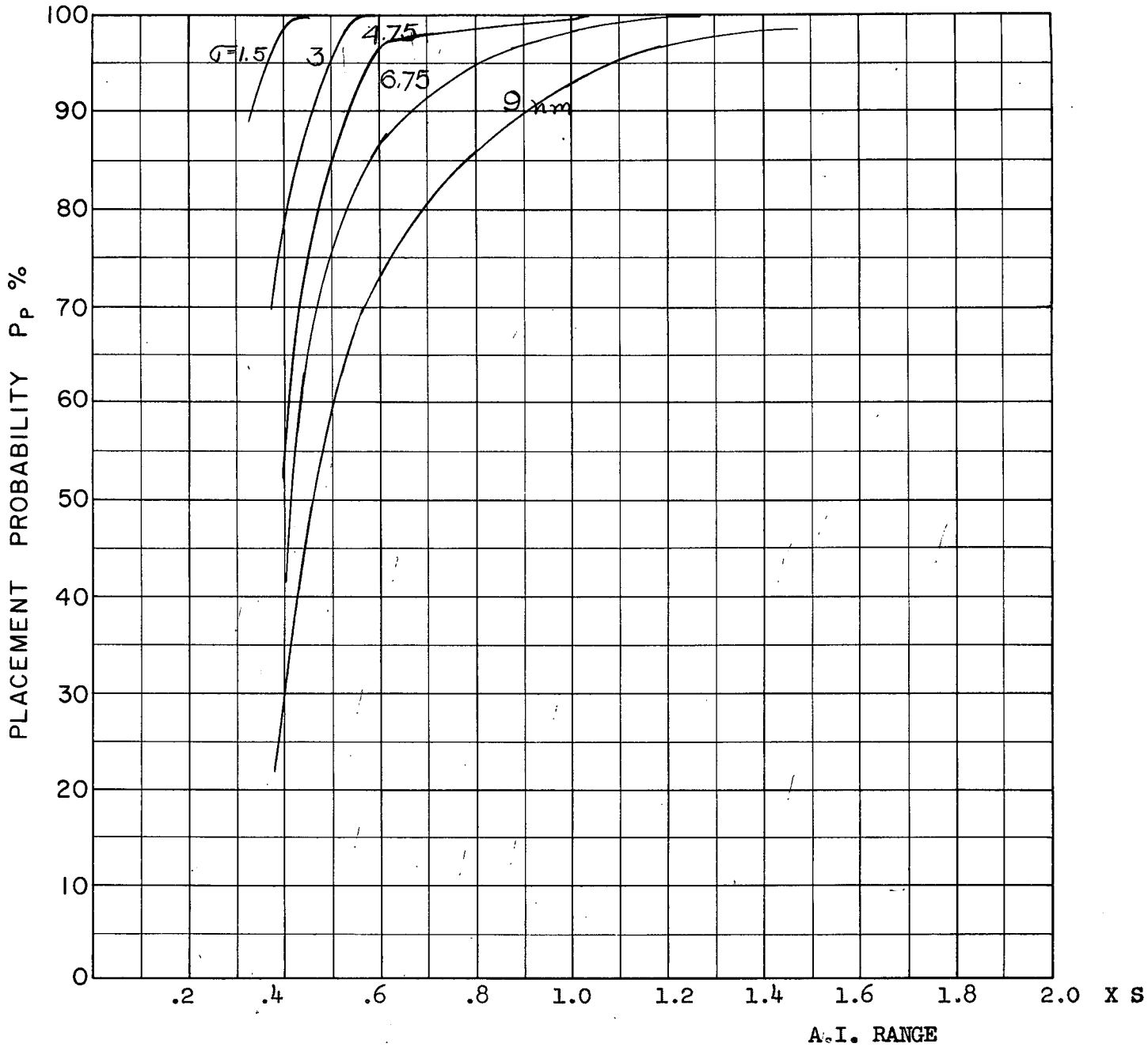

COURSE DIFFERENCE: 180°
TARGET EVASION: 0.5
TARGET MACH NO.: 2.0
INTERCEPTOR LATERAL G's: 3.0
INTERCEPTOR MACH NO.: 1.5
σ OF G.C.I. ACCURACY: 5 Values
A.I. DETECTION RANGE AS FRACTION OF SPECIFICATION RANGE, S: ABSCISSA
A.I. DETECTION RANGE CONTOUR: Delta
ALTITUDE: 50 K

D34
C

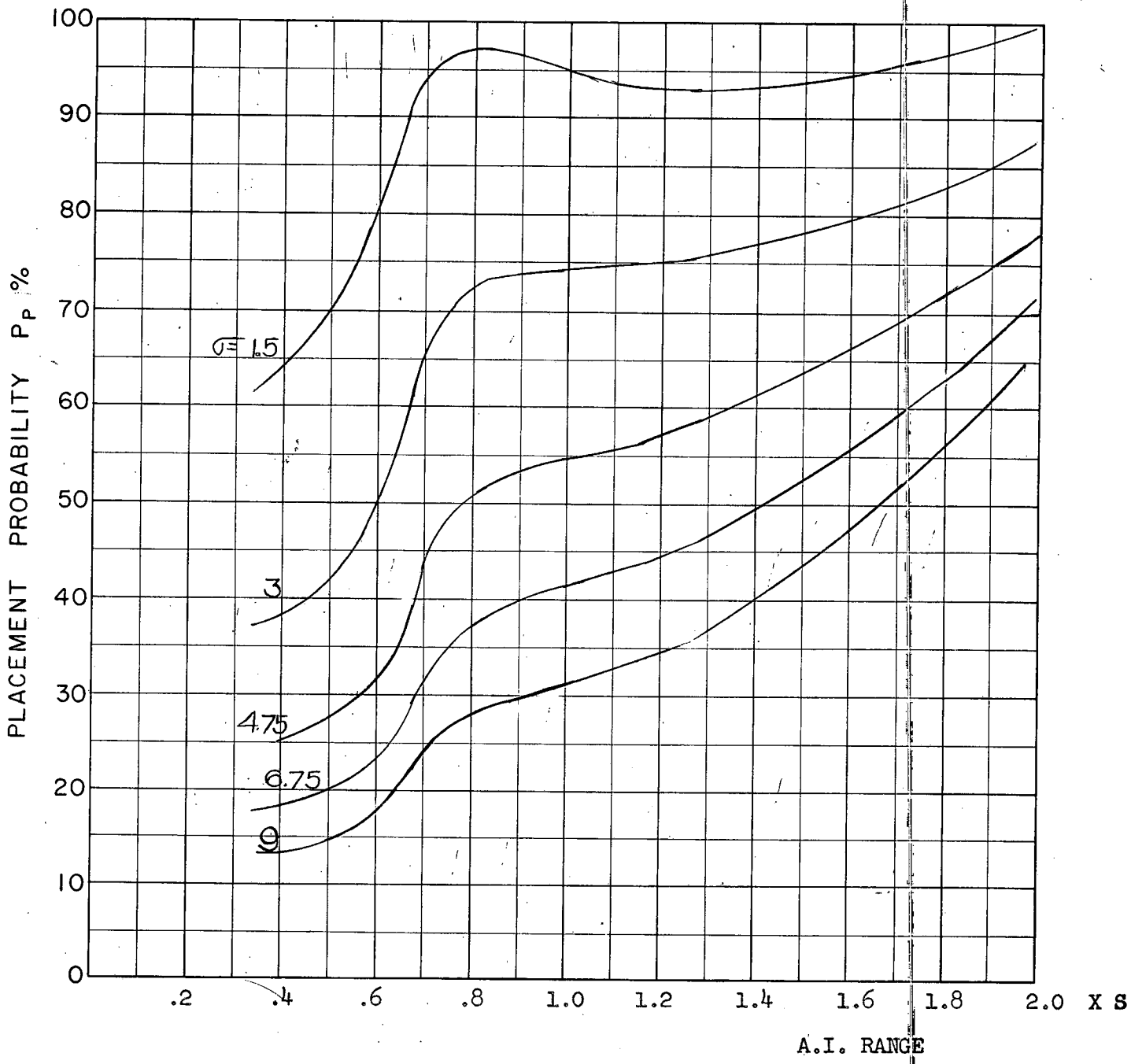

COURSE DIFFERENCE: 110°
TARGET EVASION: 0.4
TARGET MACH NO.: 1.5
INTERCEPTOR LATERAL G's: 0.85
INTERCEPTOR MACH NO.: 1.5
σ OF G.C.I. ACCURACY: 5 Values
A.I. DETECTION RANGE AS FRACTION OF SPECIFICATION RANGE, S: ABSCISSA
A.I. DETECTION RANGE CONTOUR: Straight
ALTITUDE: 50 K

S-3
C

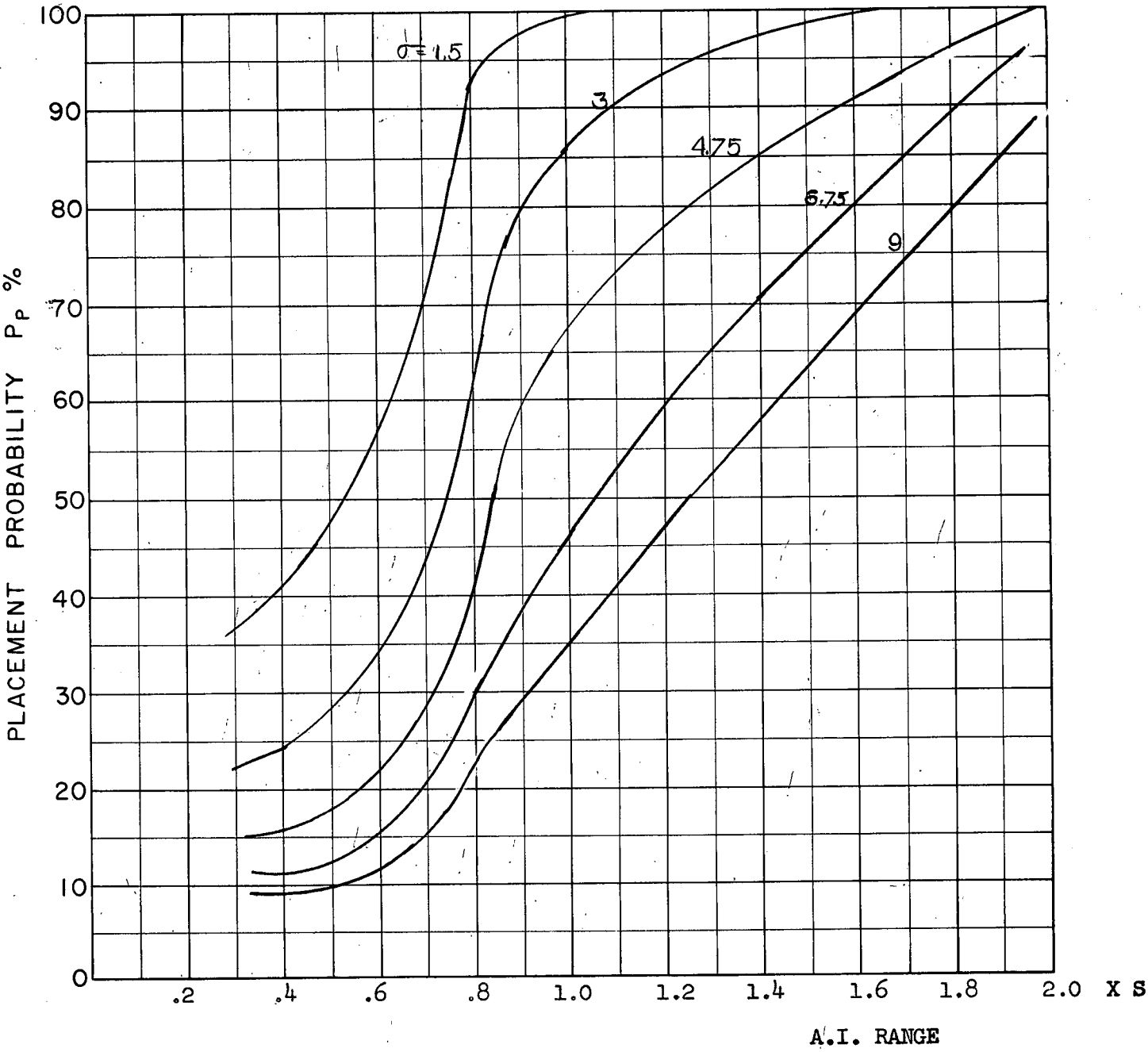

COURSE DIFFERENCE: 135°
TARGET EVASION: 0.4
TARGET MACH NO.: 1.5
INTERCEPTOR LATERAL G's: 0.85
INTERCEPTOR MACH NO.: 1.5
σ OF G.C.I. ACCURACY: 5 Values
A.I. DETECTION RANGE AS FRACTION OF SPECIFICATION RANGE, S: ABSCISSA
A.I. DETECTION RANGE CONTOUR: Straight
ALTITUDE: 50 K

S 4 c

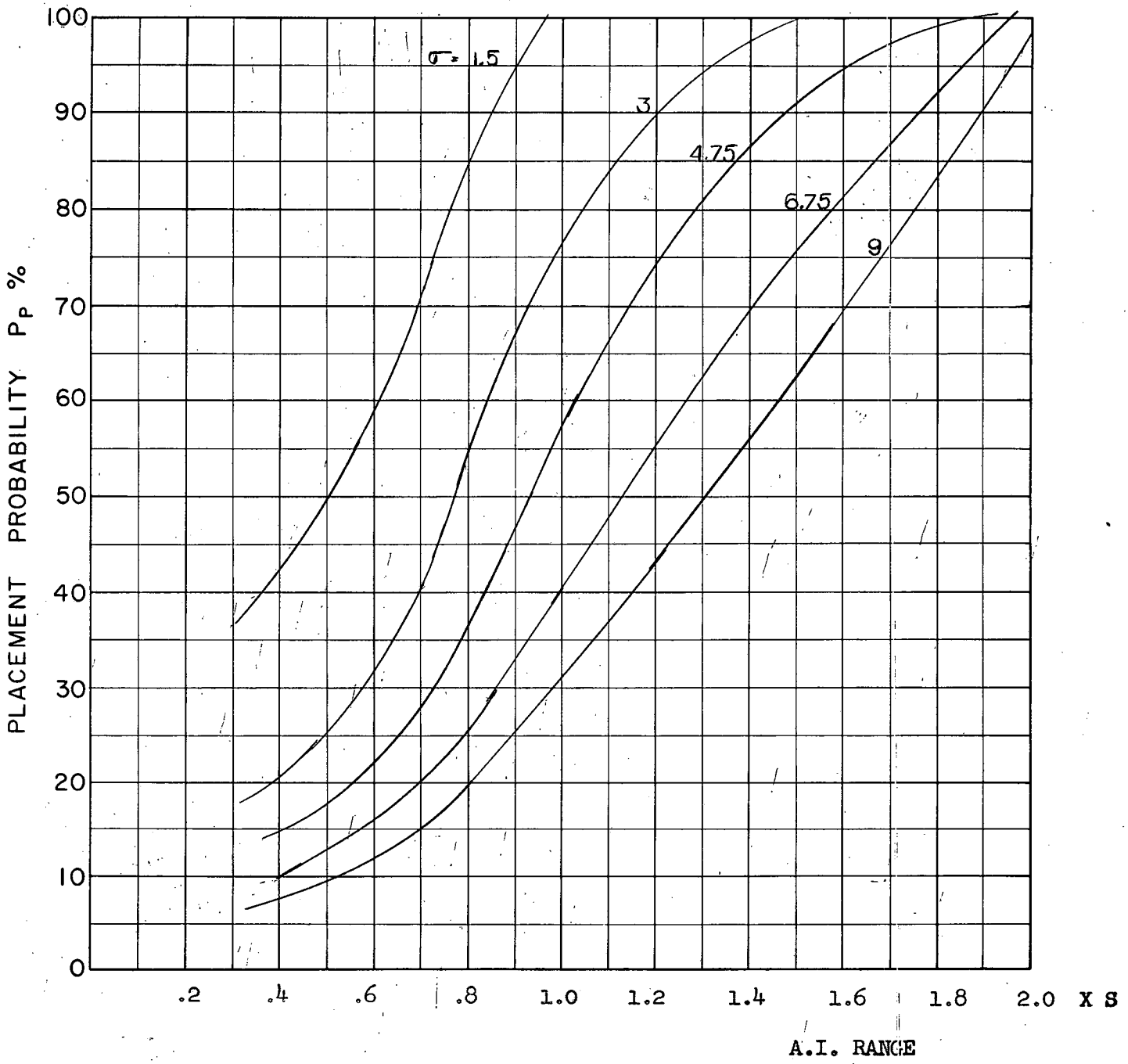

COURSE DIFFERENCE: 160°
TARGET EVASION: 0.4
TARGET MACH NO.: 1.5
INTERCEPTOR LATERAL G's: 0.85
INTERCEPTOR MACH NO.: 1.5
σ OF G.C.I. ACCURACY: 5 Values
A.I. DETECTION RANGE AS FRACTION OF SPECIFICATION RANGE, S ABSCISSA
A.I. DETECTION RANGE CONTOUR: Straight
ALTITUDE: 50 K

S-5
C

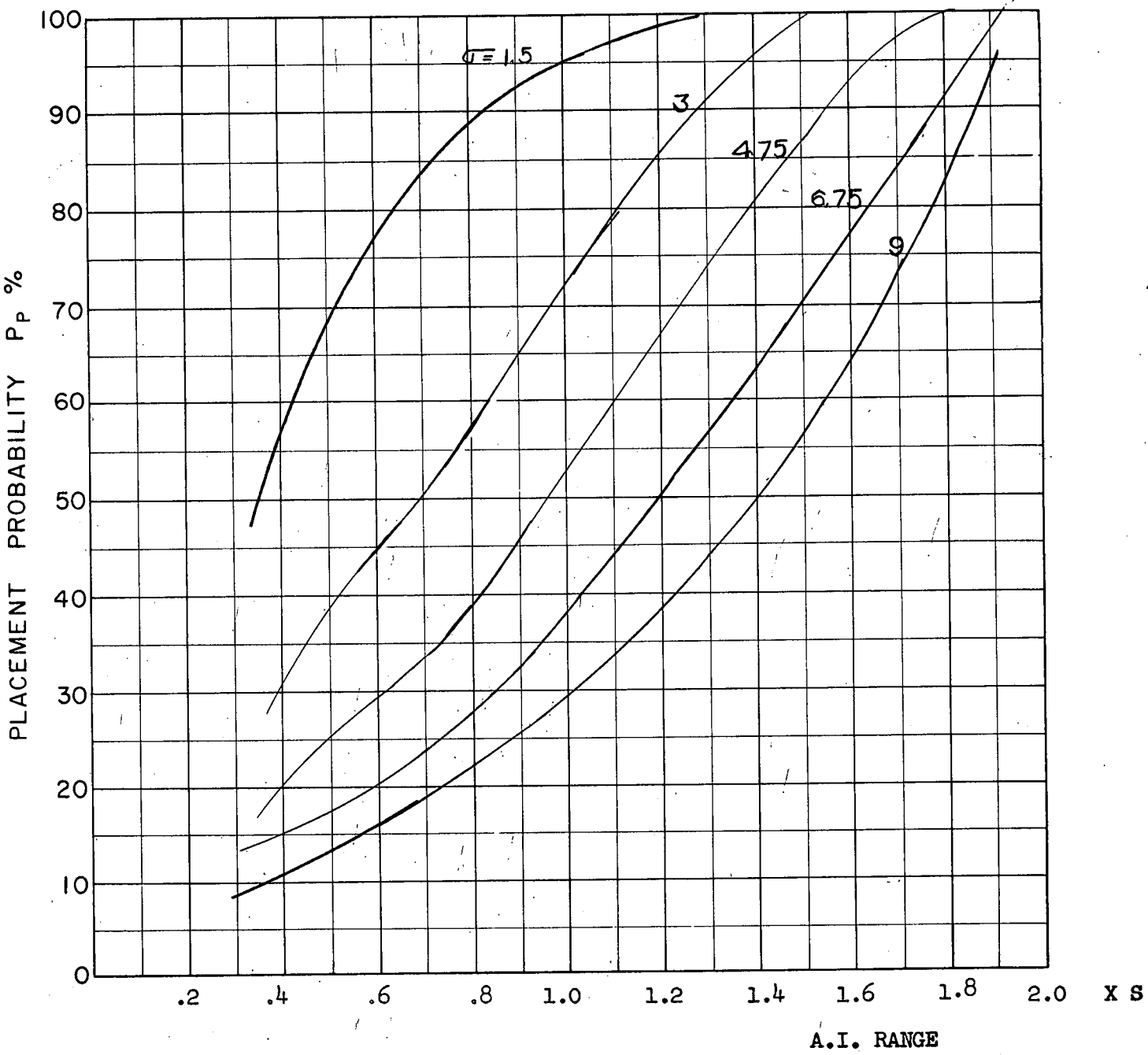

COURSE DIFFERENCE: 180°
TARGET EVASION: 0.4
TARGET MACH NO.: 1.5
INTERCEPTOR LATERAL G's: 0.85
INTERCEPTOR MACH NO.: 1.5
σ OF G.C.I. ACCURACY: 5 Values
A.I. DETECTION RANGE AS FRACTION OF SPECIFICATION RANGE, S: ABSCISSA
A.I. DETECTION RANGE CONTOUR: Straight
ALTITUDE: 50 K

S-6
C

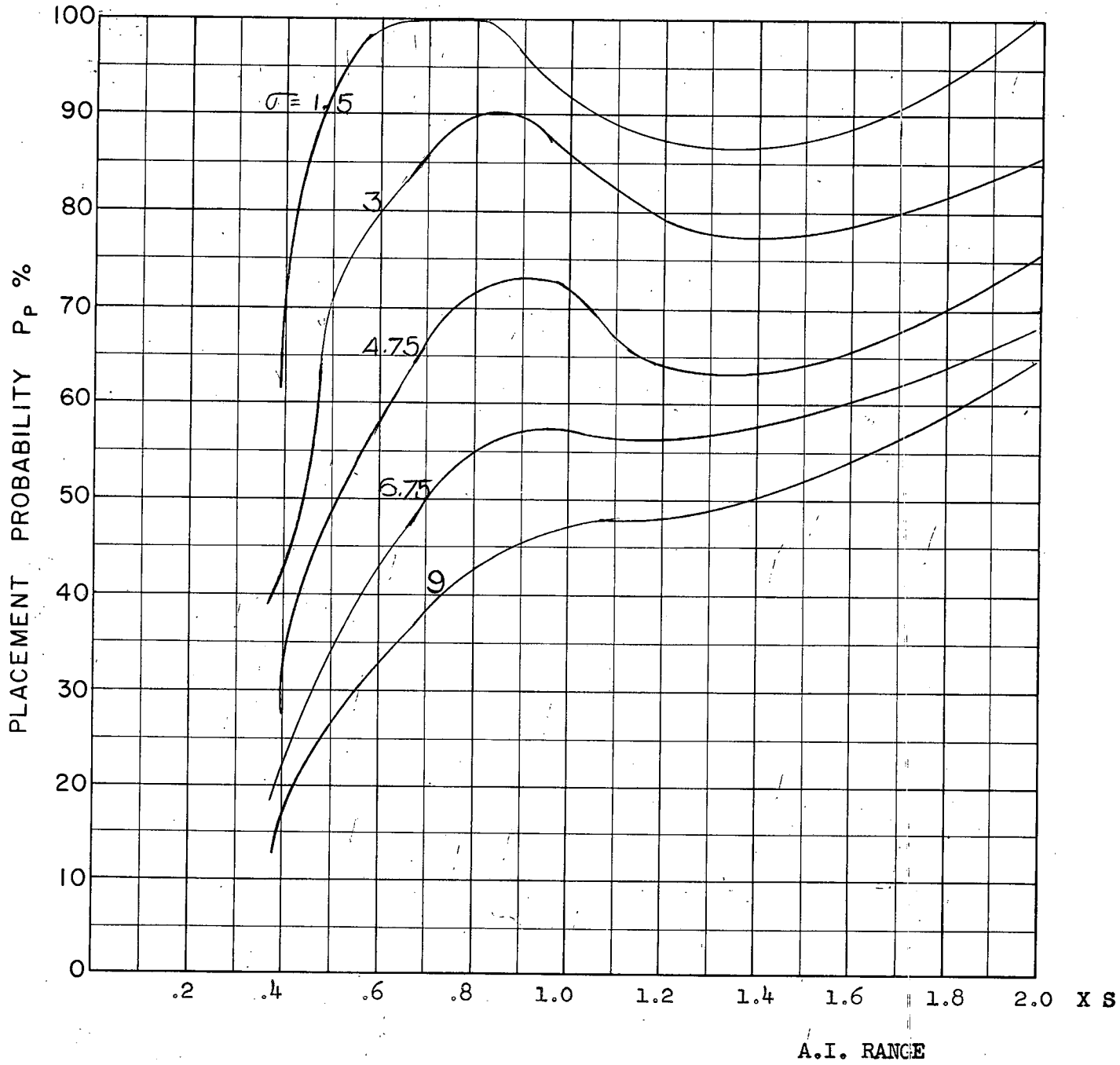

COURSE DIFFERENCE: 110°
TARGET EVASION: 0.4
TARGET MACH NO.: 1.5
INTERCEPTOR LATERAL G's: 1.6
INTERCEPTOR MACH NO.: 1.5
σ OF G.C.I. ACCURACY: 5 Values
A.I. DETECTION RANGE AS FRACTION OF SPECIFICATION RANGE, S: ABSCISSA
A.I. DETECTION RANGE CONTOUR: Straight
ALTITUDE: 50 K

S.7 C

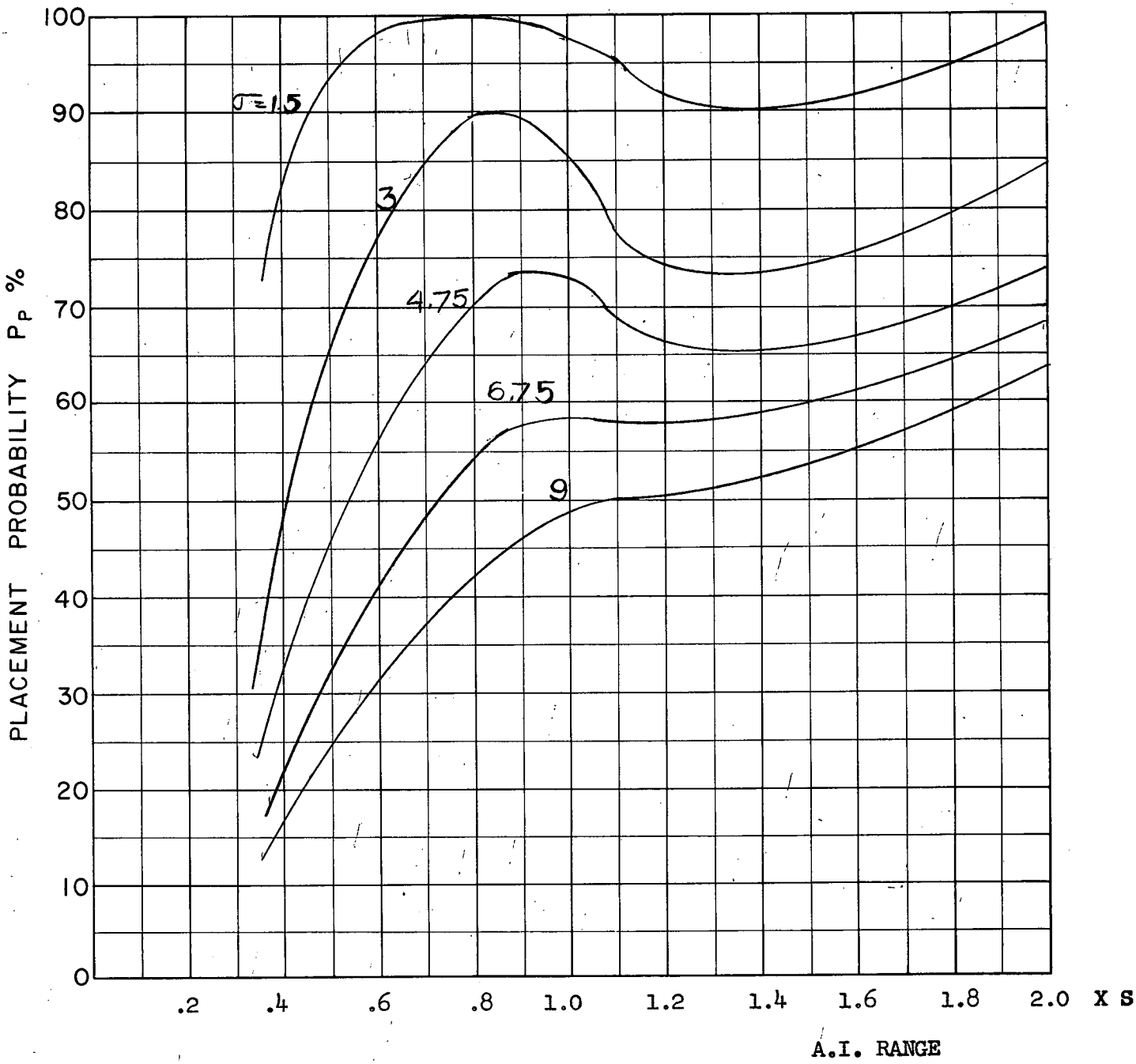

COURSE DIFFERENCE: 110°
TARGET EVASION: .4
TARGET MACH NO.: 1.5
INTERCEPTOR LATERAL G's: 1.6
INTERCEPTOR MACH NO.: 1.5
σ OF G.C.I. ACCURACY: 5 Values
A.I. DETECTION RANGE AS FRACTION OF SPECIFICATION RANGE, S: ABSCISSA
A.I. DETECTION RANGE CONTOUR: Straight
ALTITUDE: 50 K
LOOK ANGLE LIMIT = 75°

58 C

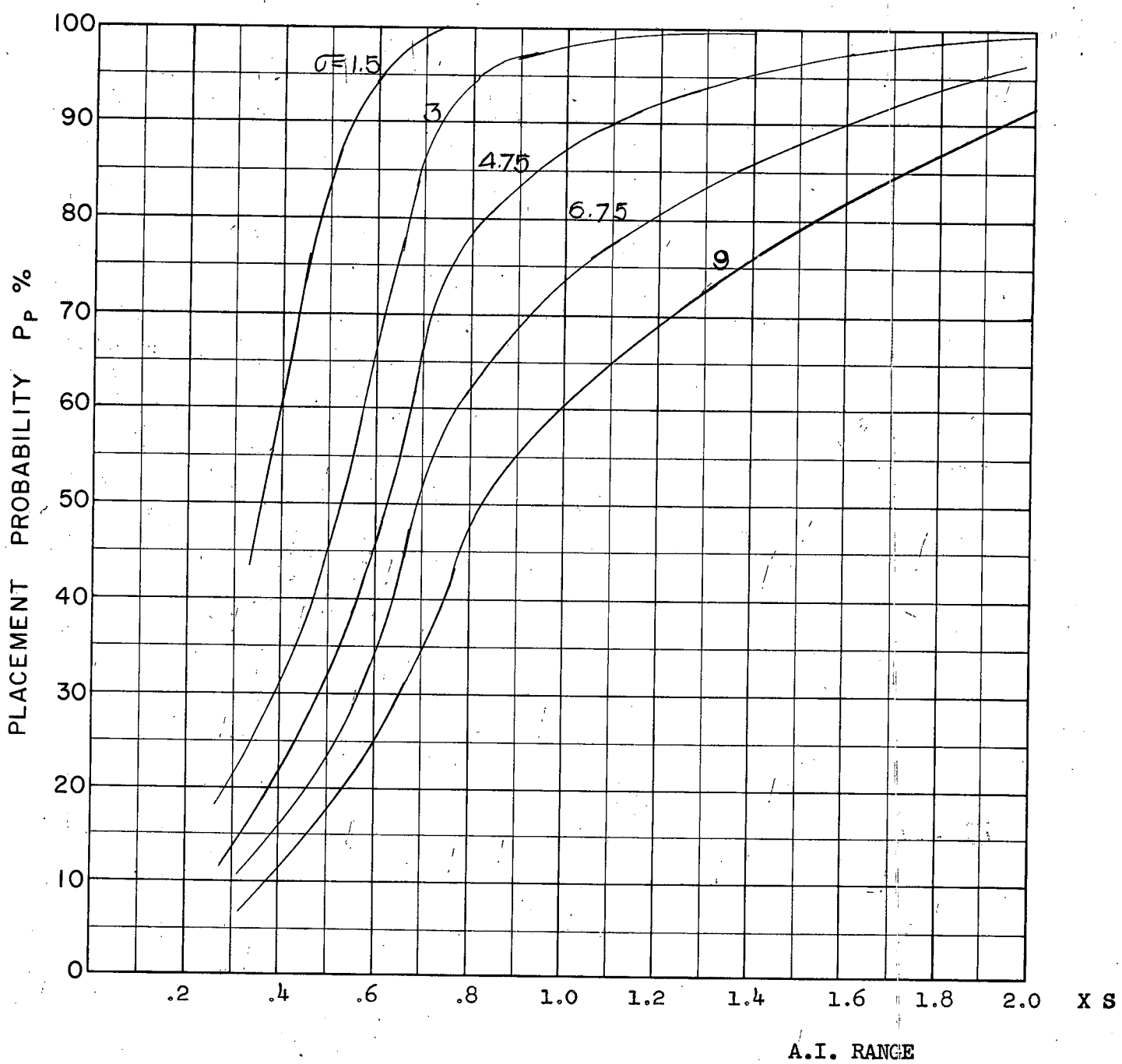

COURSE DIFFERENCE: 135°
TARGET EVASION: 0.4
TARGET MACH NO.: 1.5
INTERCEPTOR LATERAL G's: 1.6
INTERCEPTOR MACH NO.: 1.5
σ OF G.C.I. ACCURACY: 5 Values
A.I. DETECTION RANGE AS FRACTION OF SPECIFICATION RANGE, S: ABSCISSA
A.I. DETECTION RANGE CONTOUR: Straight
ALTITUDE: 50 K

S-9 C

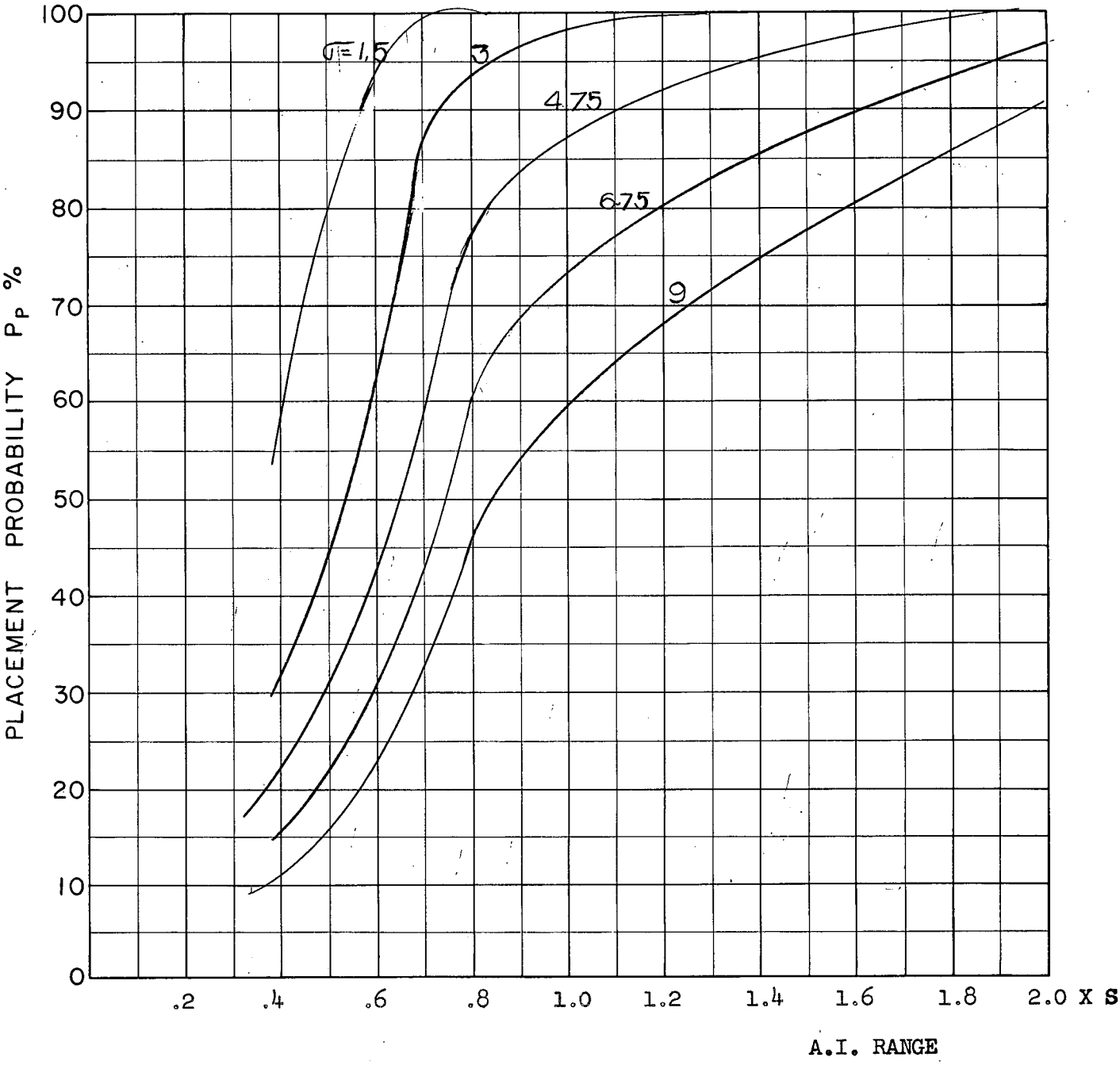

COURSE DIFFERENCE: 135°
TARGET EVASION: 0.4
TARGET MACH NO.: 1.5
INTERCEPTOR LATERAL G's: 1.6
INTERCEPTOR MACH NO.: 1.5
σ OF G.C.I. ACCURACY: 5 Values
A.I. DETECTION RANGE AS FRACTION OF SPECIFICATION RANGE, S: ABSCISSA
A.I. DETECTION RANGE CONTOUR: Straight
ALTITUDE: 50 K
LOOK ANGLE LIMIT = 75°

S-10
C

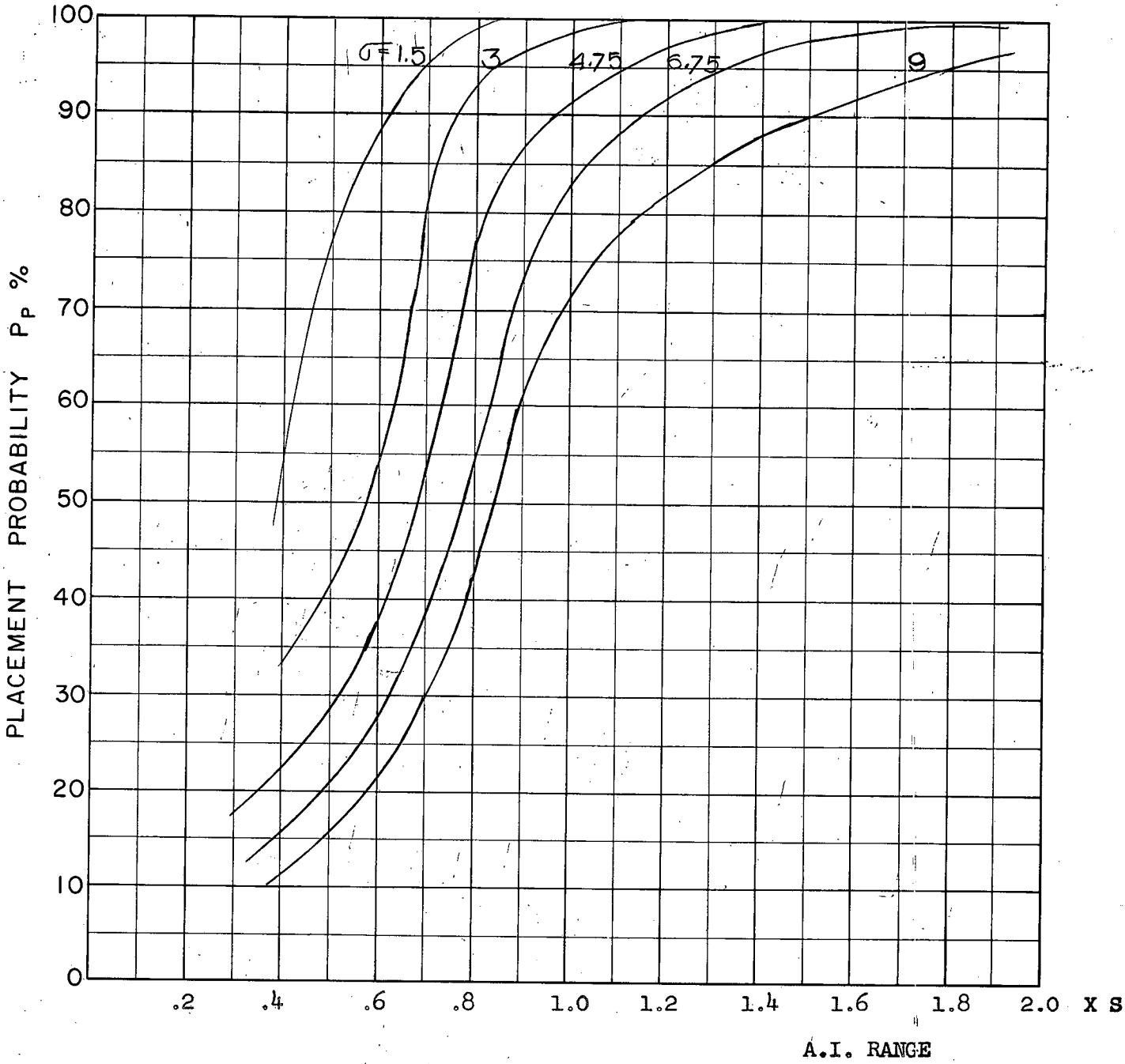

COURSE DIFFERENCE: 160°
TARGET EVASION: 0.4
TARGET MACH NO.: 1.5
INTERCEPTOR LATERAL G's: 1.6
INTERCEPTOR MACH NO.: 1.5
σ OF G.C.I. ACCURACY: 5 Values
A.I. DETECTION RANGE AS FRACTION OF SPECIFICATION RANGE, S: ABSCISSA
A.I. DETECTION RANGE CONTOUR: Straight
ALTITUDE: 50 K

S 11 C

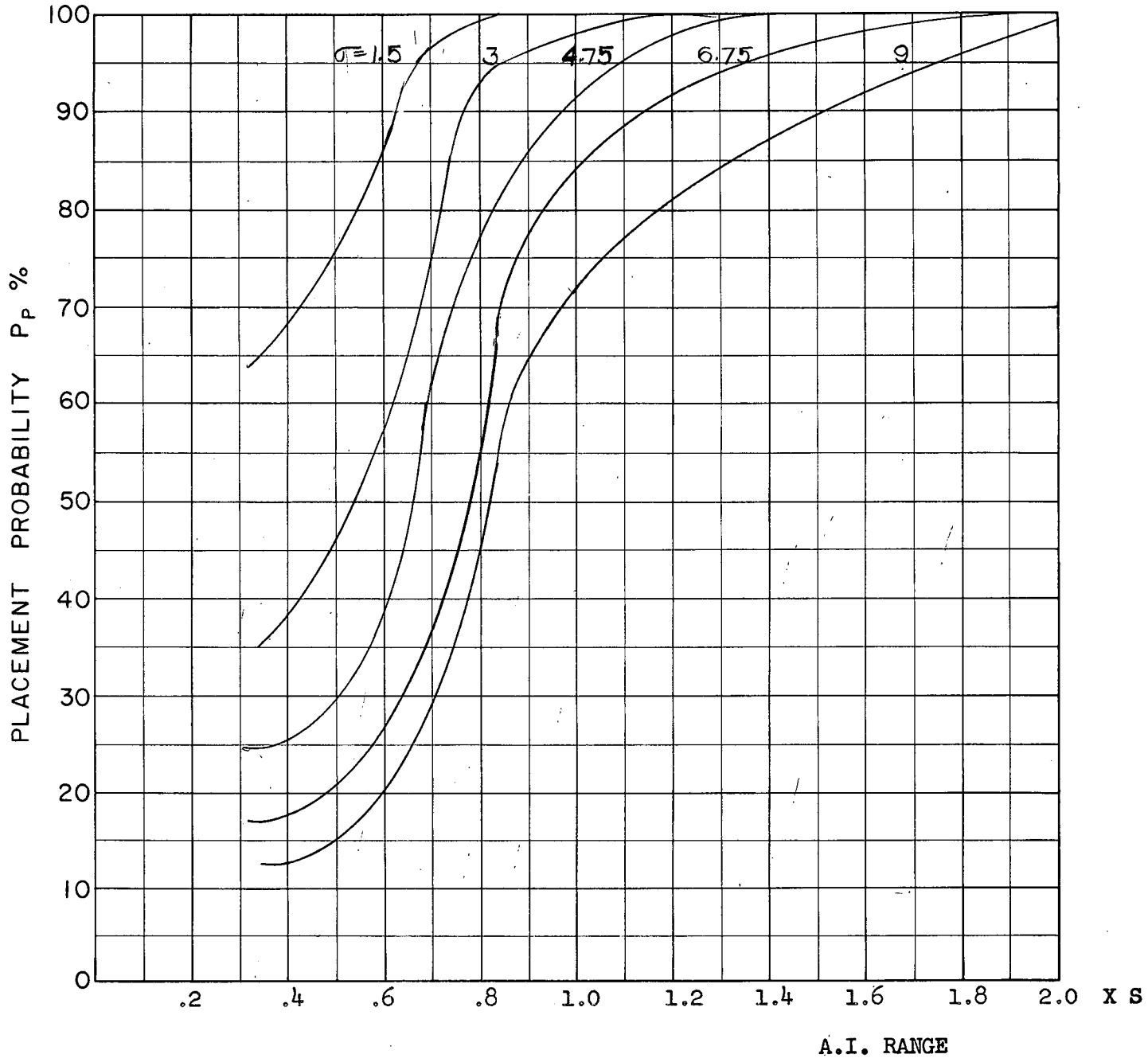

COURSE DIFFERENCE: 160°
TARGET EVASION: 0.4
TARGET MACH NO.: 1.5
INTERCEPTOR LATERAL G's: 1.6
INTERCEPTOR MACH NO.: 1.5
σ OF G.C.I. ACCURACY: 5 Values
A.I. DETECTION RANGE AS FRACTION OF SPECIFICATION RANGE, S: ABSCISSA
A.I. DETECTION RANGE CONTOUR: Straight
ALTITUDE: 50 K
LOOK ANGLE LIMIT = 75°

S12
C

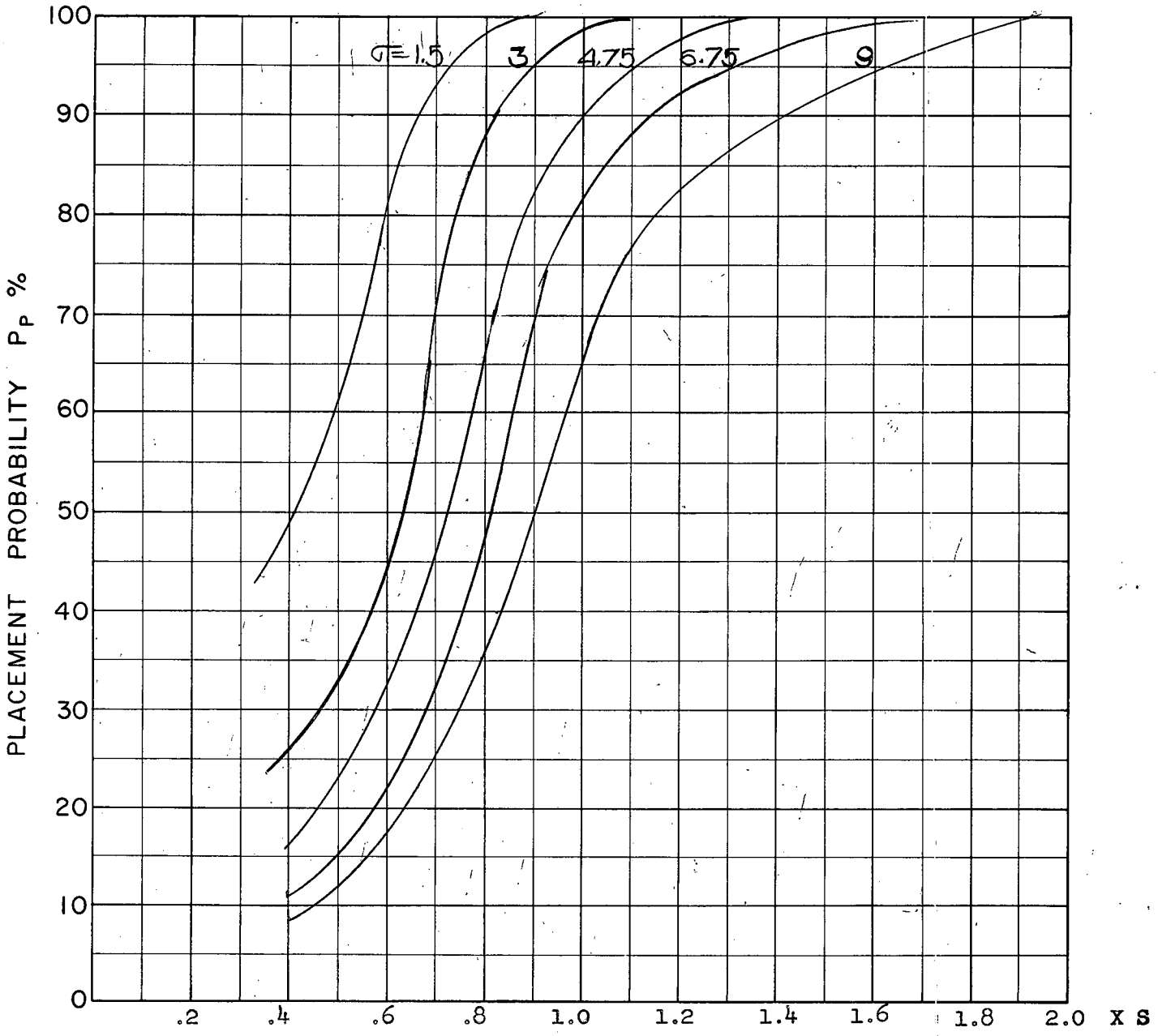

COURSE DIFFERENCE: 180°
TARGET EVASION: 0.4
TARGET MACH NO.: 1.5
INTERCEPTOR LATERAL G's: 1.6
INTERCEPTOR MACH NO.: 1.5
σ OF G.C.I. ACCURACY: 5 Values
A.I. DETECTION RANGE AS FRACTION OF SPECIFICATION RANGE, S: ABSCISSA
A.I. DETECTION RANGE CONTOUR: Straight
ALTITUDE: 50 K

S13
C

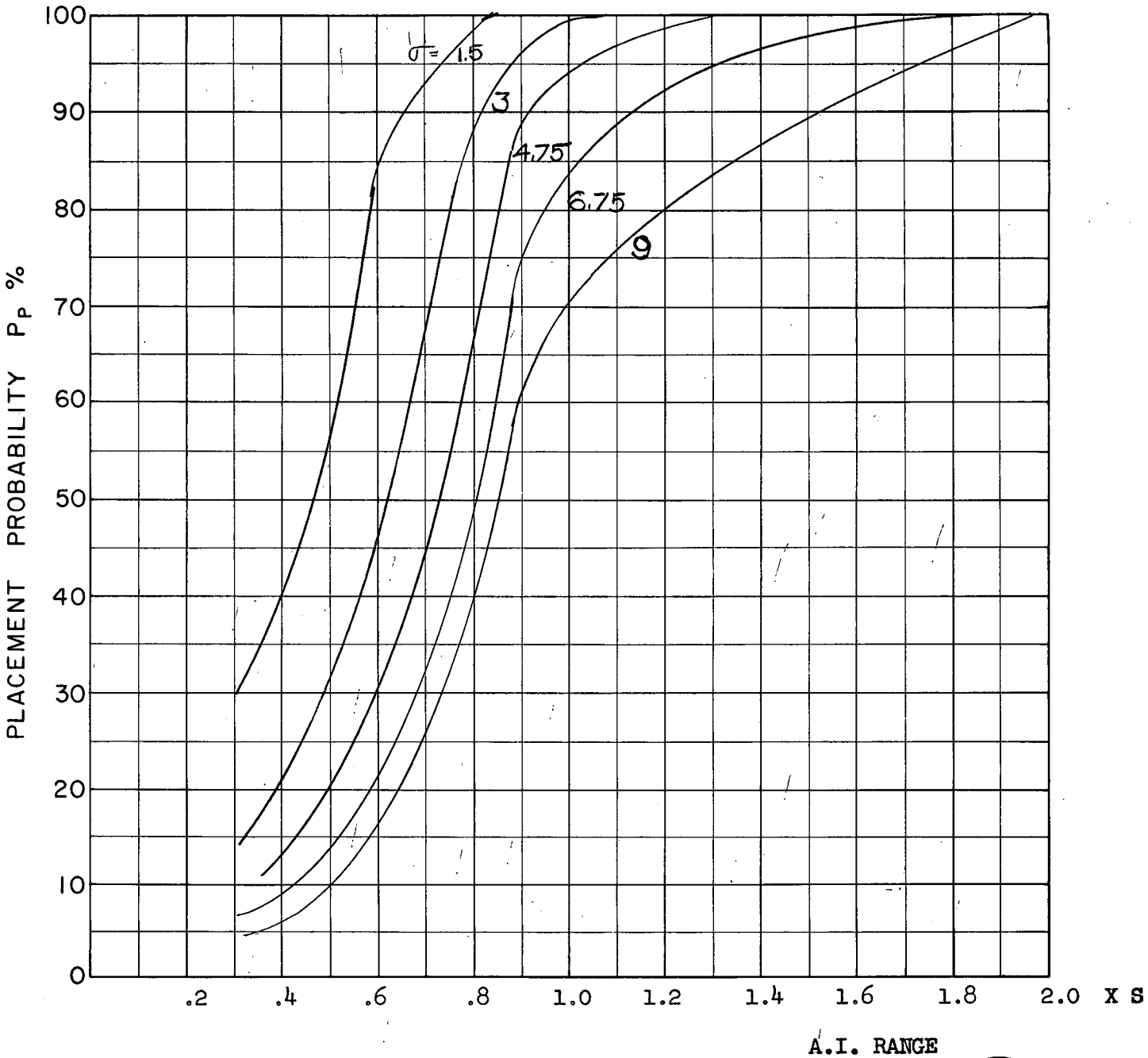

COURSE DIFFERENCE: 180°
TARGET EVASION: 0.4
TARGET MACH NO.: 1.5
INTERCEPTOR LATERAL G's: 1.6
INTERCEPTOR MACH NO.: 1.5
σ OF G.C.I. ACCURACY: 5 Values
A.I. DETECTION RANGE AS FRACTION OF SPECIFICATION RANGE, S: ABSCISSA
A.I. DETECTION RANGE CONTOUR: Straight
ALTITUDE: 50 K
LOOK ANGLE LIMIT = 75°

S 14 c

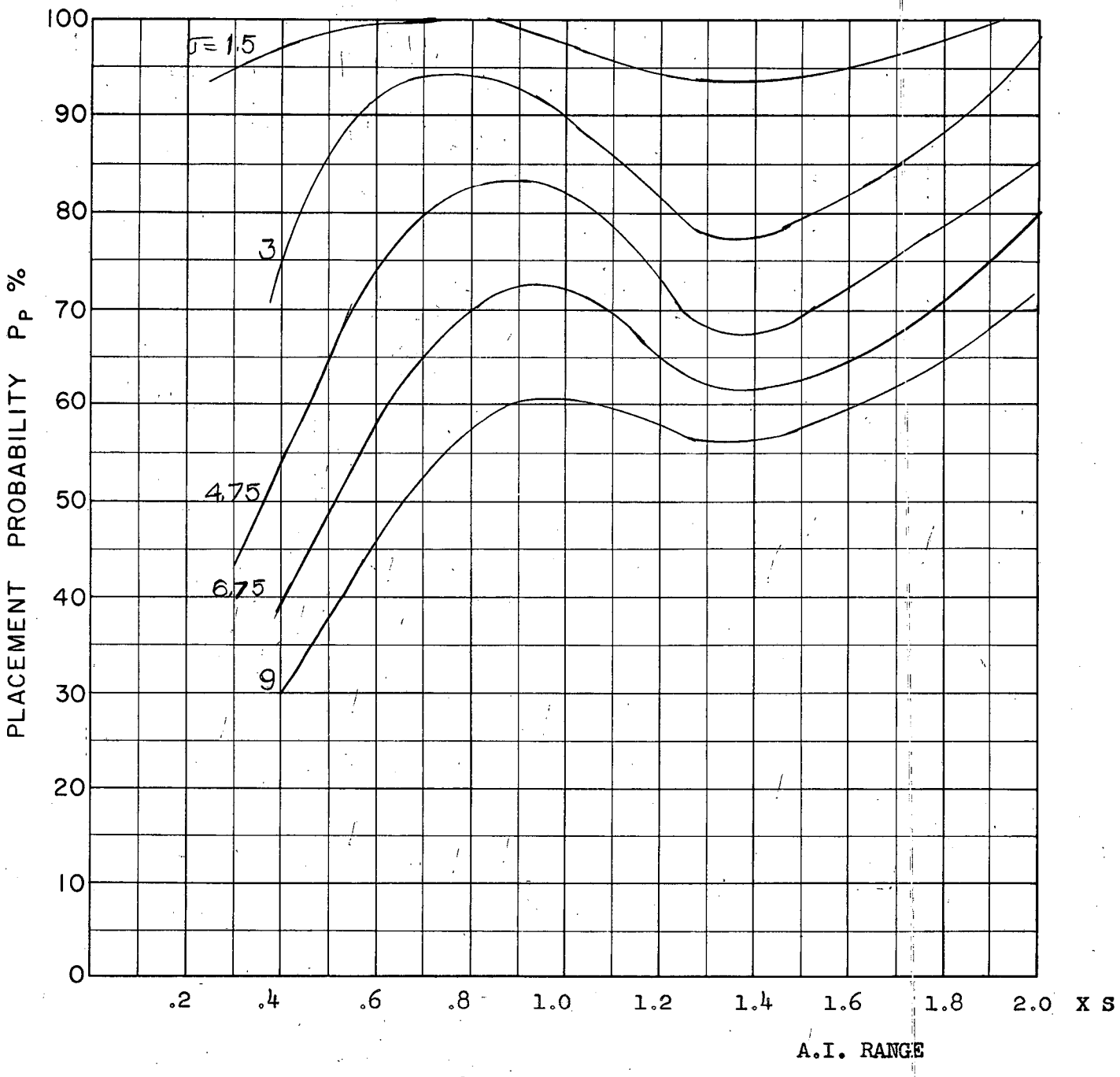

COURSE DIFFERENCE: 110°
TARGET EVASION: 0.4
TARGET MACH NO.: 1.5
INTERCEPTOR LATERAL G's: 3.0
INTERCEPTOR MACH NO.: 1.5
σ OF G.C.I. ACCURACY: 5 Values
A.I. DETECTION RANGE AS FRACTION OF SPECIFICATION RANGE, S: ABSCISSA
A.I. DETECTION RANGE CONTOUR: Straight
ALTITUDE: 50 K

S15
C

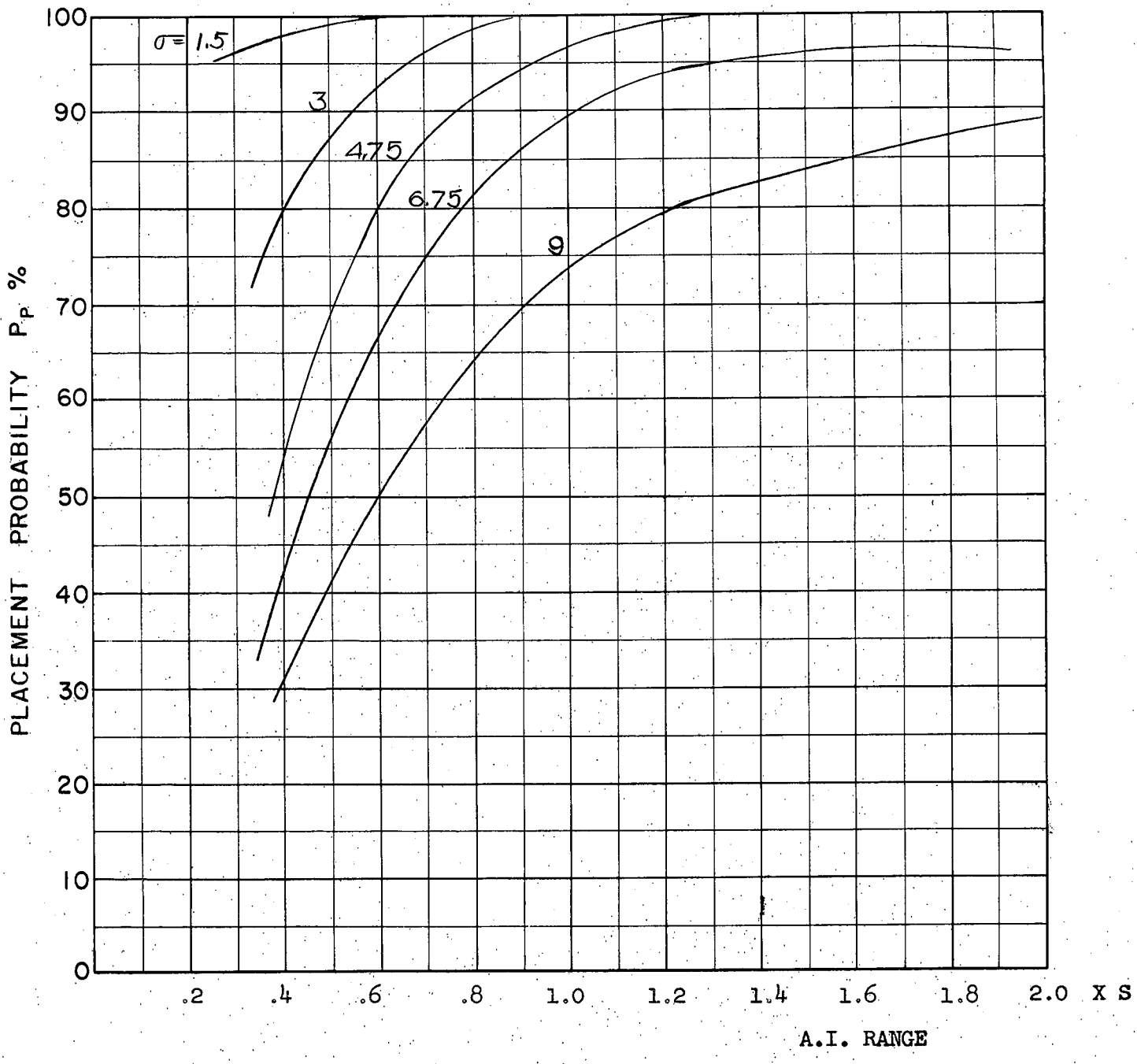

COURSE DIFFERENCE: 135°
TARGET EVASION: 0.4
TARGET MACH NO.: 1.50
INTERCEPTOR LATERAL G's: 3.0
INTERCEPTOR MACH NO.: 1.5
σ OF G.C.I. ACCURACY: 5 Values
A.I. DETECTION RANGE AS FRACTION OF SPECIFICATION RANGE, S ABSCISSA
A.I. DETECTION RANGE CONTOUR: Straight
ALTITUDE: 50 K

S16
C

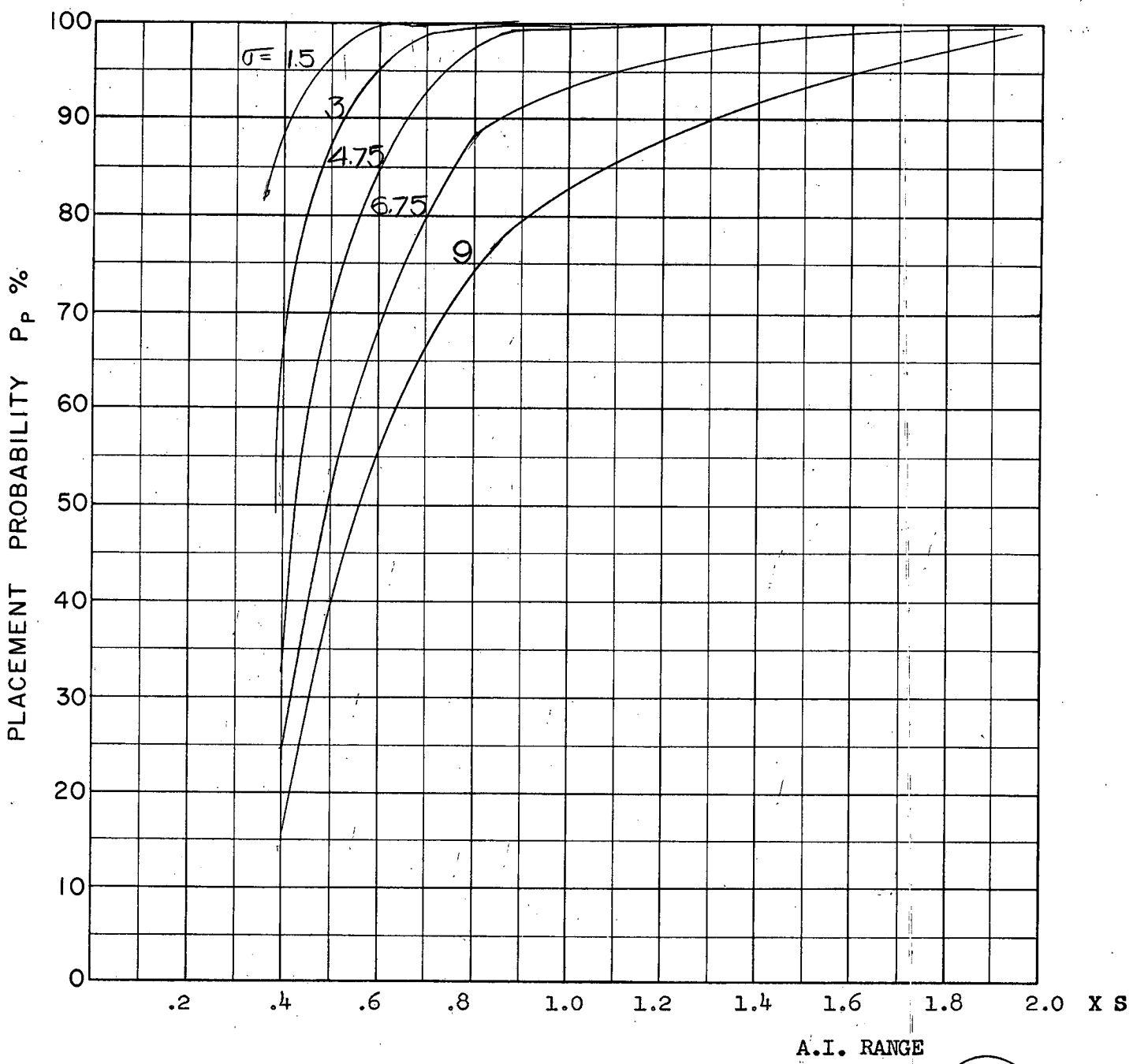

S-17
C

COURSE DIFFERENCE: 160°
TARGET EVASION: 0.4
TARGET MACH NO.: 2.0
INTERCEPTOR LATERAL G's: 3.0
INTERCEPTOR MACH NO.: 1.5
σ OF G.C.I. ACCURACY: 5 Values
A.I. DETECTION RANGE AS FRACTION OF SPECIFICATION RANGE, S: ABSCISSA
A.I. DETECTION RANGE CONTOUR: Straight
ALTITUDE: 50 K

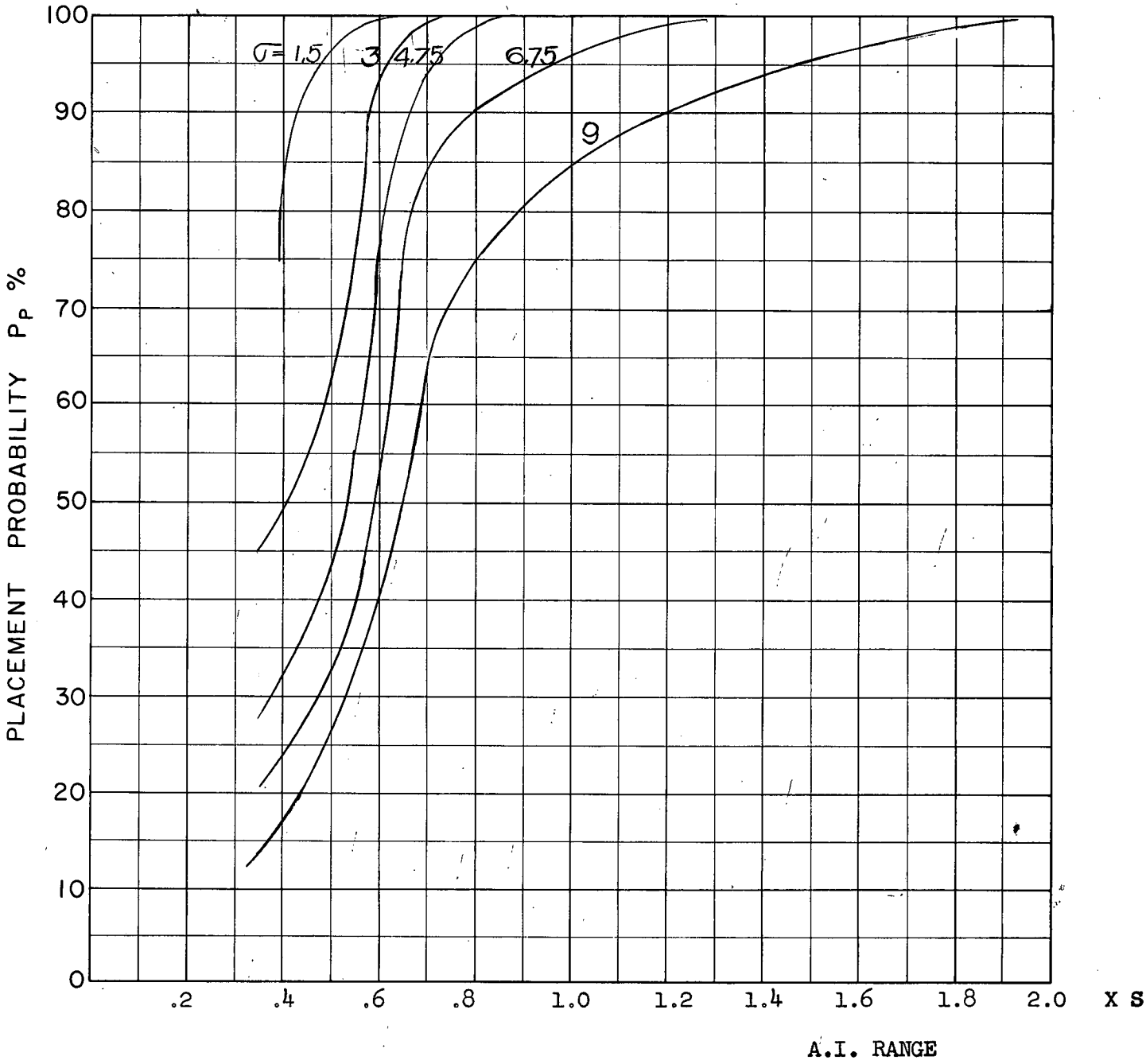

COURSE DIFFERENCE: 180°
TARGET EVASION: 0.4
TARGET MACH NO.: 1.5
INTERCEPTOR LATERAL G's: 3.0
INTERCEPTOR MACH NO.: 1.5
σ OF G.C.I. ACCURACY: 5 Values
A.I. DETECTION RANGE AS FRACTION OF SPECIFICATION RANGE, S: ABSCISSA
A.I. DETECTION RANGE CONTOUR: Straight
ALTITUDE: 50 K

S 18
C

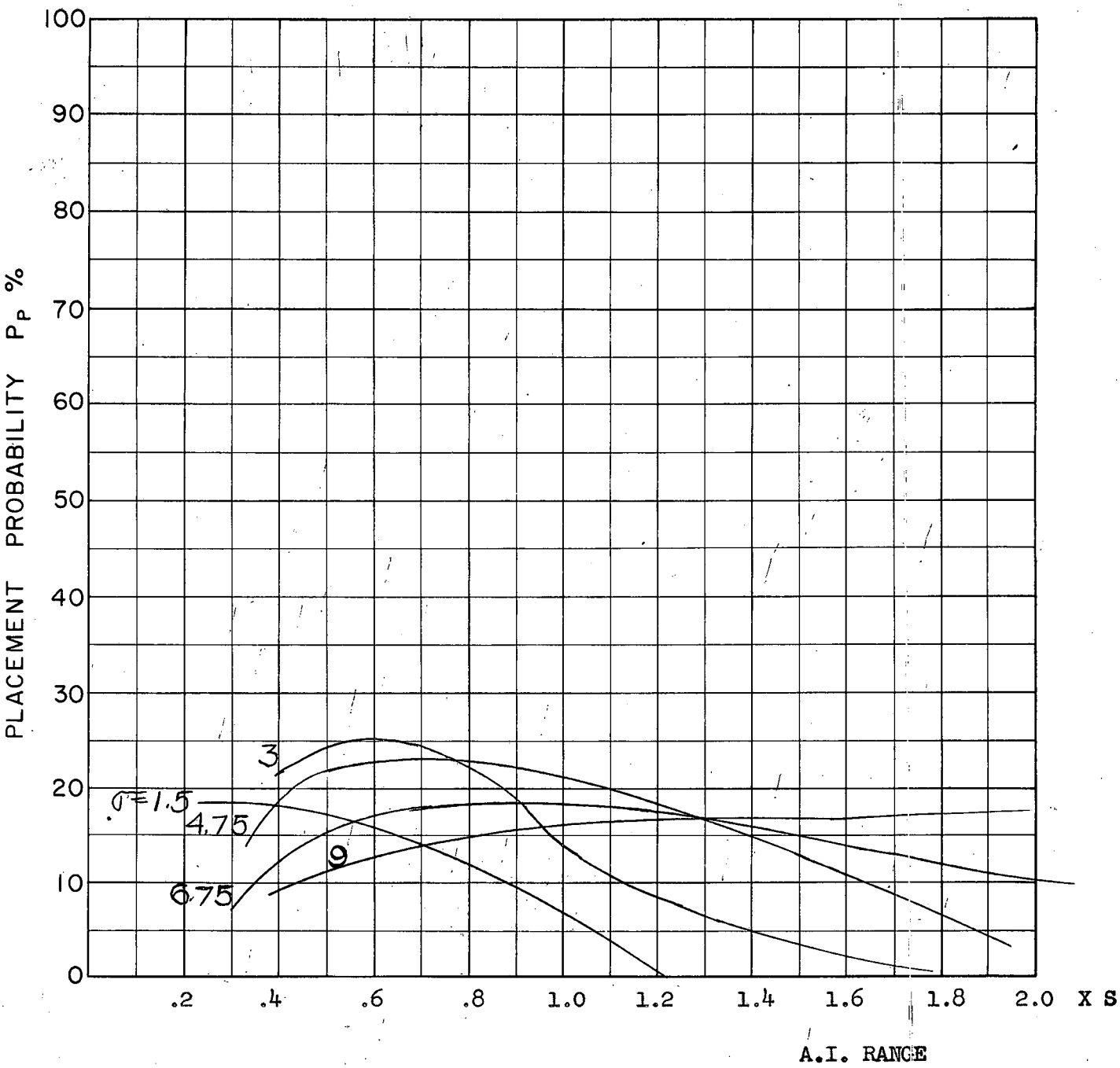

COURSE DIFFERENCE: 110°
TARGET EVASION: 0.5
TARGET MACH NO.: 2.0
INTERCEPTOR LATERAL G's: 0.85
INTERCEPTOR MACH NO.: 1.5
σ OF G.C.I. ACCURACY: 5 Values
A.I. DETECTION RANGE AS FRACTION OF SPECIFICATION RANGE, S: ABSCISSA
A.I. DETECTION RANGE CONTOUR: Straight
ALTITUDE: 50 K

S19
c

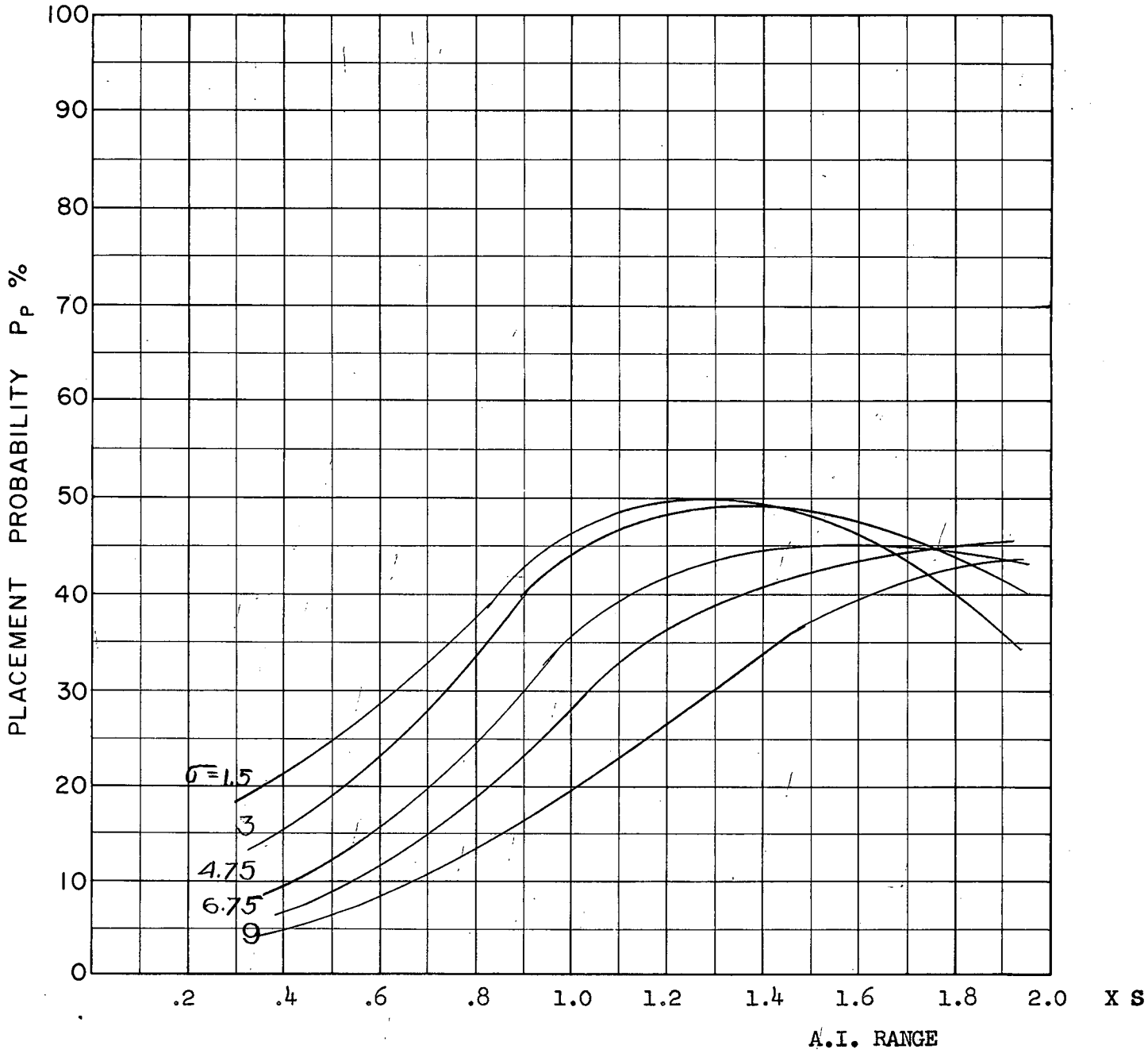

COURSE DIFFERENCE: 135°
TARGET EVASION: 0.5
TARGET MACH NO.: 2.0
INTERCEPTOR LATERAL G's: 0.85
INTERCEPTOR MACH NO.: 1.5
σ OF G.C.I. ACCURACY: 5 Values
A.I. DETECTION RANGE AS FRACTION OF SPECIFICATION RANGE, S: ABSCISSA
A.I. DETECTION RANGE CONTOUR: Straight
ALTITUDE: 50 K

S 20 C

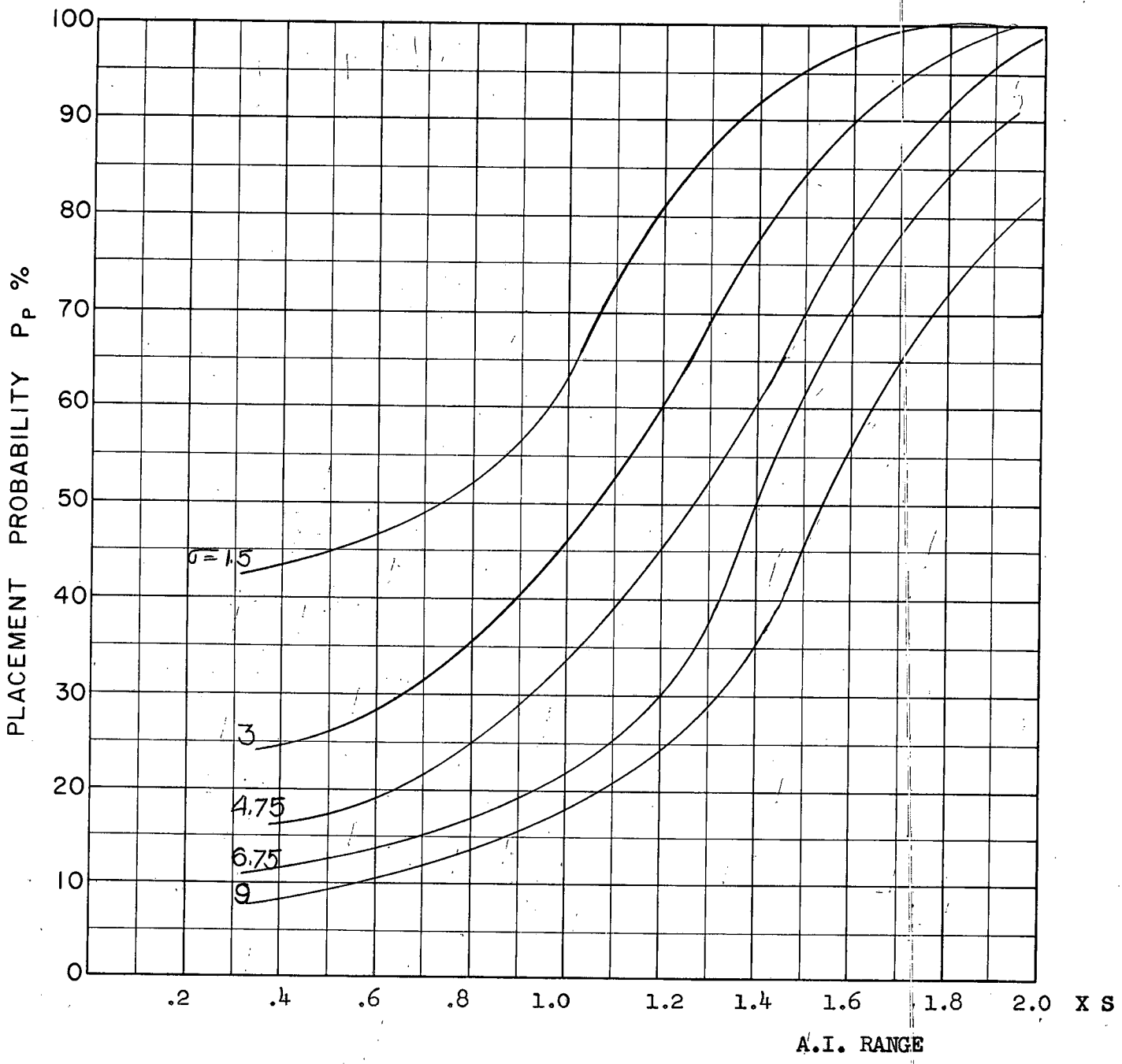

COURSE DIFFERENCE: 160°
TARGET EVASION: 0.5
TARGET MACH NO.: 2.0
INTERCEPTOR LATERAL G's: 0.85
INTERCEPTOR MACH NO.: 1.5
σ OF G.C.I. ACCURACY: 5 Values
A.I. DETECTION RANGE AS FRACTION OF SPECIFICATION RANGE, S : ABSCISSA
A.I. DETECTION RANGE CONTOUR: Straight
ALTITUDE: 50 K

S-21
C

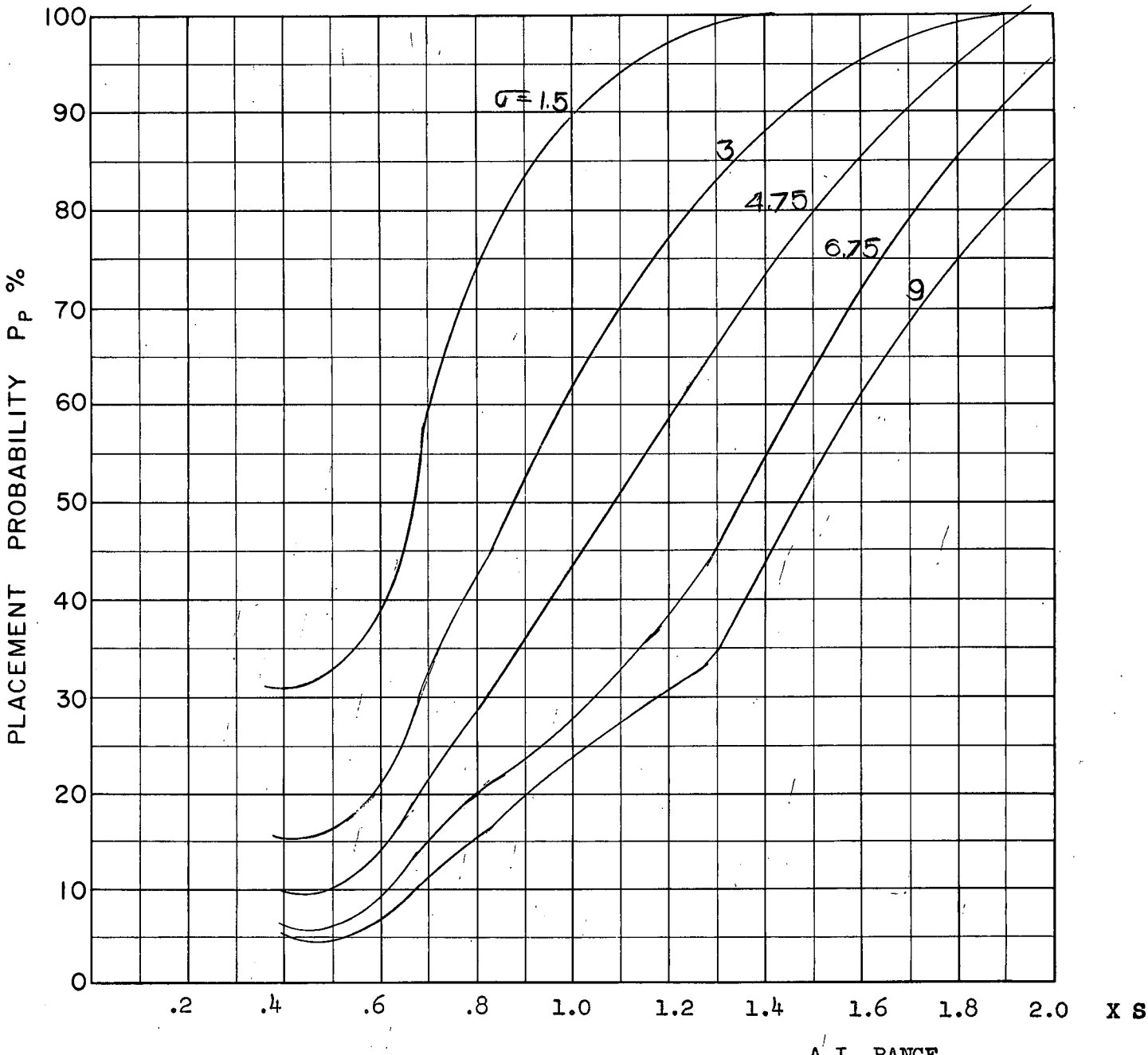

COURSE DIFFERENCE: 180°
TARGET EVASION: 0.5
TARGET MACH NO.: 2.0
INTERCEPTOR LATERAL G's: 0.85
INTERCEPTOR MACH NO.: 1.5
σ OF G.C.I. ACCURACY: 5 Values
A.I. DETECTION RANGE AS FRACTION OF SPECIFICATION RANGE, S: ABSCISSA
A.I. DETECTION RANGE CONTOUR: Straight
ALTITUDE: 50 K

S-22
C

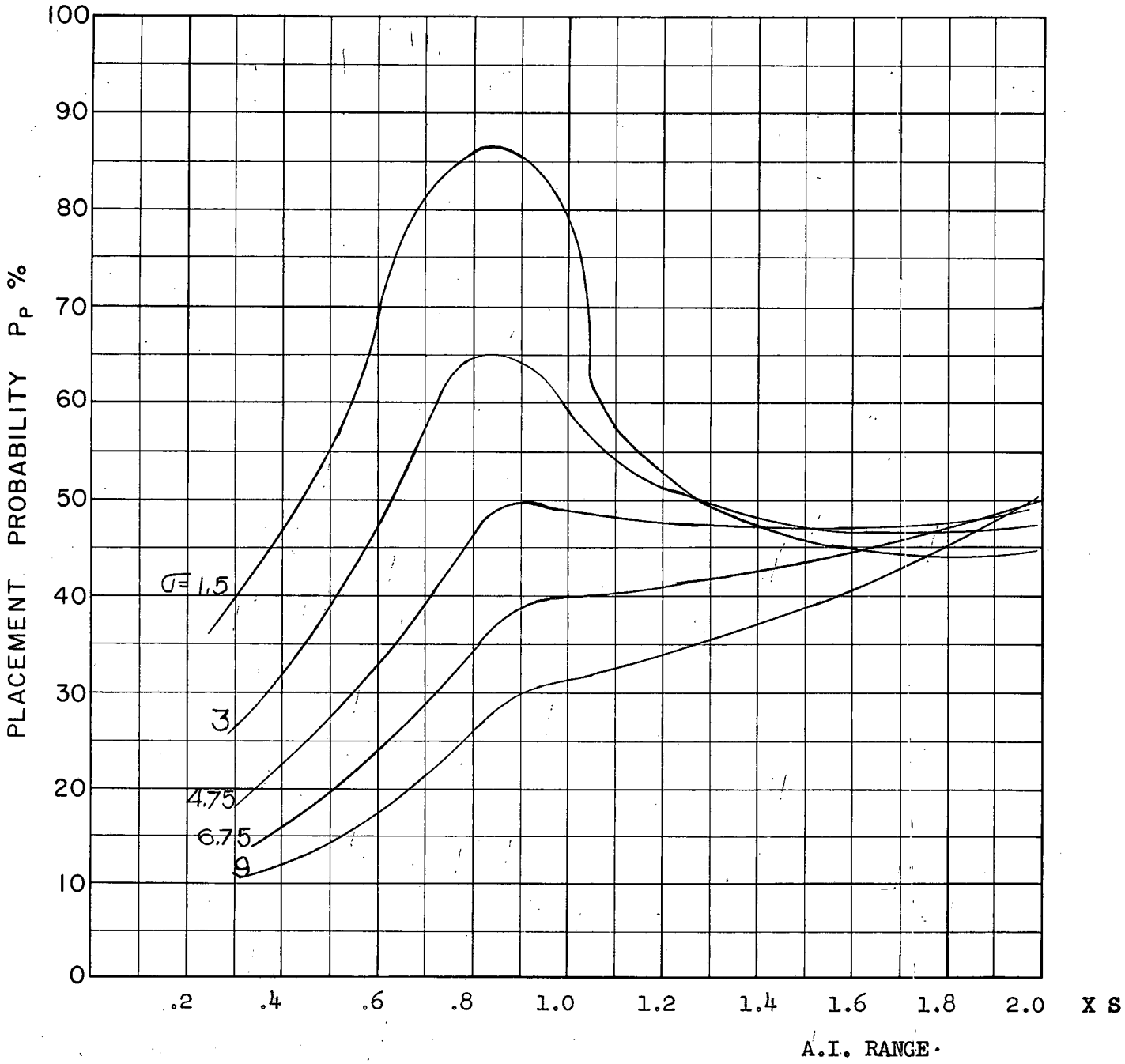

COURSE DIFFERENCE: 110°
TARGET EVASION: 0.5
TARGET MACH NO.: 2.0
INTERCEPTOR LATERAL G's: 1.6
INTERCEPTOR MACH NO.: 1.5
σ OF G.C.I. ACCURACY: 5 Values
A.I. DETECTION RANGE AS FRACTION OF SPECIFICATION RANGE, S: ABSCISSA
A.I. DETECTION RANGE CONTOUR: Straight
ALTITUDE: 50 K

S-23 C

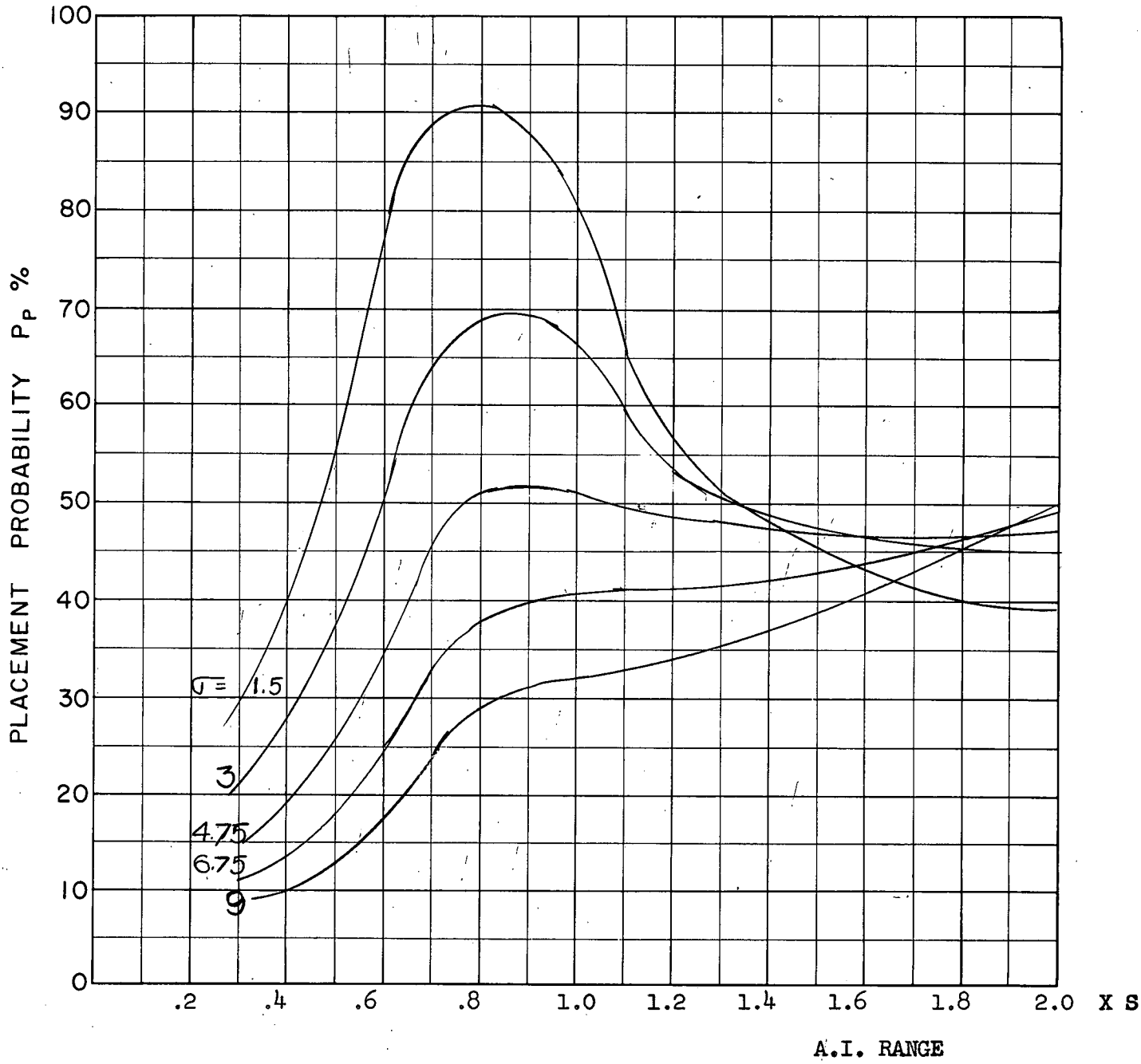

COURSE DIFFERENCE: 110°
TARGET EVASION: 0.5
TARGET MACH NO.: 2.0
INTERCEPTOR LATERAL G's: 1.6
INTERCEPTOR MACH NO.: 1.5
σ OF G.C.I. ACCURACY: 5 Values
A.I. DETECTION RANGE AS FRACTION OF SPECIFICATION RANGE, S : ABSCISSA
A.I. DETECTION RANGE CONTOUR: Straight
ALTITUDE: 50 K
LOOK ANGLE LIMIT - 75°

S24
C

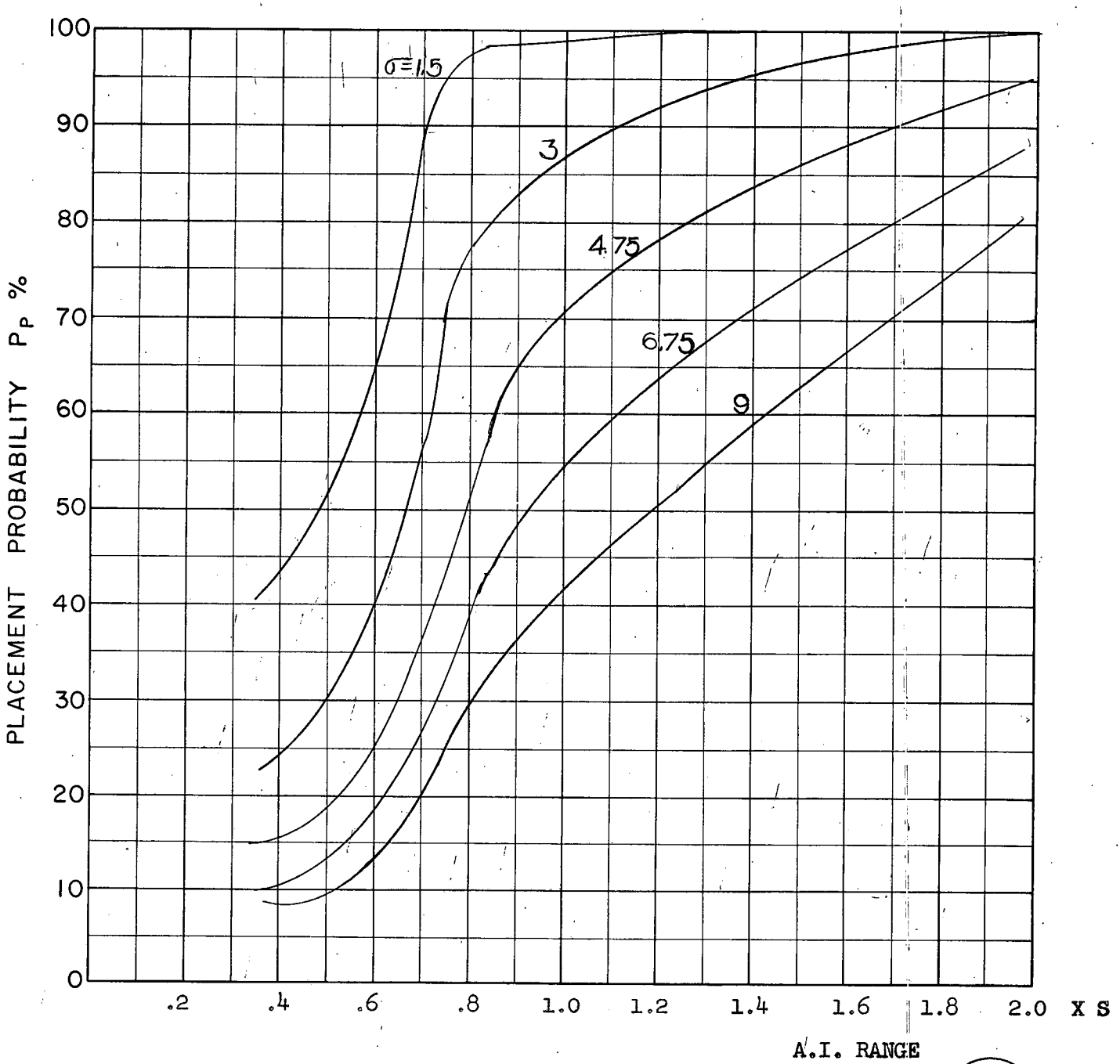

S25
C

COURSE DIFFERENCE: 135°
TARGET EVASION: 0.5
TARGET MACH NO.: 2.0
INTERCEPTOR LATERAL G's: 1.6
INTERCEPTOR MACH NO.: 1.5
σ OF G.C.I. ACCURACY: 5 Values
A.I. DETECTION RANGE AS FRACTION OF SPECIFICATION RANGE, S: ABSCISSA
A.I. DETECTION RANGE CONTOUR: Straight
ALTITUDE: 50 K

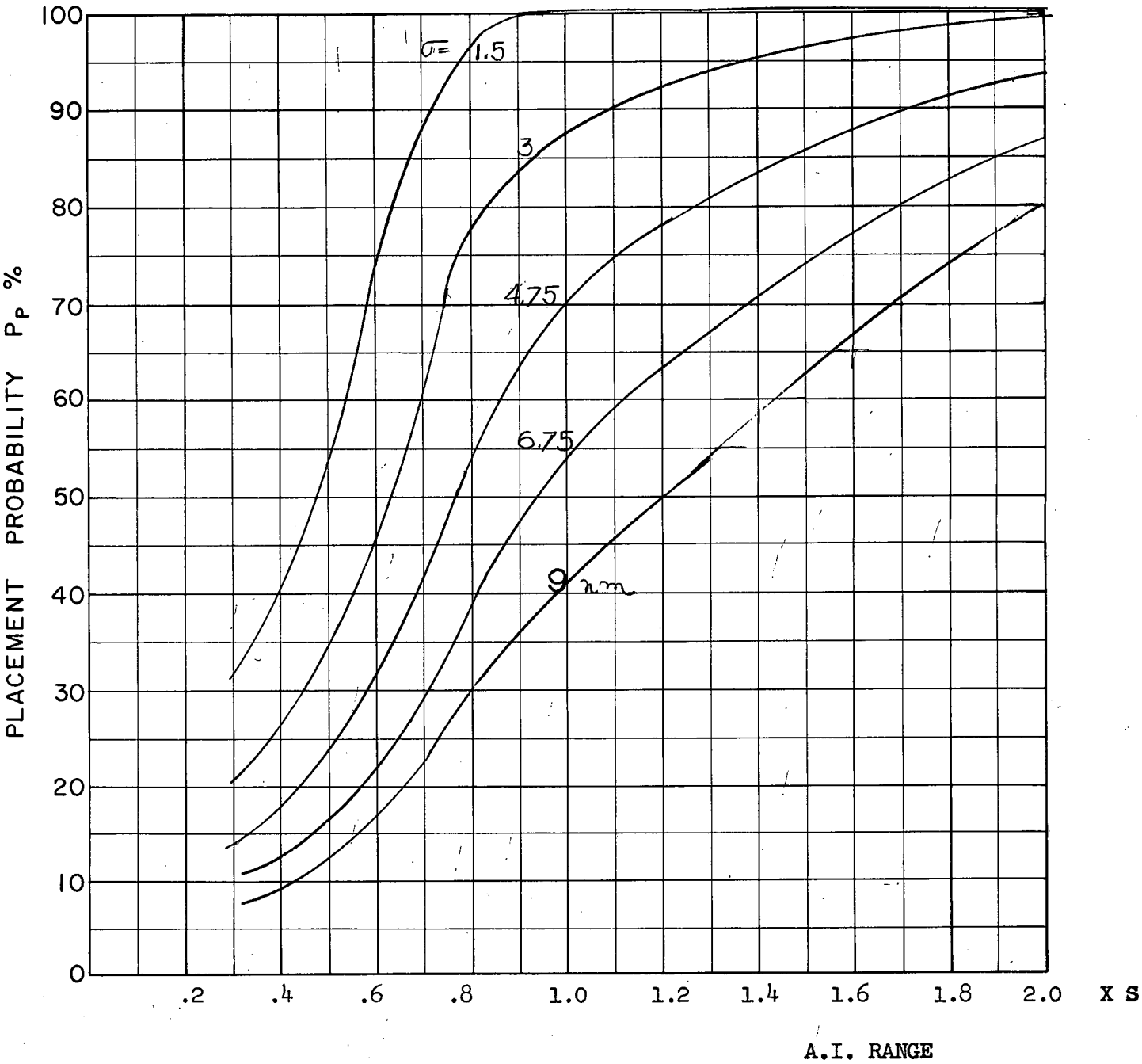

COURSE DIFFERENCE: 135°
TARGET EVASION: 0.5
TARGET MACH NO.: 2.0
INTERCEPTOR LATERAL G's: 1.6
INTERCEPTOR MACH NO.: 1.5
σ OF G.C.I. ACCURACY: 5 Values
A.I. DETECTION RANGE AS FRACTION OF SPECIFICATION RANGE, S: ABSCISSA
A.I. DETECTION RANGE CONTOUR: Straight
ALTITUDE: 50 K
LOOK ANGLE LIMIT = 75°

S26
C

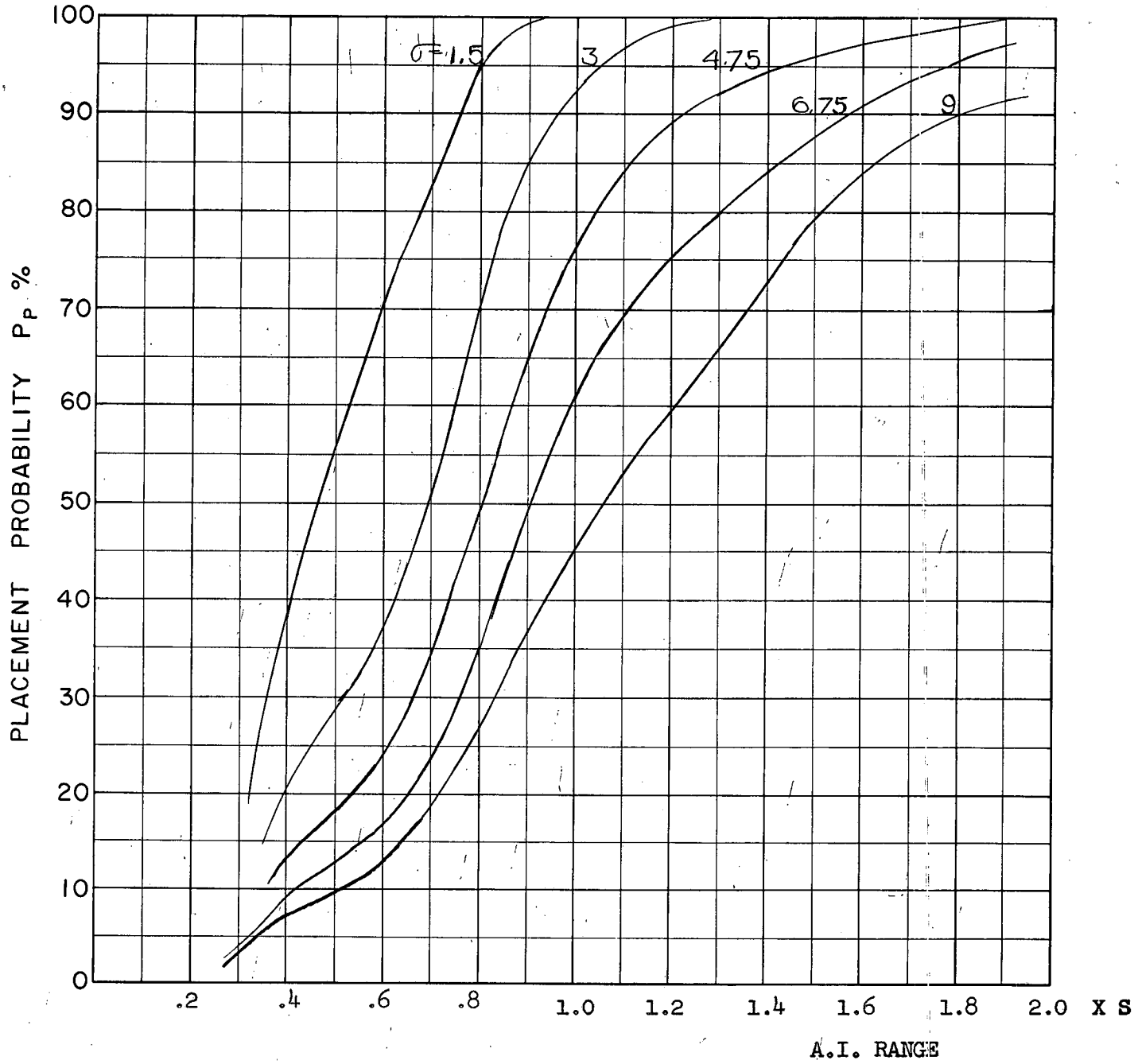

COURSE DIFFERENCE: 160°
TARGET EVASION: 0.5
TARGET MACH NO.: 2.0
INTERCEPTOR LATERAL G's: 1.6
INTERCEPTOR MACH NO.: 1.5
σ OF G.C.I. ACCURACY: 5 Values
A.I. DETECTION RANGE AS FRACTION OF SPECIFICATION RANGE, S: ABSCISSA
A.I. DETECTION RANGE CONTOUR: Straight
ALTITUDE: 50 K

S-27
C

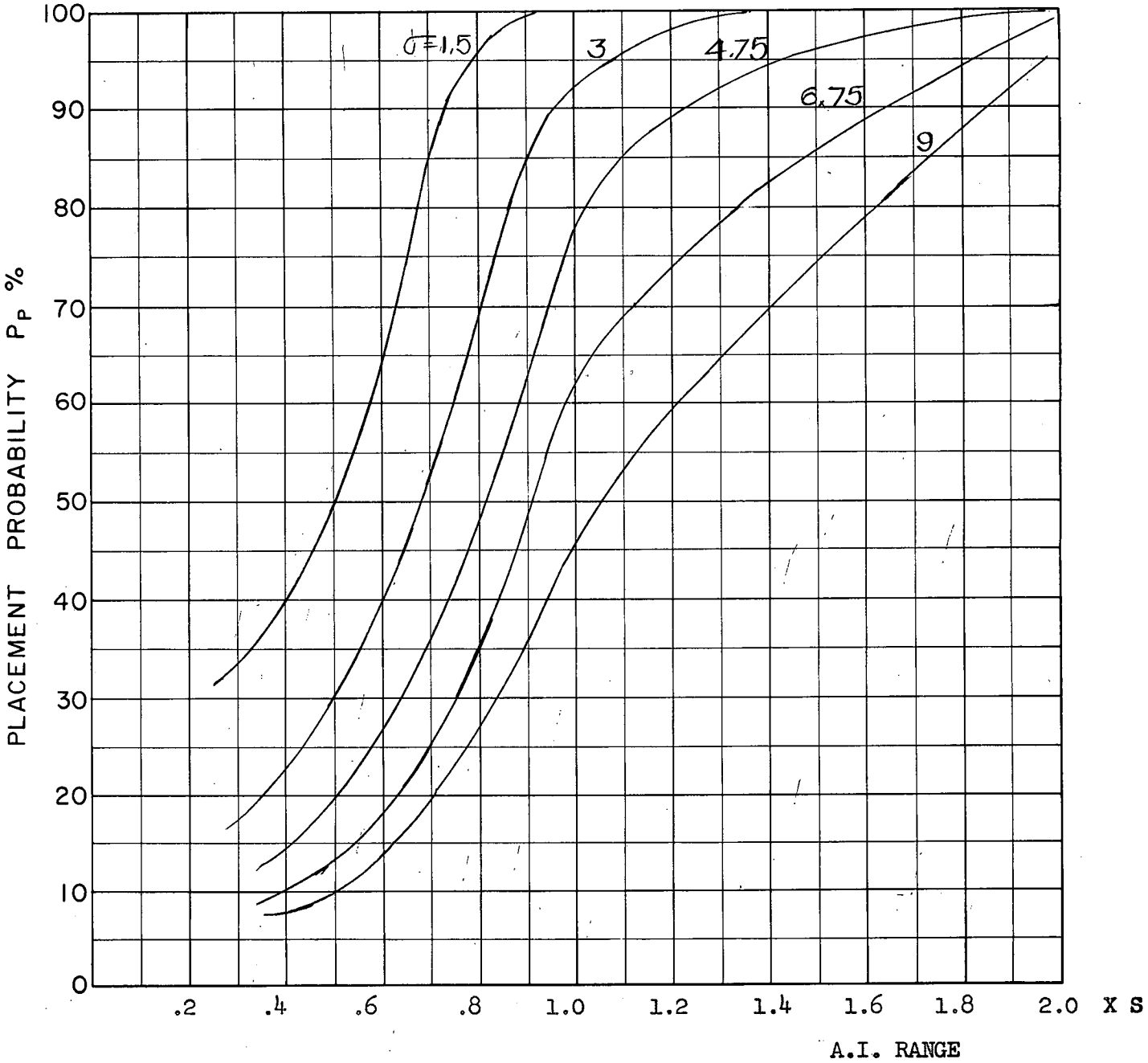

COURSE DIFFERENCE: 160°
TARGET EVASION: 0.5
TARGET MACH NO.: 2.0
INTERCEPTOR LATERAL G's: 1.6
INTERCEPTOR MACH NO.: 1.5
σ OF G.C.I. ACCURACY: 5 Values
A.I. DETECTION RANGE AS FRACTION OF SPECIFICATION RANGE, S: ABSCISSA
A.I. DETECTION RANGE CONTOUR: Straight
ALTITUDE: 50 K
LOOK ANGLE LIMIT = 75°

S28 C

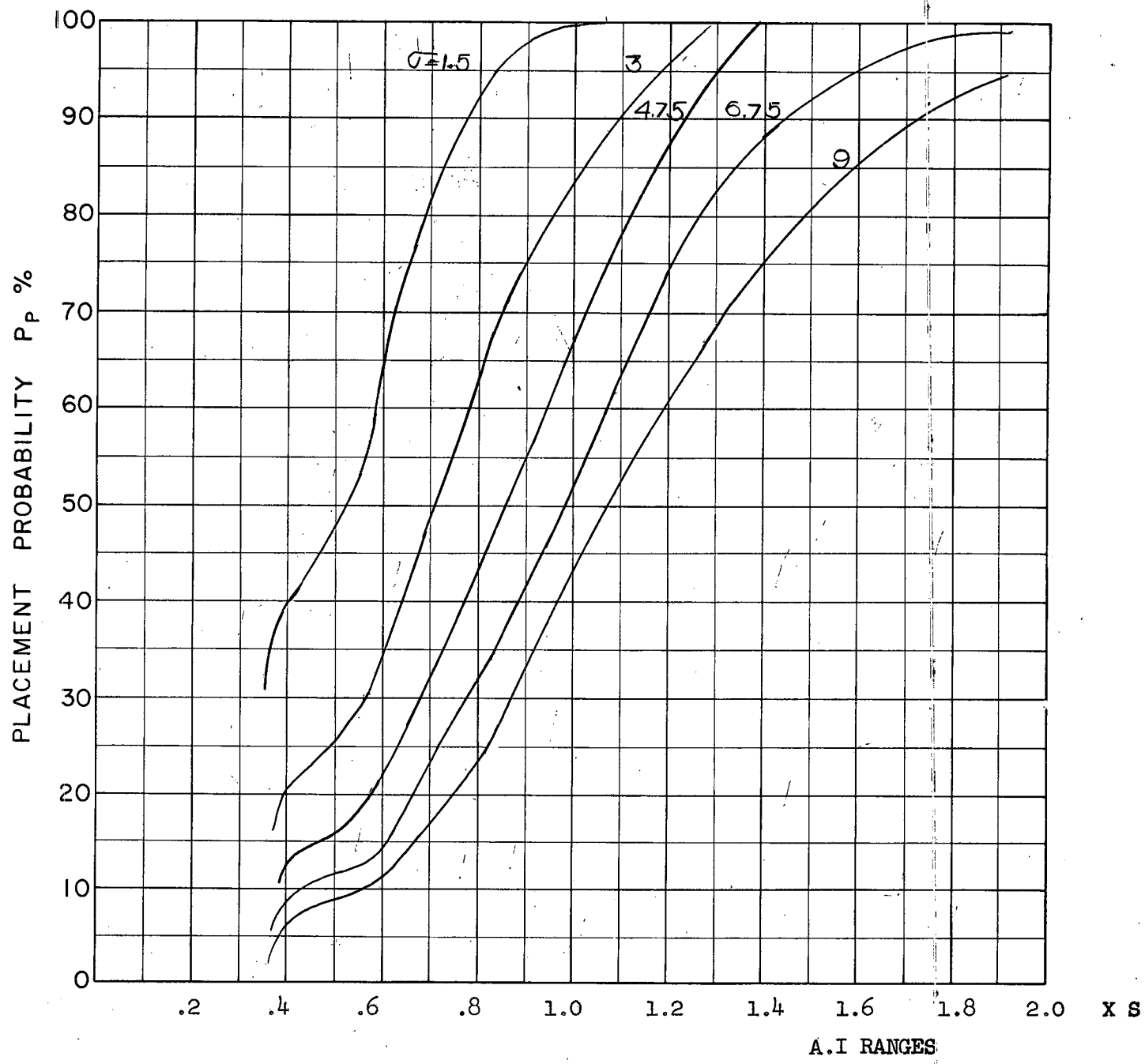

COURSE DIFFERENCE: 180°
TARGET EVASION: 0.5
TARGET MACH NO.: 2.0
INTERCEPTOR LATERAL G's: 1.6
INTERCEPTOR MACH NO.: 1.5
σ OF G.C.I. ACCURACY: 5 Values
A.I. DETECTION RANGE AS FRACTION OF SPECIFICATION RANGE, S: ABSCISSA
A.I. DETECTION RANGE CONTOUR: Straight
ALTITUDE: 50 K

S 29
C

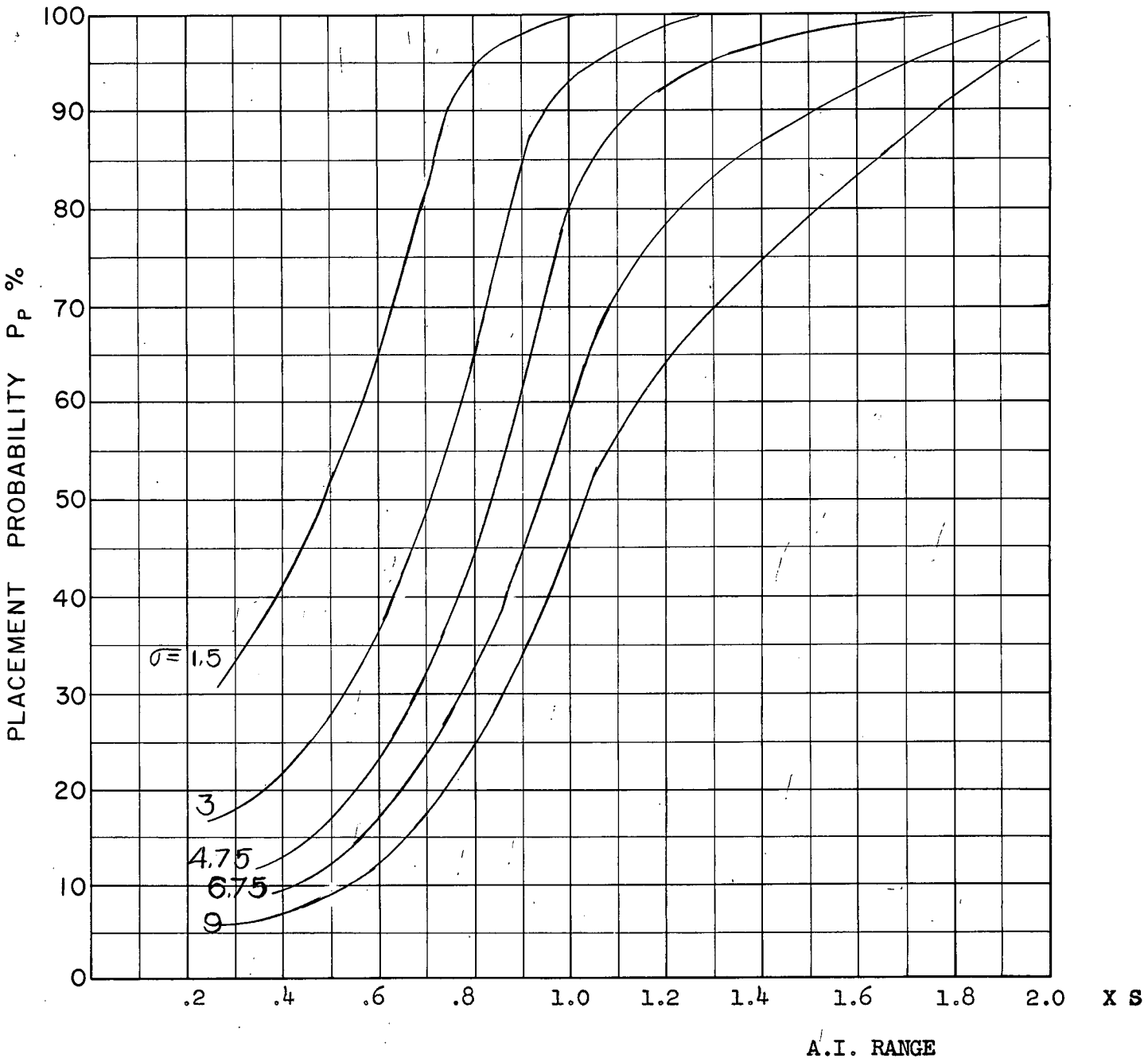

COURSE DIFFERENCE: 180°
TARGET EVASION: 0.5
TARGET MACH NO.: 2.0
INTERCEPTOR LATERAL G's: 1.6
INTERCEPTOR MACH NO.: 1.5
σ OF G.C.I. ACCURACY: 5 Values
A.I. DETECTION RANGE AS FRACTION OF SPECIFICATION RANGE, S : ABSCISSA
A.I. DETECTION RANGE CONTOUR: Straight
ALTITUDE: 50 K
LOOK ANGLE LIMIT = 75°

S 30 c

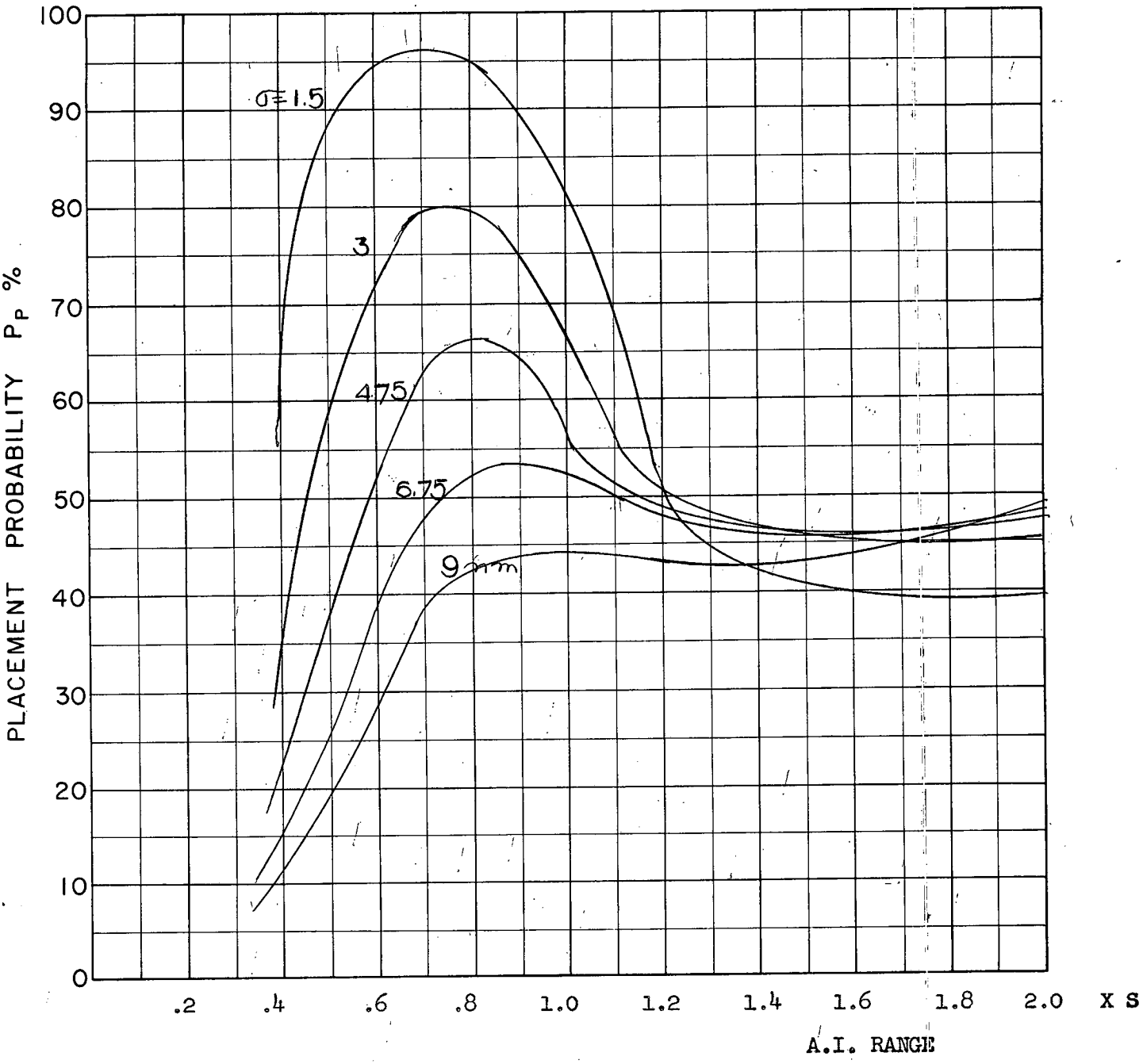

COURSE DIFFERENCE: 110°
TARGET EVASION: 0.5
TARGET MACH NO.: 2.0
INTERCEPTOR LATERAL G's: 3.0
INTERCEPTOR MACH NO.: 1.5
σ OF G.C.I. ACCURACY: 5 Values
A.I. DETECTION RANGE AS FRACTION OF SPECIFICATION RANGE, S: ABSCISSA
A.I. DETECTION RANGE CONTOUR: Straight
ALTITUDE: 50 K

S31
c

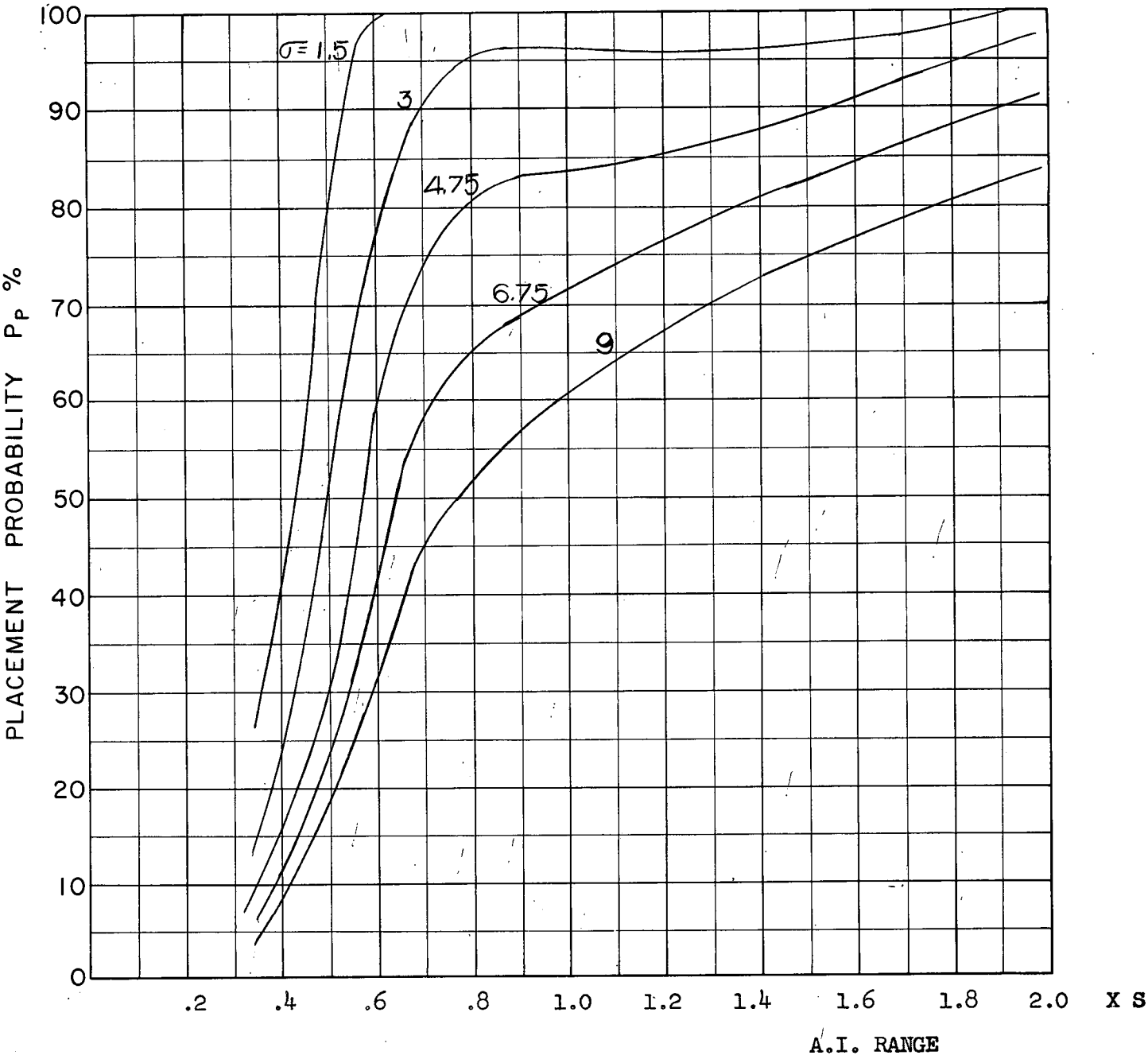

COURSE DIFFERENCE: 135°
TARGET EVASION: 0.5
TARGET MACH NO.: 2.0
INTERCEPTOR LATERAL G's: 3.0
INTERCEPTOR MACH NO.: 1.5
σ OF G.C.I. ACCURACY: 5 Values
A.I. DETECTION RANGE AS FRACTION OF SPECIFICATION RANGE, S : ABSCISSA
A.I. DETECTION RANGE CONTOUR: Straight
ALTITUDE: 50 K

S32
C

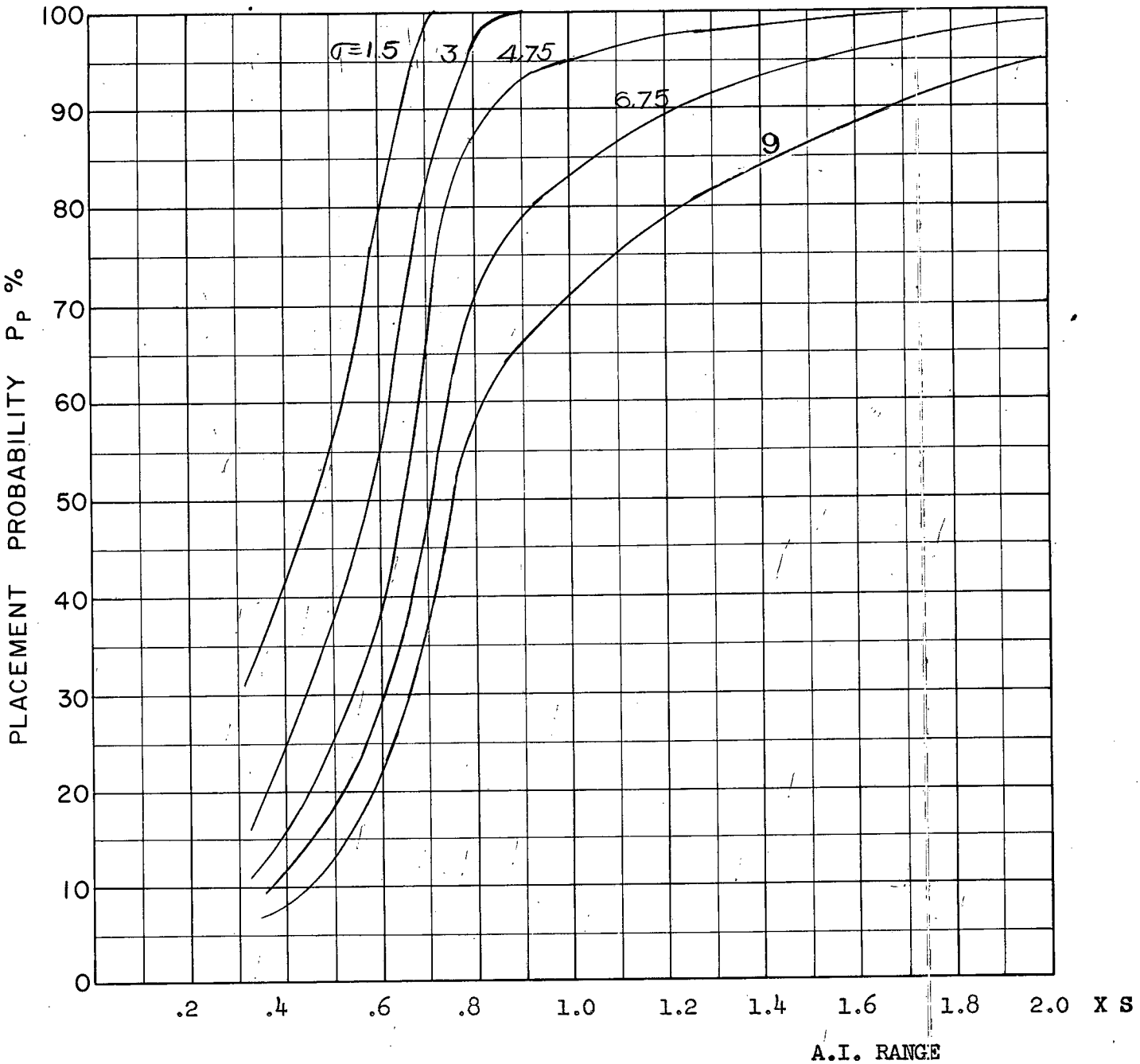

S 33
C

COURSE DIFFERENCE: 160°
TARGET EVASION: 0.5
TARGET MACH NO.: 2.0
INTERCEPTOR LATERAL G's: 3.0
INTERCEPTOR MACH NO.: 1.5
σ OF G.C.I. ACCURACY: 5 Values
A.I. DETECTION RANGE AS FRACTION OF SPECIFICATION RANGE, S: ABSCISSA
A.I. DETECTION RANGE CONTOUR: Straight
ALTITUDE: 50 K

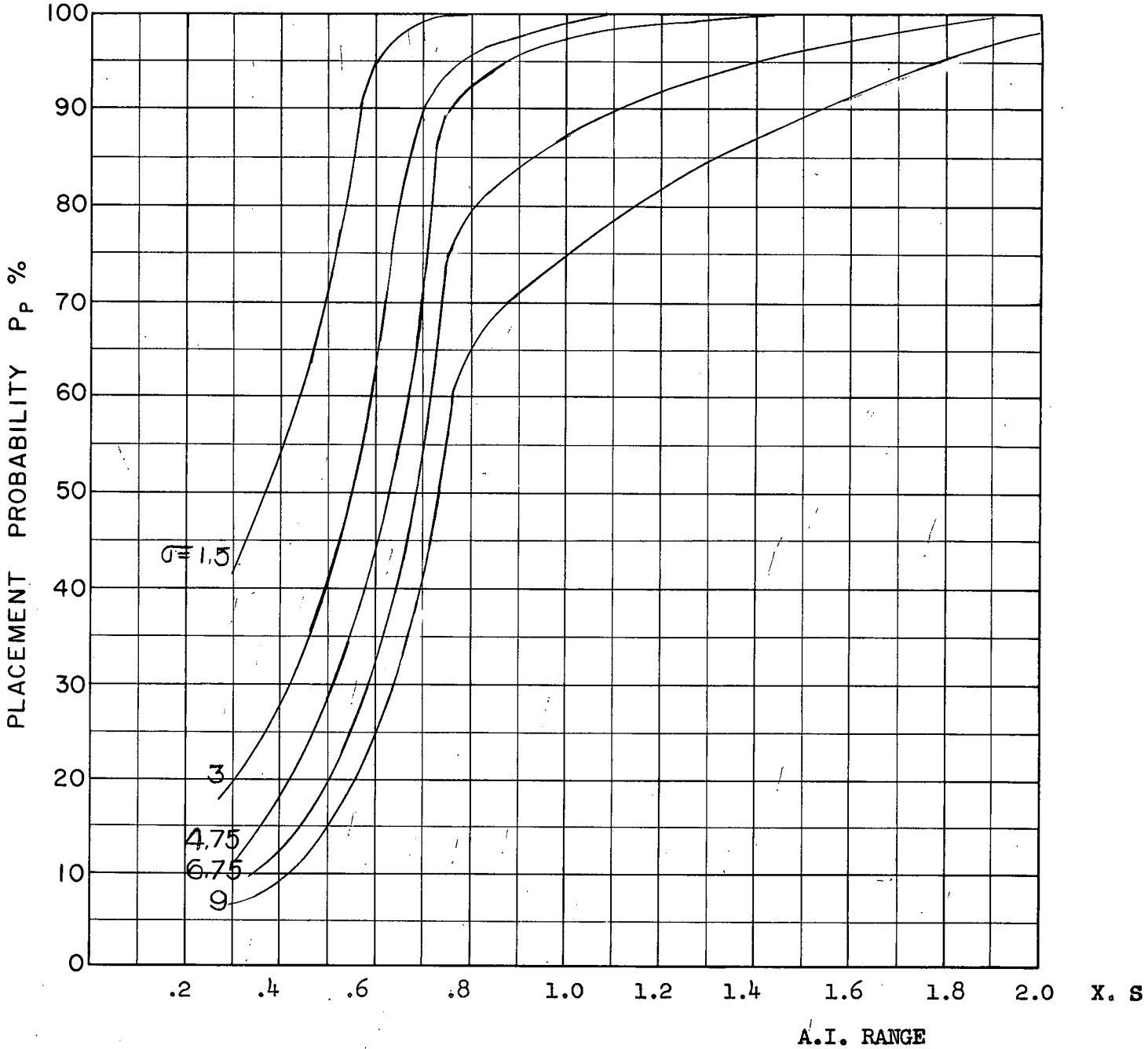

COURSE DIFFERENCE: 180°
TARGET EVASION: 0.5
TARGET MACH NO.: 2.0
INTERCEPTOR LATERAL G's: 3.0
INTERCEPTOR MACH NO.: 1.5
σ OF G.C.I. ACCURACY: 5 Values
A.I. DETECTION RANGE AS FRACTION OF SPECIFICATION RANGE, S: ABSCISSA
A.I. DETECTION RANGE CONTOUR: Straight
ALTITUDE: 50 K

S 34
C

APPENDIX 'D'

2-D Graphical Placement Study for a Decelerating Interceptor Against a Non-evading Target.

by J.A. Ockenden.

1. Scope and Purpose

Previous graphical placement studies conducted at CARDE have concerned only an interceptor flying constant rate, constant speed turns. The studies were valuable in providing an understanding of the effect of various parameters, but the results were thought to be unrealistic because fighter deceleration, caused by excess drag in high rate turns, was not considered. Several estimates of CF-105 thrust/drag characteristics are now available, and two of these have been used to construct trajectories of a fighter turning at maximum rate. The trajectories have been transformed into target coordinates for various target speeds, initial fighter speeds and course differences, and used to construct placement charts from which placement probabilities are computed.

Similar studies with decelerating fighter turns have been conducted on the REAC, and in some respects the REAC results should be more realistic. The time taken to prepare each placement chart graphically is comparable with the REAC time, and the trajectory construction time may roughly be set against REAC setting-up and fault-correction time. It is considered that the graphical study is complementary to the REAC work. Firstly, it provides a check of allowable approach zones in problem areas where the studies are comparable. In addition, the graphical method is readily adaptable to various aerodynamic estimates, whereas much time would be required to change aerodynamic functions on the REAC.

A minimum study program was drawn up to provide basic trends at one altitude. Two sets of aerodynamic estimates were considered, to point out their effect on the placement problem. The effect of altitude was investigated briefly for one set of aerodynamics.

The two aerodynamic estimates used were N.A.E. "Pessimistic" and AVRO "Elastic" (also referred to as AVRO 2.2). The annex to this appendix specifies the estimates in detail.

The four initial course differences used throughout were 180°, 160°, 135° and 110°. Initial fighter speeds of Mach 2.0 and Mach 1.5 were combined with target speeds of Mach 2.0 and Mach 1.5. Effort was concentrated on an altitude of 50,000 feet. For the AVRO "Elastic" aerodynamics the speed

combination $M_{F_o} = 1.5$ and $M_T = 2.0$ was considered at 40,000 feet, and $M_T = M_{F_o} = 2.0$ at 60,000 feet altitude.

The results are discussed in Section 3, and presented graphically in Figures 5 to 45.

2. Graphical Method with Maximum g Fighter Turns

2.1 General Considerations

The principles of the placement chart method of computing placement probabilities are described in detail in Appendix "C" of CARDE Tech. Letter N-47-8. In the current study, techniques were developed for the use of decelerating fighter relative trajectories to determine the locus of the limiting point at which a corrective turn must be started to allow missile launch. The fighter deceleration results from the increased drag occurring in high rate turns.

Several factors influenced the initial choice of certain parameters and of the method employed. It was considered desirable, to some extent, for the study to progress in parallel with the 3-D simulation on the REAc, so that comparisons in the horizontal plane would be possible. Thus various parameters and assumptions are common to both studies. The speed combinations and initial course differences were chosen from values used in drawing the relative trajectories for NAE aerodynamics, which were already available when the work began. The graphical method is inevitably a compromise, involving several assumptions which must be made in the interest of simplicity and speed. The effect on the placement probability results of all the assumptions is considered to be small.

2.2 Assumptions Involved in the Graphical Method

2.2.1 Launch Zone - CARDE Tech. Letter N-47-2 provides maximum and minimum launch contours for a hypothetical missile similar to Sparrow II. The curves are polar plots in target coordinates, drawn for various speed combinations, altitudes and allowable heading errors. Since the curve shapes depend on fighter speed, no single launch zone may be used in the present study to determine a limiting approach path. Unless the fighter is on the ideal approach line, the necessary turn will gradually reduce the fighter speed. Thus for any one initial fighter speed, a set of launch zones must be drawn for various fighter speeds less than the initial speed, and the appropriate one used to define a successful firing position.

The problem is simplified if a launching circle is used instead of a zone. If lead collision navigation is determining the fighter course, a firing circle of radius $F + V_F t_f$, centred $V_T t_f$ ahead of the target, is defined. The fighter is in an ideal firing position, kinematically, anywhere on this circle, if its speed is V_F and it is heading towards the

centre, and if t_f is the time the missile will take to travel a distance F relative to the fighter. Thus a set of concentric circles, corresponding to various V_F values, is required, with the target a distance $V_T t_f$ from the centre. Radial lines from the centre, every 10^o from 0 to 360^o anti-clockwise starting at the target, show immediately the ideal course difference at any point on any circle. (A full treatment of the theory of lead collision navigation may be found in Hughes Aircraft Co. TM 339.)

It remains, then, to choose values of F and t_f in such a way that the resulting launch circle is in fair agreement with the relevant launch zone in N-47-2. The agreement should apply to range at launch and heading at launch, at all aspects. The results of N-47-2 show that it is not possible to choose a lead collision launch circle which agrees with the launch zone in ideal heading, if the missile performance is taken into account. A closer approximation results from using an artificially small t_f value. F may be chosen to give reasonable launch range agreement at all aspects. A frontal aspect range limit of about 45,000 feet is imposed by the maximum range of the missile seeker.

Since lead collision launch range is a function of fighter and target speeds, if, for instance, frontal launch range must not exceed 45,000 feet, either a small F must be chosen, or F must be a function of V_F and V_T. If F was made sufficiently small, the launch range would be less than minimum launch range in many cases, and it was considered impractical in this study to vary F with V_F and V_T. Hence a compromise value of 15,000 feet was chosen for F. Missile performance would give a corresponding t_f value of 17.3 seconds, but a smaller value results in better agreement with empirical ideal headings from N-47-2. 12.87 seconds was chosen, to give an average incremental missile speed of Mach 1.2. It is important to realize that in high speed cases these values produce frontal launch ranges in excess of 45,000 feet. The worst case is 65,000 feet head-on, where $M_T = M_F = 2.0$. The exact effect of this situation on the probability figures is not known, but it seems likely that probabilities would increase slightly, rather than decrease if firing was prevented outside 45,000 feet. If firing was kinematically possible at 60,000 feet, the situation should not deteriorate if the attack was continued, against a non-evading target, although it would be necessary to switch to lead pursuit navigation at the lead collision firing time.

2.2.2 Heading Error - The maximum and minimum launch contours in N-47-2 are, in most cases, drawn for an allowable heading error of 15^o and 5^o respectively. Ideally, the launching circle of the present study should lie between these contours, so that a reasonable heading error would be 10^o, and this value has been used throughout.

It was stated above that lead collision navigation leads to firing on a circle of radius $F + V_F t_f$. This is true only in the ideal case of no heading error at launch. If there is a heading error, at $T = t_f$ the fighter will

not be on the circle, but will in fact lie on a curve whose equation is

$$R = V_T t_f \left(\cos\epsilon\sqrt{\frac{V_M}{V_T}^2 - \mathrm{Sin}^2 A} - \cos A - \mathrm{Sin}\, A \,\mathrm{Sin}\,\epsilon\right)$$

where ϵ is the heading error at $T = t_f$

V_M is the average missile speed

A is the aspect at $T = t_f$

R is the range at $T = t_f$

For small ϵ values the curve approximates to a circle, lying inside the circle at front and rear aspects. On the beam it lies inside the circle for positive ϵ (too much lead) and outside for negative ϵ (too little lead). Certain assumptions are made in the derivation of the equation which are valid only for small ϵ values.

For the purpose of the present study, the above effect has been neglected, and launch circles used. The increase in complexity resulting from the use of the above curves instead of circles did not appear to be justified, in view of the small effect on probability. Probability figures would be affected at low AI ranges only, where manoeuvre barriers are significant, and then only to the extent of a few percent. However, it should be noted that the exact effect of the simplification has not been assessed.

2.2.3 Look Angle Limit - The look angle limit is 66° throughout, measured between the line of sight and the fighter velocity vector. The assumption of a constant look angle limit, measured in this way, is somewhat unrealistic. The maximum angle between the line of sight and the aircraft datum may be constant, but the angle between the datum and the velocity vector changes as the fighter manoeuvres. Thus the 66° angle used may contain an error of the order of 10°, in either sense, in some cases. The resulting errors in placement probability are not known, but the assumption may explain some differences between look angle barriers of this study and those of the 3-D REAC simulation, where angle of attack and bank angle are taken into account.

2.2.4 Fighter Speed Changes - It has been assumed throughout that the fighter flies either maximum g decelerating turns, if there is a steering error, or straight at constant speed if there is no steering error. In practice, or in a REAC study, whenever the fighter flies straight or turns slowly, its speed will increase, unless it is already at maximum.

A speed increase will occur towards the end of all successful lead collision trajectories except those starting on a manoeuvre barrier. In these cases, the real fighter would accelerate during the "on aim" period of the trajectory, so that the relative path would curve forward slightly, and the fighter would fire at higher speed, further forward and sooner than indicated in the graphical

study. However, unless the mode of navigation were changed, this does not mean that the initial turn could be started later, enabling the approach lane to be widened. If the turn started behind the existing minimum fallback barrier, the fighter would never eliminate the steering error, so there would be no straight flight to allow acceleration. The turn would continue until the look angle was exceeded. If the turn started behind the existing look angle barrier, the look angle would be exceeded before straight flight became possible. Hence it is considered that the look angle and minimum fallback barriers of the study give a good representation of the practical case, where unmodified lead collision navigation is used.

2.2.5 Probabilities - Placement probabilities were evaluated as described in Appendix "C" to CARDE Tech. Letter N-47-8. However it should be noted that the 80% probability AI acquisition contours are being used, rather than delayed contours. Also, standard deviation values, , of GCI accuracy are assumed independent of aspect and course difference. The effect of these assumptions is thought to be insignificant.

2.3 Details of Graphical Method

2.3.1 Target coordinate fighter turn trajectories - Trajectories for maximum rate fighter turns in target coordinates have been donstructed by the Analysis Group, using N.A.E. 28% C.G. position pessimistic estimates and AVRO "Elastic" estimates of CF-105 aerodynamics. Some of the N.A.E. space curves were drawn by the REAC, and transformed to target coordinates, for various target speeds and initial course differences, on the drawing board. The others were drawn in target coordinates by the REAC. The REAC relative trajectories were published in CARDE Tech Letter N-47-12. The AVRO space curves were hand calculated and transformed to target coordinates by a drawing board technique.

The N.A.E. trajectories were marked at five second intervals, and values of Mach number and angle turned were available for these points. For the present study, points spaced equally in Mach number were required, at intervals of Mach 0.1. Such points were inserted by interpolation, using the existing time points and values. The AVRO trajectories were drawn using points of 0.1 Mach number spacing, as required, and the Mach number and course difference were shown beside each point. The method is described in detail in the Annex to this Appendix.

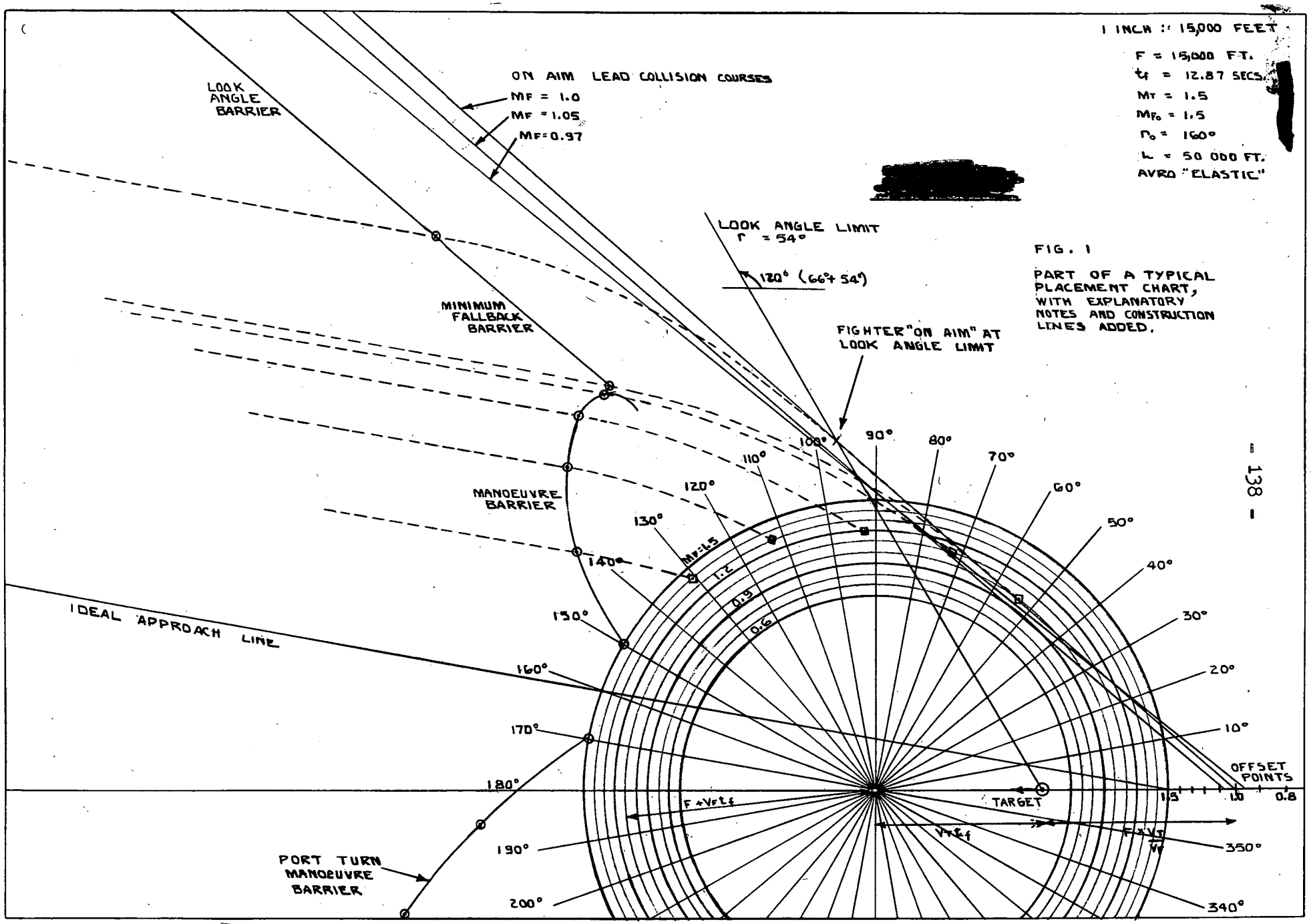

FIG. 1

PART OF A TYPICAL PLACEMENT CHART, WITH EXPLANATORY NOTES AND CONSTRUCTION LINES ADDED.

2.3.2 Placement Charts - Figure 1 is a reproduction of part of a typical placement chart, illustrating the method of obtaining the placement barriers. The fighter trajectories in target coordinates corresponding to each experimental point on the barriers are shown as broken lines. The barrier points are circled, and it is seen that the fighter starts turning at the circled point. The firing point, at the end of each trajectory, is shown. The manoeuvre barrier trajectory firing points have 10° heading error, while the other (only one is shown, being the end point of two trajectories) is an "on aim" firing point.

In the case illustrated, the target speed and initial fighter speed are both Mach 1.5, and the initial course difference (Γ_o) is 160°. Firing circles of radius $F + V_F t_f$ are drawn for the same V_F values corresponding to $M_F = 0.6$ to $M_F = 1.5$, at Mach 0.1 intervals. Offset points, a distance $F.\ V_T/V_F$ behind the target, are drawn for the same V_F range. The target is a distance $V_T t_f$ from the circle centre.

The cut-out relative trajectory for $\Gamma_o = 160^{\circ}$ shows the Γ value at each M_F value. Thus the firing points of the manoeuvre barrier trajectories may be marked on each firing circle, taking into account the allowable heading error at launch of 10°. Then the manoeuvre barrier may be constructed using the cut-out, in the usual way. The charts are drawn on graph paper, which facilitates alignment of the baseline, drawn on the translucent cut-out, in the direction of target velocity.

Three ideal lead collision courses at constant Mach numbers of 0.97, 1.0 and 1.05 are shown. The course differences of these three straight line courses are those that a fighter, starting to turn at Mach 1.5 and 160° course difference, would have at these speeds. Thus it is seen that when the initial conditions of speed and course difference are specified, there is only one final straight line lead collision course for each final speed. The Mach 1.0 course is the farthest back, and hence it may be called the minimum fallback line. If the fighter falls behind this line, it will have no chance of successful firing. A course difference of 54° is required to fly down this straight line. A minimum fallback barrier may be constructed parallel to the minimum fallback line, on which the fighter must start turning.

The look angle limit of 66° prevents indefinite extension of the minimum fallback barrier. For any course difference, Γ, the fighter must lie between target aspects of $\Gamma + 66^{\circ}$ and $\Gamma - 66^{\circ}$, or the look angle will be exceeded. Thus, on the minimum fallback line, aspect must not exceed 120°, and this defines the extreme minimum fallback trajectory, and the start of the look angle barrier, as shown. The look angle barrier is almost a straight line continuation of the minimum fallback barrier. Further points, not shown, are found by finding the look angle limit points on the ideal lead collision courses of higher Mach number than the minimal fallback line. The barrier points move out very rapidly with increasing final Mach number.

The port turn half of the placement chart is drawn in the same way. A difference appears at smaller initial course difference, in that the initial look angle barrier determines the outer part of the approach lane. The initial look angle limit is the target aspect line at $\Gamma_o + 66^\circ$. In the zone of interest it determines part of the approach lane for all $\Gamma_o = 110^\circ$ cases, and some $\Gamma_o = 135^\circ$ cases.

3. Discussion of Results

3.1 The dependent variable of the study is placement probability, expressed as a percentage. The placement probability is the chance of manoeuvring the interceptor, placed with a certain course difference by G.C.I., into a position in which missiles may be fired with a certain probability of kill. The allowable missile firing conditions are determined from the results of a separate missile study.

There remain seven parameters, any one of which may be considered the independent variable. The results are best considered in terms of these seven parameters in turn. They are AI range, initial fighter speed, target speed, initial course difference, fighter aerodynamics, altitude and GCI accuracy. Several additional factors have been varied in other studies, but are constants of the present work. They include target evasion, target type, look angle limits, allowable launch heading error, type of fire control navigation and navigation constants. Non-evading, delta wing targets only are considered. The look angle limit is 66°, and the allowable heading error at launch is 10°. The mode of fire control navigation is lead collision, with constants described in Subsection 2.2.1.

The results will now be considered in terms of the seven parameters.

3.2 A.I. Range

It is considered that the best graphical presentation of the probability of placement results is in terms of AI range as abscissa. Forty graphs in this form, Figs. 5 to 44, comprise 120 probability curves with various combinations of values of the other six variables.

A.I. range is expressed as a fraction of the specification range, S, against the particular target chosen. S has a value of 34 nautical miles head-on for a delta wing target. Five values of AI range are used, namely 0.4S, 0.6S, 0.85S, S and 1.28S and it is assumed that the fighter starts the corrective turn on the contour concerned.

A general result, well known for non-evading targets, is the steady increase in probability with increasing AI range. The increase is steep in the region of 0.4S, and flattens out between 0.6S and S. For AI ranges greater than S, the probability is usually at least 95%, except in some cases with the most pessimistic GCI accuracy.

3.3 Target Speed and Initial Fighter Speed

These two variables are best considered together, so that basically there are three cases, equal speed, fighter speed advantage, and fighter speed disadvantage. With the values chosen, Mach 1.5 and 2.0 for fighter and target, there are two equal speed cases and one each of advantage and disadvantage. It is instructive to consider one set of aerodynamics (AVRO), 50,000 feet altitude and one GCI σ (the pessimistic figure gives probabilities which do not reach 100% except at high AI range). Under these conditions, the highest probabilities result from a fighter speed advantage, while a fighter speed disadvantage gives lowest figures. An exception occurs for frontal attacks with low AI range, where highest probabilities occur in the equal speed Mach 1.5 case, and lowest in the Mach 2.0 equal speed case. The trends are identical for the N.A.E. aerodynamics.

3.4 Initial Course Difference

Attacks with four values of initial course difference, 180°, 160°, 135° and 110° were considered. The resulting trends are closely associated with those described in the previous subsection. In general, probabilities are highest in frontal attacks. However, for low A.I. range, with equal speeds of Mach 2.0 or a fighter speed advantage, beam attacks are better than frontal.

3.5 Fighter Aerodynamics

In all the cases considered, the AVRO "Elastic" aerodynamics, which give better turn rates, result in higher placement probabilities than the N.A.E. 28% C.G. pessimistic estimates. The increase is most significant at low A.I. ranges, where manoeuvre barriers determine the allowable approach lane, and particularly for frontal attacks with a speed disadvantage. Under these conditions, typical probability increases are 29% to 39% and 52% to 67%.

3.6 Altitude

The bulk of the results presented are for 50,000 ft. co-altitude attacks. Equal speed (Mach 2.0) attacks were investigated for AVRO aerodynamics at 60,000 feet, and the speed disadvantage case at 40,000 feet. It is worth noting that an initial fighter speed of Mach 1.5 was investigated at 60,000 feet, but was considered to be impractical. The rate of turn is low, and in extreme approaches the fighter speed would fall below Mach 0.8 (near the stall speed at this altitude) before the corrective turn was completed. A fighter speed of Mach 2.0 at 60,000 ft. may not be possible in practice, but it is useful to have information at this altitude. The situation at slightly lower altitudes may be assessed by interpolation.

The results at 40,000 feet are almost identical to the corresponding case at 50,000 feet. The 60,000 feet probabilities are consistently lower than those for 50,000 feet, the difference being most significant at A.I. ranges below 0.85.

3.7 G.C.I. Accuracy

Of the three standard deviations of GCI accuracy, 9 n.m., which results in some low probabilities, is considered pessimistic. Using 1.5 n.m., the lowest placement probability found was 84% at 0.4 S AI range, but this value of σ is thought to be an optimistic estimate of GCI radar performance. The intermediate value, 4.75 n.m., is probably realistic, and gives intermediate probabilities, ranging from 35% to 90% at 0.4 S.

It is clear then that the value achieved in practice is very significant if A.I. radar range is low. Above specification A.I. range the placement probability is usually above 90%, even with σ = 9 n.m., so that G.C.I. accuracy is not important in this range against a non-evading delta wing target.

4. Conclusions

The graphical method described provides results, at a competitive speed, in the simple case of a coaltitude attack against a non-evading target. It may be used to point out basic trends, such as the effect on placement probability of a change in fighter aerodynamics. From a knowledge of such an effect in the simple case studied, it may be possible to predict the effect of the same change in a more sophisticated study, for instance in three dimensions with an evading target, so saving considerable time and repetition.

ANNEX to Appendix 'D'

The Methods of Obtaining Fighter Trajectories

in Target Coordinates

by CF-105 Analysis Group

Introduction and Summary

The purpose of this section is to describe the methods used to obtain, in the case of non-evading targets, the trajectories of the fighter in target coordinates when it is turning at the maximum rate determined only by lift limits, not by thrust limits. Because the lift limits allow higher rates of turn than do the thrust limits, the fighter will necessarily decelerate. It is then sometimes referred to as a decelerating fighter or a fighter making a decelerating turn. This does not imply that the fighter is deliberately decelerated by closing the throttle or using dive brakes.

Two separate methods and a combination of the two were used. In the first, the REAC (Reeves Electronic Analogue Computer) was used to simulate the aerodynamics of the fighter and to solve the equations of motion so as to produce on an XY plotting board the trajectories in target coordinates. In the second method, the forces acting on the fighter were calculated by hand and the equations of motion were solved numerically to obtain the trajectories in space, from which the trajectories in target coordinates were obtained by graphical means. In the combination of the two methods, the space trajectories were obtained by the REAC and the target coordinate trajectories were obtained graphically.

Two estimates of the aerodynamic performance of the CF-105 were used. One estimate, now obsolete, was based on the "pessimistic" data provided by the National Aeronautical Establishment for a center of gravity position of 28% MAC, Ref. (1), and an aircraft weight of 50,000 lb. The other estimate, sometimes referred to as AVRO 2.2, was based on AVRO "Elastic" data for a center of gravity position of 29.5% M.A.C., Ref. (1); an aircraft weight of 51,600 lb, and thrust data for an Iroquois engine with rematched compressors and a 49 inch ejector, Ref. (3)*. A measure of the turning performance of the CF-105 which is often used is the normal load factor obtainable in a constant speed turn at Mach Number 1.5 at 50,000 feet. This is 1.29 according to

*The AVRO 2.2 estimate is essentially the same as the latest AVRO data given in Ref.(2) and (3), except at Mach numbers less than 1.15. Below M = 1.15 the drag estimate is different because at the time it was made, the preliminary AVRO "Elastic" drag carpet available did not cover the high lift cases at speeds less than M = 1.15 and hence had to be extrapolated. The extrapolated estimate does not agree with the newer data of Ref. (2) but the resulting differences are not likely to have an appreciable effect on the placement probabilities for fighters having initial speeds of M = 1.5 or greater.

the NAE estimate and 1.63 according to the AVRO estimate. It should be noted that the specification of the turning performance at one flight condition does not define the turning performance in general, nor does it necessarily identify the particular aircraft and engine performance estimates from which the turning performance is calculated. For example, the thrust of two different engines may be the same at Mach number 1.5 but different at Mach number 2.0. This is actually the case for two versions of the Iroquois engine.

For the cases listed below, fighter trajectories in target coordinates have been obtained for port and starboard turns beginning at various course differences. These initial course differences were 75, 90, 110, 135, 160 and 180 degrees, except in the cases marked with an asterisk in which the first two, 75 and 90 degrees, were omitted. Some of the cases at 60,000 feet are not practical in the sense that with the performance estimates used, the CF-105 could not fly steadily at the initial conditions stated. However, these cases are worth study since they may be attainable by zooming and in any case they enable trends with increasing altitude to be estimated.

Aerodynamics and Weight	Initial Fighter Mach No.	Target Mach No.	Altitudes (feet)	Methods Used	Remarks
NAE 28% e.g. "pessimistic" 50,000 lb.	1.5	0.85	40,000 50,000	REAC	Published in Ref(1)
		1.2 1.5 2.0	50,000		
	2.0	0.85	60,000 40,000 50,000	REAC graphical	Not published but available at CARDE.
		1.2 1.5 2.0	50,000 60,000		
AVRO"Elastic" 51,600 lb.	1.5	1.5	50,000	numerical graphical	Not published but available at CARDE.
	1.5	2.0	40,000* 50,000 60,000*		
	2.0	1.5	50,000		
	2.0	2.0	50,000 60,000*		

Description of Method

The fighter is assumed to make horizontal coordinated turns at maximum lift as defined below and at maximum thrust with full reheat, decelerating as required when the drag exceeds the thrust. The NACA standard atmosphere is used and only altitudes in the stratosphere are considered.

Maximum Lift

The maximum lift is limited by stall, buffet, maximum control deflection, maximum control hinge moment and by the maximum that the pilot or autopilot will demand. Because the first three of these are each proportional to the atmospheric pressure, it is convenient to denote their combined limit by one symbol, Lm_B, and write

$$Lm_B = \left[\frac{Lm_B}{p_o}\right] \times p_t \qquad (1)$$

where $\frac{Lm_B}{p_o}$ is a function of Mach number, M, only, and p_o is the atmospheric pressure. The hinge moment limit is given by

$$Lm_{HM} = Lm_{HM1} + \left[\frac{Lm_{HM2}}{p_o}\right] \cdot p_o \qquad (2)$$

where Lm_{HM1} and $\frac{Lm_{HM2}}{p_o}$ are functions of M only.

The limit imposed by the pilot or autopilot is given by

$$Lm_P = n_P W \qquad (3)$$

where n_P is the pilot or autopilot limited load factor.

The maximum lift is the smaller of Lm_B, Lm_{HM}, and Lm_P,

that is: $Lm \leqslant Lm_B$, $Lm \leqslant Lm_{HM}$, $Lm \leqslant Lm_P$. (4)

Drag

In general, drag is given by

$$D = p_o \cdot f\left(M, \frac{L}{p_o}\right) . \qquad (5)$$

f is often given graphically as a function of M and L/p_o by means of a drag carpet. Over a useful range of L/p_o, f is approximately a quadratic function of L/p_o. Then D can be written

$$D = \frac{D_o}{p_o} p_o + K_1 L + \frac{F}{p_o} L^2 \qquad (6)$$

where $\frac{D_o}{p_o}$, K_1 and F are functions of M only.

Thrust

Maximum thrust with afterburner is a function of Mach number and altitude. In the case of the NAE aerodynamics the thrust is given by

$$T = \frac{T}{p_o} . p_o \qquad (7)$$

where $\frac{T}{p_o}$ is a function of M only, in the stratosphere.

In the case of the AVRO aerodynamics, equation (7) is an approximation and the thrust carpets of Ref.(3) should be used when possible.

Use of the REAC to Obtain Fighter Trajectories

The REAC circuit used is shown in Figure (2). The forces Lm, D, and T were simulated according to equations (1), (2), (4), (6), (7). Because of difficulties in generating the function $\frac{Lm_B}{po}$ in the neighbourhood of M = 1, it was expressed as

$$\frac{Lm_B}{po} = C_1 + C_2 V_F + \Delta \frac{Lm_B}{p_o} \qquad (8)$$

where C_1 and C_2 are constants. In the case of NAE 28% cg. "pessimistic" aerodynamics, C_1 = 88 ft.^{2}, and C_2 = 0.3553 ft.sec. No pilot limited load factor as such was used, but in no case done on the REAC did Lm_B and Lm_{HM} exceed 200,000 lb. which is equivalent to n = 4.

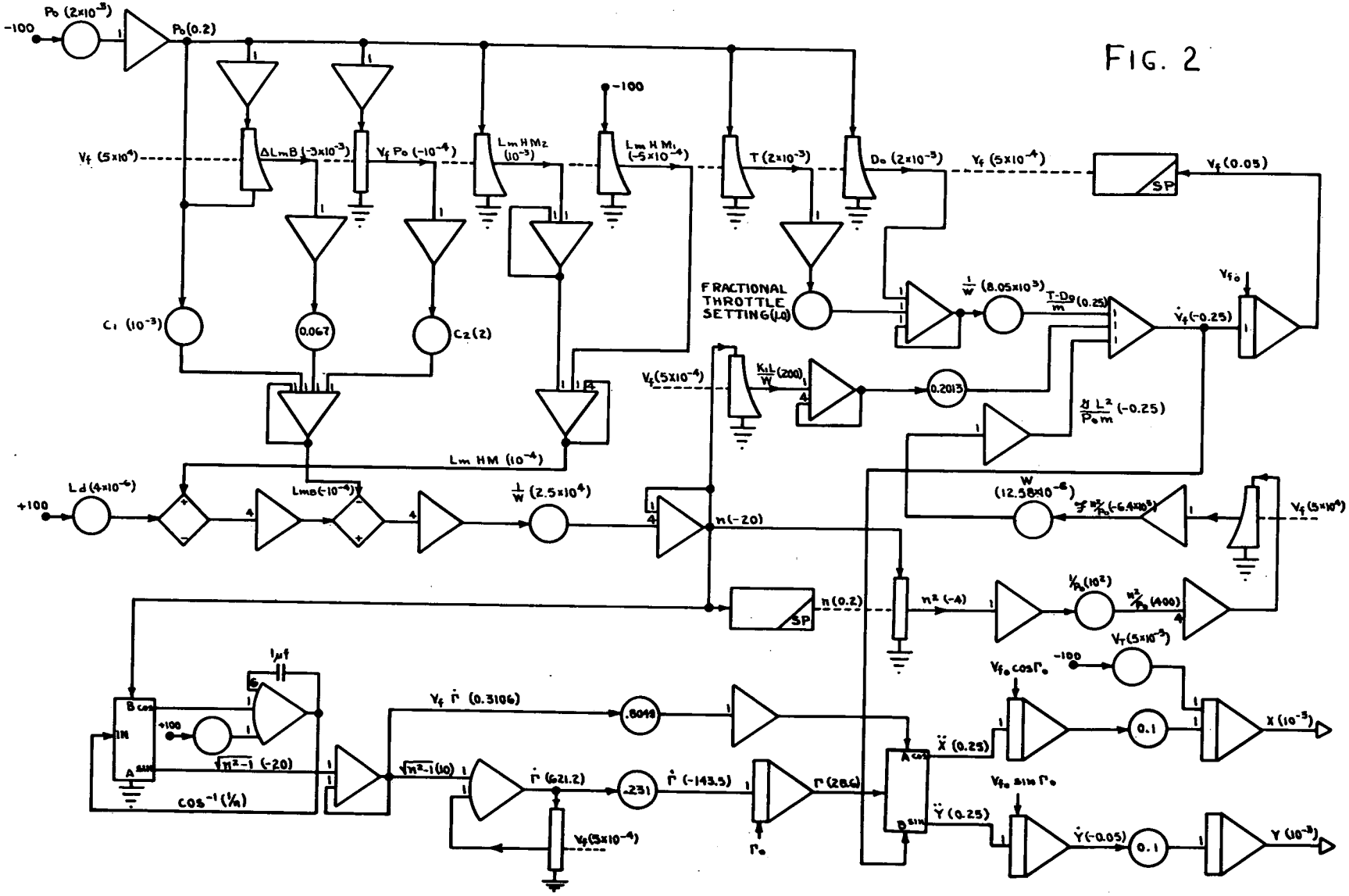
-100
P_o (2×10^{-3})
P_o(0.2)
V_f (5×10^{-4})
$\Delta L_m B$ (-3×10^{-3})
$V_f P_o$ (-10^{-4})
$L_m H M_2$ (10^{-3})
$L_m H M_1$ (-5×10^{-4})
T (2×10^{-3})
D_o (2×10^{-3})
V_f (5×10^{-4})
SP
V_f(0.05)
C_1 (10^{-3})
0.067
C_2(2)
FRACTIONAL THROTTLE SETTING(1.0)
$\frac{1}{W}$ (8.05×10^{3})
$\frac{T-D_o}{m}$(0.25)
$\dot{V}_f$(-0.25)
V_{f_o}
V_f(5×10^{-4})
$\frac{K_1 L}{W}$(200)
0.2013
$\frac{J L^2}{P_o m}$(-0.25)
$L_m HM$ (10^{-4})
+100
L_d(4×10^{-4})
$L_m B$(10^{-4})
$\frac{1}{W}$ (2.5×10^{4})
n(-20)
W (12.58×10^{-6})
V_f(5×10^{-4})
n(0.2)
n^2(-4)
$\frac{V}{P_o}$(10^2)
$\frac{n^2}{P_o}$(400)
V_T(5×10^{-5})
1μf
$V_f \dot{\Gamma}$ (0.3106)
.8048
$V_{f_o}\cos\Gamma_o$
-100
$\ddot{X}$ (0.25)
0.1
X (10^{-5})
$\sqrt{n^2-1}$ (-20)
$\cos^{-1}(1/n)$
$\sqrt{n^2-1}$(10)
$\dot{\Gamma}$ (621.2)
-231
$\dot{\Gamma}$ (-143.5)
Γ (28.6)
Γ_o
$V_{f_o}\sin\Gamma_o$
$\ddot{Y}$ (0.25)
$\dot{Y}$(-0.05)
0.1
Y (10^{-3})

FIG. 2

The equations of motion given below were solved by the REAC and the trajectories were drawn directly in target coordinates by an XY plotter. See Figure (3).

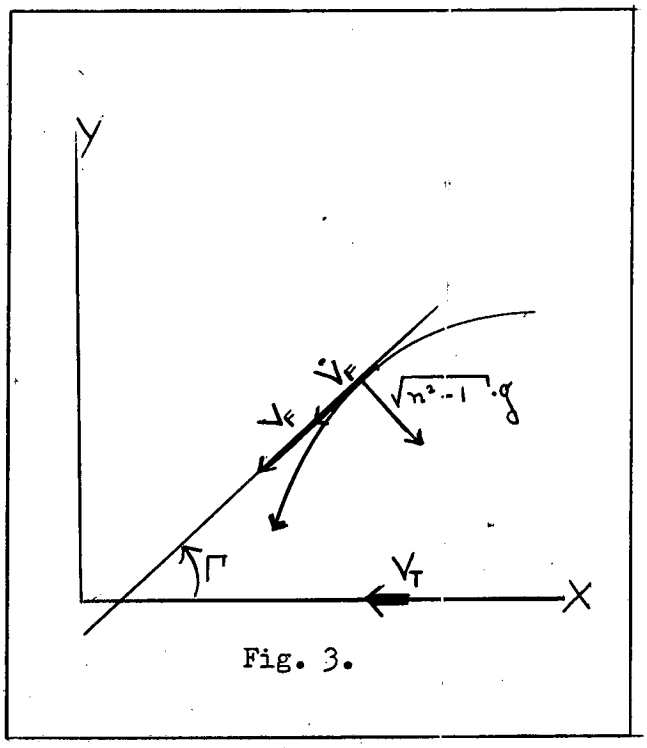

Fig. 3.

Equations of Motion

$$\dot{V}_F = \frac{T - D}{m} \qquad (9)$$

where $m = \frac{W}{g}$. (The small variation of W with time is ignored).

$$V_F \dot{\Gamma} = \sqrt{n^2 - 1} \cdot g \qquad (10)$$

where $n = \frac{Lm}{W}$. (For starboard turns the sign of $\dot{\Gamma}$ is reversed).

Γ is the course difference.

$$\ddot{x} = -\dot{V}_F \cos\Gamma + \dot{\Gamma} V_F \sin\Gamma \qquad (11)$$

$$\ddot{y} = -\dot{V}_F \sin\Gamma - \dot{\Gamma} V_F \cos\Gamma \qquad (12)$$

Initial conditions:

V_{Fo} and Γ_o are parameters to be varied.

x_o and y_o were chosen as required in setting up the XY plotter.

$$\dot{x}_o = -V_{Fo} \cos\Gamma_o + V_T \qquad (13)$$

$$\dot{y}_o = -V_{Fo} \sin\Gamma_o \qquad (14)$$

In equation (13) the addition of V_T to $\dot{x}_o$ causes the solution to be in target coordinates.

Because this REAC computation is open loop, all errors developed are integrated and become steadily greater as the motion proceeds. The errors in the region of M = 1.0 are somewhat larger than at higher speeds because of difficulties in generating some of the aerodynamic functions. Therefore the

parts of the trajectories at speeds less than M = 0.85 are not considered to be reliable. This is not important, however, except in the case of initial fighter speeds less than M = 1.5.

Numerical and Graphical Method of Obtaining Fighter Trajectories

The forces Lm and D were calculated using equations (1), (3), (4), (5). The AVRO data showed that there was no hinge moment limit. The pilot or autopilot limited load factor, n_p, was taken to be 4.0 in accordance with an informal communication from AVRO Aircraft Limited. The thrust was obtained from thrust carpets in Ref. (3). The equations of motion given below were integrated numerically to obtain the trajectories in space coordinates at Mach number intervals of 0.1. See Fig. (4).

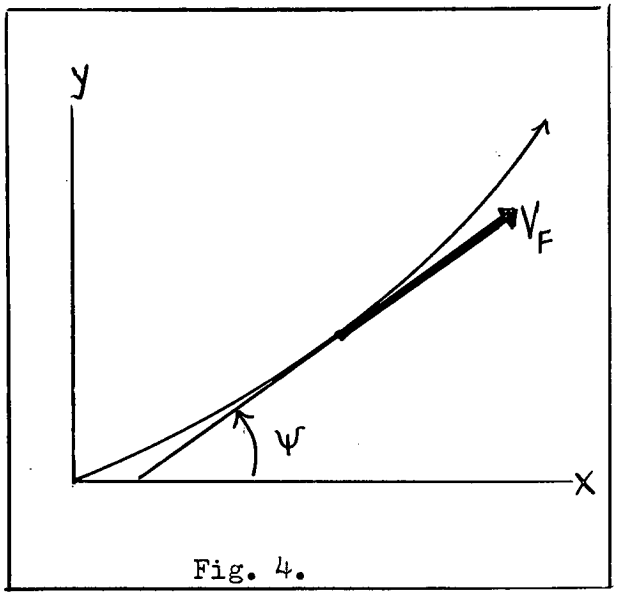

Fig. 4.

$$\frac{dt}{dM} = \frac{-a}{g}\frac{W}{(D - T)} \qquad (15)$$

where a is the speed of sound and g = 32.2.

$$\frac{d\psi}{dt} = \frac{g}{aM}\sqrt{n^2 - 1} \qquad (16)$$

where $n = \frac{Lm}{W}$

$$\dot{x} = aM \cos\psi \qquad (17)$$

$$\dot{y} = aM \sin\psi \qquad (18)$$

Because the small variation of W with time can be ignored and D - T is a function of M only at constant altitude, equation (15) can be solved by a simple numerical integration.

To obtain the trajectories in target coordinates from the ones in space coordinates, it is necessary to subtract the target motion in a direction determined by the initial course difference. This was done by using a standard drafting machine with a specially prepared paper scale attached, showing the distance travelled by the target during the time it took the fighter to reach each point on the space trajectory. Only one scale is required for all initial course differences, at a given altitude and target speed. The same method can be used to obtain the trajectories in target coordinates from the space trajectories obtained from the REAC, thus reducing the number of REAC runs required. In order to do this the time taken to reach given points on the space trajectory must be available from the REAC.

From the experience gained with the two methods it appears that the fighter trajectories in target coordinates for non-evading targets can be obtained more efficiently by the numerical-graphical method.

References

1. CARDE Technical Letter N-47-12 "Second Quarterly Report on CF-105 Weapon System Assessment". Appendix B "Aerodynamics" by B. Cheers, Nov. 1956. SECRET. U.

2. AVRO Aircraft Limited, "CF-105 Periodic Performance Report No. 9". Nov/Dec 1956. SECRET.

3. AVRO Aircraft Limited "CF-105 Periodic Performance Report No. 10". Dec. 1956. SECRET.

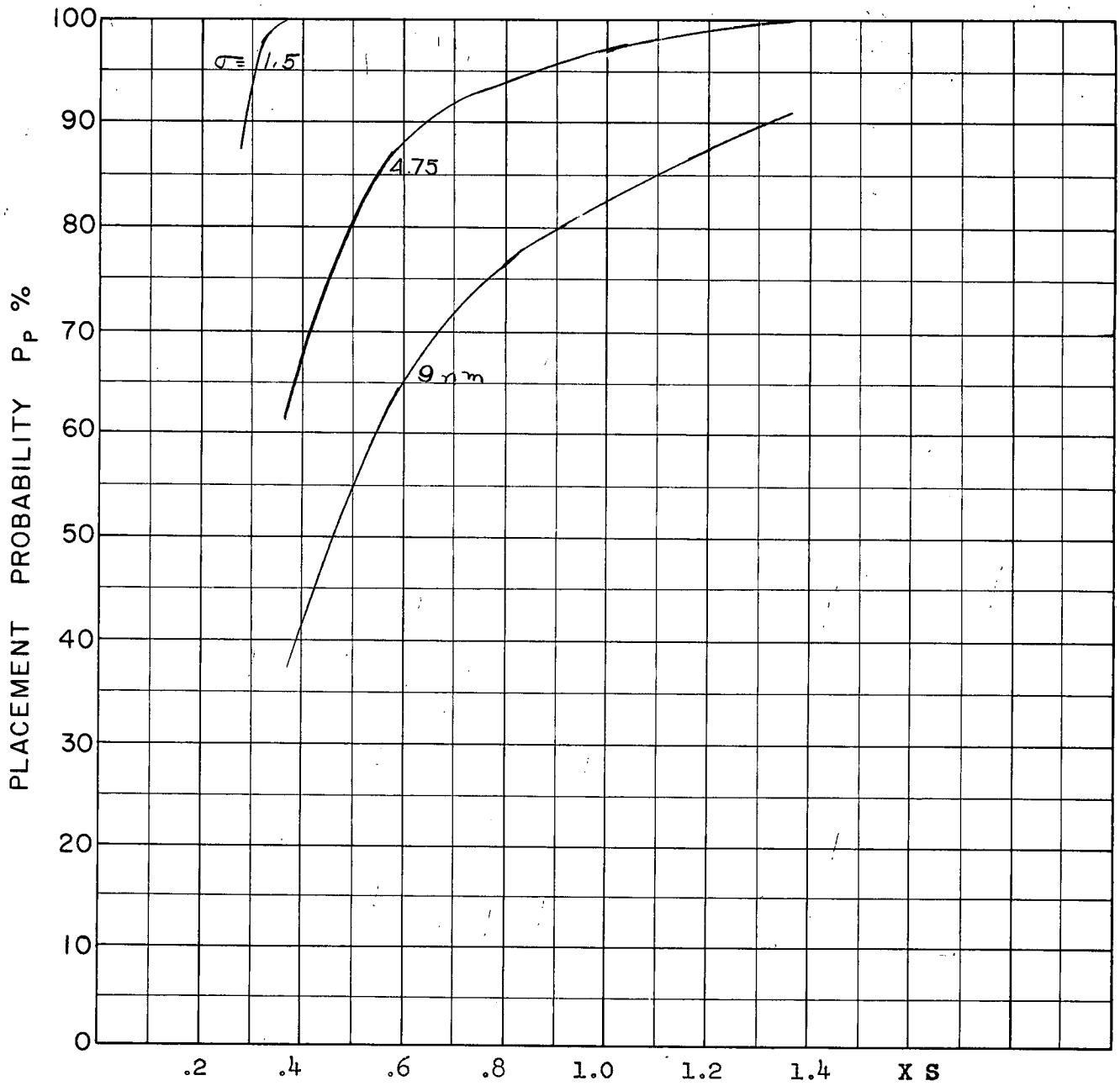

A.I. RANGE

FIG 5
D

COURSE DIFFERENCE: 110°
TARGET EVASION: 0
TARGET MACH NO.: 1.5
INTERCEPTOR LATERAL G's: N.A.E. 28% Pessimistic Aerodynamics
INTERCEPTOR MACH NO.: 1.5 Initial
σ OF G.C.I. ACCURACY: 3 Values
A.I. DETECTION RANGE AS FRACTION OF SPECIFICATION RANGE, S: ABSCISSA
A.I. DETECTION RANGE CONTOUR: Delta
ALTITUDE: 50 K

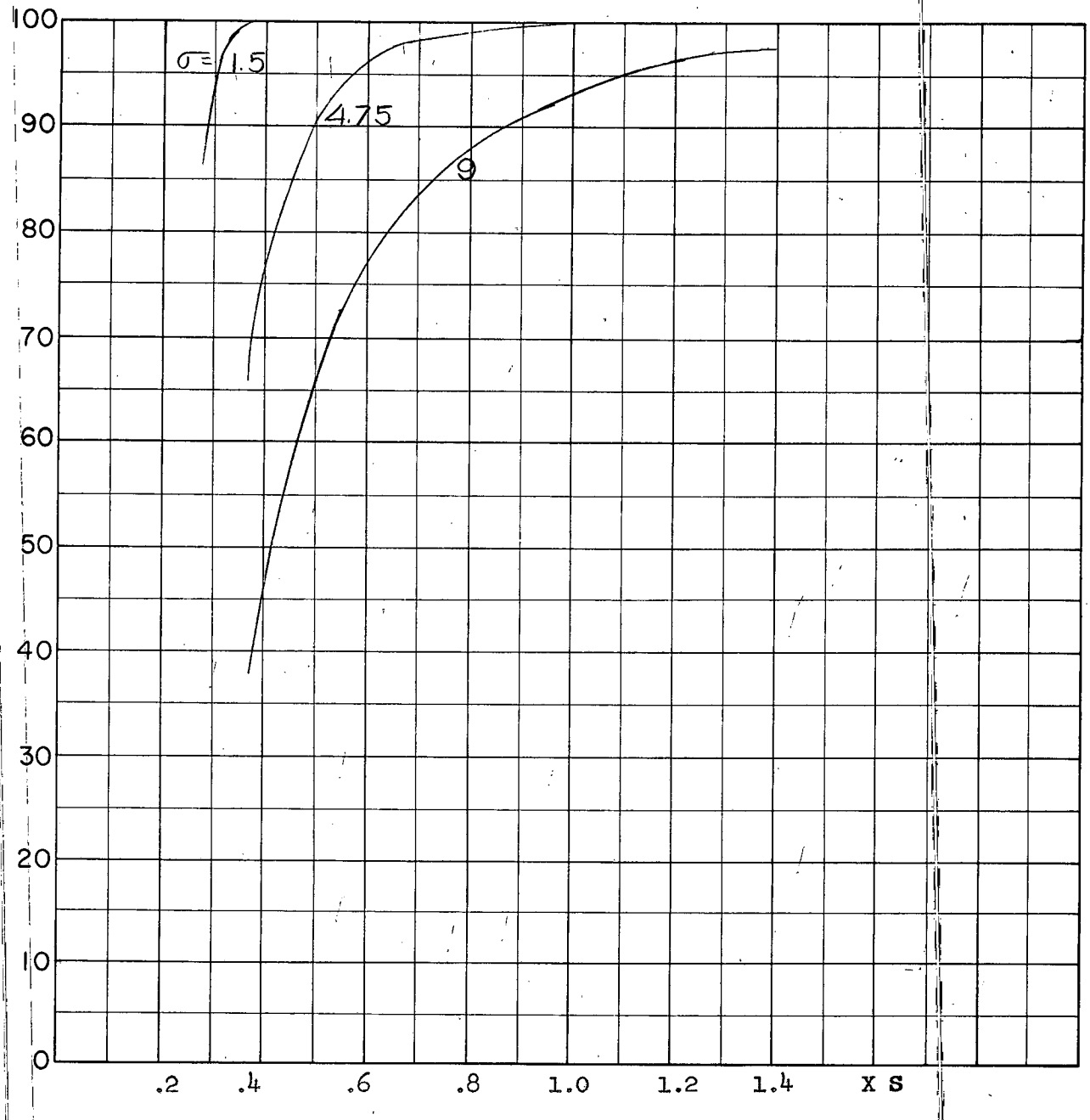

FIG 6 D

COURSE DIFFERENCE: 135°
TARGET EVASION: 0
TARGET MACH NO.: 1.5
INTERCEPTOR LATERAL G's: N.A.E. 28% Pessimistic Aerodynamics
INTERCEPTOR MACH NO.: 1.5 Initial
σ OF G.C.I. ACCURACY: 3 Values
A.I. DETECTION RANGE AS FRACTION OF SPECIFICATION RANGE, S: ABSCISSA
A.I. DETECTION RANGE CONTOUR: Delta
ALTITUDE: 50 K

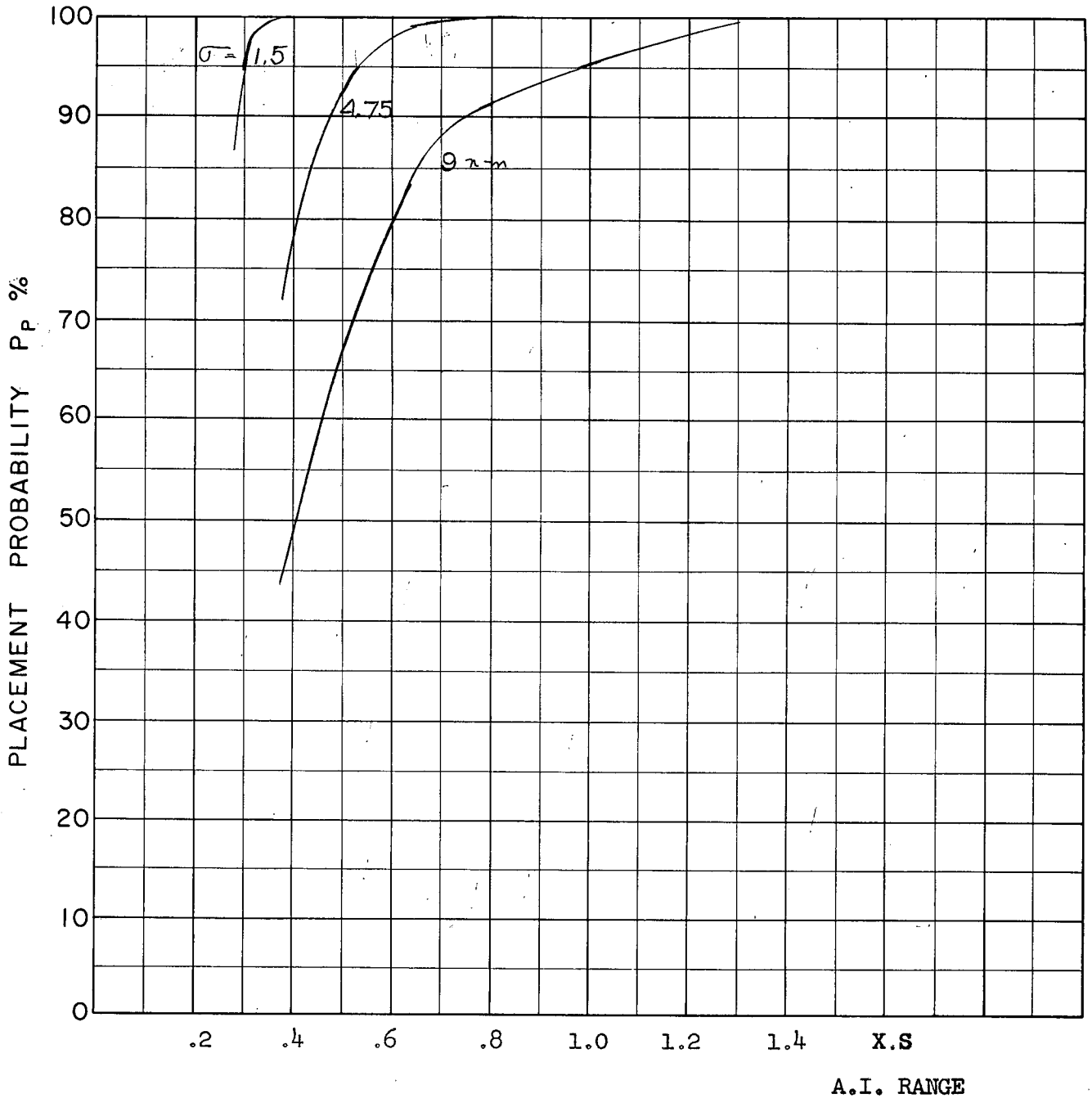

COURSE DIFFERENCE: 160°
TARGET EVASION: 0
TARGET MACH NO.: 1.5
INTERCEPTOR LATERAL G's: N.A.E. 28% Pessimistic Aerodynamics
INTERCEPTOR MACH NO.: 1.5 Initial
σ OF G.C.I. ACCURACY: 3 Values
A.I. DETECTION RANGE AS FRACTION OF SPECIFICATION RANGE, S: ABSCISSA
A.I. DETECTION RANGE CONTOUR: Delta
ALTITUDE: 50K

FIG 7
D

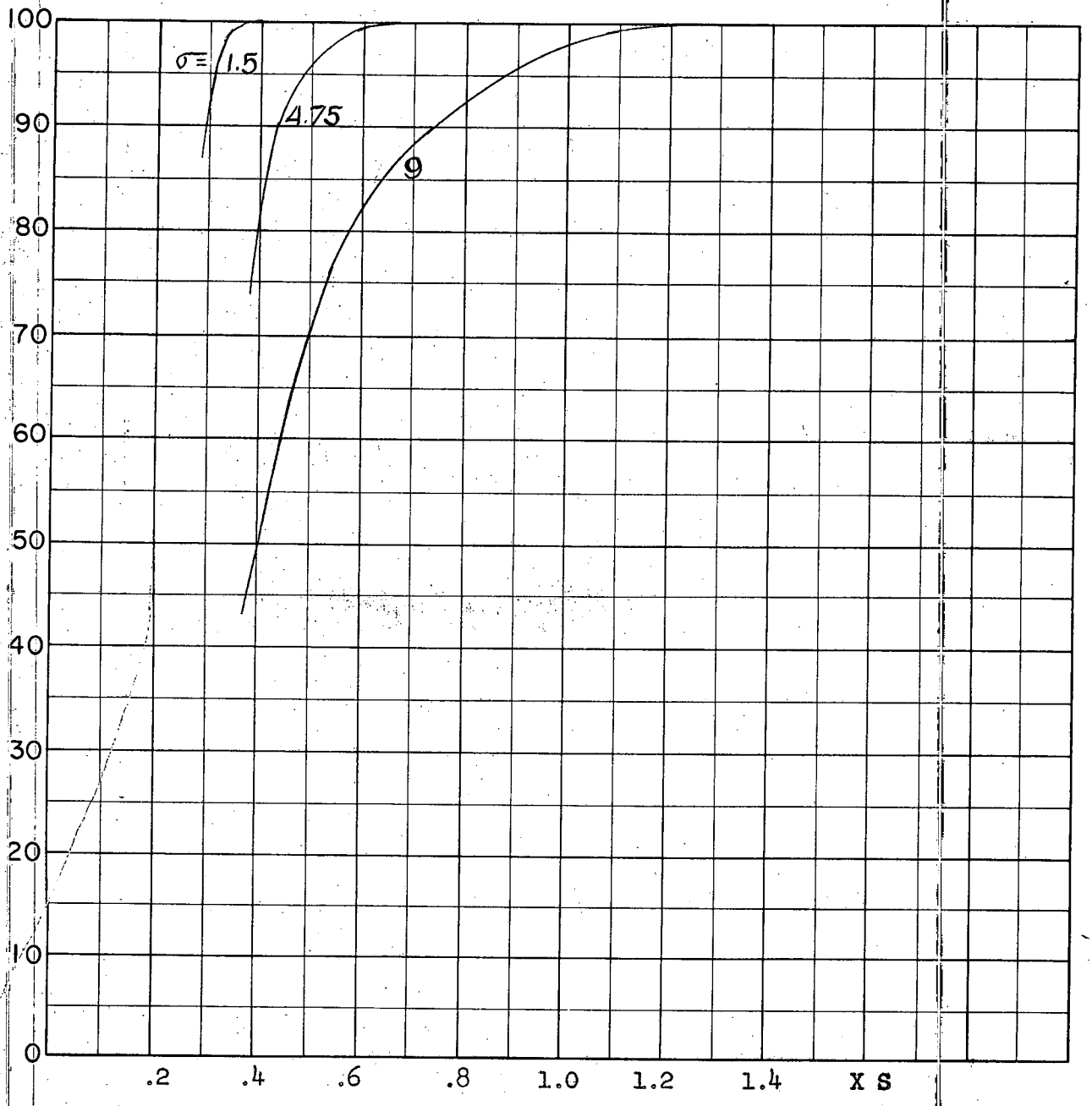

COURSE DIFFERENCE: 180°
TARGET EVASION: 0
TARGET MACH NO.: 1.5
INTERCEPTOR LATERAL G's: N.A.E. 28% Pessimistic Aerodynamics
INTERCEPTOR MACH NO.: 1.5 Initial
σ OF G.C.I. ACCURACY: 3 Values
A.I. DETECTION RANGE AS FRACTION OF SPECIFICATION RANGE, S: ABSCISSA
A.I. DETECTION RANGE CONTOUR: Delta
ALTITUDE: 50 K

FIG 8 D

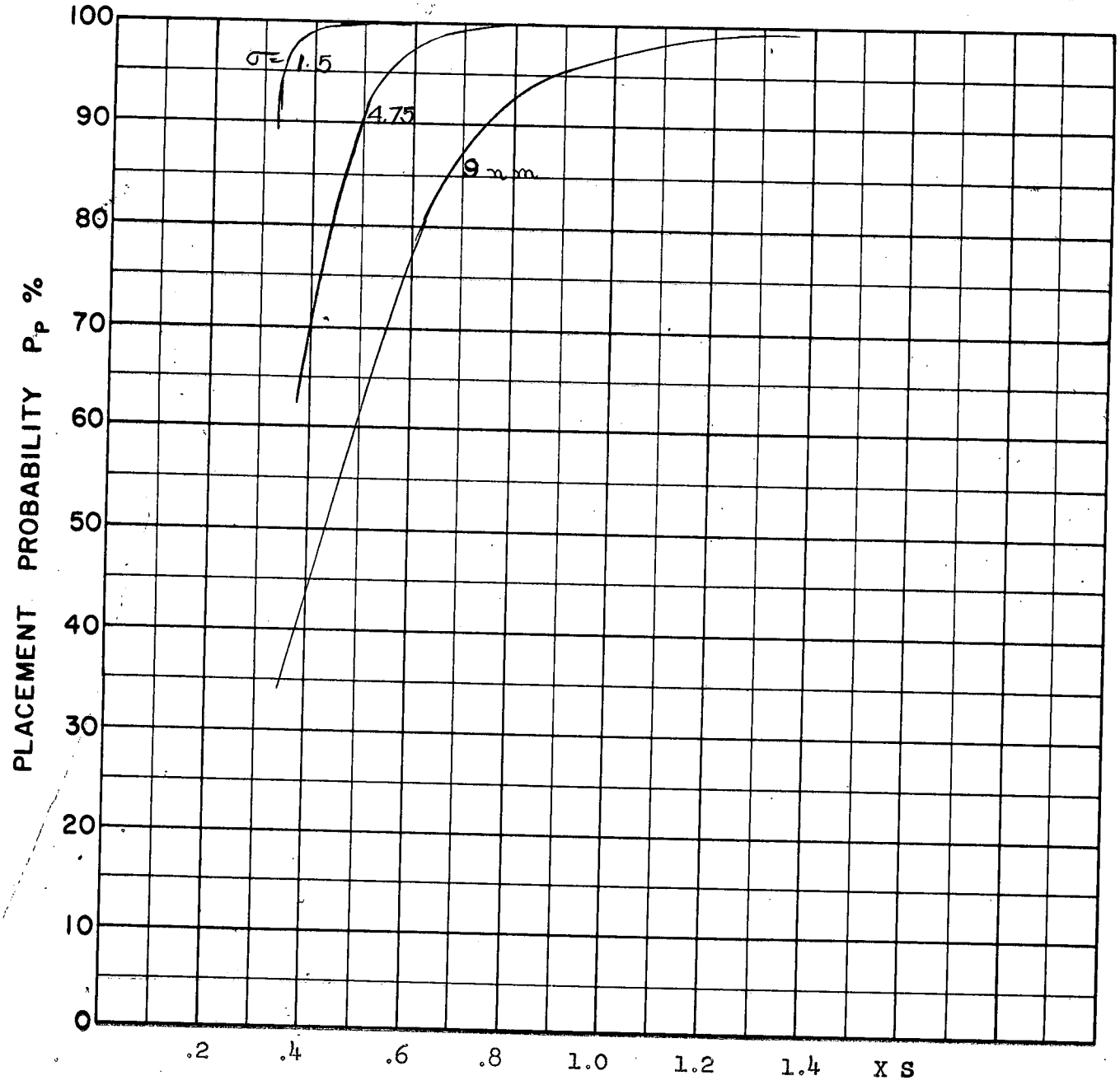

COURSE DIFFERENCE: 110°
TARGET EVASION: 0
TARGET MACH NO.: 1.5
INTERCEPTOR LATERAL G's: N.A.E. 28 % Pessimistic Aerodynamics
INTERCEPTOR MACH NO.: 2.0 Initial
σ OF G.C.I. ACCURACY: 3 Values
A.I. DETECTION RANGE AS FRACTION OF SPECIFICATION RANGE, S: ABSCISSA
A.I. DETECTION RANGE CONTOUR: Delta
ALTITUDE: 50 K

FIG. 9 D

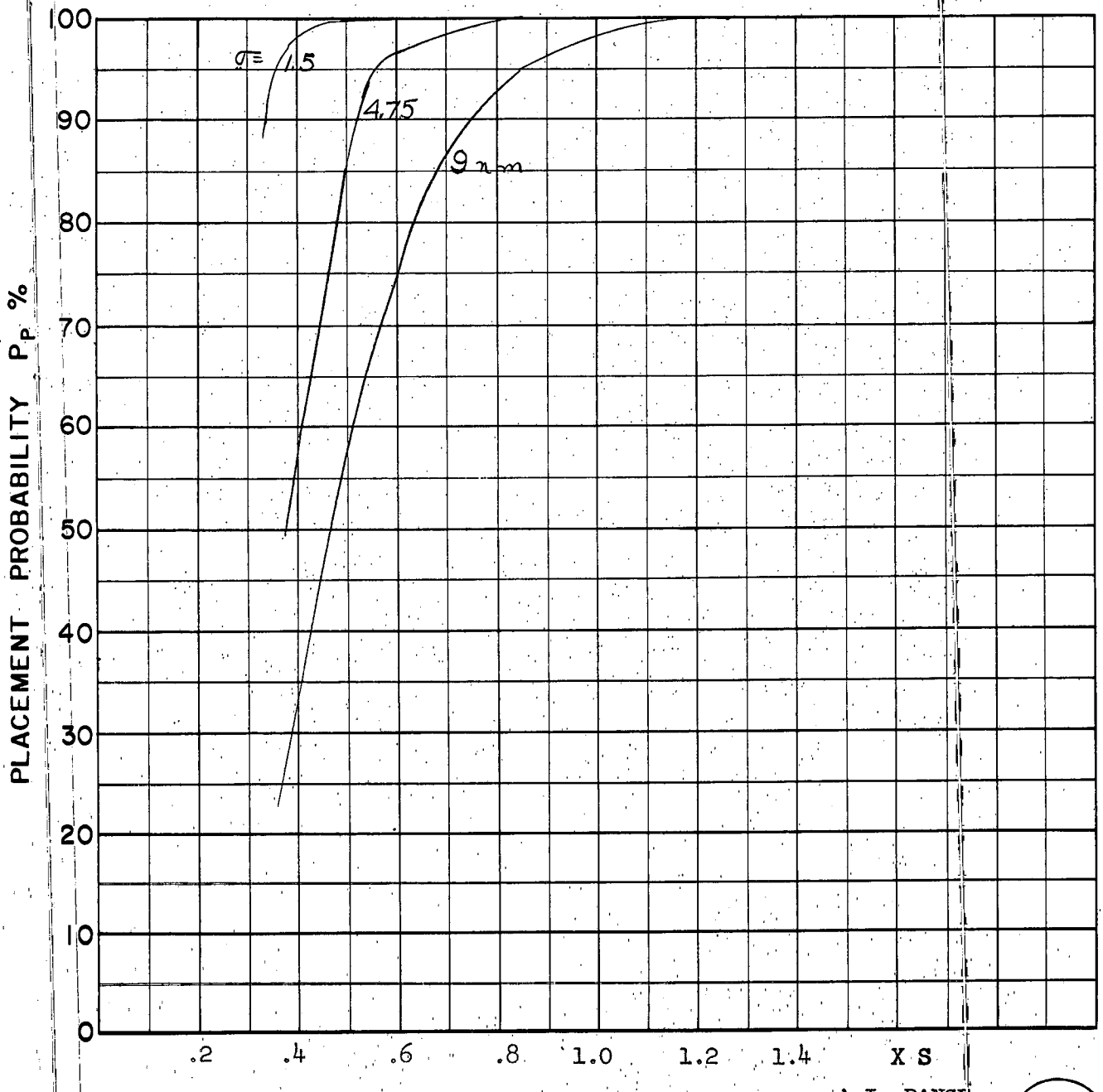

FIG 10 D

COURSE DIFFERENCE: 135°
TARGET EVASION: 0
TARGET MACH NO.: 1.5
INTERCEPTOR LATERAL G's: N.A.E. 28% Pessimistic Aerodynamics
INTERCEPTOR MACH NO.: 2.0 Initial
σ OF G.C.I. ACCURACY: 3 Values
A.I. DETECTION RANGE AS FRACTION OF SPECIFICATION RANGE, S: ABSCISSA
A.I. DETECTION RANGE CONTOUR: Delta
ALTITUDE: 50 K

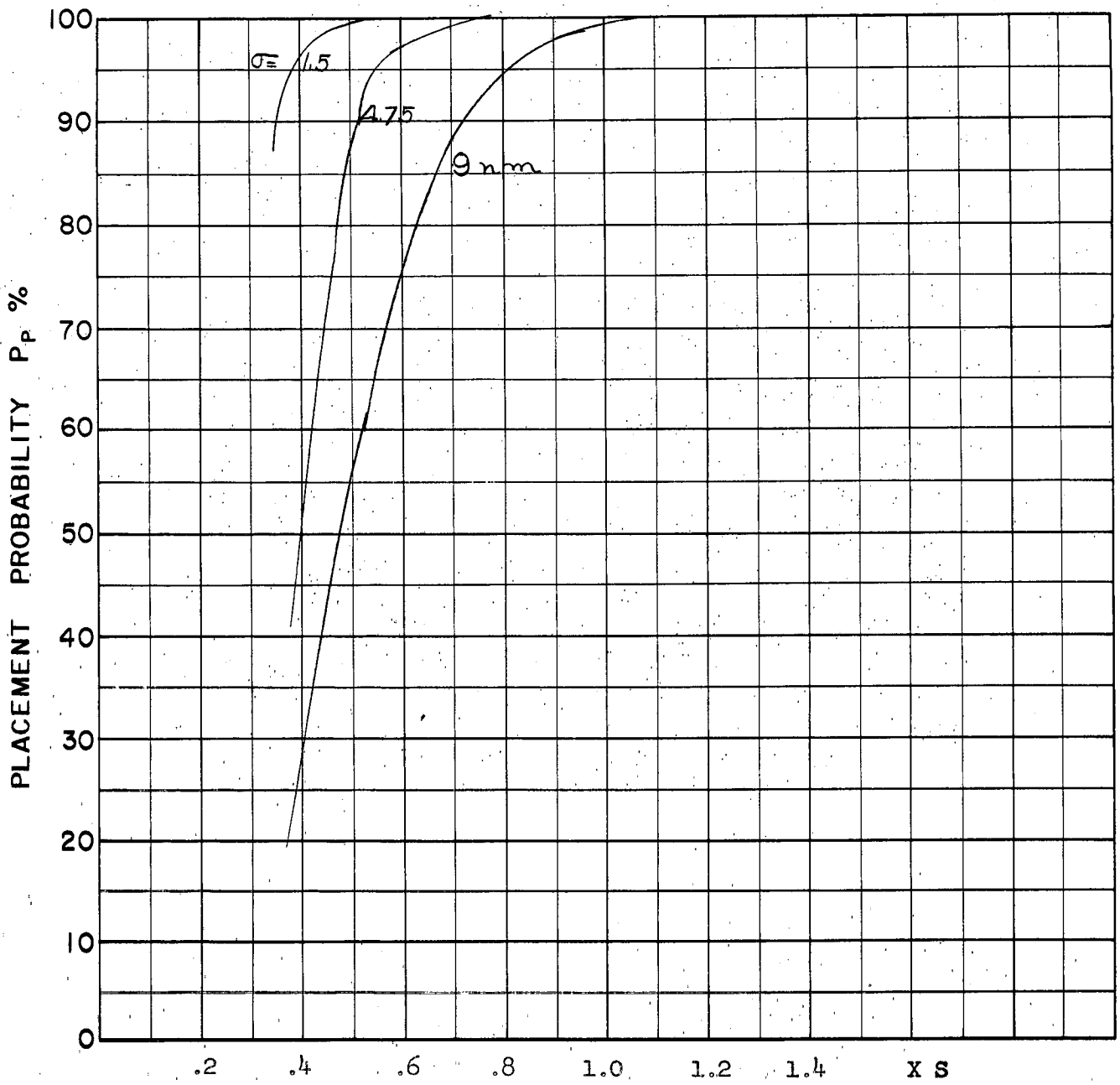

A.I. RANGE

FIG 11 D

COURSE DIFFERENCE: 160°
TARGET EVASION: 0
TARGET MACH NO.: 1.5
INTERCEPTOR LATERAL G's: N.A.E. 28 % Pessimistic Aerodynamics
INTERCEPTOR MACH NO.: 2.0 Initial
σ OF G.C.I. ACCURACY: 3 Values
A.I. DETECTION RANGE AS FRACTION OF SPECIFICATION RANGE, S: ABSCISSA
A.I. DETECTION RANGE CONTOUR: Delta
ALTITUDE: 50 K

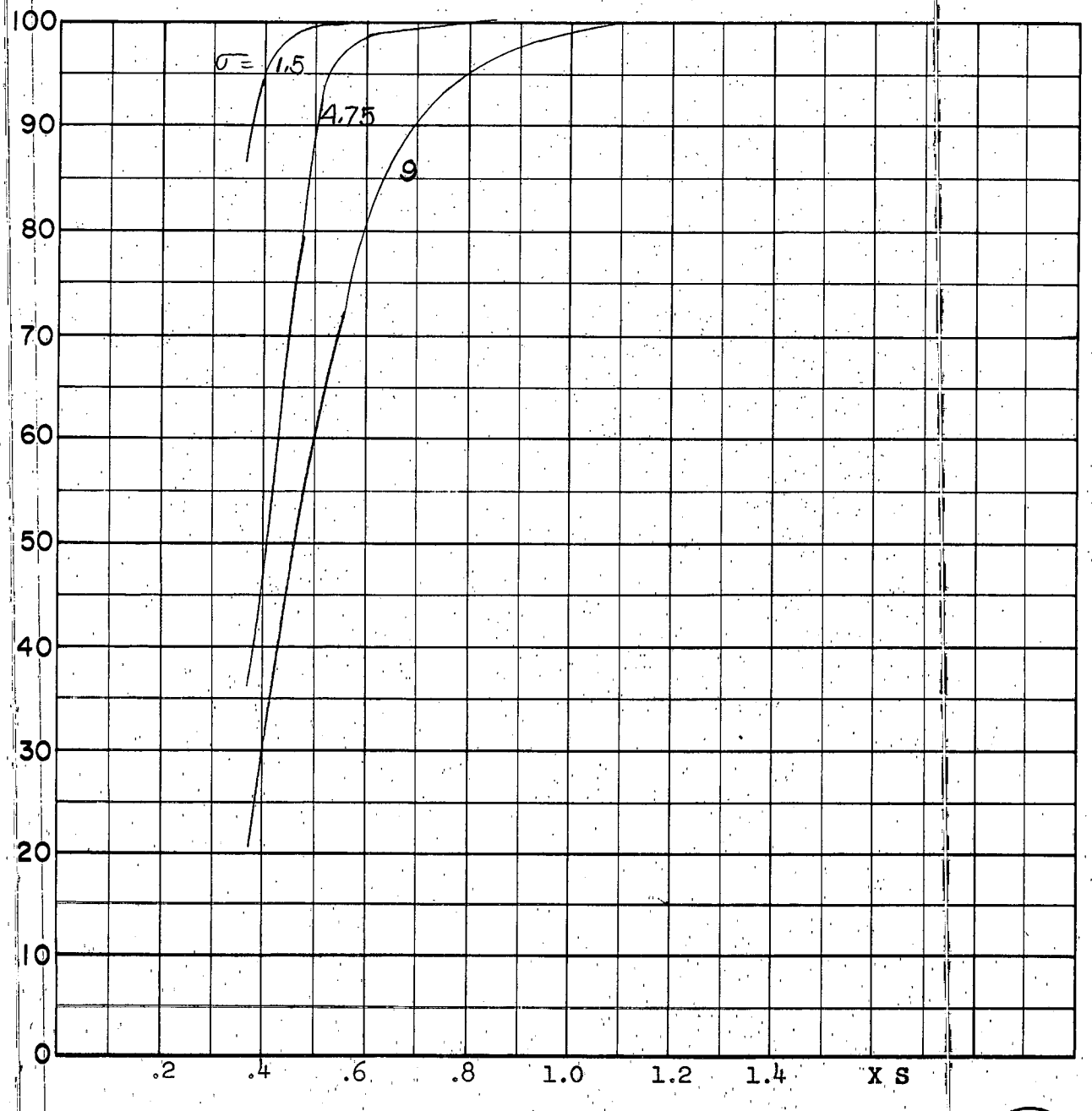

FIG 12 D

COURSE DIFFERENCE: 180°
TARGET EVASION: 0
TARGET MACH NO.: 1.5
INTERCEPTOR LATERAL G's: N.A.E. 28% Pessimistic Aerodynamics
INTERCEPTOR MACH NO.: 2.0 Initial
σ OF G.C.I. ACCURACY: 3 Values
A.I. DETECTION RANGE AS FRACTION OF SPECIFICATION RANGE, S: ABSCISSA
A.I. DETECTION RANGE CONTOUR: Delta
ALTITUDE: 50 K

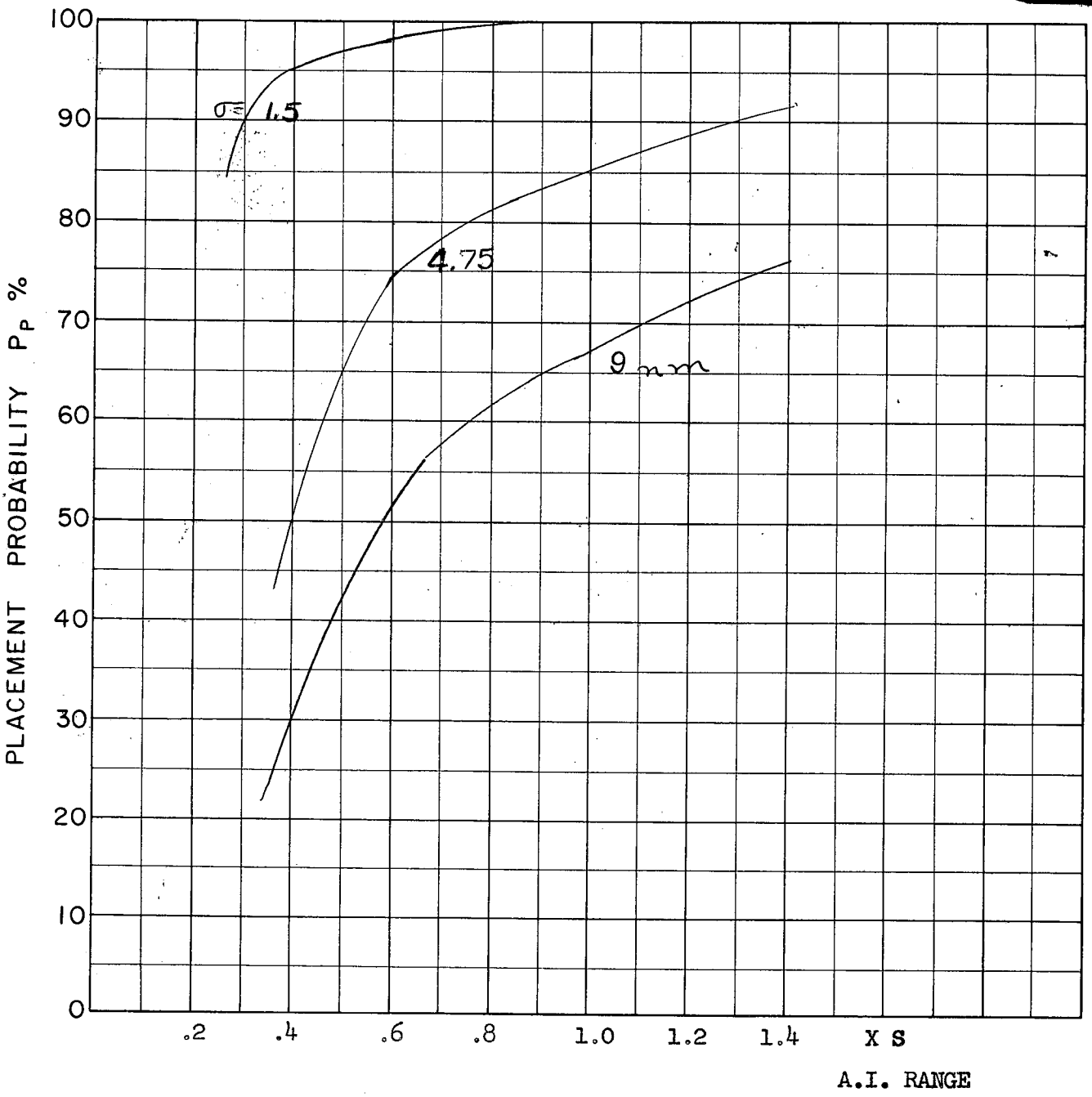

COURSE DIFFERENCE: 110°
TARGET EVASION: 0
TARGET MACH NO.: 2.0
INTERCEPTOR LATERAL G's: N.A.E. 28% Pessimistic Aerodynamics
INTERCEPTOR MACH NO.: 1.5 Initial
σ OF G.C.I. ACCURACY: 3 Values
A.I. DETECTION RANGE AS FRACTION OF SPECIFICATION RANGE, S: ABSCISSA
A.I. DETECTION RANGE CONTOUR: Delta
ALTITUDE: 50 K

FIG 13 D

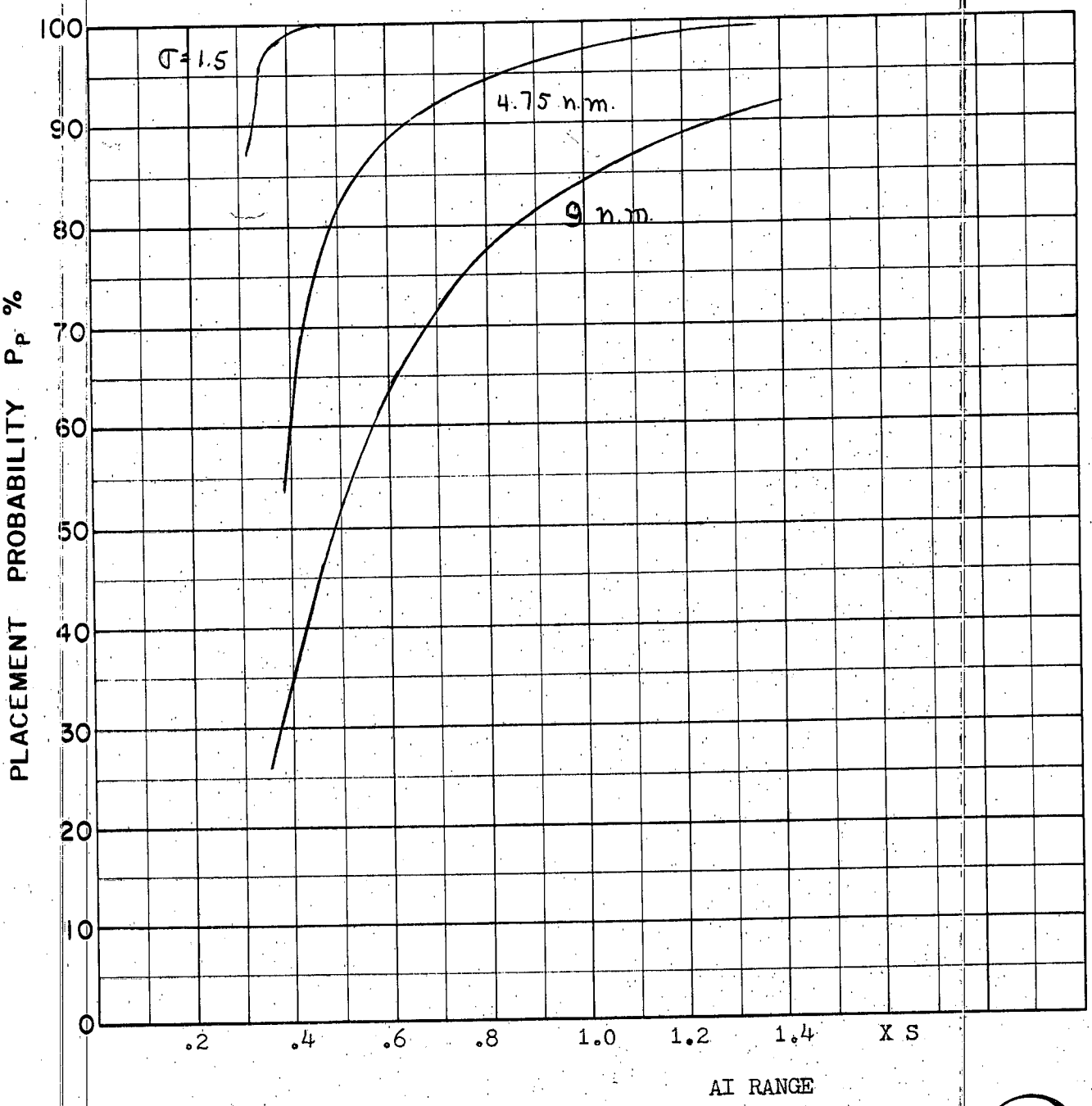

FIG 14 D

COURSE DIFFERENCE: 135°
TARGET EVASION: 0
TARGET MACH NO.: 2.0
INTERCEPTOR LATERAL G's: NAE 28% Pessimistic Aerodynamics
INTERCEPTOR MACH NO.: 1.5 Initial
σ OF G.C.I. ACCURACY: 3 Values
A.I. DETECTION RANGE AS FRACTION OF SPECIFICATION RANGE, S: Abscissa
A.I. DETECTION RANGE CONTOUR: Delta
ALTITUDE: 50 K

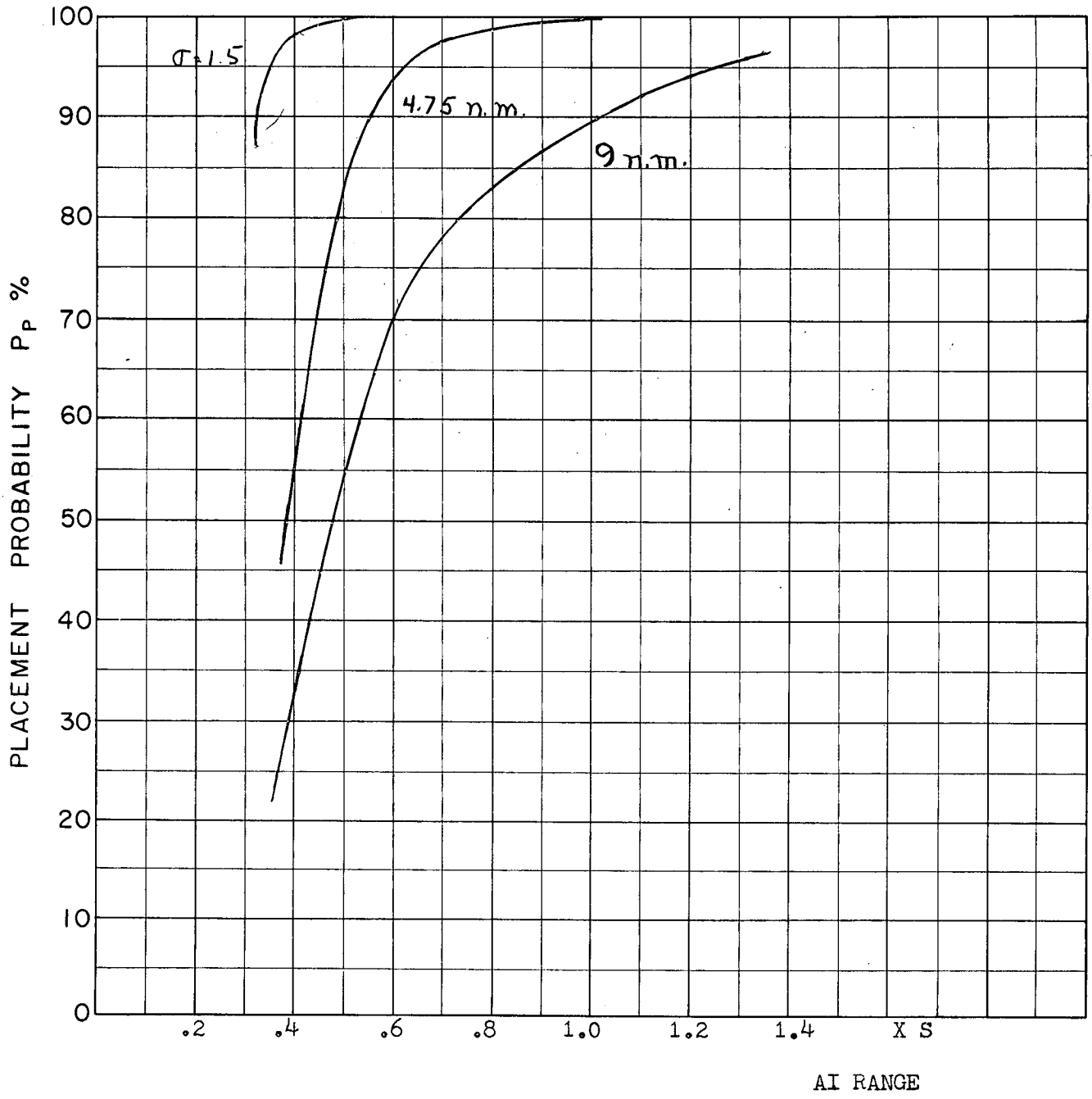

COURSE DIFFERENCE: 160°
TARGET EVASION: 0
TARGET MACH NO.: 2.0
INTERCEPTOR LATERAL G's: NAE 28% Pessimistic Aerodynamics
INTERCEPTOR MACH NO.: 1.5 Initial
σ OF G.C.I. ACCURACY: 3 values
A.I. DETECTION RANGE AS FRACTION OF SPECIFICATION RANGE, S: Abscissa
A.I. DETECTION RANGE CONTOUR: Delta
ALTITUDE: 50 K

F16 15 D

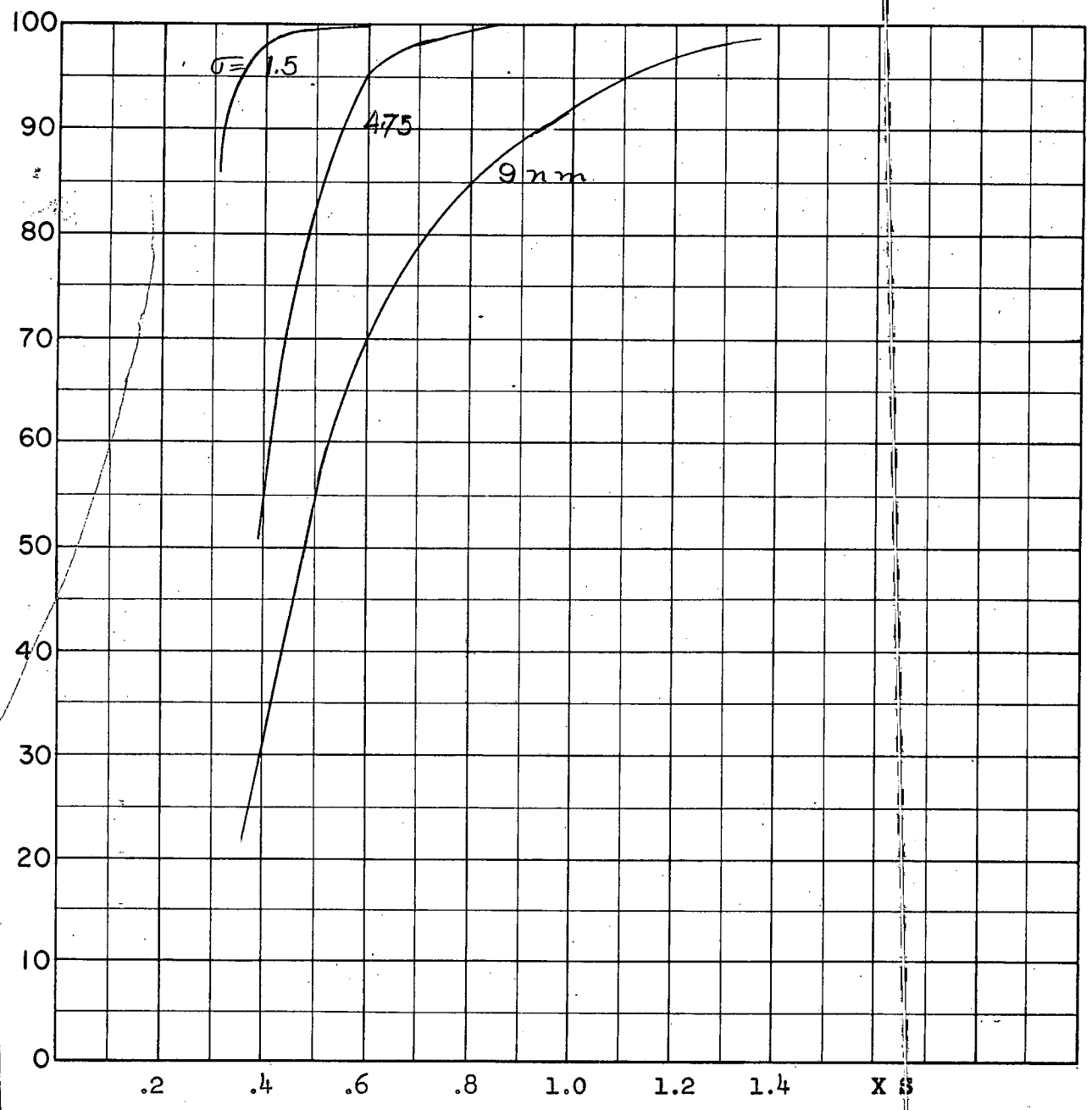

FIG 16 D

COURSE DIFFERENCE: 180°
TARGET EVASION: 0
TARGET MACH NO.: 2.0
INTERCEPTOR LATERAL G's: N.A.E. 28% Pessimistic Aerodynamics
INTERCEPTOR MACH NO.: 1.5 Initial
σ OF G.C.I. ACCURACY: 3 Values
A.I. DETECTION RANGE AS FRACTION OF SPECIFICATION RANGE, S: ABSCISSA
A.I. DETECTION RANGE CONTOUR: Delta
ALTITUDE: 50 K

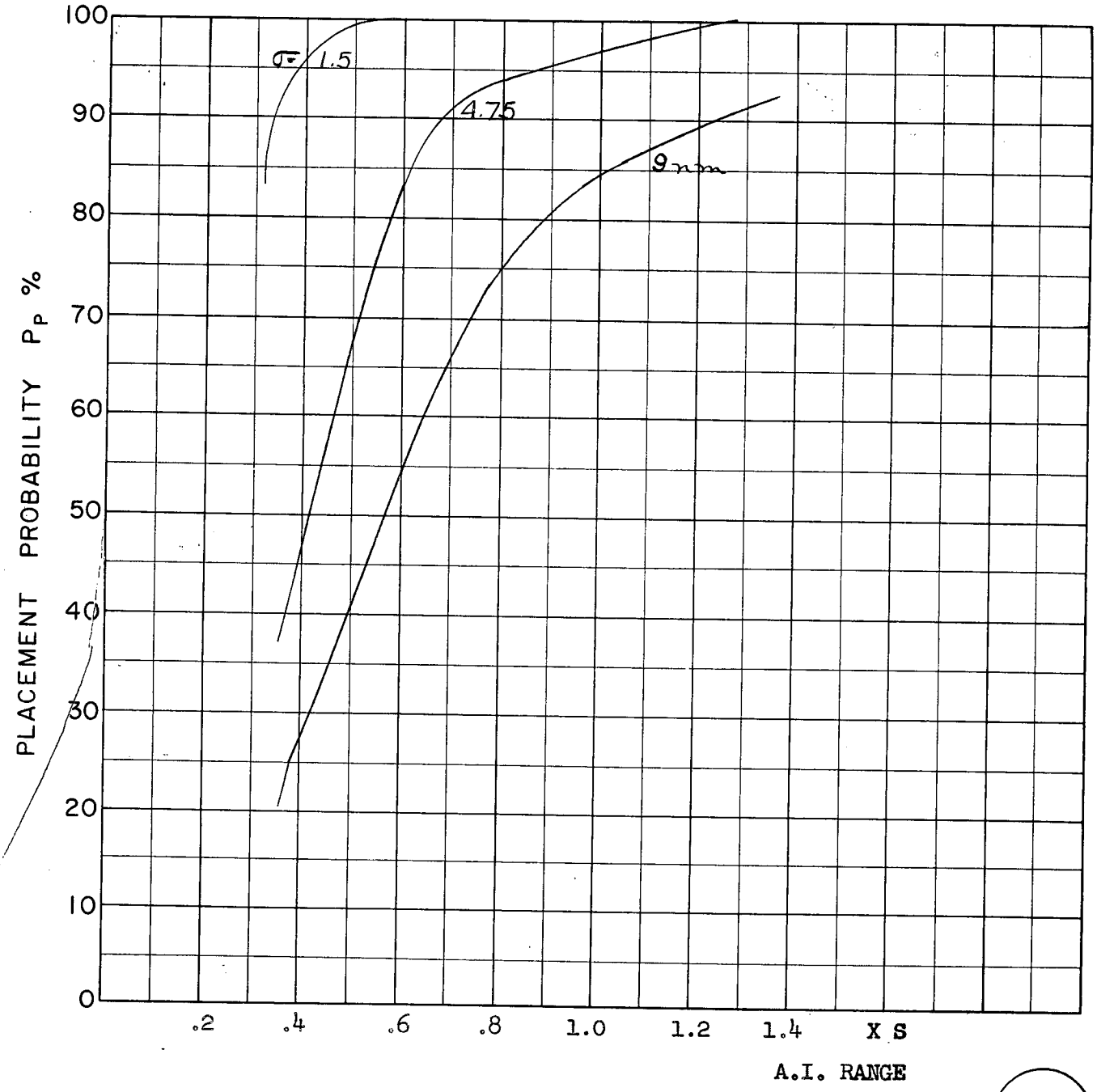

FIG 17
D

COURSE DIFFERENCE: 110°
TARGET EVASION: 0
TARGET MACH NO.: 2.0
INTERCEPTOR LATERAL G's: N.A.E. 28% Pessimistic Aerodynamics
INTERCEPTOR MACH NO.: 2.0 Initial
σ OF G.C.I. ACCURACY: 3 Values
A.I. DETECTION RANGE AS FRACTION OF SPECIFICATION RANGE, S: ABSCISSA
A.I. DETECTION RANGE CONTOUR: Delta
ALTITUDE: 50 K

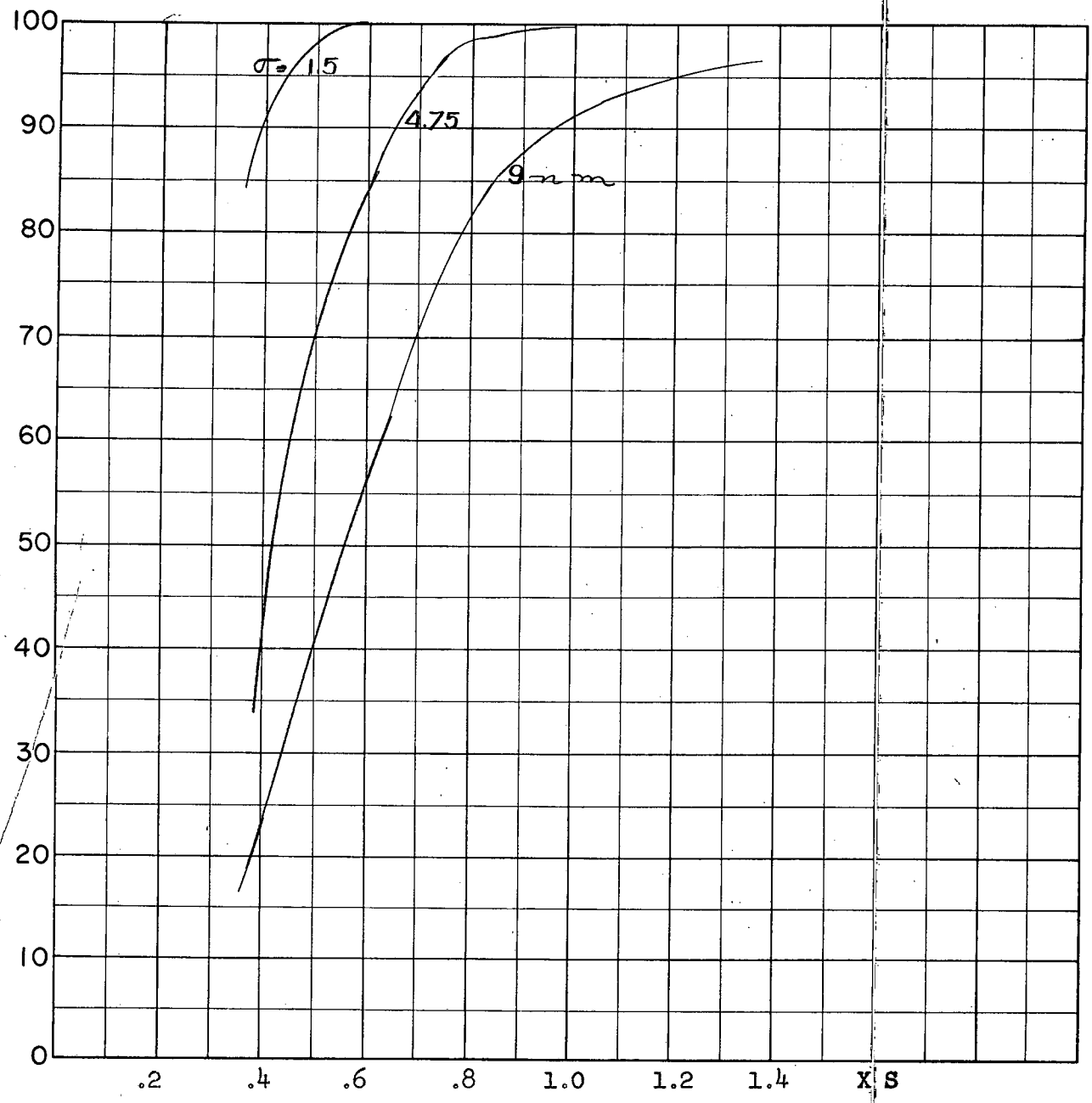

FIG 18 D

COURSE DIFFERENCE: 135°
TARGET EVASION: 0
TARGET MACH NO.: 2.0
INTERCEPTOR LATERAL G's: N.A.E. 28% Pessimistic Aerodynamics
INTERCEPTOR MACH NO.: 2.0 Initial
σ OF G.C.I. ACCURACY: 3 Values
A.I. DETECTION RANGE AS FRACTION OF SPECIFICATION RANGE, S: ABSCISSA
A.I. DETECTION RANGE CONTOUR: Delta
ALTITUDE: 50 K

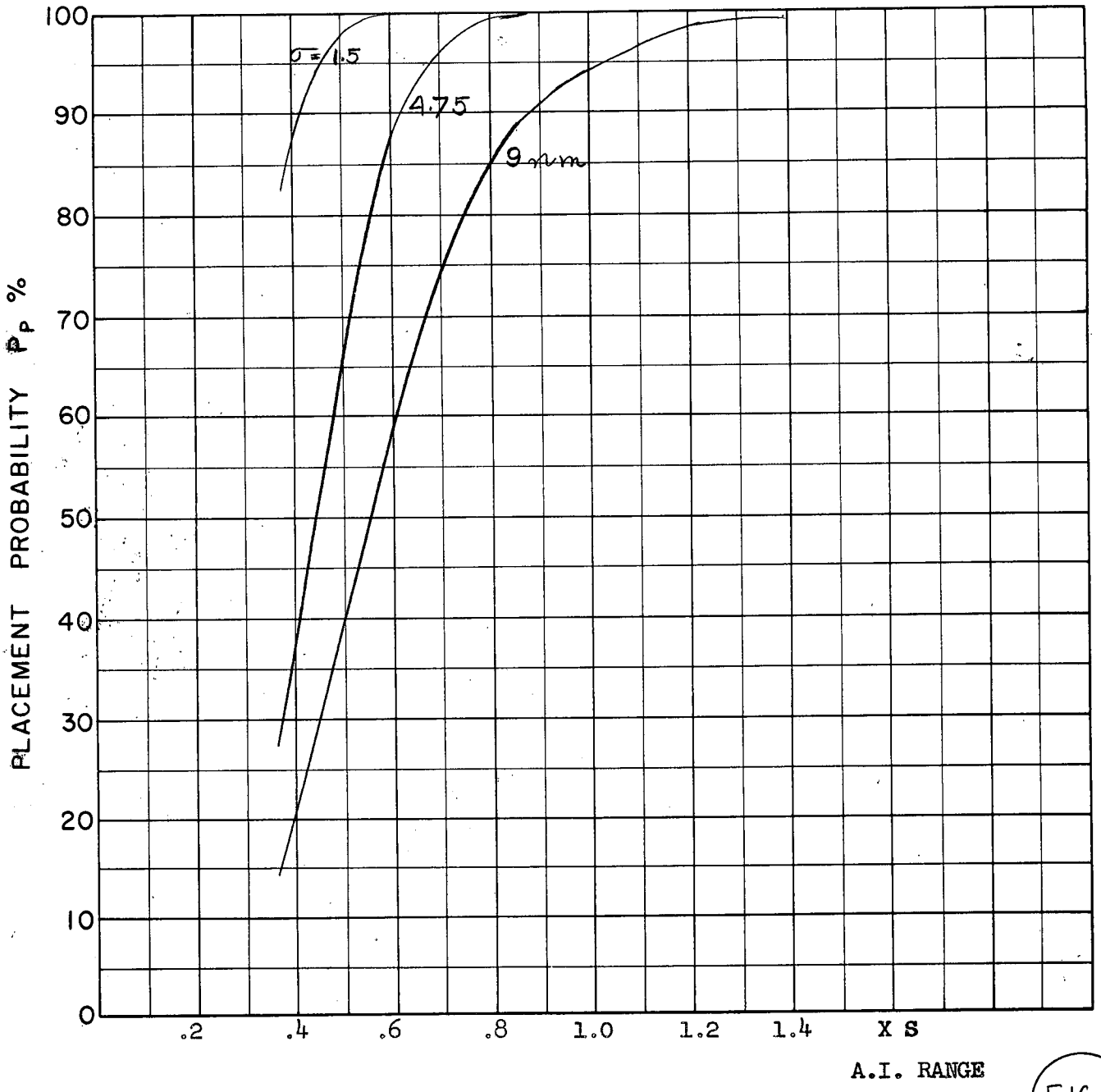

FIG 19 D

COURSE DIFFERENCE: 160°
TARGET EVASION: 0
TARGET MACH NO.: 2.0
INTERCEPTOR LATERAL G's: N.A.E. 28% Pessimistic Aerodynamics
INTERCEPTOR MACH NO.: 2.0 Initial
σ OF G.C.I. ACCURACY: 3 Values
A.I. DETECTION RANGE AS FRACTION OF SPECIFICATION RANGE, S: ABSCISSA
A.I. DETECTION RANGE CONTOUR: Delta
ALTITUDE: 50 K

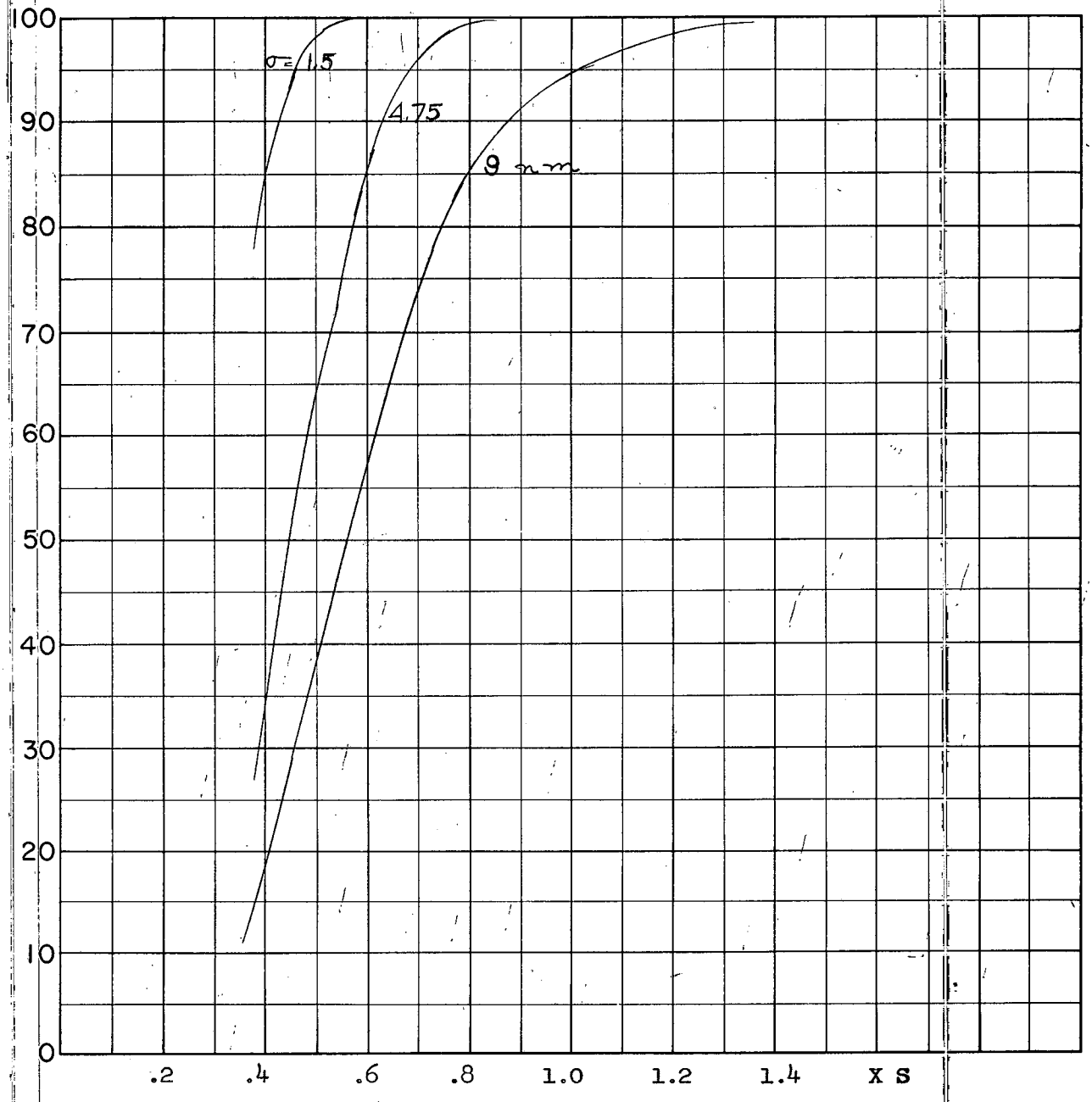

FIG 20 D

COURSE DIFFERENCE: 180°
TARGET EVASION: 0
TARGET MACH NO.: 2.0
INTERCEPTOR LATERAL G's: N.A.E. 28% Pessimistic Aerodynamics
INTERCEPTOR MACH NO.: 2.0 Initial
σ OF G.C.I. ACCURACY: 3 Values
A.I. DETECTION RANGE AS FRACTION OF SPECIFICATION RANGE, S: ABSCISSA
A.I. DETECTION RANGE CONTOUR: Delta
ALTITUDE: 50 K

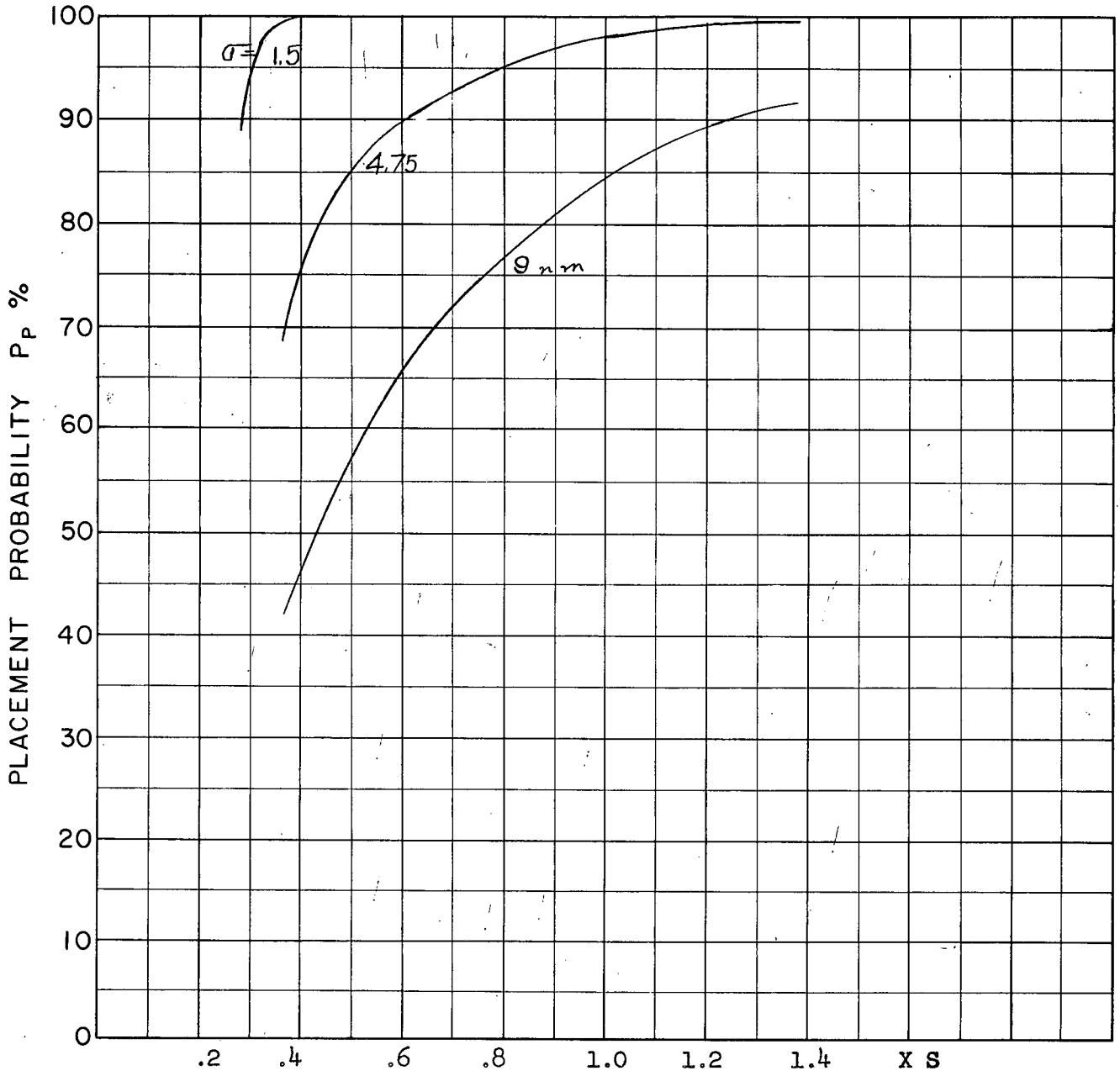

FIG 21 D

COURSE DIFFERENCE: 110°
TARGET EVASION: 0
TARGET MACH NO.: 1.5
INTERCEPTOR LATERAL G's: Avro 2.2 Aerodynamics
INTERCEPTOR MACH NO.: 1.5 Initial
σ OF G.C.I. ACCURACY: 3 Values
A.I. DETECTION RANGE AS FRACTION OF SPECIFICATION RANGE, S: ABSCISSA
A.I. DETECTION RANGE CONTOUR: Delta
ALTITUDE: 50 K

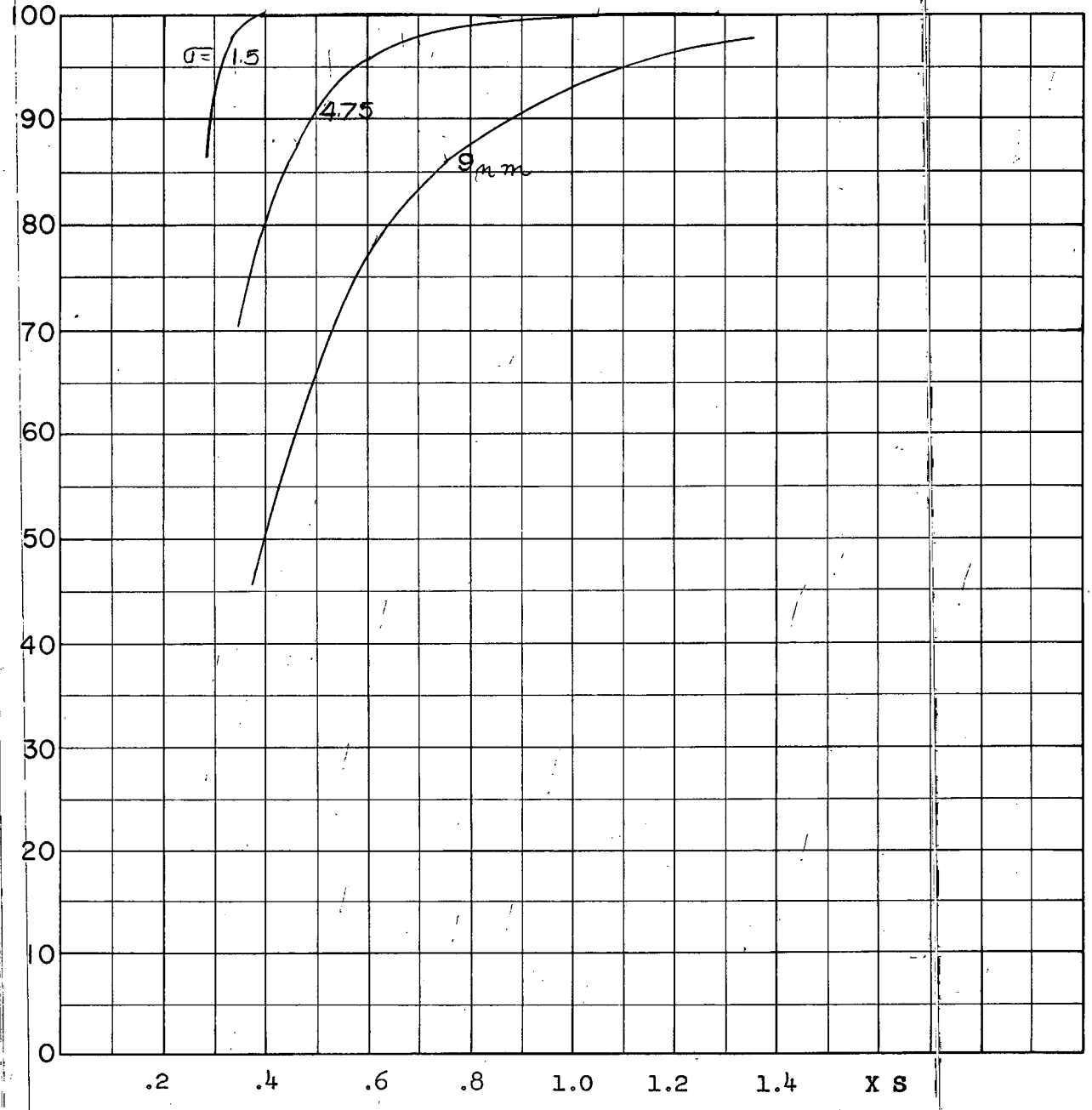

COURSE DIFFERENCE: 135°
TARGET EVASION: 0
TARGET MACH NO.: 1.5
INTERCEPTOR LATERAL G's: Avro 2.2 Aerodynamics
INTERCEPTOR MACH NO.: 1.5 Initial
σ OF G.C.I. ACCURACY: 3 Values
A.I. DETECTION RANGE AS FRACTION OF SPECIFICATION RANGE, S: ABSCISSA
A.I. DETECTION RANGE CONTOUR: Delta
ALTITUDE: 50 K

FIG 22 (D)

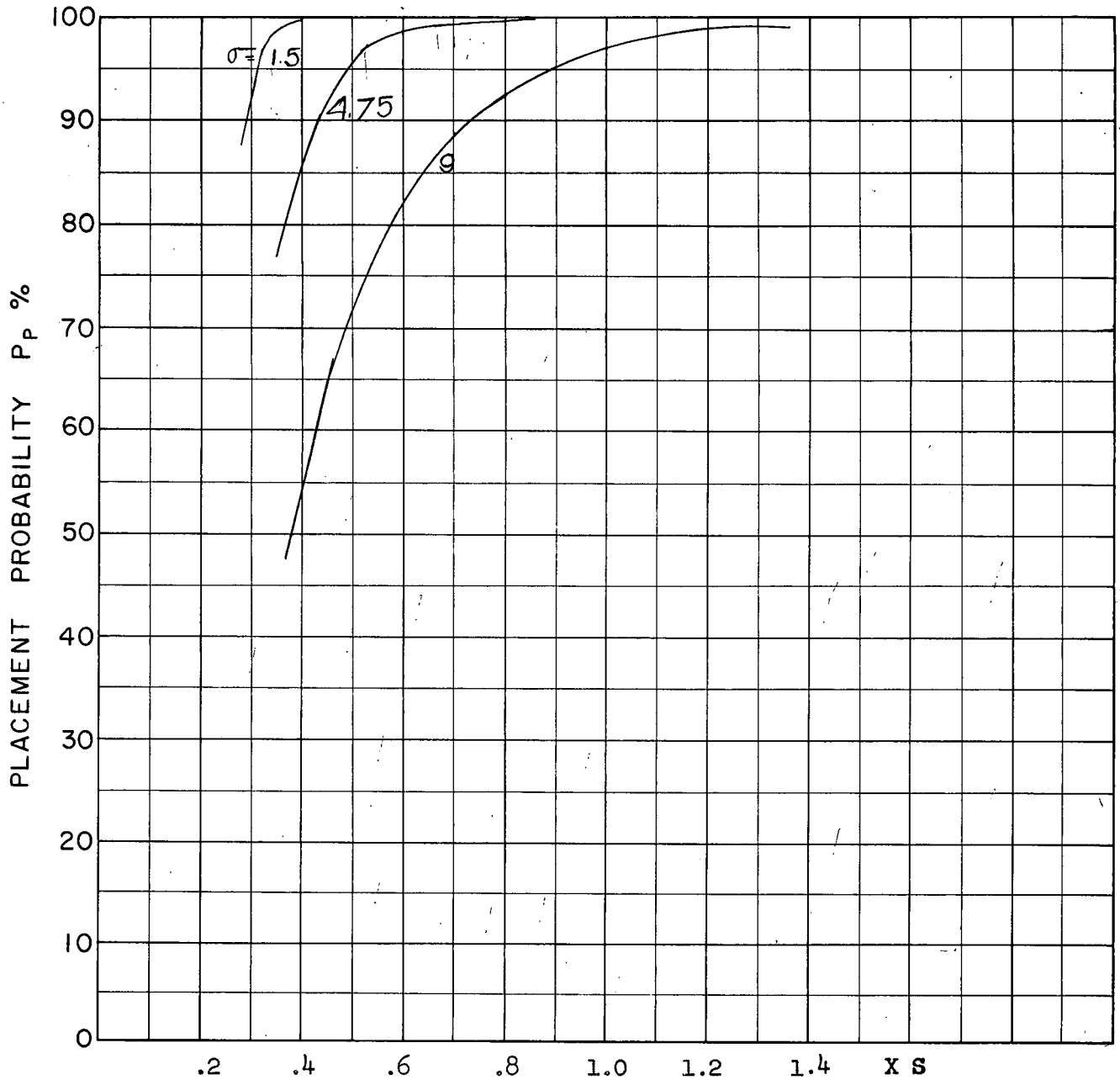

FIG 23 D

COURSE DIFFERENCE: 160°
TARGET EVASION: 0
TARGET MACH NO.: 1.5
INTERCEPTOR LATERAL G's: Avro 2.2 Aerodynamics
INTERCEPTOR MACH NO.: 1.5 Initial
σ OF G.C.I. ACCURACY: 3 Values
A.I. DETECTION RANGE AS FRACTION OF SPECIFICATION RANGE, S: ABSCISSA
A.I. DETECTION RANGE CONTOUR: Delta
ALTITUDE: 50 K

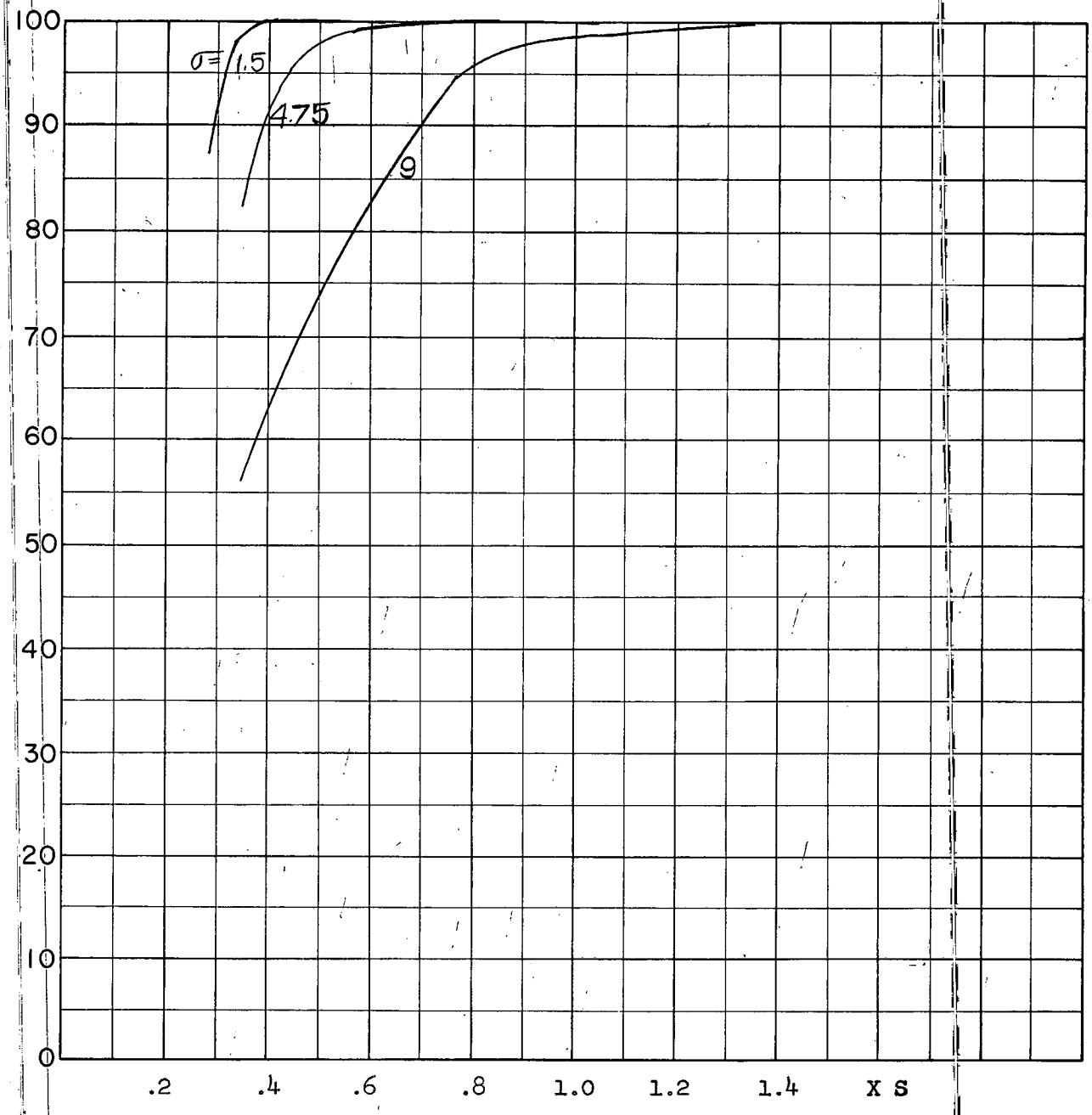

COURSE DIFFERENCE: 180°
TARGET EVASION: 0
TARGET MACH NO.: 1.5
INTERCEPTOR LATERAL G's: Avro 2.2 Aerodynamics
INTERCEPTOR MACH NO.: 1.5 Initial
σ OF G.C.I. ACCURACY: 3 Values
A.I. DETECTION RANGE AS FRACTION OF SPECIFICATION RANGE, S: ABSCISSA
A.I. DETECTION RANGE CONTOUR: Delta
ALTITUDE: 50 K

FIG 24 D

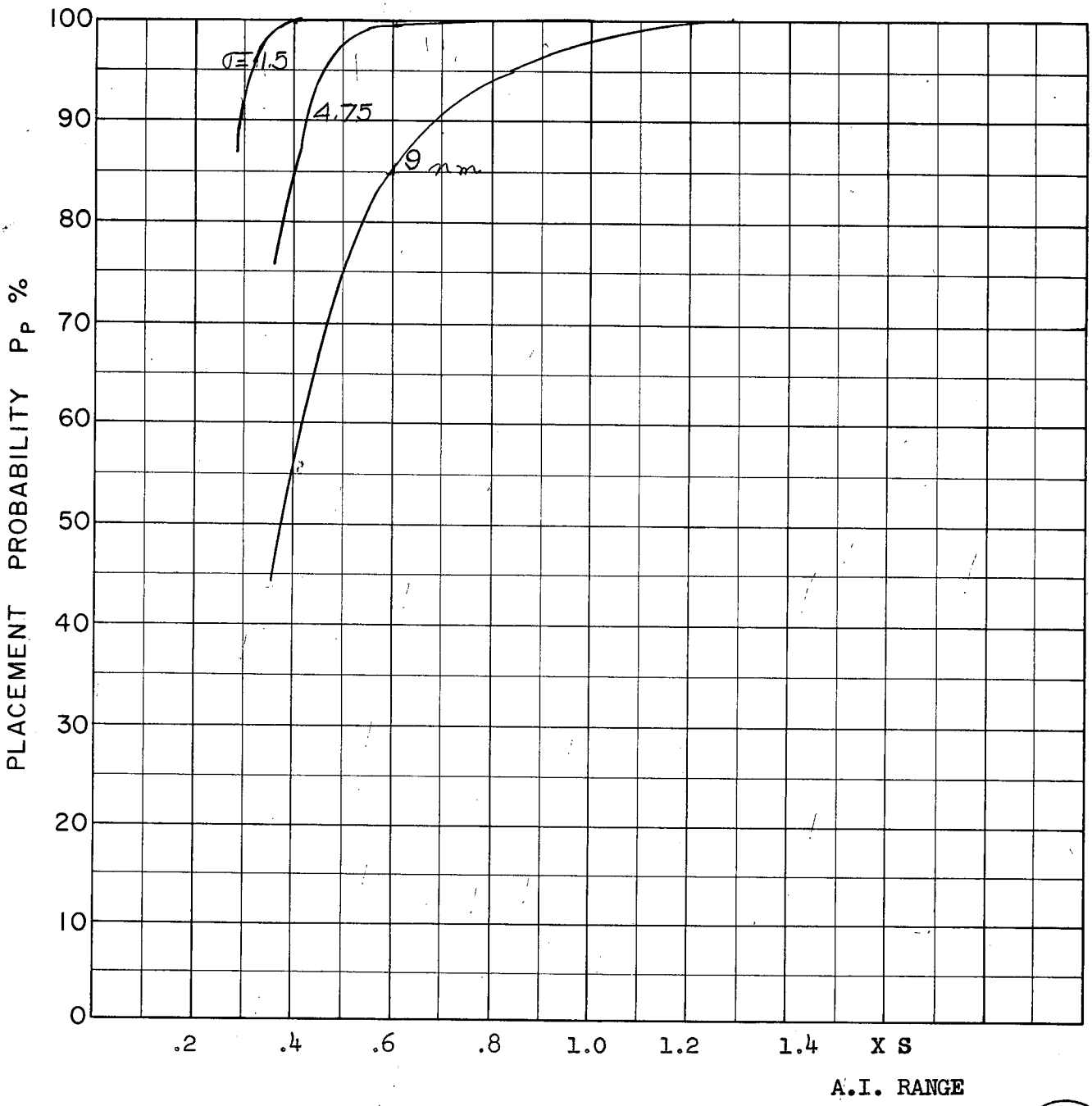

COURSE DIFFERENCE: 110°
TARGET EVASION: 0
TARGET MACH NO.: 1.5
INTERCEPTOR LATERAL G's: Avro 2.2 Aerodynamics
INTERCEPTOR MACH NO.: 2.0 Initial
σ OF G.C.I. ACCURACY: 3 Values
A.I. DETECTION RANGE AS FRACTION OF SPECIFICATION RANGE, S: ABSCISSA
A.I. DETECTION RANGE CONTOUR: Delta
ALTITUDE: 50 K

FIG 25 D

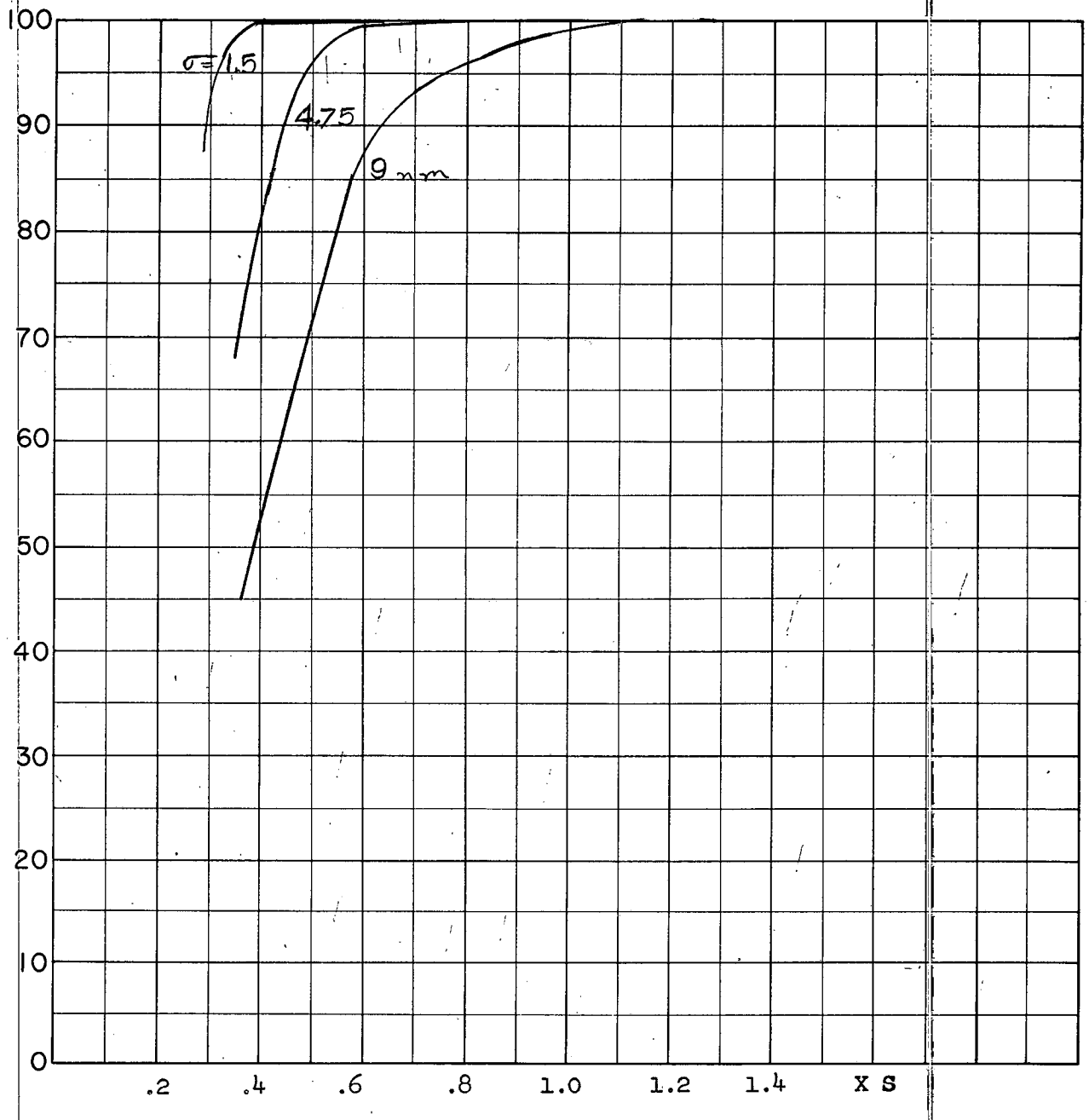

FIG 26 D

COURSE DIFFERENCE: 135°
TARGET EVASION: 0
TARGET MACH NO.: 1.5
INTERCEPTOR LATERAL G's: Avro 2.2 Aerodynamics
INTERCEPTOR MACH NO.: 2.0 Initial
σ OF G.C.I. ACCURACY: 3 Values
A.I. DETECTION RANGE AS FRACTION OF SPECIFICATION RANGE, S: ABSCISSA
A.I. DETECTION RANGE CONTOUR: Delta
ALTITUDE: 50 K

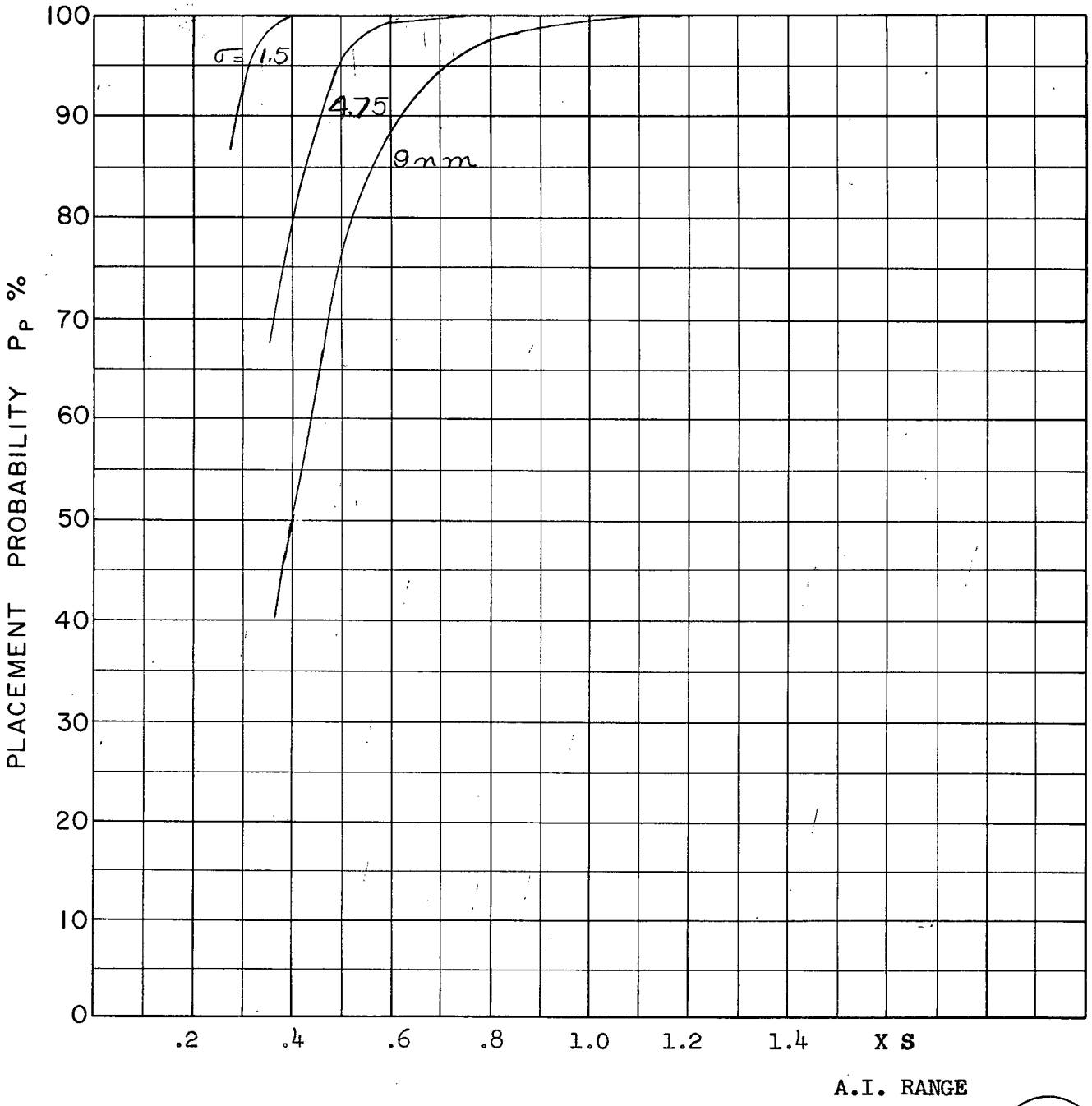

FIG 27 D

COURSE DIFFERENCE: 160°
TARGET EVASION: 0
TARGET MACH NO.: 1.5
INTERCEPTOR LATERAL G's: Avro 2.2 Aerodynamics
INTERCEPTOR MACH NO.: 2.0 Initial
σ OF G.C.I. ACCURACY: 3 Values
A.I. DETECTION RANGE AS FRACTION OF SPECIFICATION RANGE, S: ABSCISSA
A.I. DETECTION RANGE CONTOUR: Delta
ALTITUDE: 50 K

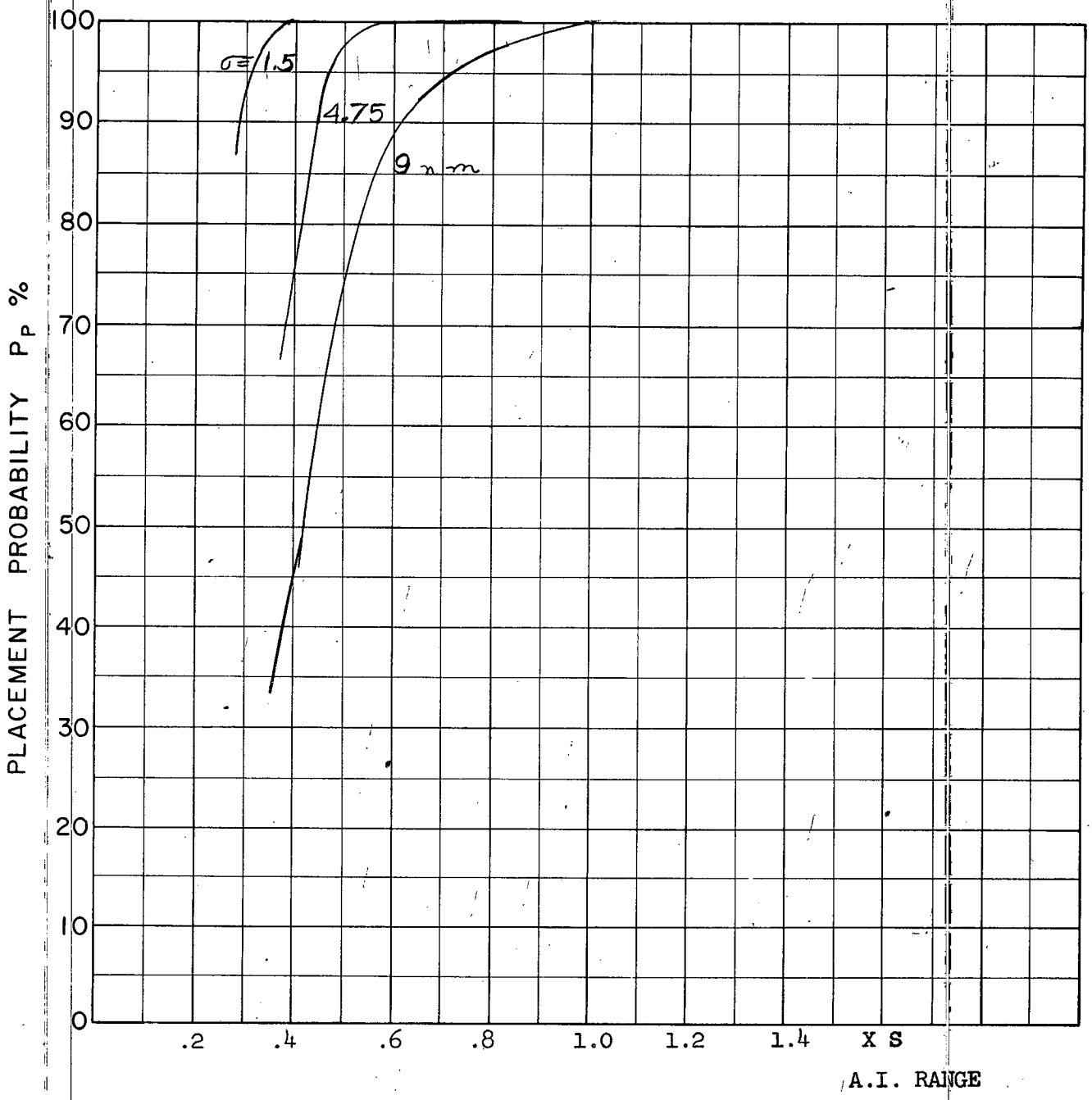

COURSE DIFFERENCE: 180°
TARGET EVASION: 0
TARGET MACH NO.: 1.5
INTERCEPTOR LATERAL G's: Avro 2.2 Aerodynamics
INTERCEPTOR MACH NO.: 2.0 Initial
σ OF G.C.I. ACCURACY: 3 Values
A.I. DETECTION RANGE AS FRACTION OF SPECIFICATION RANGE, S: ABSCISSA
A.I. DETECTION RANGE CONTOUR: Delta
ALTITUDE: 50 K

FIG 28 D

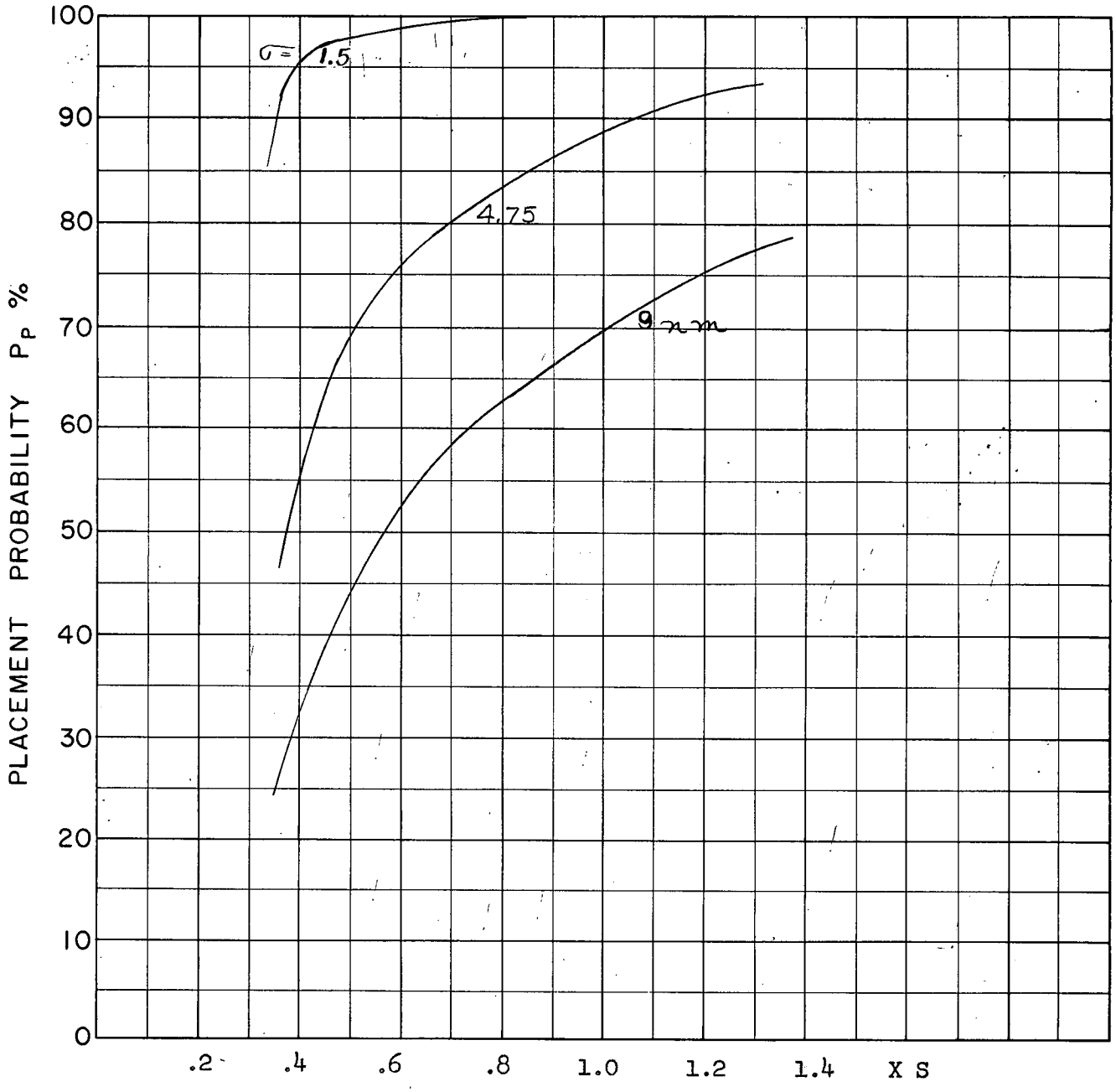

FIG 29 D

COURSE DIFFERENCE: 110°
TARGET EVASION: 0
TARGET MACH NO.: 2.0
INTERCEPTOR LATERAL G's: Avro 2.2 Aerodynamics
INTERCEPTOR MACH NO.: 1.5 Initial
σ OF G.C.I. ACCURACY: 3 Values
A.I. DETECTION RANGE AS FRACTION OF SPECIFICATION RANGE, S: ABSCISSA
A.I. DETECTION RANGE CONTOUR: Delta
ALTITUDE: 50 K

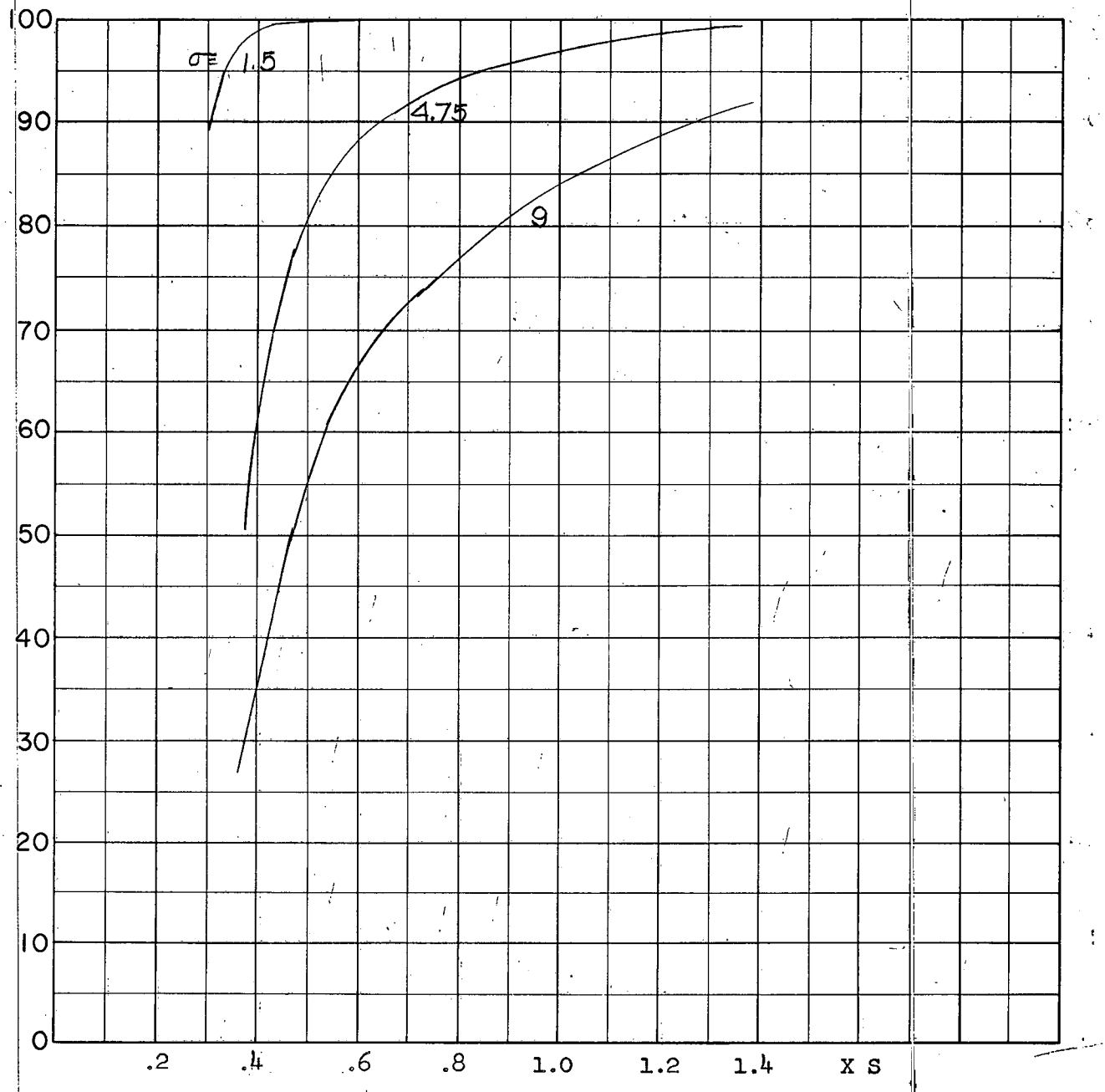

COURSE DIFFERENCE: 135°
TARGET EVASION: 0
TARGET MACH NO.: 2.0
INTERCEPTOR LATERAL G's: Avro 2.2 Aerodynamics
INTERCEPTOR MACH NO.: 1.5 Initial
σ OF G.C.I. ACCURACY: 3 Values
A.I. DETECTION RANGE AS FRACTION OF SPECIFICATION RANGE, S: ABSCISSA
A.I. DETECTION RANGE CONTOUR: Delta
ALTITUDE: 50 K

FIG 30 D

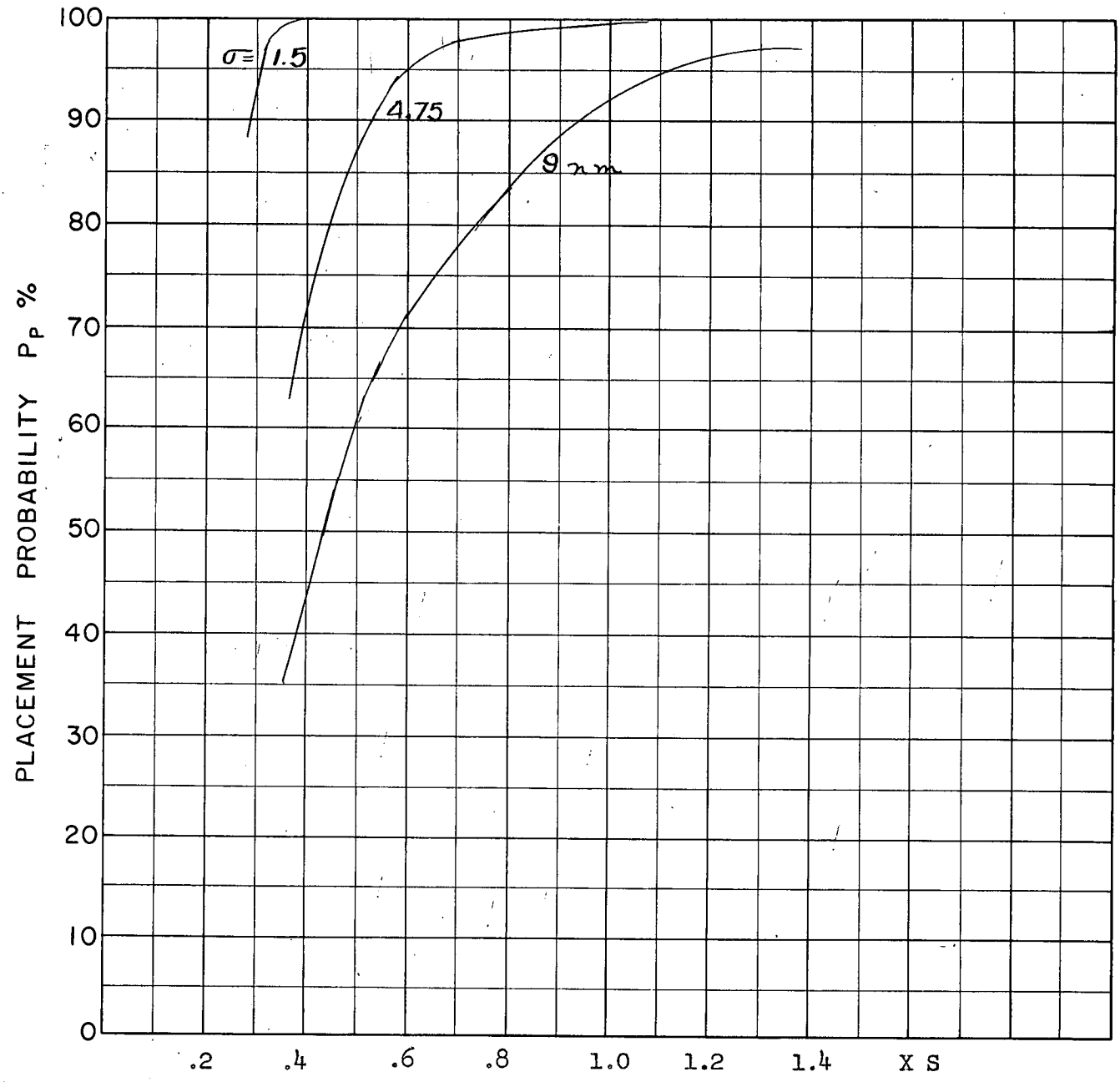

FIG 31 D

COURSE DIFFERENCE: 160°
TARGET EVASION: 0
TARGET MACH NO.: 2.0
INTERCEPTOR LATERAL G's: Avro 2.2 Aerodynamics
INTERCEPTOR MACH NO.: 1.5 Initial
σ OF G.C.I. ACCURACY: 3 Values
A.I. DETECTION RANGE AS FRACTION OF SPECIFICATION RANGE, S: ABSCISSA
A.I. DETECTION RANGE CONTOUR: Delta
ALTITUDE: 50 K

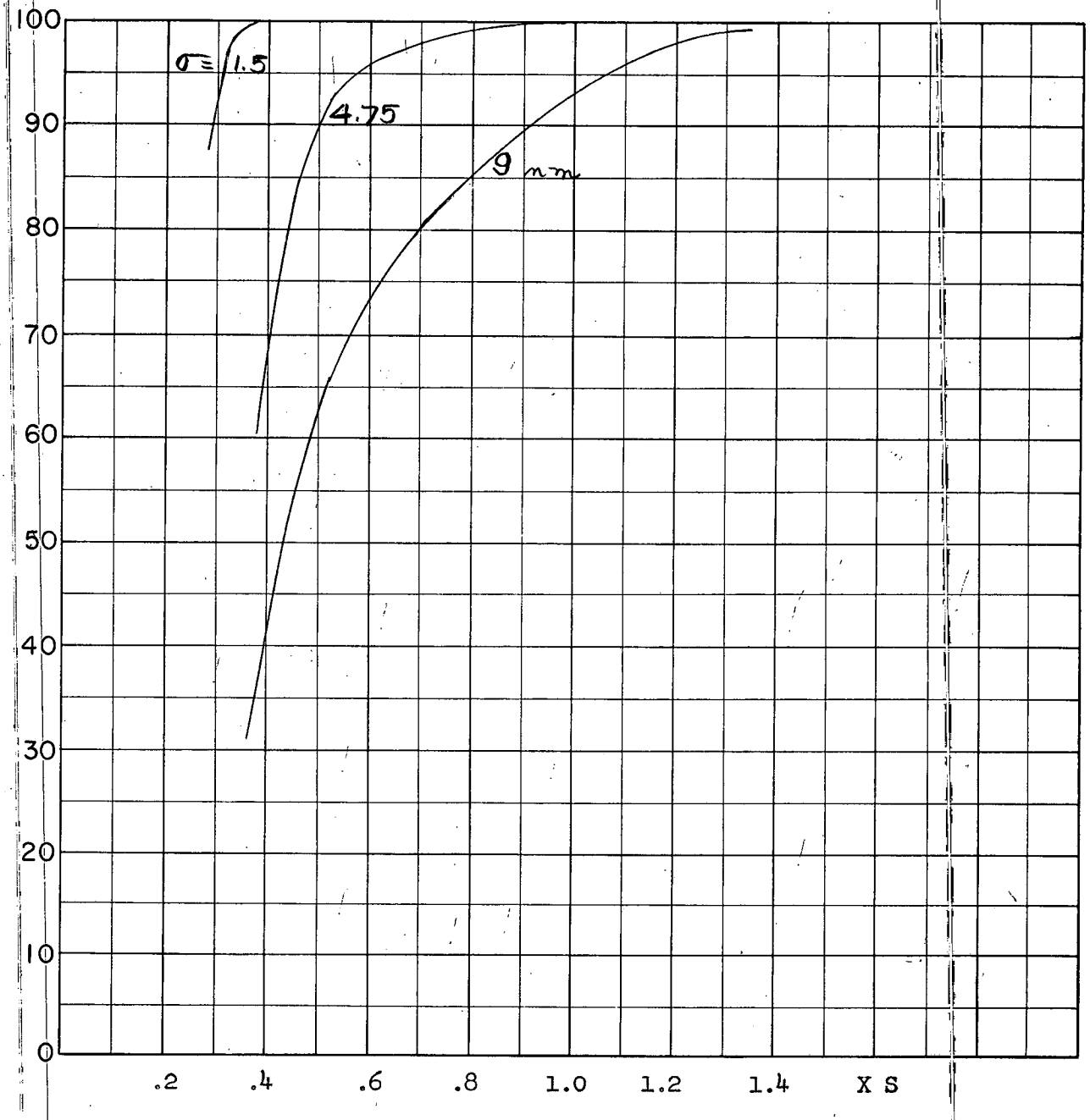

FIG32 D

COURSE DIFFERENCE: 180°
TARGET EVASION: 0
TARGET MACH NO.: 2.0
INTERCEPTOR LATERAL G's: Avro 2.2 Aerodynamics
INTERCEPTOR MACH NO.: 1.5 Initial
σ OF G.C.I. ACCURACY: 3 Values
A.I. DETECTION RANGE AS FRACTION OF SPECIFICATION RANGE, S: ABSCISSA
A.I. DETECTION RANGE CONTOUR: Delta
ALTITUDE: 50 K

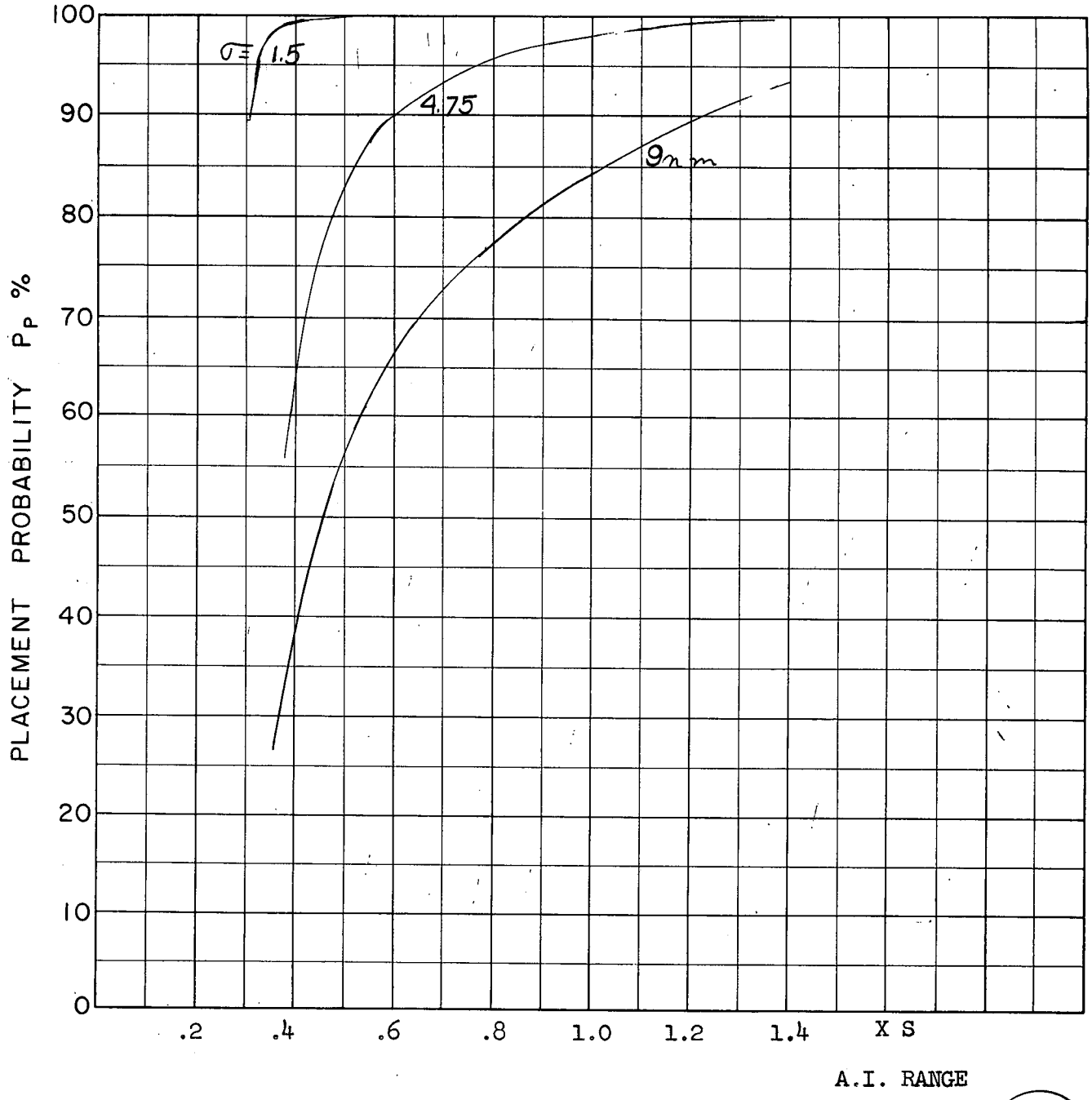

COURSE DIFFERENCE: 110°
TARGET EVASION: 0
TARGET MACH NO.: 2.0
INTERCEPTOR LATERAL G's: Avro 2.2 Aerodynamics
INTERCEPTOR MACH NO.: 2.0 Initial
σ OF G.C.I. ACCURACY: 3 Values
A.I. DETECTION RANGE AS FRACTION OF SPECIFICATION RANGE, S: ABSCISSA
A.I. DETECTION RANGE CONTOUR: Delta
ALTITUDE: 50 K

FIG 33 D

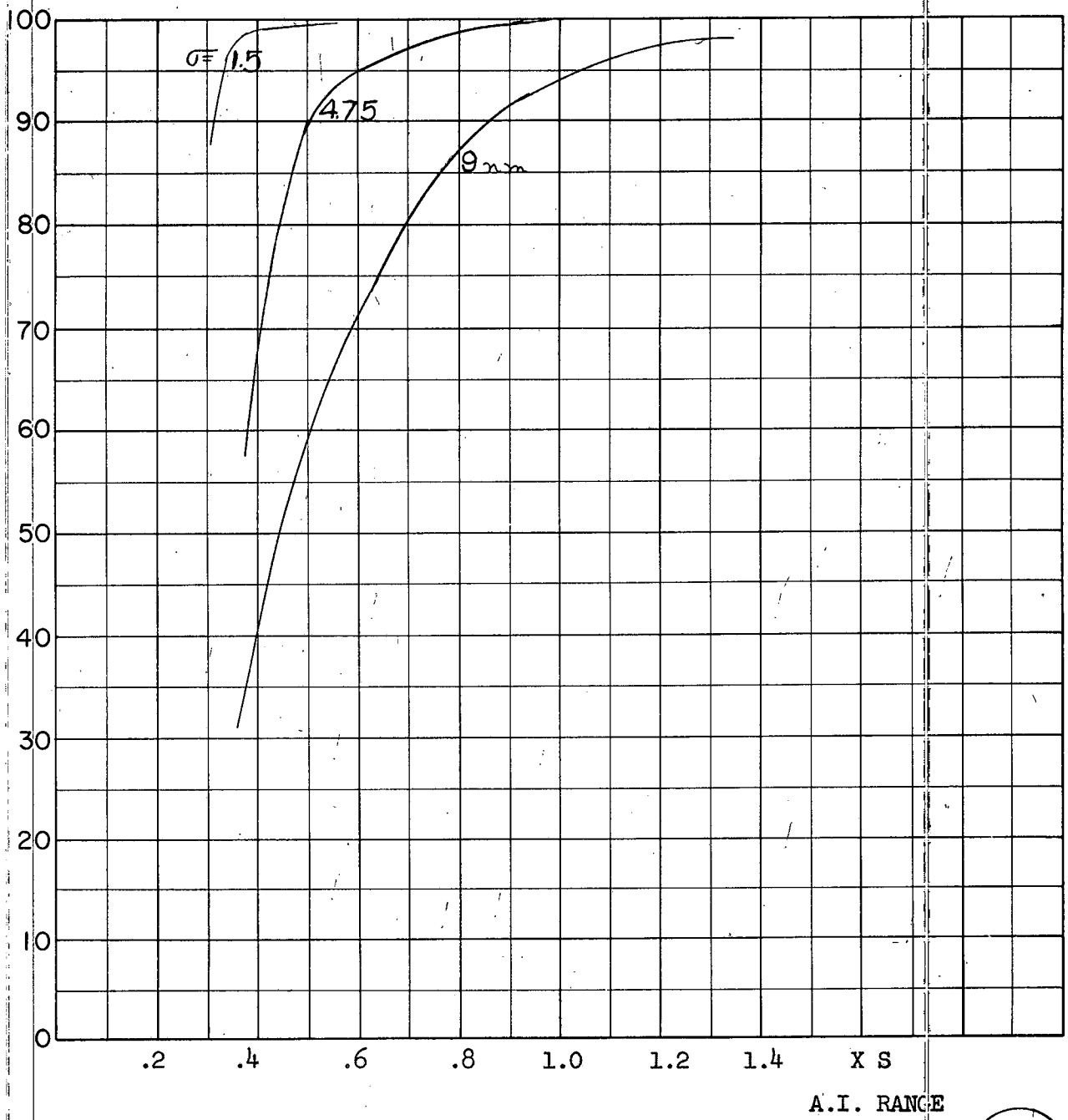

FIG 34 D

COURSE DIFFERENCE: 135°
TARGET EVASION: 0
TARGET MACH NO.: 2.0
INTERCEPTOR LATERAL G's: Avro 2.2 Aerodynamics
INTERCEPTOR MACH NO.: 2.0 Initial
σ OF G.C.I. ACCURACY: 3 Values
A.I. DETECTION RANGE AS FRACTION OF SPECIFICATION RANGE, S: ABSCISSA
A.I. DETECTION RANGE CONTOUR: Delta
ALTITUDE: 50 K

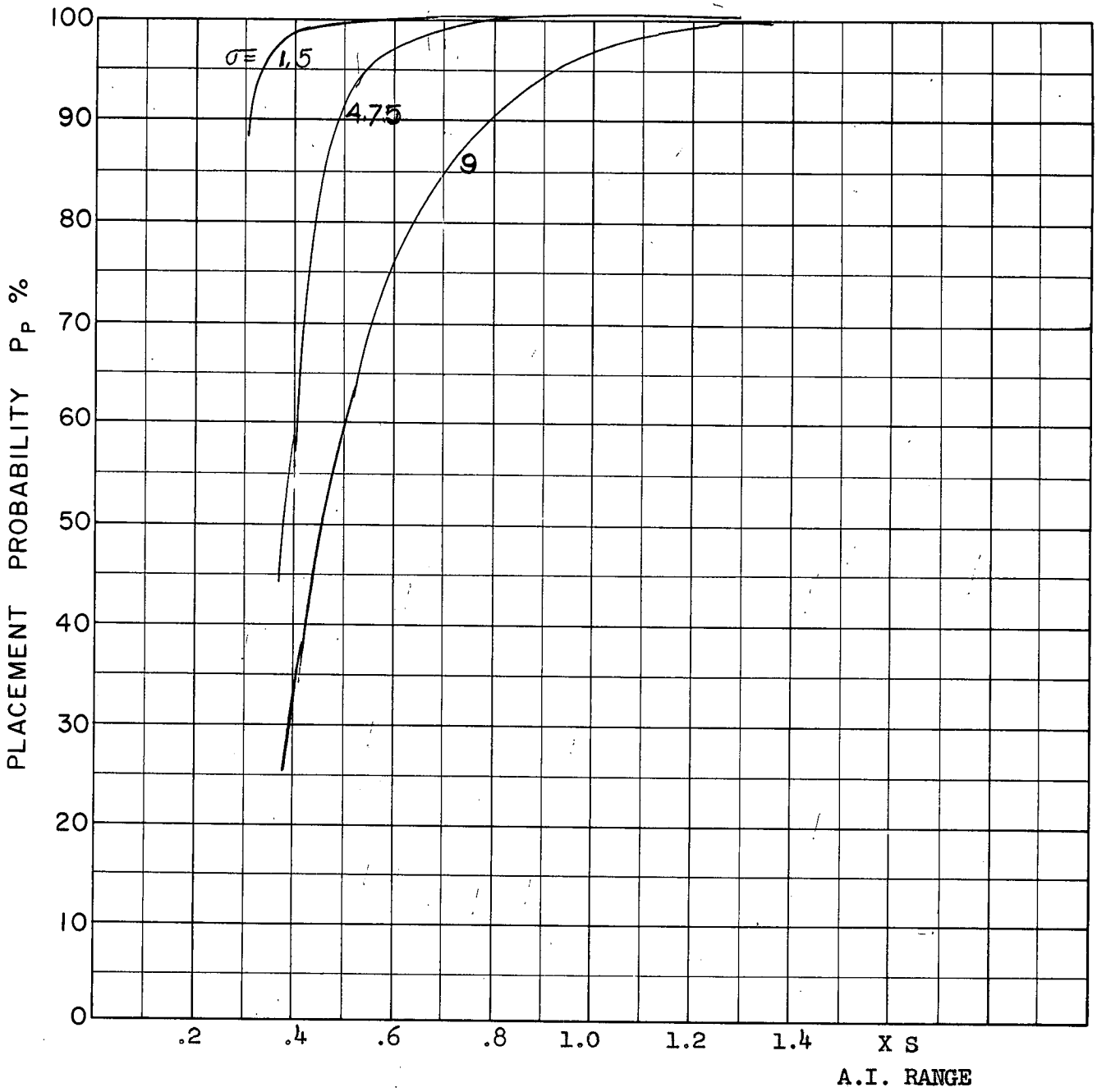

COURSE DIFFERENCE: 160°
TARGET EVASION: 0
TARGET MACH NO.: 2,0
INTERCEPTOR LATERAL G's: Avro 2.2 Aerodynamics
INTERCEPTOR MACH NO.: 2.0 Initial
σ OF G.C.I. ACCURACY: 3 values
A.I. DETECTION RANGE AS FRACTION OF SPECIFICATION RANGE, S: ABSCISSA
A.I. DETECTION RANGE CONTOUR: Delta
ALTITUDE: 50 K

FIG35 D

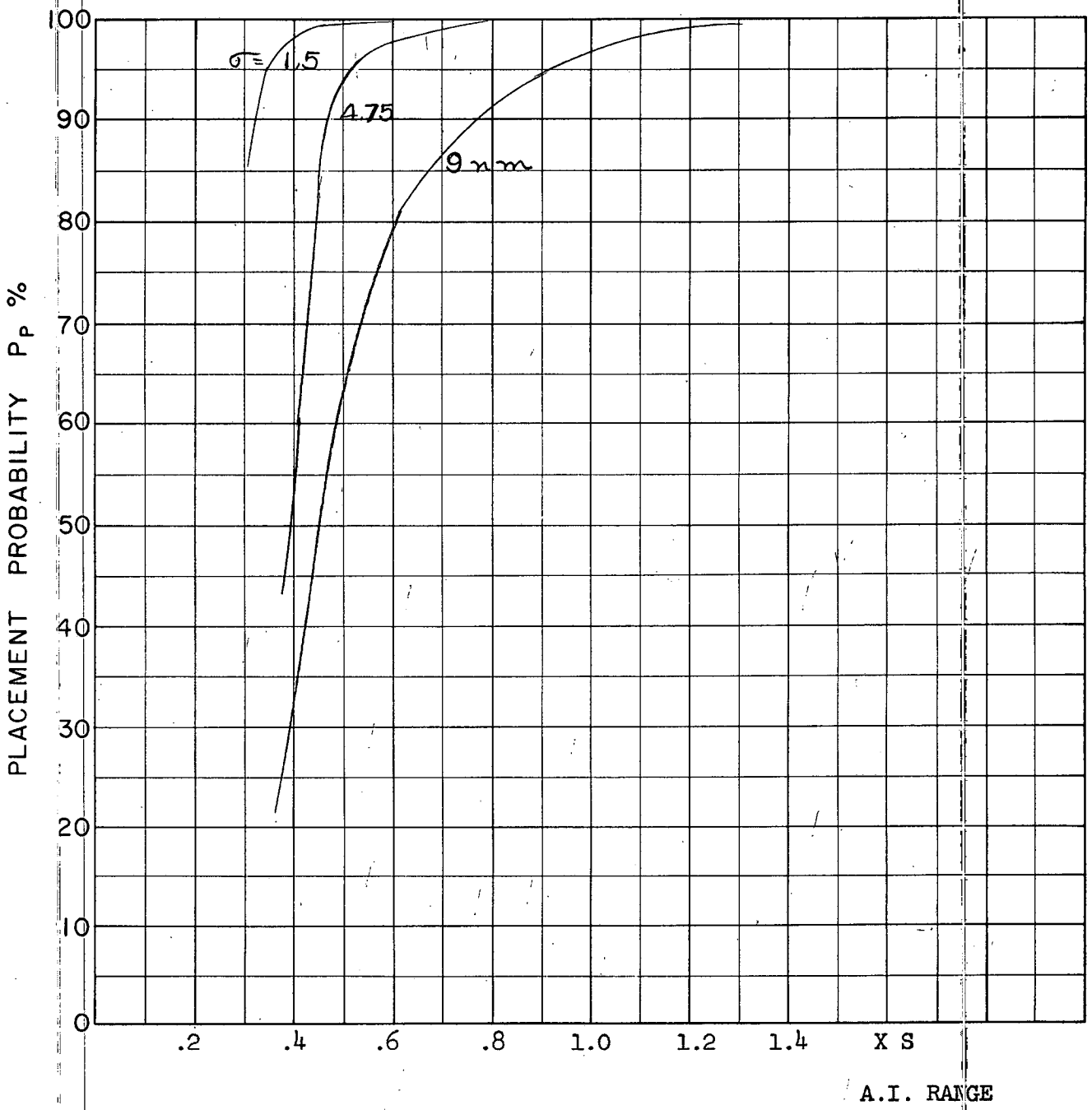

COURSE DIFFERENCE: 180°
TARGET EVASION: 0
TARGET MACH NO.: 2.0
INTERCEPTOR LATERAL G's: Avro 2.2 Aerodynamics
INTERCEPTOR MACH NO.: 2.0 Initial
σ OF G.C.I. ACCURACY: 3 values
A.I. DETECTION RANGE AS FRACTION OF SPECIFICATION RANGE, S: ABSCISSA
A.I. DETECTION RANGE CONTOUR: Delta
ALTITUDE: 50 K

FIG 36 D

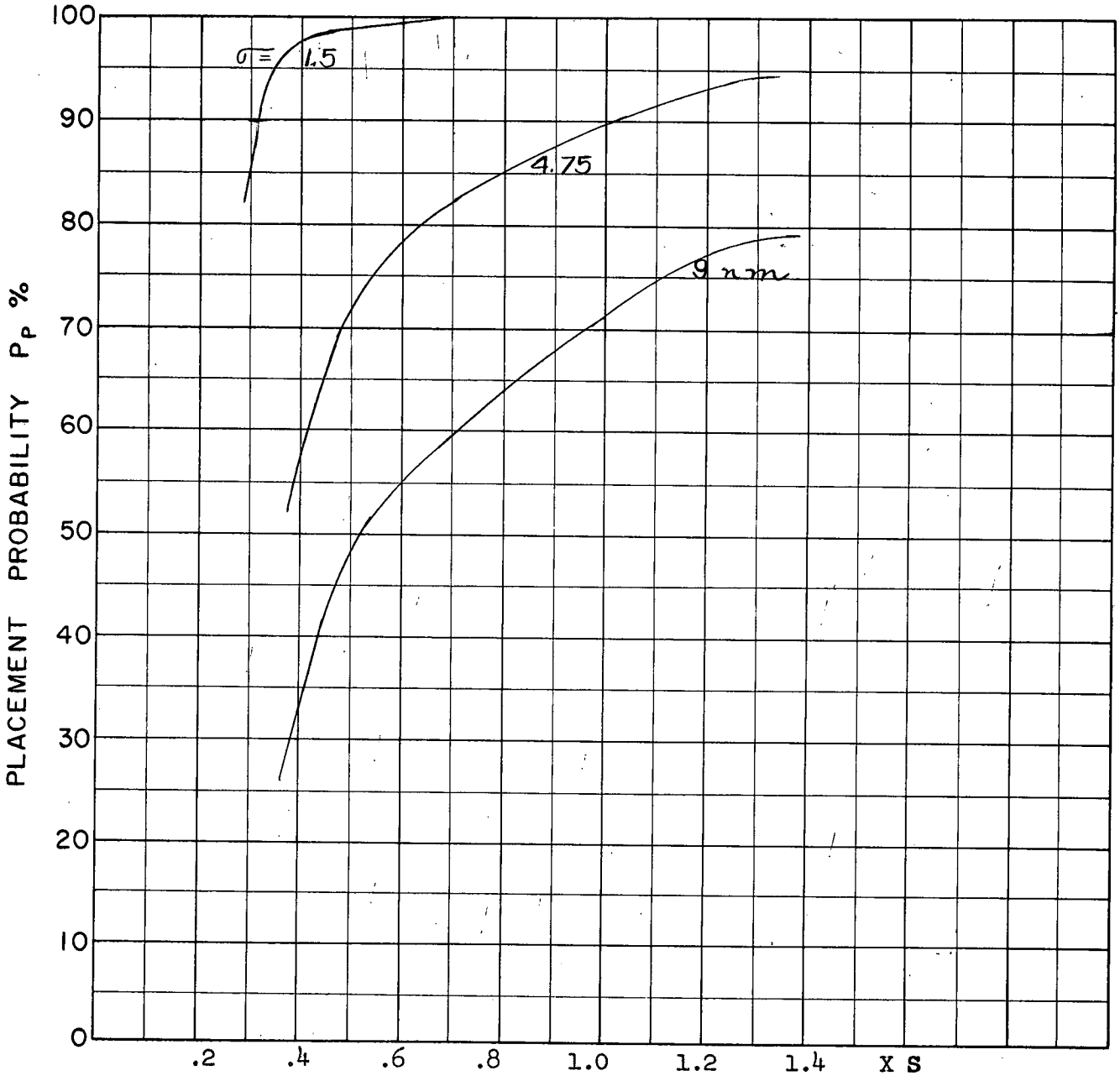

COURSE DIFFERENCE: 110°
TARGET EVASION: 0
TARGET MACH NO.: 2.0
INTERCEPTOR LATERAL G's: Avro 2.2 Aerodynamics
INTERCEPTOR MACH NO.: 1.5 Initial
σ OF G.C.I. ACCURACY: 3 Values
A.I. DETECTION RANGE AS FRACTION OF SPECIFICATION RANGE, S: ABSCISSA
A.I. DETECTION RANGE CONTOUR: Delta
ALTITUDE: 40 K

FIG 37 D

FIG 38 D

COURSE DIFFERENCE: 135°
TARGET EVASION: 0
TARGET MACH NO.: 2.0
INTERCEPTOR LATERAL G's: Avro 2.2 Aerodynamics
INTERCEPTOR MACH NO.: 1.5 Initial
σ OF G.C.I. ACCURACY: 3 Values
A.I. DETECTION RANGE AS FRACTION OF SPECIFICATION RANGE, S: ABSCISSA
A.I. DETECTION RANGE CONTOUR: Delta
ALTITUDE: 40 K

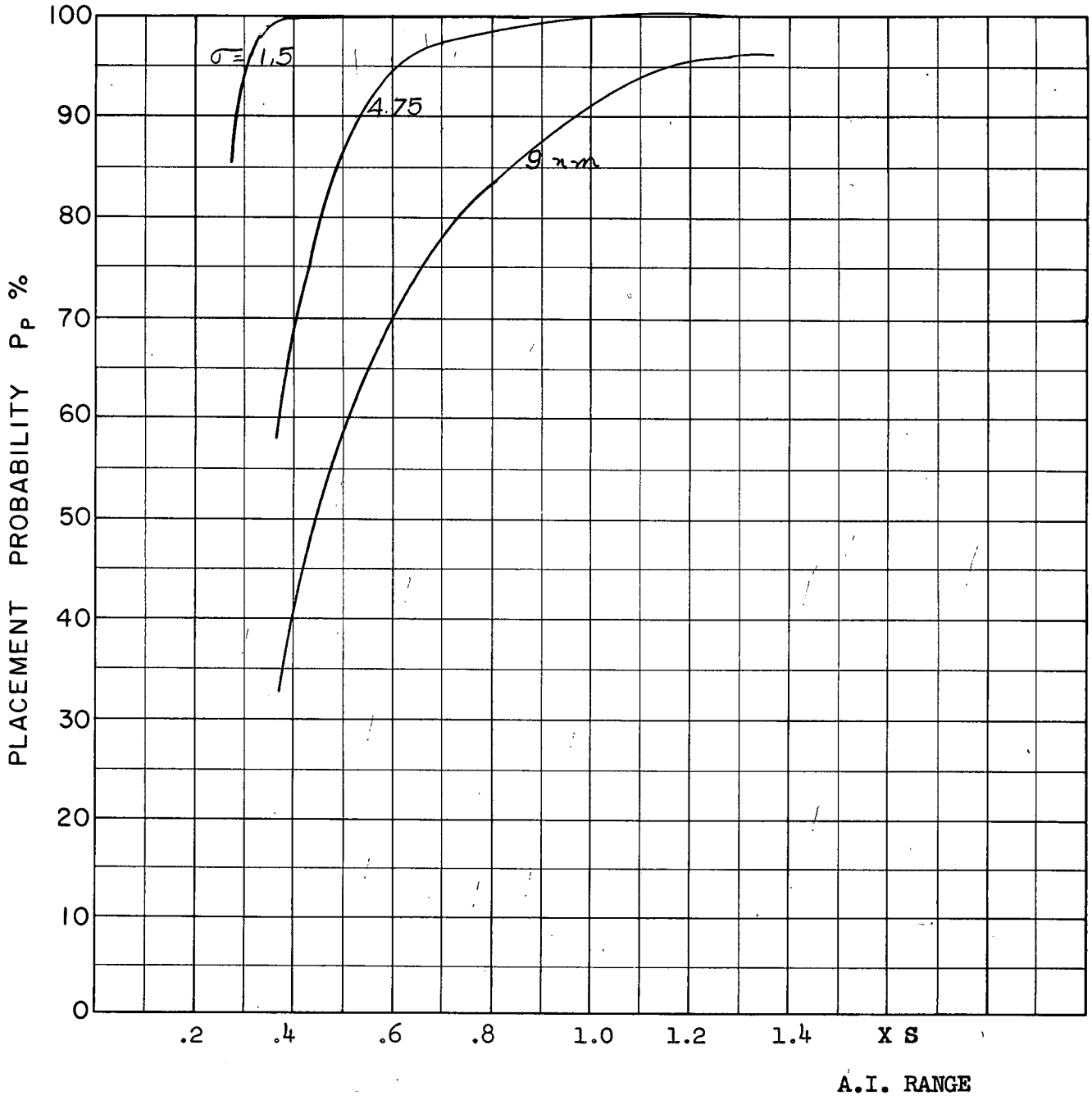

COURSE DIFFERENCE: 160°
TARGET EVASION: 0
TARGET MACH NO.: 2.0
INTERCEPTOR LATERAL G's: Avro 2.2 Aerodynamics
INTERCEPTOR MACH NO.: 1.5 Initial
σ OF G.C.I. ACCURACY: 3 Values
A.I. DETECTION RANGE AS FRACTION OF SPECIFICATION RANGE, S: ABSCISSA
A.I. DETECTION RANGE CONTOUR: Delta
ALTITUDE: 40 K

FIG 39 D

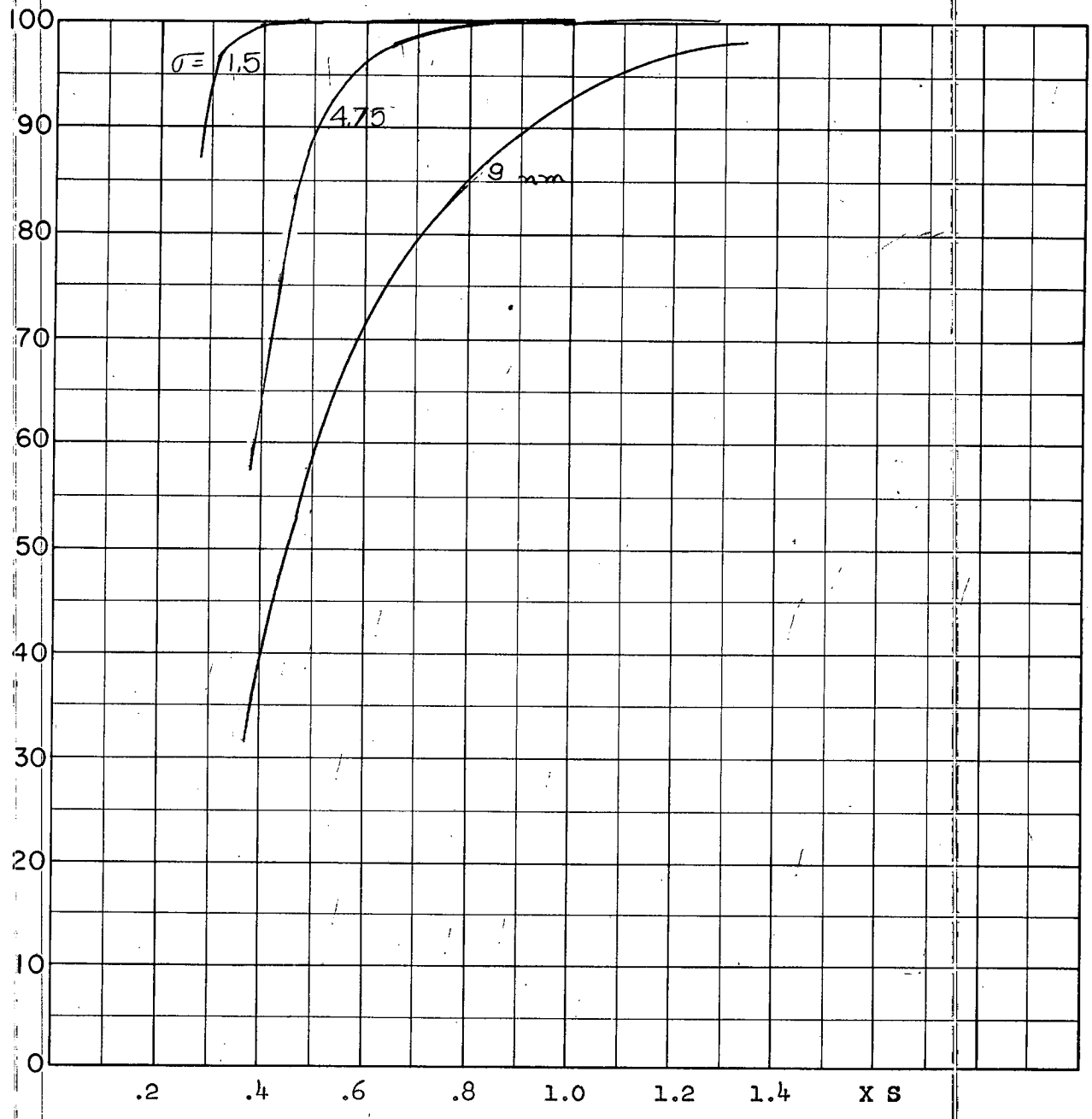

COURSE DIFFERENCE: 180°
TARGET EVASION: 0
TARGET MACH NO.: 2.0
INTERCEPTOR LATERAL G's: Avro 2.2 Aerodynamics
INTERCEPTOR MACH NO.: 1.5 Initial
σ OF G.C.I. ACCURACY: 3 Values
A.I. DETECTION RANGE AS FRACTION OF SPECIFICATION RANGE, S: ABSCISSA
A.I. DETECTION RANGE CONTOUR: Delta
ALTITUDE: 40 K

FIG 40 D

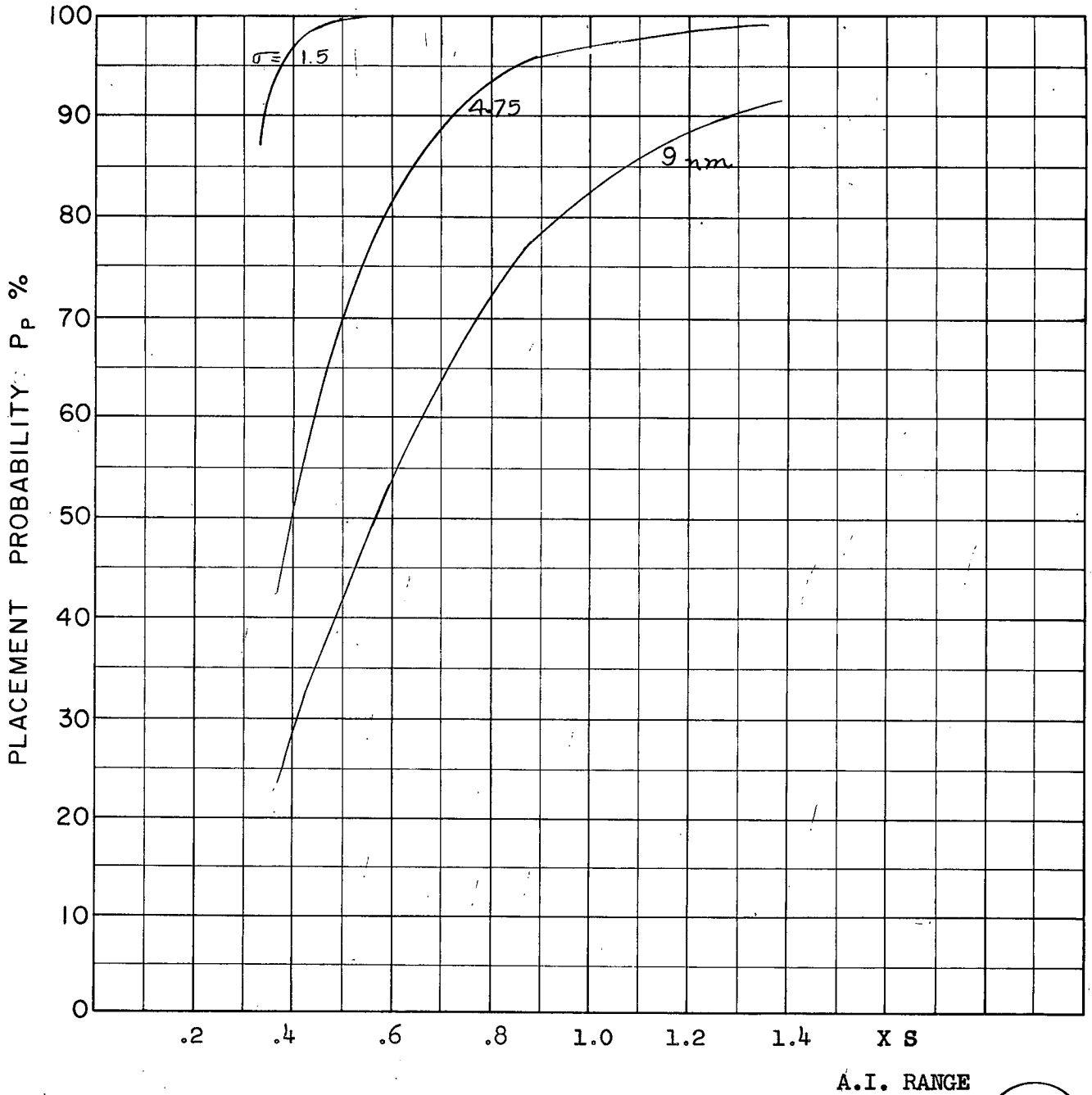

FIG 41 D

COURSE DIFFERENCE: 110°
TARGET EVASION: 0
TARGET MACH NO.: 2.0
INTERCEPTOR LATERAL G's: Avro 2.2 Aerodynamics
INTERCEPTOR MACH NO.: 2.0 Initial
σ OF G.C.I. ACCURACY: 3 Values
A.I. DETECTION RANGE AS FRACTION OF SPECIFICATION RANGE, S: ABSCISSA
A.I. DETECTION RANGE CONTOUR: Delta
ALTITUDE: 60 K

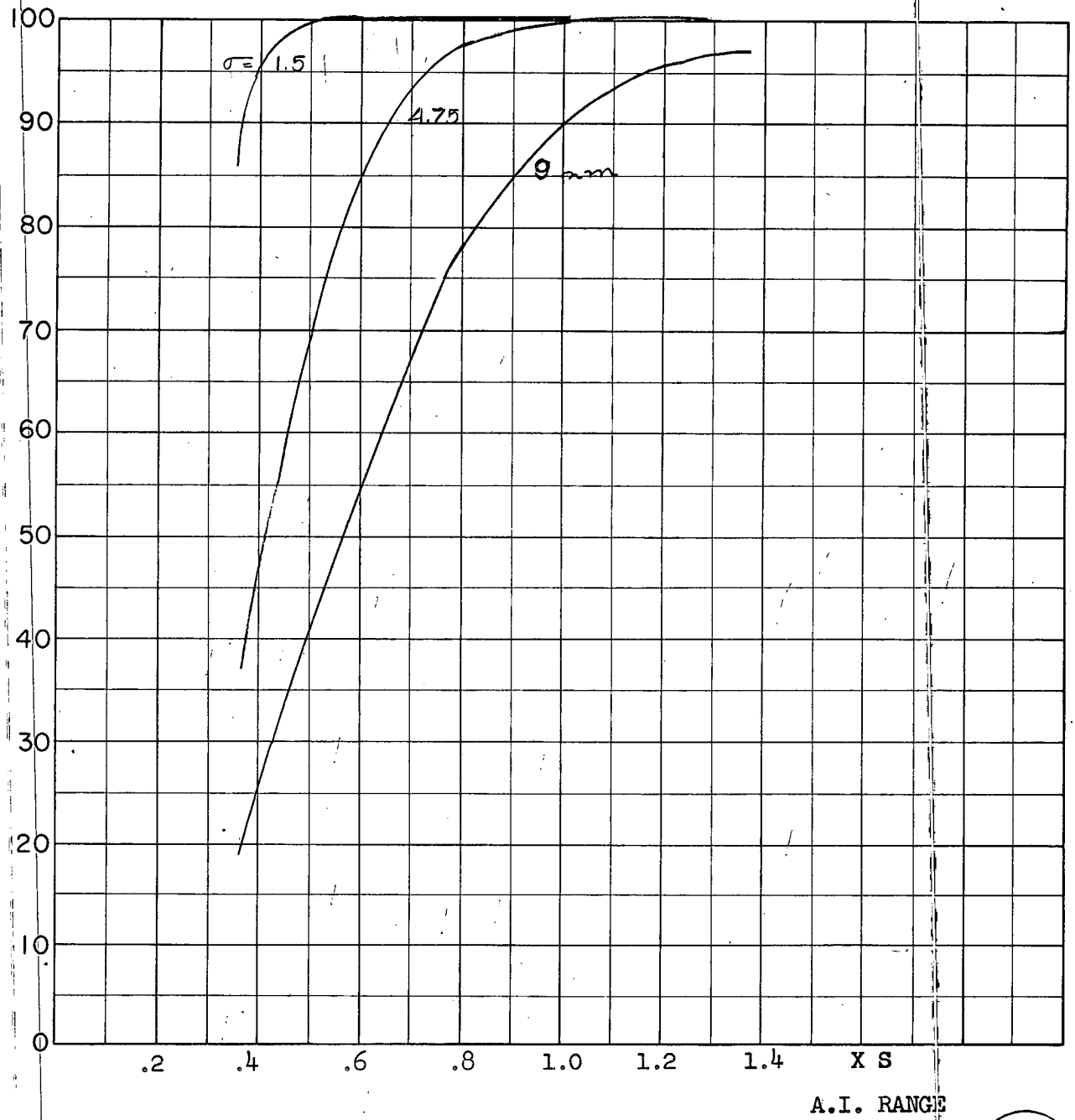

FIG 42 D

COURSE DIFFERENCE: 135°
TARGET EVASION: 0
TARGET MACH NO.: 2.0
INTERCEPTOR LATERAL G's: Avro 2.2 Aerodynamics
INTERCEPTOR MACH NO.: 2.0 Initial
σ OF G.C.I. ACCURACY: 3 Values
A.I. DETECTION RANGE AS FRACTION OF SPECIFICATION RANGE, S: ABSCISSA
A.I. DETECTION RANGE CONTOUR: Delta
ALTITUDE: 60 K

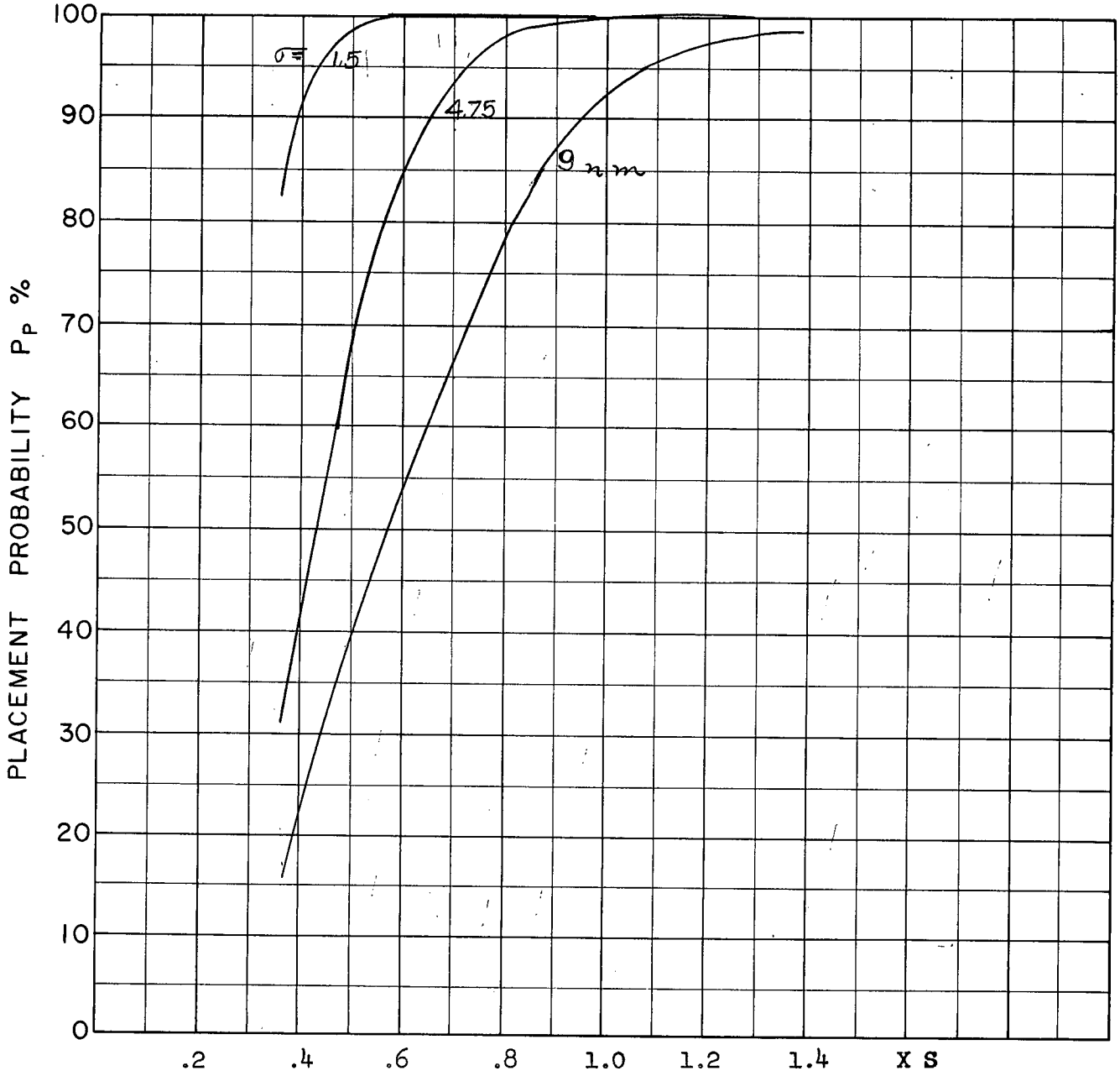

COURSE DIFFERENCE: 160°
TARGET EVASION: 0
TARGET MACH NO.: 2.0
INTERCEPTOR LATERAL G's: Avro 2.2 Aerodynamics
INTERCEPTOR MACH NO.: 2.0 Initial
σ OF G.C.I. ACCURACY: 3 Values
A.I. DETECTION RANGE AS FRACTION OF SPECIFICATION RANGE, S: ABSCISSA
A.I. DETECTION RANGE CONTOUR: Delta
ALTITUDE: 60 K

FIG 43 D

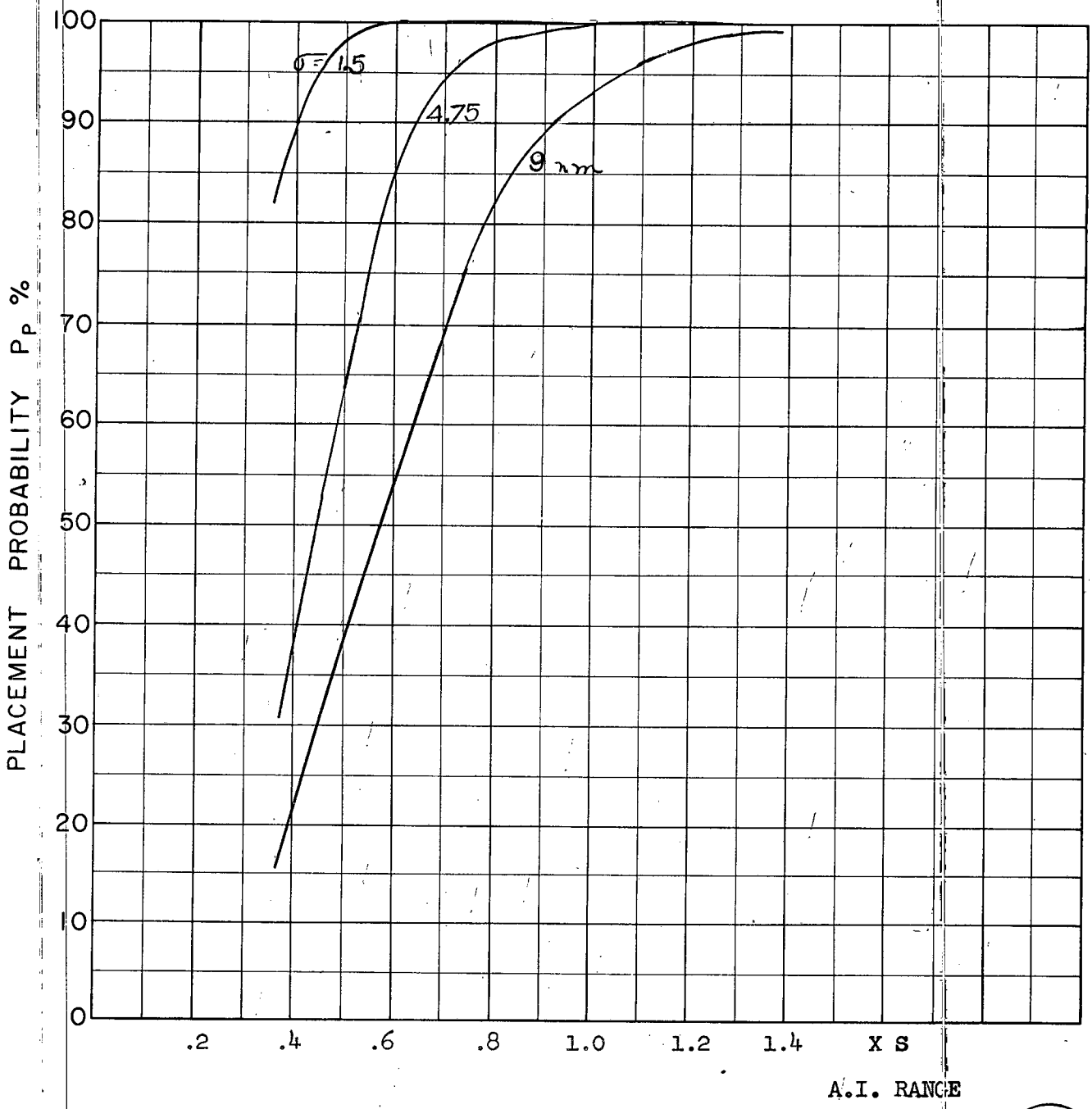

COURSE DIFFERENCE: 180°
TARGET EVASION: 0
TARGET MACH NO.: 2.0
INTERCEPTOR LATERAL G's: Avro 2.2 Aerodynamics
INTERCEPTOR MACH NO.: 2.0 Initial
σ OF G.C.I. ACCURACY: 3 Values
A.I. DETECTION RANGE AS FRACTION OF SPECIFICATION RANGE, S: ABSCISSA
A.I. DETECTION RANGE CONTOUR: Delta
ALTITUDE: 60 K

FIG 44 D

APPENDIX 'E'

Interceptor Placement in Two Dimensions Using CF-105 Aerodynamic Performance Estimates

by B. Hughes

1. Introduction

In the CF-105 Assessment Study extensive placement studies have been done, both for evading and non-evading targets, under the assumption that the interceptor speed maintains constant. A range of turn capabilities have been considered, and so the placement probability for the CF-105 may be found by interpolation in the results, when a given power limited performance is assumed. The most recent estimates predict a power-limited load factor of 1.63 at Mach number 1.5 at 50,000 feet altitude; this corresponds to a lateral turn rate of 1.3 g's, which is towards the lower end of the range of values used, and in a region where variations in probabilities due to this parameter are linear.

References 1 and 2 describe the work which has been done. Results are published in Reference 2 for non-evading and gently evading targets and in appendices B and C of this report for evading targets.

A model of the CF-105 based on performance estimates made at N.A.E. (references 4 and 5) has been incorporated into a similar two-dimensional placement study on the REAC. The aircraft may manoeuvre to the aerodynamic limit (or to any lesser arbitrary limit) with consequent deceleration. A more realistic set of placement probability values is obtained in this way. The methods used and results obtained for this one set of aerodynamic estimates are given in this appendix.

The N.A.E. estimates used for this work credit the CF-105 with ability to make a 1.29 load factor limited turn at 50,000 feet at Mach 1.5. These data have been superseded by the later AVRO estimates; appendices D and F describe work with this more optimistic set of aerodynamic characteristics.

2. REAC Simulation

Figure 1 gives the circuit which was used to simulate the attack geometry. The equations were similar to those used in the constant speed cases (Reference 1, Appendix D; see also Reference 3). The lead collision steering mode was used, with conversion to lead pursuit outside maximum missile launch range.

Figure 2 gives the circuit used to simulate the CF-105 aerodynamics. The method of mechanizing the data was similar to that described in Appendix D of this report, and described also in Appendix D of Reference 2. The data used are referred to as "the 28% MAC. pessimistic data of N.A.E.".

The equations used are given in association with the figures.

3. Missile Launch Zones

The launch zones used were similar to those used in other REAC work (see Appendix C above, and Reference 2), having been derived from those obtained in Reference 6.

An interceptor Mach number of 1.5 at missile launch was assumed in choosing the launch zones, although the initial interceptor Mach number was 1.8 in all cases. The interceptor speed is variable, depending on the degree and duration of manoeuvre. Mach numbers in the range 1.1 to 1.9 were observed at the end of the attack runs, but in most cases the final speed corresponded closely to Mach 1.5. Any variations due to this effect were neglected. The maximum permissible launch range is restricted by missile seeker range at front aspects, and fighter speed has little effect on this limit. The launch zone is affected only slightly by interceptor speed variations at rear aspects.

4. Symbols

R	-	range
V_f	-	interceptor velocity
V_t	-	target velocity
Vm	-	missile velocity
A	-	aspect angle
θ	-	look angle

F	-	missile travel relative to fighter - stick length
T	-	time-to-go, as defined by equation (iii) or (iii)*
ΔV	-	difference between mean missile velocity and fighter velocity at launch
M	-	expected miss-distance
δ	-	approximate heading error
Γ	-	course difference
ψ	-	angle between space reference axes and target axes
$\dot{\Gamma} + \dot{\psi}$	-	rate of turn of interceptor, space coordinates
$(\dot{\Gamma} + \dot{\psi})_d$	-	demanded rate of turn
g	-	acceleration due to gravity
n	-	load factor
n_{max}	-	maximum permissible load factor
θ_i	-	ideal look angle - no heading error
Th	-	thrust
P_o	-	atmospheric pressure
D	-	drag
D_o	-	zero lift drag
L	-	lift
L_{max}	-	maximum permissible lift
K_1	-	functions of Mach number in the drag equation
$\mathcal{F}$	-	functions of Mach number in the drag equation
L_{mB}	-	maximum lift, buffet and elevator deflection limit
L_mHM	-	maximum lift, hinge-moment limit
W	-	weight of interceptor

5. Equations for Geometry

$$\dot{R} = V_t \cos A - V_f \cos \theta \qquad \text{(i)}$$

$$R(\dot{A} + \dot{\psi}) = V_f \sin \theta - V_t \sin A \qquad \text{(ii)}$$

When $F/T < \Delta V$, flying a lead collision course:

$$\frac{R}{T} = (V_f + F/T) \cos \theta - V_t \cos A \qquad \text{(iii)}$$

$$\frac{M}{T} = (V_f + F/T) \sin \theta - V_t \sin A \qquad \text{(iv)}$$

$$\delta = \frac{M}{T} \cdot \frac{1}{V_f + F/T} \qquad \text{(v)}$$

and when $F/T \geq \Delta V$, after conversion to lead pursuit:

$$\frac{R}{T} = V_m \cos \theta - V_t \cos A \qquad \text{(iii)*}$$

$$\frac{M}{T} = V_m \sin \theta - V_t \sin A \qquad \text{(iv)*}$$

$$\delta = \frac{M}{T} \cdot \frac{1}{V_m} \qquad \text{(v)*}$$

where $V_m = V_f + \Delta V$.

$$(\dot{\Gamma} + \dot{\psi})_d = \frac{K}{1 + \tau S} \cdot \frac{1 + \tau_1 S}{1 + \tau_2 S} \cdot \qquad \text{(vi)}$$

where $K = 4 \text{ sec.}^{-1}$

$\tau = 2$ sec.

$\tau_1 = 1.625$ sec.

$\tau_2 = 1$ sec.

When $(\dot{\Gamma} + \dot{\psi})_d \leq \frac{g}{V_f}\sqrt{n_{max}^2 - 1}$,

$$(\dot{\Gamma} + \dot{\psi}) \equiv \frac{g}{V_f}\sqrt{n^2 - 1} = (\dot{\Gamma} + \dot{\psi})_d \; ; \qquad \text{(vii)}$$

when $(\dot{\Gamma} + \dot{\psi})_d > \frac{g}{V_f}\sqrt{n_{max}^2 - 1}$, $(\dot{\Gamma} + \dot{\psi}) = \frac{g}{V_f}\sqrt{n_{max}^2 - 1}$ (vii)*

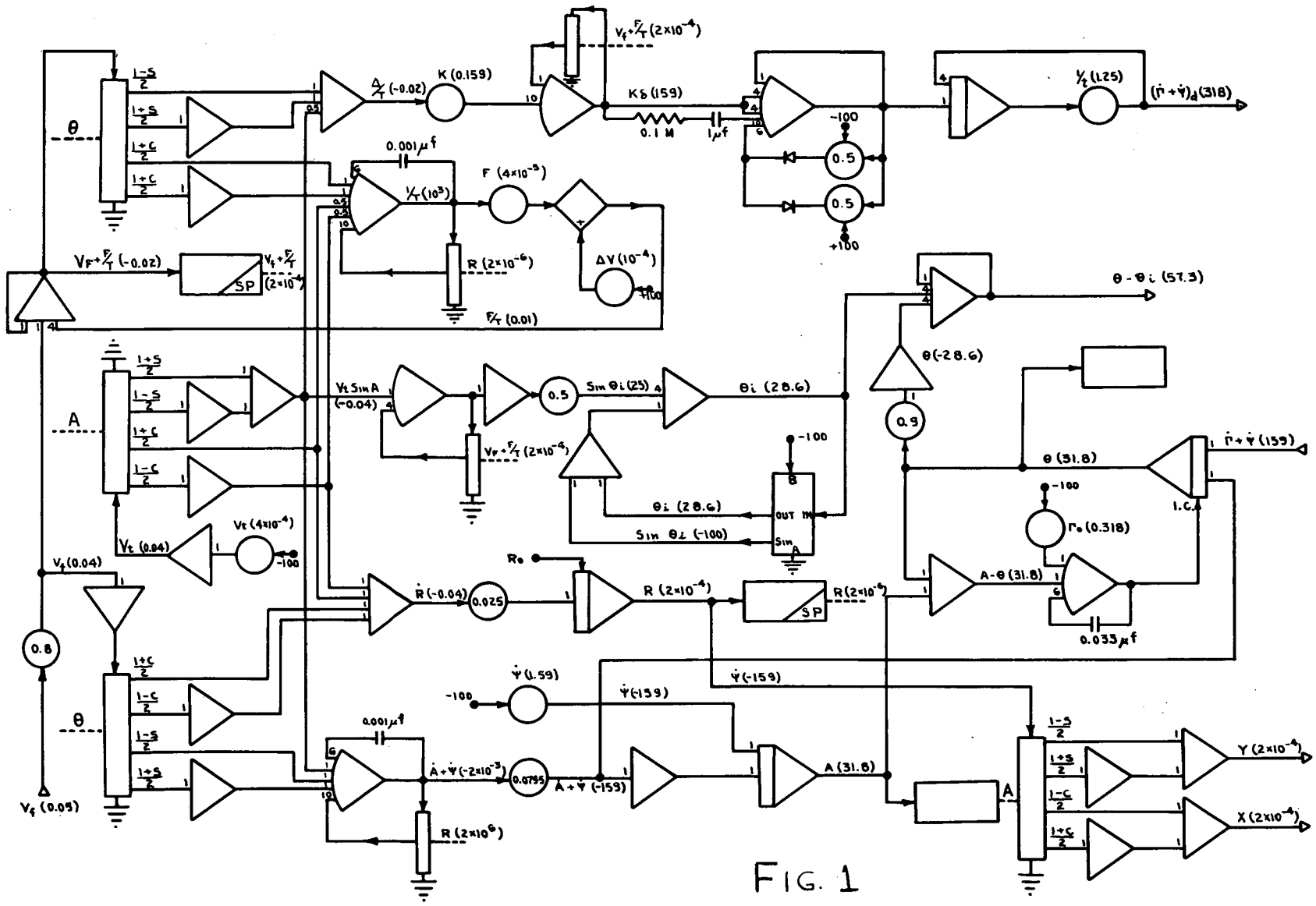
θ
A
θ
K (0.159)
Kδ (159)
0.1 M
1 μf
0.001 μf
F (4×10⁻³)
R (2×10⁻⁶)
ΔV (10⁻⁴)
F/T (0.01)
SP
-100
0.5
+100
1/T (L25)
(ṙ+ψ̇)d (318)
θ - θi (57.3)
θ(-28.6)
0.9
θ (31.8)
ṙ+ψ̇ (159)
I.C.
r₀ (0.318)
A-θ (31.8)
0.033 μf
θi (28.6)
Sin θi (25)
Sin θi (-100)
OUT IN
Sin
Vt Sin A (-0.04)
Vt (4×10⁻⁴)
Vt (0.04)
Vf (0.04)
Vf (0.09)
0.8
Ṙ (-0.04)
0.025
R (2×10⁻⁴)
R₀
ψ̇ (1.59)
ψ̇ (-159)
Ȧ+ψ̇ (-2×10⁻³)
0.0795
A+ψ̇ (-159)
A (31.8)
Y (2×10⁻⁴)
X (2×10⁻⁴)

FIG. 1

When $F/T < \Delta V$,

$$\theta_i = \sin^{-1} \left(\frac{V_t}{(V_f + F/T)} . \sin A \right) \qquad \text{(viii)}$$

and when $F/T \geq \Delta V$,

$$\theta_i = \sin^{-1} \left(\frac{V_t}{V_m} . \sin A \right) \qquad \text{(viii)*}$$

The heading error at any time is $\theta - \theta_i$; this must be distinguished from δ which is an approximate value of heading error, used in the navigation computer.

6. Equations for Aerodynamics

$$Th = \frac{Th}{Po} . Po \qquad \text{(ix)}$$

$$D = Po. \frac{Do}{po} + K_1 L + \frac{\mathcal{F} L^2}{Po} \qquad \text{(x)}$$

$$L_{max} \leqslant \frac{L_{mB}}{Po} . Po \qquad \text{(xi)}$$

$$L_{max} \leqslant L_{mHM_1} + \frac{L_{mHM_2}}{Po} . Po \qquad \text{(xii)}$$

$$L_{max} \leqslant 4W \qquad \text{(xiii)}$$

$$n_{max} = \frac{L_{max}}{W} \qquad \text{(xiv)}$$

$$n = \frac{L}{W} \qquad \text{(xv)}$$

$\frac{Th}{Po}$, $\frac{Do}{po}$, K_1, $\mathcal{F}$, $\frac{L_{mB}}{Po}$, L_{mHM_1}, $\frac{L_{mHM_2}}{Po}$ are functions of Mach No.

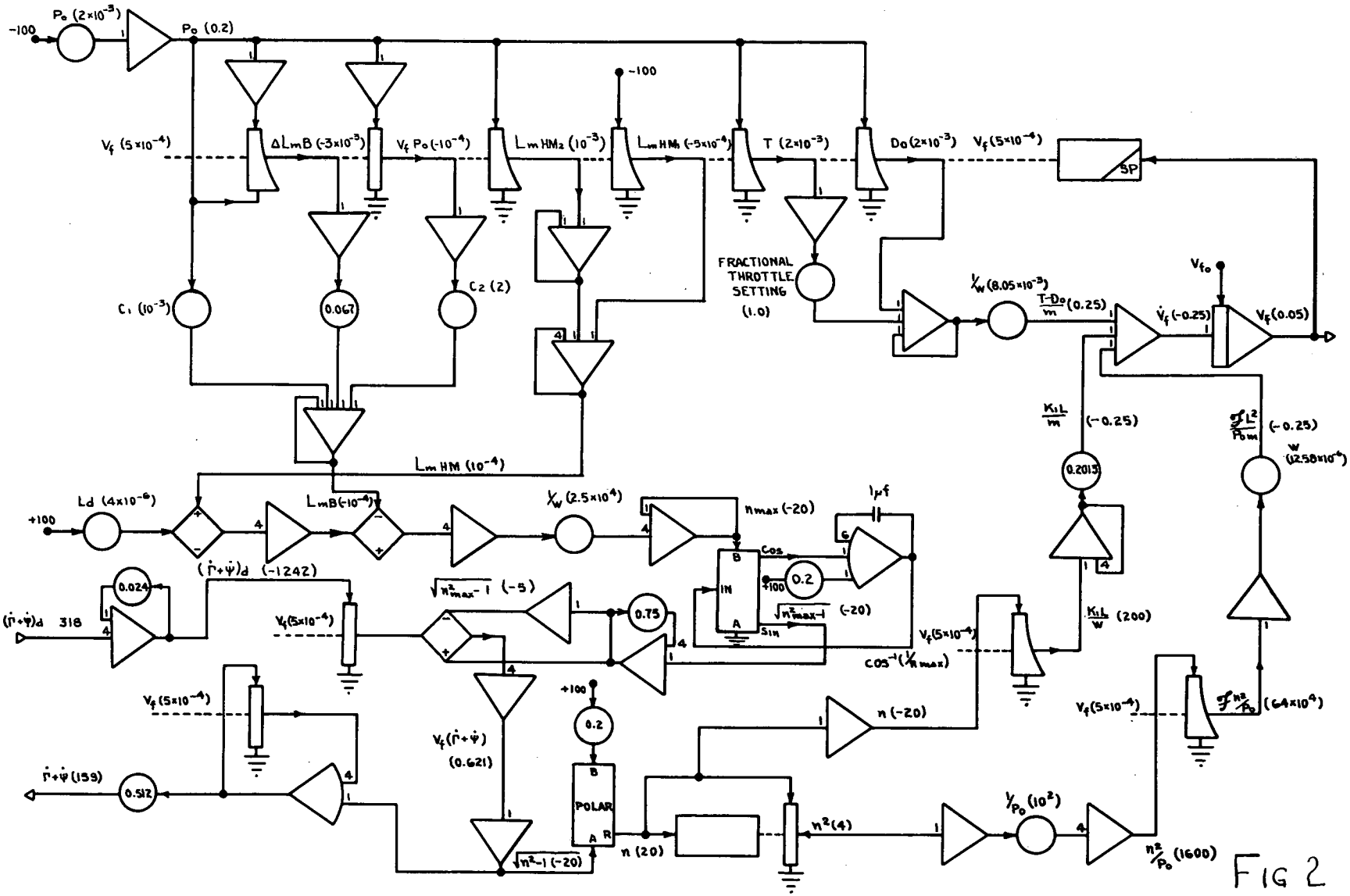
-100
P_o (2×10^{-3})
P_o (0.2)
V_f (5×10^{-4})
ΔL_{mB} (-3×10^{-3})
$V_f P_o$ (-10^{-4})
L_{mHM_2} (10^{-3})
L_{mHM_1} (-5×10^{-4})
T (2×10^{-3})
D_o (2×10^{-3})
V_f (5×10^{-4})
SP
C_1 (10^{-3})
0.067
C_2 (2)
FRACTIONAL THROTTLE SETTING (1.0)
K_w (8.05×10^{-3})
$\frac{T-D_o}{m}$ (0.25)
$\dot{V}_f$ (-0.25)
V_f (0.05)
V_{f_o}
L_{mHM} (10^{-4})
$\frac{K_1 L}{m}$ (-0.25)
0.2015
$\frac{K_2 L^2}{P_o m}$ (-0.25)
W (12.58×10^{-4})
Ld (4×10^{-6})
+100
L_{mB} (-10^{-4})
K_w (2.5×10^{4})
n_{max} (-20)
1μf
$(\dot{r}+\dot{\psi})_d$ (-1242)
0.024
$(\dot{r}+\dot{\psi})_d$ 318
$\sqrt{n^2_{max}-1}$ (-5)
V_f(5×10^{-4})
0.75
Cos
IN
Sin
+100
0.2
$\sqrt{n^2_{max}-1}$ (-20)
$\cos^{-1}(\frac{1}{n_{max}})$
$\frac{K_1 L}{W}$ (200)
$V_f(\dot{r}+\dot{\psi})$ (0.621)
+100
0.2
POLAR
$\dot{r}+\dot{\psi}$ (159)
0.512
$\sqrt{n^2-1}$ (-20)
n (20)
n (-20)
n^2(4)
$\frac{1}{P_o}$ (10^2)
$\frac{n^2}{P_o}$ (1600)
$\frac{fn^2}{P_o}$ (64×10^{-4})

FIG 2

7. Results and Discussion

Placement diagrams have been obtained under the conditions detailed in Table 1. Probabilities of successful placement, P_p, have been obtained from these diagrams by the method outlined in Reference 2. The page numbers on which the curves of placement probability vs. AI range are printed are also given in Table 1.

7.1 Target Evasion

The targets considered in this work were assumed to fly at Mach Nos. 1.5 or 2.0. These targets made constant turn rate conversion manoeuvres during the interceptor's approach beginning at detection by the interceptor. In many cases it was found that a target can turn sufficiently to place the interceptor astern and then escape because of its high speed. Target turns limited to 30° and 60°, as well as unlimited target turns, were considered to determine how far off course a target needs to turn to avoid attack.

The greatest degradation of placement probabilities took place when the interceptor made beam attacks on Mach 2.0 targets. A target turn through 30° in the optimum direction reduces the width of the allowable placement zone seriously in these cases. Probability of placement has been plotted against target's change of course in a number of cases. (See Table 1).

In calculating placement probabilities it has been assumed that the target makes an intelligent manoeuvre, turning in such a direction as to reduce placement probability rather than to increase it. With this assumption placement probability appears to rise from zero to a maximum and then fall to zero again as the AI radar range increases. Of course this will only happen in practice if the target always begins an intelligent conversion manoeuvre at the time of AI detection. The abscissa of each of these placement probability curves could also be labelled "Range at which target evasion begins," in order to make it clear that the fall in the value of placement probability is due to the target's manoeuvre beginning at long range, not to improved AI radar range. On the other hand improved AI radar performance, leading to greater lock-on ranges, will give a target an earlier opportunity to begin evasion. When attacking a target which could turn and escape because of its high speed, it may be advisable to delay lock-on or even hand tracking of the AI radar and thus avoid giving early warning of attack to the target.

[redacted]

7.2 Altitude

Only a limited altitude programme has been carried out, some work being done at 50,000 ft. altitude, some at 55,000 feet. The estimated ceiling of the CF-105 (N.A.E. 28% pessimistic) is about 58,000 feet and the maximum altitude at which Mach number 1.8 can be maintained in straight and level flight is about 55,000 feet.

7.3 Restriction of Interceptor g's

The gain used in the navigation control loop was such that the interceptor would make its corrective turns at the highest possible g's. At high g's, near to the aerodynamic limits, the deceleration due to induced drag is also high and the interceptor velocity falls very considerably in a prolonged turn. Velocity decreases of this nature make interception difficult when the fighter begins its attack from a point behind the ideal approach line, when maximum velocity should be maintained in order to catch up with the target.

It had been tentatively concluded from the earlier work with a constant speed model of the interceptor that placement probability increases only slowly with interceptor lateral g capability above 1.5 (load factor 1.8; see Ref.2). Consequently some cases were studied with a fixed limit on interceptor load factor which lay below the normal aerodynamic limits in the range of velocities considered. This procedure increases the allowable placement on the rear side of the ideal approach line, but tends to degrade it on the front side. These results indicate that it may be desirable to manoeuvre to the aerodynamic limit when ahead of the ideal line, but to manoeuvre only to the power limit when behind this line. This matter is discussed further in Appendix K of this report.

8. References

1. CARDE Technical Letter N-47-8, "First Quarterly Report on CF-105 Weapon System Assessment", Appendices C and D. SECRET.

2. CARDE Technical Letter N-47-12, "Second Quarterly Report on CF-105 Weapon System Assessment", Appendix K. SECRET.

3. CARDE Technical Letter N-47-14, "CF-105 Aircraft Interceptor Placement Problem - A Method of Solution using the REAC for the 2-Dimensional Constant Fighter Speed Case", SECRET.

4. N.A.E. Lab. Memo. No. AE-82, "The Problem of Representing the High-Altitude Performance of a Turbo-jet Aircraft on an Analogue Computer", by R.J. Templin. CONFIDENTIAL.

5. N.A.E. Lab. Memo. No. AE-46g, "High Altitude Performance Data for the CF-105 Aircraft", by O.E. Michaelsen. SECRET.

6. CARDE Technical Letter N-47-2, "Launch Zones for a Hypothetical Constant Bearing Missile" by J.T. Macfarlane.

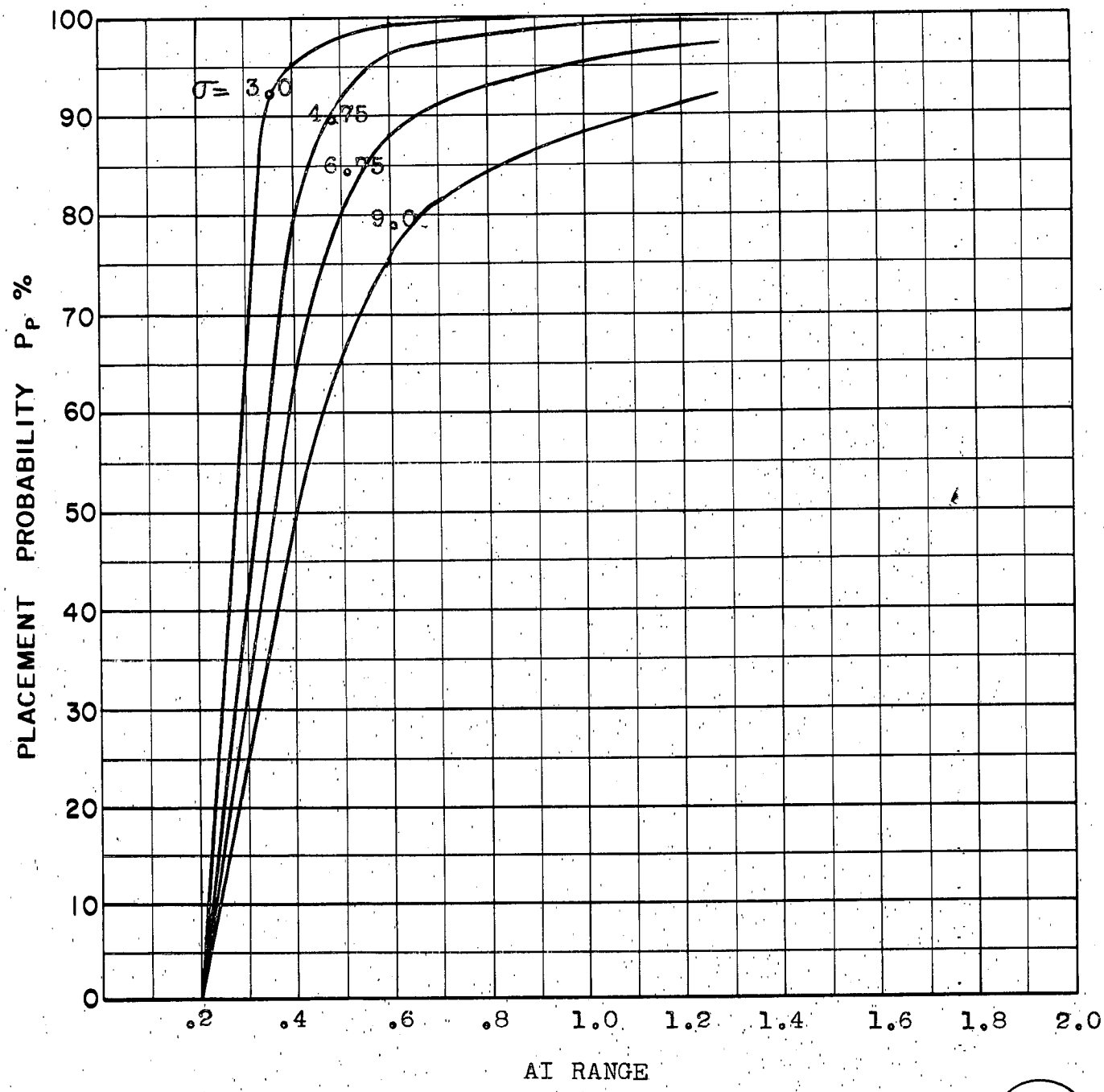

COURSE DIFFERENCE: 110°
TARGET EVASION: 0.75g (30° & 60°) change of course
TARGET MACH NO.: 1.5
INTERCEPTOR LATERAL G's: 28 % pess
INTERCEPTOR MACH NO.: 1.8
σ OF G.C.I. ACCURACY: 5 Values
A.I. DETECTION RANGE AS FRACTION OF SPECIFICATION RANGE, S: Abscissa
A.I. DETECTION RANGE CONTOUR: Delta Wing
ALTITUDE: 50K

D.1 E

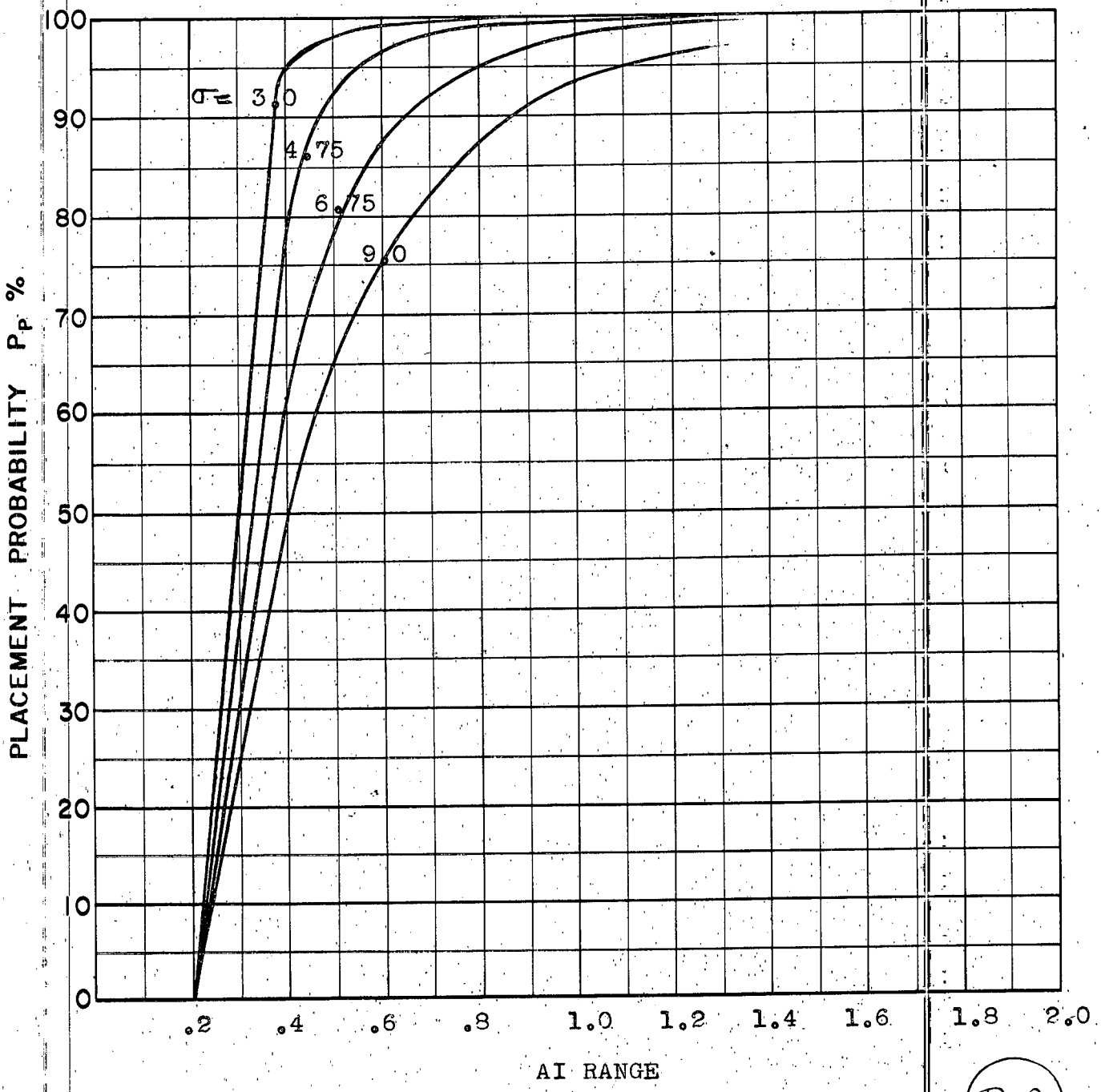

D-2
E

COURSE DIFFERENCE: 135°
TARGET EVASION: 0.75g (30° & 60°) change of course
TARGET MACH NO.: 1.5
INTERCEPTOR LATERAL G's: 2 8% Pess
INTERCEPTOR MACH NO.: 1.8
σ OF G.C.I. ACCURACY: 5 Values
A.I. DETECTION RANGE AS FRACTION OF SPECIFICATION RANGE, S: Abscissa
A.I. DETECTION RANGE CONTOUR: Delta Wing
ALTITUDE: 50K

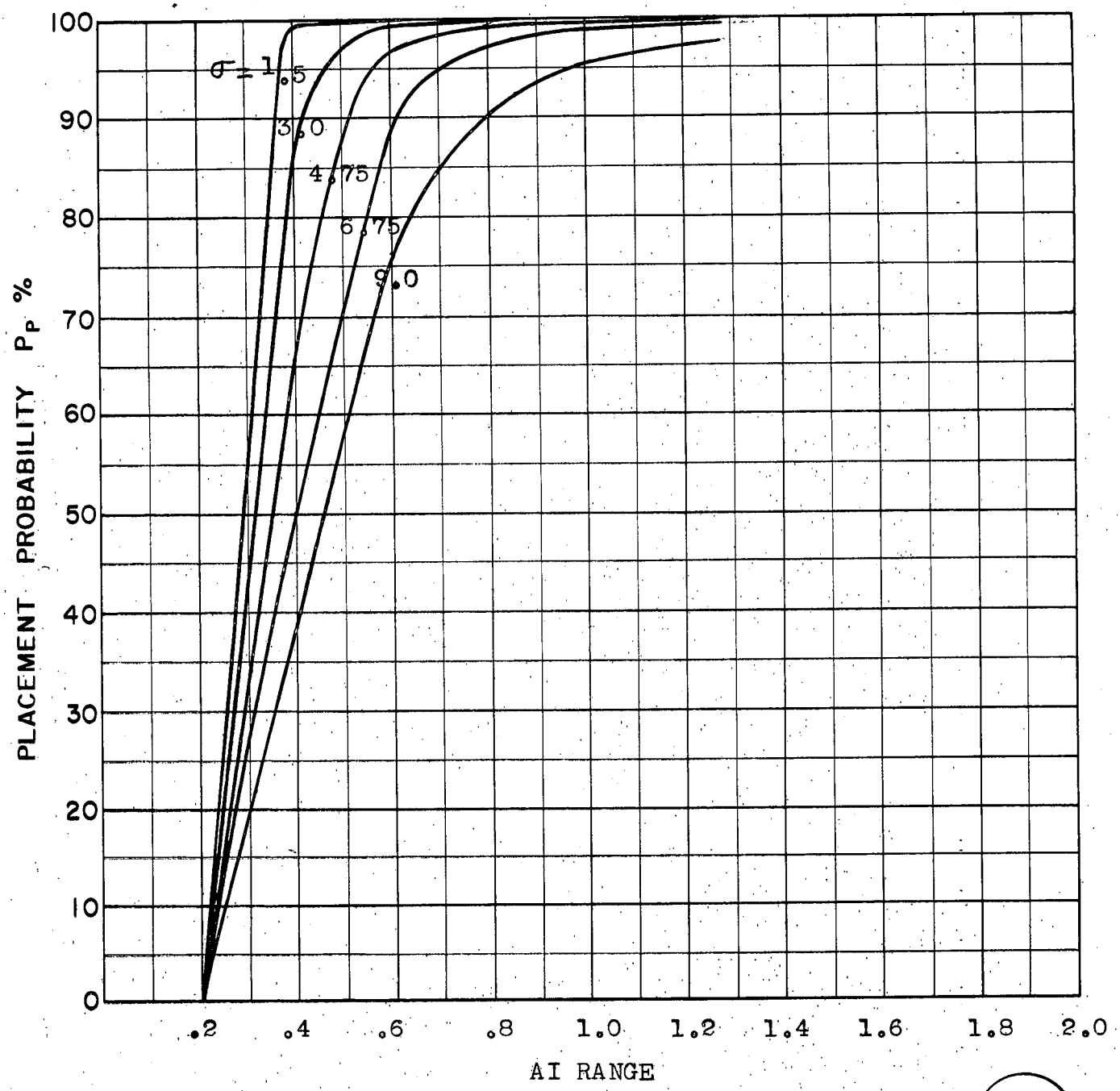

COURSE DIFFERENCE: 160°
TARGET EVASION: 0.75g (30° & 60°) change of course
TARGET MACH NO.: 1.5
INTERCEPTOR LATERAL G's: 28% pess.
INTERCEPTOR MACH NO.: 1.8
σ OF G.C.I. ACCURACY: 5 Values
A.I. DETECTION RANGE AS FRACTION OF SPECIFICATION RANGE, S: Abscissa
A.I. DETECTION RANGE CONTOUR: Delta Wing
ALTITUDE: 50K

D-3
ε

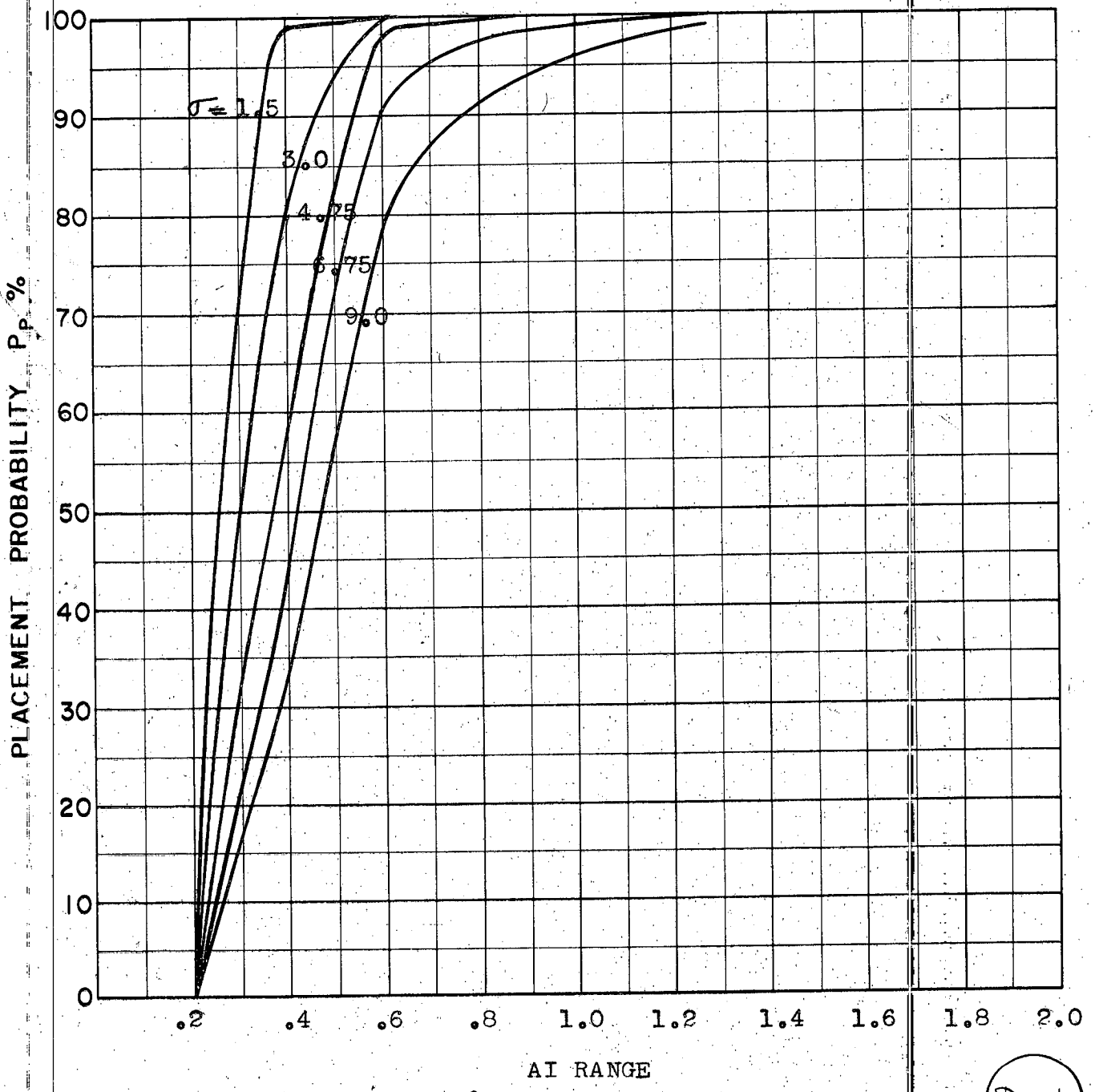

D-4
ε

COURSE DIFFERENCE: 180°
TARGET EVASION: 0.75g (30° & 60°) change of course
TARGET MACH NO.: 1.5
INTERCEPTOR LATERAL G's: 28% pess.
INTERCEPTOR MACH NO.: 1.8
σ OF G.C.I. ACCURACY: 5 Values
A.I. DETECTION RANGE AS FRACTION OF SPECIFICATION RANGE, S: Abscissa
A.I. DETECTION RANGE CONTOUR: Delta Wing
ALTITUDE: 50K

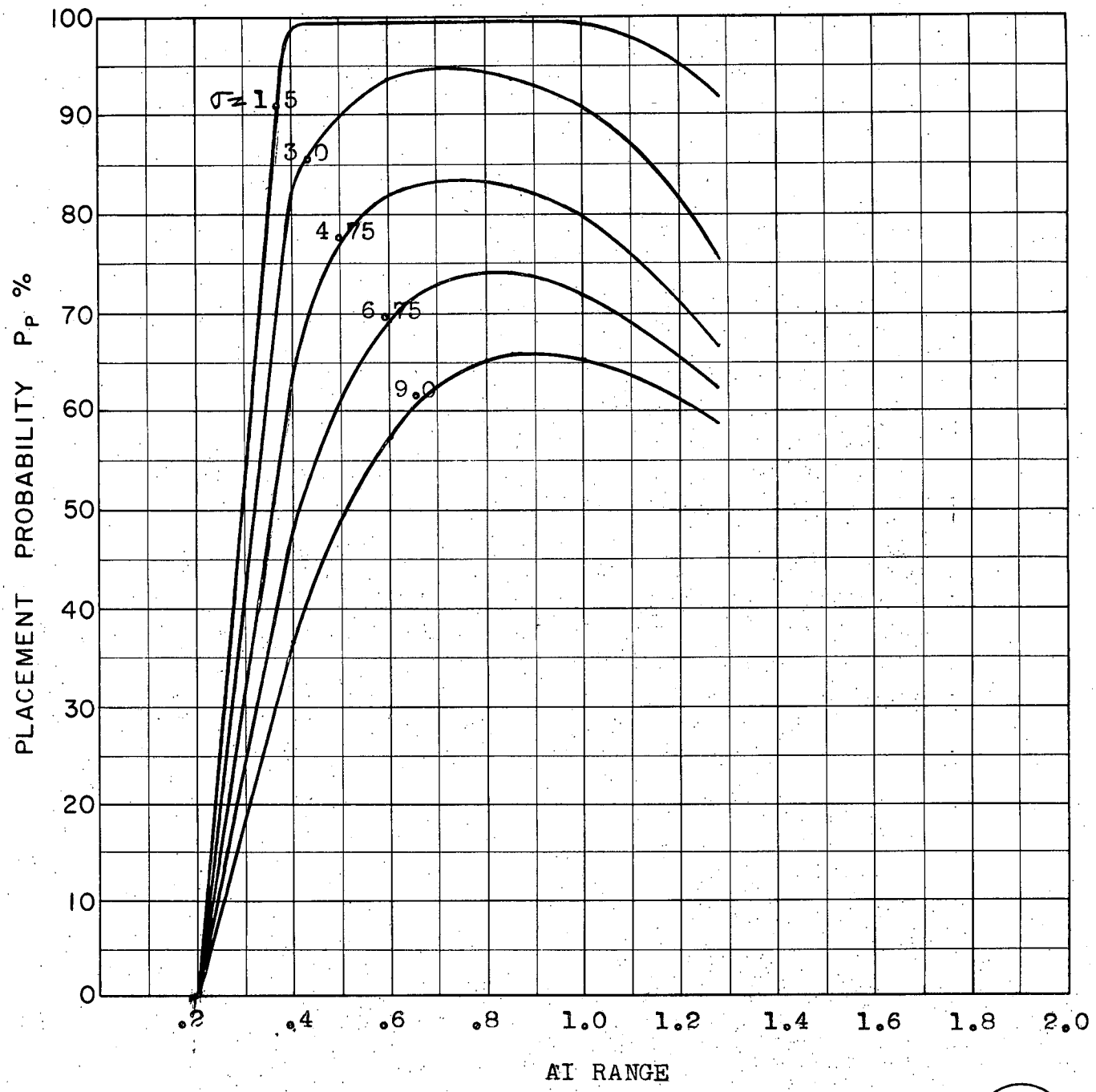

COURSE DIFFERENCE: 110°
TARGET EVASION: 0.25g
TARGET MACH NO.: 2.0
INTERCEPTOR LATERAL G's: 28% pess.
INTERCEPTOR MACH NO.: 1.8
σ OF G.C.I. ACCURACY: 5 Values
A.I. DETECTION RANGE AS FRACTION OF SPECIFICATION RANGE, S: Abscissa
A.I. DETECTION RANGE CONTOUR: Delta Wing
ALTITUDE: 50K

D-5

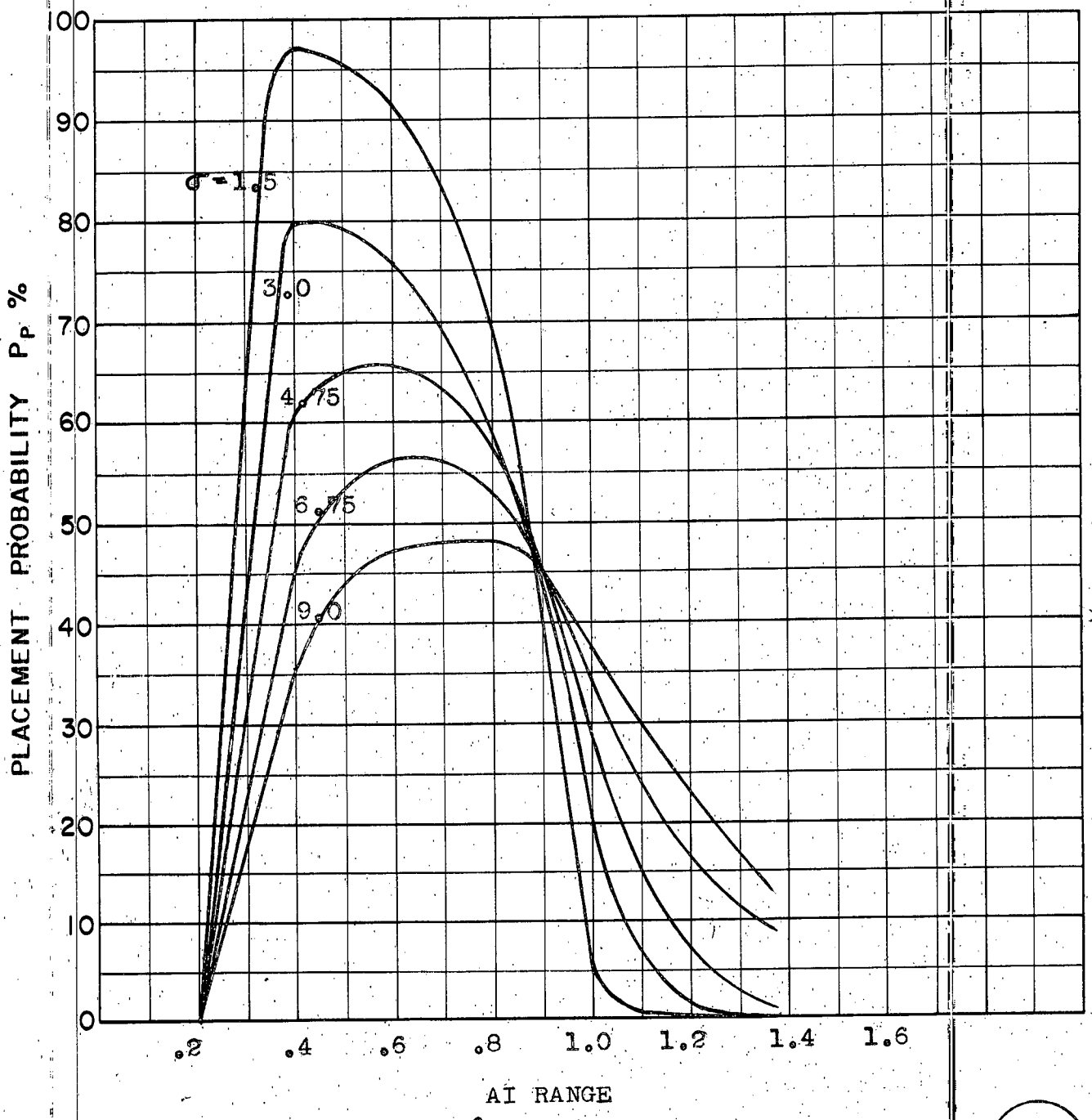

COURSE DIFFERENCE: 110°
TARGET EVASION: 0.5g
TARGET MACH NO.: 2.0
INTERCEPTOR LATERAL G's: 28% pess.
INTERCEPTOR MACH NO.: 1.8
σ OF G.C.I. ACCURACY: 5 Values
A.I. DETECTION RANGE AS FRACTION OF SPECIFICATION RANGE, S: Abscissa
A.I. DETECTION RANGE CONTOUR: Delta Wing
ALTITUDE: 50K

D-6a
E

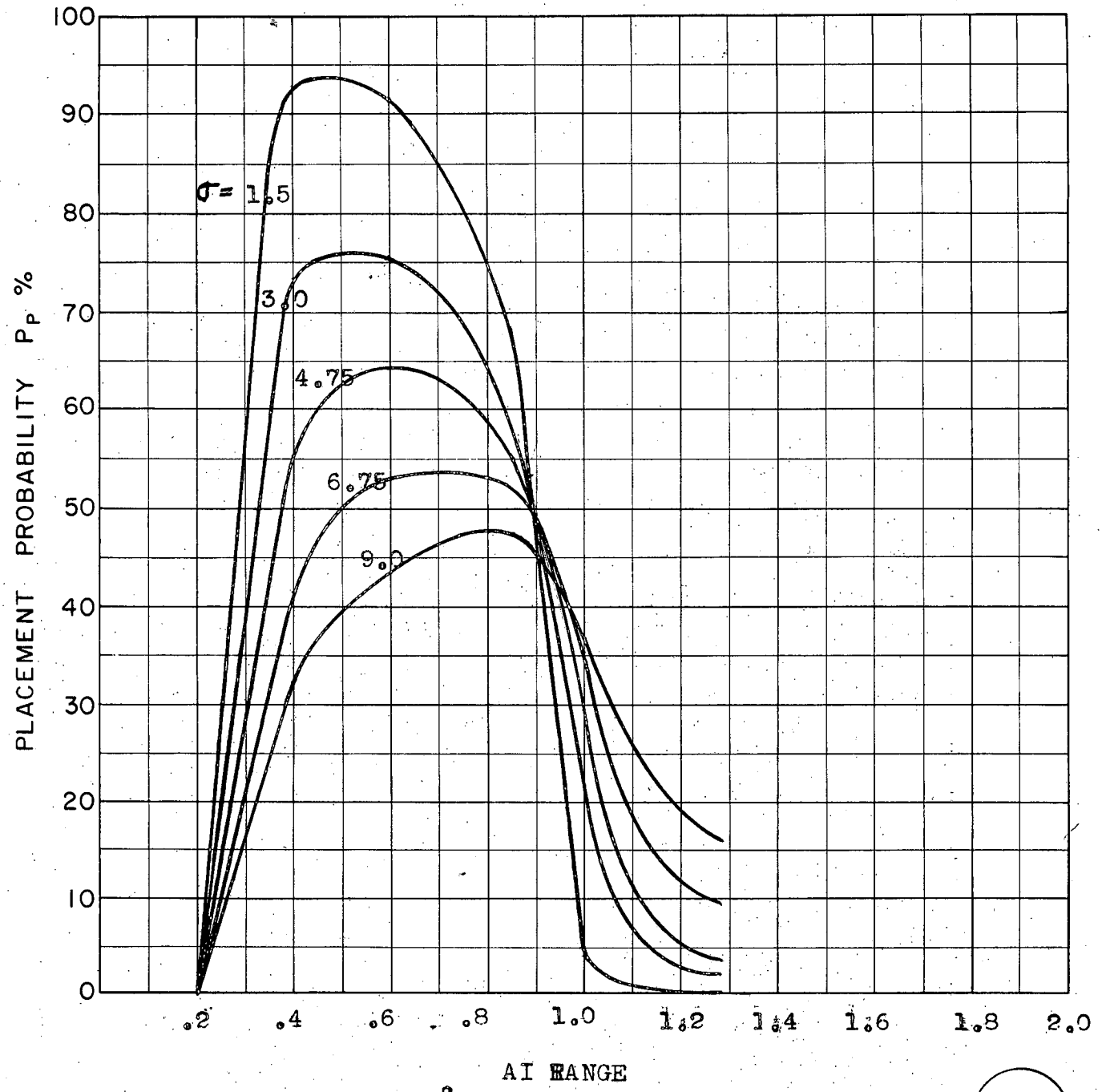

COURSE DIFFERENCE: 110°
TARGET EVASION: 0.5g
TARGET MACH NO.: 2.0
INTERCEPTOR LATERAL G's: 2.0g Limit; 28% pess.
INTERCEPTOR MACH NO.: 1.8
σ OF G.C.I. ACCURACY: 5 Values
A.I. DETECTION RANGE AS FRACTION OF SPECIFICATION RANGE, S: Abscissa
A.I. DETECTION RANGE CONTOUR: Delta Wing
ALTITUDE: 50K

D.6b
E

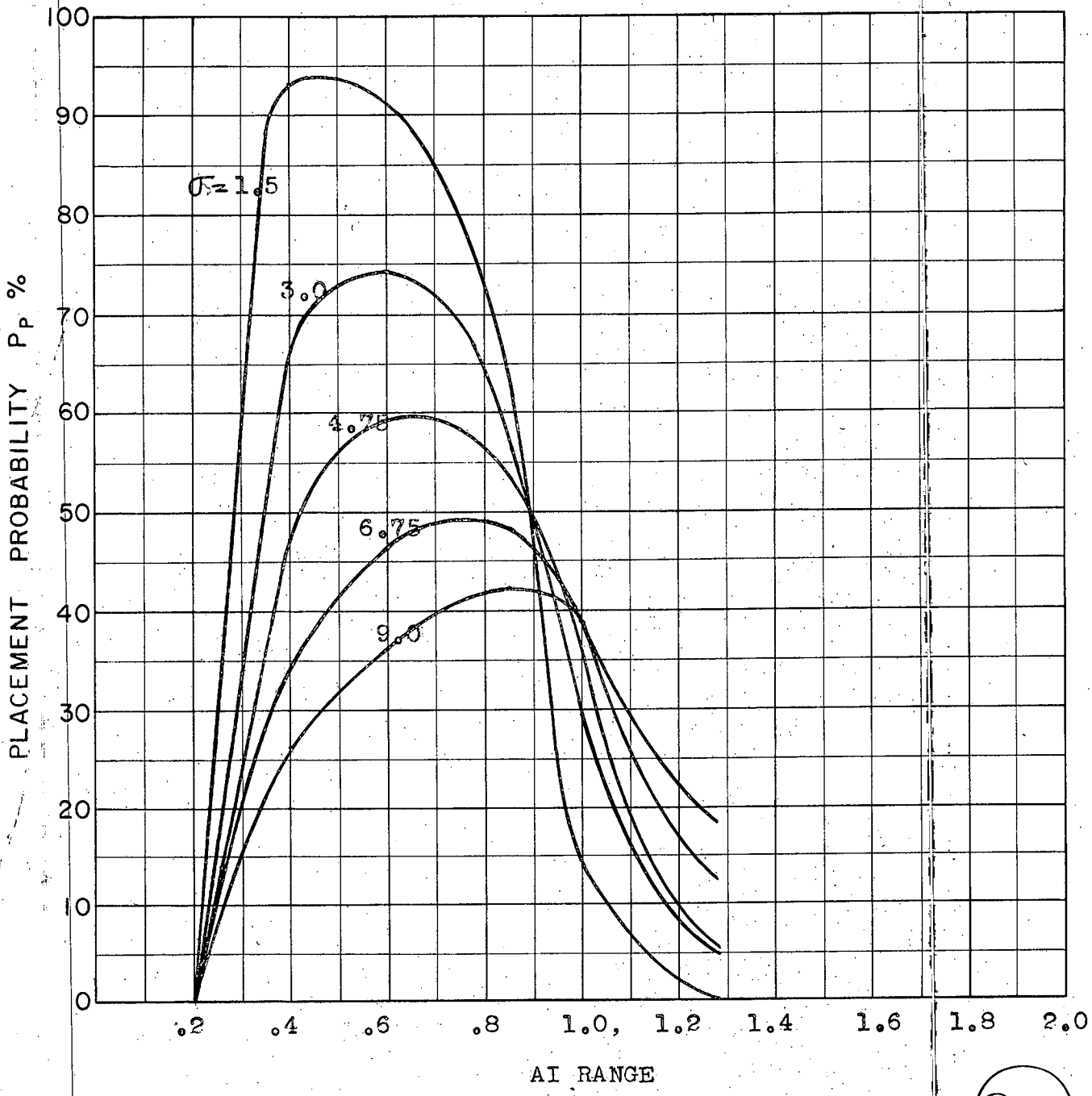

D-6c
E

COURSE DIFFERENCE: 110°
TARGET EVASION: 0.5g
TARGET MACH NO.: 2.0
INTERCEPTOR LATERAL G's: 1.5g Limit; 28% pess.
INTERCEPTOR MACH NO.: 1.8
σ OF G.C.I. ACCURACY: 5 Values
A.I. DETECTION RANGE AS FRACTION OF SPECIFICATION RANGE, S: Abscissa
A.I. DETECTION RANGE CONTOUR: Delta Wing
ALTITUDE: 50K

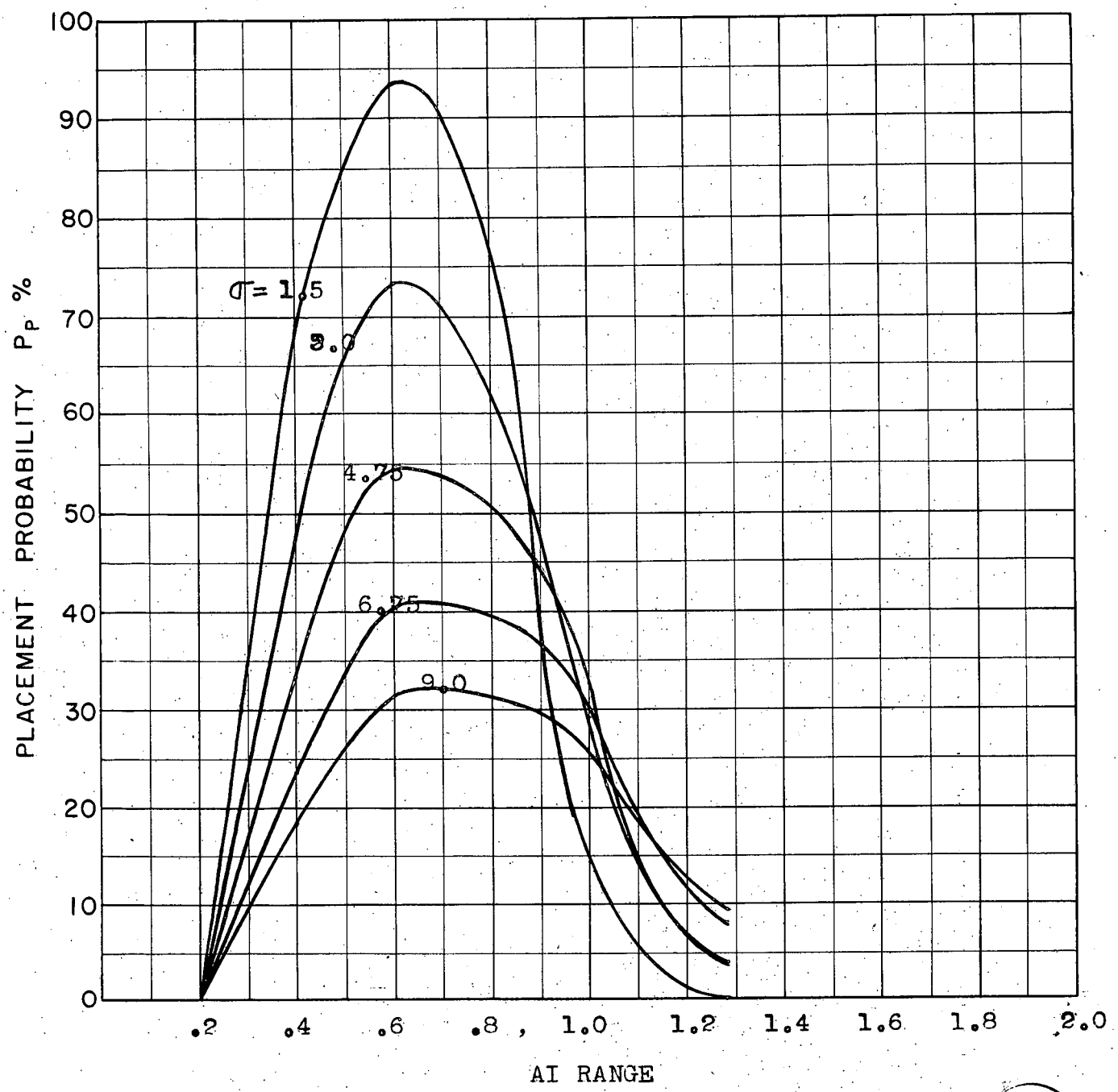

COURSE DIFFERENCE: 110°
TARGET EVASION: 0.5g
TARGET MACH NO.: 2.0
INTERCEPTOR LATERAL G's: 1.0 Limit; 28% pess.
INTERCEPTOR MACH NO.: 1.8
σ OF G.C.I. ACCURACY: 5 Values
A.I. DETECTION RANGE AS FRACTION OF SPECIFICATION RANGE, S: Abscissa
A.I. DETECTION RANGE CONTOUR: Delta Wing
ALTITUDE: 50K

D-6d
E

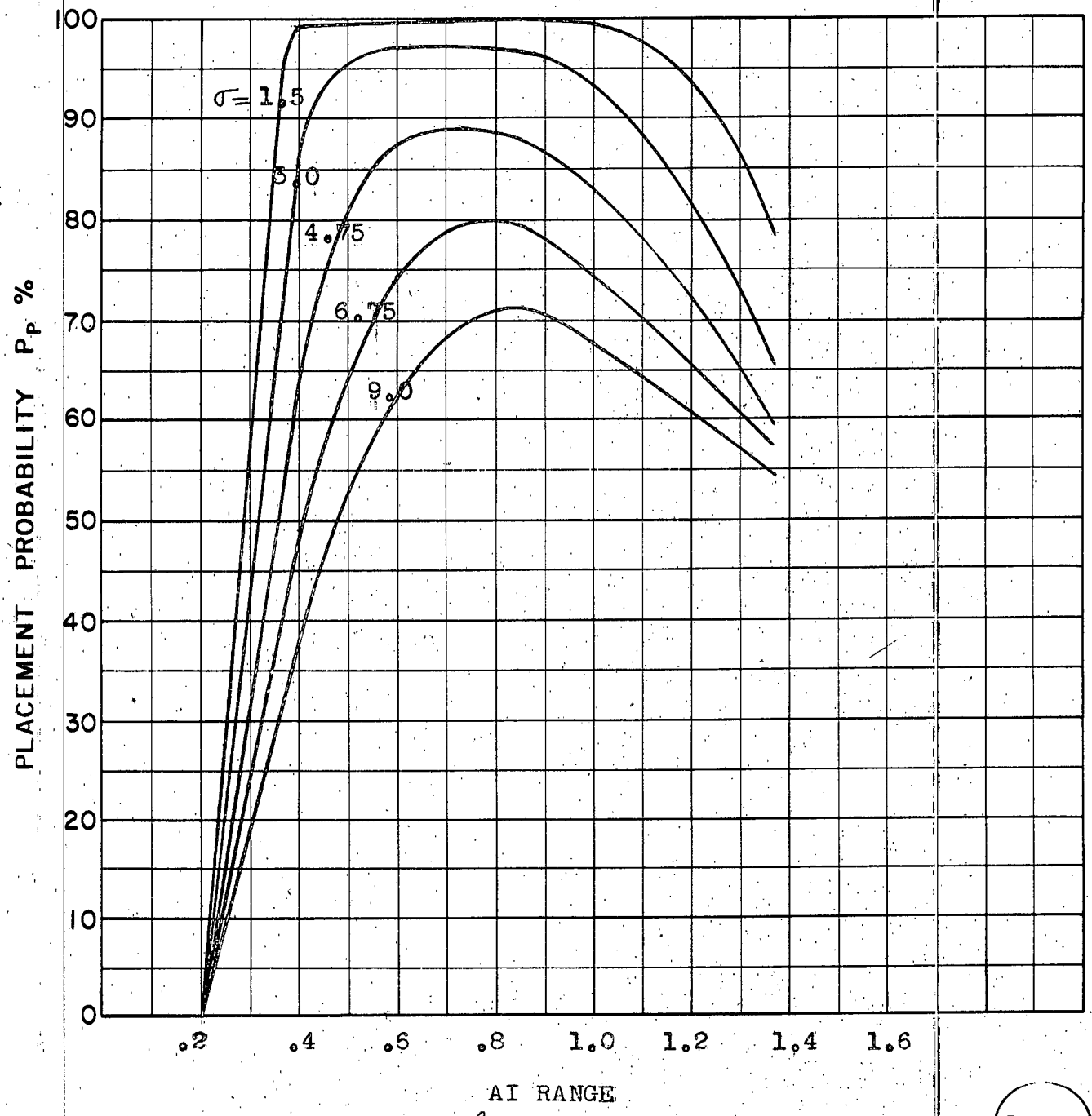

D-7 E

COURSE DIFFERENCE: 135°
TARGET EVASION: 0.5g
TARGET MACH NO.: 2.0
INTERCEPTOR LATERAL G's: 28% pess.
INTERCEPTOR MACH NO.: 1.8
σ OF G.C.I. ACCURACY: 5 Values
A.I. DETECTION RANGE AS FRACTION OF SPECIFICATION RANGE, S: Abscissa
A.I. DETECTION RANGE CONTOUR: Delta Wing
ALTITUDE: 50K

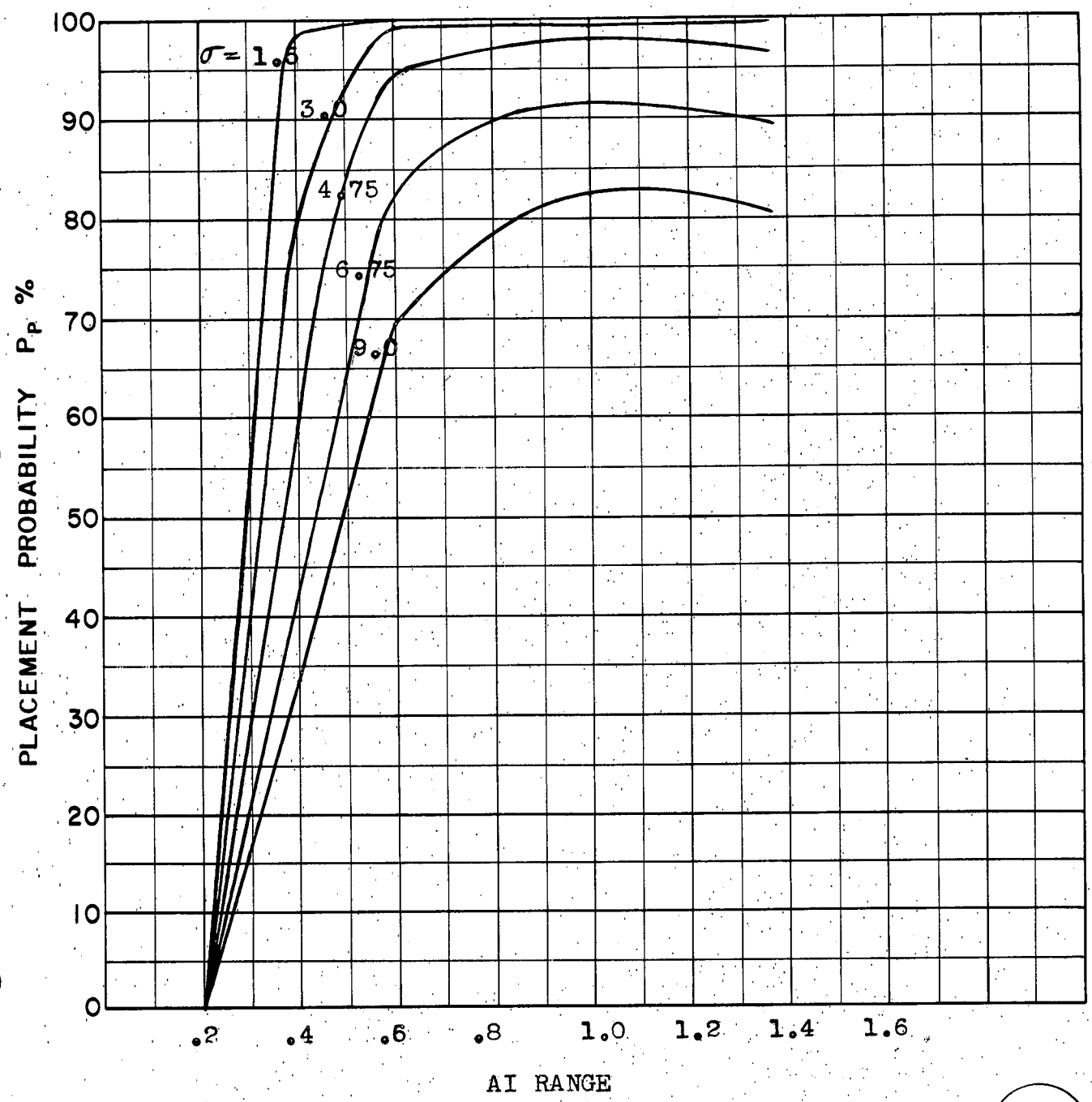

COURSE DIFFERENCE: 160°
TARGET EVASION: 0.5g
TARGET MACH NO.: 2.0
INTERCEPTOR LATERAL G's: 28% pos.
INTERCEPTOR MACH NO.: 1.8
σ OF G.C.I. ACCURACY: 5 Values
A.I. DETECTION RANGE AS FRACTION OF SPECIFICATION RANGE, S: Abscissa
A.I. DETECTION RANGE CONTOUR: Delta Wing
ALTITUDE: 50K

D-8 E

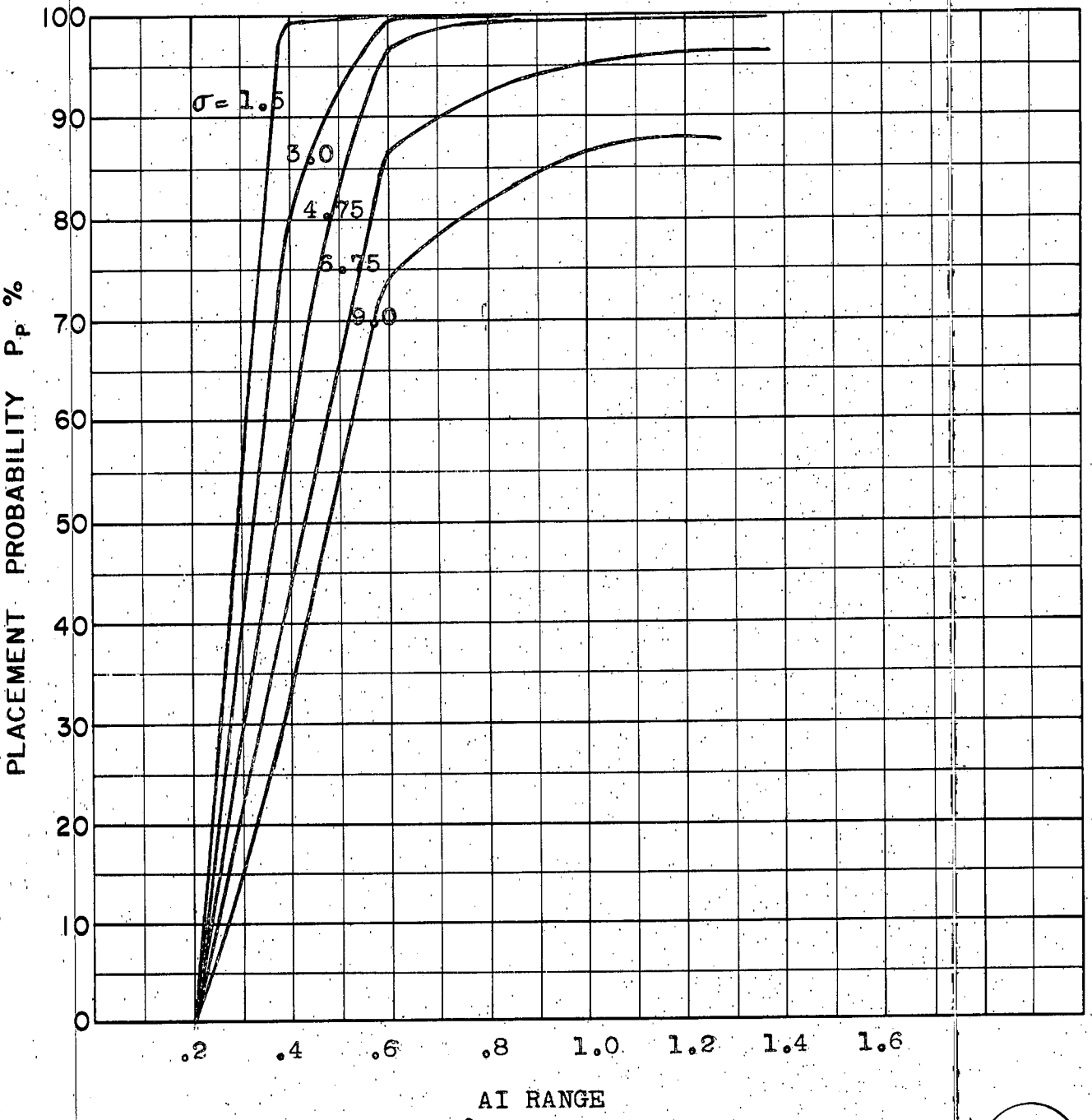

COURSE DIFFERENCE: 180°
TARGET EVASION: 0.5g
TARGET MACH NO.: 2.0
INTERCEPTOR LATERAL G's: 28% pess.
INTERCEPTOR MACH NO.: 1.8
σ OF G.C.I. ACCURACY: 5 Values
A.I. DETECTION RANGE AS FRACTION OF SPECIFICATION RANGE, S: Abscissa
A.I. DETECTION RANGE CONTOUR: Delta Wing
ALTITUDE: 50K

D.9a
E

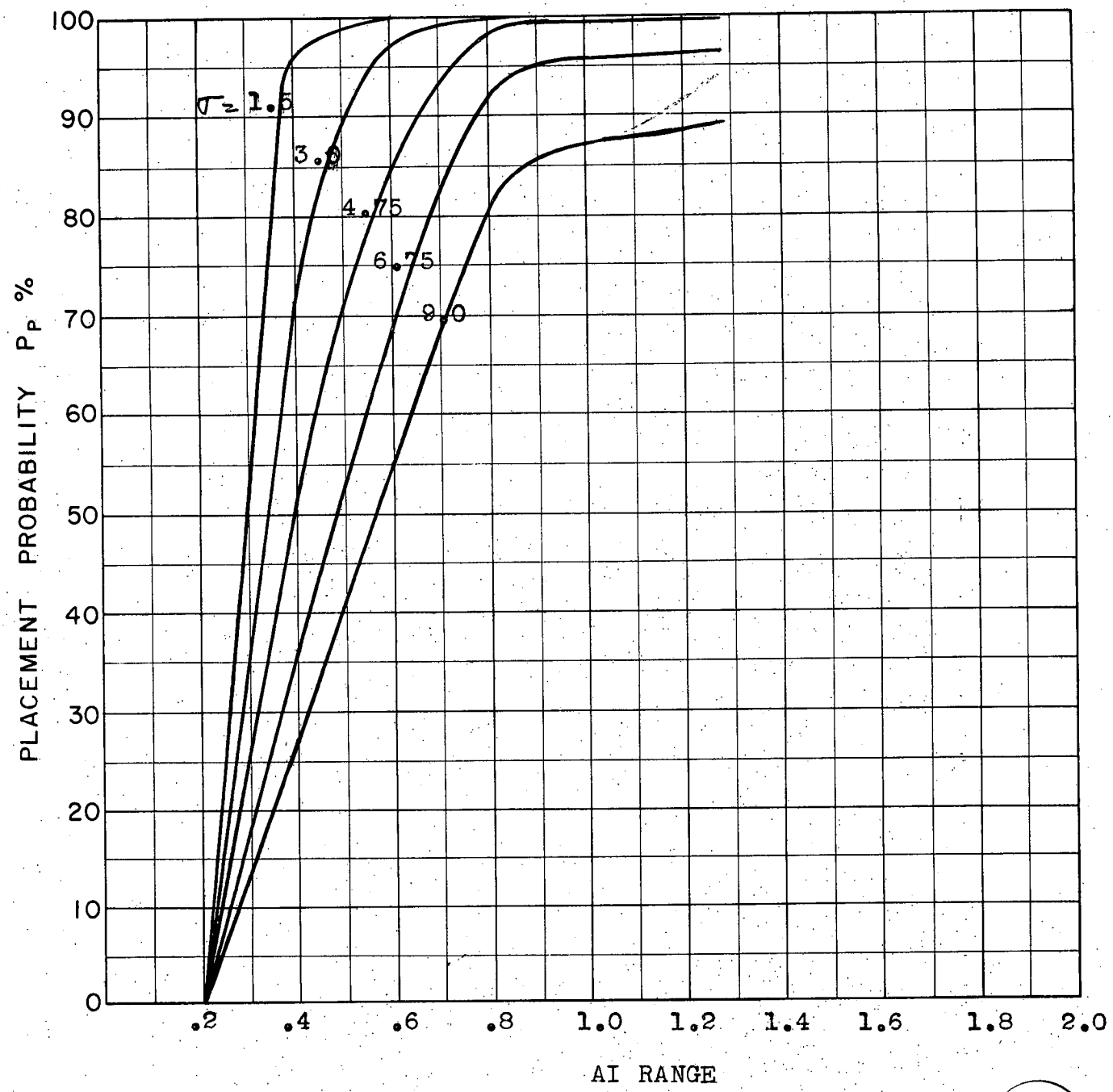

COURSE DIFFERENCE: 180°
TARGET EVASION: 0.5g
TARGET MACH NO.: 2.0
INTERCEPTOR LATERAL G's: 2.0g Limit; 28% pess.
INTERCEPTOR MACH NO.: 1.8
σ OF G.C.I. ACCURACY: 5 Values
A.I. DETECTION RANGE AS FRACTION OF SPECIFICATION RANGE, S: Abscissa
A.I. DETECTION RANGE CONTOUR: Delta Wing
ALTITUDE: 50K

D-9b
E

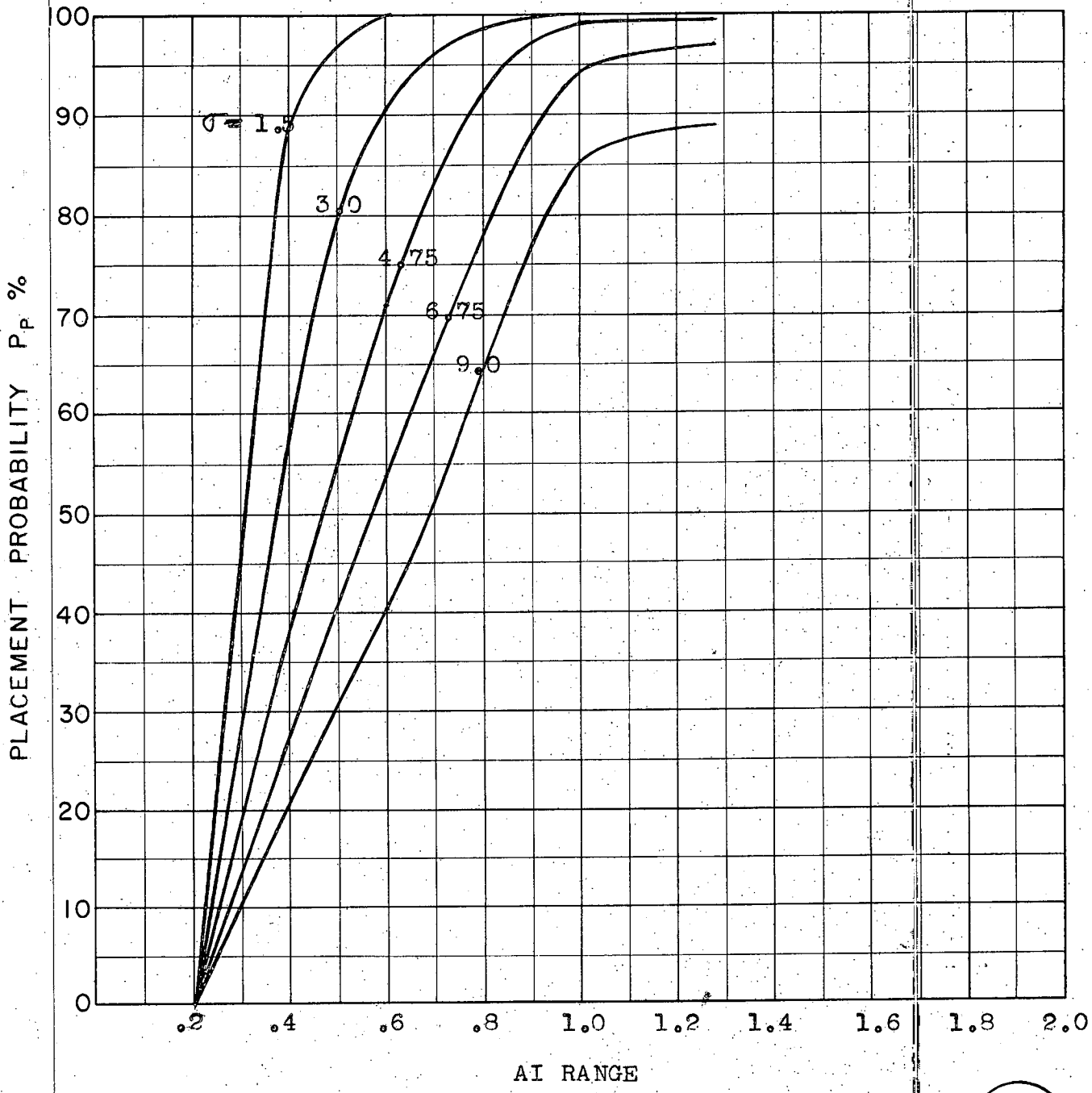

COURSE DIFFERENCE: 180°
TARGET EVASION: 0.5g
TARGET MACH NO.: 2.0
INTERCEPTOR LATERAL G's: 1.5g Limit 28% pess.
INTERCEPTOR MACH NO.: 1.8
σ OF G.C.I. ACCURACY: 5 Values
A.I. DETECTION RANGE AS FRACTION OF SPECIFICATION RANGE, S: Abscissa
A.I. DETECTION RANGE CONTOUR: Delta Wing
ALTITUDE: 50K

D-9c
E

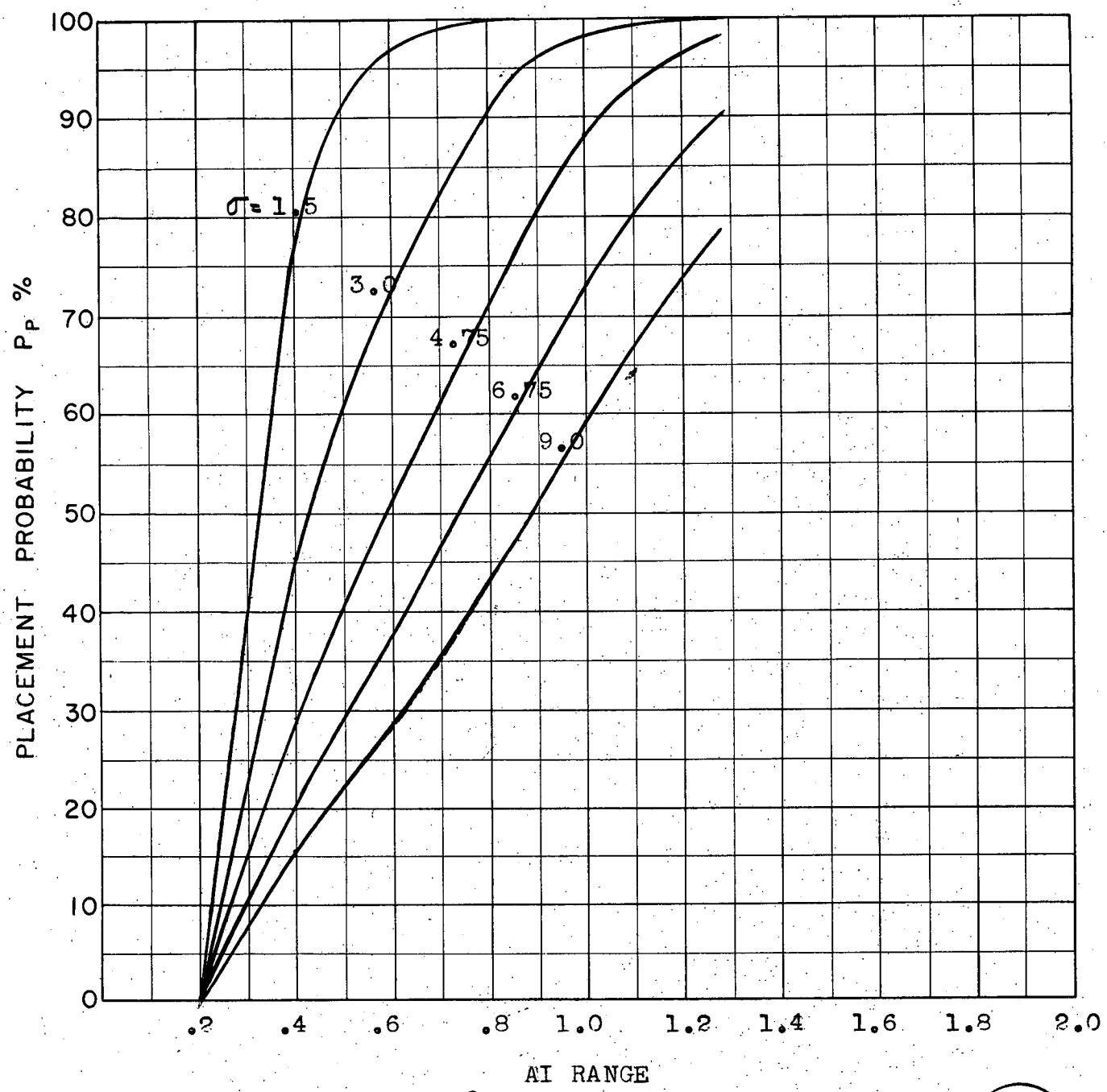

COURSE DIFFERENCE: 180°
TARGET EVASION: 0.5g
TARGET MACH NO.: 2.0
INTERCEPTOR LATERAL G's: 1.0g Limit: 28% pess.
INTERCEPTOR MACH NO.: 1.8
σ OF G.C.I. ACCURACY: 5 Values
A.I. DETECTION RANGE AS FRACTION OF SPECIFICATION RANGE, S: Abscissa
A.I. DETECTION RANGE CONTOUR: Delta Wing
ALTITUDE: 50K

D-9d
E

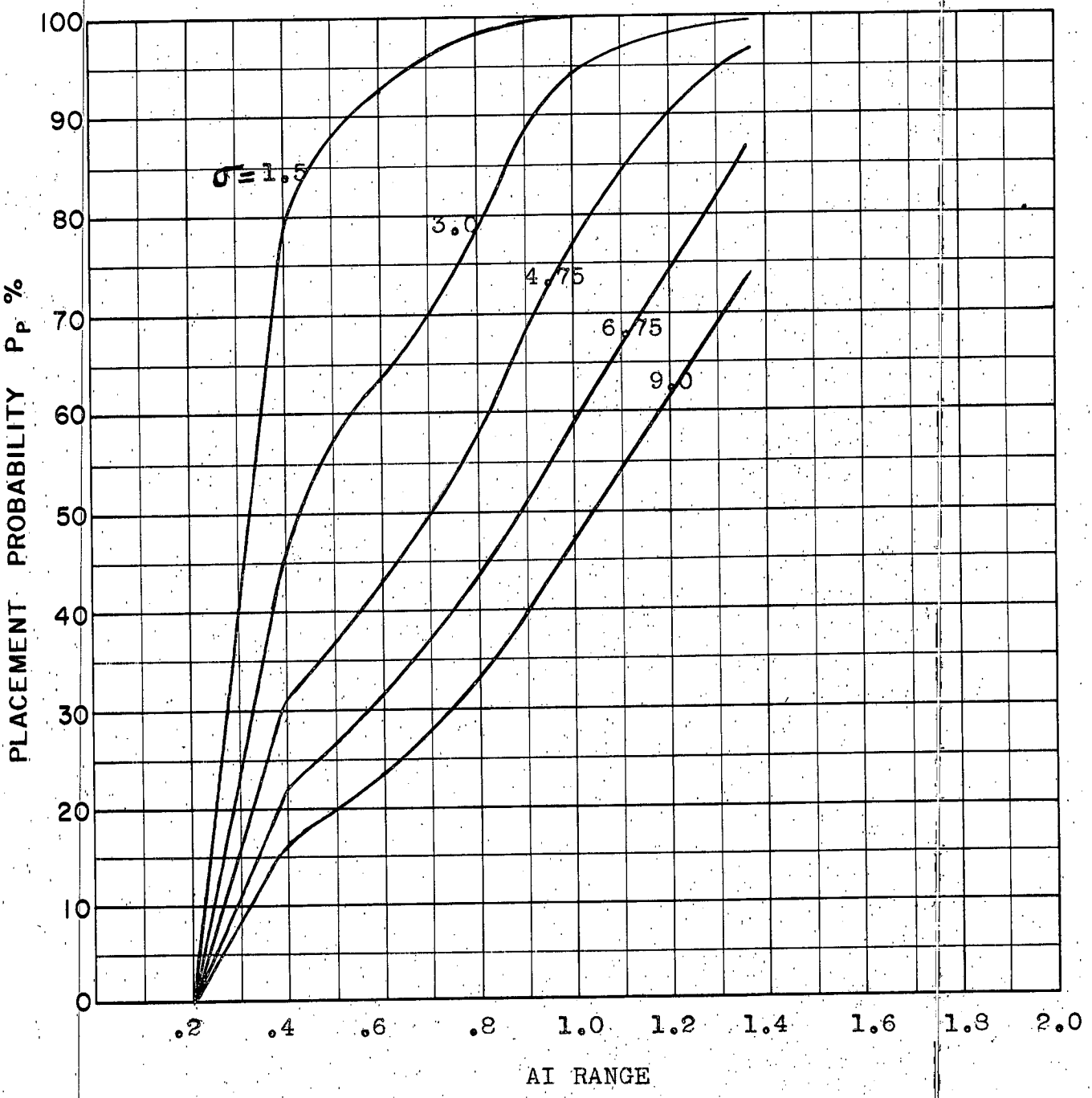

COURSE DIFFERENCE: 180°
TARGET EVASION: 0.5g
TARGET MACH NO.: 2.0
INTERCEPTOR LATERAL G's: Limited to 0.75g (28% pess.)
INTERCEPTOR MACH NO.: 1.8
σ OF G.C.I. ACCURACY: 5 Values
A.I. DETECTION RANGE AS FRACTION OF SPECIFICATION RANGE, S: Abscissa
A.I. DETECTION RANGE CONTOUR: Delta Wing
ALTITUDE: 50K

D.9e
E

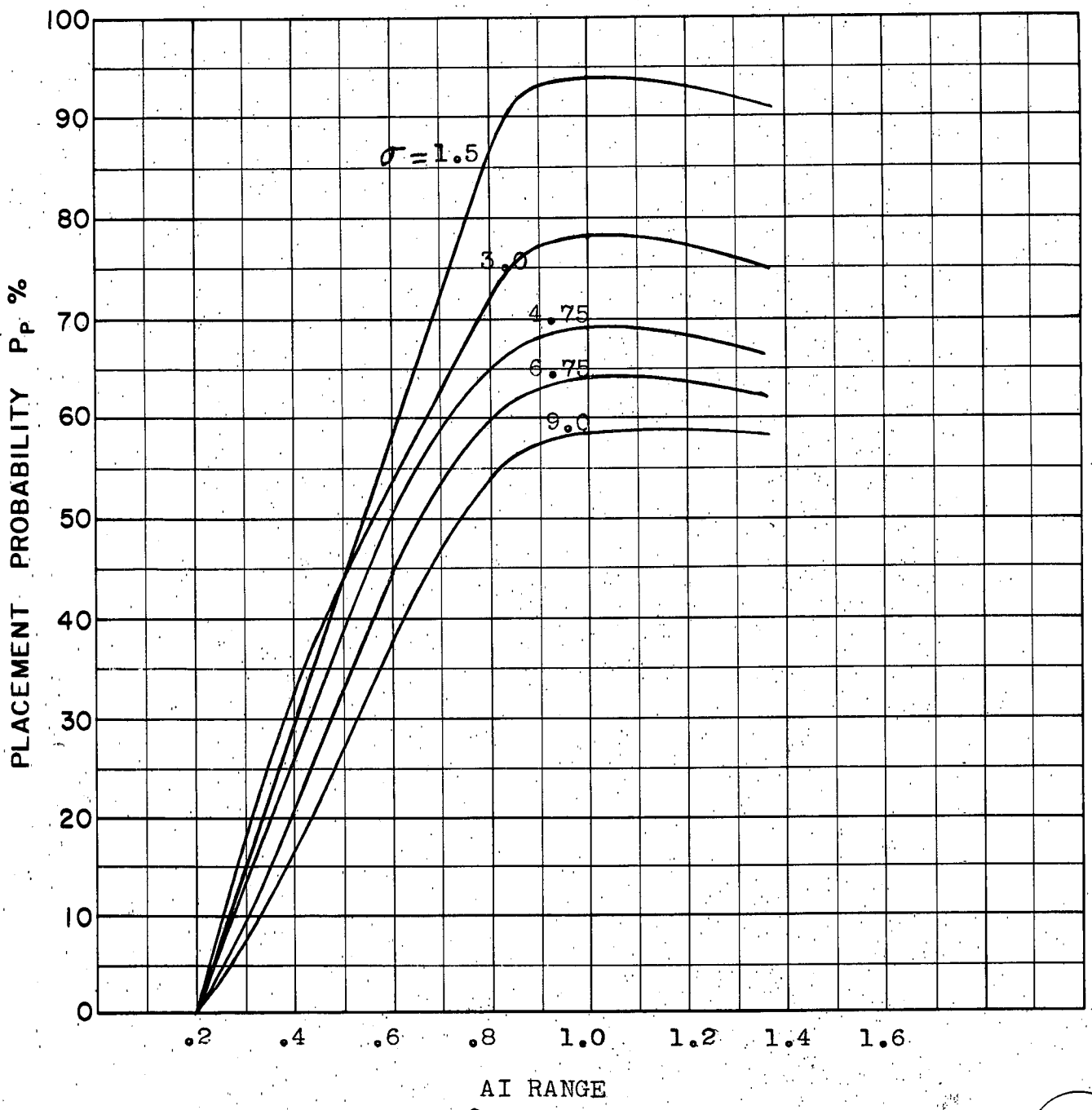

COURSE DIFFERENCE: 110°
TARGET EVASION: 0.75g Limited to 30° change of course
TARGET MACH NO.: 2.0
INTERCEPTOR LATERAL G's: 28% pess.
INTERCEPTOR MACH NO.: 1.8
σ OF G.C.I. ACCURACY: 5 Values
A.I. DETECTION RANGE AS FRACTION OF SPECIFICATION RANGE, S: Abscissa
A.I. DETECTION RANGE CONTOUR: Delta Wing
ALTITUDE: 50K

D-10a
E

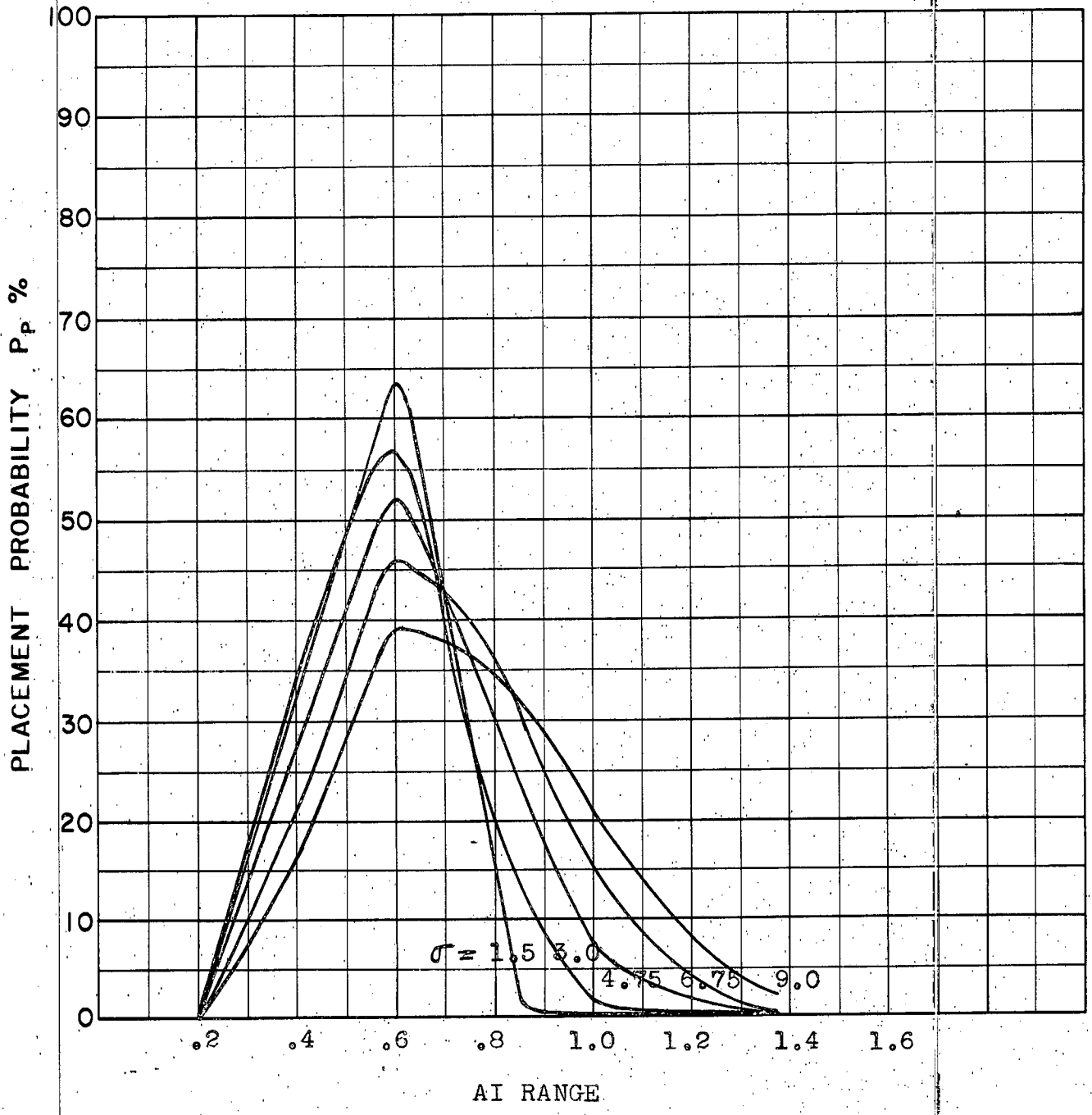

COURSE DIFFERENCE: 110°
TARGET EVASION: 0.75g Limited to 60° change of course
TARGET MACH NO.: 2.0
INTERCEPTOR LATERAL G's: 28% pess.
INTERCEPTOR MACH NO.: 1.8
σ OF G.C.I. ACCURACY: 5 Values
A.I. DETECTION RANGE AS FRACTION OF SPECIFICATION RANGE, S: Abscissa
A.I. DETECTION RANGE CONTOUR: Delta
ALTITUDE: 50K

D10b
E

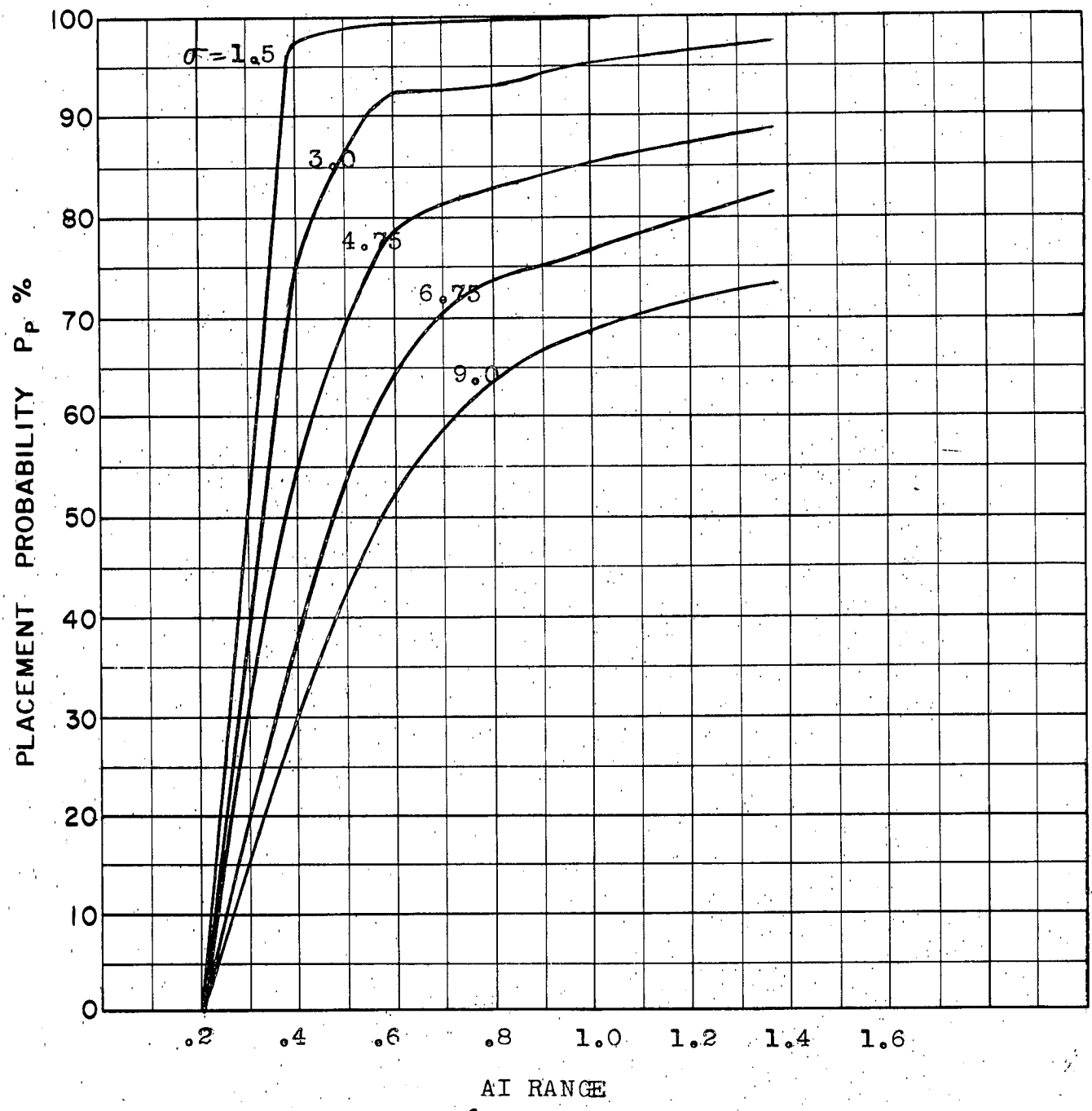

COURSE DIFFERENCE: 135°
TARGET EVASION: 0.75g Limited to 30° change of course
TARGET MACH NO.: 2.0
INTERCEPTOR LATERAL G's: 28% pess.
INTERCEPTOR MACH NO.: 1.8
σ OF G.C.I. ACCURACY: 5 Values
A.I. DETECTION RANGE AS FRACTION OF SPECIFICATION RANGE, S Abscissa
A.I. DETECTION RANGE CONTOUR: Delta Wing
ALTITUDE: 50K

D11a
E

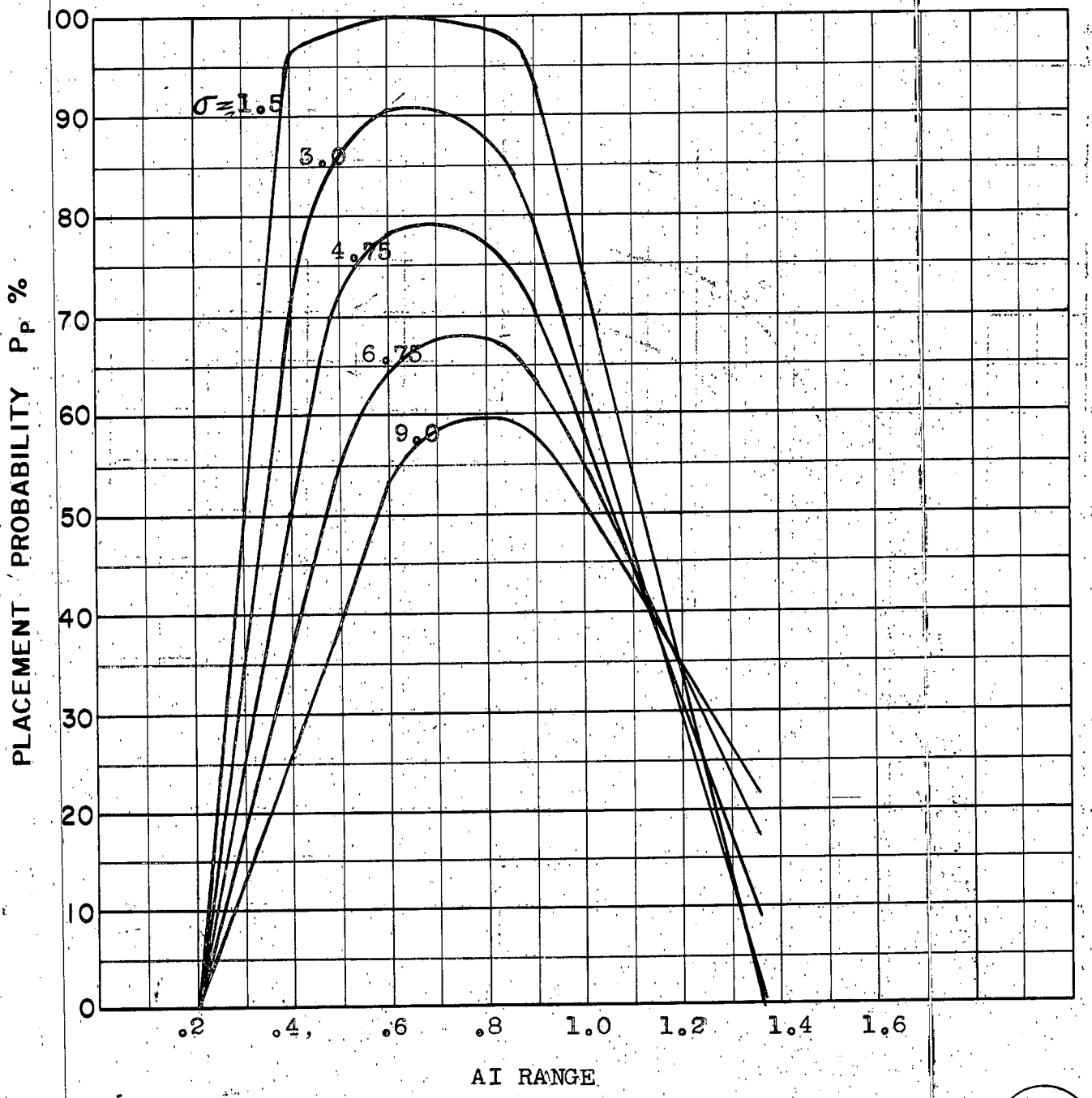

COURSE DIFFERENCE: 135°
TARGET EVASION: 0.75g Limited to 60° change of course
TARGET MACH NO.: 2.0
INTERCEPTOR LATERAL G's: 28% pess.
INTERCEPTOR MACH NO.: 1.8
σ OF G.C.I. ACCURACY: 5 Values
A.I. DETECTION RANGE AS FRACTION OF SPECIFICATION RANGE, S: Abscissa
A.I. DETECTION RANGE CONTOUR: Delta Wing
ALTITUDE: 50K

D11b
E

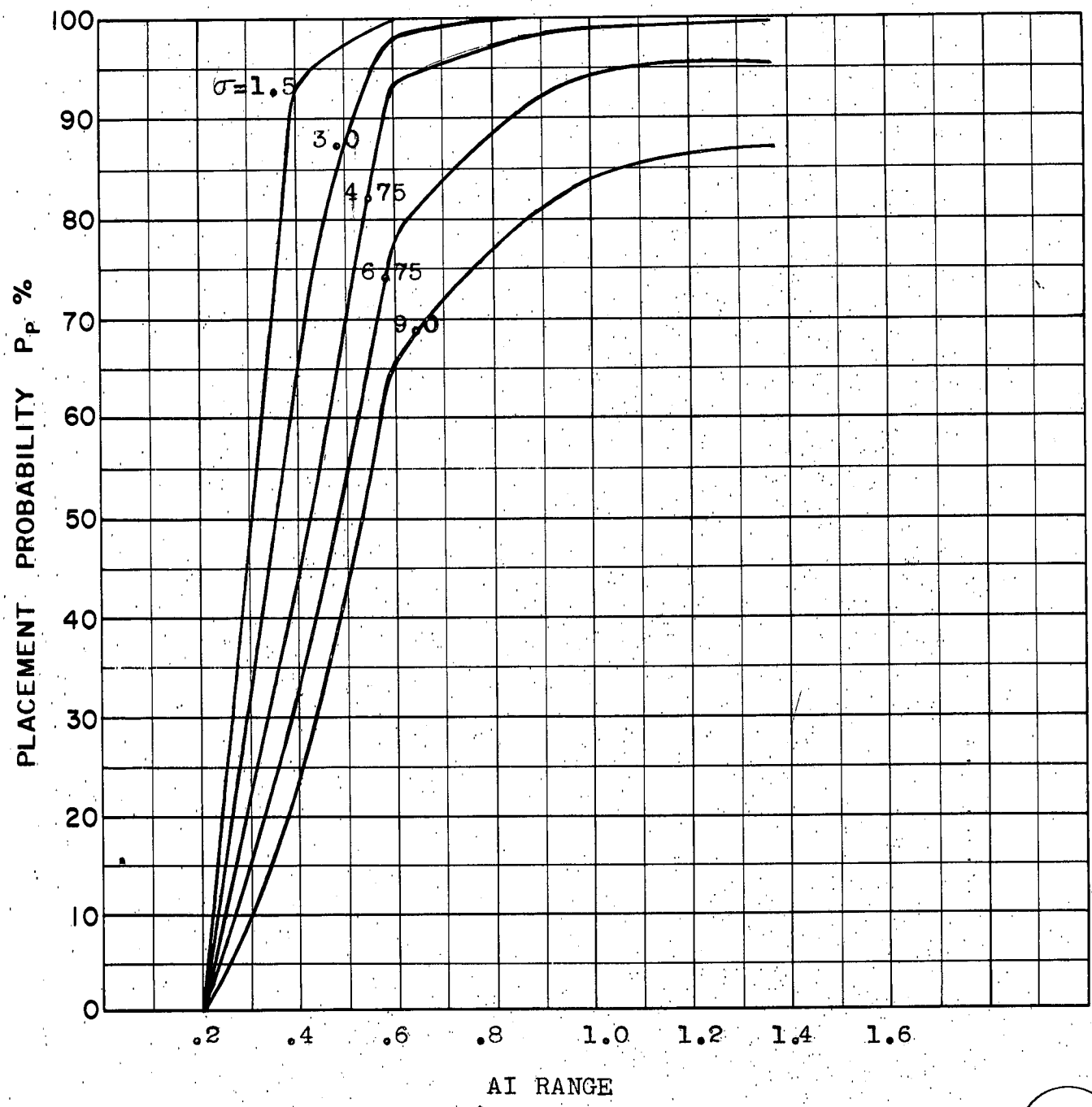

COURSE DIFFERENCE: 160°
TARGET EVASION: 0.75g Limited to 30° change of course
TARGET MACH NO.: 2.0
INTERCEPTOR LATERAL G's: 28% pess.
INTERCEPTOR MACH NO.: 1.8
σ OF G.C.I. ACCURACY: 5 Values
A.I. DETECTION RANGE AS FRACTION OF SPECIFICATION RANGE, S: Abscissa
A.I. DETECTION RANGE CONTOUR: Delta Wing
ALTITUDE: 50K

D12a
E

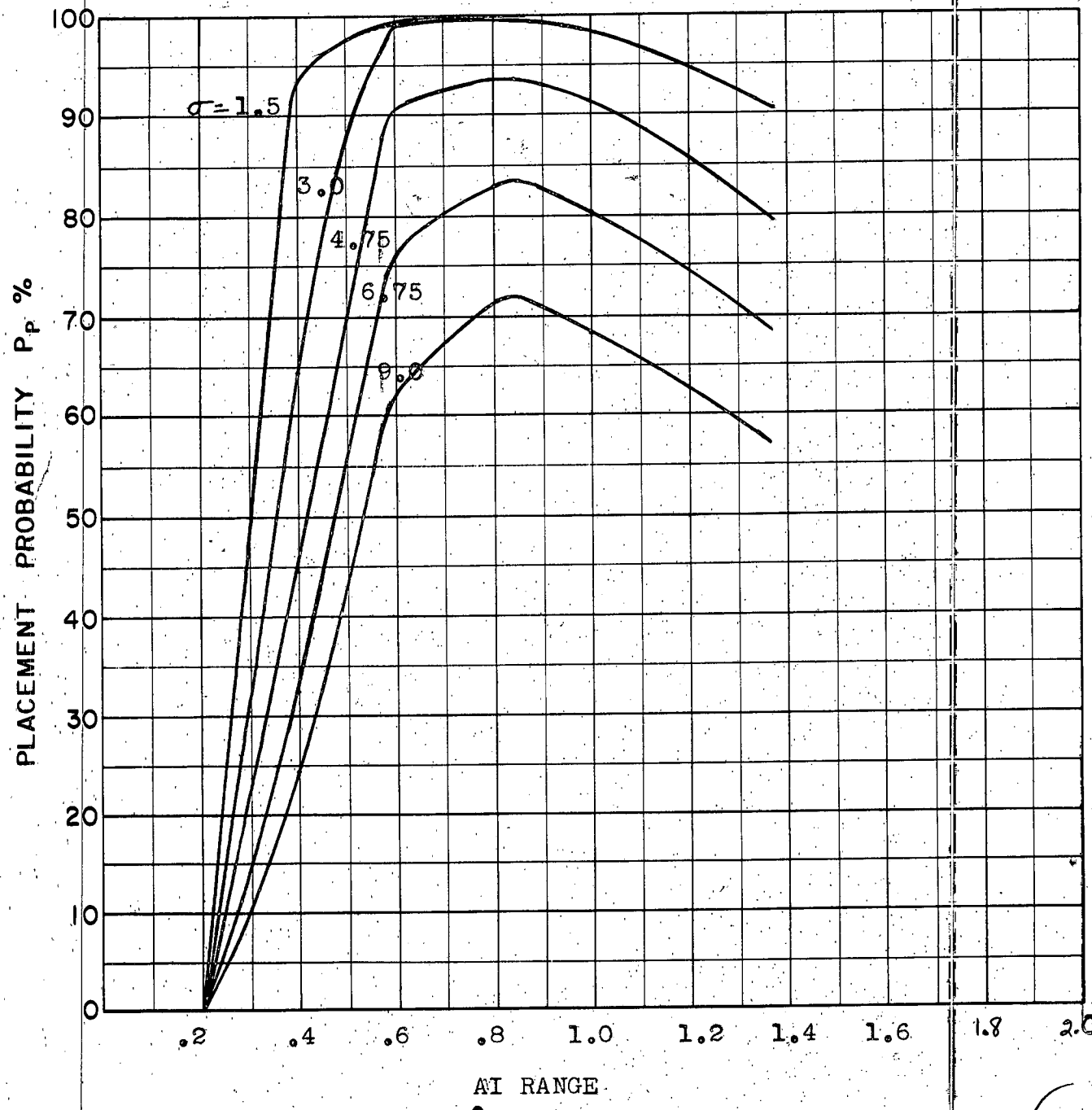

COURSE DIFFERENCE: 160°
TARGET EVASION: 0.75g Limited to 60° change of course
TARGET MACH NO.: 2.0
INTERCEPTOR LATERAL G's: 28% pess.
INTERCEPTOR MACH NO.: 1.8
σ OF G.C.I. ACCURACY: 5 Values
A.I. DETECTION RANGE AS FRACTION OF SPECIFICATION RANGE, S: Abscissa
A.I. DETECTION RANGE CONTOUR: Delta Wing
ALTITUDE: 50K

D126

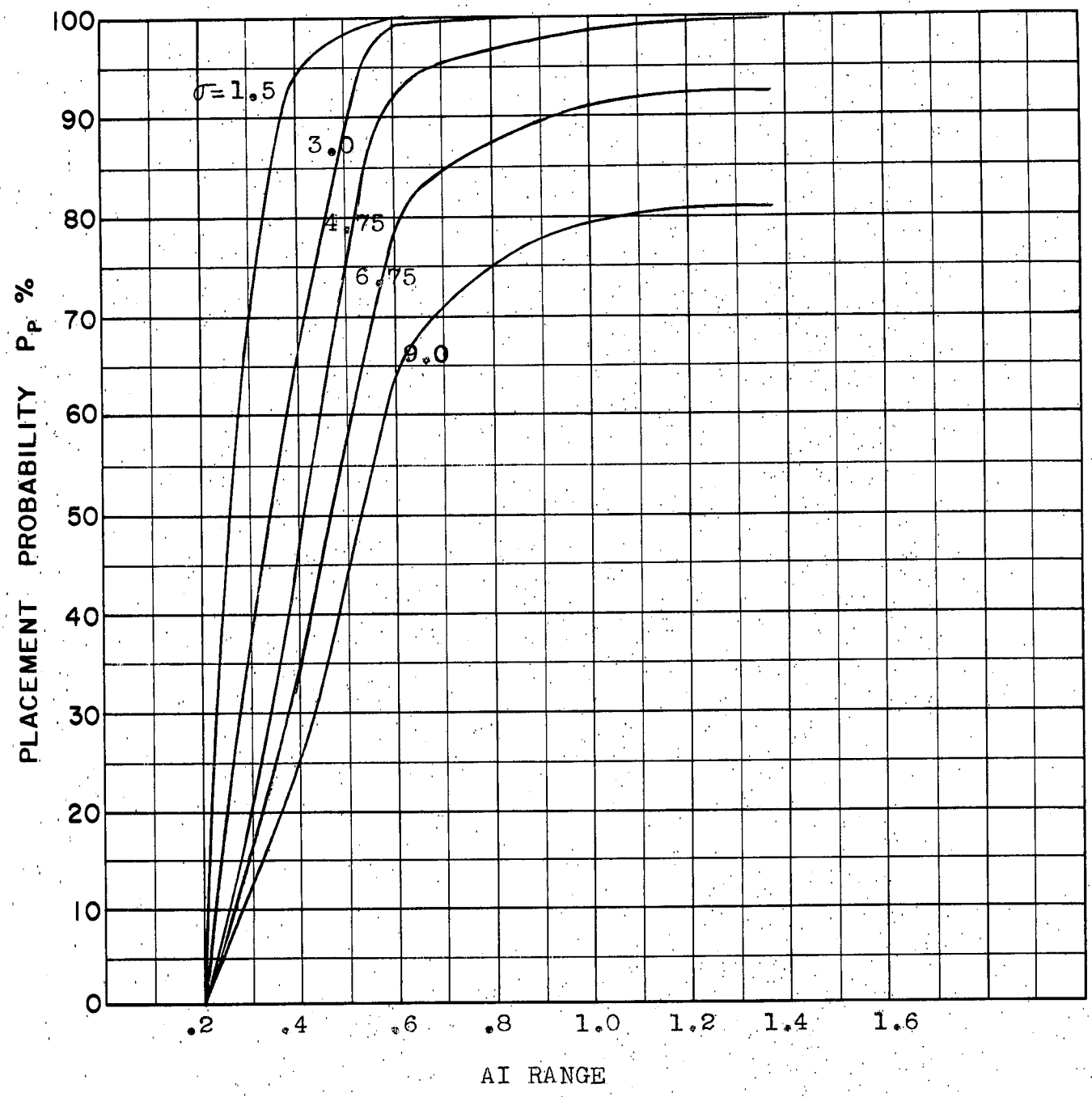

COURSE DIFFERENCE: 180°
TARGET EVASION: 0.75g Limited to 30° change of course
TARGET MACH NO.: 2.0
INTERCEPTOR LATERAL G's: 28% pess.
INTERCEPTOR MACH NO.: 1.8
σ OF G.C.I. ACCURACY: 5 Values
A.I. DETECTION RANGE AS FRACTION OF SPECIFICATION RANGE, S: Abscissa
A.I. DETECTION RANGE CONTOUR: Delta Wing
ALTITUDE: 50K

D13a
E

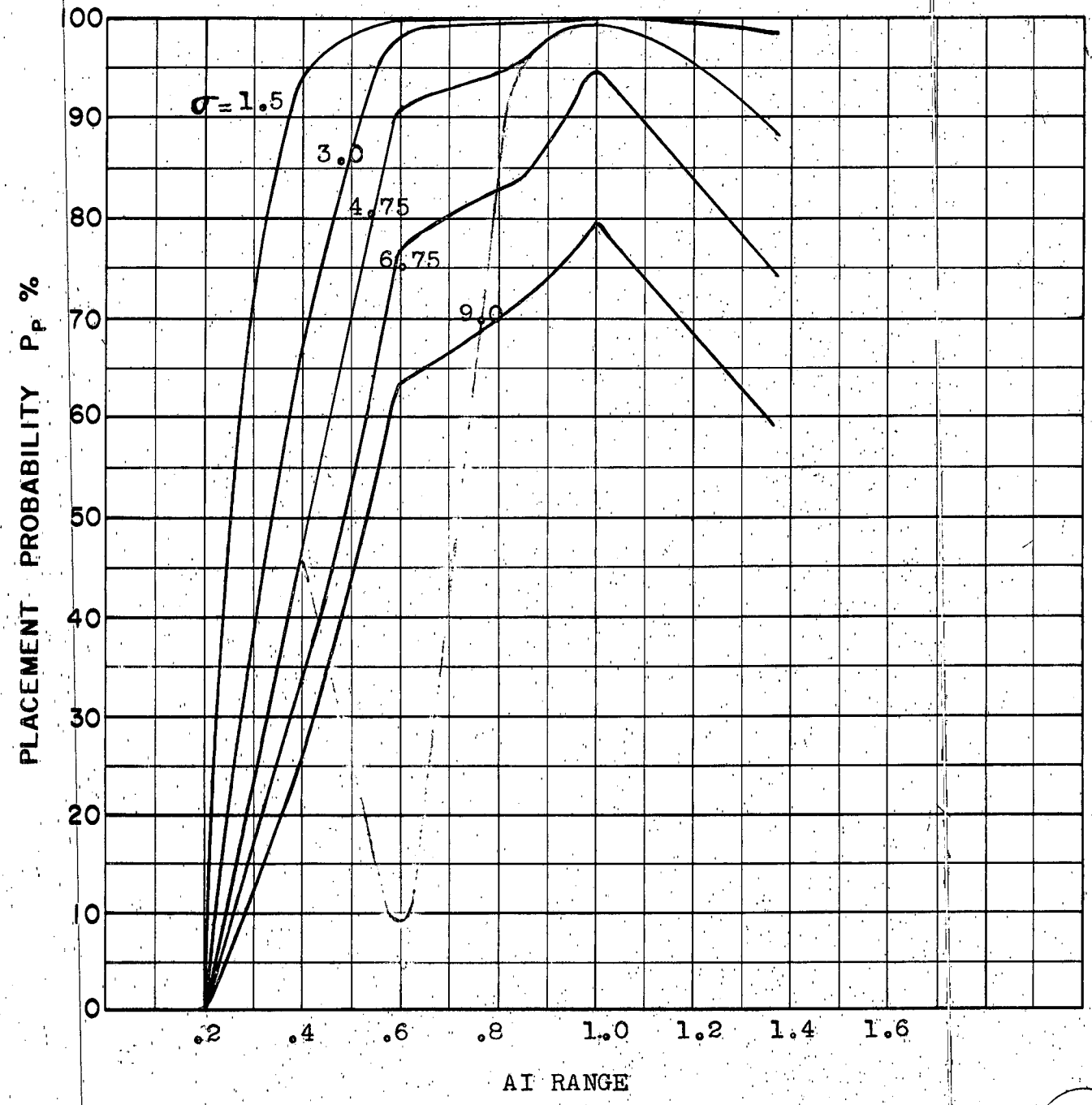

COURSE DIFFERENCE: 180°
TARGET EVASION: 0.75g Limited to 60° change of course
TARGET MACH NO.: 2.0
INTERCEPTOR LATERAL G's: 28% pess.
INTERCEPTOR MACH NO.: 1.8
σ OF G.C.I. ACCURACY: 5 Values
A.I. DETECTION RANGE AS FRACTION OF SPECIFICATION RANGE, S: Abscissa
A.I. DETECTION RANGE CONTOUR: Delta Wing
ALTITUDE: 50K

D13.6 E

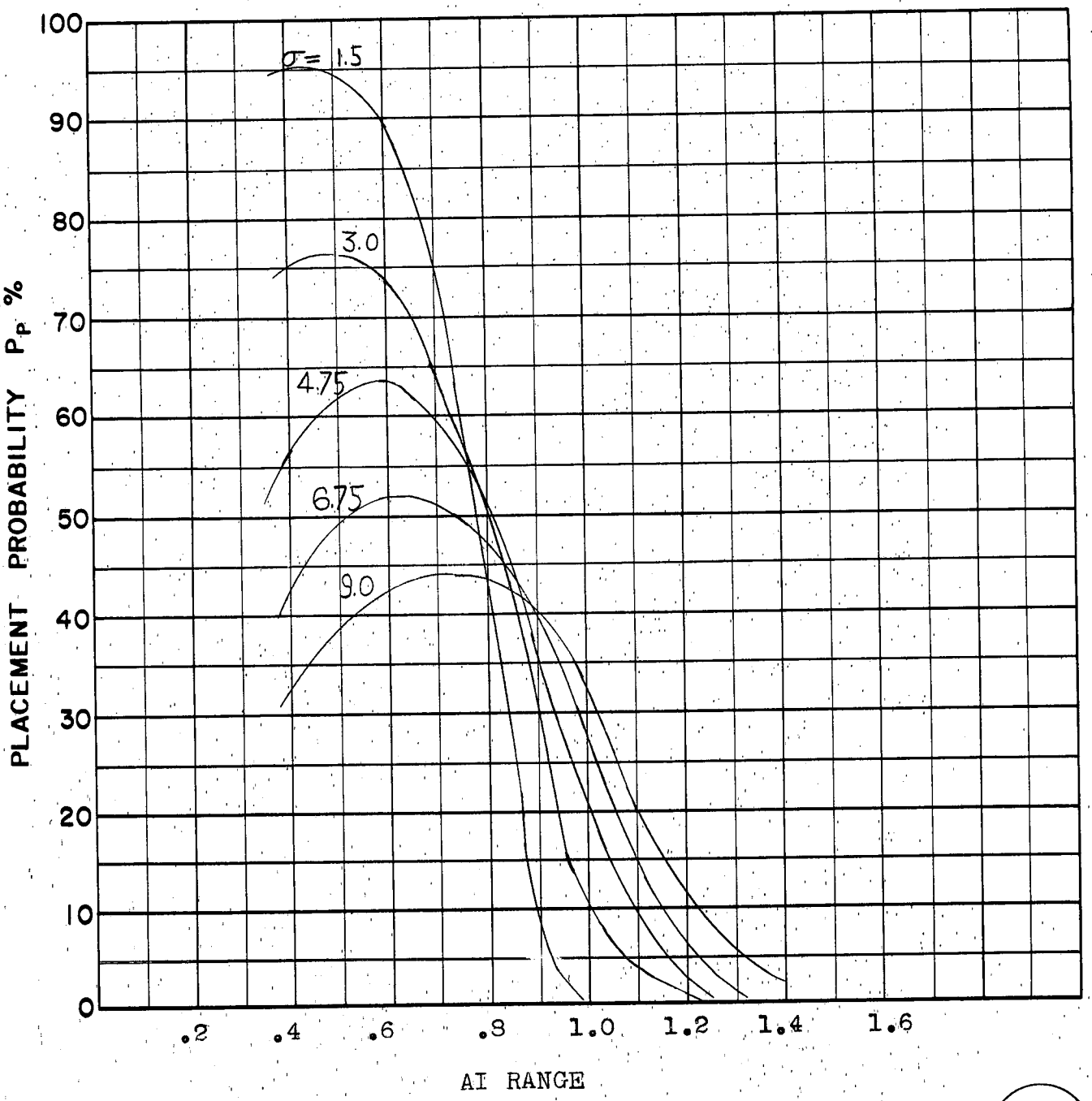

COURSE DIFFERENCE: 110°
TARGET EVASION: 0.5g
TARGET MACH NO.: 2.0
INTERCEPTOR LATERAL G's: 28% pess.
INTERCEPTOR MACH NO.: 1.8
σ OF G.C.I. ACCURACY: 5 Values
A.I. DETECTION RANGE AS FRACTION OF SPECIFICATION RANGE, S: Abscissa
A.I. DETECTION RANGE CONTOUR: Delta Wing
ALTITUDE: 55K

D14
E

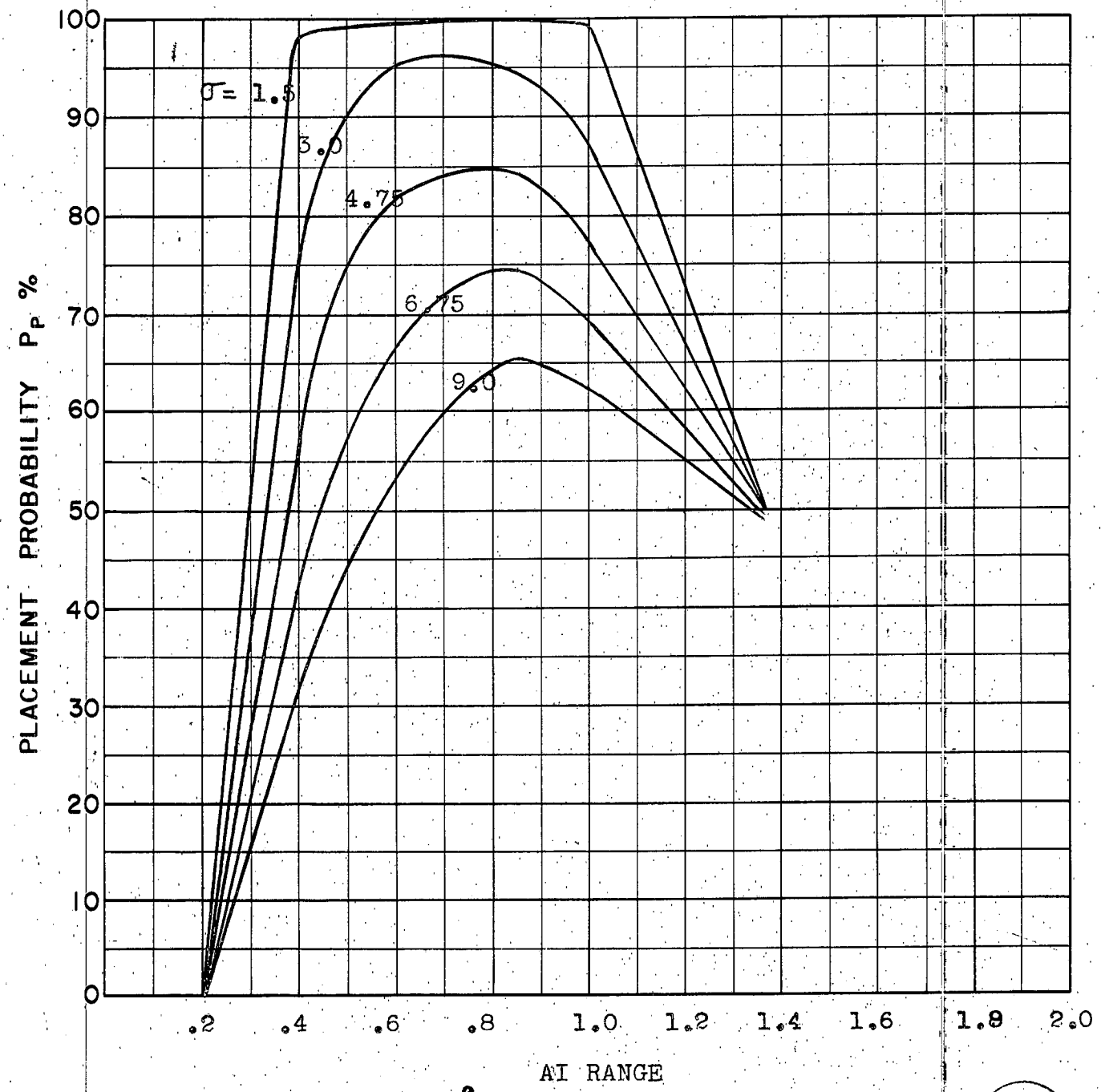

COURSE DIFFERENCE: 135°
TARGET EVASION: 0.5g
TARGET MACH NO.: 2.0
INTERCEPTOR LATERAL G's: 28% pess.
INTERCEPTOR MACH NO.: 1.8
σ OF G.C.I. ACCURACY: 5 Values
A.I. DETECTION RANGE AS FRACTION OF SPECIFICATION RANGE, S: Abscissa
A.I. DETECTION RANGE CONTOUR: Delta Wing
ALTITUDE: 55K

D15
E

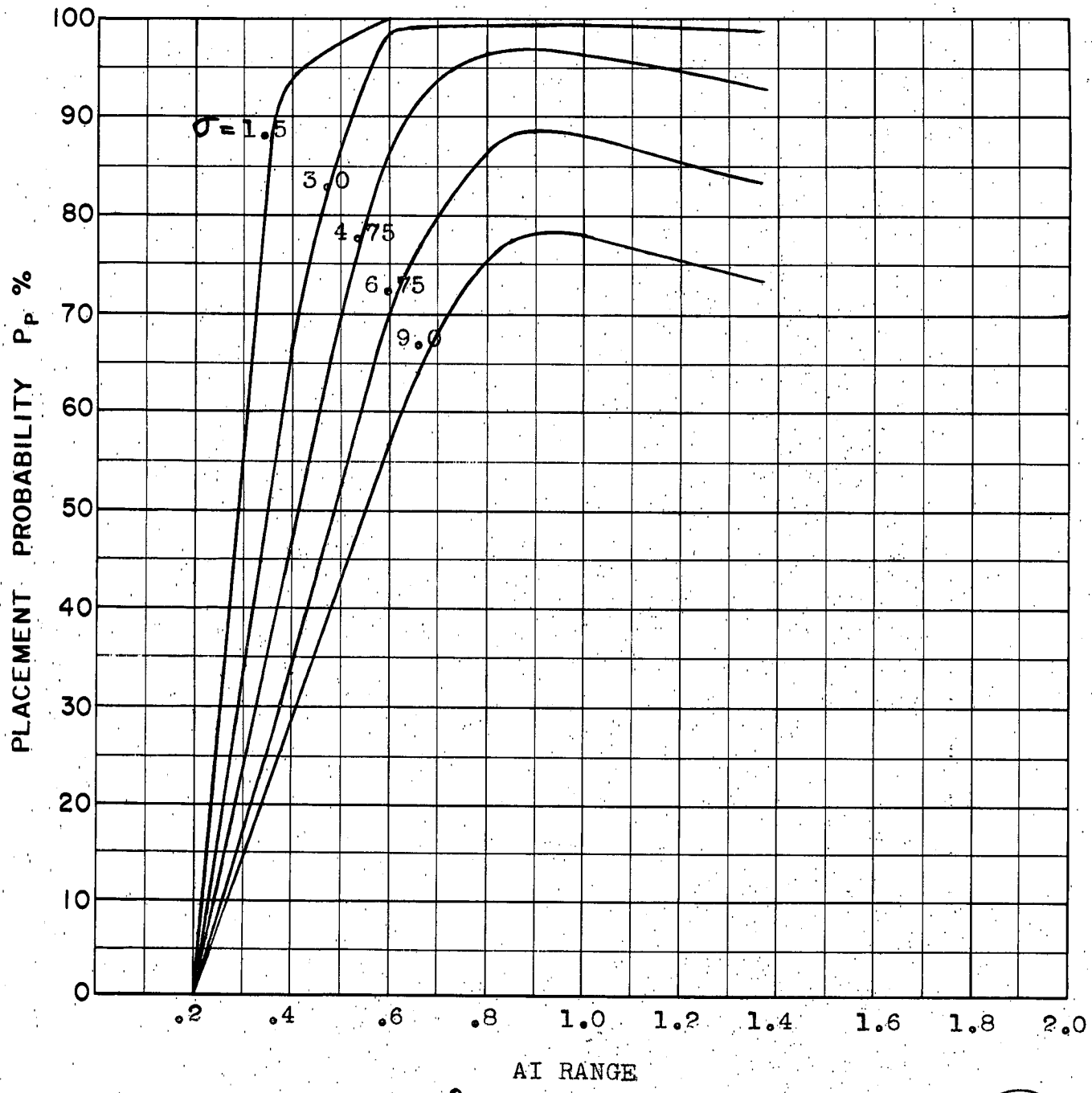

COURSE DIFFERENCE: 160°
TARGET EVASION: 0.5g
TARGET MACH NO.: 2.0
INTERCEPTOR LATERAL G's: 28% pess.
INTERCEPTOR MACH NO.: 1.8
σ OF G.C.I. ACCURACY: 5 Values
A.I. DETECTION RANGE AS FRACTION OF SPECIFICATION RANGE, S: Abscissa
A.I. DETECTION RANGE CONTOUR: Delta Wing
ALTITUDE: 55K

D16
E

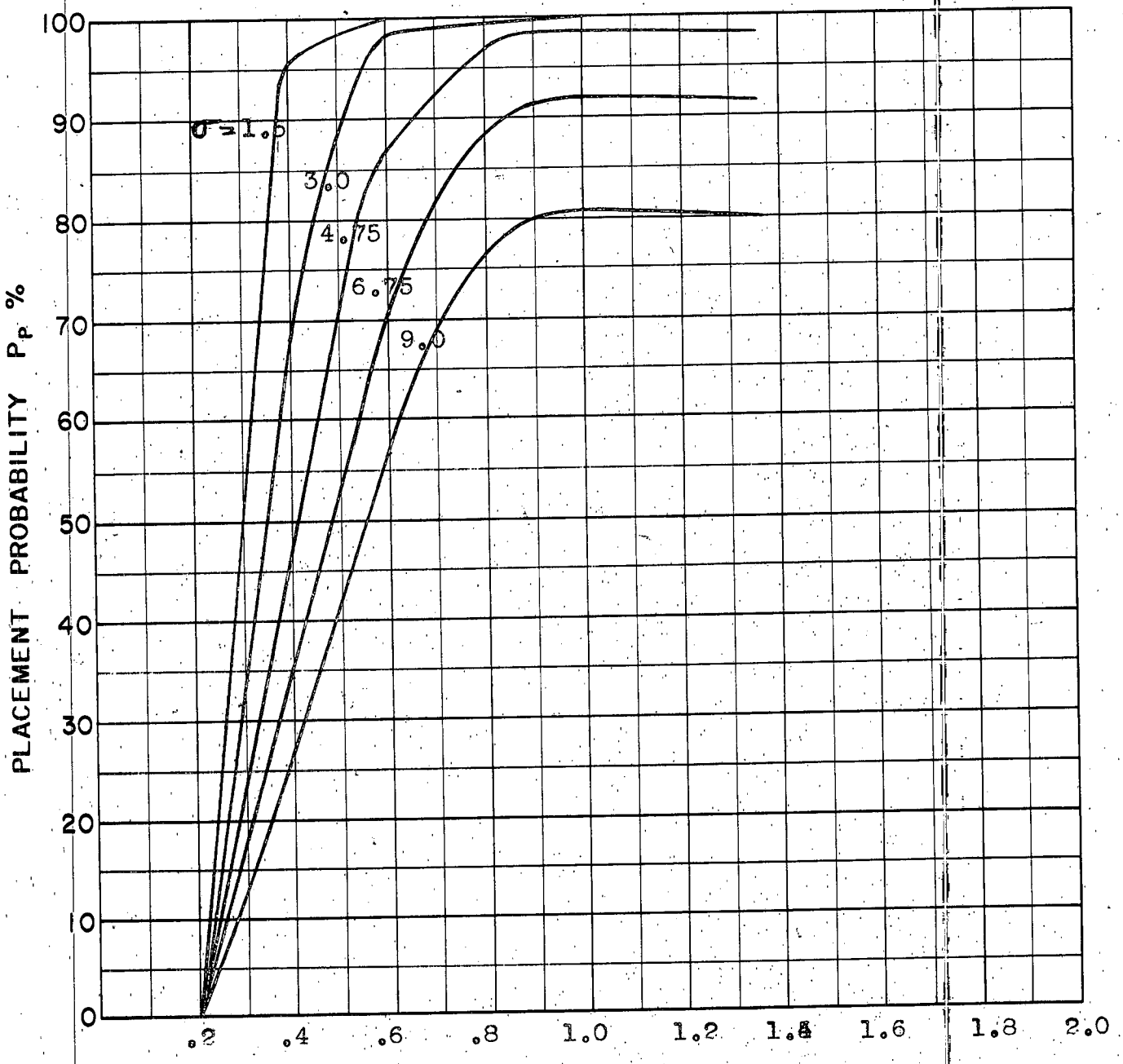

COURSE DIFFERENCE: 180°
TARGET EVASION: 0.5g
TARGET MACH NO.: 2.0
INTERCEPTOR LATERAL G's: 28% pess.
INTERCEPTOR MACH NO.: 1.8
σ OF G.C.I. ACCURACY: 5 Values
A.I. DETECTION RANGE AS FRACTION OF SPECIFICATION RANGE, S: Abscissa
A.I. DETECTION RANGE CONTOUR: Delta Wing
ALTITUDE: 55K

D17
E

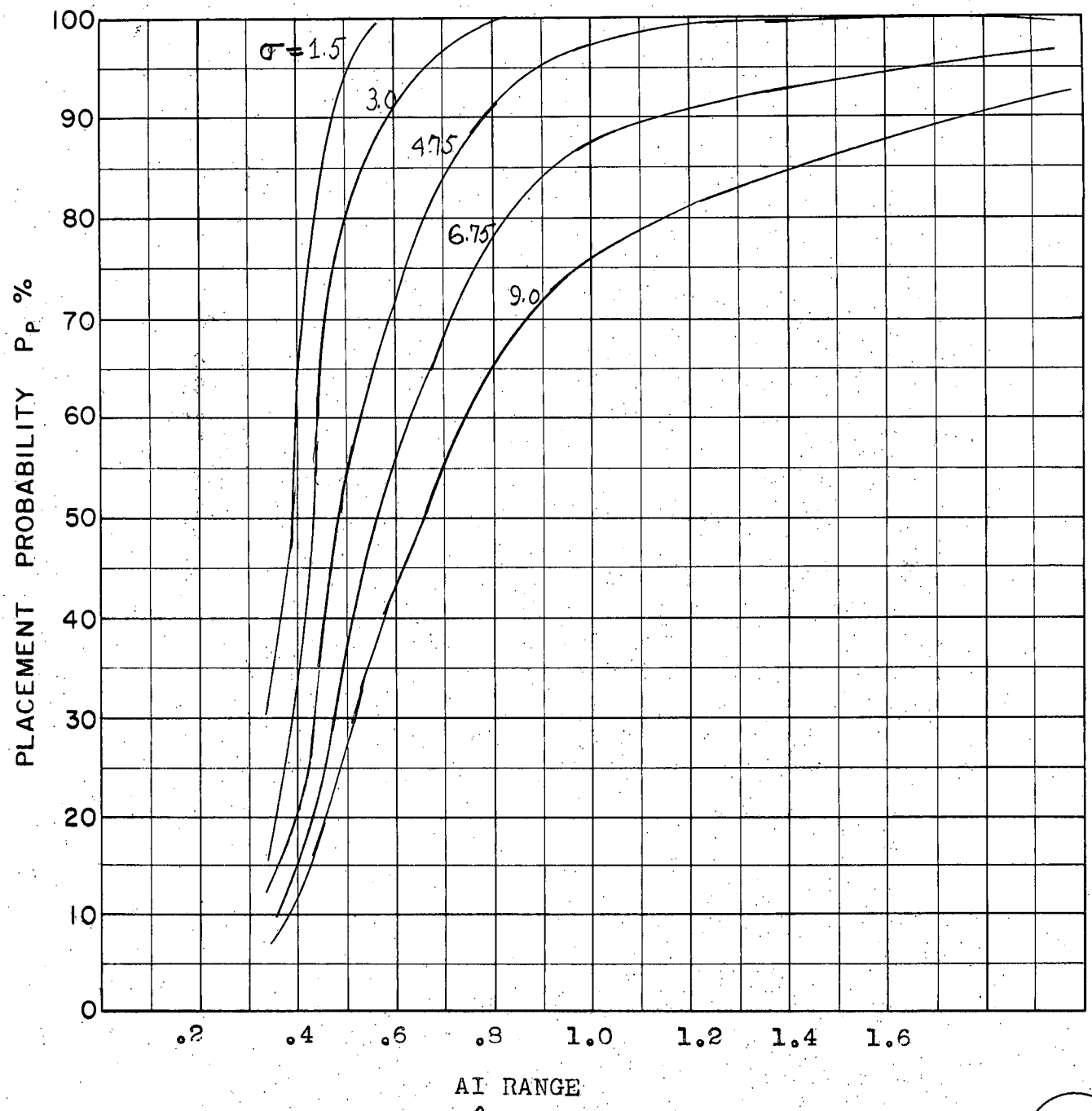

COURSE DIFFERENCE: 110°
TARGET EVASION: 0.75g (30° & 60°) change of course
TARGET MACH NO.: 1.5
INTERCEPTOR LATERAL G's: 28% pess.
INTERCEPTOR MACH NO.: 1.8
σ OF G.C.I. ACCURACY: 5 Values
A.I. DETECTION RANGE AS FRACTION OF SPECIFICATION RANGE, S: Abscissa
A.I. DETECTION RANGE CONTOUR: Straight Wing
ALTITUDE: 50K

S-1 E

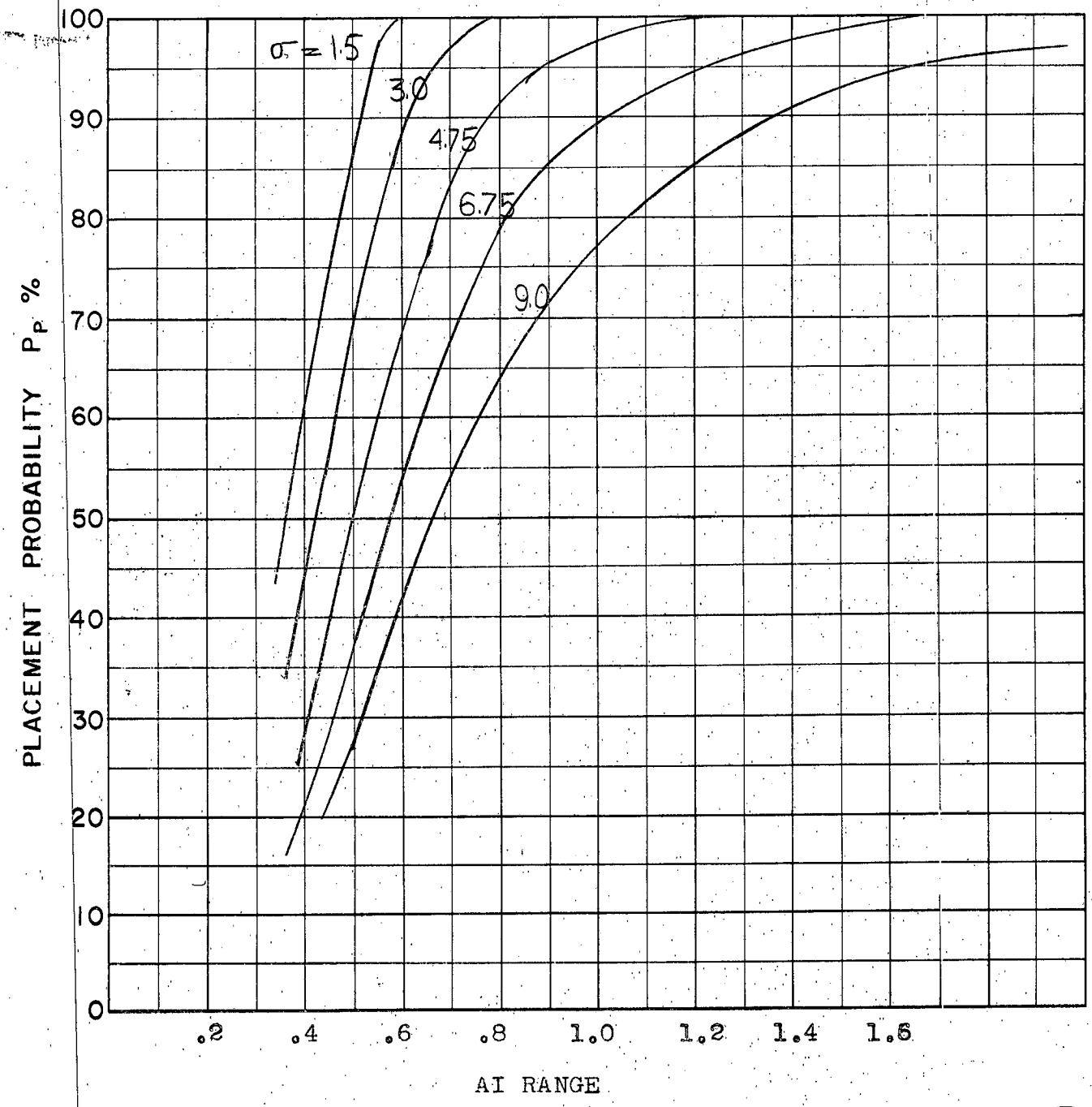

COURSE DIFFERENCE: 135°
TARGET EVASION: 0.75g (30° & 60°) change of course
TARGET MACH NO.: 1.5
INTERCEPTOR LATERAL G's: 28% pess.
INTERCEPTOR MACH NO.: 2.0
σ OF G.C.I. ACCURACY: 5 Values
A.I. DETECTION RANGE AS FRACTION OF SPECIFICATION RANGE, S Abscissa
A.I. DETECTION RANGE CONTOUR: Straight Wing
ALTITUDE: 50K

S-12
E

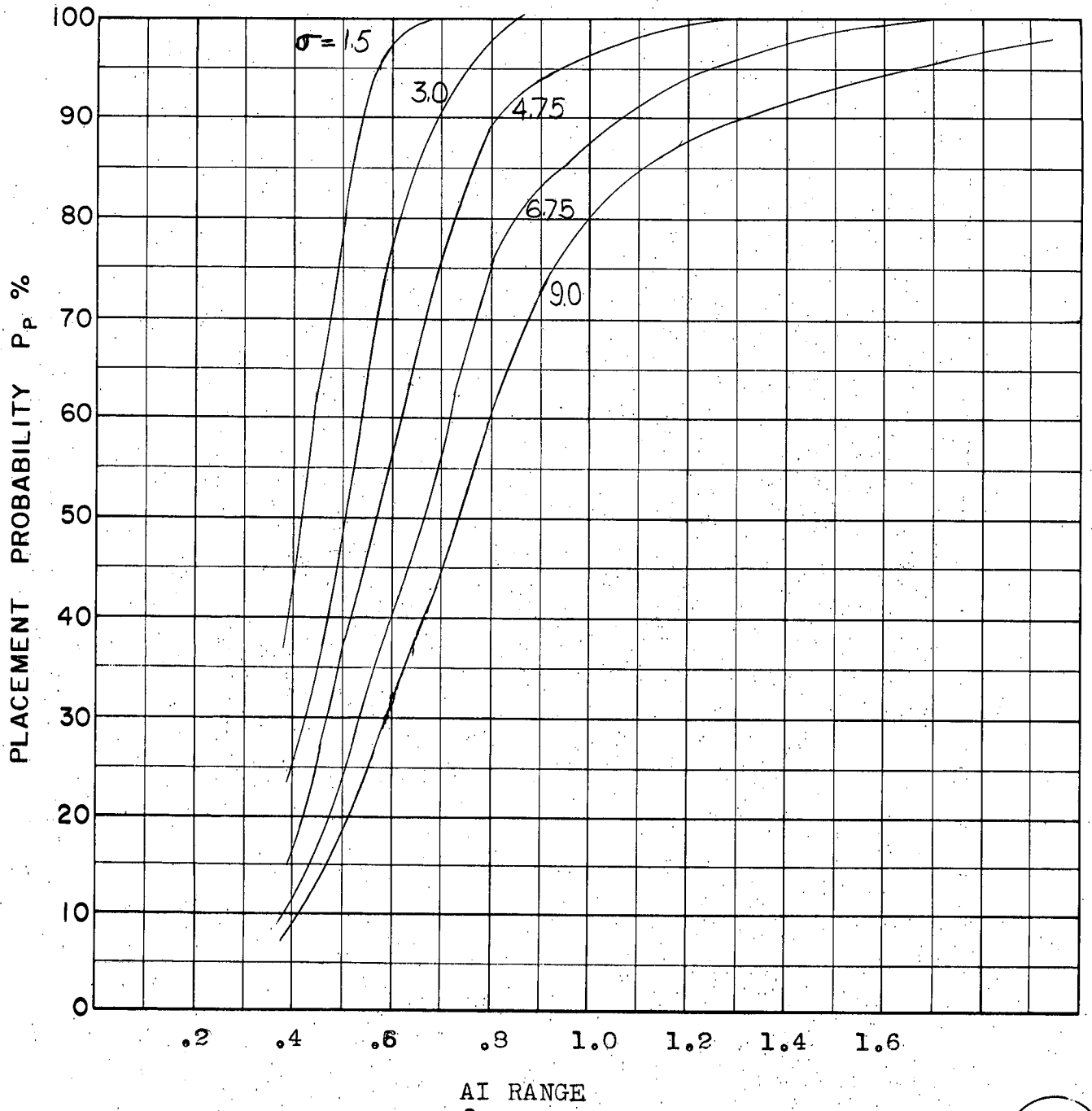

COURSE DIFFERENCE: 160°
TARGET EVASION: 0.75g (30° & 60°) change of course
TARGET MACH NO.: 1.5
INTERCEPTOR LATERAL G's: 28% pess.
INTERCEPTOR MACH NO.: 2.0
σ OF G.C.I. ACCURACY: 5 Values
A.I. DETECTION RANGE AS FRACTION OF SPECIFICATION RANGE, S: Abscissa
A.I. DETECTION RANGE CONTOUR: Straight Wing
ALTITUDE: 50K

S-3
E

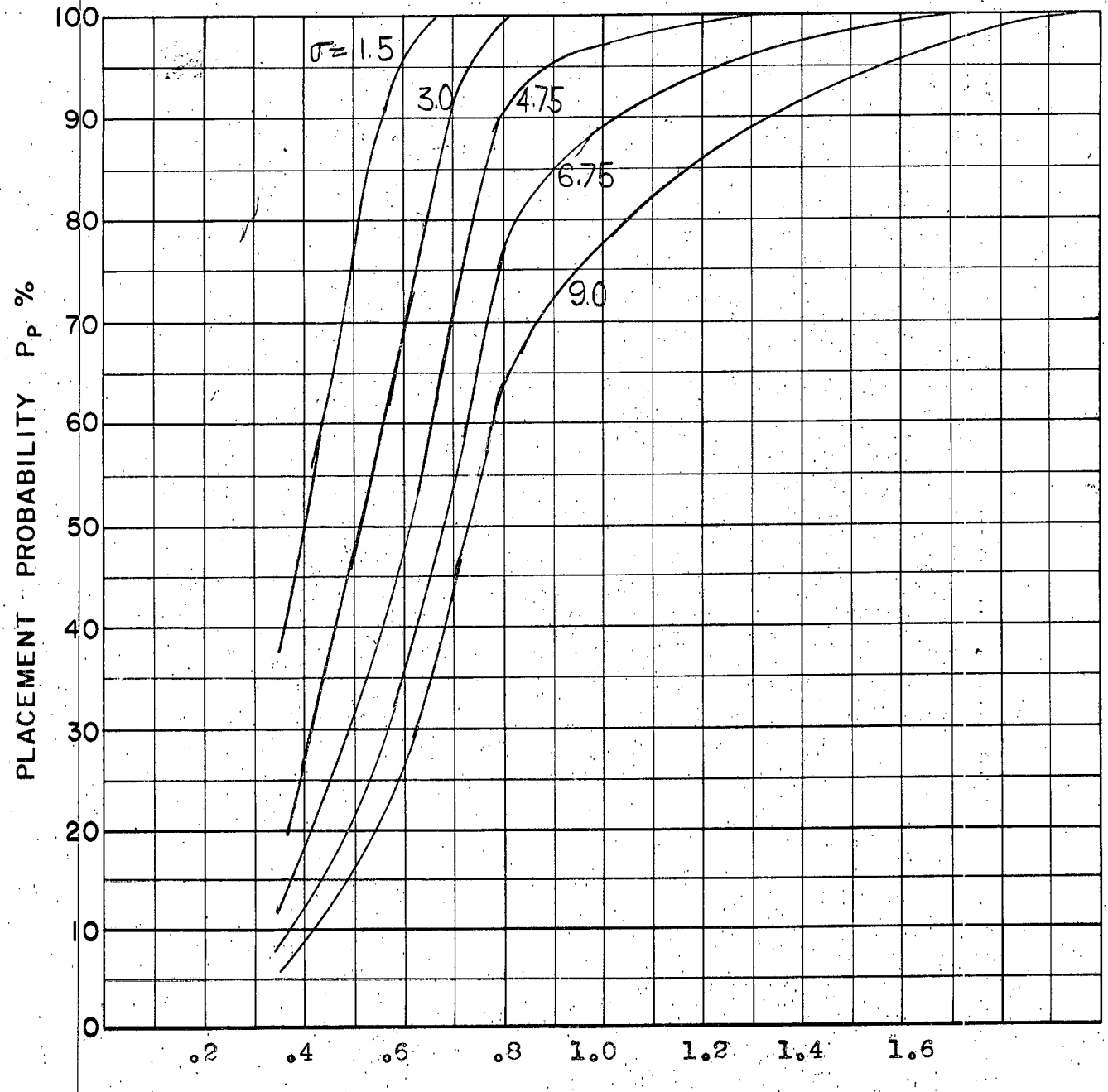

COURSE DIFFERENCE: 180°
TARGET EVASION: 0.75g (30° & 60°) change of course
TARGET MACH NO.: 1.5
INTERCEPTOR LATERAL G's: 28% pess.
INTERCEPTOR MACH NO.: 1.8
σ OF G.C.I. ACCURACY: 5 Values
A.I. DETECTION RANGE AS FRACTION OF SPECIFICATION RANGE, S: Abscissa
A.I. DETECTION RANGE CONTOUR: Straight Wing
ALTITUDE: 50K

S-4 E

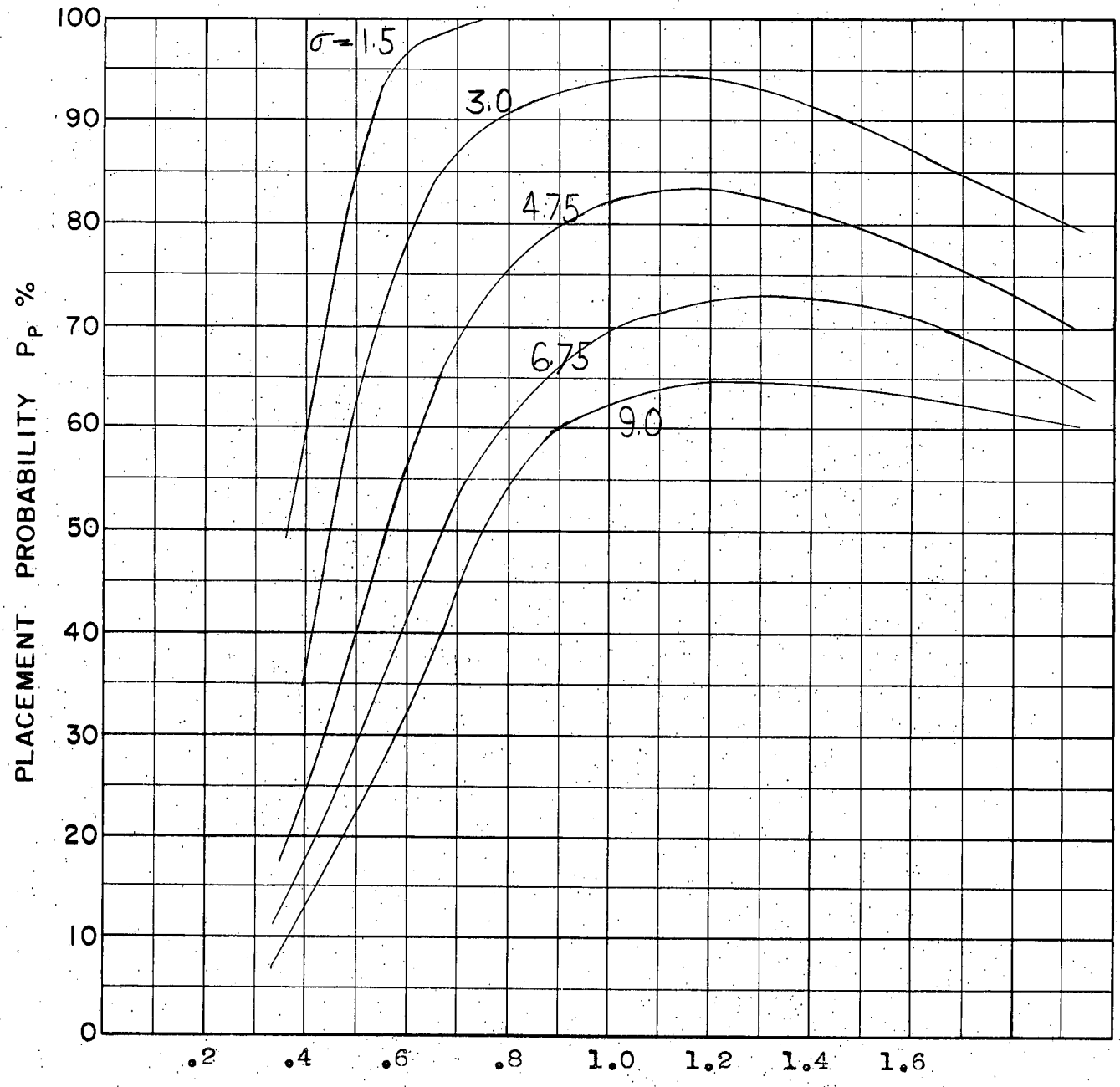

COURSE DIFFERENCE: 110°
TARGET EVASION: 0.25g
TARGET MACH NO.: 2.0
INTERCEPTOR LATERAL G's: 28% pess.
INTERCEPTOR MACH NO.: 1.8
σ OF G.C.I. ACCURACY: 5 Values
A.I. DETECTION RANGE AS FRACTION OF SPECIFICATION RANGE, S: Abscissa
A.I. DETECTION RANGE CONTOUR: Straight Wing
ALTITUDE: 50K

S-5
E

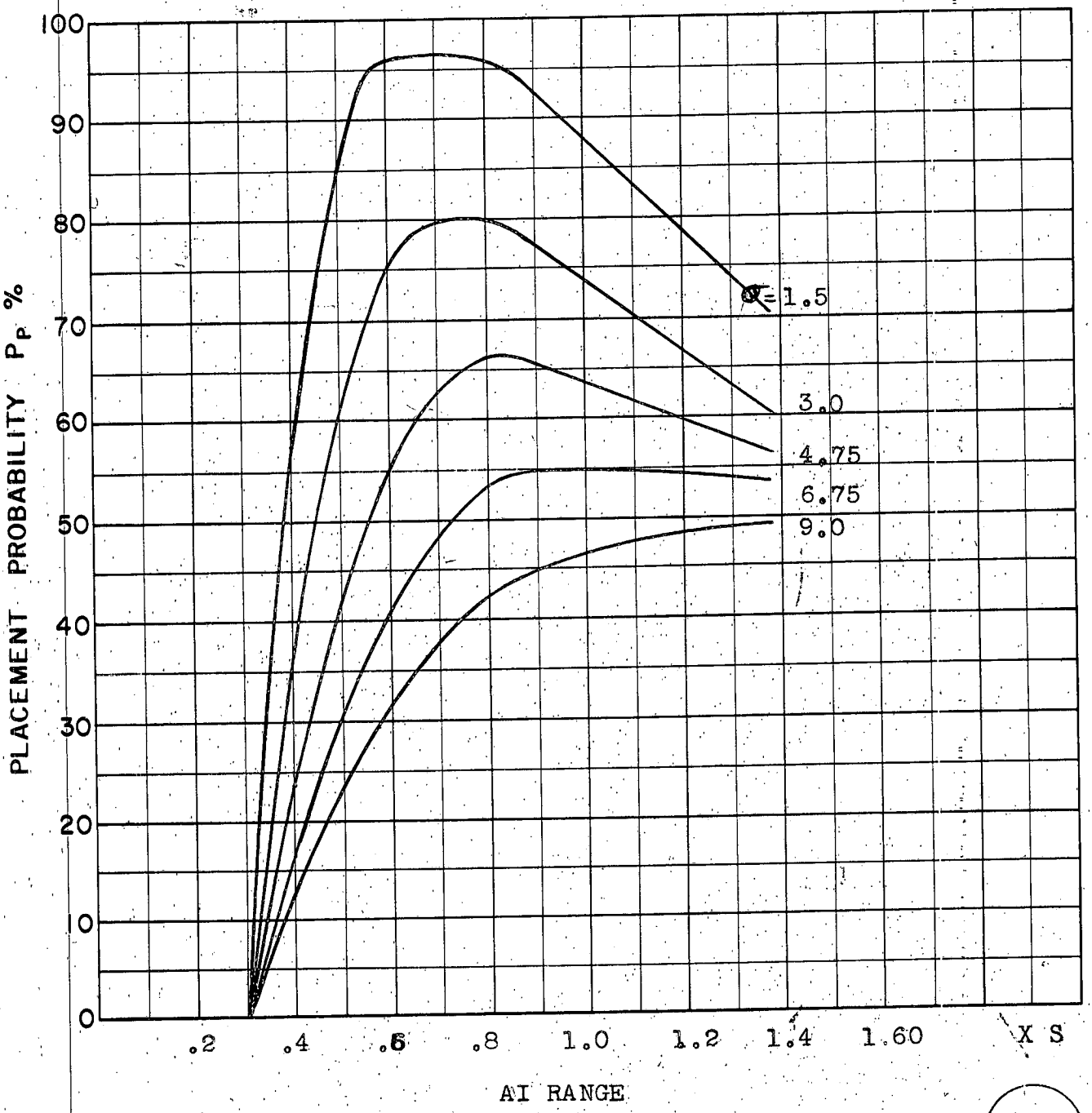

S.6a

COURSE DIFFERENCE: 110°
TARGET EVASION: 0.5g
TARGET MACH NO.: 2.0
INTERCEPTOR LATERAL G's: 28% pess.
INTERCEPTOR MACH NO.: 1.8
σ OF G.C.I. ACCURACY: 5 Values
A.I. DETECTION RANGE AS FRACTION OF SPECIFICATION RANGE, S: Abscissa
A.I. DETECTION RANGE CONTOUR: STRAIGHT WING
ALTITUDE: 50K

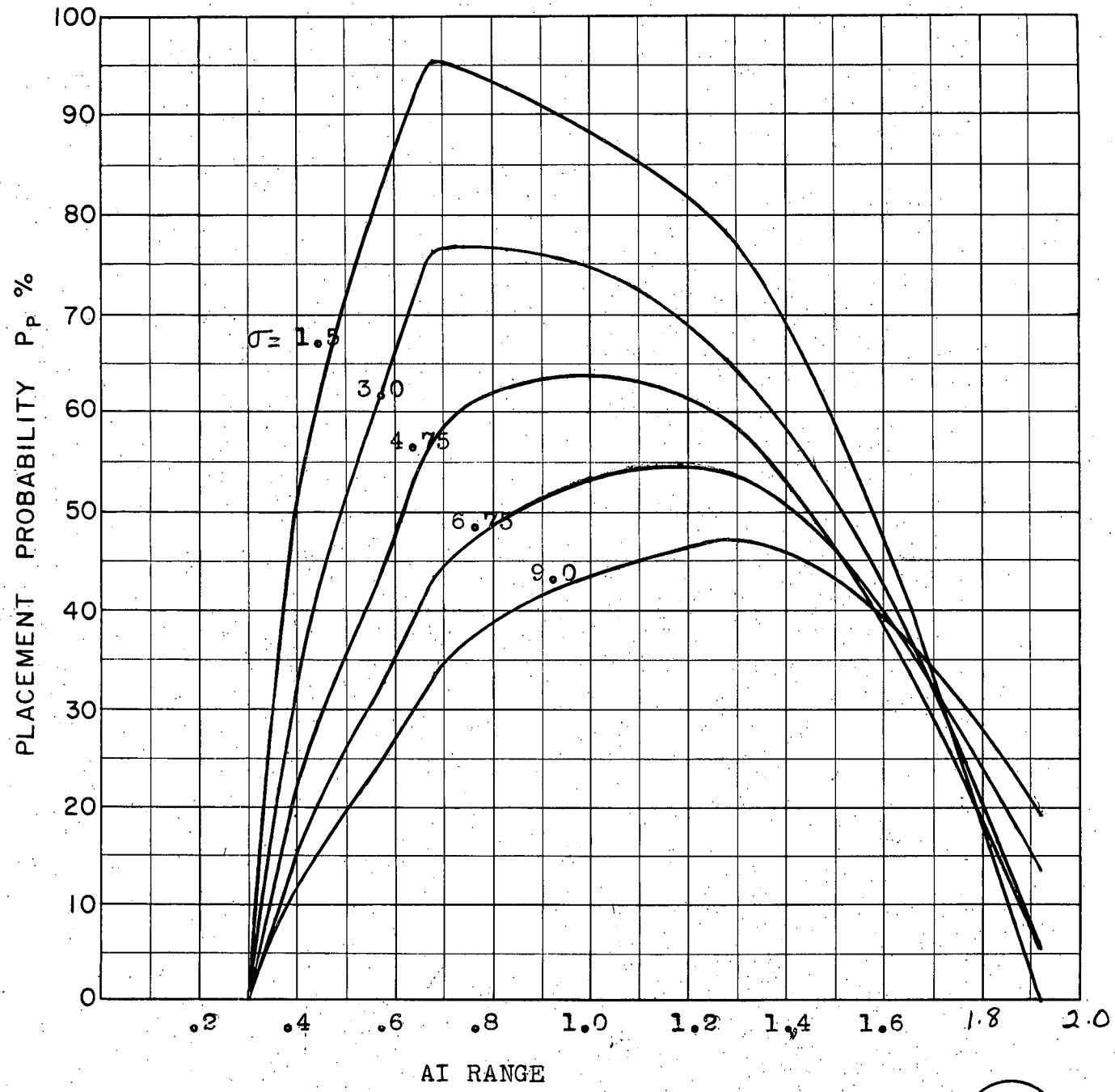

S-6b

COURSE DIFFERENCE: 110°
TARGET EVASION: 0.5g
TARGET MACH NO.: 2.0
INTERCEPTOR LATERAL G's: 2.0g limit, 28% pess.
INTERCEPTOR MACH NO.: 1.8
σ OF G.C.I. ACCURACY: 5 Values
A.I. DETECTION RANGE AS FRACTION OF SPECIFICATION RANGE, S: Abscissa
A.I. DETECTION RANGE CONTOUR: Straight Wing
ALTITUDE: 50K

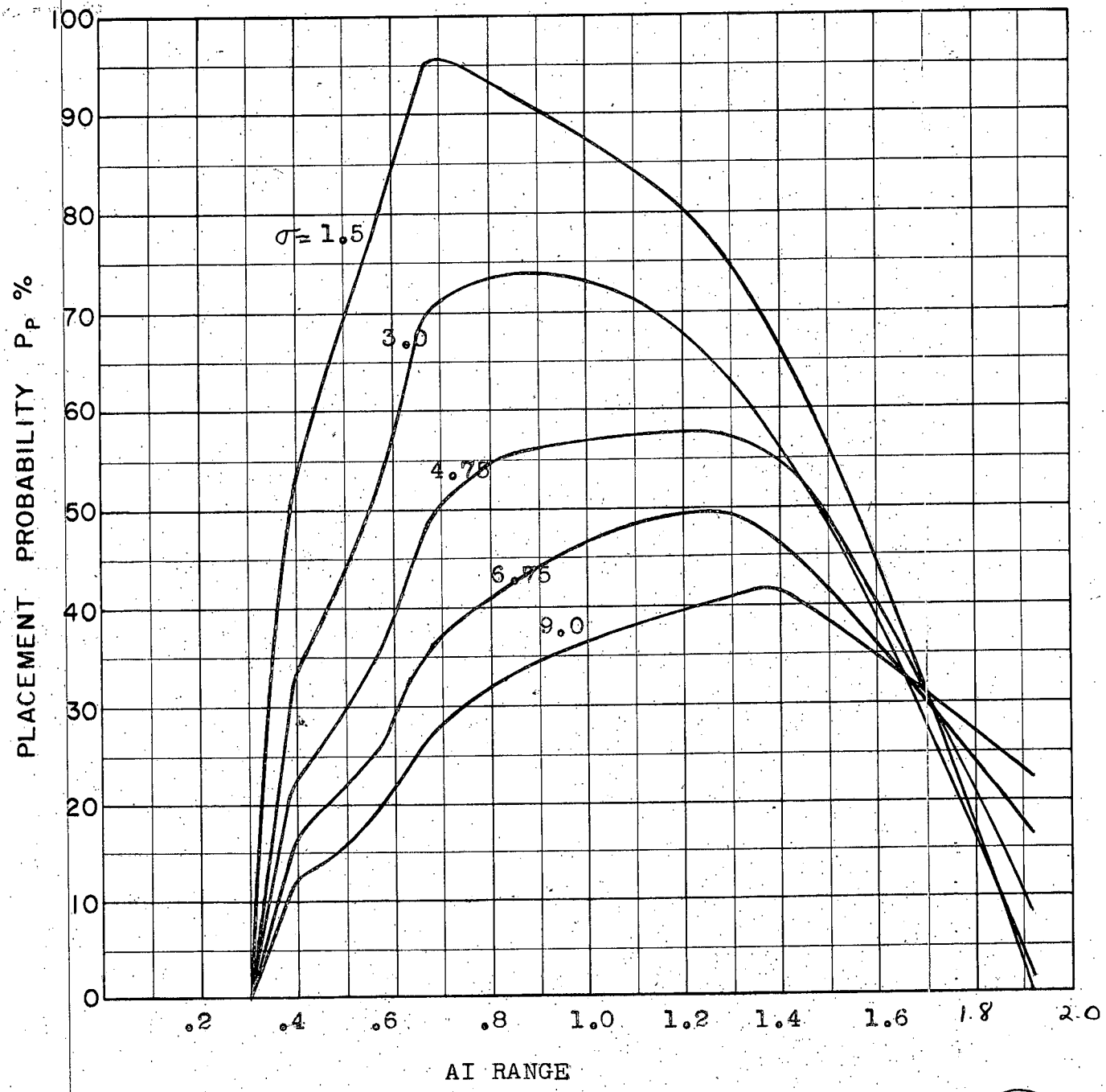

COURSE DIFFERENCE: 110°
TARGET EVASION: 0.5g
TARGET MACH NO.: 2.0
INTERCEPTOR LATERAL G's: 1.5 Limit ; 28% pess.
INTERCEPTOR MACH NO.: 1.8
σ OF G.C.I. ACCURACY: 5 Values
A.I. DETECTION RANGE AS FRACTION OF SPECIFICATION RANGE, S: Abscissa
A.I. DETECTION RANGE CONTOUR: Straight Wing
ALTITUDE: 50K

S-6c
E

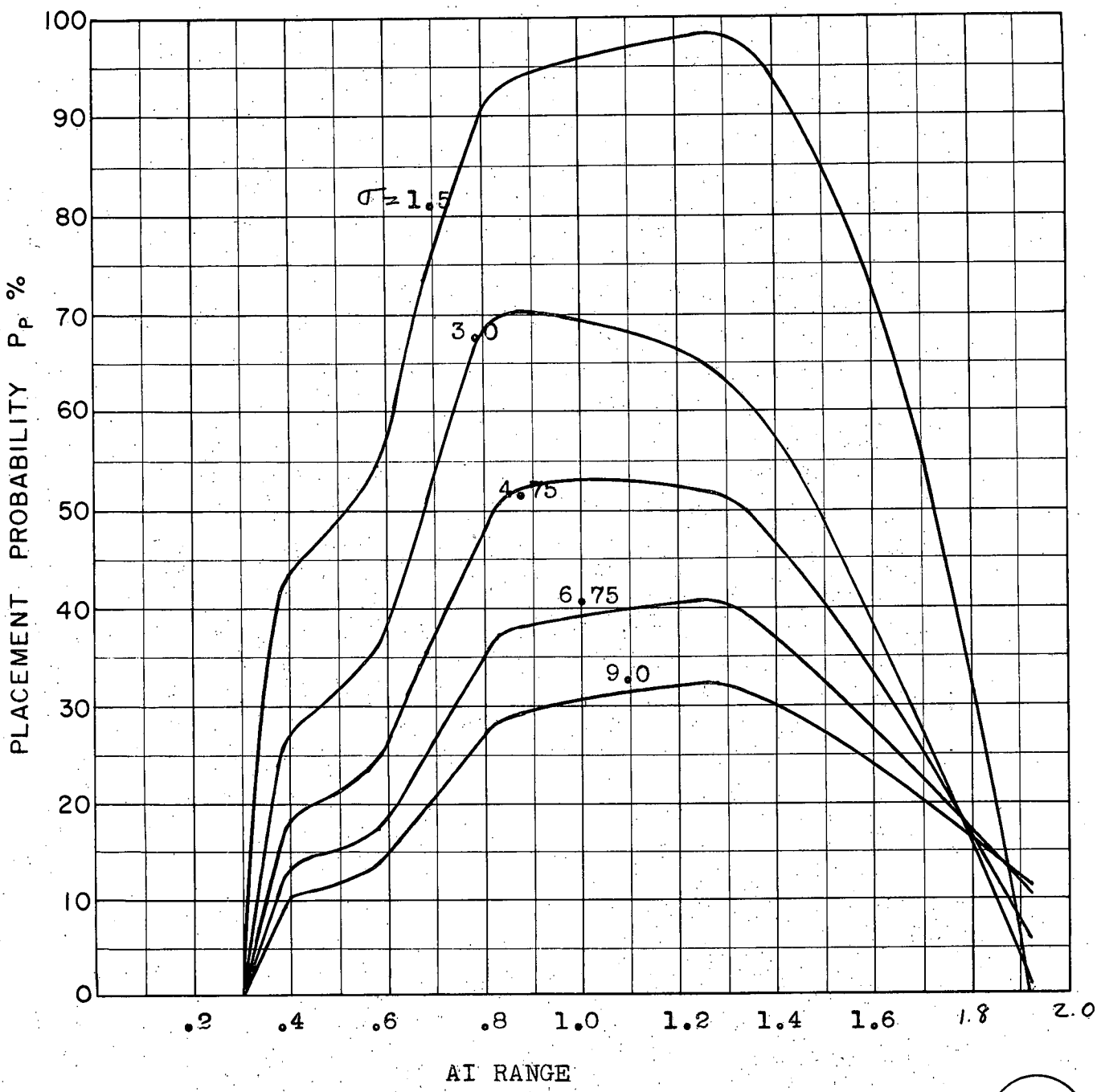

COURSE DIFFERENCE: 110°
TARGET EVASION: 0.5g
TARGET MACH NO.: 2.0
INTERCEPTOR LATERAL G's: 1.0 Limit; 28% pess.
INTERCEPTOR MACH NO.: 1.8
σ OF G.C.I. ACCURACY: 5 Values
A.I. DETECTION RANGE AS FRACTION OF SPECIFICATION RANGE, S: Abscissa
A.I. DETECTION RANGE CONTOUR: Straight Wing
ALTITUDE: 50K

S-6d
E

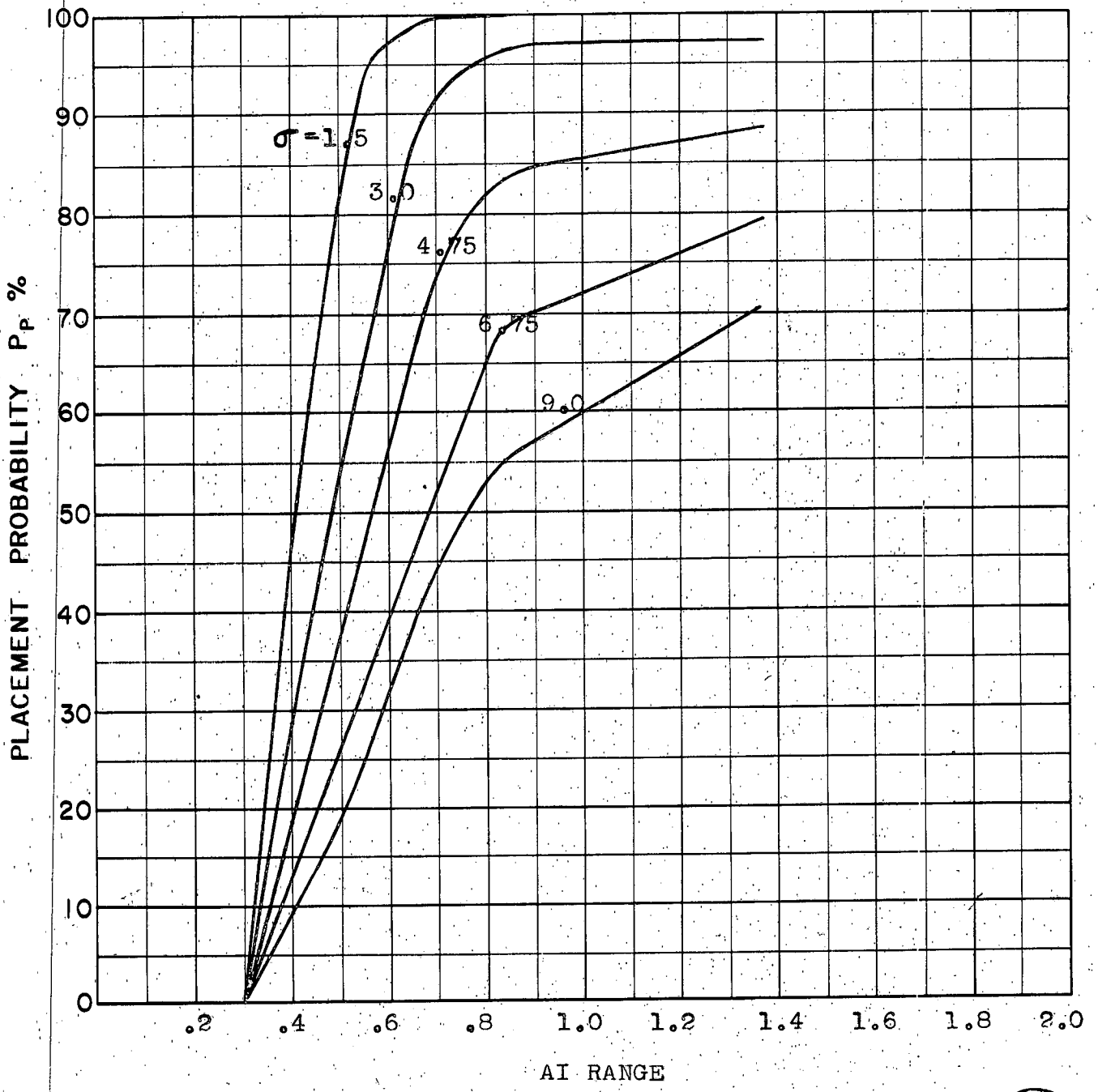

COURSE DIFFERENCE: 135°
TARGET EVASION: 0.5g
TARGET MACH NO.: 2.0
INTERCEPTOR LATERAL G's: 28% pess.
INTERCEPTOR MACH NO.: 1.8
σ OF G.C.I. ACCURACY: 5 Values
A.I. DETECTION RANGE AS FRACTION OF SPECIFICATION RANGE, S: Abscissa
A.I. DETECTION RANGE CONTOUR: Straight Wing
ALTITUDE: 50K

S-7
E

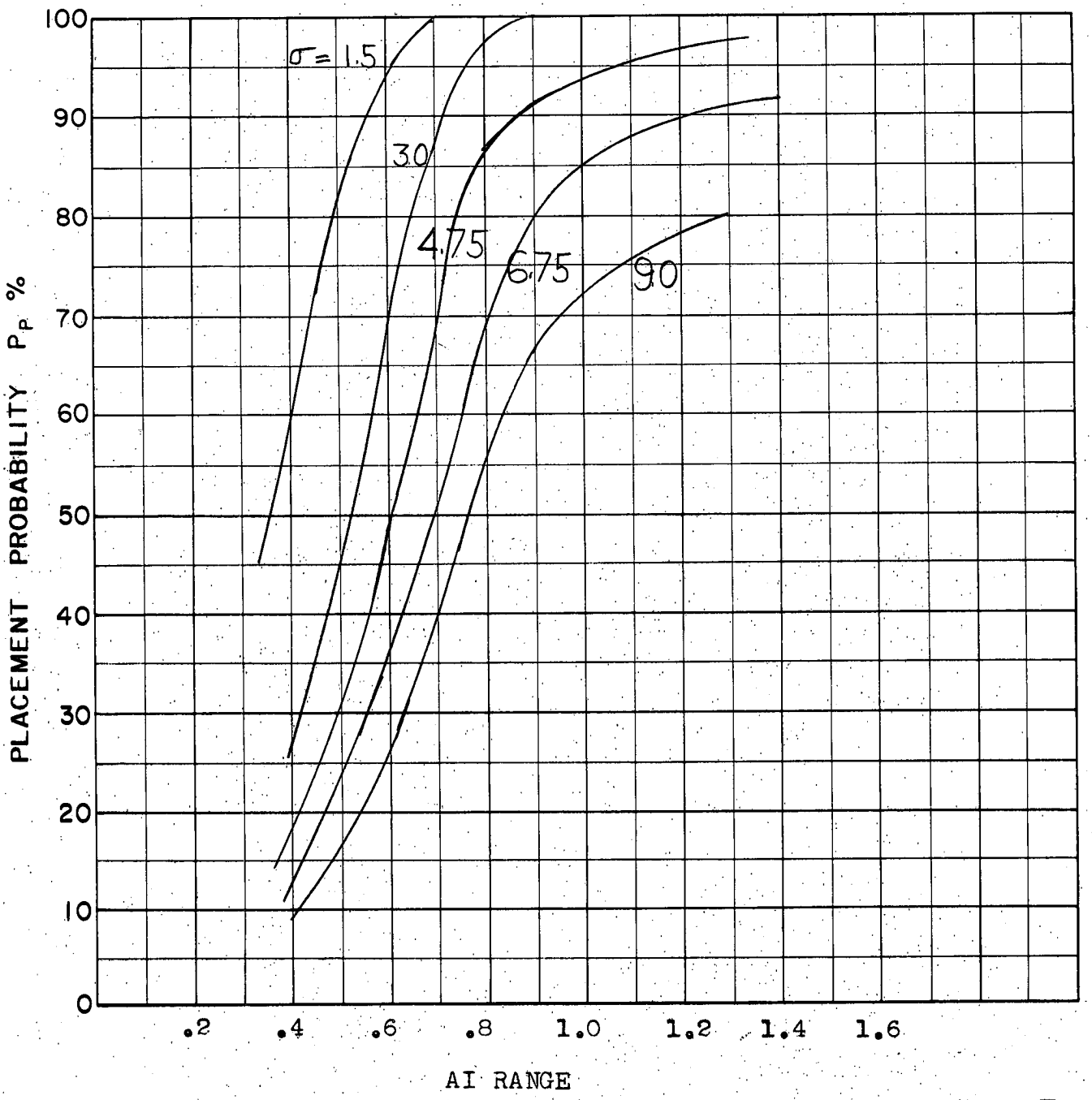

COURSE DIFFERENCE: 160°
TARGET EVASION: 0.5g
TARGET MACH NO.: 2.0
INTERCEPTOR LATERAL G's: 28% peak.
INTERCEPTOR MACH NO.: 1.8
σ OF G.C.I. ACCURACY: 5 Values
A.I. DETECTION RANGE AS FRACTION OF SPECIFICATION RANGE, S: Abscissa
A.I. DETECTION RANGE CONTOUR: Straight Wing
ALTITUDE: 50K

S-8
E

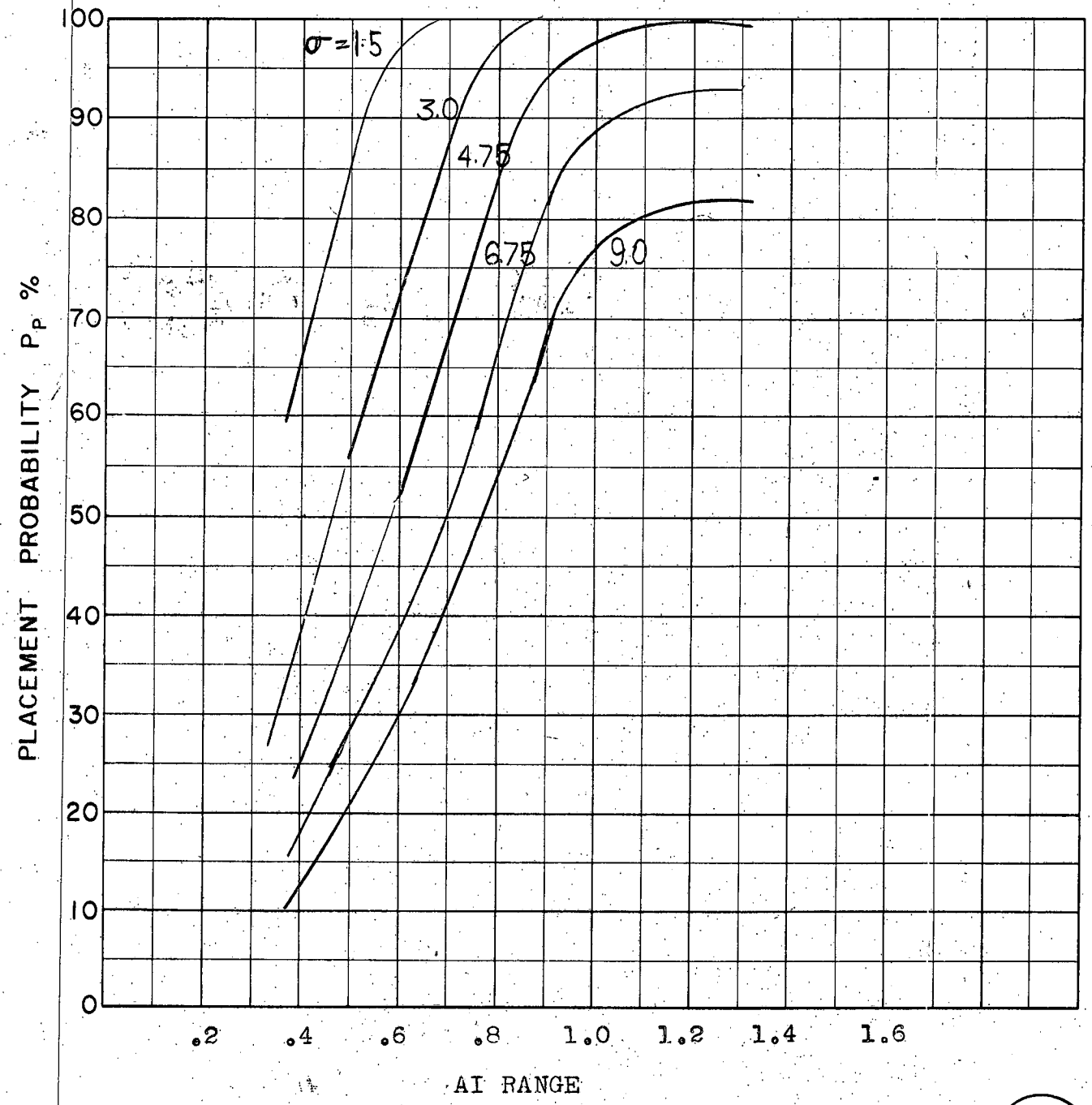

COURSE DIFFERENCE: 180°
TARGET EVASION: 0.5g
TARGET MACH NO.: 2.0
INTERCEPTOR LATERAL G's: 28% pess.
INTERCEPTOR MACH NO.: 1.8
σ OF G.C.I. ACCURACY: 5 Values
A.I. DETECTION RANGE AS FRACTION OF SPECIFICATION RANGE, S: Abscissa
A.I. DETECTION RANGE CONTOUR: Straight Wing
ALTITUDE: 50K

S-9a
E

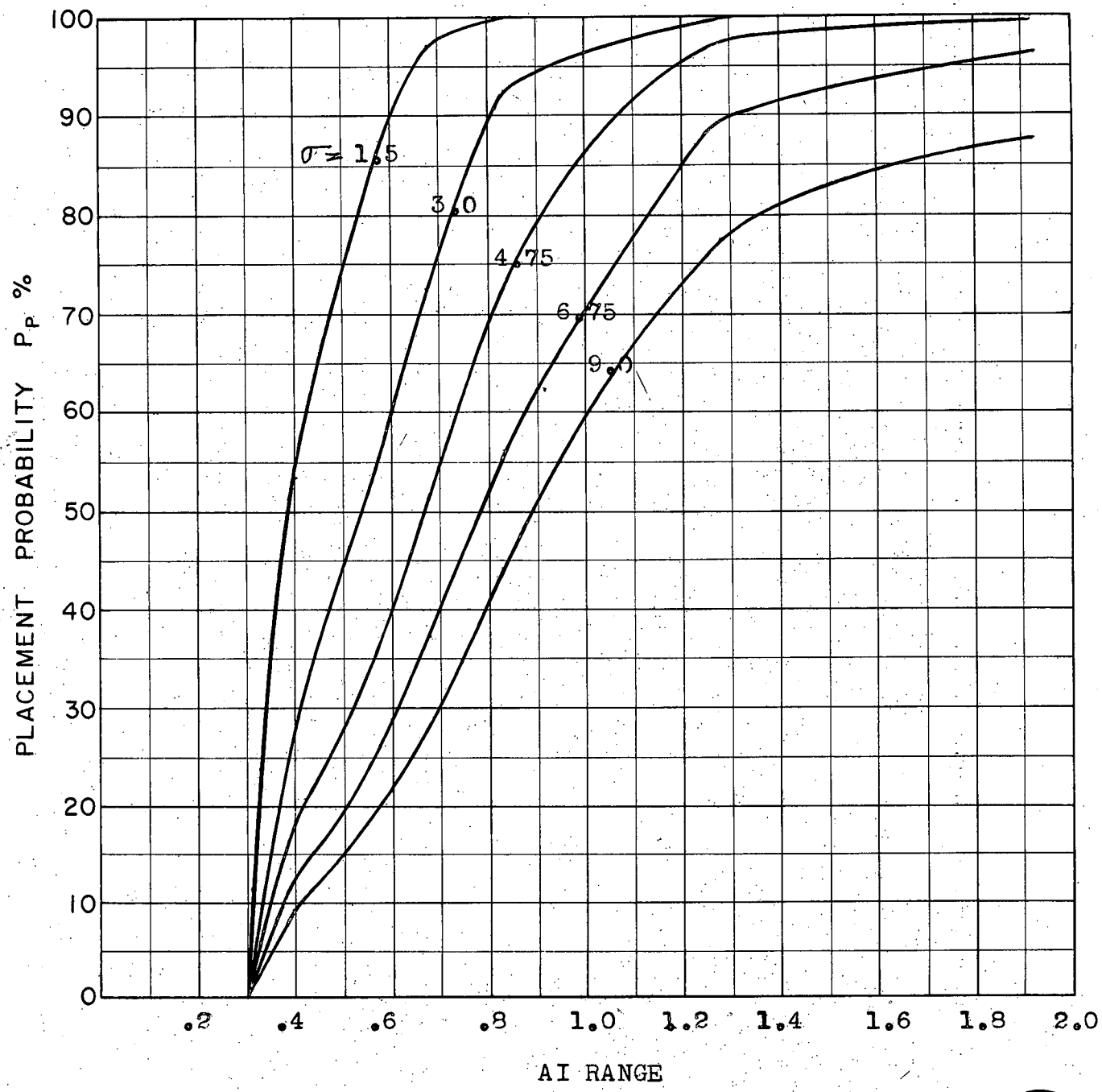

COURSE DIFFERENCE: 180°
TARGET EVASION: 0.5g
TARGET MACH NO.: 2.0
INTERCEPTOR LATERAL G's: 2.0 Limit; 28% pess.
INTERCEPTOR MACH NO.: 1.8
σ OF G.C.I. ACCURACY: 5 Values
A.I. DETECTION RANGE AS FRACTION OF SPECIFICATION RANGE, S: Abscissa
A.I. DETECTION RANGE CONTOUR: Straight Wing
ALTITUDE: 50K

S9b
E

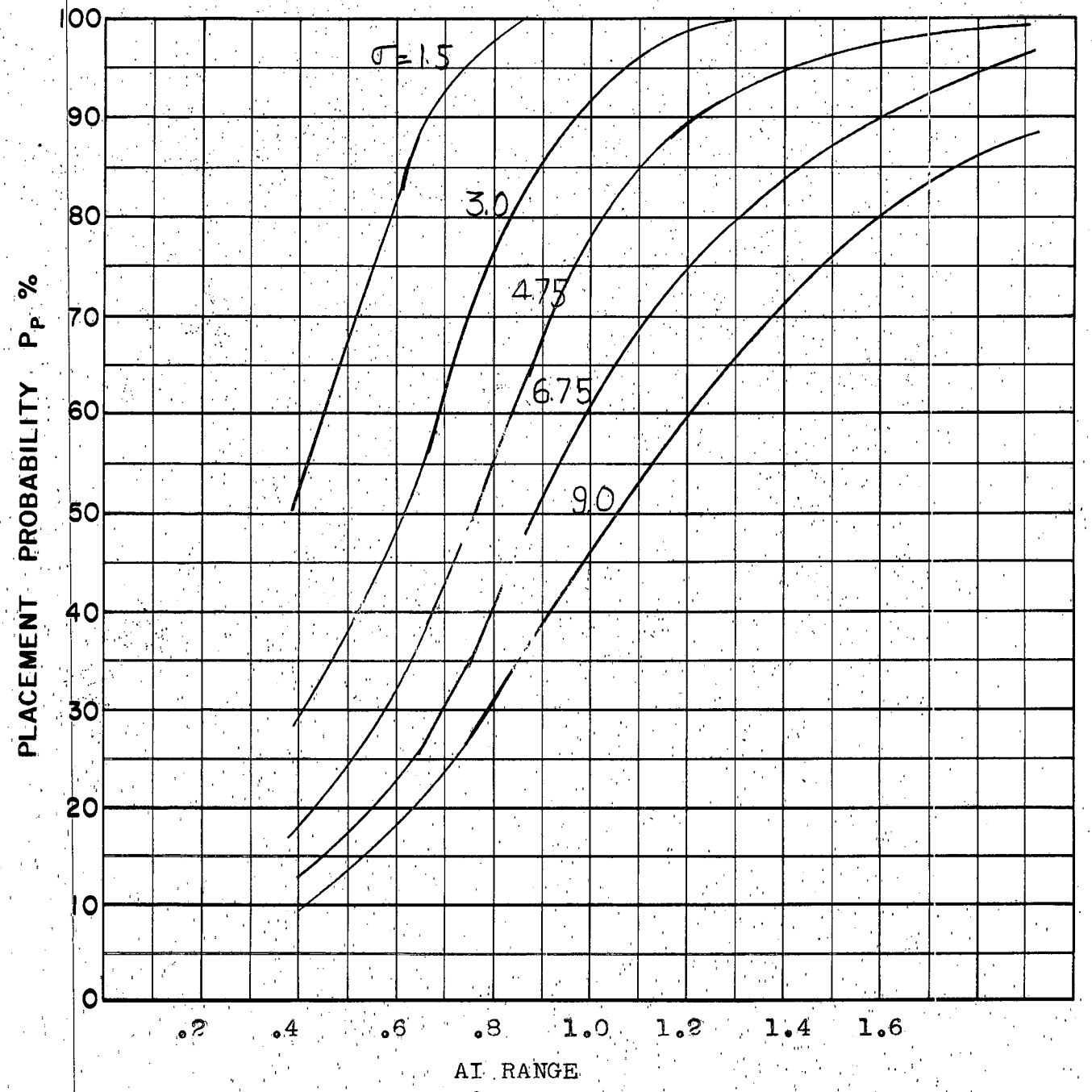

COURSE DIFFERENCE: 180°
TARGET EVASION: 0.5g
TARGET MACH NO.: 2.0
INTERCEPTOR LATERAL G's: 1.5g Limit; 28% pess.
INTERCEPTOR MACH NO.: 1.8
σ OF G.C.I. ACCURACY: 5 Values
A.I. DETECTION RANGE AS FRACTION OF SPECIFICATION RANGE, S: Abscissa
A.I. DETECTION RANGE CONTOUR: Straight Wing
ALTITUDE: 50K

S-9c
E

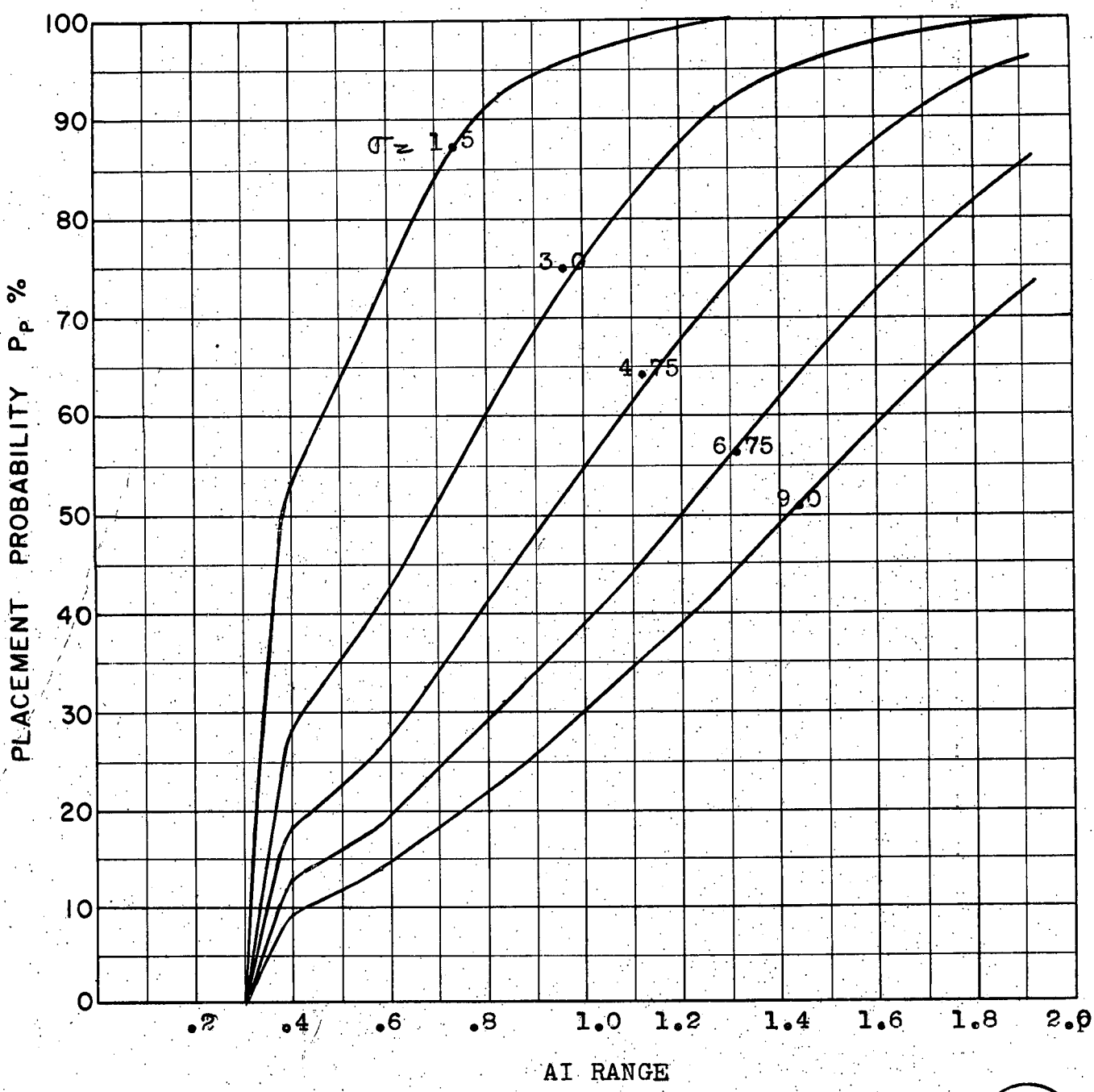

COURSE DIFFERENCE: 180°
TARGET EVASION: 0.5g
TARGET MACH NO.: 2.0
INTERCEPTOR LATERAL G's: 1.0 Limit; 28% pess.
INTERCEPTOR MACH NO.: 1.8
σ OF G.C.I. ACCURACY: 5 Values
A.I. DETECTION RANGE AS FRACTION OF SPECIFICATION RANGE, S: Abscissa
A.I. DETECTION RANGE CONTOUR: Straight Wing
ALTITUDE: 50K

S-9d
E

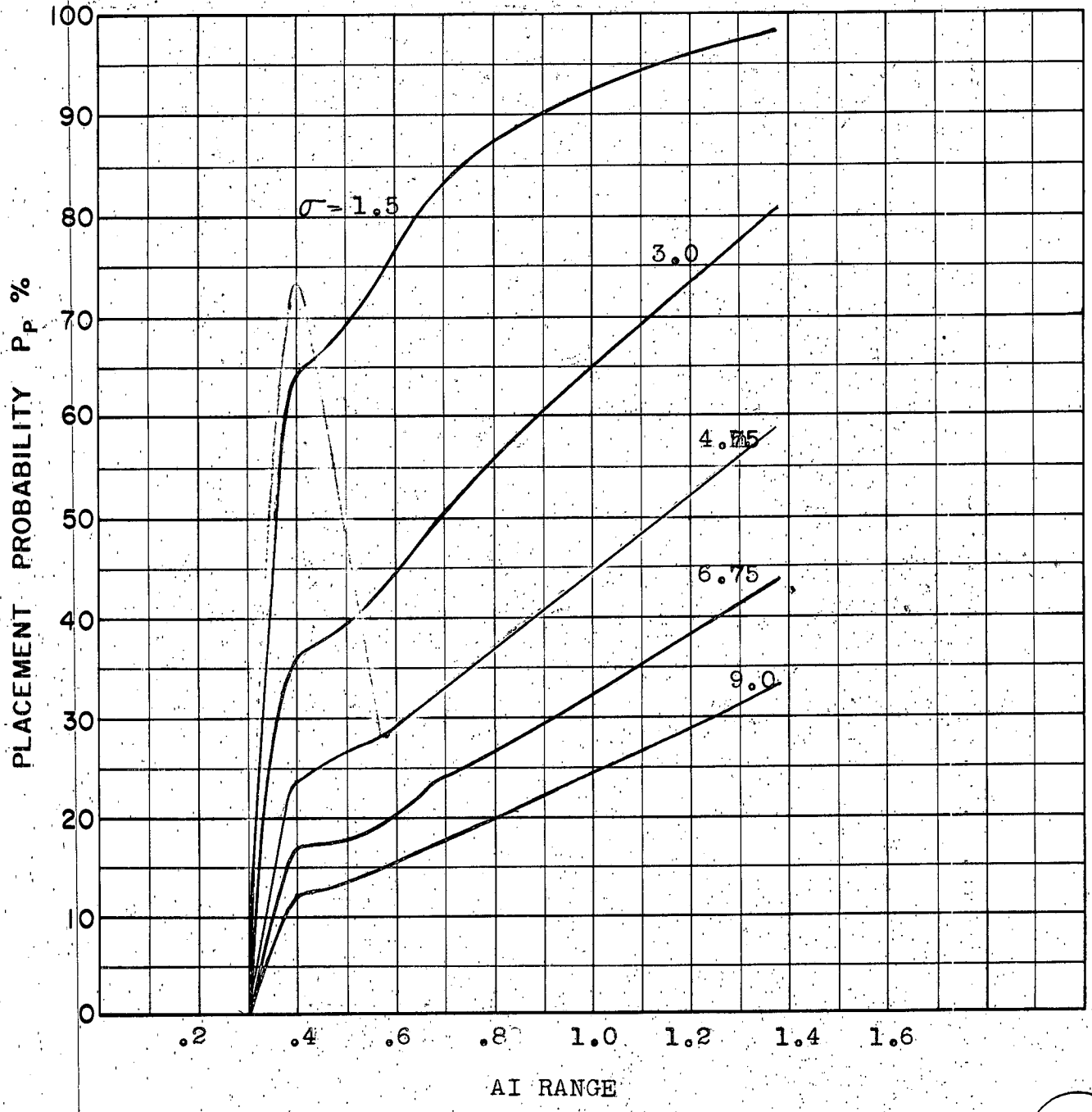

COURSE DIFFERENCE: 180°
TARGET EVASION: 0.5g
TARGET MACH NO.: 2.0
INTERCEPTOR LATERAL G's: Limited to 0.75g (28% pess.)
INTERCEPTOR MACH NO.: 1.8
σ OF G.C.I. ACCURACY: 5 Values
A.I. DETECTION RANGE AS FRACTION OF SPECIFICATION RANGE, S: Abscissa
A.I. DETECTION RANGE CONTOUR: Sraight Wing
ALTITUDE: 50K

S-9e
E

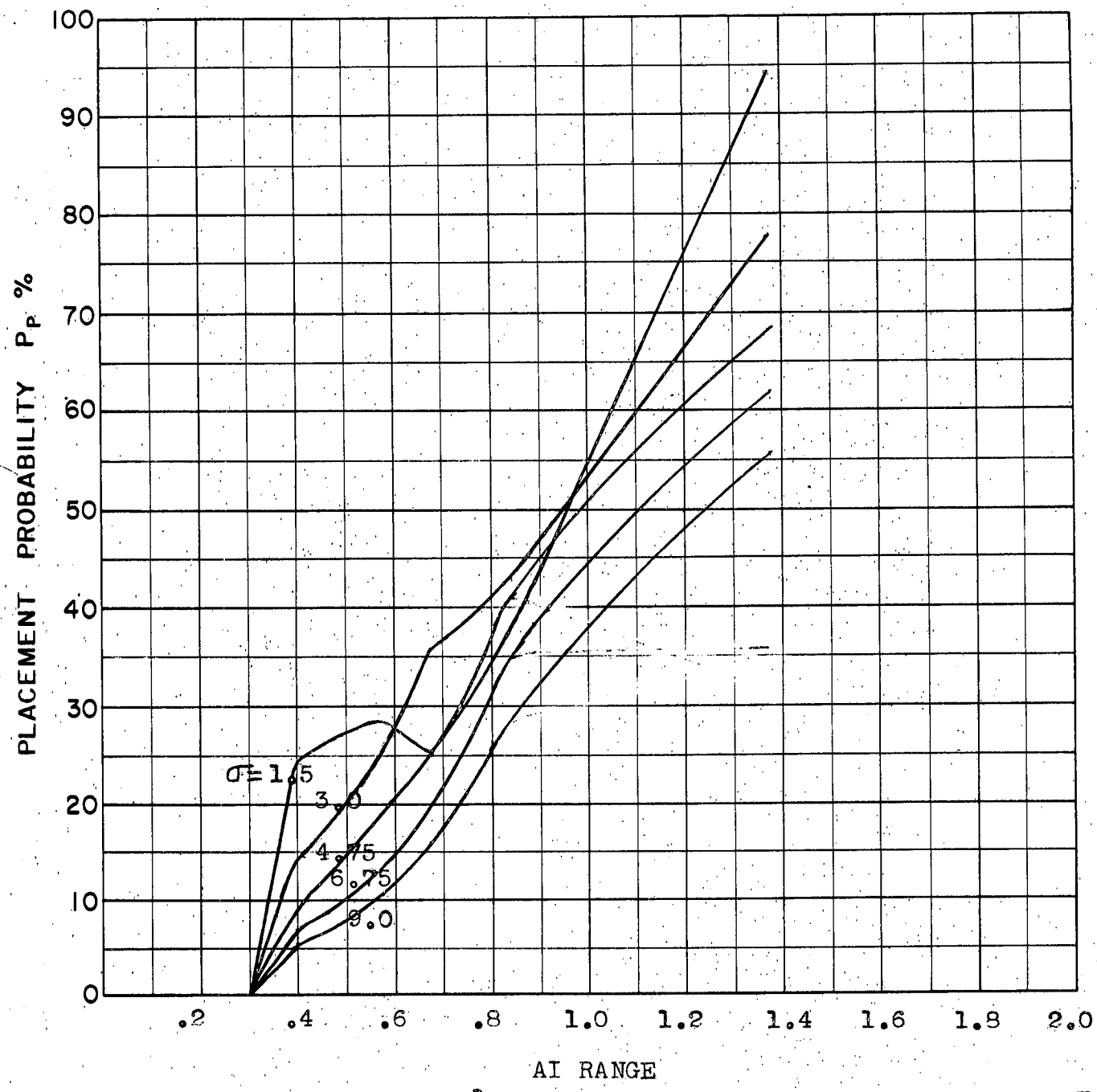

COURSE DIFFERENCE: 110°
TARGET EVASION: 0.75g Limited to 30° change of course
TARGET MACH NO.: 2.0
INTERCEPTOR LATERAL G's: 28% pess.
INTERCEPTOR MACH NO.: 1.8
σ OF G.C.I. ACCURACY: 5 Values
A.I. DETECTION RANGE AS FRACTION OF SPECIFICATION RANGE, S: Abscissa
A.I. DETECTION RANGE CONTOUR: Straight Wing
ALTITUDE: 50K

S10a
E

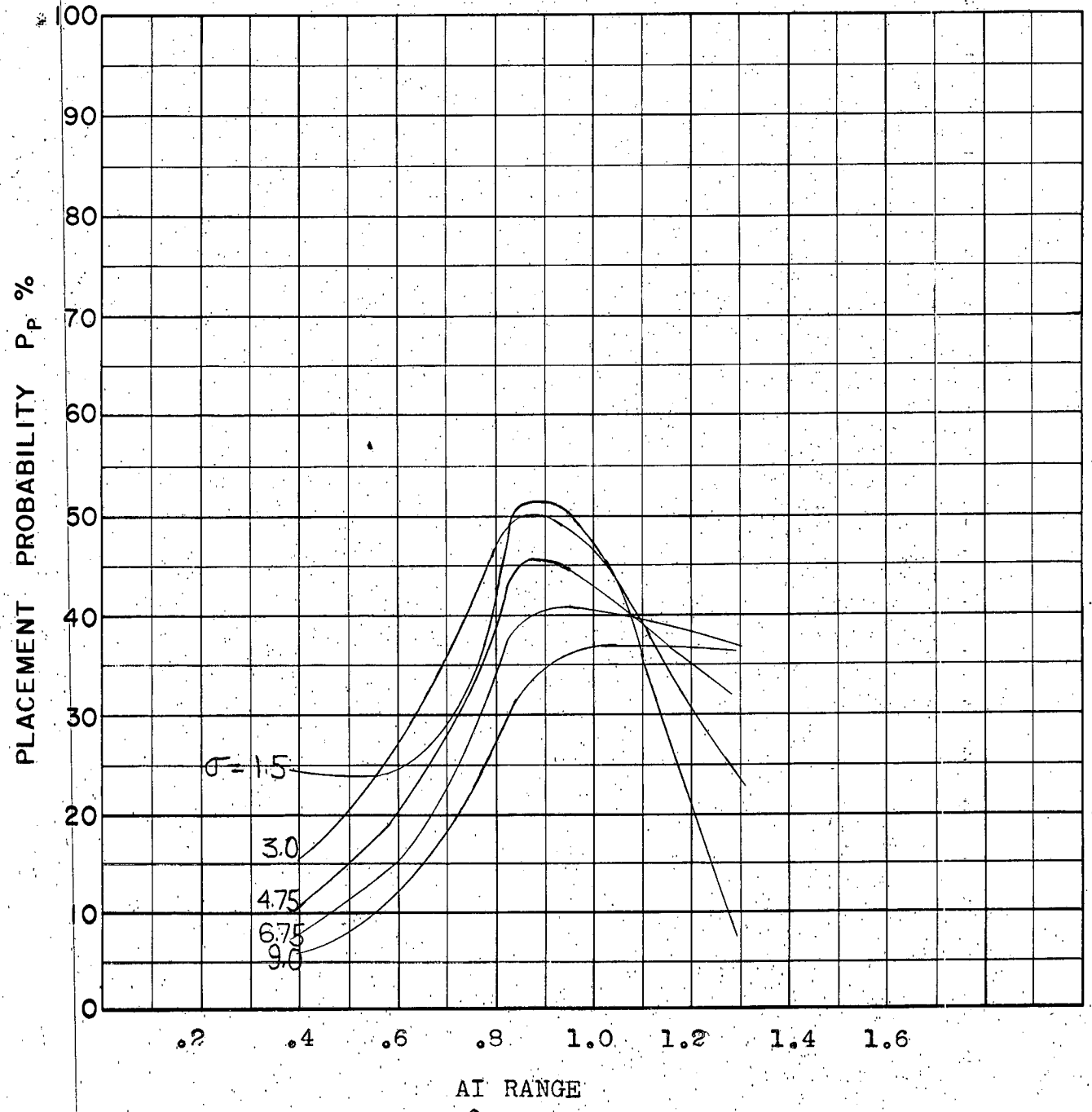

COURSE DIFFERENCE: 110°
TARGET EVASION: 0.75g Limited to 60° change of course
TARGET MACH NO.: 2.0
INTERCEPTOR LATERAL G's: 28% pess.
INTERCEPTOR MACH NO.: 1.8
σ OF G.C.I. ACCURACY: 5 Values
A.I. DETECTION RANGE AS FRACTION OF SPECIFICATION RANGE, S: Abscissa
A.I. DETECTION RANGE CONTOUR: Straight Wing
ALTITUDE: 50K

S-10b
E

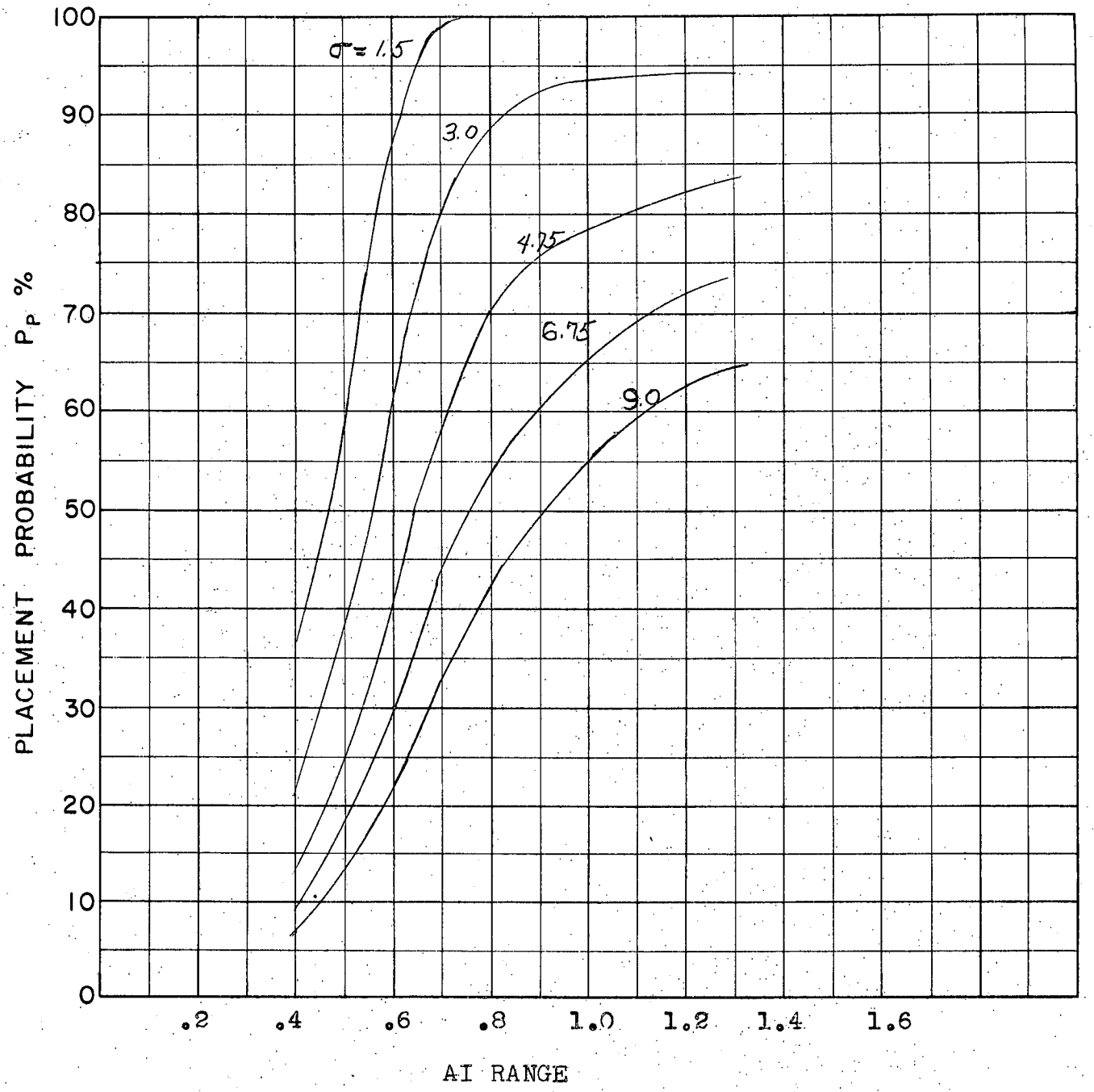

COURSE DIFFERENCE: 135°
TARGET EVASION: 0.75g Limited to 30° change of course
TARGET MACH NO.: 2.0
INTERCEPTOR LATERAL G's: 28% pess.
INTERCEPTOR MACH NO.: 1.8
σ OF G.C.I. ACCURACY: 5 Values
A.I. DETECTION RANGE AS FRACTION OF SPECIFICATION RANGE, S: Abscissa
A.I. DETECTION RANGE CONTOUR: Straight Wing
ALTITUDE: 50K

S-11a
E

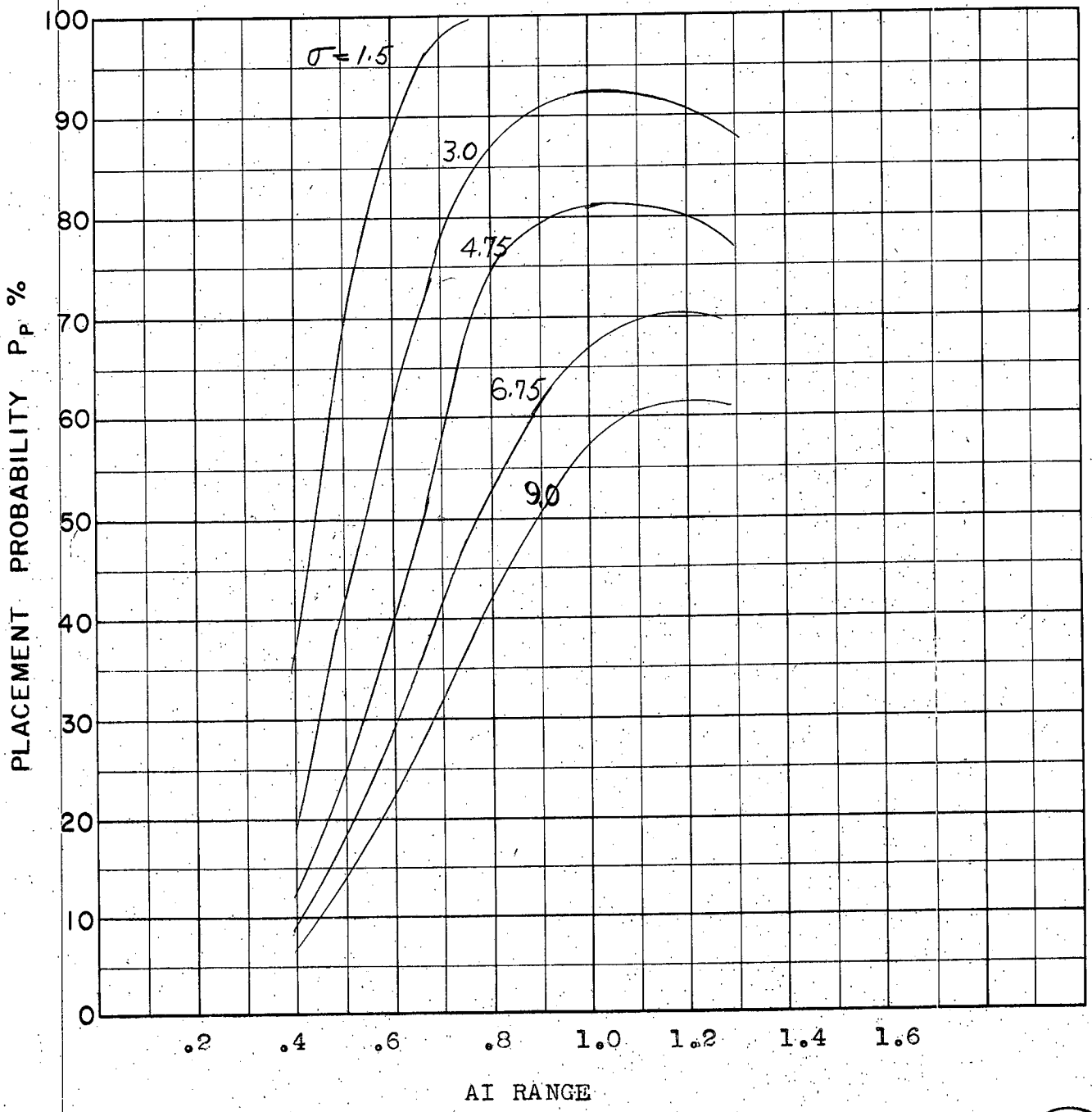

COURSE DIFFERENCE: 135°
TARGET EVASION: 0.75g Limited to 60° change of course
TARGET MACH NO.: 2.0
INTERCEPTOR LATERAL G's: 28% pess.
INTERCEPTOR MACH NO.: 1.8
σ OF G.C.I. ACCURACY: 5 Values
A.I. DETECTION RANGE AS FRACTION OF SPECIFICATION RANGE, S: Abscissa
A.I. DETECTION RANGE CONTOUR: Straight Wing
ALTITUDE: 50K

S-11b
E

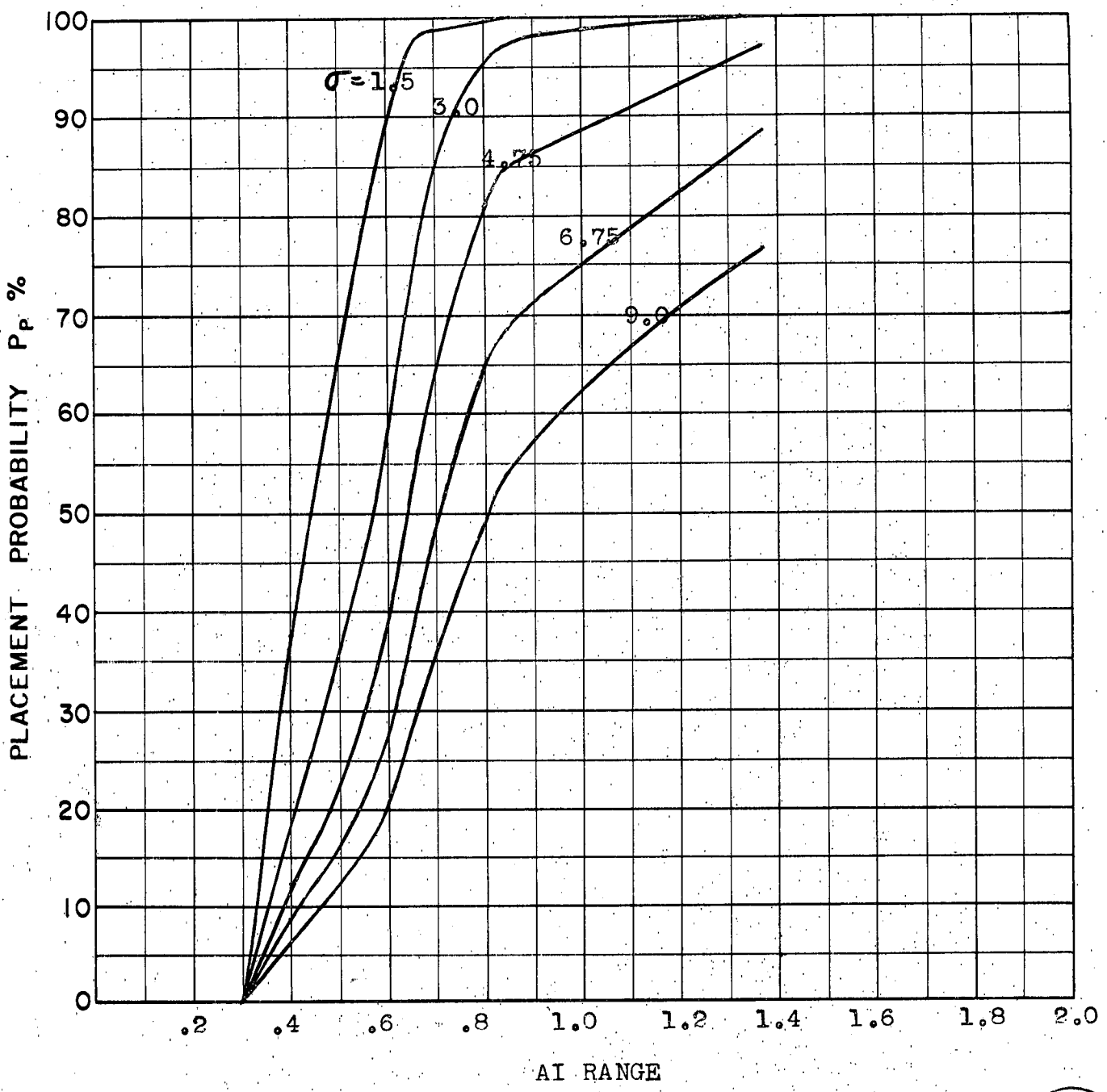

COURSE DIFFERENCE: 160°
TARGET EVASION: 0.75g Limited to 30° change of course
TARGET MACH NO.: 2.0
INTERCEPTOR LATERAL G's: 28% peak.
INTERCEPTOR MACH NO.: 1.8
σ OF G.C.I. ACCURACY: 5 Values
A.I. DETECTION RANGE AS FRACTION OF SPECIFICATION RANGE, S: Abscissa
A.I. DETECTION RANGE CONTOUR: Straight Wing
ALTITUDE: 50K

S12a
E

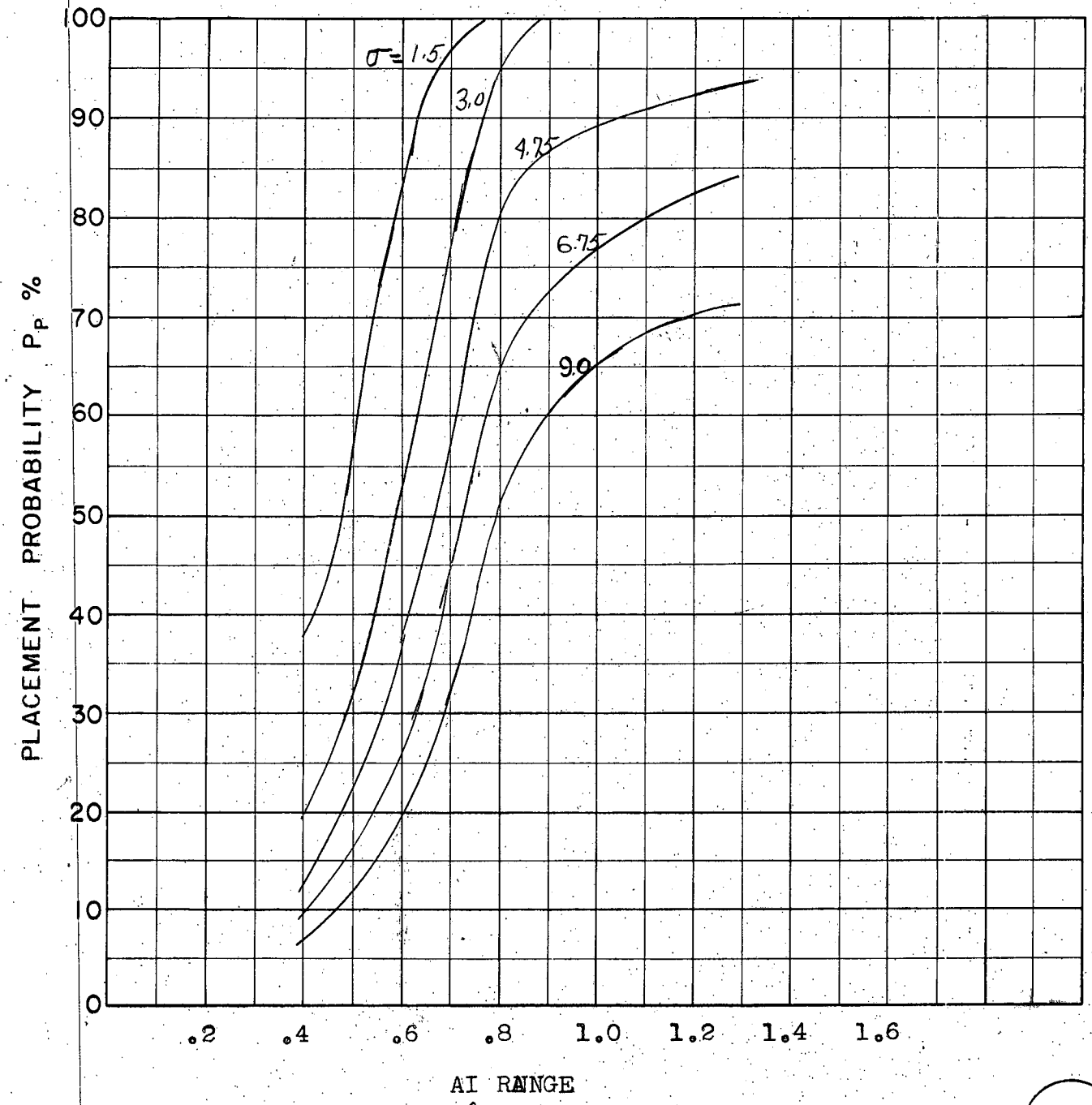

COURSE DIFFERENCE: 160°
TARGET EVASION: 0.75g Limited to 60° change of course
TARGET MACH NO.: 2.0
INTERCEPTOR LATERAL G's: 28% pess.
INTERCEPTOR MACH NO.: 1.8
σ OF G.C.I. ACCURACY: 5 Values
A.I. DETECTION RANGE AS FRACTION OF SPECIFICATION RANGE, S: Abscissa
A.I. DETECTION RANGE CONTOUR: Straight Wing
ALTITUDE: 50K

S12b
E

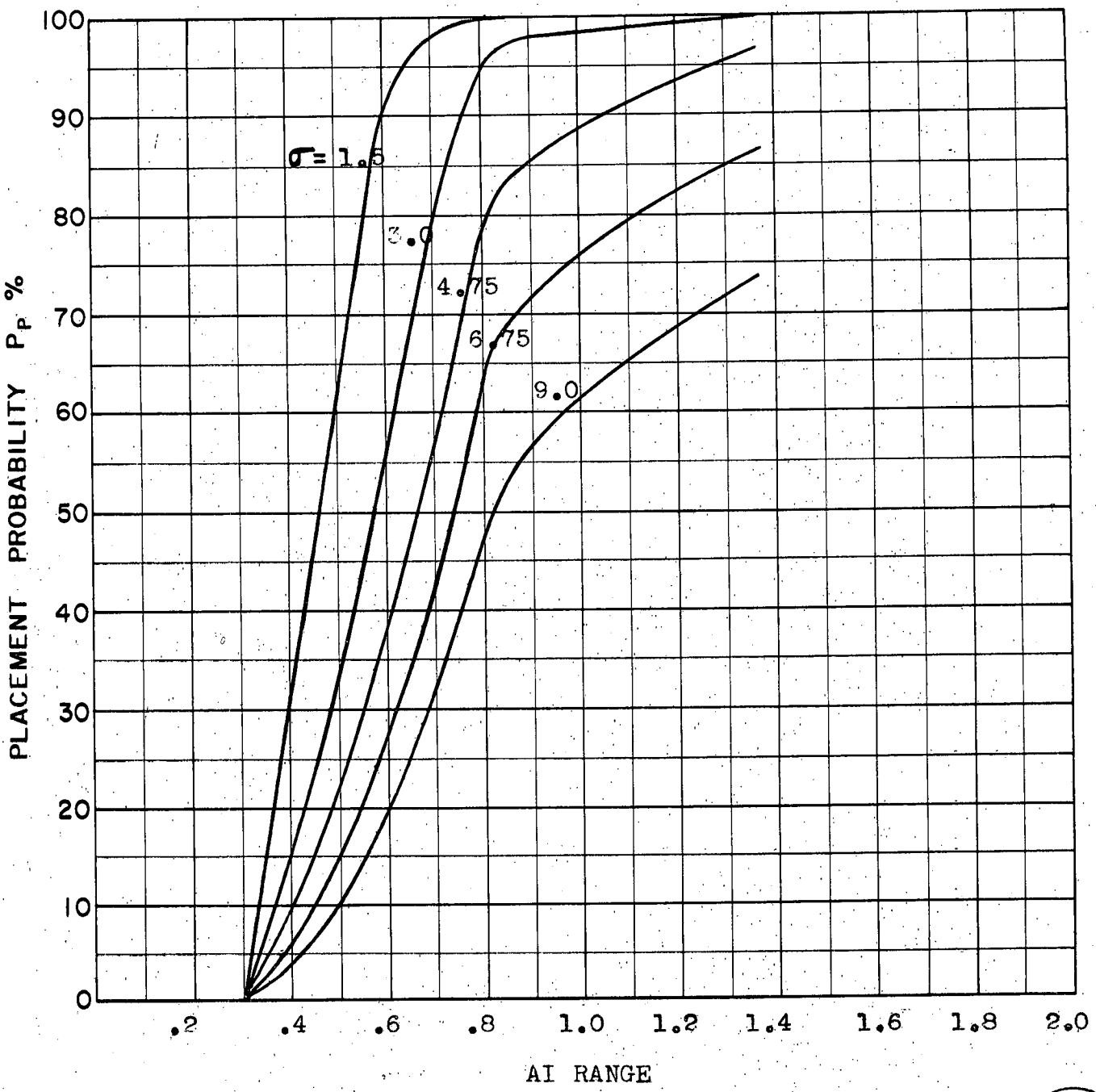

COURSE DIFFERENCE: 180°
TARGET EVASION: 0.75g Limited to 30° change of course
TARGET MACH NO.: 2.0
INTERCEPTOR LATERAL G's: 28% pess.
INTERCEPTOR MACH NO.: 1.8
σ OF G.C.I. ACCURACY: 5 Values
A.I. DETECTION RANGE AS FRACTION OF SPECIFICATION RANGE, S: Abscissa
A.I. DETECTION RANGE CONTOUR: Straight Wing
ALTITUDE: 50K

S-13a
E

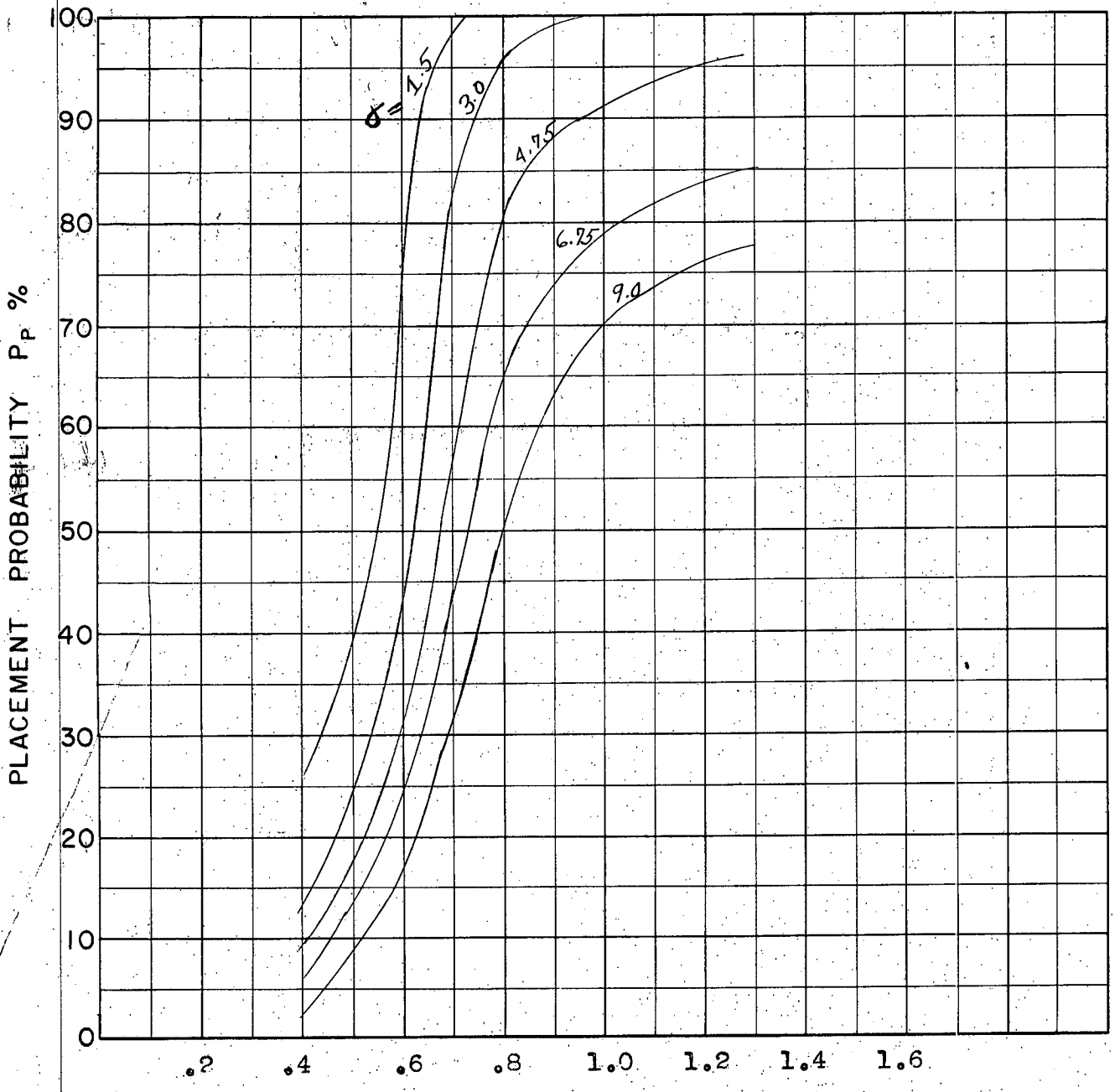

COURSE DIFFERENCE: 180°
TARGET EVASION: 0.75g Limited to 60° change of course
TARGET MACH NO.: 2.0
INTERCEPTOR LATERAL G's: 28% pegs.
INTERCEPTOR MACH NO.: 1.8
σ OF G.C.I. ACCURACY: 5 Values
A.I. DETECTION RANGE AS FRACTION OF SPECIFICATION RANGE, S: Abscissa
A.I. DETECTION RANGE CONTOUR: Straight Wing
ALTITUDE: 50K

S-136 E

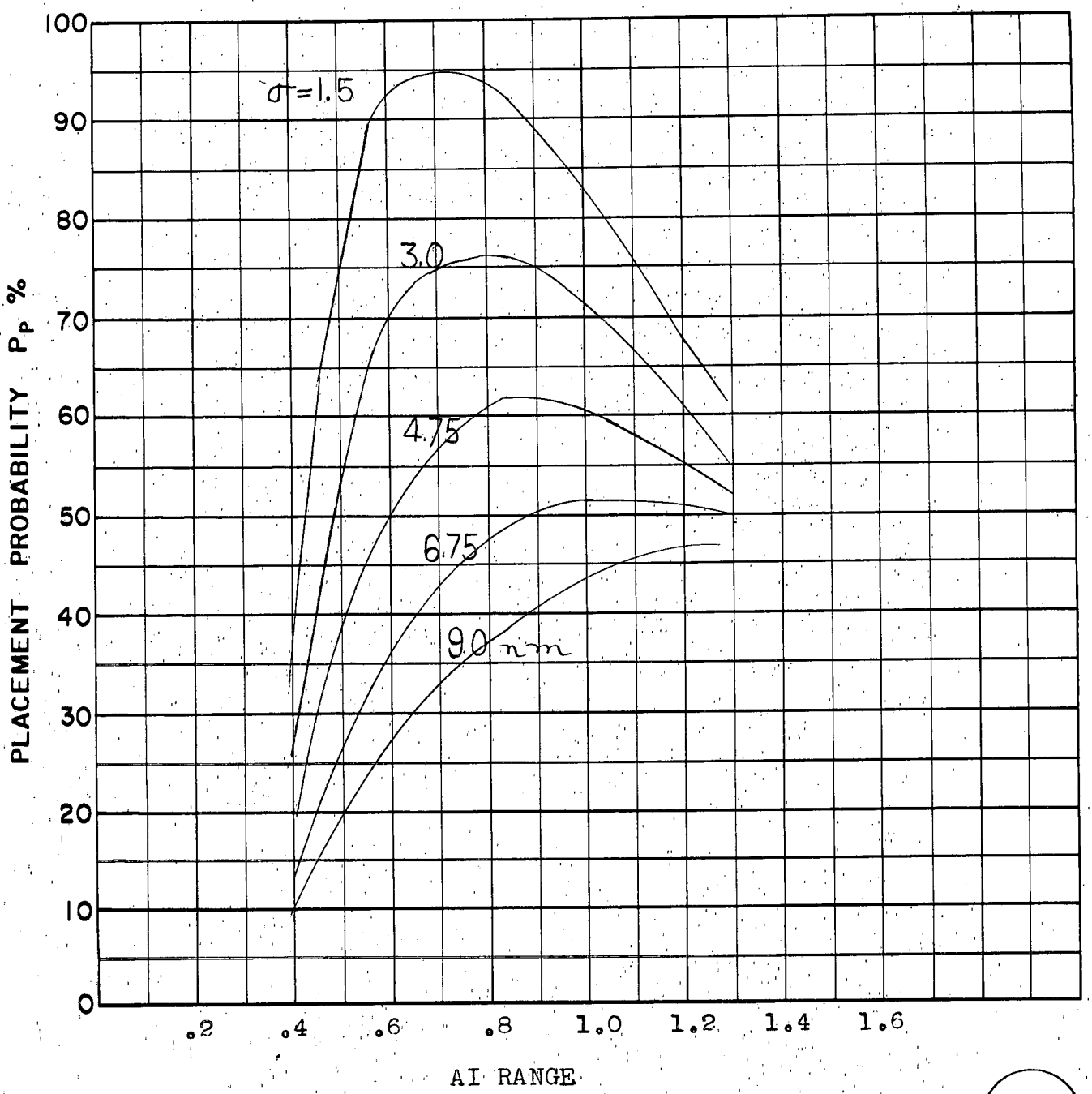

S.14
E

COURSE DIFFERENCE: 110°
TARGET EVASION: 0.5g
TARGET MACH NO.: 2.0
INTERCEPTOR LATERAL G's: 28% poss.
INTERCEPTOR MACH NO.: 1.8
σ OF G.C.I. ACCURACY: 5 Values
A.I. DETECTION RANGE AS FRACTION OF SPECIFICATION RANGE, S Abscissa
A.I. DETECTION RANGE CONTOUR: Straight Wing
ALTITUDE: 55K

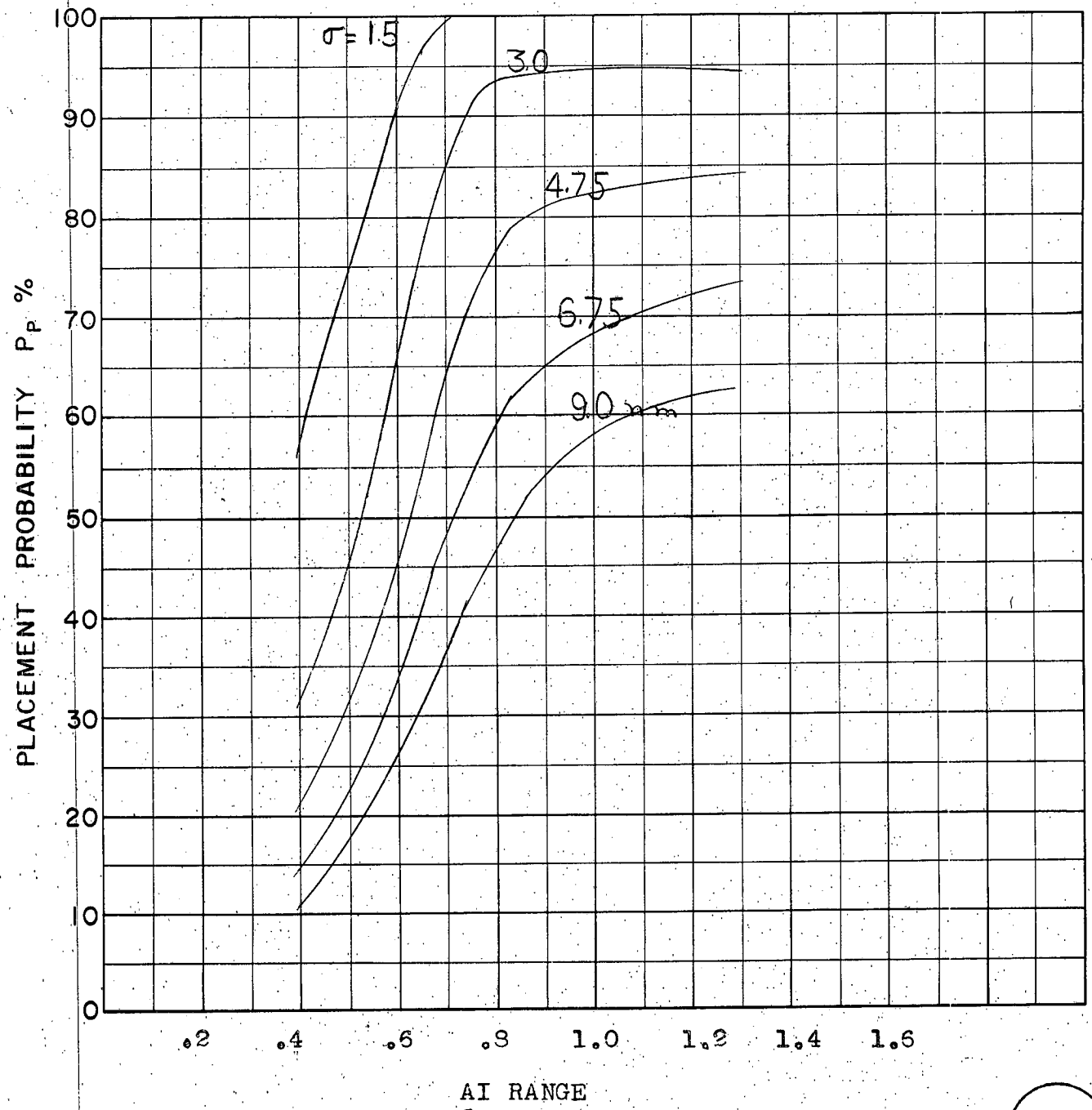

S.15 E

COURSE DIFFERENCE: 135°
TARGET EVASION: 0.5g
TARGET MACH NO.: 2.0
INTERCEPTOR LATERAL G's: 28% pess.
INTERCEPTOR MACH NO.: 1.8
σ OF G.C.I. ACCURACY: 5 Values
A.I. DETECTION RANGE AS FRACTION OF SPECIFICATION RANGE, S: Abscissa
A.I. DETECTION RANGE CONTOUR: Straight Wing
ALTITUDE: 55K

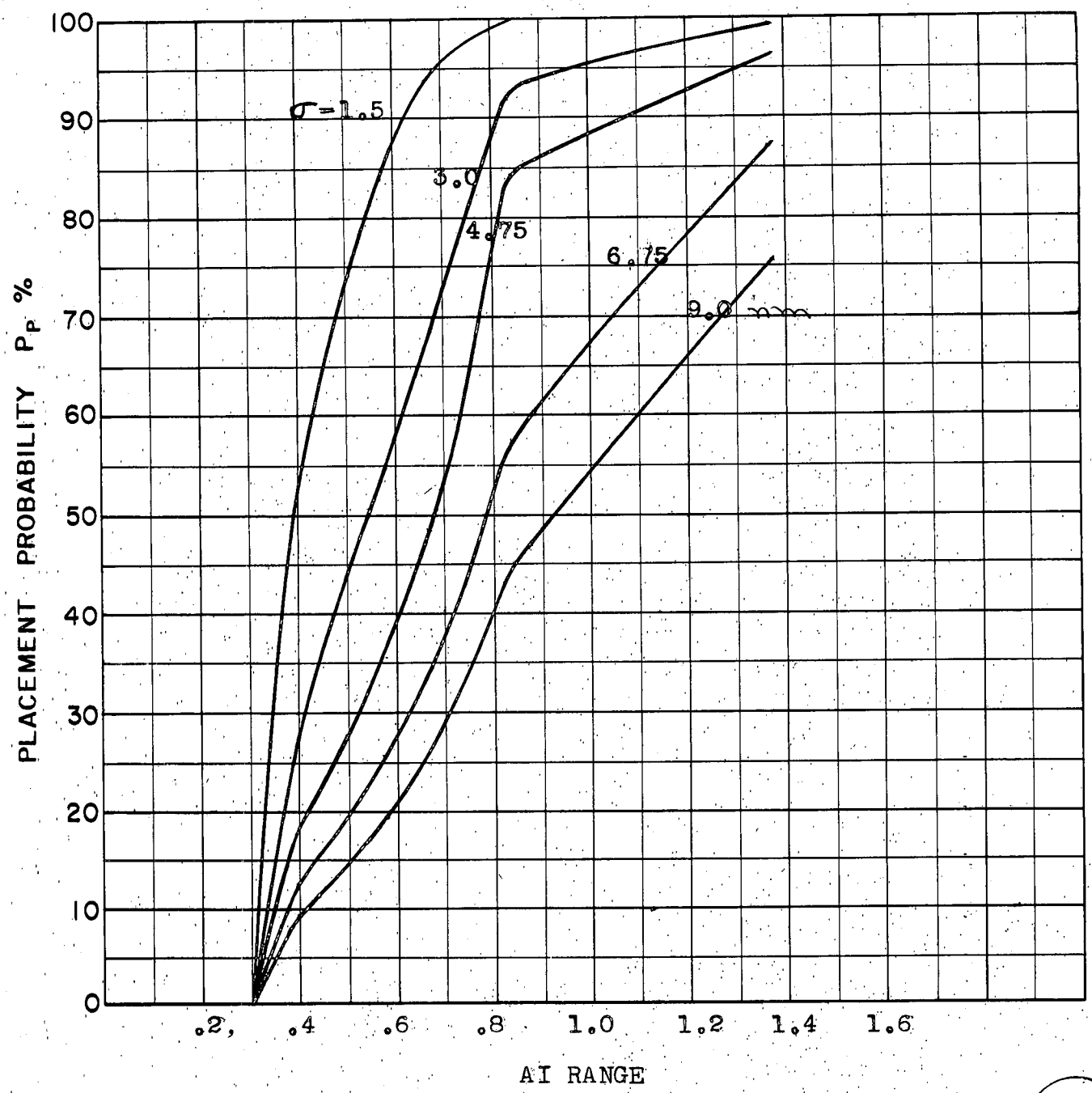

COURSE DIFFERENCE: 160°
TARGET EVASION: 0.5g
TARGET MACH NO.: 2.0
INTERCEPTOR LATERAL G's: 28% pess.
INTERCEPTOR MACH NO.: 1.8
σ OF G.C.I. ACCURACY: 5 Values
A.I. DETECTION RANGE AS FRACTION OF SPECIFICATION RANGE, S: Abscissa
A.I. DETECTION RANGE CONTOUR: Straight Wing
ALTITUDE: 55K

S 16
E

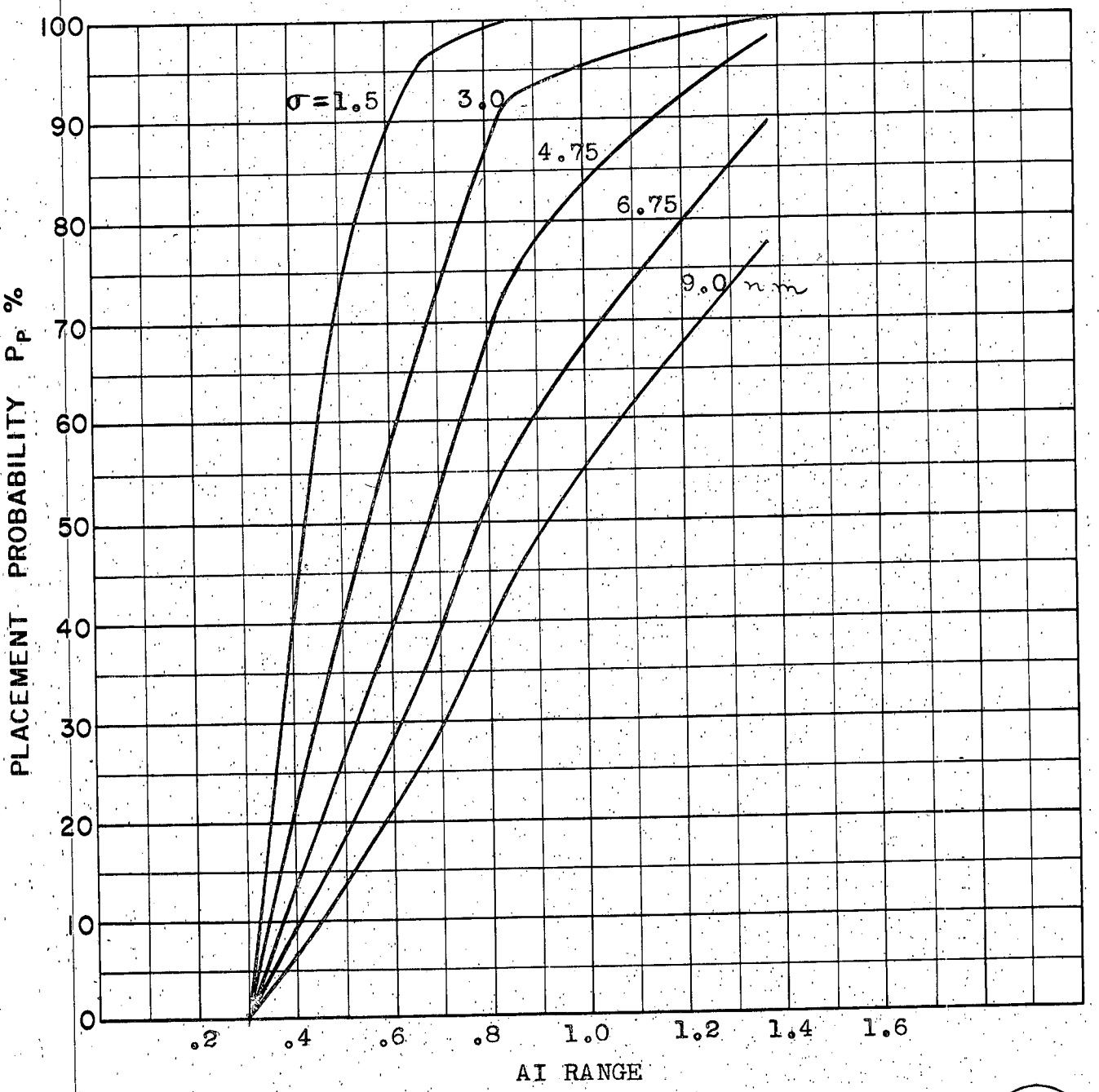

S-17 E

COURSE DIFFERENCE: 180°
TARGET EVASION: 0.5g
TARGET MACH NO.: 2.0
INTERCEPTOR LATERAL G's: 28% pess.
INTERCEPTOR MACH NO.: 1.8
σ OF G.C.I. ACCURACY: 5 Values
A.I. DETECTION RANGE AS FRACTION OF SPECIFICATION RANGE, S: Abscissa
A.I. DETECTION RANGE CONTOUR: STRAIGHT WING
ALTITUDE: 55K

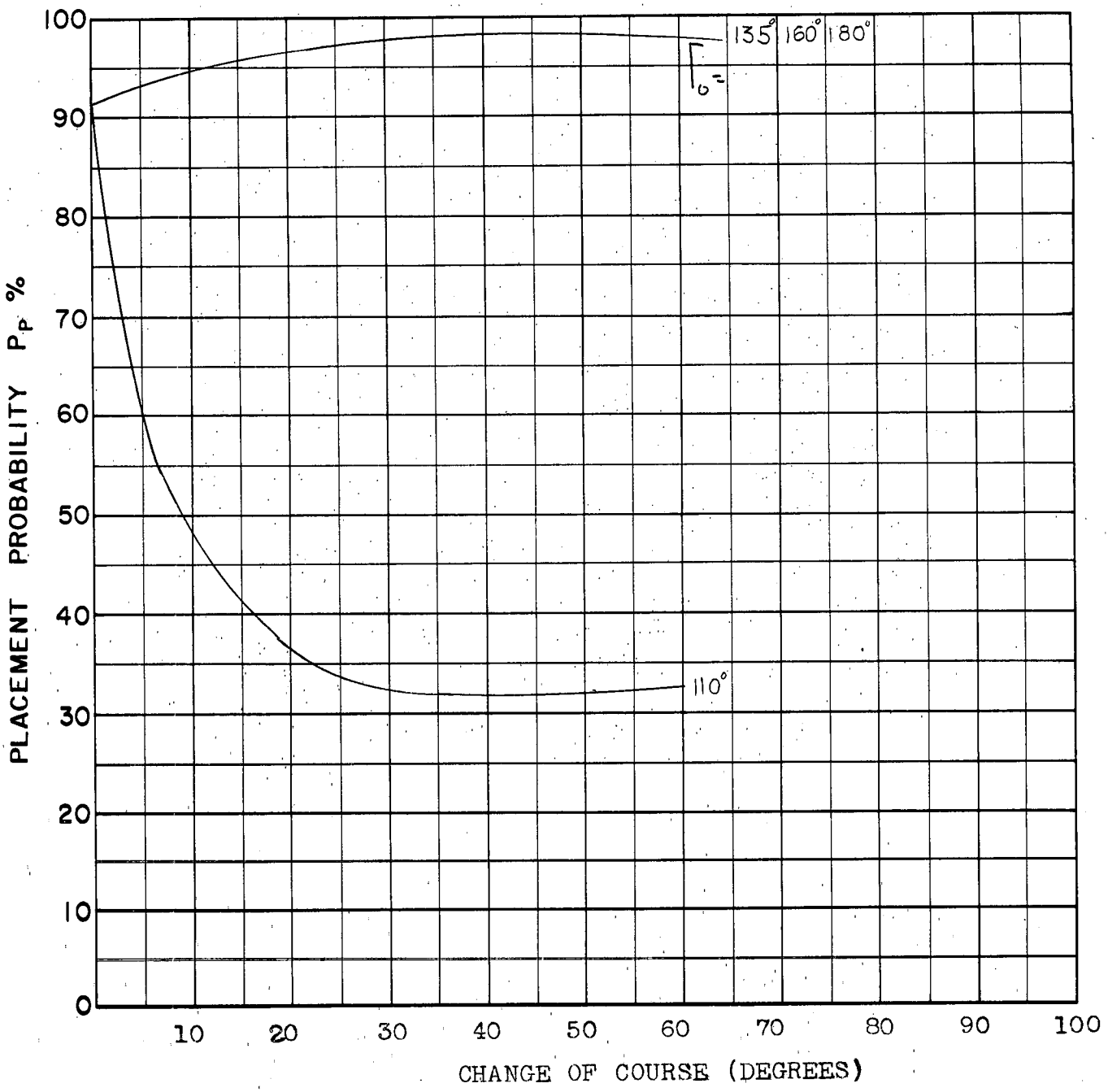

COURSE DIFFERENCE: 4 Values
TARGET EVASION: 0.75g
TARGET MACH NO.: 2.0
INTERCEPTOR LATERAL G's: 28% pess.
INTERCEPTOR MACH NO.: 1.8
σ OF G.C.I. ACCURACY: 1.5
A.I. DETECTION RANGE AS FRACTION OF SPECIFICATION RANGE, S: 0.4
A.I. DETECTION RANGE CONTOUR: Delta Wing
ALTITUDE: 50K

D18

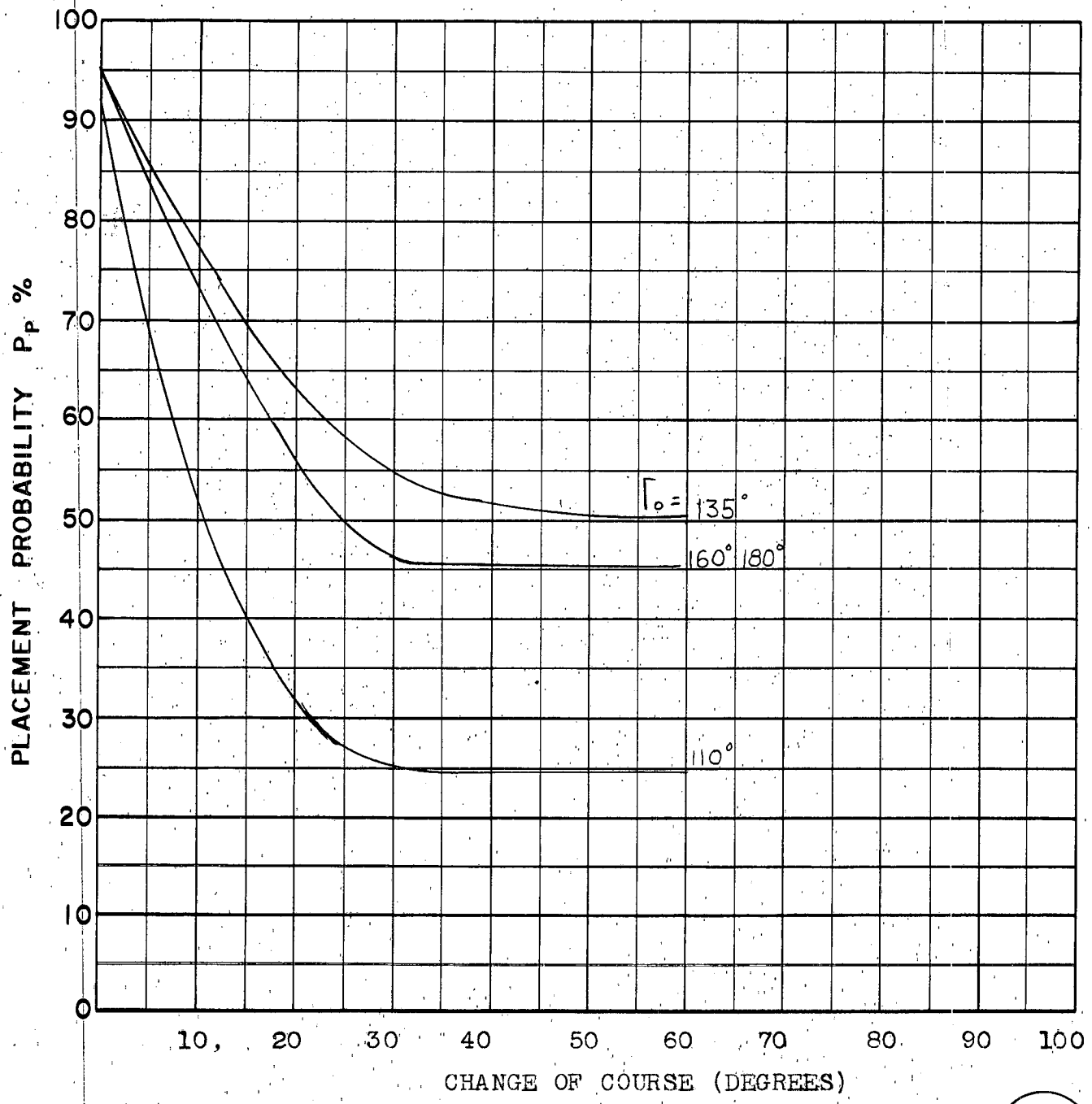

COURSE DIFFERENCE: 4 Values
TARGET EVASION: 0.75g
TARGET MACH NO.: 2.0
INTERCEPTOR LATERAL G's: 28% Pess.
INTERCEPTOR MACH NO.: 1.8
σ OF G.C.I. ACCURACY: 4.75
A.I. DETECTION RANGE AS FRACTION OF SPECIFICATION RANGE, S: 0.4
A.I. DETECTION RANGE CONTOUR: Delta Wing
ALTITUDE: 50K

D19

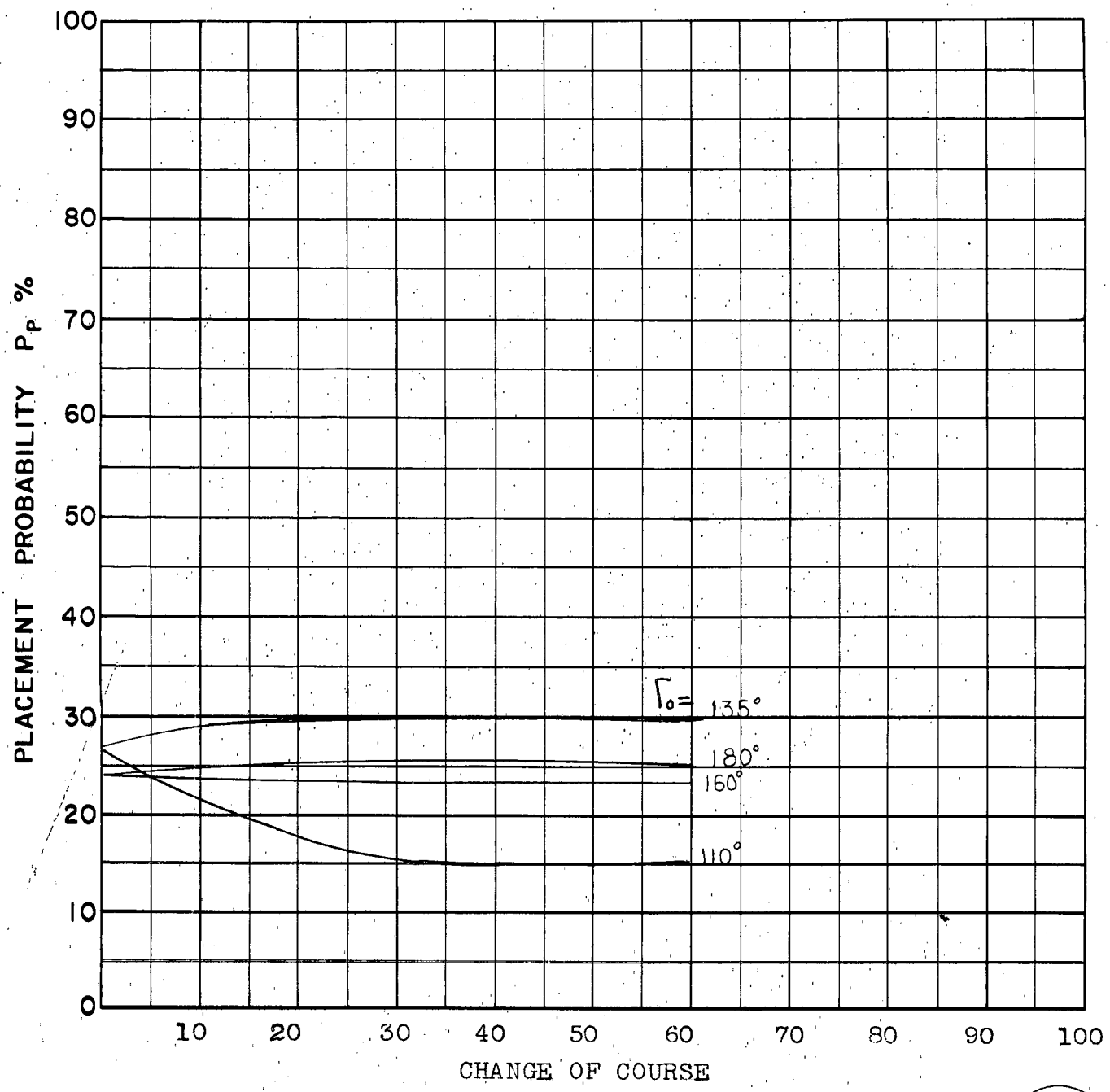

D20

COURSE DIFFERENCE: 4 Values
TARGET EVASION: 0.75g
TARGET MACH NO.: 2.0
INTERCEPTOR LATERAL G's: 28% pess.
INTERCEPTOR MACH NO.: 1.8
σ OF G.C.I. ACCURACY: 9.0
A.I. DETECTION RANGE AS FRACTION OF SPECIFICATION RANGE, S: 0.4
A.I. DETECTION RANGE CONTOUR: Delta Wing
ALTITUDE: 50K

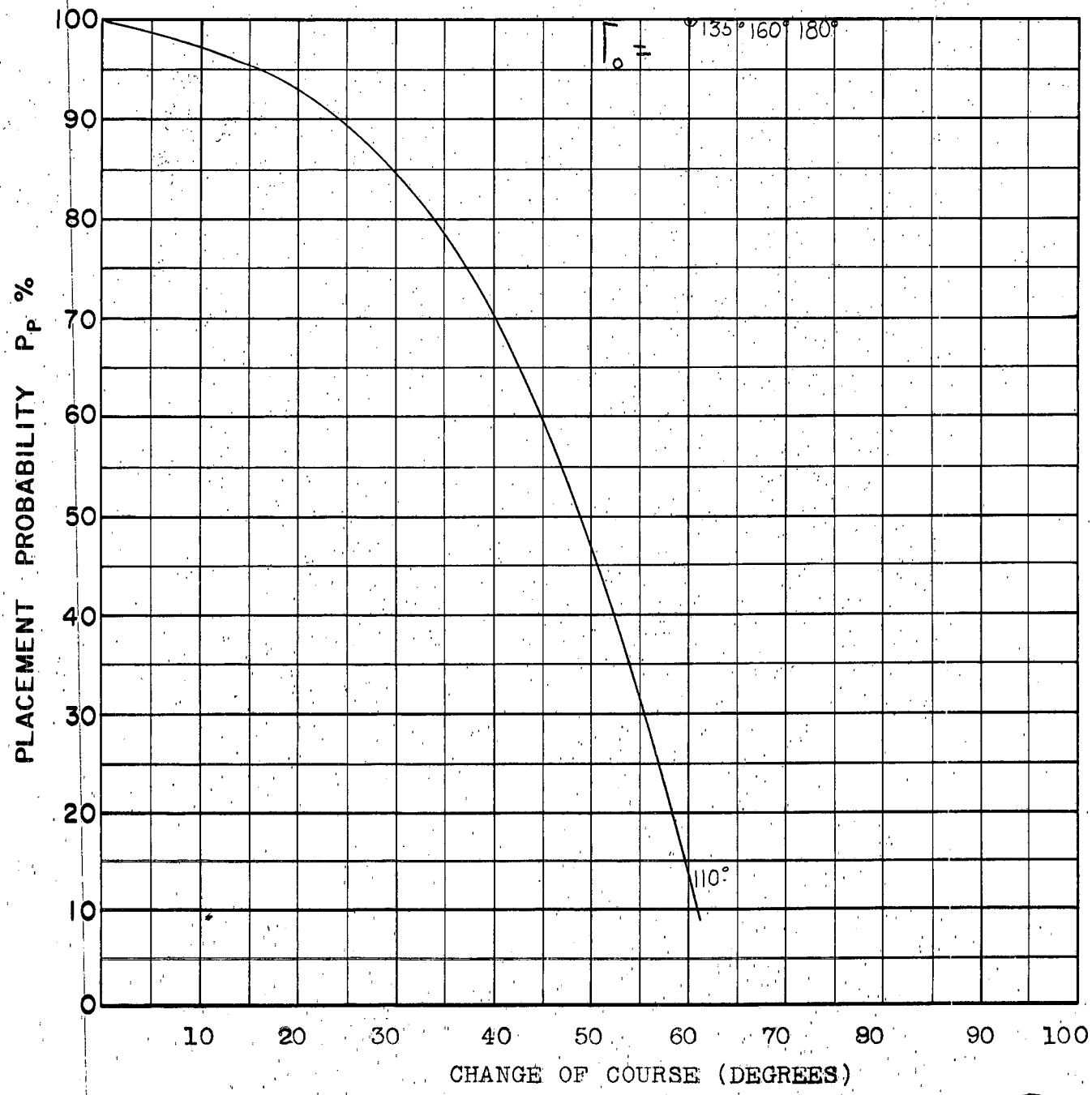

COURSE DIFFERENCE: 4 Values
TARGET EVASION: 0.75
TARGET MACH NO.: 2
INTERCEPTOR LATERAL G's: 28% pess
INTERCEPTOR MACH NO.: 1.8
σ OF G.C.I. ACCURACY: 1.5
A.I. DETECTION RANGE AS FRACTION OF SPECIFICATION RANGE, S: 0.8
A.I. DETECTION RANGE CONTOUR: Delta Wing
ALTITUDE: 50K

D21

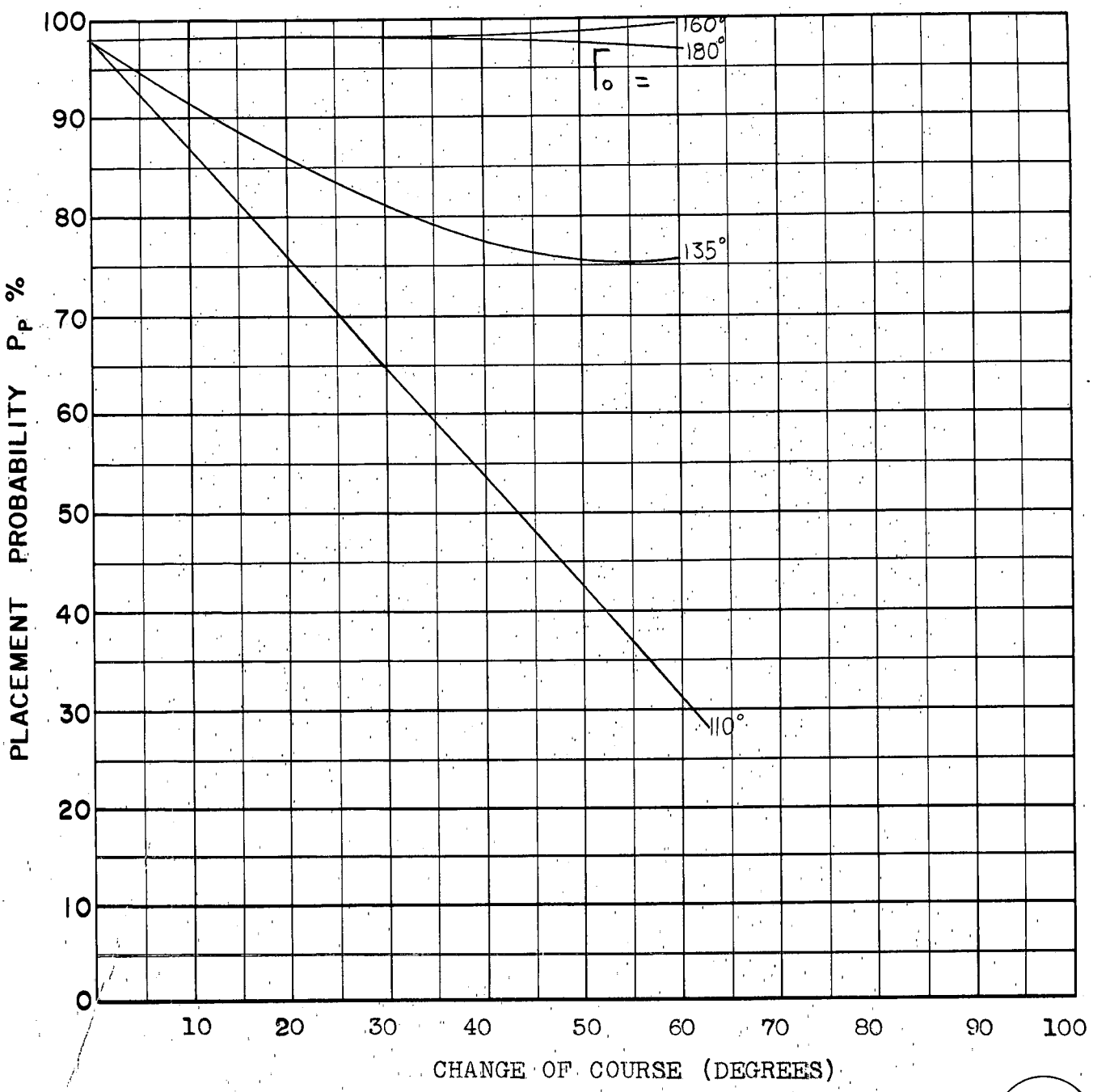

D-22

COURSE DIFFERENCE: 4 Values
TARGET EVASION: 0.75g
TARGET MACH NO.: 2.0
INTERCEPTOR LATERAL G's: 28% pess.
INTERCEPTOR MACH NO.: 1.8
σ OF G.C.I. ACCURACY: 4.75
A.I. DETECTION RANGE AS FRACTION OF SPECIFICATION RANGE, S: 0.8
A.I. DETECTION RANGE CONTOUR: Delta Wing
ALTITUDE: 50K

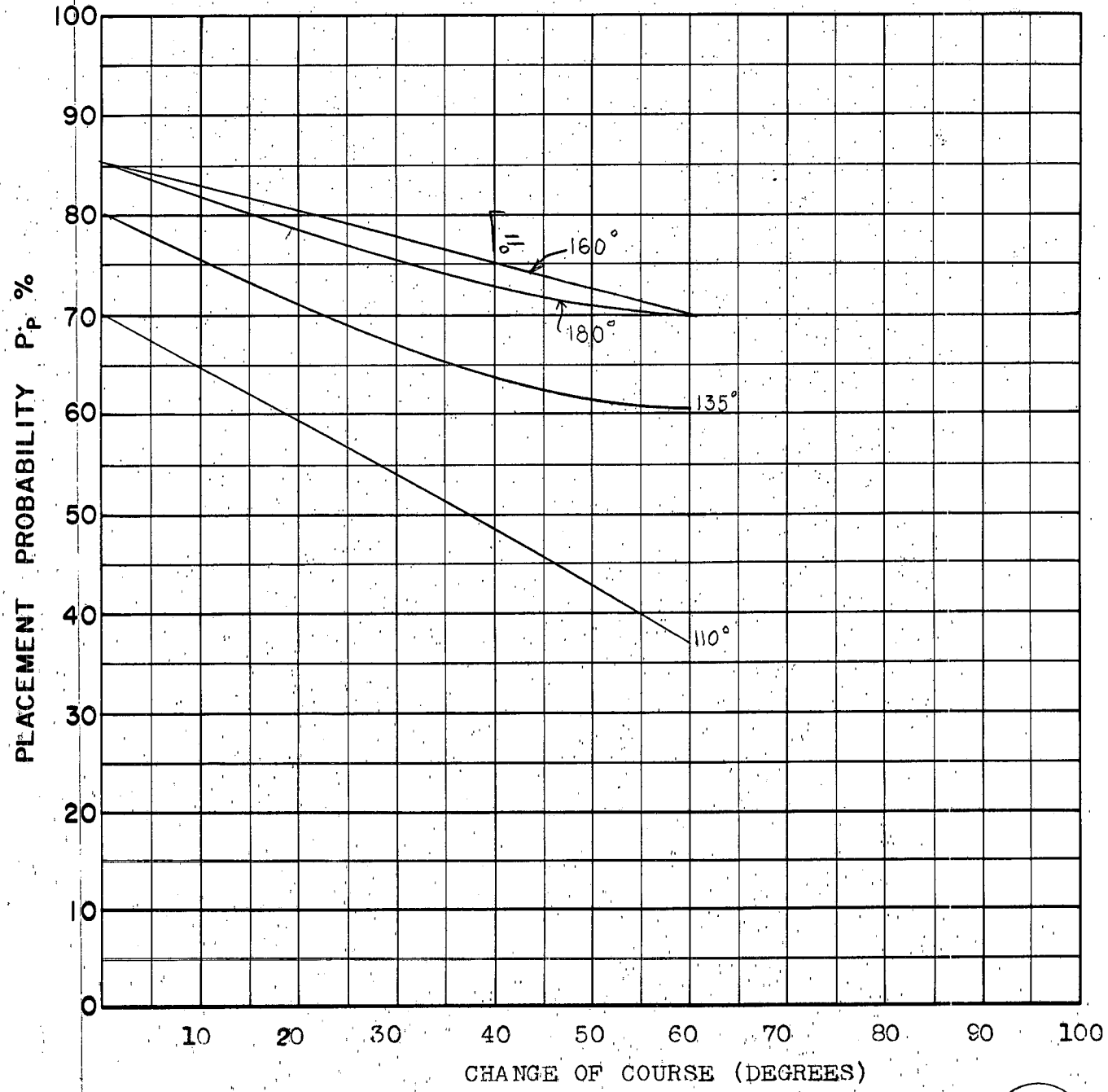

COURSE DIFFERENCE: 4 Values
TARGET EVASION: 0.75g
TARGET MACH NO.: 2.0
INTERCEPTOR LATERAL G's: 28% pess.
INTERCEPTOR MACH NO.: 1.8
σ OF G.C.I. ACCURACY: 9.0
A.I. DETECTION RANGE AS FRACTION OF SPECIFICATION RANGE, S: 0.8
A.I. DETECTION RANGE CONTOUR: Delta Wing
ALTITUDE: 50K

D-23

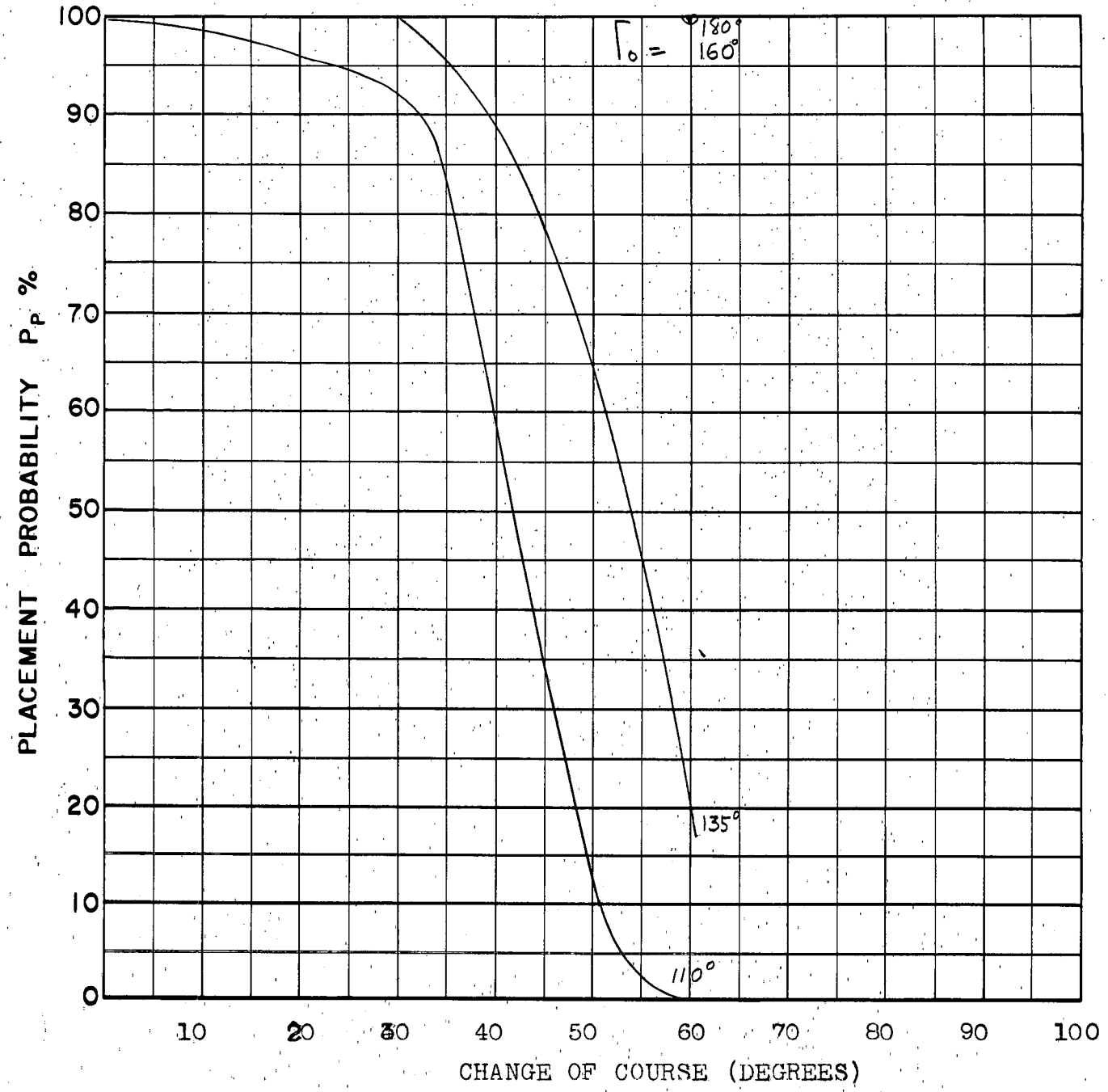

COURSE DIFFERENCE: 4 Values
TARGET EVASION: 0.75g
TARGET MACH NO.: 2.0
INTERCEPTOR LATERAL G's: 28% pess.
INTERCEPTOR MACH NO.: 1.8
σ OF G.C.I. ACCURACY: 1.5
A.I. DETECTION RANGE AS FRACTION OF SPECIFICATION RANGE, S: 1.2
A.I. DETECTION RANGE CONTOUR: Delta Wing
ALTITUDE: 50K

D-24

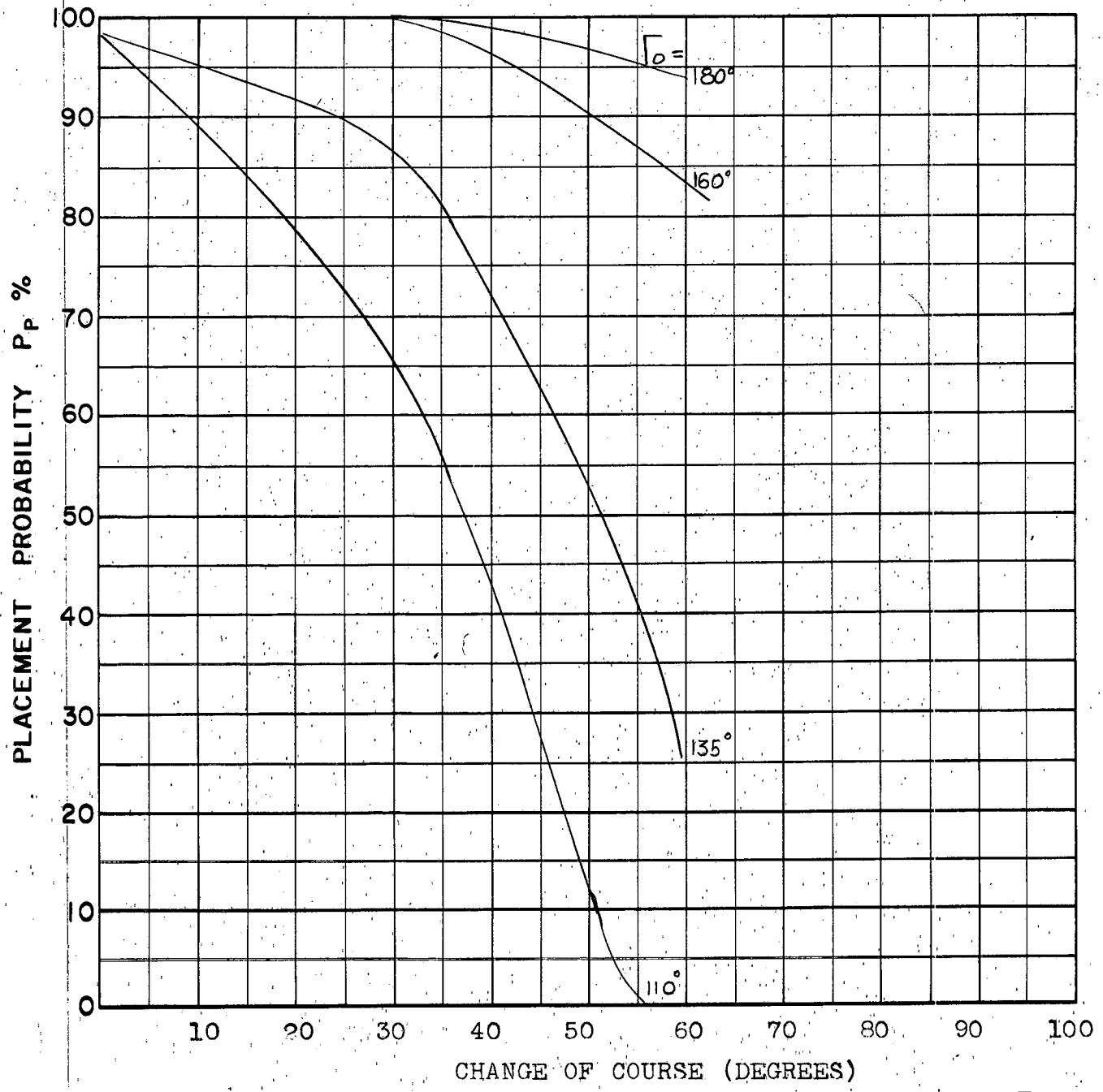

COURSE DIFFERENCE: 4 Values
TARGET EVASION: 0.75g
TARGET MACH NO.: 2.0
INTERCEPTOR LATERAL G's: 28% pess.
INTERCEPTOR MACH NO.: 1.8
σ OF G.C.I. ACCURACY: 4.75
A.I. DETECTION RANGE AS FRACTION OF SPECIFICATION RANGE, S: 1.2
A.I. DETECTION RANGE CONTOUR: Delta Wing
ALTITUDE: 50K

D.25

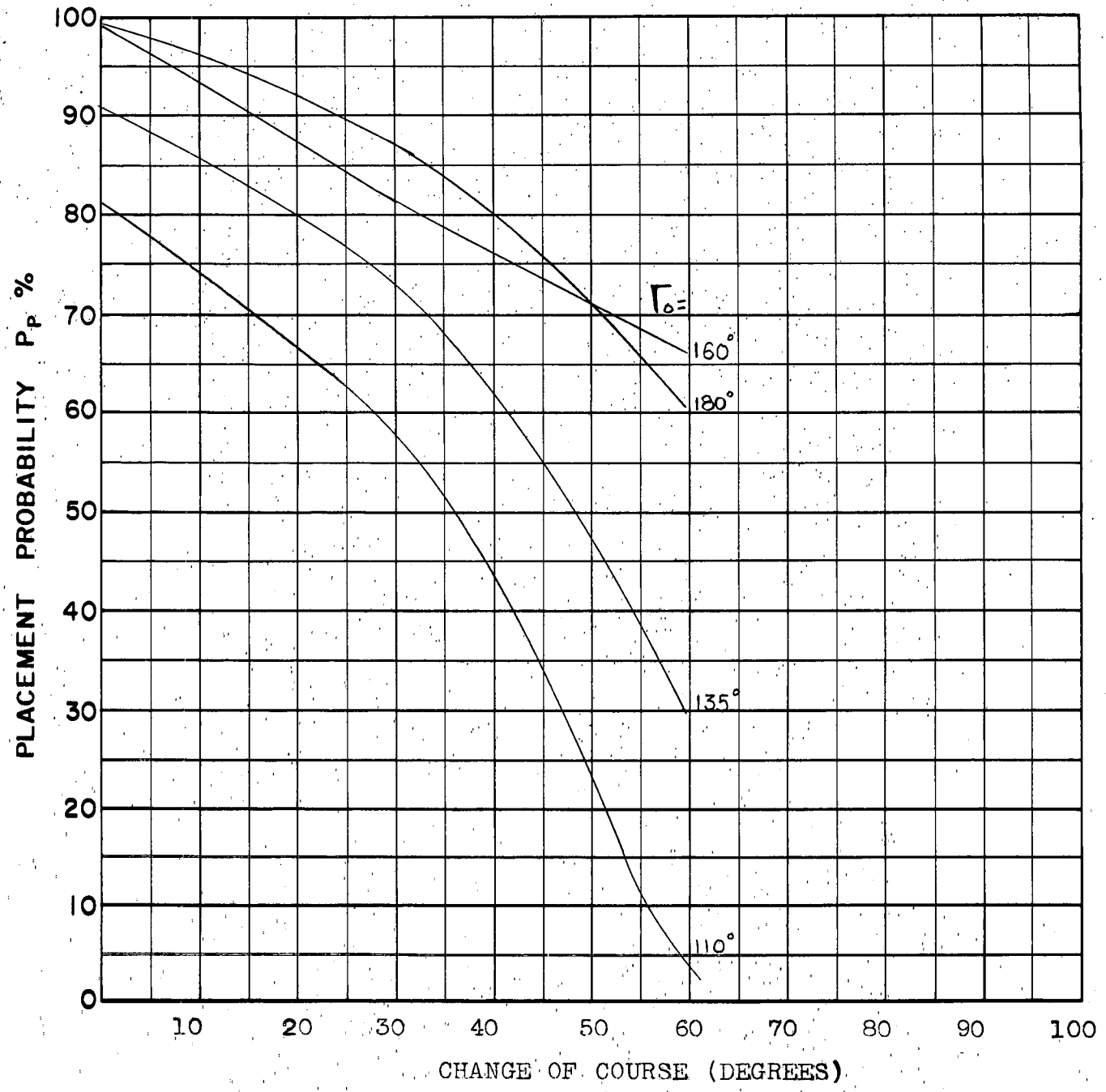

COURSE DIFFERENCE: 4 Values
TARGET EVASION: 0.75g
TARGET MACH NO.: 2.0
INTERCEPTOR LATERAL G's: 28% pess.
INTERCEPTOR MACH NO.: 1.8
σ OF G.C.I. ACCURACY: 9.0
A.I. DETECTION RANGE AS FRACTION OF SPECIFICATION RANGE, S: 1.2
A.I. DETECTION RANGE CONTOUR: Delta Wing
ALTITUDE: 50K

D26

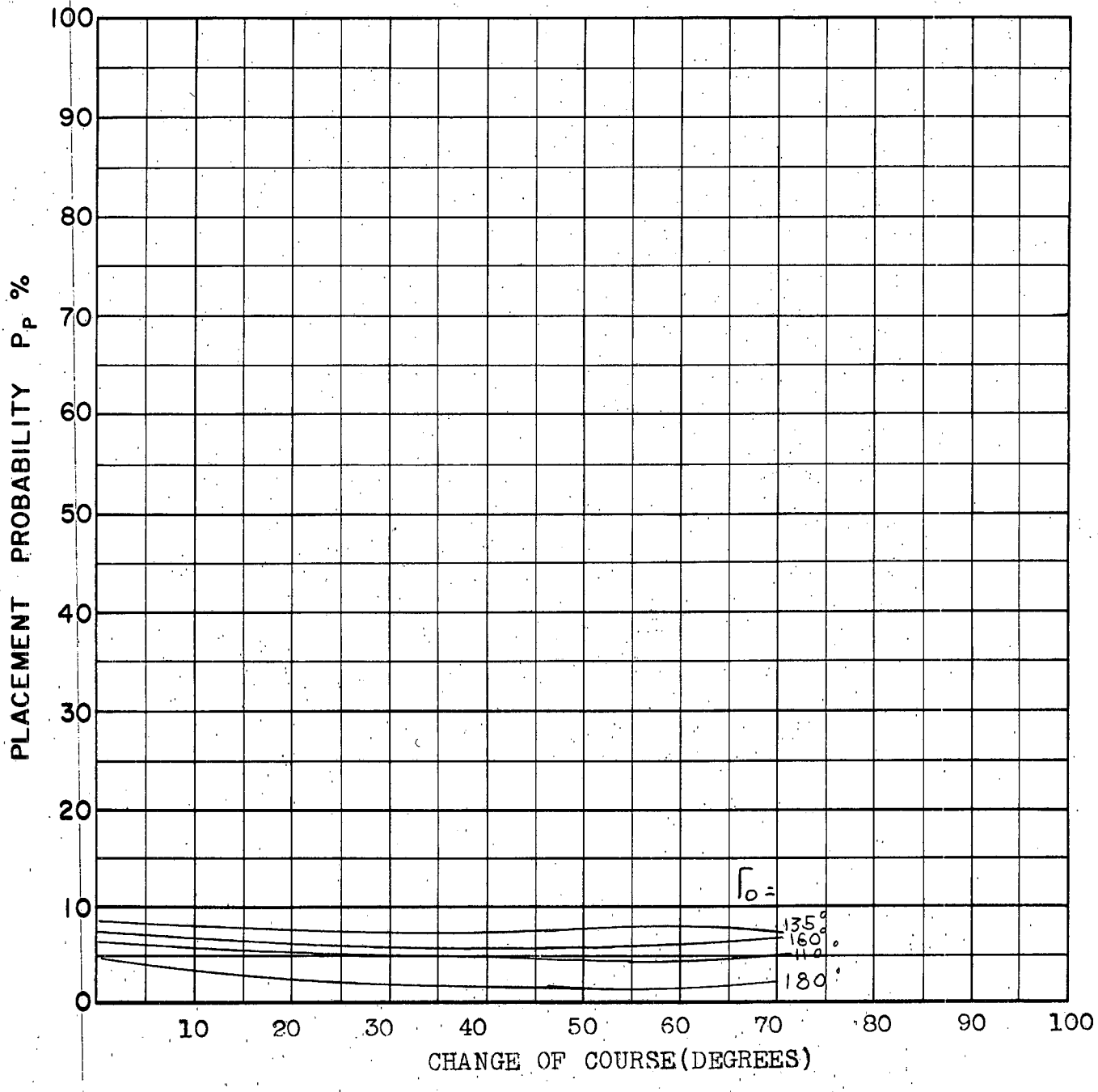

COURSE DIFFERENCE: 4 Values
TARGET EVASION: 0.75g
TARGET MACH NO.: 2.0
INTERCEPTOR LATERAL G's: 28% pess.
INTERCEPTOR MACH NO.: 1.8
σ OF G.C.I. ACCURACY: 9.0
A.I. DETECTION RANGE AS FRACTION OF SPECIFICATION RANGE, S: 0.4
A.I. DETECTION RANGE CONTOUR: Straight Wing
ALTITUDE: 50K

S-18

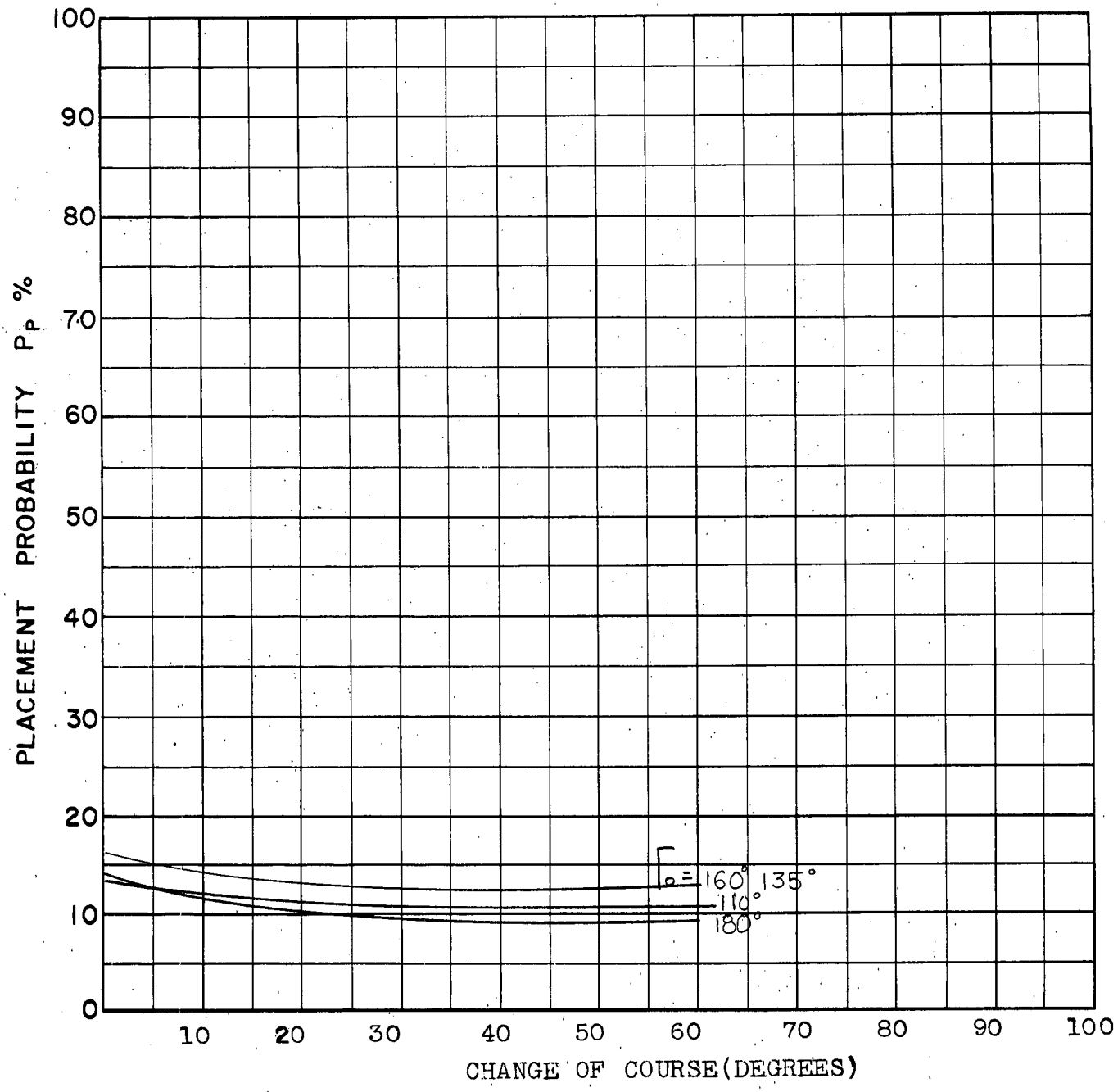

COURSE DIFFERENCE: 4 Values
TARGET EVASION: 0.75g
TARGET MACH NO.: 2.0
INTERCEPTOR LATERAL G's: 28% pess.
INTERCEPTOR MACH NO.: 1.8
σ OF G.C.I. ACCURACY: 4.75
A.I. DETECTION RANGE AS FRACTION OF SPECIFICATION RANGE, S: 0.4
A.I. DETECTION RANGE CONTOUR: Straight Wing
ALTITUDE: 50K

S 19

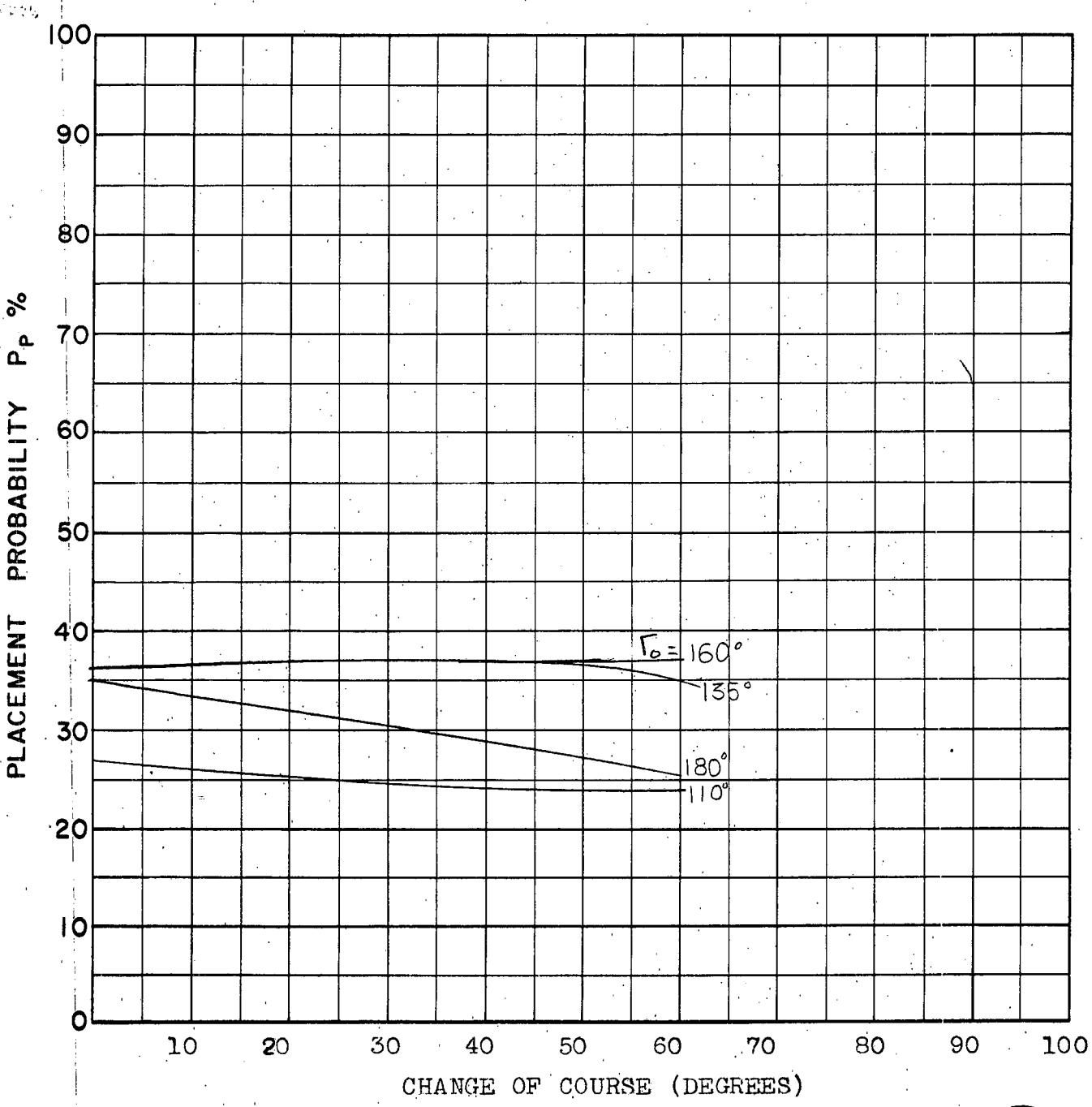

S 20

COURSE DIFFERENCE: 4 Values
TARGET EVASION: 0.75g
TARGET MACH NO.: 2.0
INTERCEPTOR LATERAL G's: 28% pess.
INTERCEPTOR MACH NO.: 1.8
σ OF G.C.I. ACCURACY: 1.5
A.I. DETECTION RANGE AS FRACTION OF SPECIFICATION RANGE, S: 0.4
A.I. DETECTION RANGE CONTOUR: Straight Wing
ALTITUDE: 50K

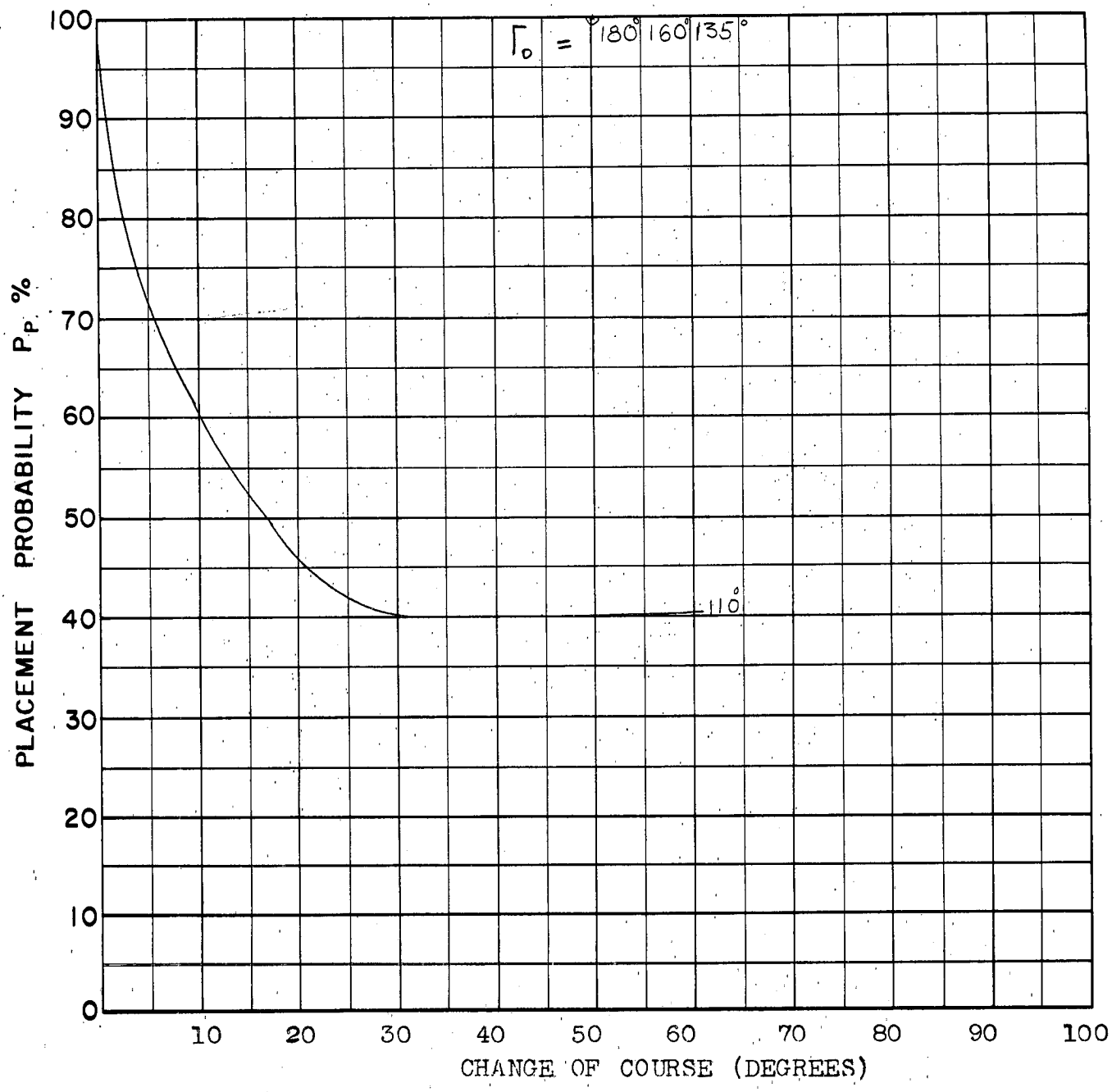

COURSE DIFFERENCE: 4 Values
TARGET EVASION: 0.75g
TARGET MACH NO.: 2.0
INTERCEPTOR LATERAL G's: 28% pess.
INTERCEPTOR MACH NO.: 1.8
σ OF G.C.I. ACCURACY: 1.5
A.I. DETECTION RANGE AS FRACTION OF SPECIFICATION RANGE, S: 0.8
A.I. DETECTION RANGE CONTOUR: Straight Wing
ALTITUDE: 50K

S-21

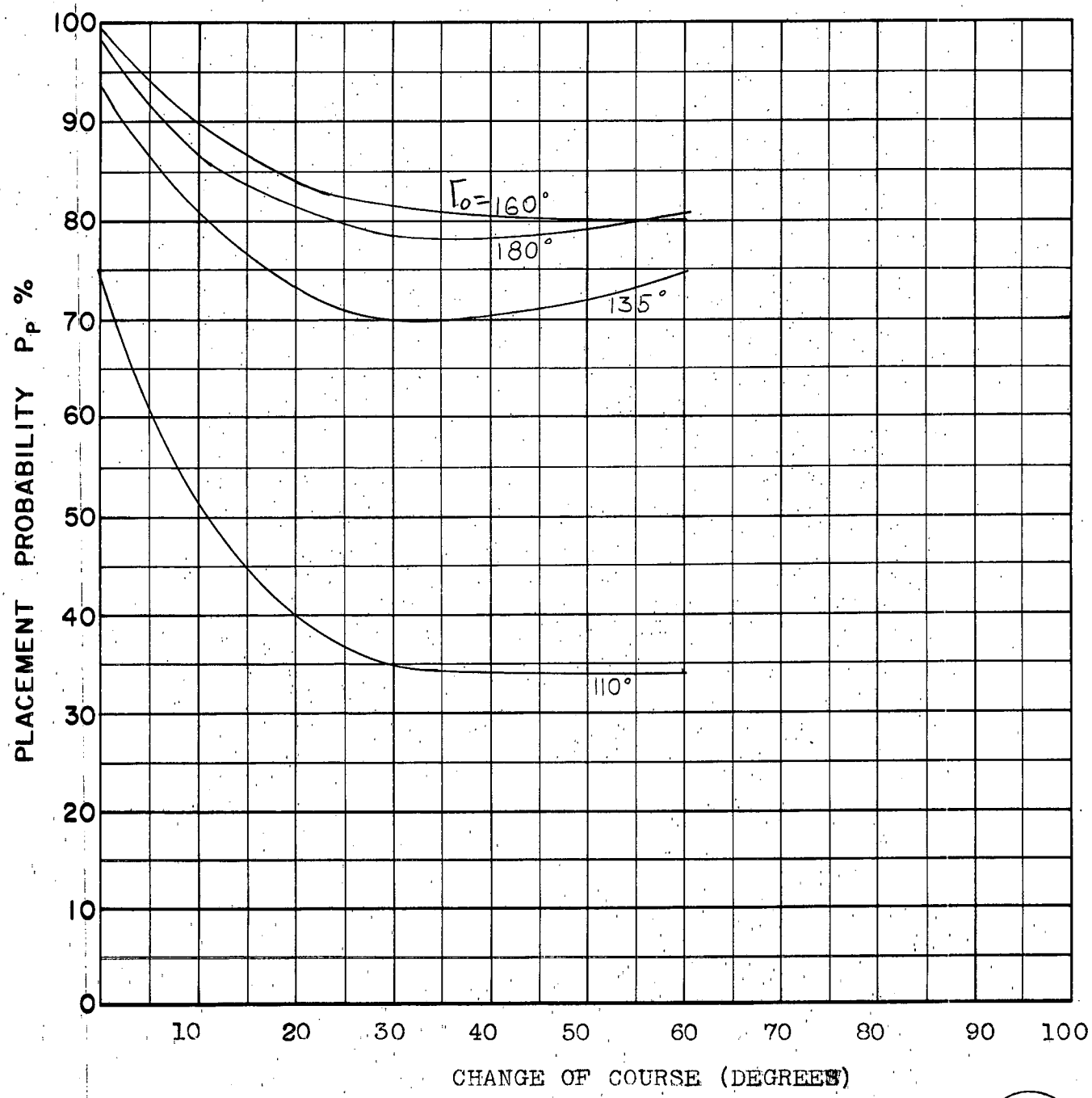

COURSE DIFFERENCE: 4 Values
TARGET EVASION: 0.75g
TARGET MACH NO.: 2.0
INTERCEPTOR LATERAL G's: 28% pess.
INTERCEPTOR MACH NO.: 1.8
σ OF G.C.I. ACCURACY: 4.75
A.I. DETECTION RANGE AS FRACTION OF SPECIFICATION RANGE, S: 0.8
A.I. DETECTION RANGE CONTOUR: Straight Wing
ALTITUDE: 50K

S22

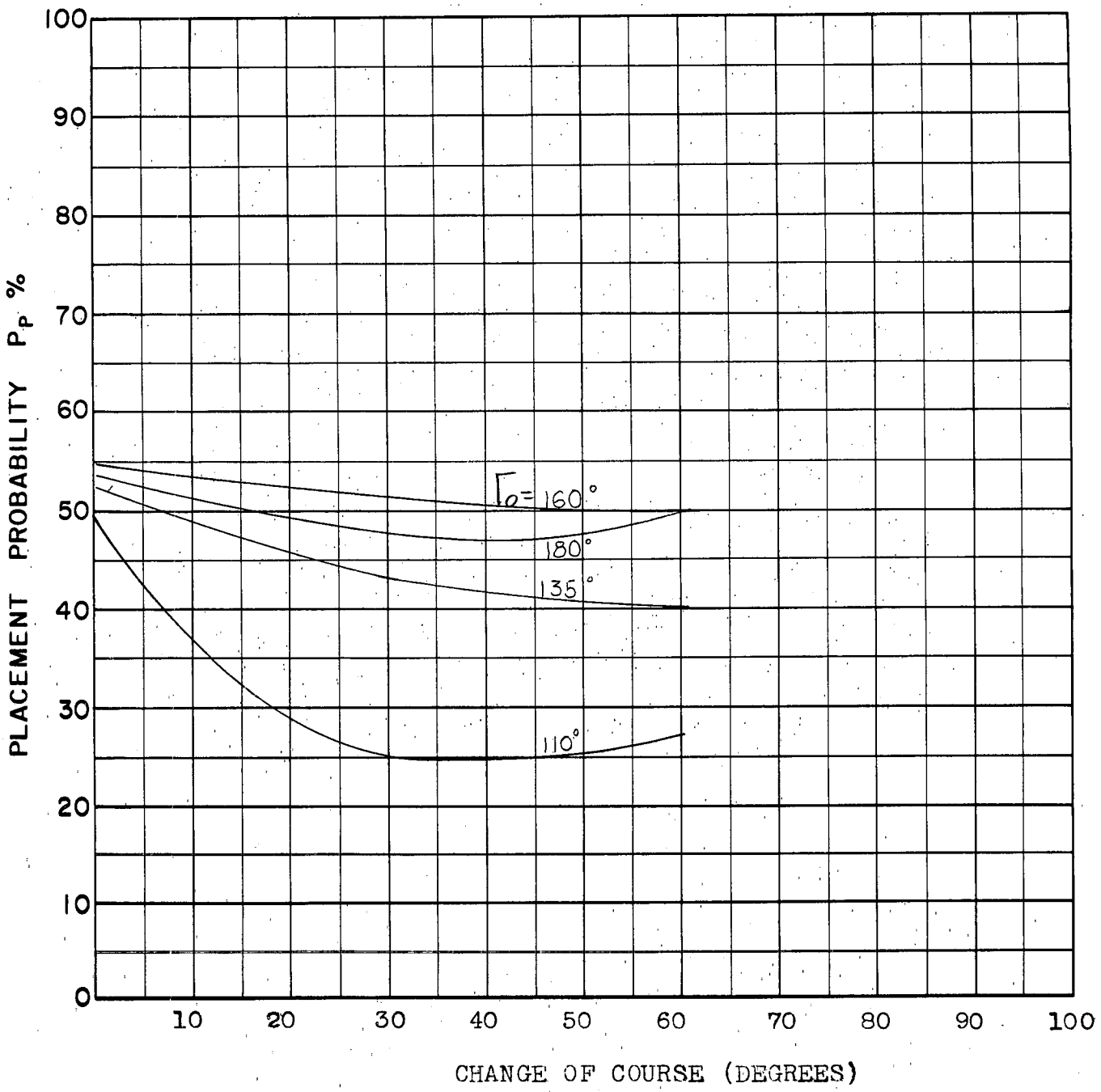

COURSE DIFFERENCE: 4 Values
TARGET EVASION: 0.75g
TARGET MACH NO.: 2.0
INTERCEPTOR LATERAL G's: 28% pess.
INTERCEPTOR MACH NO.: 1.8
σ OF G.C.I. ACCURACY: 9.0
A.I. DETECTION RANGE AS FRACTION OF SPECIFICATION RANGE, S: 0.8
A.I. DETECTION RANGE CONTOUR: Straight Wing
ALTITUDE: 50K

S 23

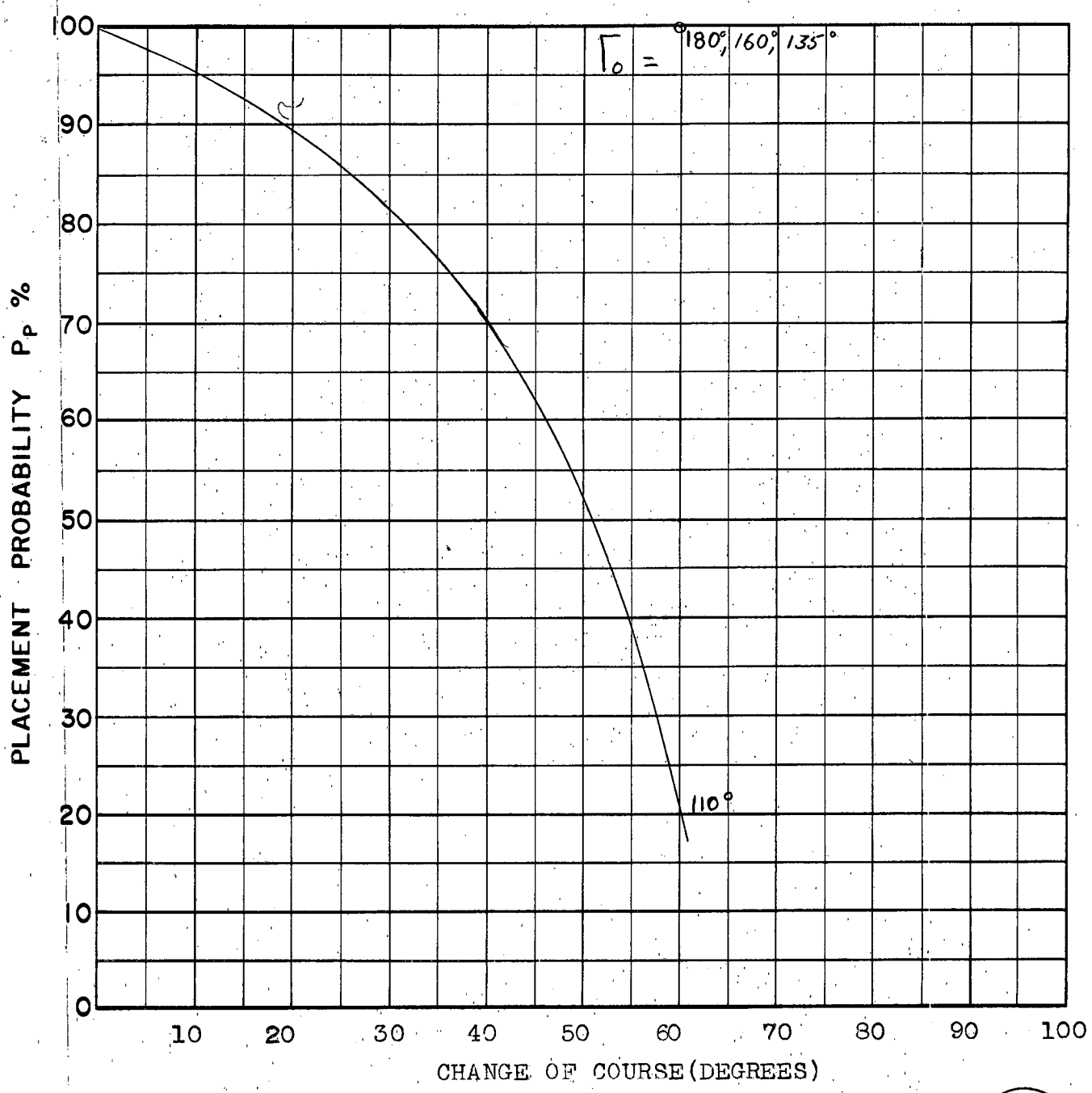

S-24

COURSE DIFFERENCE: 4 Values
TARGET EVASION: 0.75g
TARGET MACH NO.: 2.0
INTERCEPTOR LATERAL G's: 28% pess.
INTERCEPTOR MACH NO.: 1.8
σ OF G.C.I. ACCURACY: 1.5
A.I. DETECTION RANGE AS FRACTION OF SPECIFICATION RANGE, S: 1.2
A.I. DETECTION RANGE CONTOUR: Straight Wing
ALTITUDE: 50K

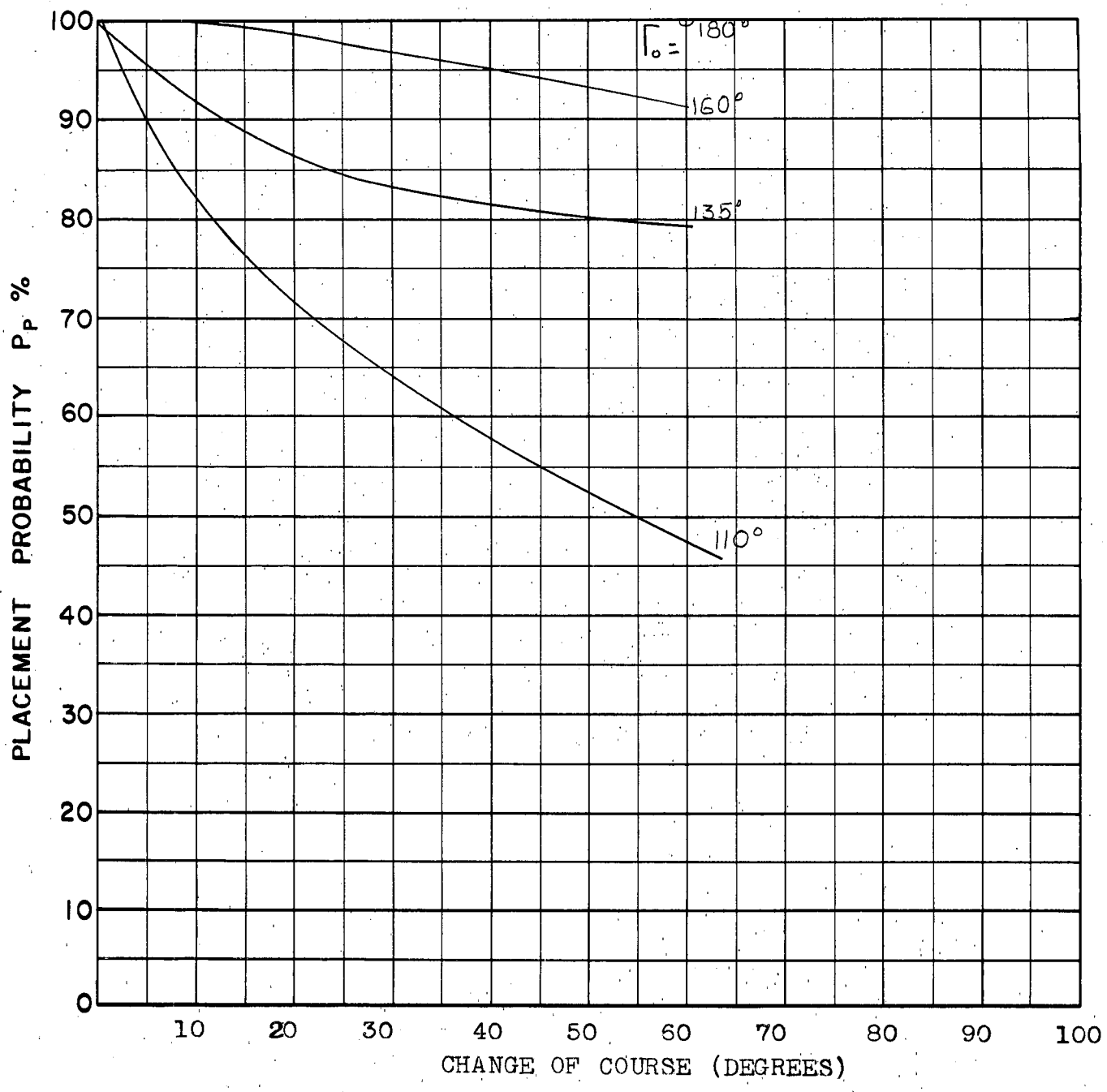

COURSE DIFFERENCE: 4 Values
TARGET EVASION: 0.75g
TARGET MACH NO.: 2.0
INTERCEPTOR LATERAL G's: 28% pess.
INTERCEPTOR MACH NO.: 1.8
σ OF G.C.I. ACCURACY: 4.75
A.I. DETECTION RANGE AS FRACTION OF SPECIFICATION RANGE, S: 1.2
A.I. DETECTION RANGE CONTOUR: Straight Wing
ALTITUDE: 50K

S25

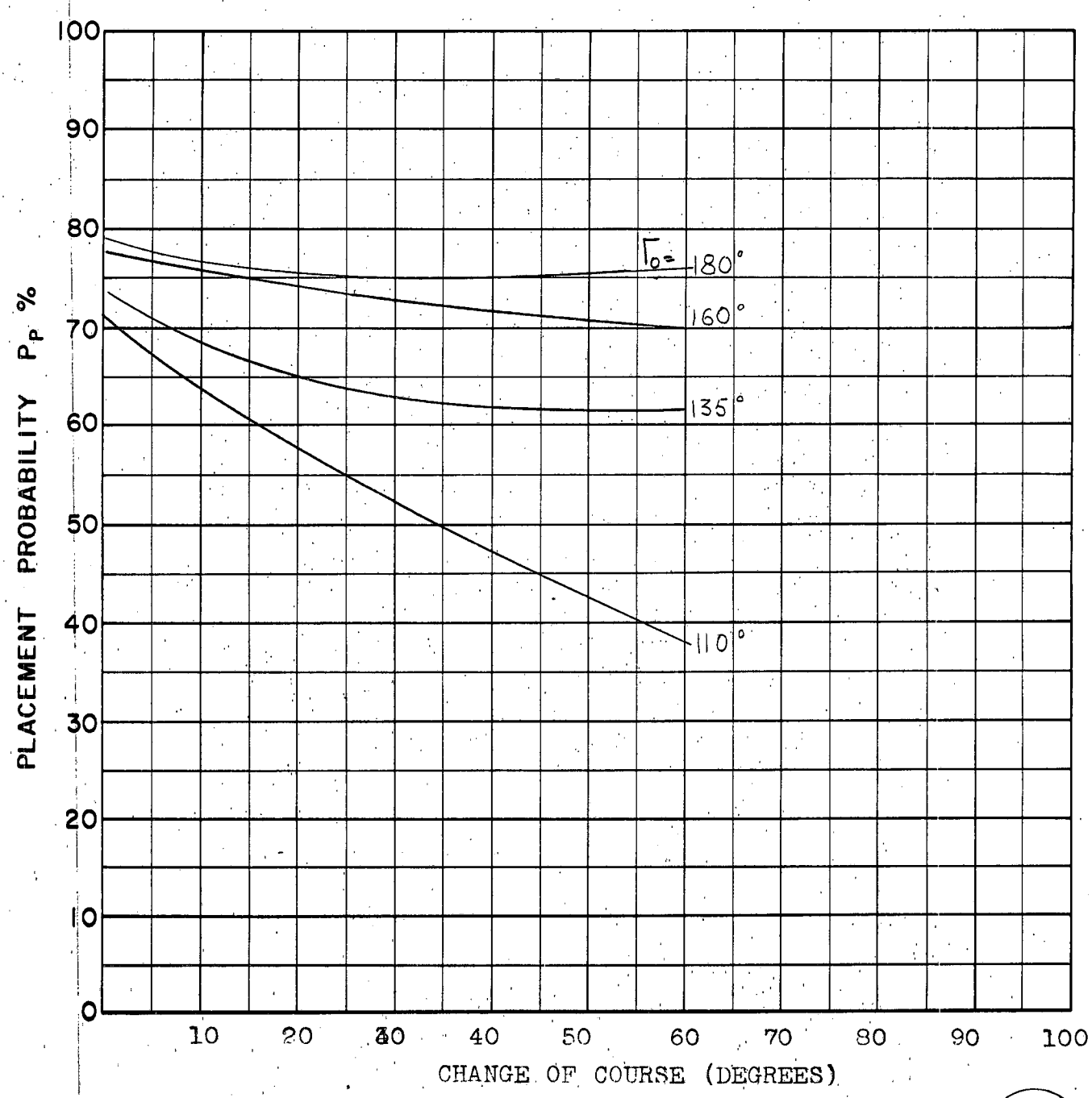

S 26

COURSE DIFFERENCE: 4 Values
TARGET EVASION: 0.75g
TARGET MACH NO.: 2.0
INTERCEPTOR LATERAL G's: 28% pess.
INTERCEPTOR MACH NO.: 1.8
σ OF G.C.I. ACCURACY: 9.0
A.I. DETECTION RANGE AS FRACTION OF SPECIFICATION RANGE, S: 1.2
A.I. DETECTION RANGE CONTOUR: Straight Wing
ALTITUDE: 50K

APPENDIX 'F'

Interceptor Placement in 2-Dimensions

Using Revised Aerodynamic Performance Estimates

by C.J. Wilson

1. Introduction

Appendix 'E' of this report describes a two-dimensional placement study which was carried out by the Analysis Group of "G" Wing using the CARDE REAC facility. A similar problem, defined in detail at CARDE, was done under contract by Computing Devices of Canada.

In the CARDE study the aircraft aerodynamics were those of N.A.E. estimates which were the only available at the time the problem was set up. Recent AVRO reports give revised estimates based on high-speed wind tunnel tests (Refs. 1, 2, 3). The CF-105 is now expected to make a 1.63 load factor power limited turn at Mach 1.5 at 50,000 ft. Recent changes to engine design increase the available thrust at higher Mach numbers, and have resulted in an estimated ceiling of 64,000 ft. at Mach 2.

2. Method and Assumptions

The target considered was a Mach 2 bomber with a $\frac{1}{2}$ g lateral evasion capability (load factor 1.12).

Reference is made to the equations given in sections 5 and 6 of Appendix 'E'. A REAC circuit was set up by Computing Devices of Canada to solve these equations. Some slight variations in conditions and conventions are described below.

2.1 Lift Limit

Maximum available lift L_{max} was not subject to a hinge-moment limit. There is no limit of the form:

$$L_{max} \leqslant L_{maxHM_1} + \frac{L_{maxHM_2}}{Po} \cdot Po$$

Instead, the lift limit is given by

$$L_{max} \leqslant \frac{L_{max}}{Po} \cdot Po$$

where $\frac{L_{max}}{Po}$ is a function of Mach number only, and

$L_{max} \leqslant NW$ where N is an arbitrary load factor limit, to which various values were assigned throughout the problem.

2.2 Launch Zones

The missiles were assumed to fly a distance F relative to the interceptor, with a relative average velocity ΔV and time of flight t_f. Permissible heading error was assumed independent of target aspect at launch, and was taken as 15° at 50,000 ft. altitude, and 8° at 60,000 ft. The depth of the launch zone was not considered. Two different sets of parameters were used:

(i) F = 15,000 ft.
ΔV = 1165 ft/sec.
t_f = 12.88 secs.

Lead-collision navigation was used until time-to-go T was equal to t_f, and actual heading error was measured at that time for comparison with the acceptable value. This launch zone was used for four charts only (Figures 9 to 12).

(ii) F = 25,000 ft.
ΔV = 1165 ft/sec.
t_f = 21.46 sec.
Missile seeker range 50,000 ft.

Lead-collision navigation was used again until time-to-go was equal to t_f, and heading error measured at that time if the range from target was less than 50,000 feet. If not, the attack was continued using lead-pursuit navigation until range was reduced to 50,000 ft., when heading error was measured.

2.3 Target Evasion

When the initial range of AI acquisition was greater than 150,000 ft., the target was assumed to start its evasive manoeuvre only when range became 150,000 feet. When initial range was less than this value, the target manoeuvre was assumed to start at the instant of AI acquisition. Thus results from this study are only comparable with those of Appendix 'E' for ranges less than 25 nautical miles.

2.4 The values of the coefficients in the REAC equations for the AVRO 2.2 or "Elastic" performance estimates are tabulated here.

AVRO 'Elastic' Performance Estimates

Mach No.	$\frac{L_{max}}{Po}$ ($ft.^2$)	$\frac{T_h}{Po}$ ($ft.^2$)	$\frac{D_o}{Po}$ ($ft.^2$)	$-K_1$	$\times 10^4$ ($ft.^{-2}$)
0.8	361	37.0	4.95	-0.0044	5.24
0.9	437	41.2	6.27	0.0050	4.53
1.0	536	46.4	14.00	0.0181	4.21
1.07	610				
1.1	609	51.9	23.4	0.0232	3.97
1.15	607	54.9			
1.2	610	57.4	33.6	0.1073	5.85
1.3	629	63.2	39.1	0.1086	5.58
1.4	643	69.1	45.2	0.1157	5.44
1.5	661	75.0	50.2	0.1098	5.17
1.6	689	82.1	56.1	0.1074	4.93
1.7	726	91.1	62.3	0.1038	4.66
1.8	767	98.6	68.7	0.0957	4.31
1.9	806	105.9	75.7	0.0898	3.99
2.0	847	112.7	83.9	0.0845	3.64

3. Results

The placement charts which were prepared by the contractor have been reduced to placement probability results at CARDE, and curves of P_p vs. σ range of acquisition are given here.

The results have not yet been fully analysed, however it is immediately obvious that the assumption that target manoeuvre begins only at 150,000 feet range at a $\frac{1}{2}$ g lateral rate restricts the effectiveness of the evasion. The target has insufficient time to turn away to a large extent unless evasion begins sooner.

Comparison with the results of Appendix 'E' is only valid in the region where target evasion assumptions are similar.

4. References

1. AVRO report "The Effect of NACA Wind Tunnel and Free Flight Tests on the Performance of the CF 1-5", Oct 1956. SECRET.

2. AVRO report "CF 105 Periodic Performance Report No.9", Nov/Dec 1956, SECRET.

3. AVRO report "CF 105 Periodic Performance Report No. 10", Dec 1956, SECRET.

4. CARDE Technical Letter N-47-12 "Second Quarterly Report on CF 105 Weapon System Assessment", Nov 1956, SECRET.

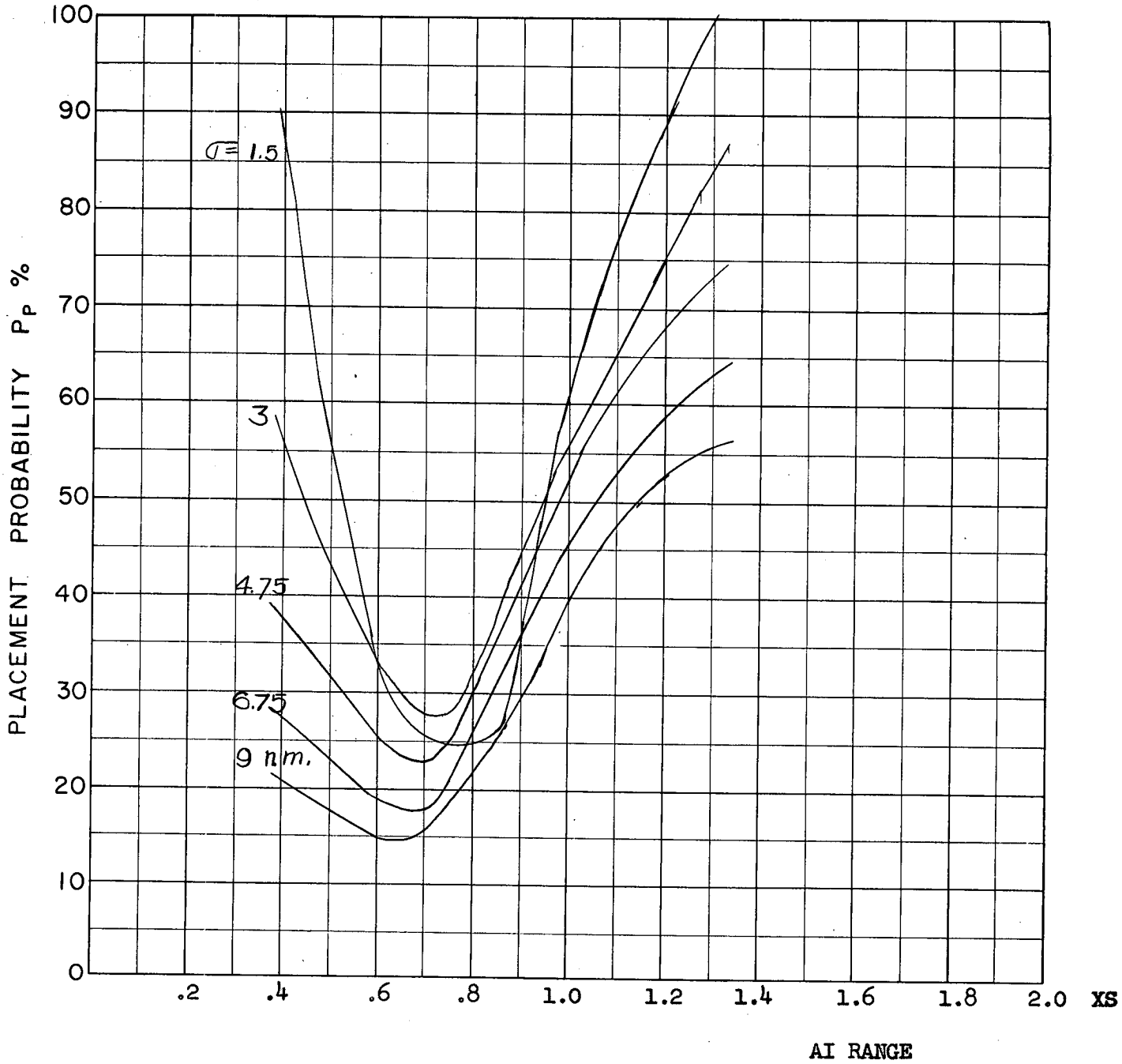

COURSE DIFFERENCE: 90°
TARGET EVASION: 0.5
TARGET MACH NO.: 2.0
INTERCEPTOR LATERAL G's: 1.414 Load Factor Limit
INTERCEPTOR MACH NO.: 1.5 Initial
σ OF G.C.I. ACCURACY: 5 Values
A.I. DETECTION RANGE AS FRACTION OF SPECIFICATION RANGE, S: ABSCISSA
A.I. DETECTION RANGE CONTOUR: Delta
ALTITUDE: 50 K
AVRO 2.2 Aerodynamics

D-1
F

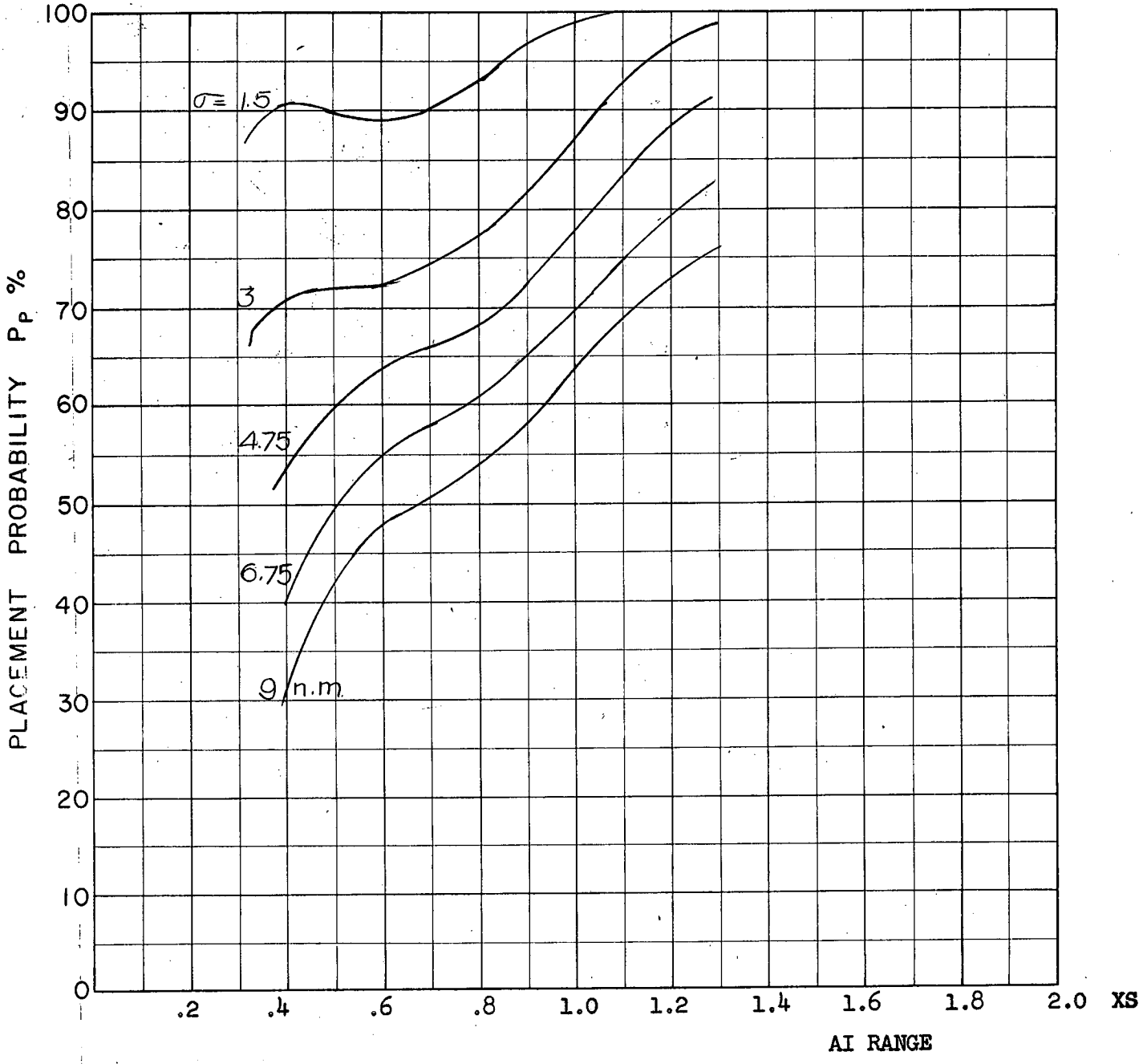

COURSE DIFFERENCE: 110°
TARGET EVASION: 0.5
TARGET MACH NO.: 2.0
INTERCEPTOR LATERAL G's: 4 Load Factor Limit
INTERCEPTOR MACH NO.: 1.5 Initial
σ OF G.C.I. ACCURACY: 5 Values
A.I. DETECTION RANGE AS FRACTION OF SPECIFICATION RANGE, S: ABSCISSA
A.I. DETECTION RANGE CONTOUR: Delta
ALTITUDE: 50 K
AVRO 2.2 Aerodynamics

D 2a
F

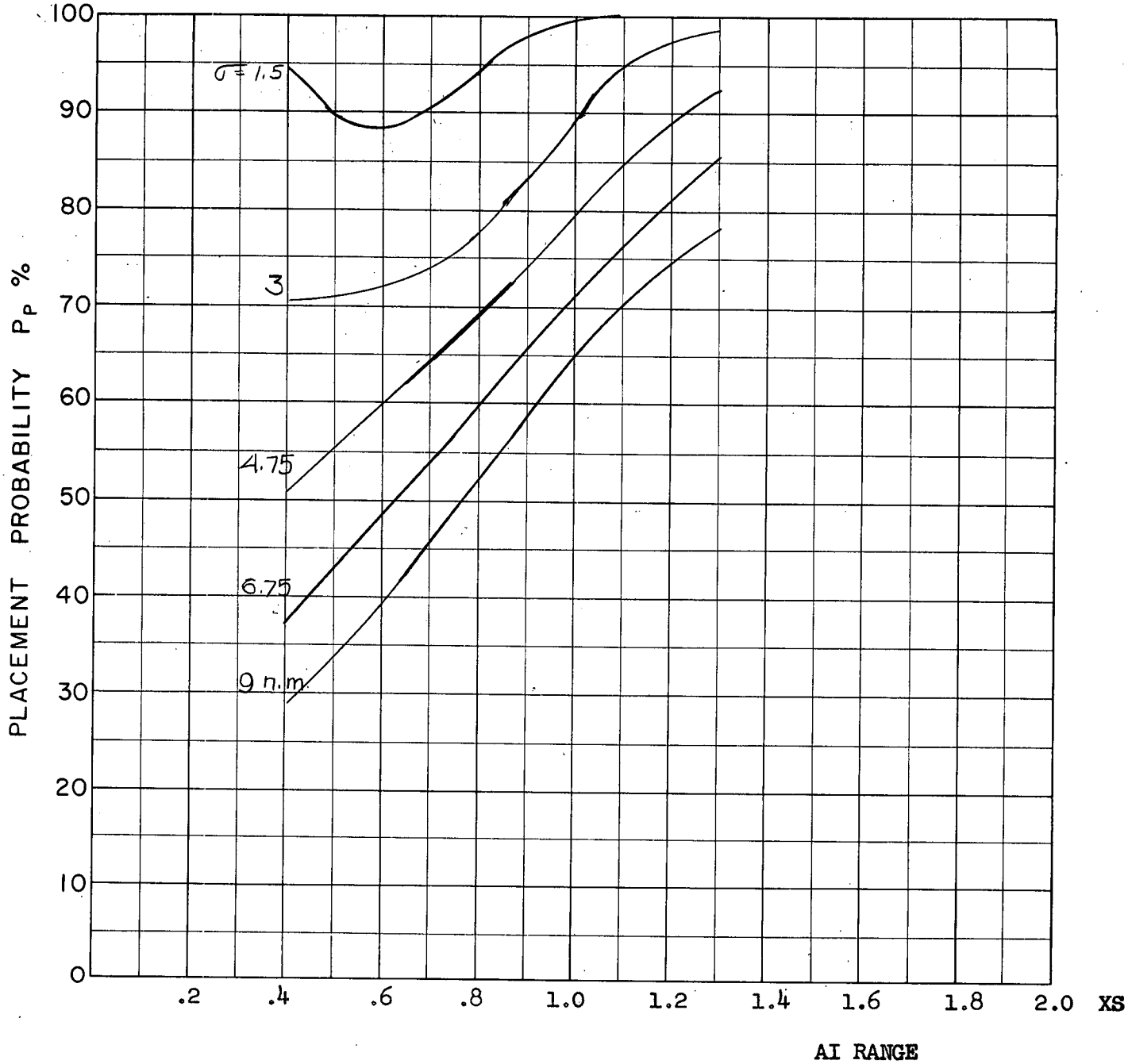

COURSE DIFFERENCE: 110°
TARGET EVASION: 0.5
TARGET MACH NO.: 2.0
INTERCEPTOR LATERAL G's: 2 1/4 Load Factor Limit
INTERCEPTOR MACH NO.: 1.5 Initial
σ OF G.C.I. ACCURACY: 5 Values
A.I. DETECTION RANGE AS FRACTION OF SPECIFICATION RANGE, S: ABSCISSA
A.I. DETECTION RANGE CONTOUR: Delta
ALTITUDE: 50 K
AVRO 2.2 Aerodynamics

D-2b
F

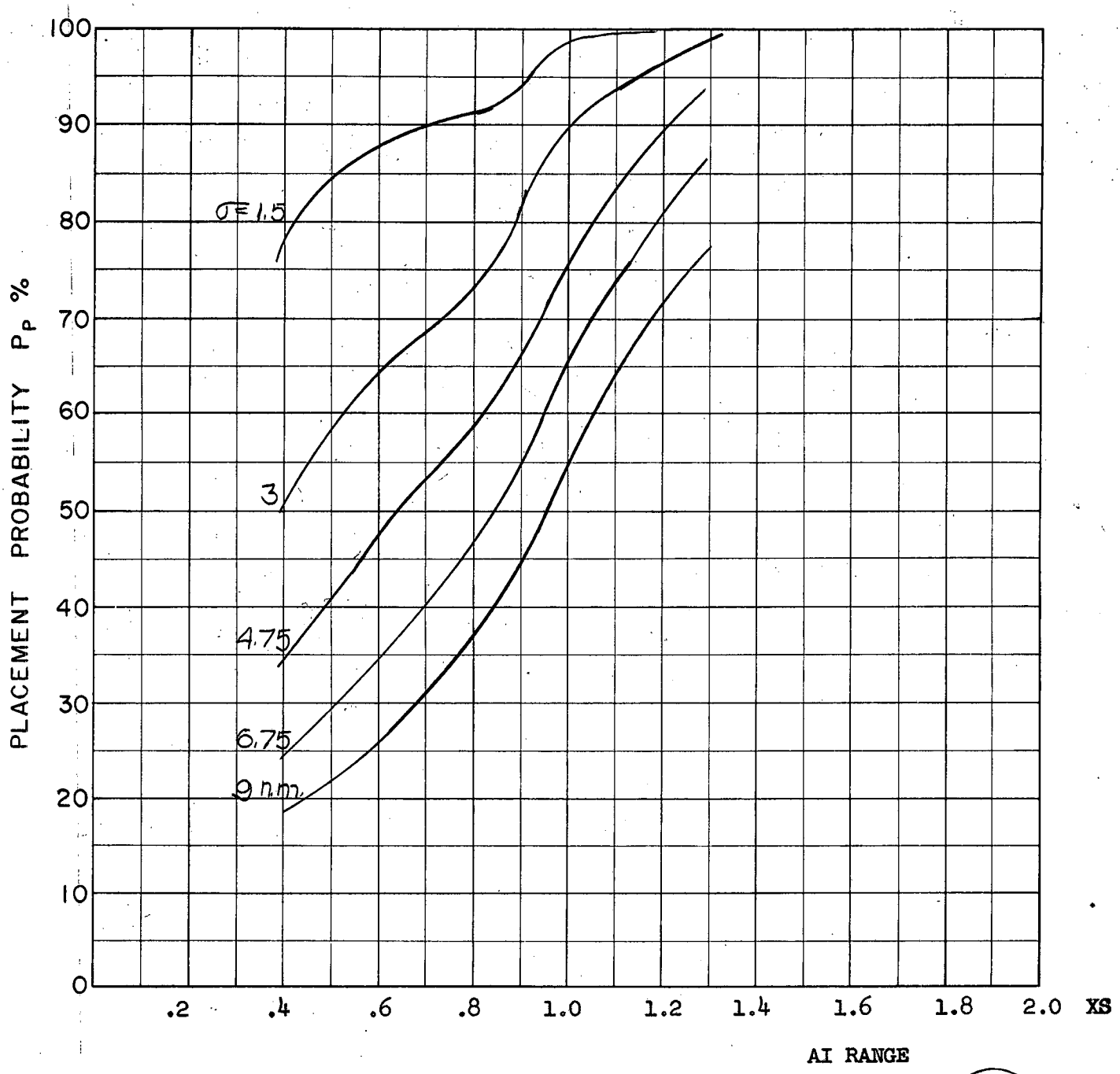

COURSE DIFFERENCE: 110°
TARGET EVASION: 0.5
TARGET MACH NO.: 2.0
INTERCEPTOR LATERAL G's: 1.414 Load Factor Limit
INTERCEPTOR MACH NO.: 1.5 Initial
σ OF G.C.I. ACCURACY: 5 Values
A.I. DETECTION RANGE AS FRACTION OF SPECIFICATION RANGE, S: ABSCISSA
A.I. DETECTION RANGE CONTOUR: Delta
ALTITUDE: 50 K
AVRO 2.2 Aerodynamics

D 2c
F

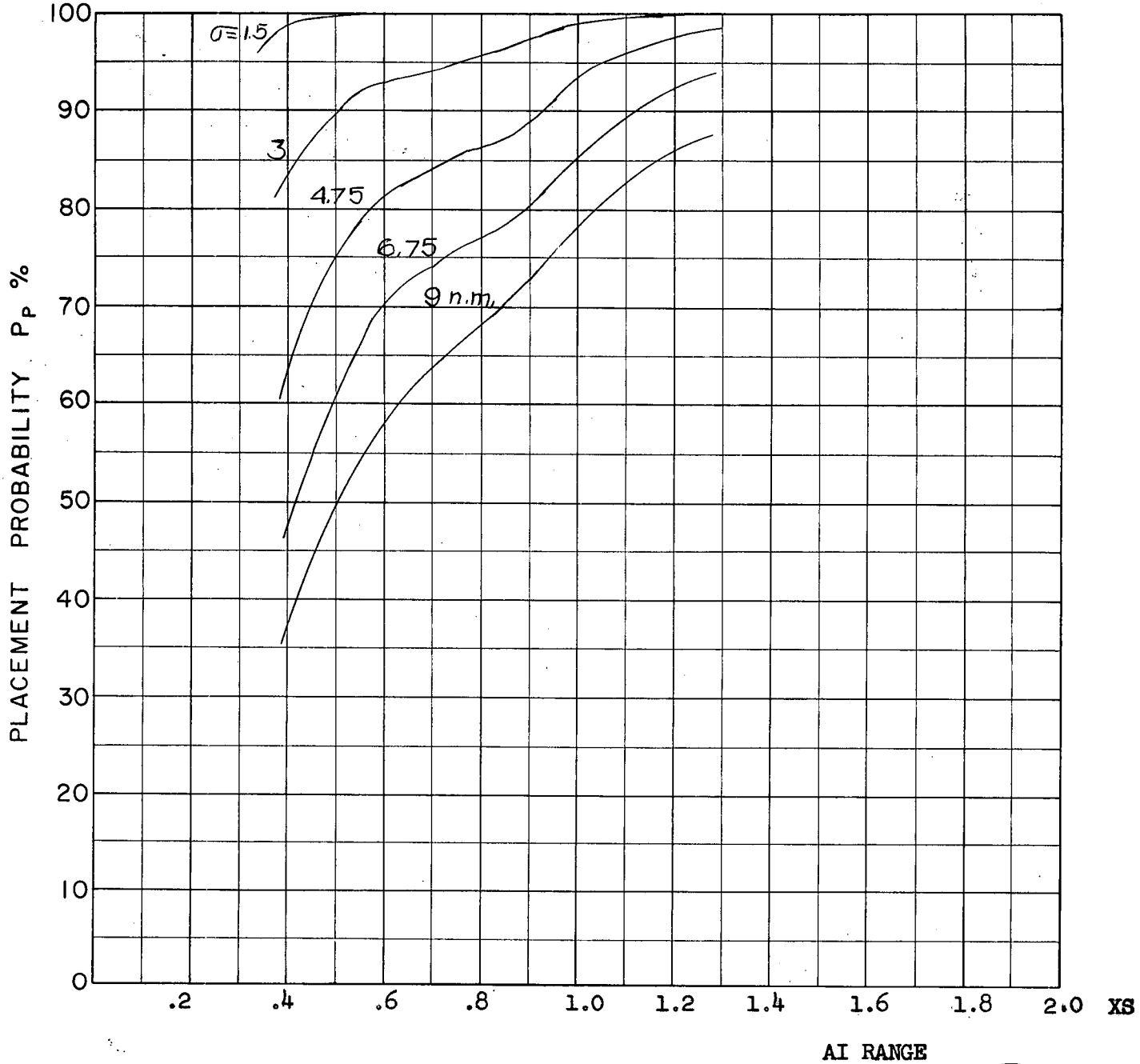

COURSE DIFFERENCE: 135°
TARGET EVASION: 0.5
TARGET MACH NO.: 2.0
INTERCEPTOR LATERAL G's: 4 Load Factor Limit
INTERCEPTOR MACH NO.: 1.5 Initial
σ OF G.C.I. ACCURACY: 5 Values
A.I. DETECTION RANGE AS FRACTION OF SPECIFICATION RANGE, S: ABSCISSA
A.I. DETECTION RANGE CONTOUR: Delta
ALTITUDE: 50 K
AVRO 2.2 Aerodynamics

D 3a
F

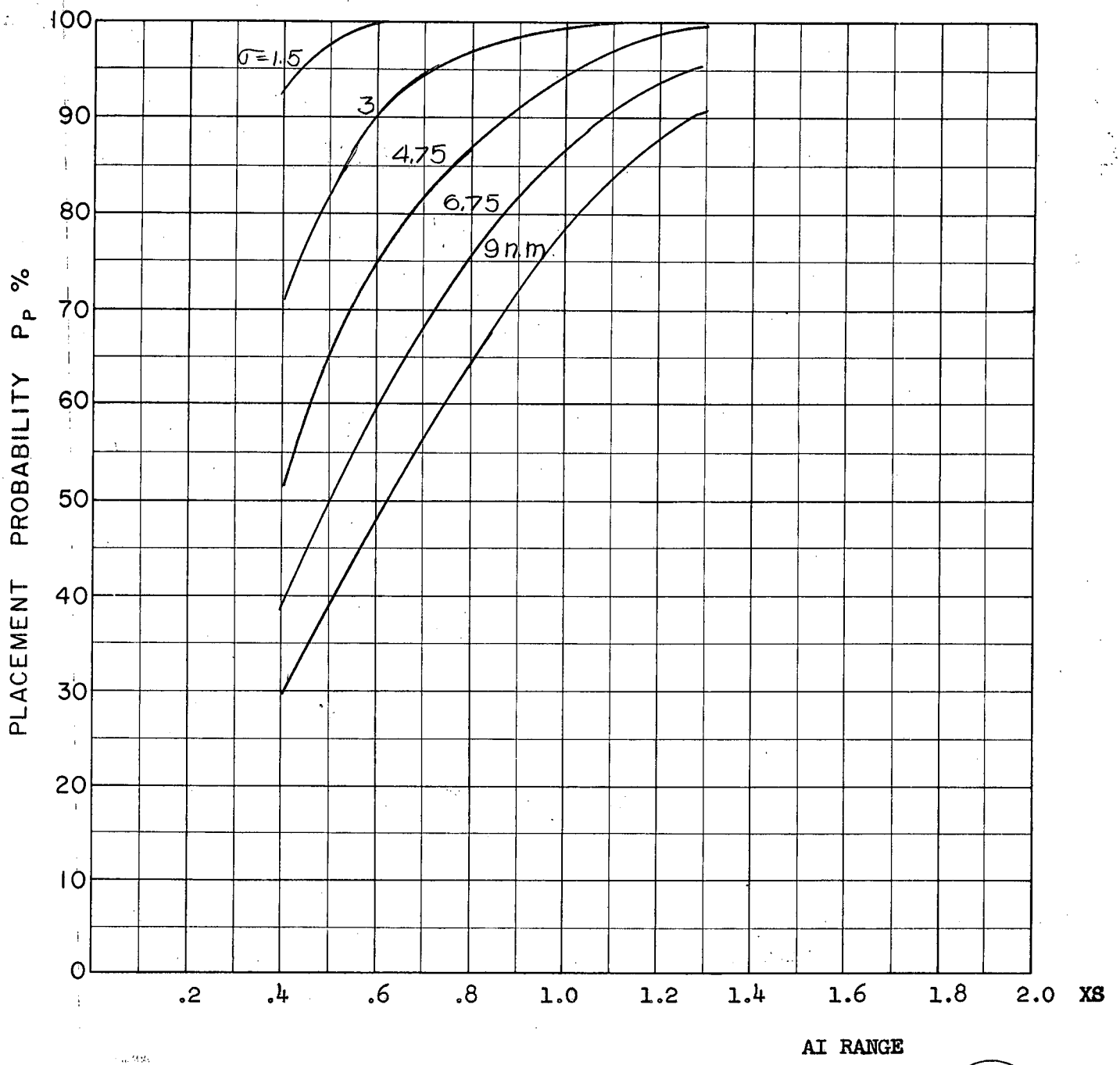

COURSE DIFFERENCE: 135°
TARGET EVASION: 0.5
TARGET MACH NO.: 2.0
INTERCEPTOR LATERAL G's: 2 1/4 Load Factor Limit
INTERCEPTOR MACH NO.: 1.5 Initial
σ OF G.C.I. ACCURACY: 5 Values
A.I. DETECTION RANGE AS FRACTION OF SPECIFICATION RANGE, S: ABSCISSA
A.I. DETECTION RANGE CONTOUR: Delta
ALTITUDE: 50 K

D.3b
F

AVRO 2.2 Aerodynamics

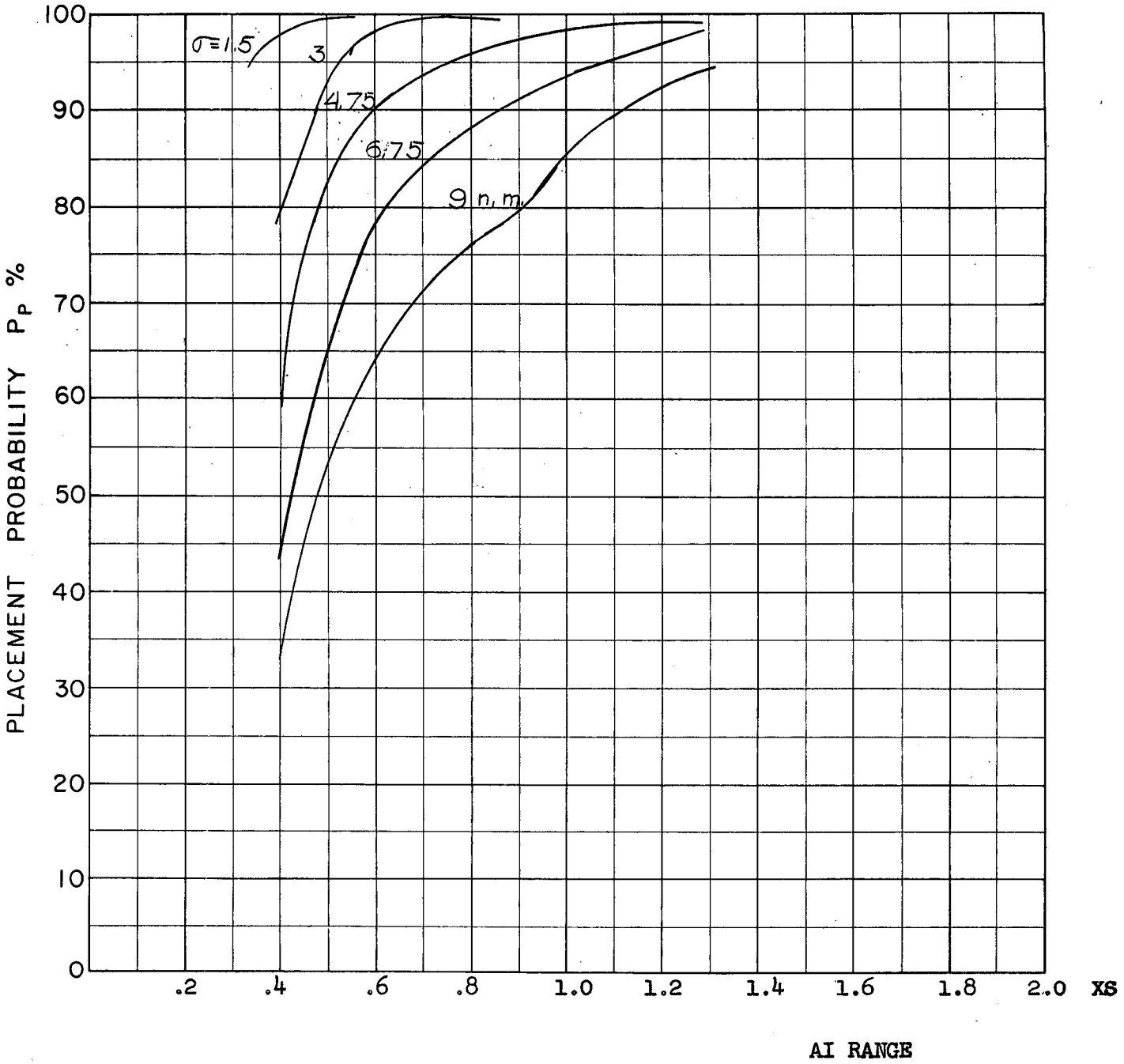

COURSE DIFFERENCE: 160°
TARGET EVASION: 0.5
TARGET MACH NO.: 2.0
INTERCEPTOR LATERAL G's: 4 Load Factor Limit
INTERCEPTOR MACH NO.: 1.5 Initial
σ OF G.C.I. ACCURACY: 5 Values
A.I. DETECTION RANGE AS FRACTION OF SPECIFICATION RANGE, S: ABSCISSA
A.I. DETECTION RANGE CONTOUR: Delta
ALTITUDE: 50 K
AVRO 2.2 Aerodynamics

D. 4a
F

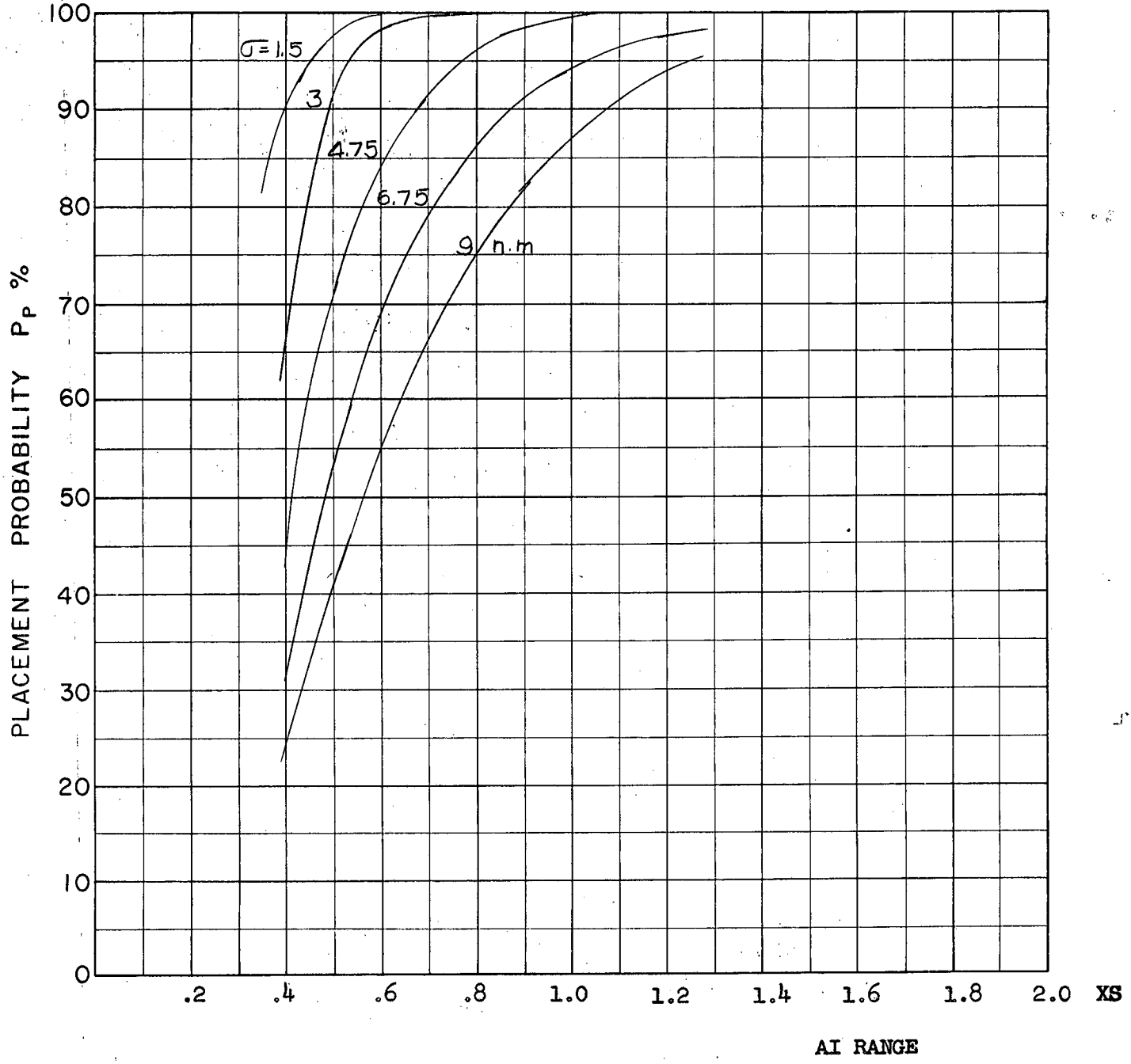

COURSE DIFFERENCE: 160°
TARGET EVASION: 0.5
TARGET MACH NO.: 2.0
INTERCEPTOR LATERAL G's: 2 1/4 Load Factor Limit
INTERCEPTOR MACH NO.: 1.5 Initial
σ OF G.C.I. ACCURACY: 5 Values
A.I. DETECTION RANGE AS FRACTION OF SPECIFICATION RANGE, S: ABSCISSA
A.I. DETECTION RANGE CONTOUR: Delta
ALTITUDE: 50 K
AVRO 2.2 Aerodynamics

D 46 F

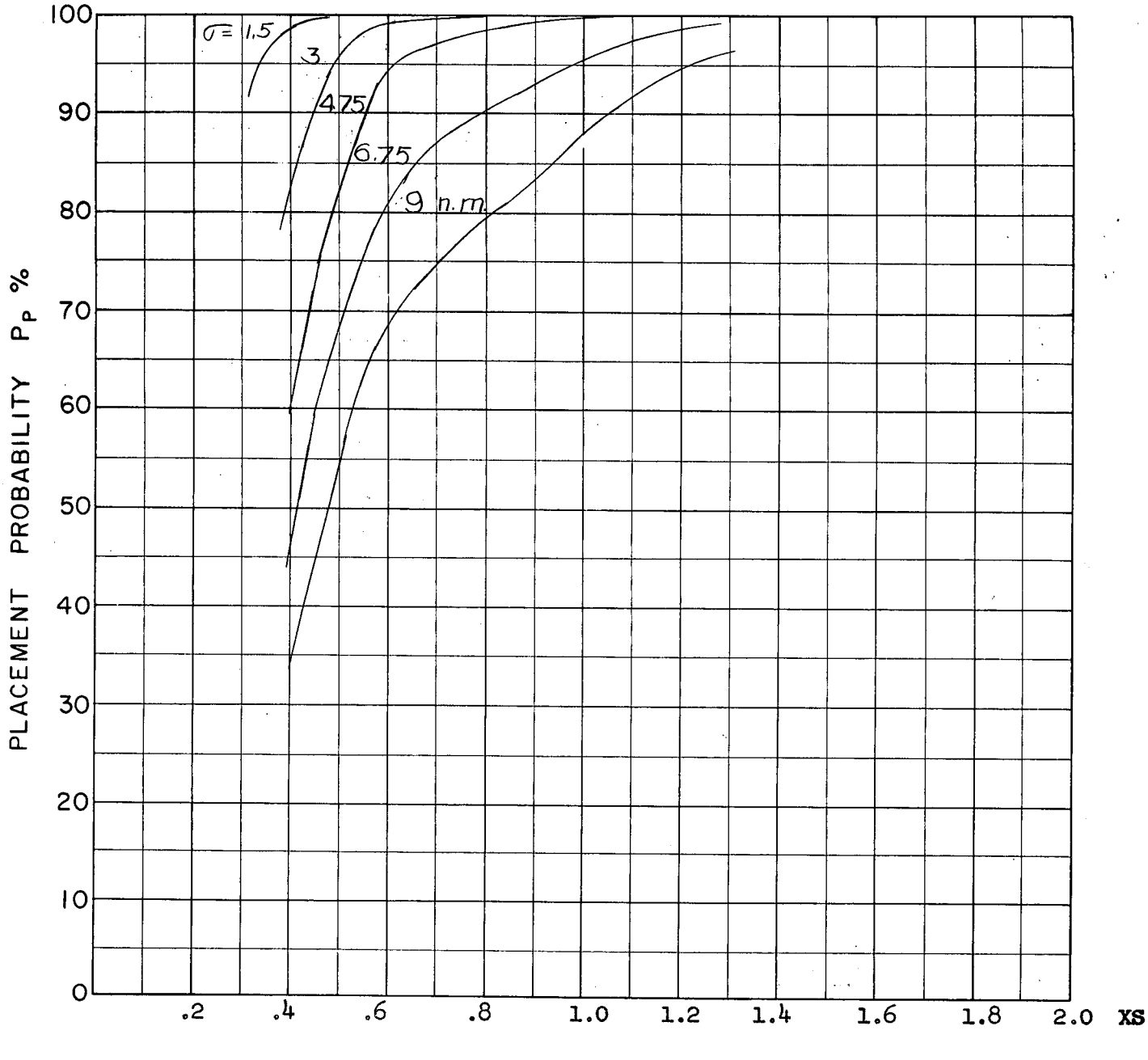

COURSE DIFFERENCE: 180°
TARGET EVASION: 0.5
TARGET MACH NO.: 2.0
INTERCEPTOR LATERAL G's: 4 Load Factor Limit
INTERCEPTOR MACH NO.: 1.5 Initial
σ OF G.C.I. ACCURACY: 5 Values
A.I. DETECTION RANGE AS FRACTION OF SPECIFICATION RANGE, S: ABSCISSA
A.I. DETECTION RANGE CONTOUR: Delta
ALTITUDE: 50 K
AVRO 2.2 Aerodynamics

D5a
F

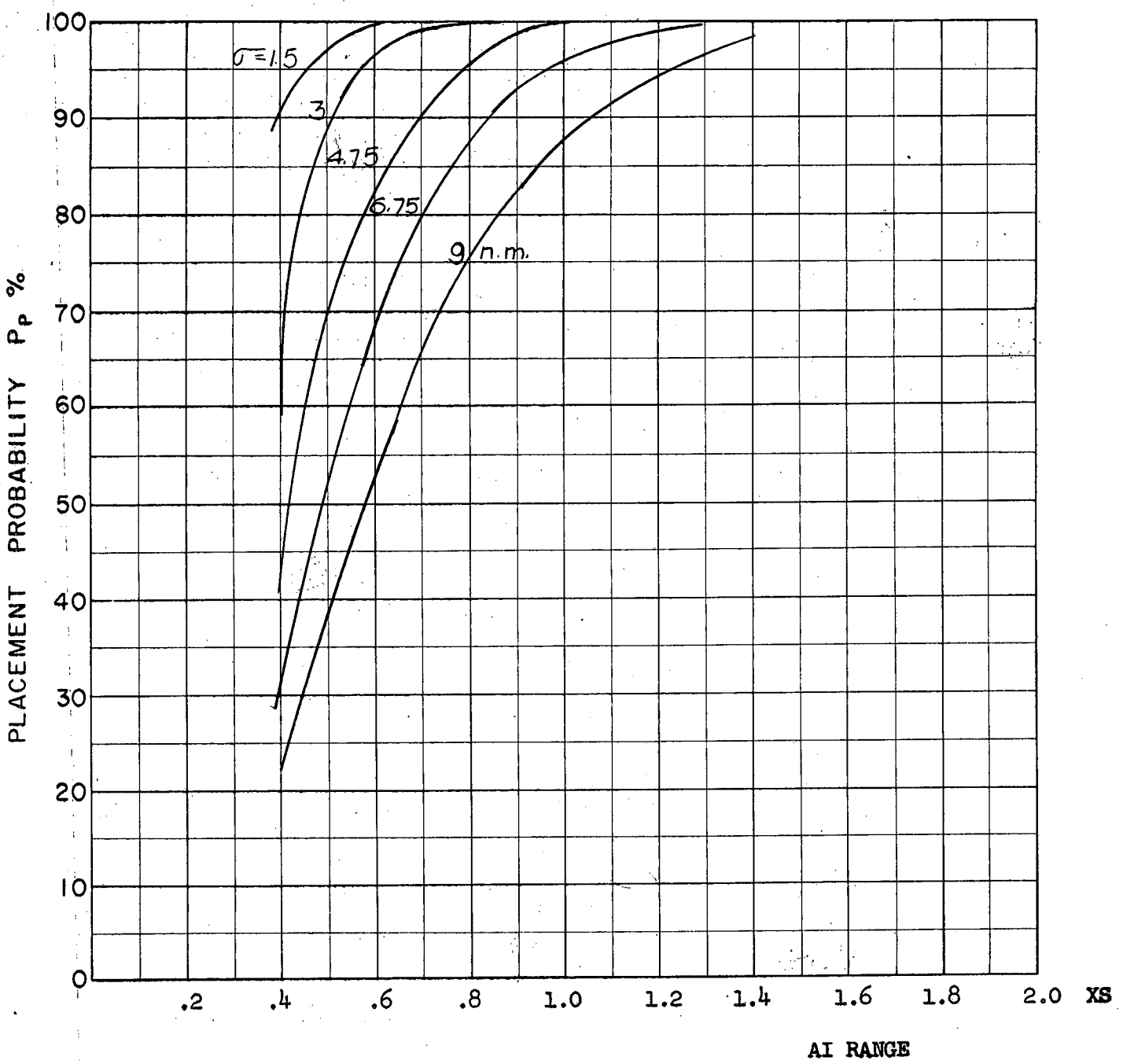

COURSE DIFFERENCE: 180°
TARGET EVASION: 0.5
TARGET MACH NO.: 2.0
INTERCEPTOR LATERAL G's: 2 1/4 Load Factor Limit
INTERCEPTOR MACH NO.: 1.5 Initial
σ OF G.C.I. ACCURACY: 5 Values
A.I. DETECTION RANGE AS FRACTION OF SPECIFICATION RANGE, S: ABSCISSA
A.I. DETECTION RANGE CONTOUR: Delta
ALTITUDE: 50 K
AVRO 2.2 Aerodynamics

D5b
F

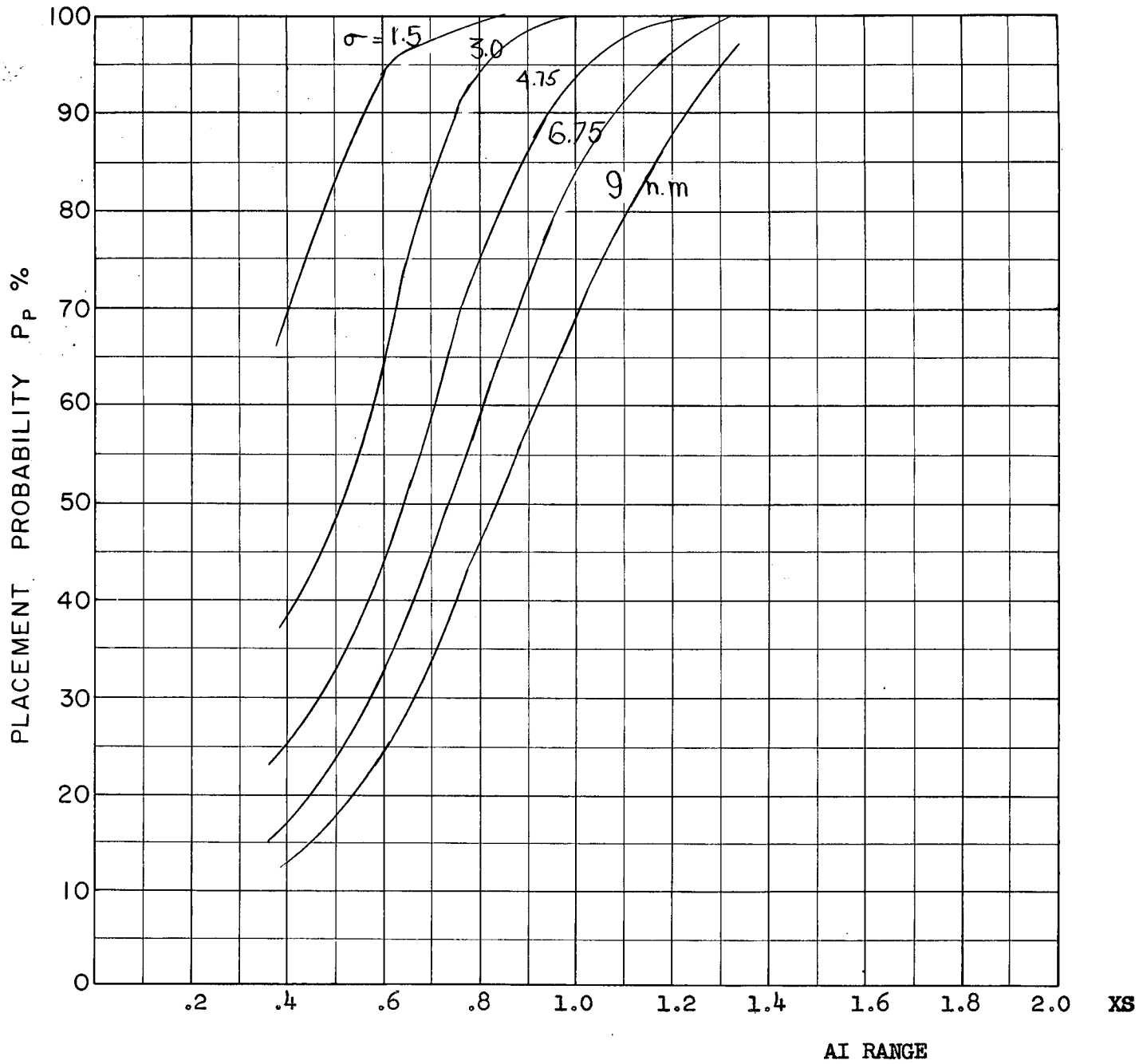

COURSE DIFFERENCE: 180°
TARGET EVASION: 0.5
TARGET MACH NO.: 2.0
INTERCEPTOR LATERAL G's: 1.414 Load Factor Limit
INTERCEPTOR MACH NO.: 1.5 Initial
σ OF G.C.I. ACCURACY: 5 Values
A.I. DETECTION RANGE AS FRACTION OF SPECIFICATION RANGE, S: ABSCISSA
A.I. DETECTION RANGE CONTOUR: Delta
ALTITUDE: 50 K
AVRO 2.2 Aerodynamics

D5 c
F

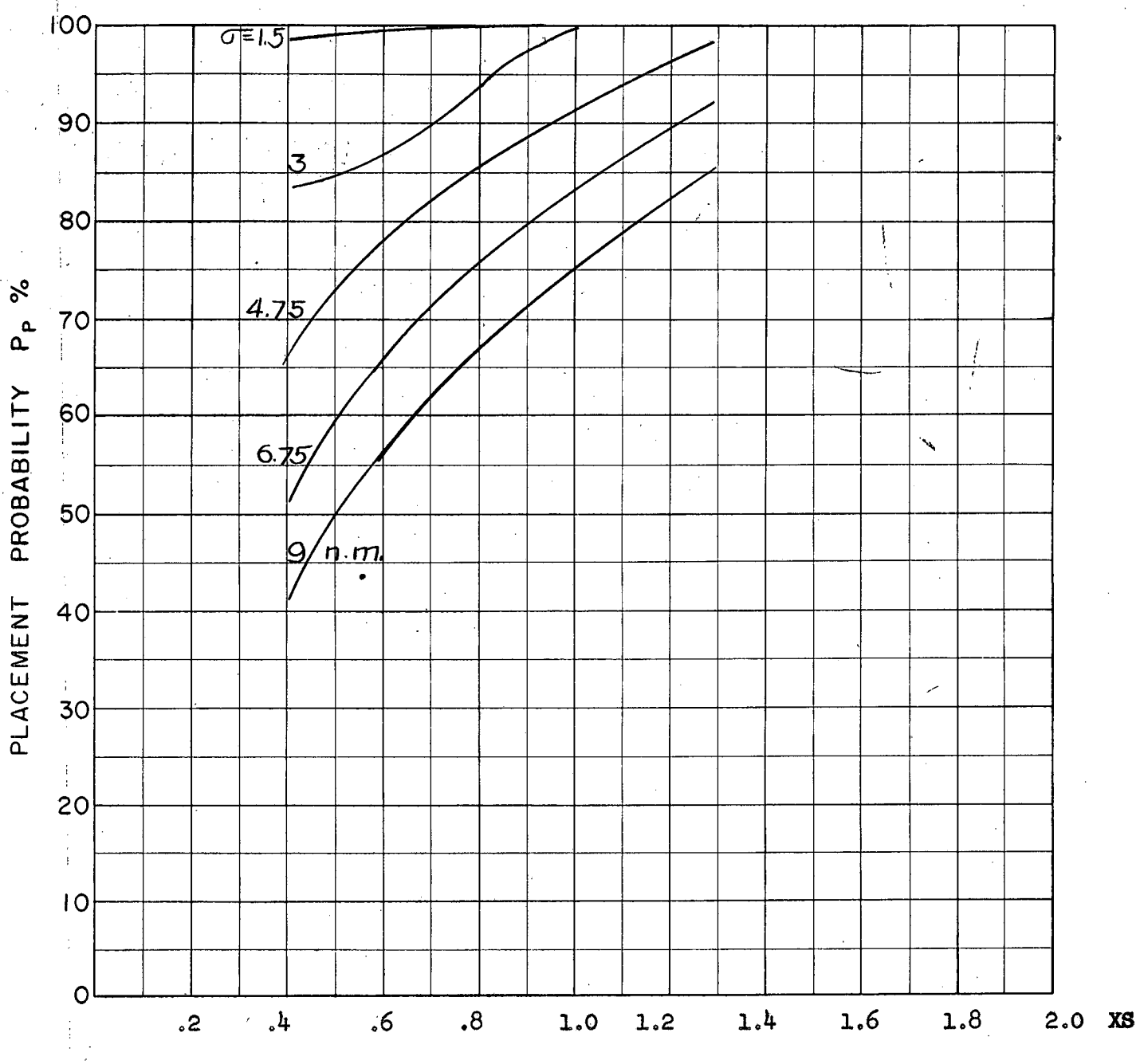

COURSE DIFFERENCE: 110°
TARGET EVASION: 0.5
TARGET MACH NO.: 2.0
INTERCEPTOR LATERAL G's: 4 Load Factor Limit
INTERCEPTOR MACH NO.: 1.8 Initial
σ OF G.C.I. ACCURACY: 5 Values
A.I. DETECTION RANGE AS FRACTION OF SPECIFICATION RANGE, S: ABSCISSA
A.I. DETECTION RANGE CONTOUR: Delta
ALTITUDE: 50K
AVRO 2.2 Aerodynamics

D6a
F

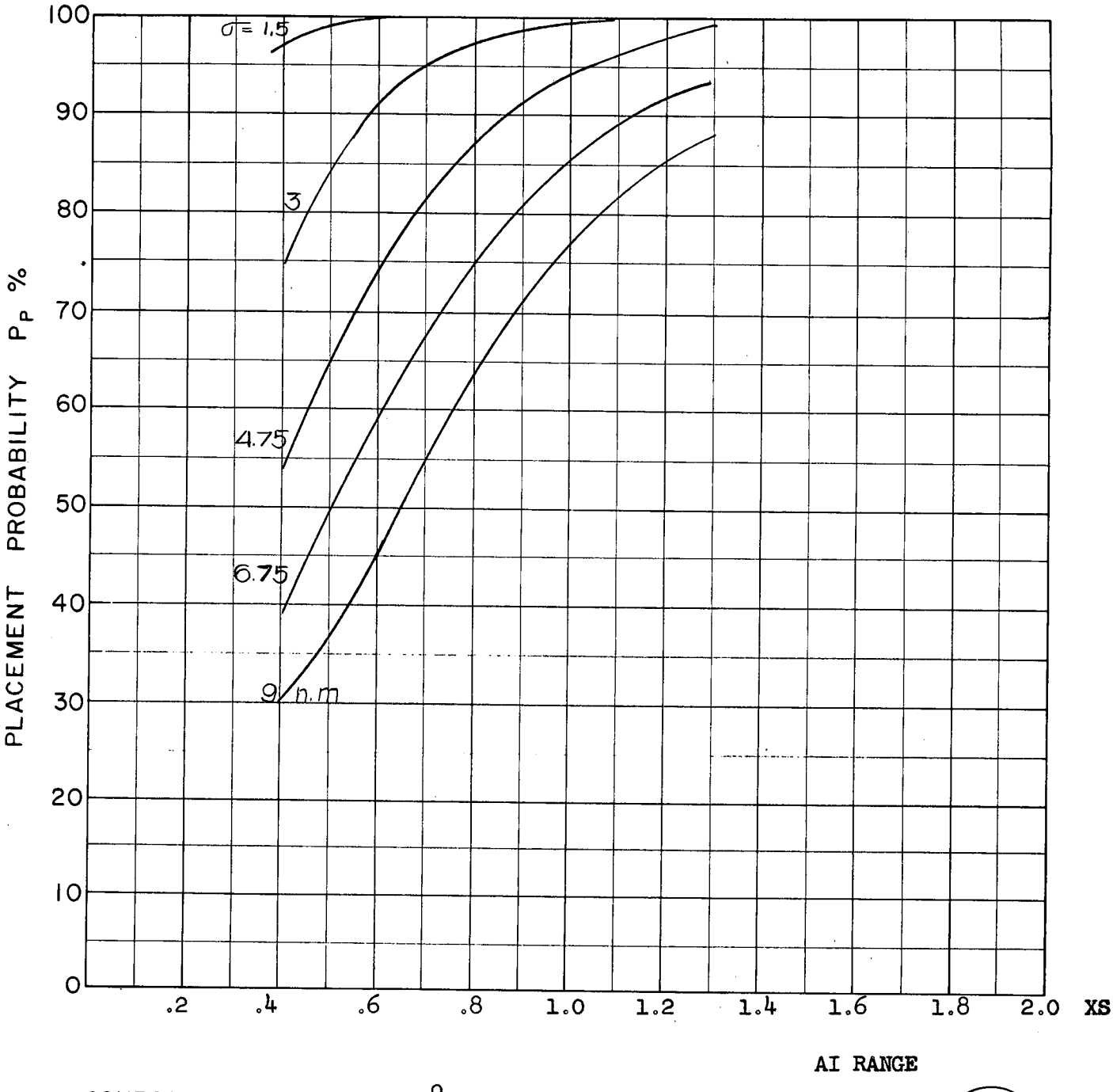

COURSE DIFFERENCE: 110°
TARGET EVASION: 0.5
TARGET MACH NO.: 2.0
INTERCEPTOR LATERAL G's: 2 1/4 Load Factor Limit
INTERCEPTOR MACH NO.: 1.8 Initial
σ OF G.C.I. ACCURACY: 5 Values
A.I. DETECTION RANGE AS FRACTION OF SPECIFICATION RANGE, S: ABSCISSA
A.I. DETECTION RANGE CONTOUR: Delta
ALTITUDE: 50 K
AVRO 2.2 Aerodynamics

D66 F

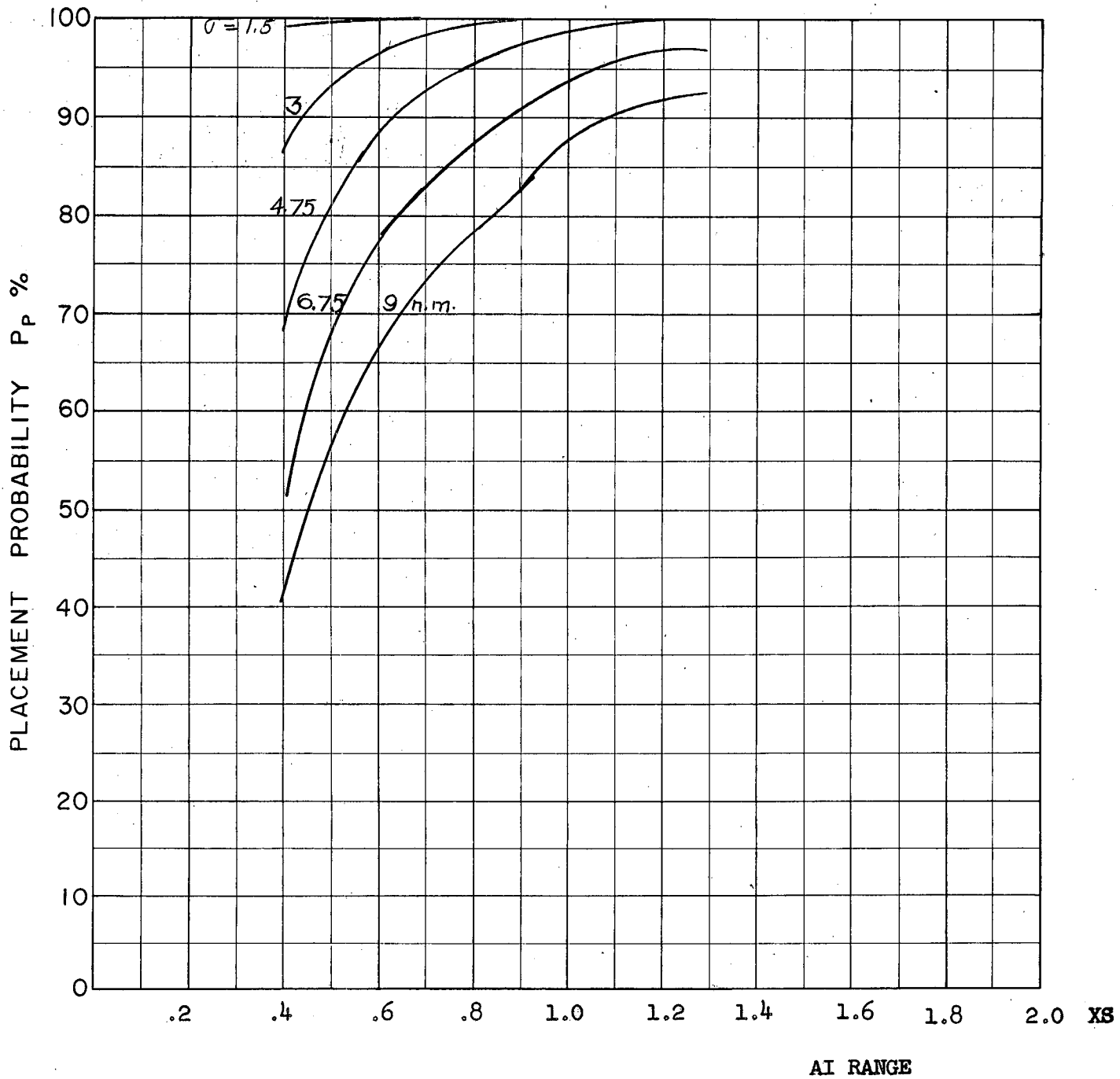

COURSE DIFFERENCE: 135°
TARGET EVASION: 0.5
TARGET MACH NO.: 2.0
INTERCEPTOR LATERAL G's: 4 Load Factor Limit
INTERCEPTOR MACH NO.: 1.8 Initial
σ OF G.C.I. ACCURACY: 5 Values
A.I. DETECTION RANGE AS FRACTION OF SPECIFICATION RANGE, S: ABSCISSA
A.I. DETECTION RANGE CONTOUR: Delta
ALTITUDE: 50K

D-7a
F

AVRO 2.2 Aerodynamics

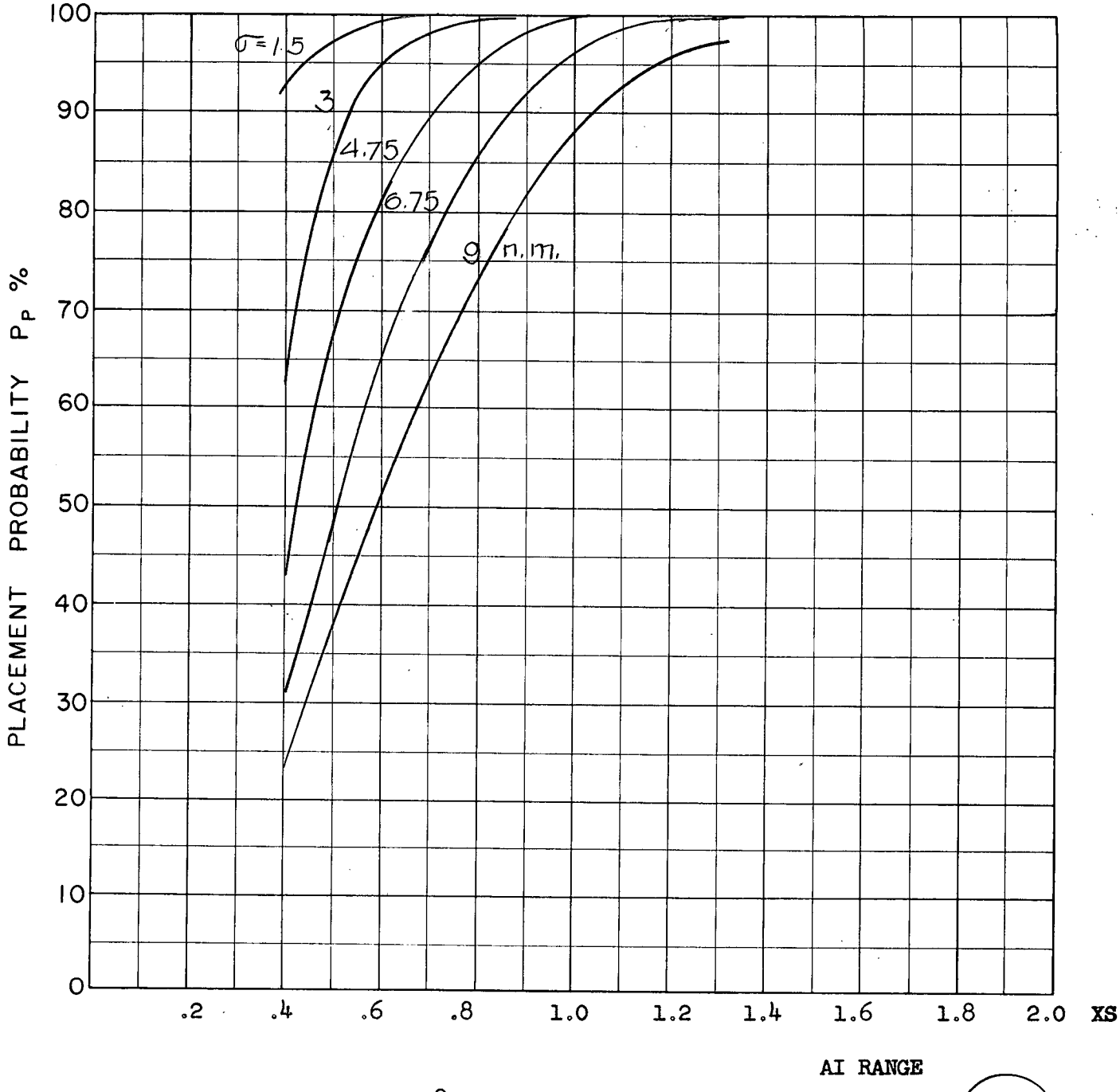

COURSE DIFFERENCE: 135°
TARGET EVASION: 0.5
TARGET MACH NO.: 2.0
INTERCEPTOR LATERAL G's: 2 1/4 Load Factor Limit
INTERCEPTOR MACH NO.: 1.8 Initial
σ OF G.C.I. ACCURACY: 5 Values
A.I. DETECTION RANGE AS FRACTION OF SPECIFICATION RANGE, S: ABSCISSA
A.I. DETECTION RANGE CONTOUR: Delta
ALTITUDE: 50 K
AVRO 2.2 Aerodynamics

D7b
F

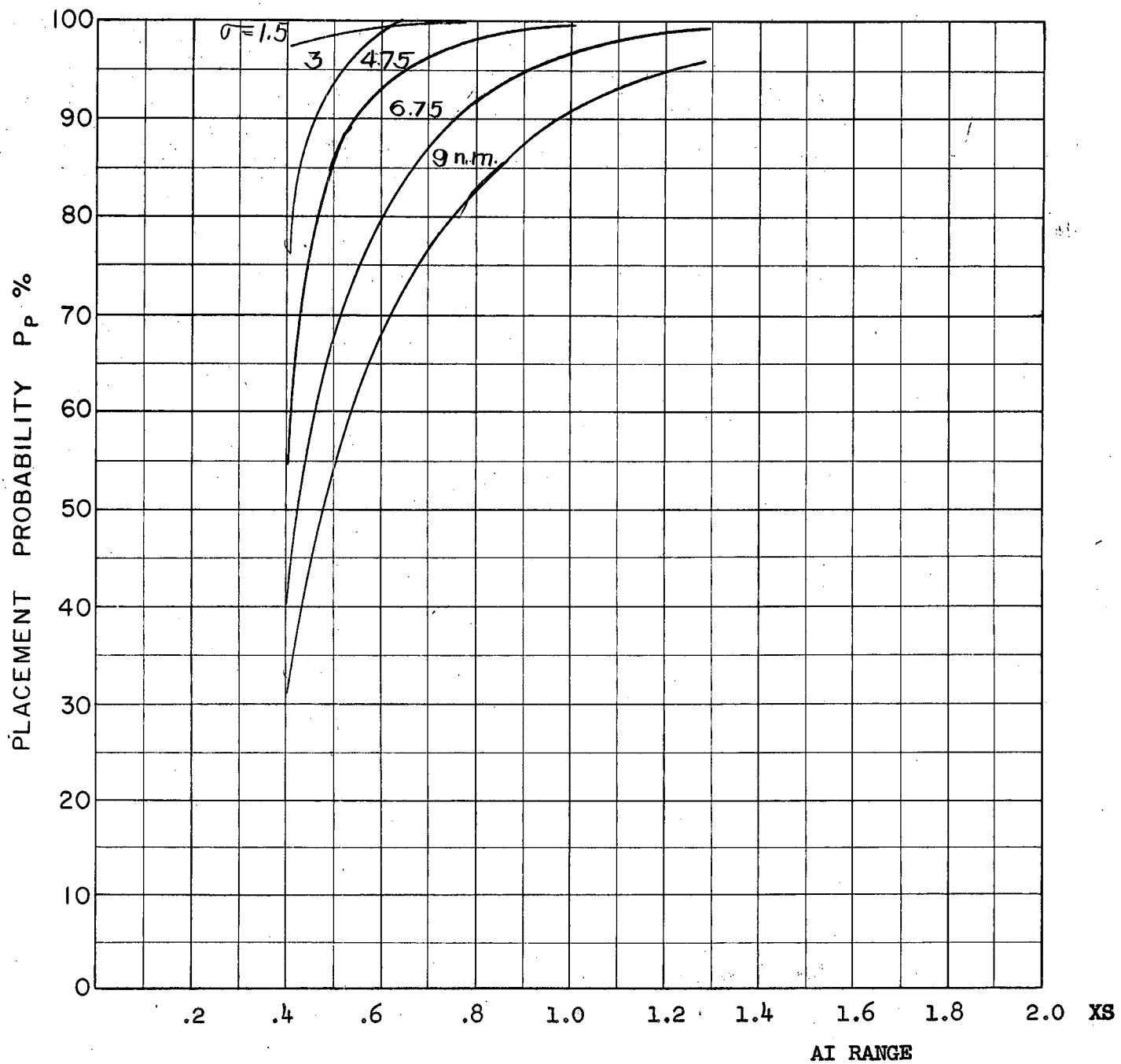

COURSE DIFFERENCE: 160°
TARGET EVASION: 0.5
TARGET MACH NO.: 2.0
INTERCEPTOR LATERAL G's: 4 Load Factor Limit
INTERCEPTOR MACH NO.: 1.8 Initial
σ OF G.C.I. ACCURACY: 5 Values
A.I. DETECTION RANGE AS FRACTION OF SPECIFICATION RANGE, S: ABSCISSA
A.I. DETECTION RANGE CONTOUR: Delta
ALTITUDE: 50 K
AVRO 2.2 Aerodynamics

D8a
P

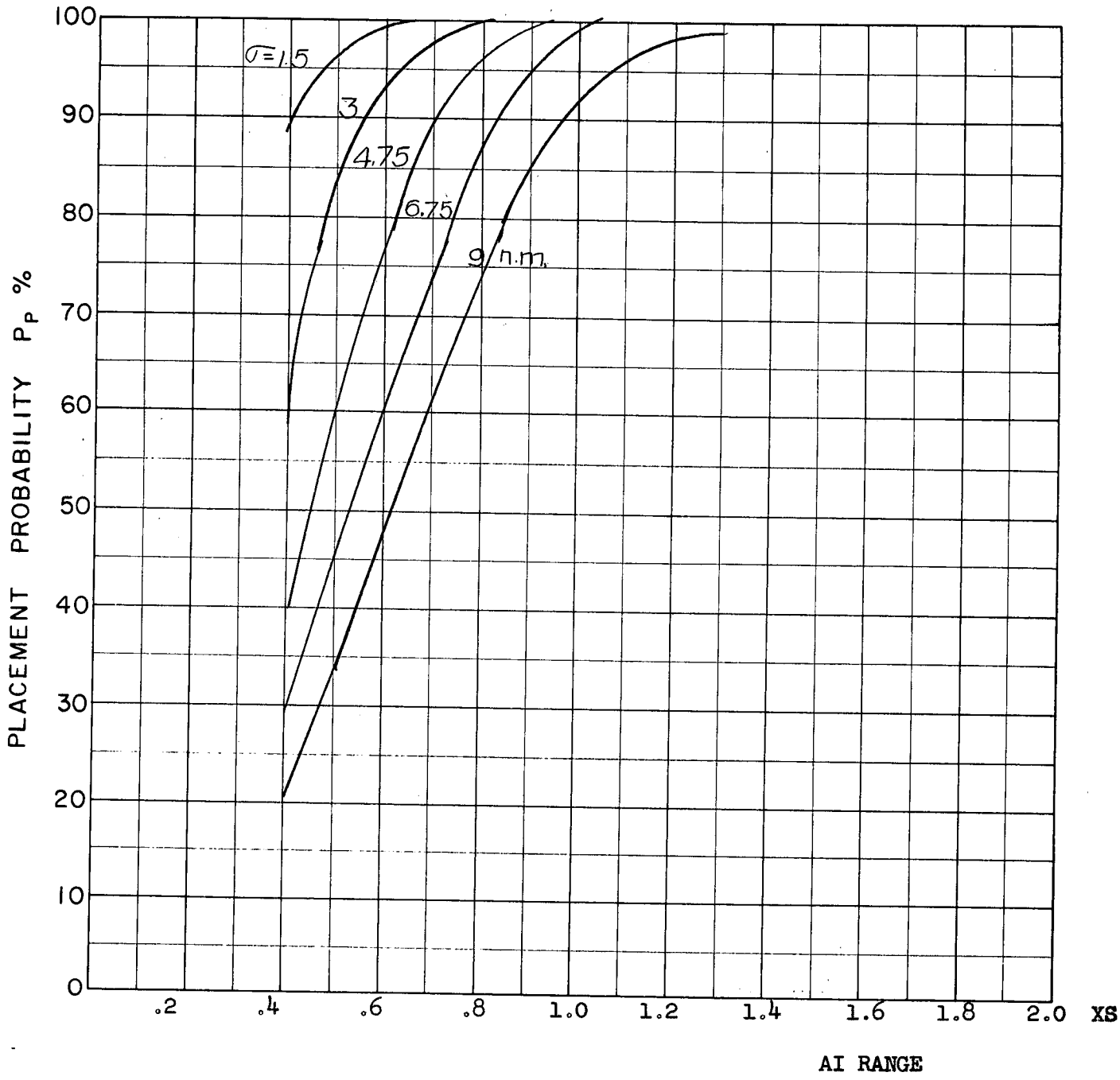

COURSE DIFFERENCE: 160°
TARGET EVASION: 0.5
TARGET MACH NO.: 2.0
INTERCEPTOR LATERAL G's: 2 1/4 Load Factor Limit
INTERCEPTOR MACH NO.: 1.8 Initial
σ OF G.C.I. ACCURACY: 5 Values
A.I. DETECTION RANGE AS FRACTION OF SPECIFICATION RANGE, S: ABSCISSA
A.I. DETECTION RANGE CONTOUR: Delta
ALTITUDE: 50 K
AVRO 2.2 Aerodynamics

D-86
F

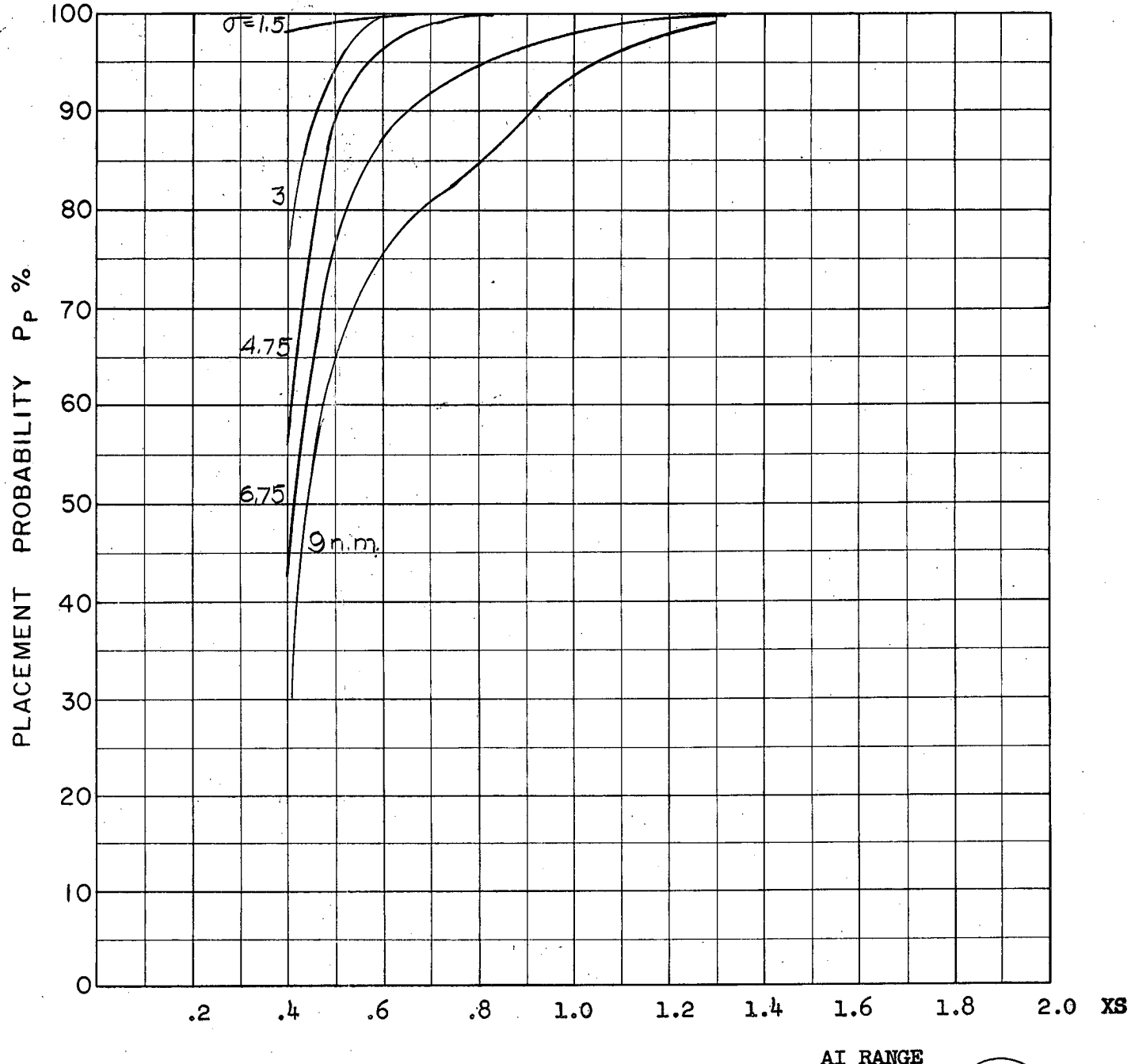

D 8 a
F

COURSE DIFFERENCE: 180°
TARGET EVASION: 0.5
TARGET MACH NO.: 2.0
INTERCEPTOR LATERAL G's: 4 Load Factor Limit
INTERCEPTOR MACH NO.: 1.8 Initial
σ OF G.C.I. ACCURACY: 5 Values
A.I. DETECTION RANGE AS FRACTION OF SPECIFICATION RANGE, S: ABSCISSA
A.I. DETECTION RANGE CONTOUR: Delta
ALTITUDE: 50 K
AVRO 2.2 Aerodynamics

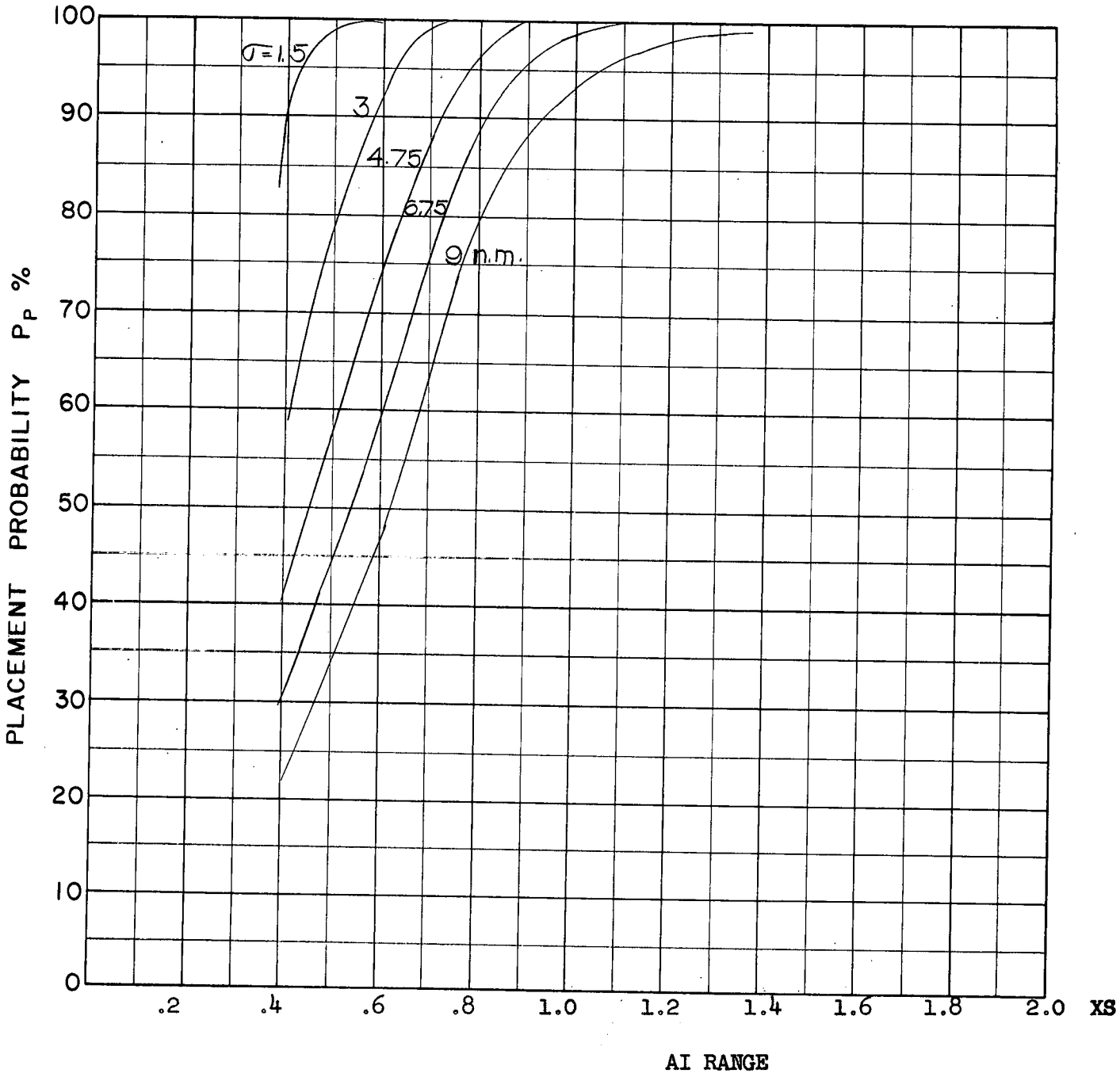

COURSE DIFFERENCE: 180°
TARGET EVASION: 0.5
TARGET MACH NO.: 2.0
INTERCEPTOR LATERAL G's: 2 1/4 Load Factor Limit
INTERCEPTOR MACH NO.: 1.8 Initial
σ OF G.C.I. ACCURACY: 5 Values
A.I. DETECTION RANGE AS FRACTION OF SPECIFICATION RANGE, S: ABSCISSA
A.I. DETECTION RANGE CONTOUR: Delta
ALTITUDE: 50 K
AVRO 2.2 Aerodynamics

D8b
F

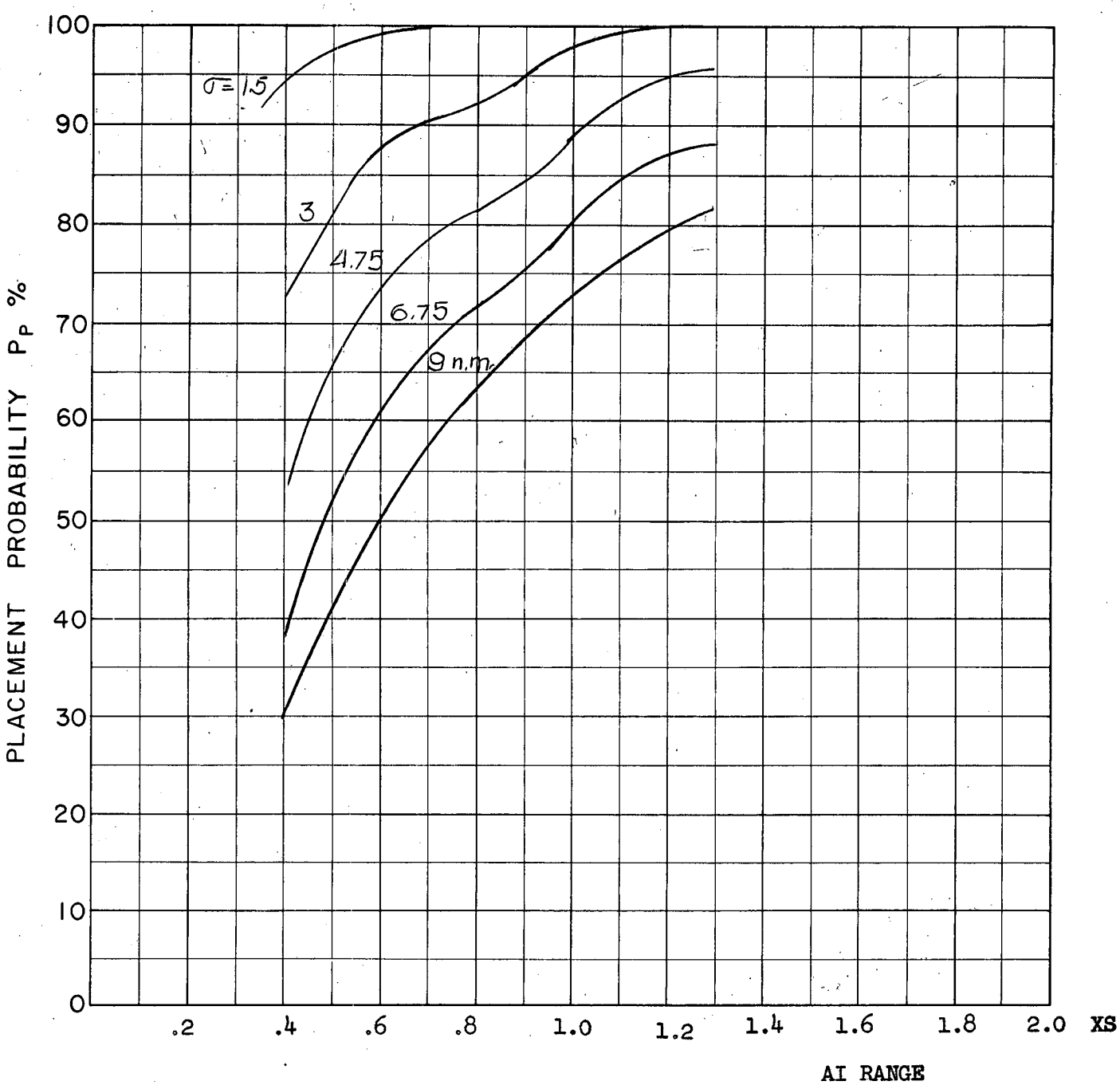

COURSE DIFFERENCE: 110°
TARGET EVASION: 0.5
TARGET MACH NO.: 2.0
INTERCEPTOR LATERAL G's: 4 Load Factor Limit
INTERCEPTOR MACH NO.: 1.8 Initial
σ OF G.C.I. ACCURACY: 5 Values
A.I. DETECTION RANGE AS FRACTION OF SPECIFICATION RANGE, S: ABSCISSA
A.I. DETECTION RANGE CONTOUR: Delta
ALTITUDE: 50 K
AVRO 2.2 Aerodynamics
LAUNCH ZONE 1

D.9
F

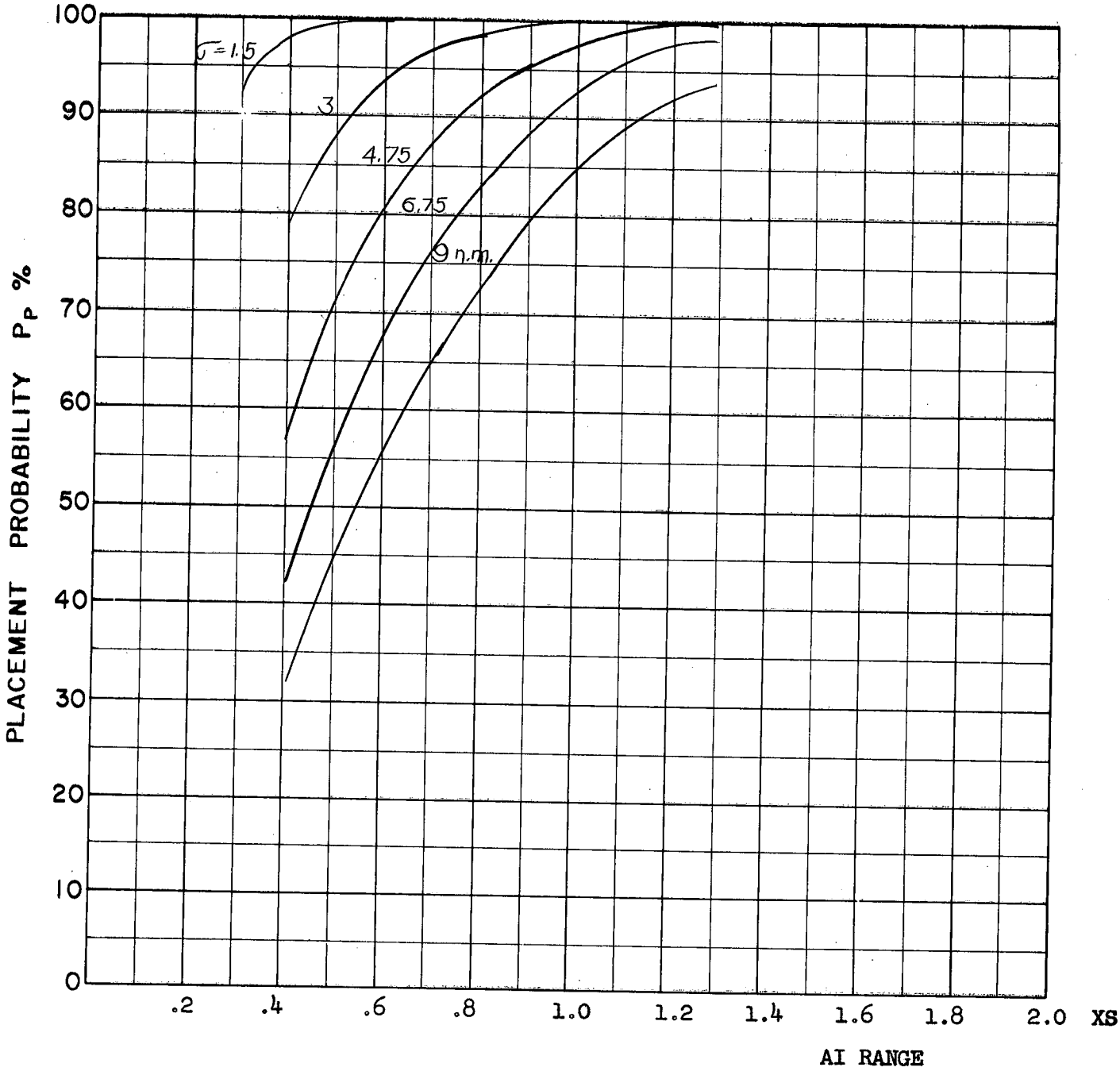

COURSE DIFFERENCE: 135°
TARGET EVASION: 0.5
TARGET MACH NO.: 2.0
INTERCEPTOR LATERAL G's: 4 Load Factor Limit
INTERCEPTOR MACH NO.: 1.8 Initial
σ OF G.C.I. ACCURACY: 5 Values
A.I. DETECTION RANGE AS FRACTION OF SPECIFICATION RANGE, S: ABSCISSA
A.I. DETECTION RANGE CONTOUR: Delta
ALTITUDE: 50 K
AVRO 2.2. Aerodynamics
LAUNCH ZONE 1

D10
F

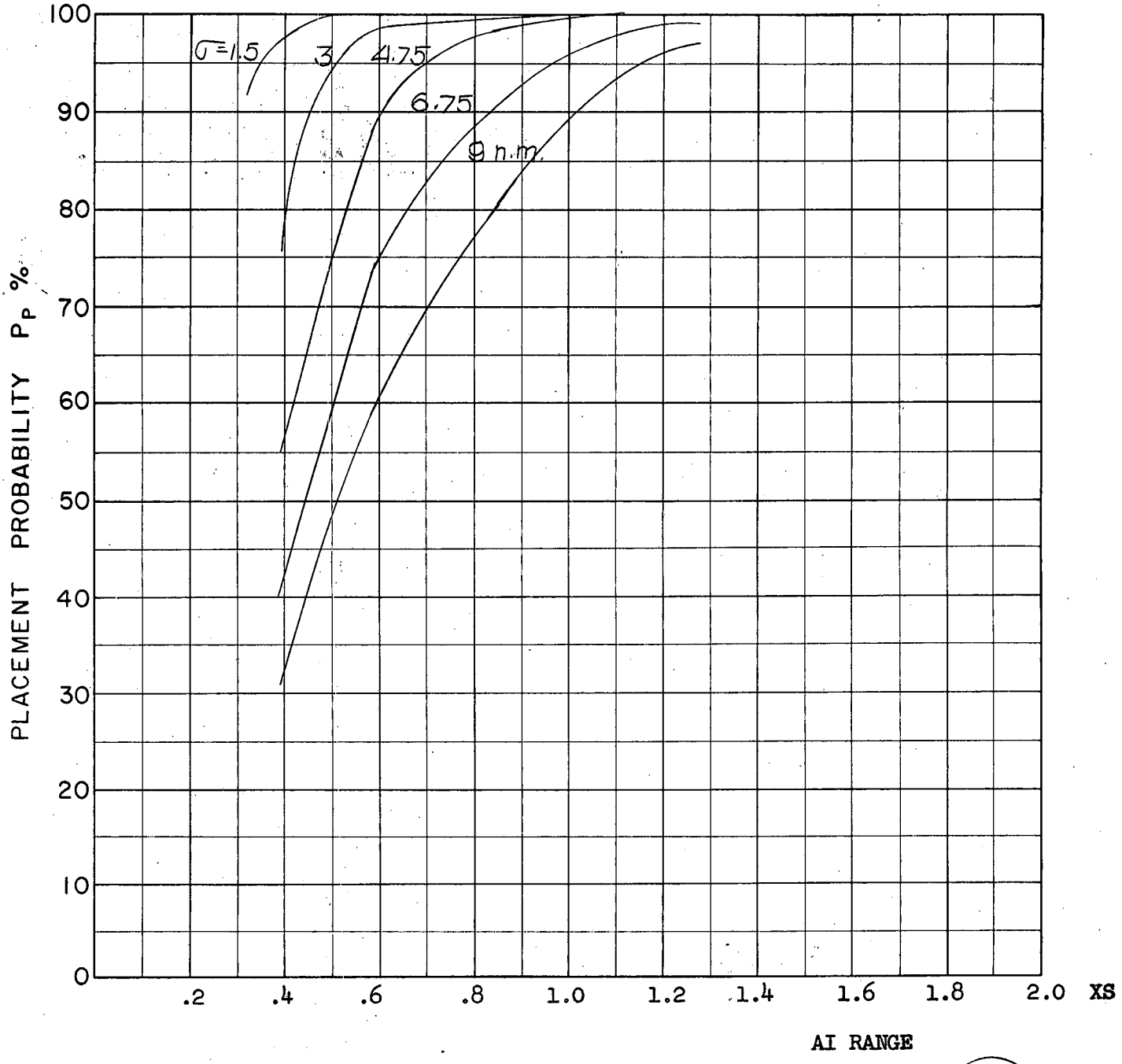

COURSE DIFFERENCE: 160°
TARGET EVASION: 0.5
TARGET MACH NO.: 2.0
INTERCEPTOR LATERAL G's: 4 Load Factor Limit
INTERCEPTOR MACH NO.: 1.8 Initial
σ OF G.C.I. ACCURACY: 5 Values
A.I. DETECTION RANGE AS FRACTION OF SPECIFICATION RANGE, S: ABSCISSA
A.I. DETECTION RANGE CONTOUR: Delta
ALTITUDE: 50 K
AVRO 2.2 Aerodynamics
LAUNCH ZONE 1

D11
F

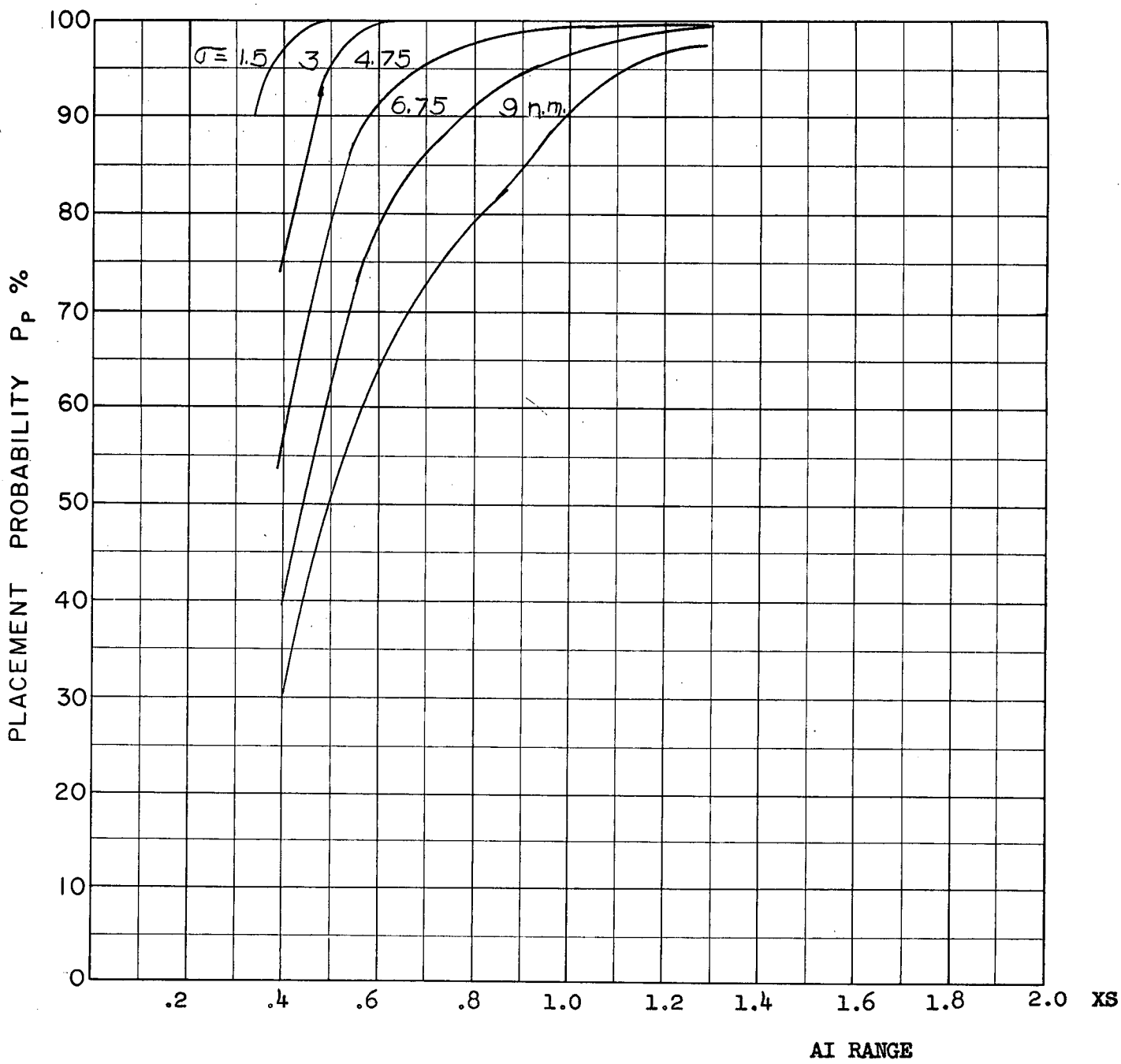

COURSE DIFFERENCE: 180°
TARGET EVASION: 0.5
TARGET MACH NO.: 2.0
INTERCEPTOR LATERAL G's: 4 Load Factor Limit
INTERCEPTOR MACH NO.: 1.8 Initial
σ OF G.C.I. ACCURACY: 5 Values
A.I. DETECTION RANGE AS FRACTION OF SPECIFICATION RANGE, S: ABSCISSA
A.I. DETECTION RANGE CONTOUR: Delta
ALTITUDE: 50 K
AVRO 2.2 Aerodynamics
Launch Zone 1

D12
E

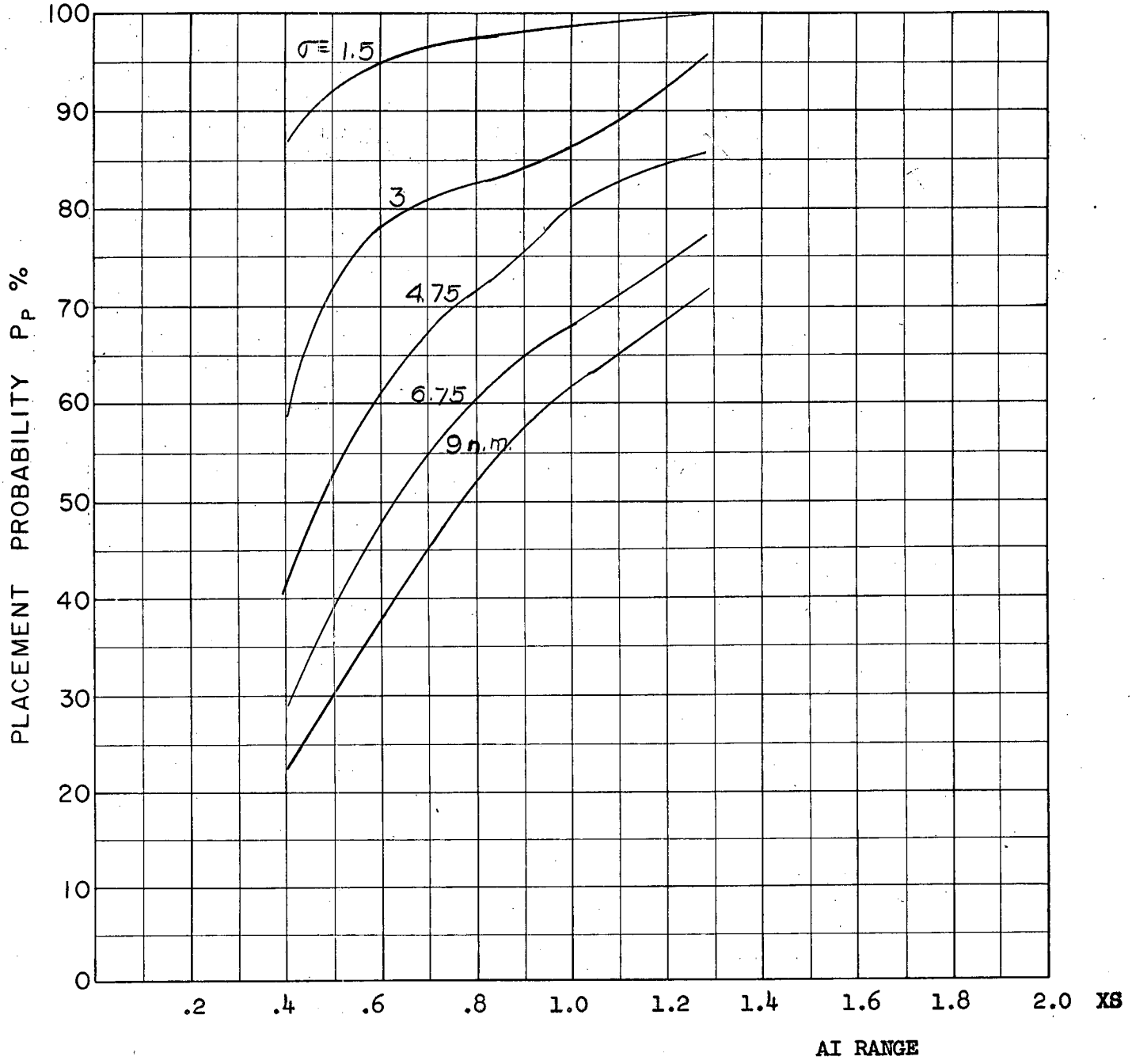

COURSE DIFFERENCE: 110°
TARGET EVASION: 0.5
TARGET MACH NO.: 2.0
INTERCEPTOR LATERAL G's: 4 Load Factor Limit
INTERCEPTOR MACH NO.: 1.8 Initial
σ OF G.C.I. ACCURACY: 5 Values
A.I. DETECTION RANGE AS FRACTION OF SPECIFICATION RANGE, S: ABSCISSA
A.I. DETECTION RANGE CONTOUR: Delta
ALTITUDE: 60 K
AVRO 2.2 Aerodynamics

D13
F

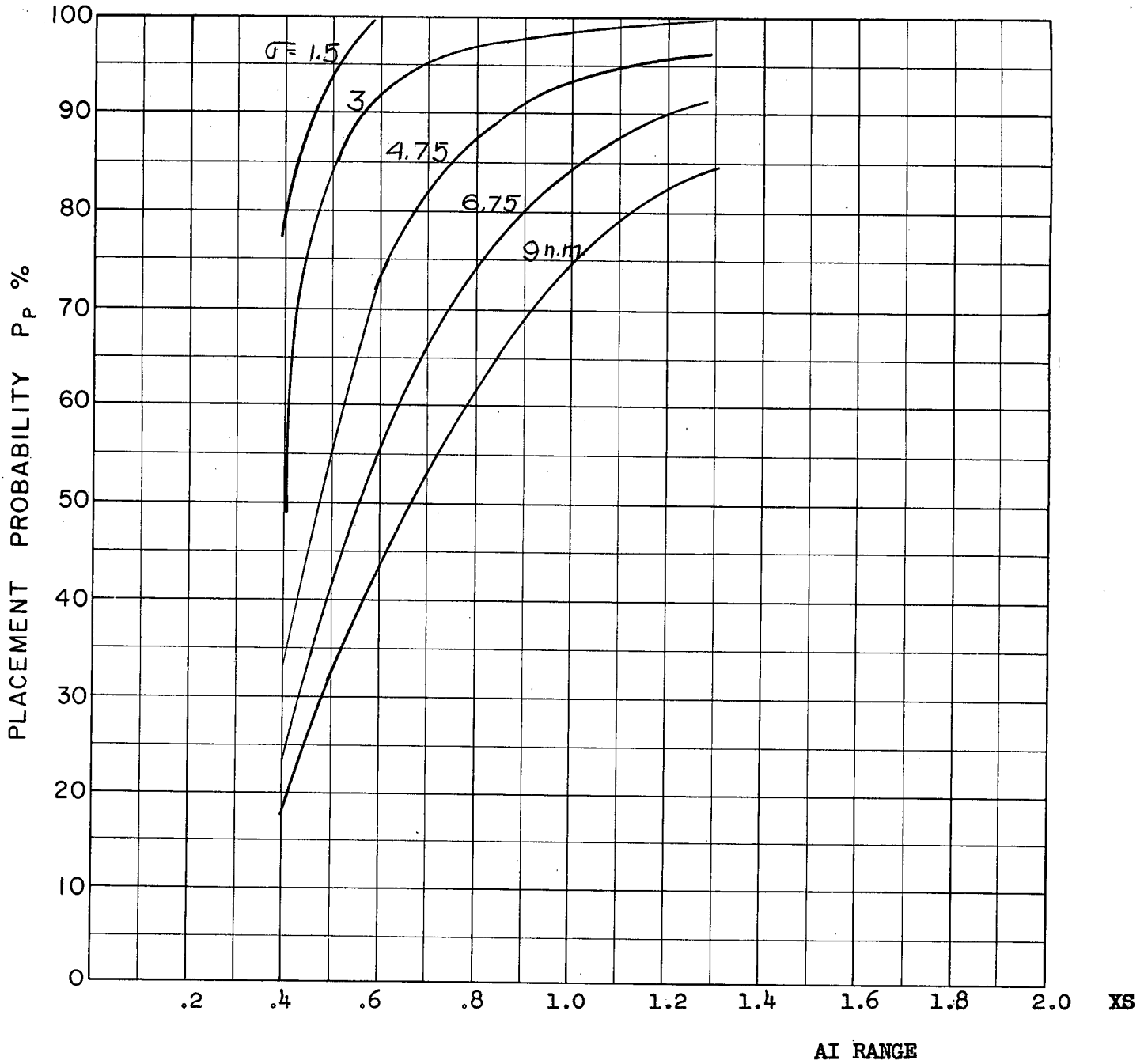

COURSE DIFFERENCE: 135°
TARGET EVASION: 0.5
TARGET MACH NO.: 2.0
INTERCEPTOR LATERAL G's: 4 Load Factor Limit
INTERCEPTOR MACH NO.: 1.8 Initial
σ OF G.C.I. ACCURACY: 5 Values
A.I. DETECTION RANGE AS FRACTION OF SPECIFICATION RANGE, S: ABSCISSA
A.I. DETECTION RANGE CONTOUR: Delta
ALTITUDE: 60 K
AVRO 2.2 Aerodynamics

D 13
F

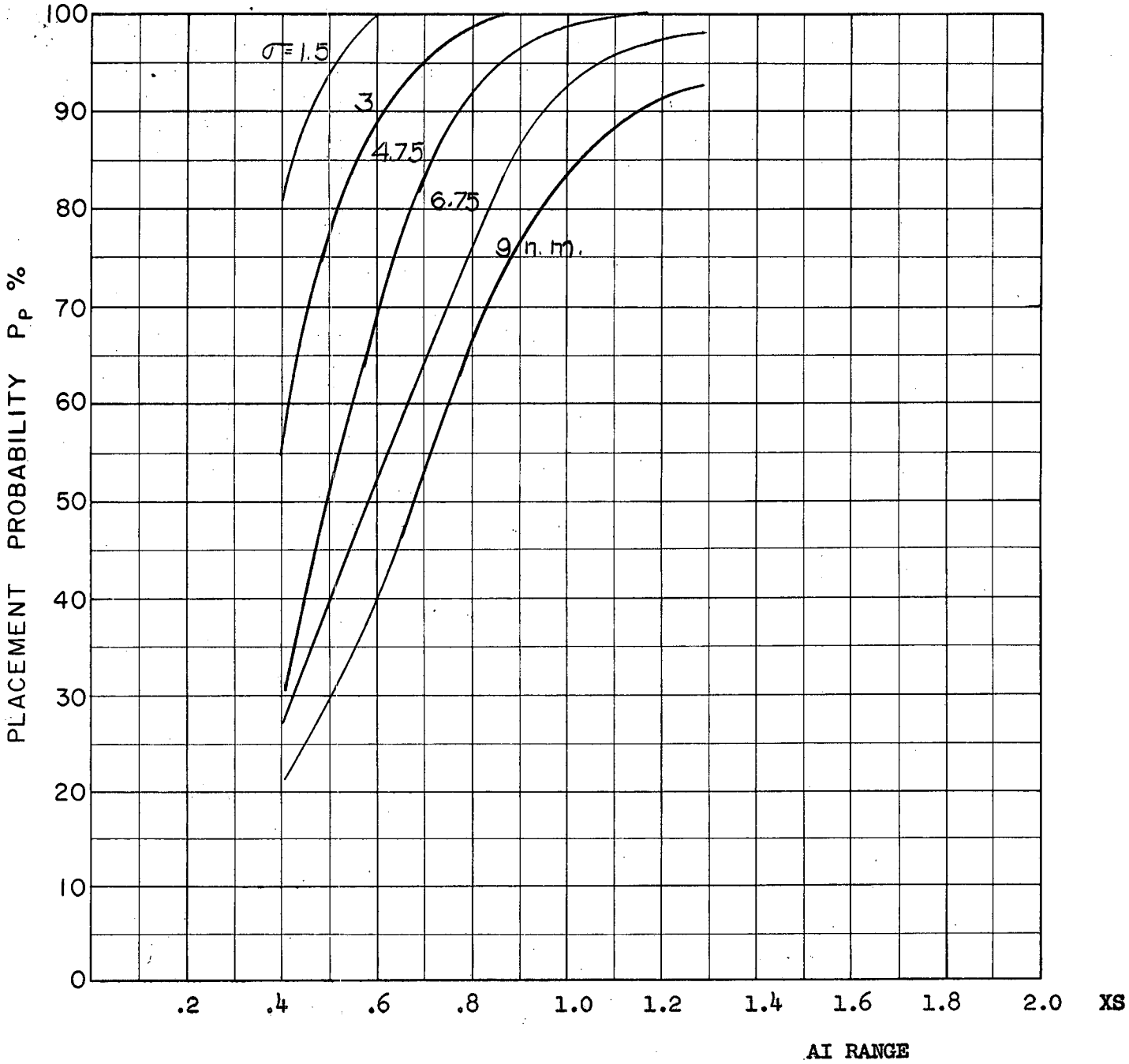

COURSE DIFFERENCE: 160°
TARGET EVASION: 0.5
TARGET MACH NO.: 2.0
INTERCEPTOR LATERAL G's: 4 Load Factor Limit
INTERCEPTOR MACH NO.: 1.8 Initial
σ OF G.C.I. ACCURACY: 5 Values
A.I. DETECTION RANGE AS FRACTION OF SPECIFICATION RANGE, S: ABSCISSA
A.I. DETECTION RANGE CONTOUR: Delta
ALTITUDE: 60 K
AVRO 2.2 Aerodynamics

D.15
F

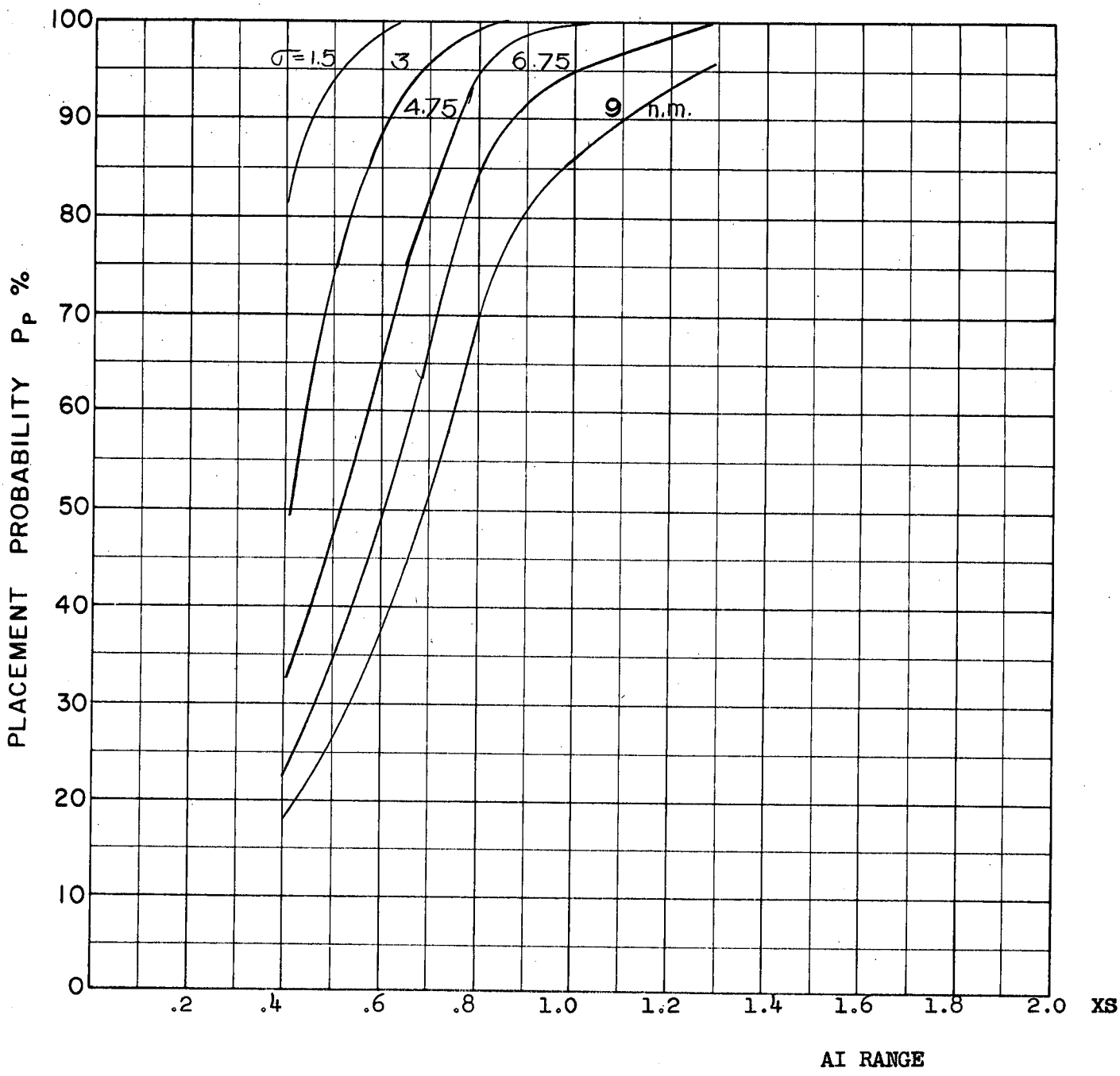

COURSE DIFFERENCE: 180°
TARGET EVASION: 0.5
TARGET MACH NO.: 2.0
INTERCEPTOR LATERAL G's: 4 Load Factor Limit
INTERCEPTOR MACH NO.: 1.8 Initial
σ OF G.C.I. ACCURACY: 5 Values
A.I. DETECTION RANGE AS FRACTION OF SPECIFICATION RANGE, S: ABSCISSA
A.I. DETECTION RANGE CONTOUR: Delta
ALTITUDE: 60K
AVRO 2.2 Aerodynamics

D 16
F

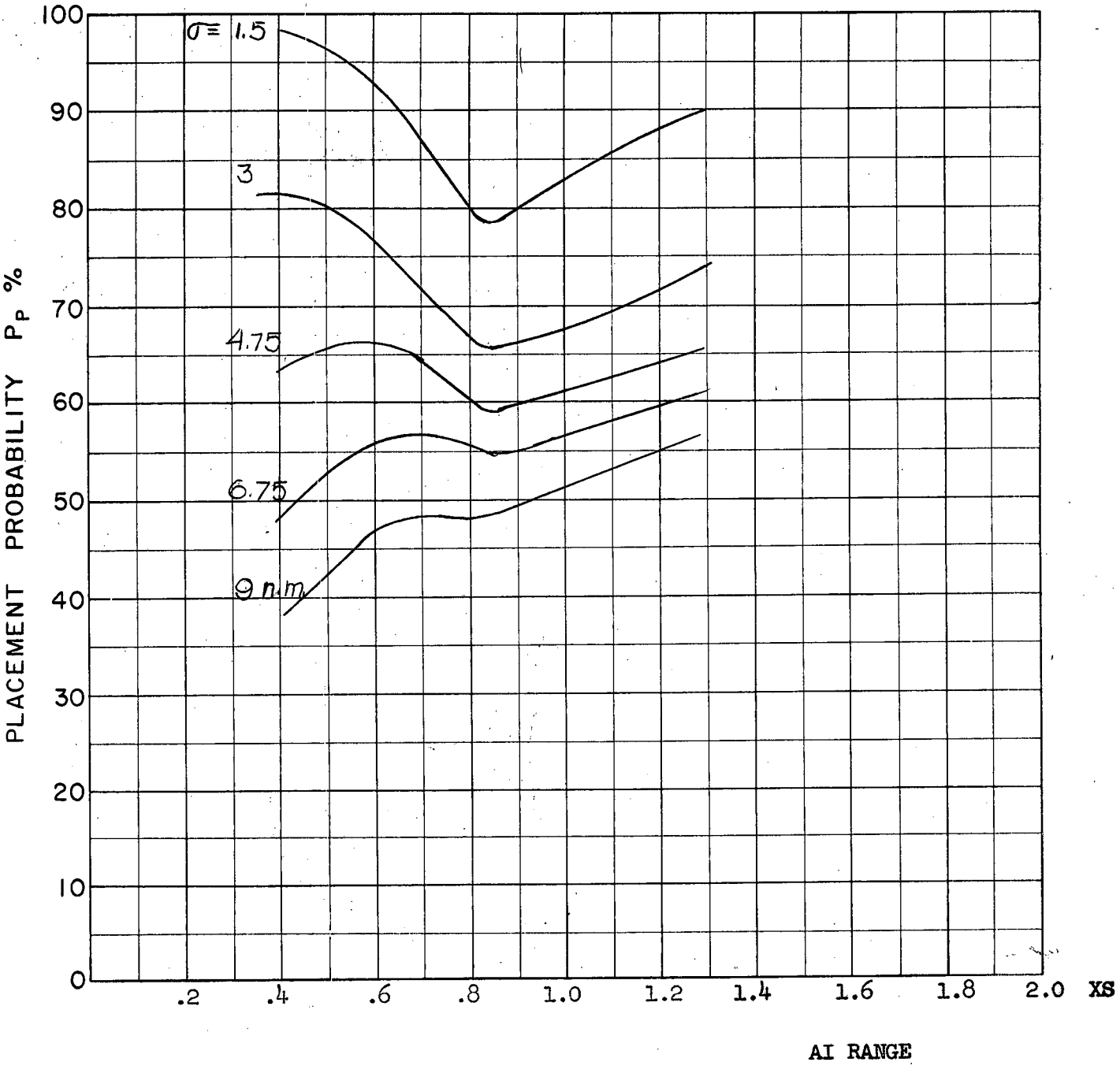

COURSE DIFFERENCE: 90°
TARGET EVASION: 0.5
TARGET MACH NO.: 2.0
INTERCEPTOR LATERAL G's: 4 Load Factor Limit
INTERCEPTOR MACH NO.: 2.0 Initial
σ OF G.C.I. ACCURACY: 5 Values
A.I. DETECTION RANGE AS FRACTION OF SPECIFICATION RANGE, S: ABSCISSA
A.I. DETECTION RANGE CONTOUR: Delta
ALTITUDE: 50 K
AVRO 2.2 Aerodynamics

D.17a
F

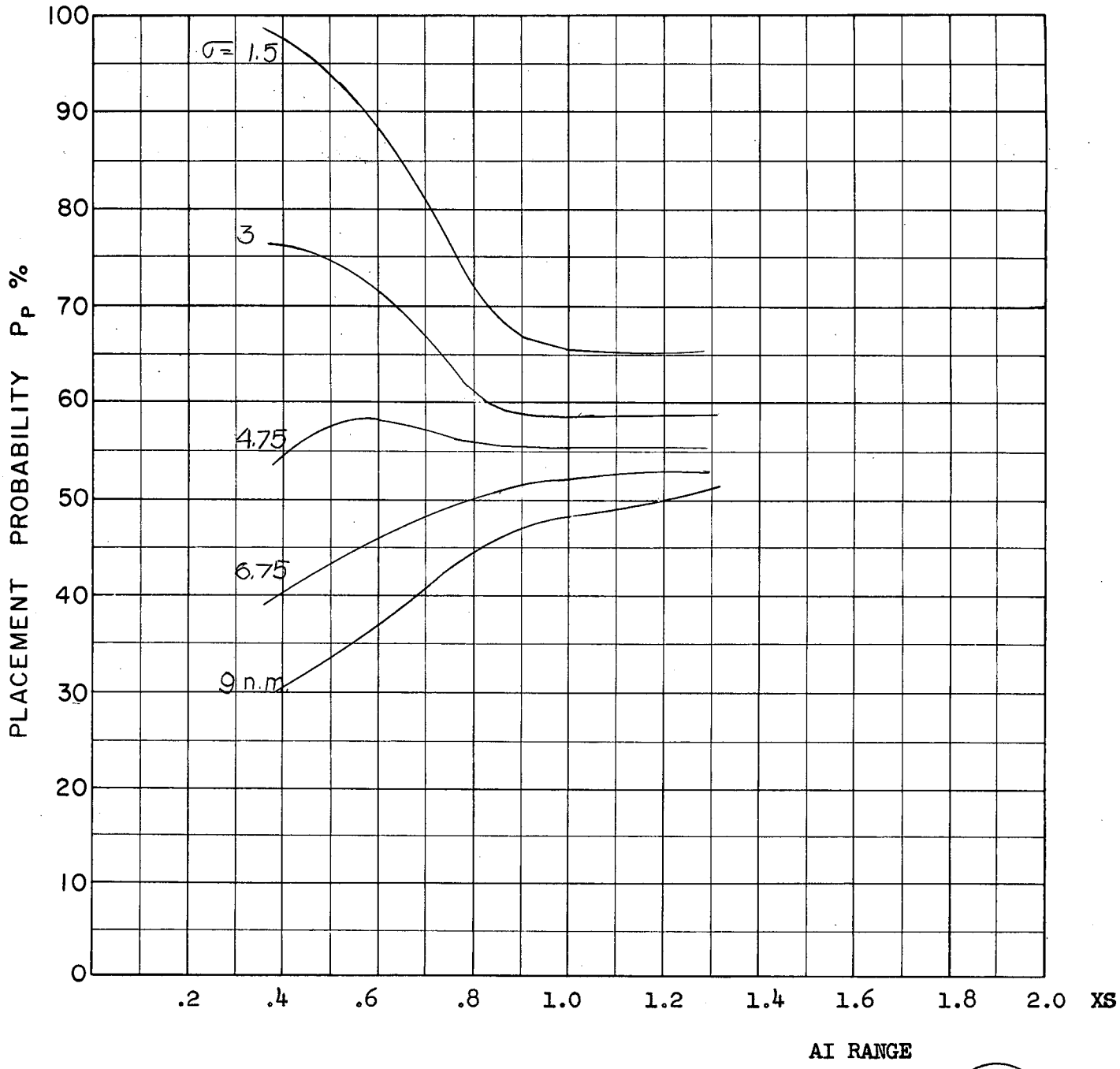

COURSE DIFFERENCE: 90°
TARGET EVASION: 0.5
TARGET MACH NO.: 2.0
INTERCEPTOR LATERAL G's: 2 1/4 Load Factor Limit
INTERCEPTOR MACH NO.: 2.0 Initial
σ OF G.C.I. ACCURACY: 5 Values
A.I. DETECTION RANGE AS FRACTION OF SPECIFICATION RANGE, S: ABSCISSA
A.I. DETECTION RANGE CONTOUR: Delta
ALTITUDE: 50 K
AVRO 2.2 Aerodynamics

D17b
F

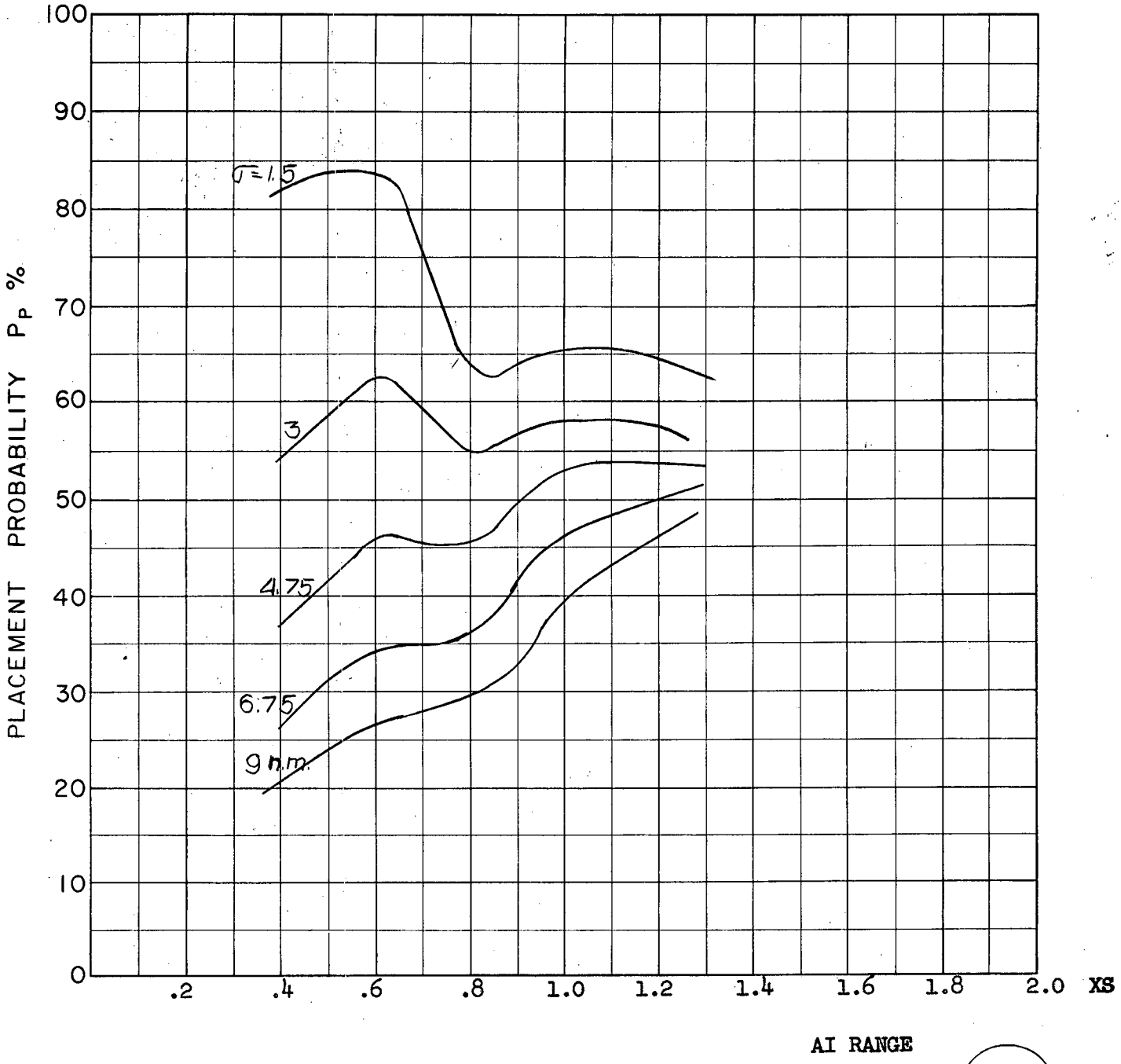

COURSE DIFFERENCE: 90°
TARGET EVASION: 0.5
TARGET MACH NO.: 2.0
INTERCEPTOR LATERAL G's: 1.414 Load Factor Limit
INTERCEPTOR MACH NO.: 2.0 Initial
σ OF G.C.I. ACCURACY: 5 Values
A.I. DETECTION RANGE AS FRACTION OF SPECIFICATION RANGE, S: ABSCISSA
A.I. DETECTION RANGE CONTOUR: Delta
ALTITUDE: 50 K
AVRO 2.2 Aerodynamics

D17c
F

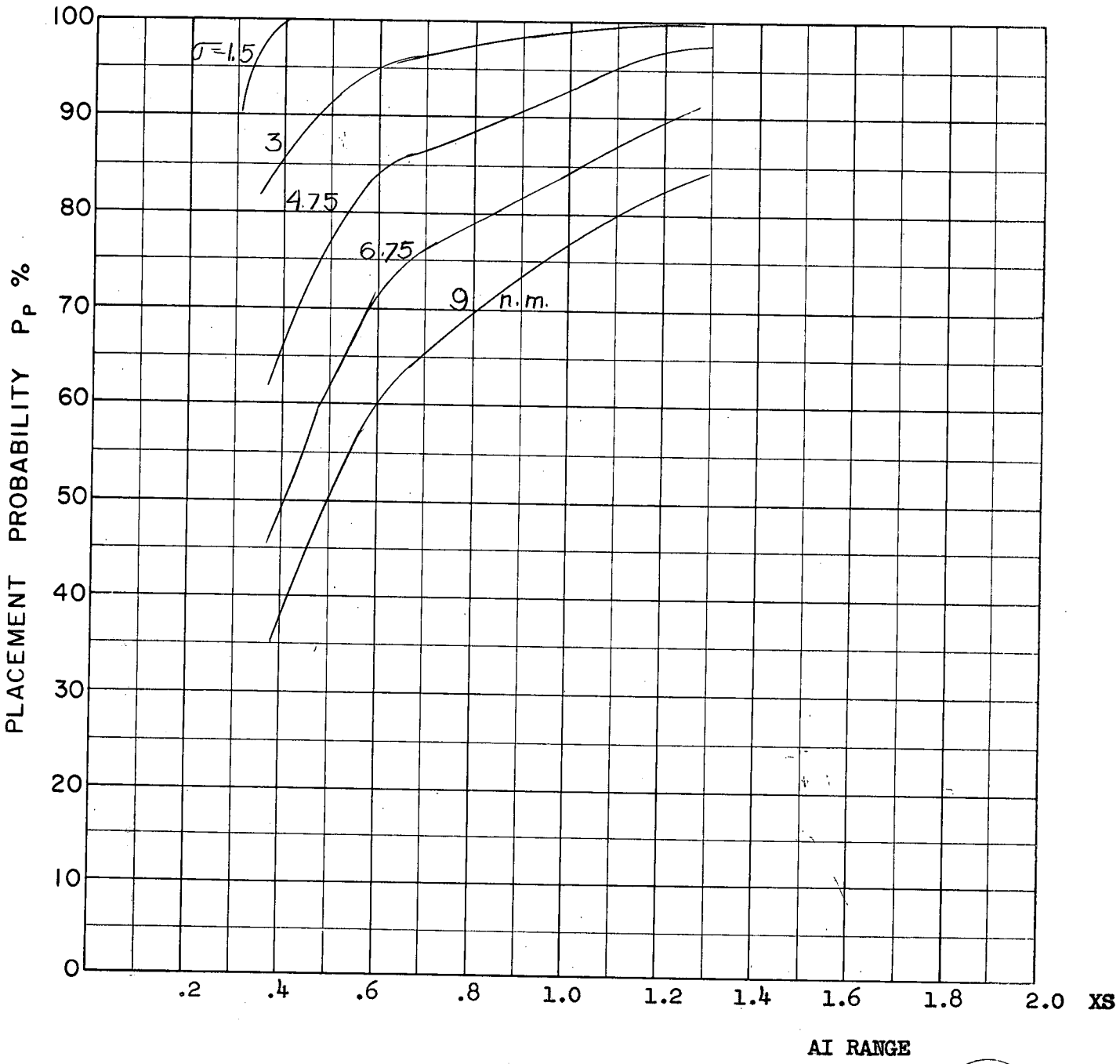

COURSE DIFFERENCE: 110°
TARGET EVASION: 0.5
TARGET MACH NO.: 2.0
INTERCEPTOR LATERAL G's: 4 Load Factor Limit
INTERCEPTOR MACH NO.: 2.0 Initial
σ OF G.C.I. ACCURACY: 5 Values
A.I. DETECTION RANGE AS FRACTION OF SPECIFICATION RANGE, S: ABSCISSA
A.I. DETECTION RANGE CONTOUR: Delta
ALTITUDE: 50 K
AVRO 2.2 Aerodynamics

D18a
F

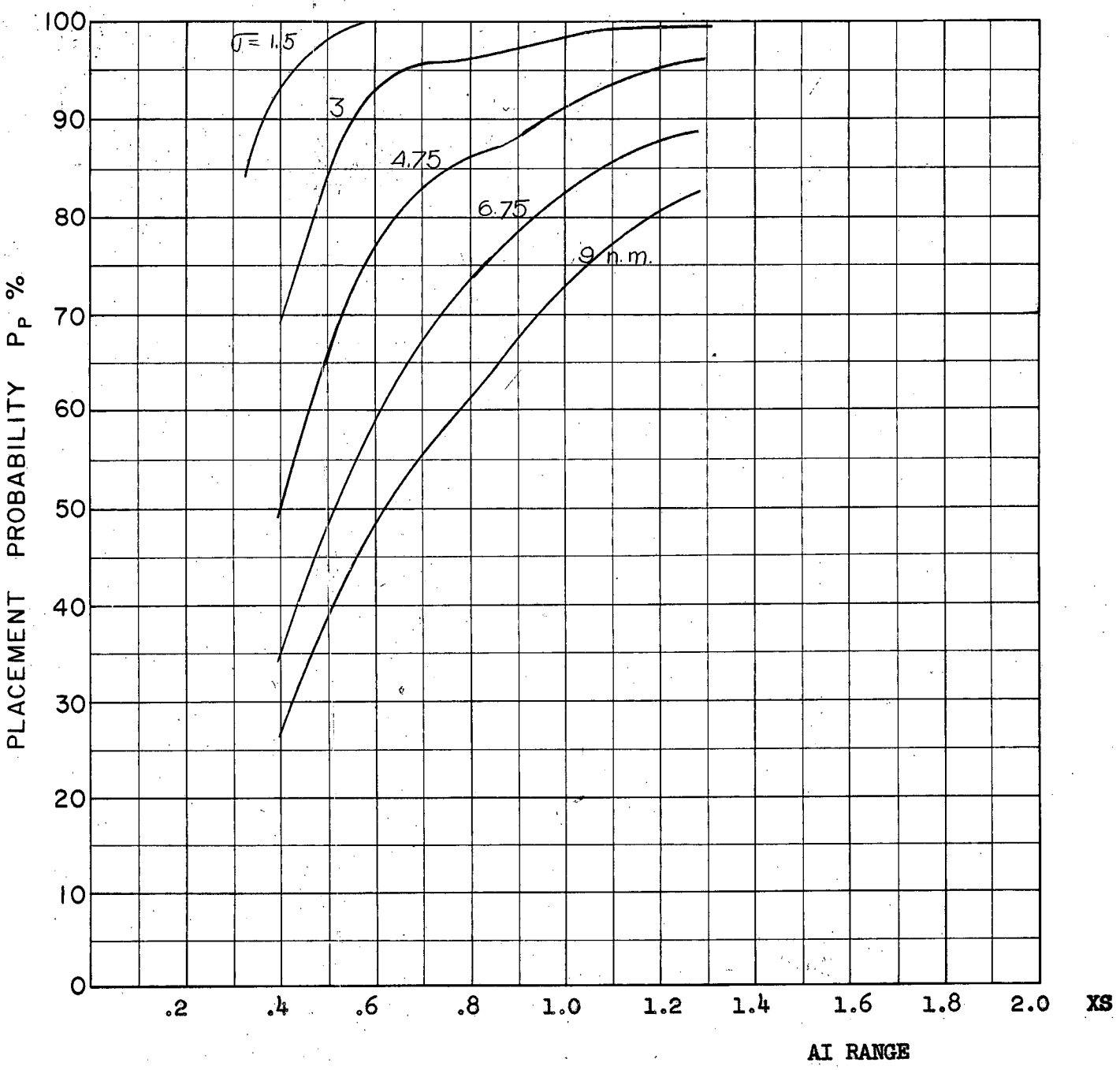

COURSE DIFFERENCE: 110°
TARGET EVASION: 0.5
TARGET MACH NO.: 2.0
INTERCEPTOR LATERAL G's: 2 1/4 Load Factor Limit
INTERCEPTOR MACH NO.: 2.0 Initial
σ OF G.C.I. ACCURACY: 5 Values
A.I. DETECTION RANGE AS FRACTION OF SPECIFICATION RANGE, S: ABSCISSA
A.I. DETECTION RANGE CONTOUR: Delta
ALTITUDE: 50 K
AVRO 2.2 Aerodynamics

D 18b
F

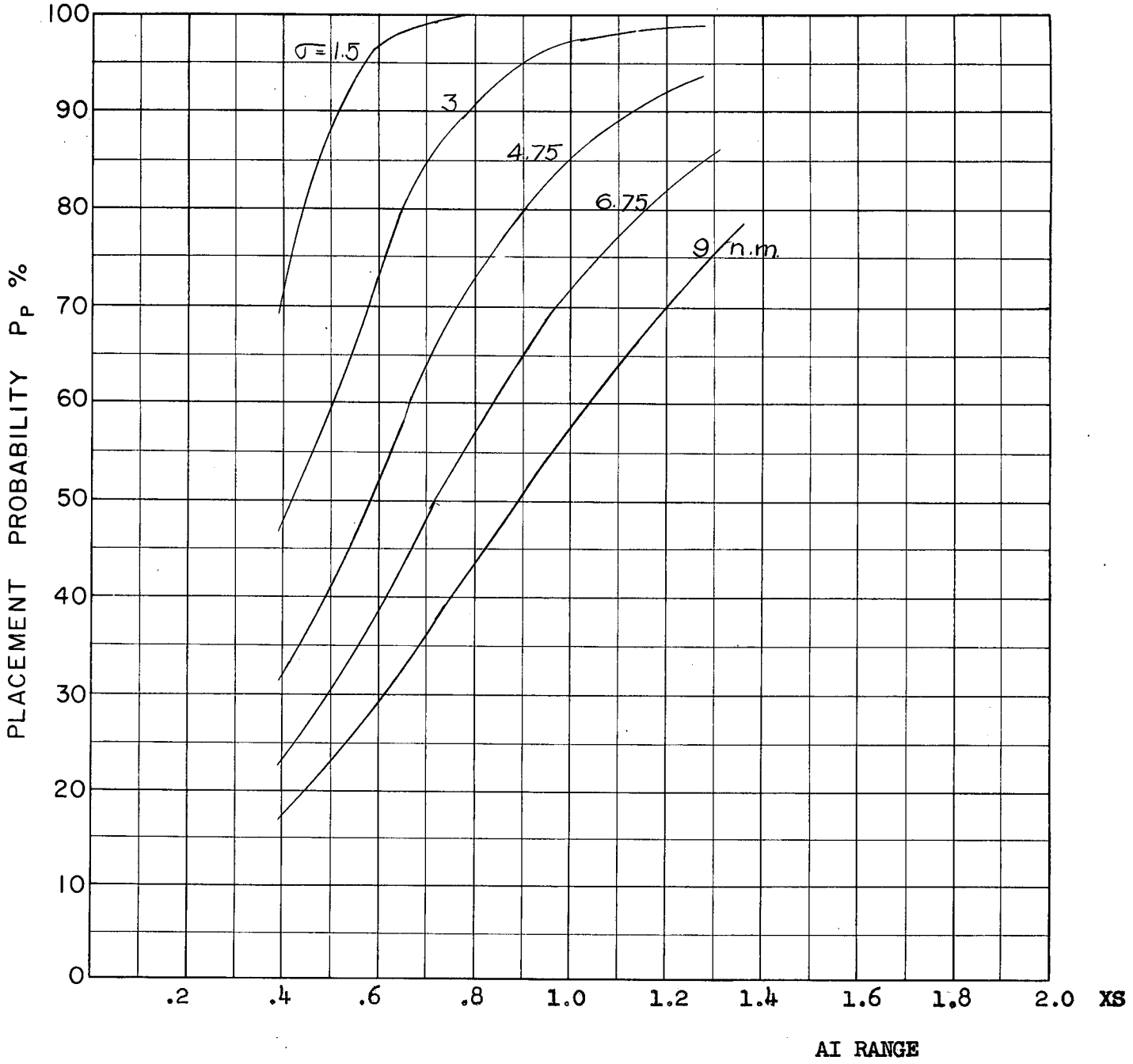

COURSE DIFFERENCE: 110°
TARGET EVASION: 0.5
TARGET MACH NO.: 2.0
INTERCEPTOR LATERAL G's: 1.414 Load Factor Limit
INTERCEPTOR MACH NO.: 2.0 Initial
σ OF G.C.I. ACCURACY: 5 Values
A.I. DETECTION RANGE AS FRACTION OF SPECIFICATION RANGE, S: ABSCISSA
A.I. DETECTION RANGE CONTOUR: Delta
ALTITUDE: 50 K
AVRO 2.2 Aerodynamics

D18c
F

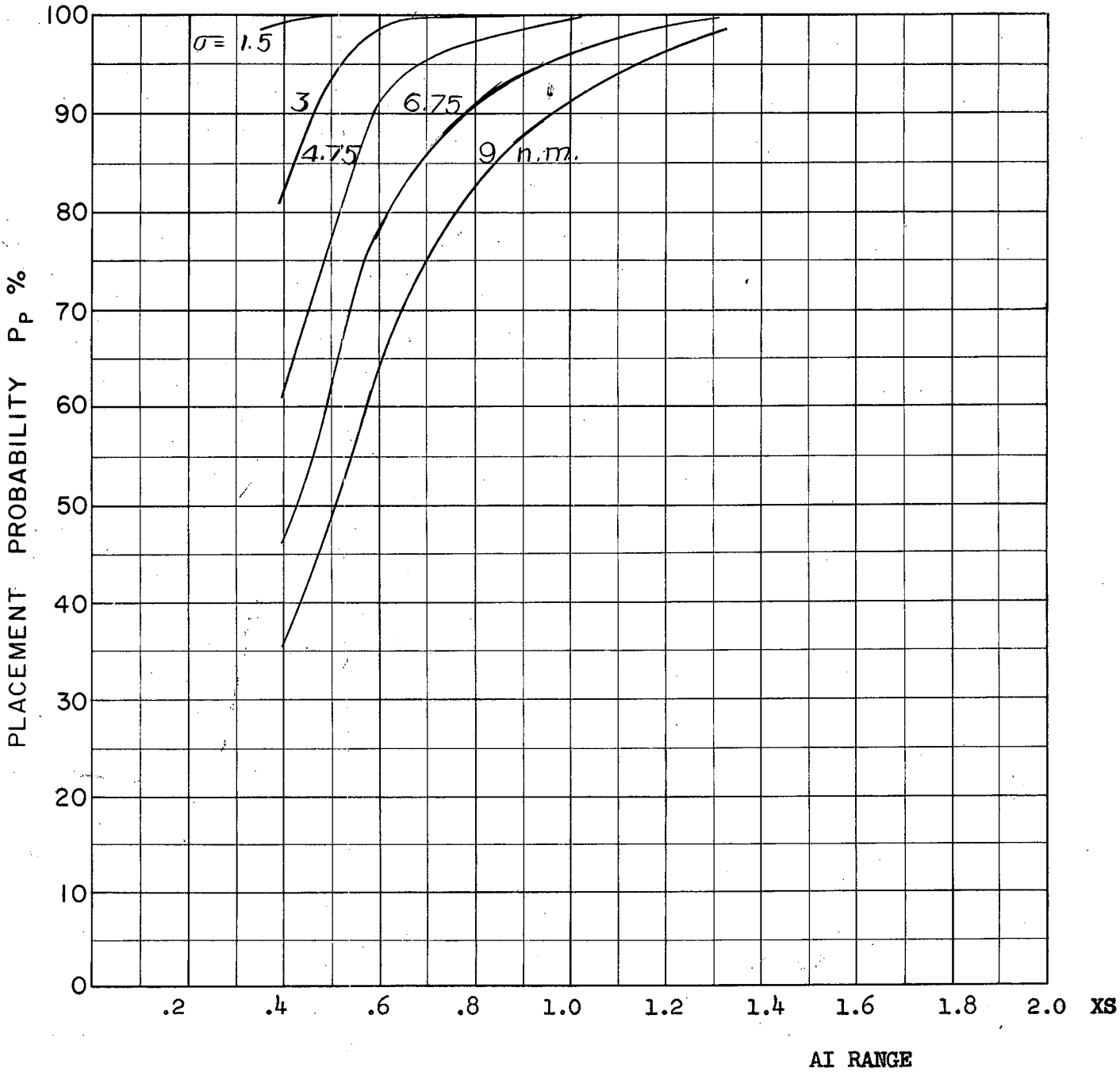

COURSE DIFFERENCE: 135°
TARGET EVASION: 0.5
TARGET MACH NO.: 2.0
INTERCEPTOR LATERAL G's: 4 Load Factor Limit
INTERCEPTOR MACH NO.: 2.0 Initial
σ OF G.C.I. ACCURACY: 5 Values
A.I. DETECTION RANGE AS FRACTION OF SPECIFICATION RANGE, S: ABSCISSA
A.I. DETECTION RANGE CONTOUR: Delta
ALTITUDE: 50 K
AVRO 2.2 Aerodynamics

D19a
F

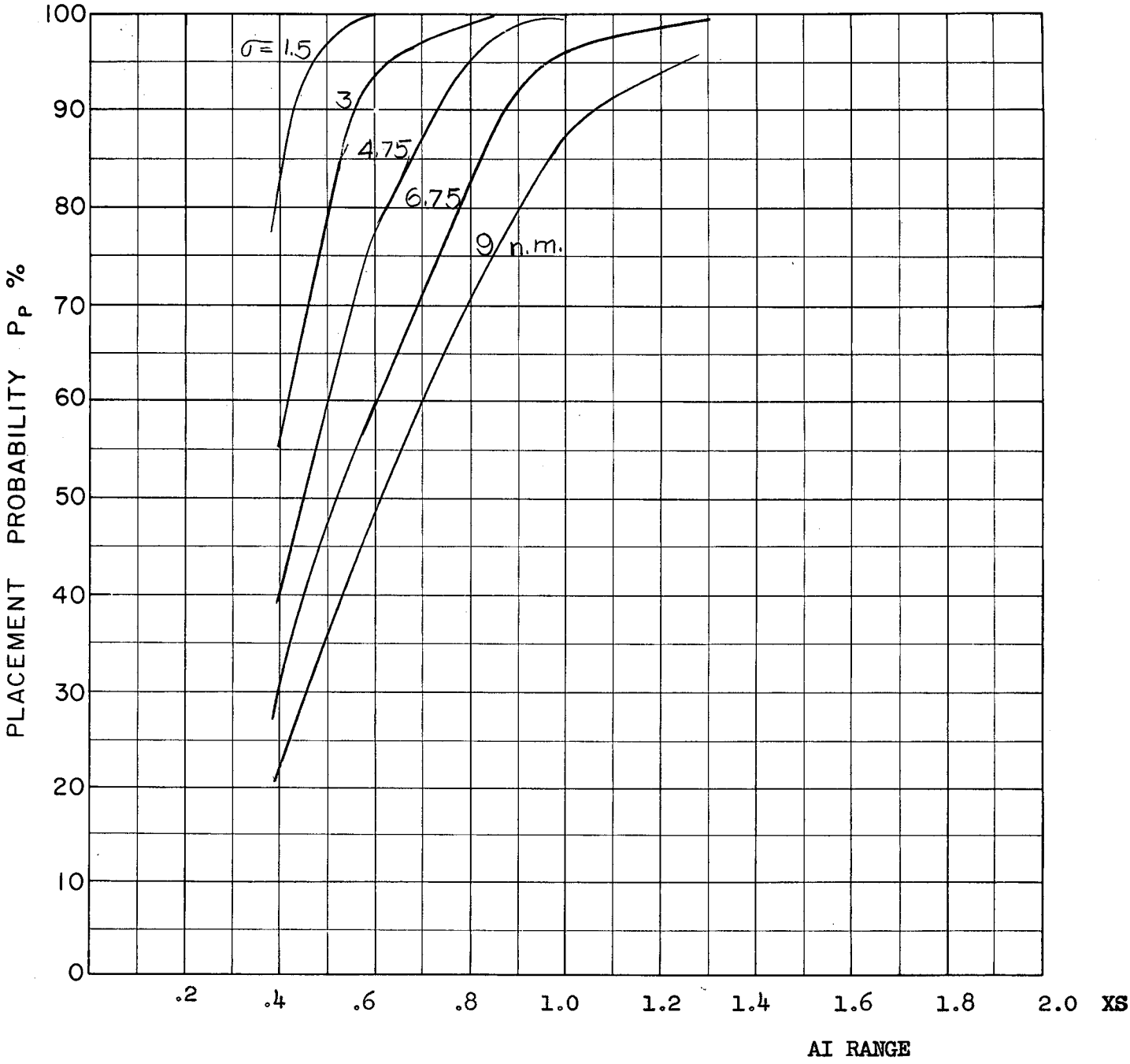

COURSE DIFFERENCE: 135°
TARGET EVASION: 0.5
TARGET MACH NO.: 2.0
INTERCEPTOR LATERAL G's: 2 1/4 Load Factor Limit
INTERCEPTOR MACH NO.: 2.0 Initial
σ OF G.C.I. ACCURACY: 5 Values
A.I. DETECTION RANGE AS FRACTION OF SPECIFICATION RANGE, S: ABSCISSA
A.I. DETECTION RANGE CONTOUR: Delta
ALTITUDE: 50 K
AVRO 2.2 Aerodynamics

D196
F

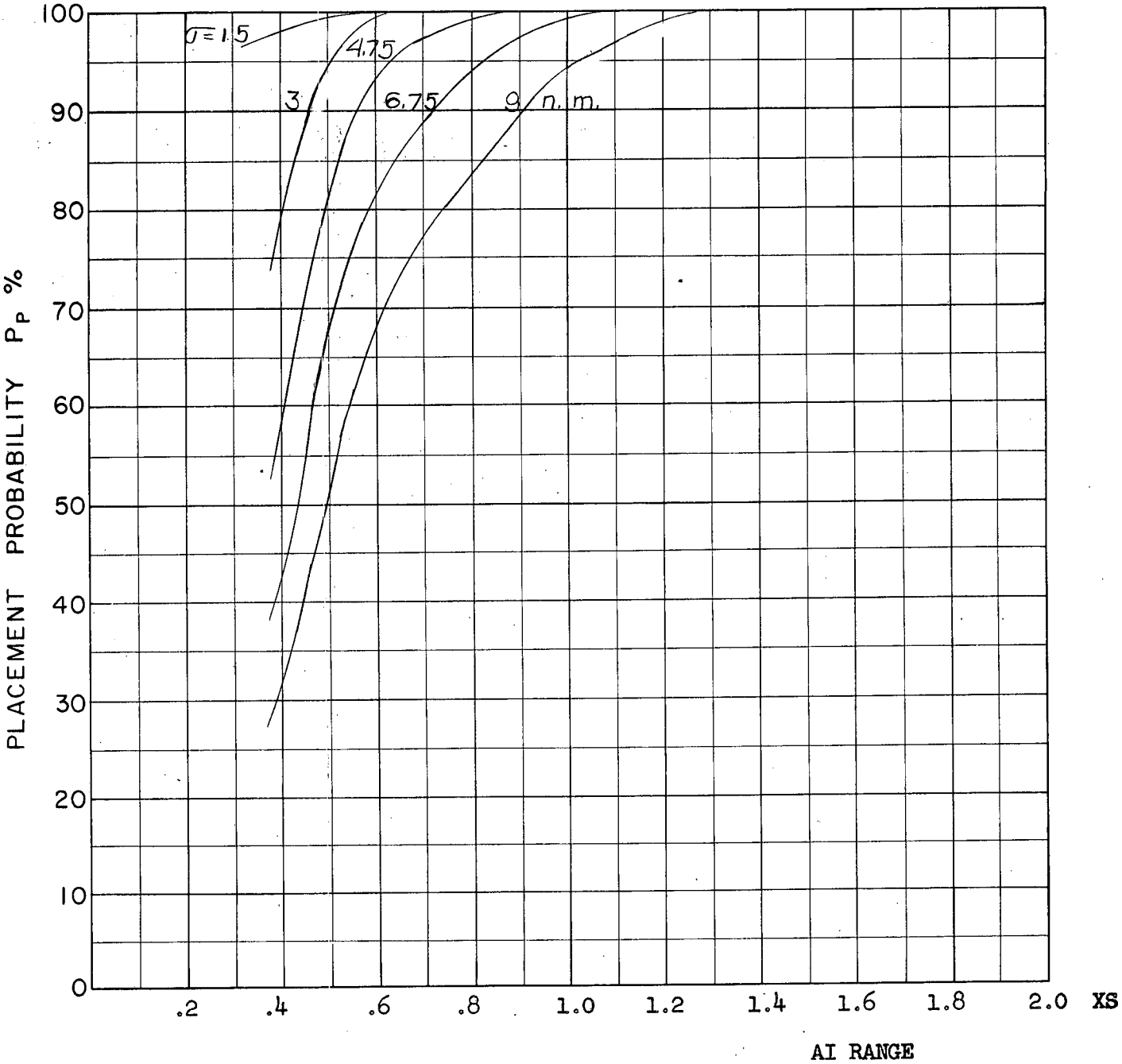

COURSE DIFFERENCE: 160°
TARGET EVASION: 0.5
TARGET MACH NO.: 2.0
INTERCEPTOR LATERAL G's: 4 Load Factor Limit
INTERCEPTOR MACH NO.: 2.0 Initial
σ OF G.C.I. ACCURACY: 5 Values
A.I. DETECTION RANGE AS FRACTION OF SPECIFICATION RANGE, S: ABSCISSA
A.I. DETECTION RANGE CONTOUR: Delta
ALTITUDE: 50 K
AVRO 2.2 Aerodynamics

D 20a
F

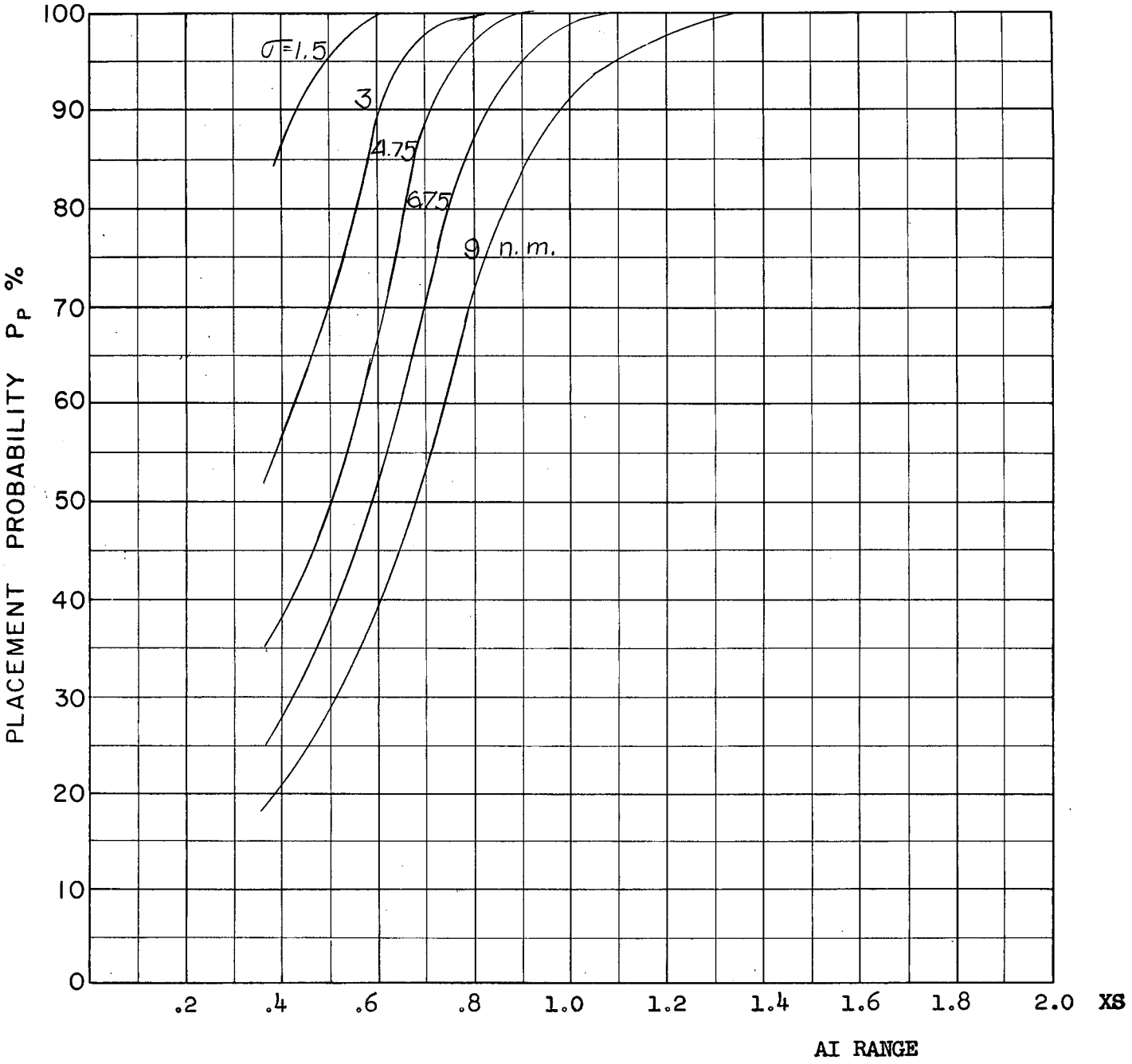

COURSE DIFFERENCE: 160°
TARGET EVASION: 0.5
TARGET MACH NO.: 2.0
INTERCEPTOR LATERAL G's: 2 1/4 Load Factor Limit
INTERCEPTOR MACH NO.: 2.0 Initial
σ OF G.C.I. ACCURACY: 5 Values
A.I. DETECTION RANGE AS FRACTION OF SPECIFICATION RANGE, S: ABSCISSA
A.I. DETECTION RANGE CONTOUR: Delta
ALTITUDE: 50 K
AVRO 2.2 Aerodynamics

D206
F

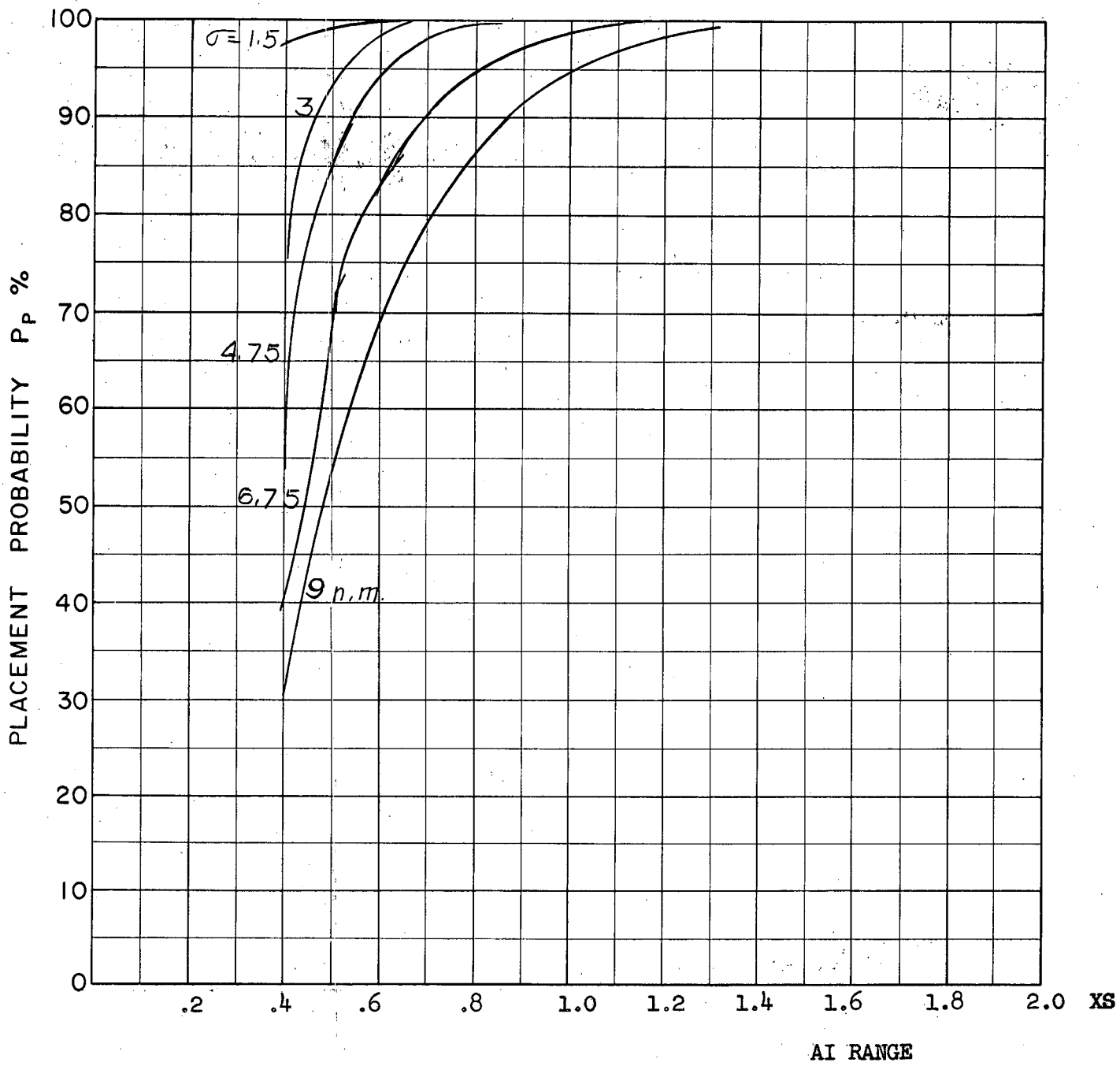

COURSE DIFFERENCE: 180°
TARGET EVASION: 0.5
TARGET MACH NO.: 2.0
INTERCEPTOR LATERAL G's: 4 Load Factor Limit
INTERCEPTOR MACH NO.: 2.0 Initial
σ OF G.C.I. ACCURACY: 5 Values
A.I. DETECTION RANGE AS FRACTION OF SPECIFICATION RANGE, S: ABSCISSA
A.I. DETECTION RANGE CONTOUR: Delta
ALTITUDE: 50 K
AVRO 2.2 Aerodynamics

D21a
F

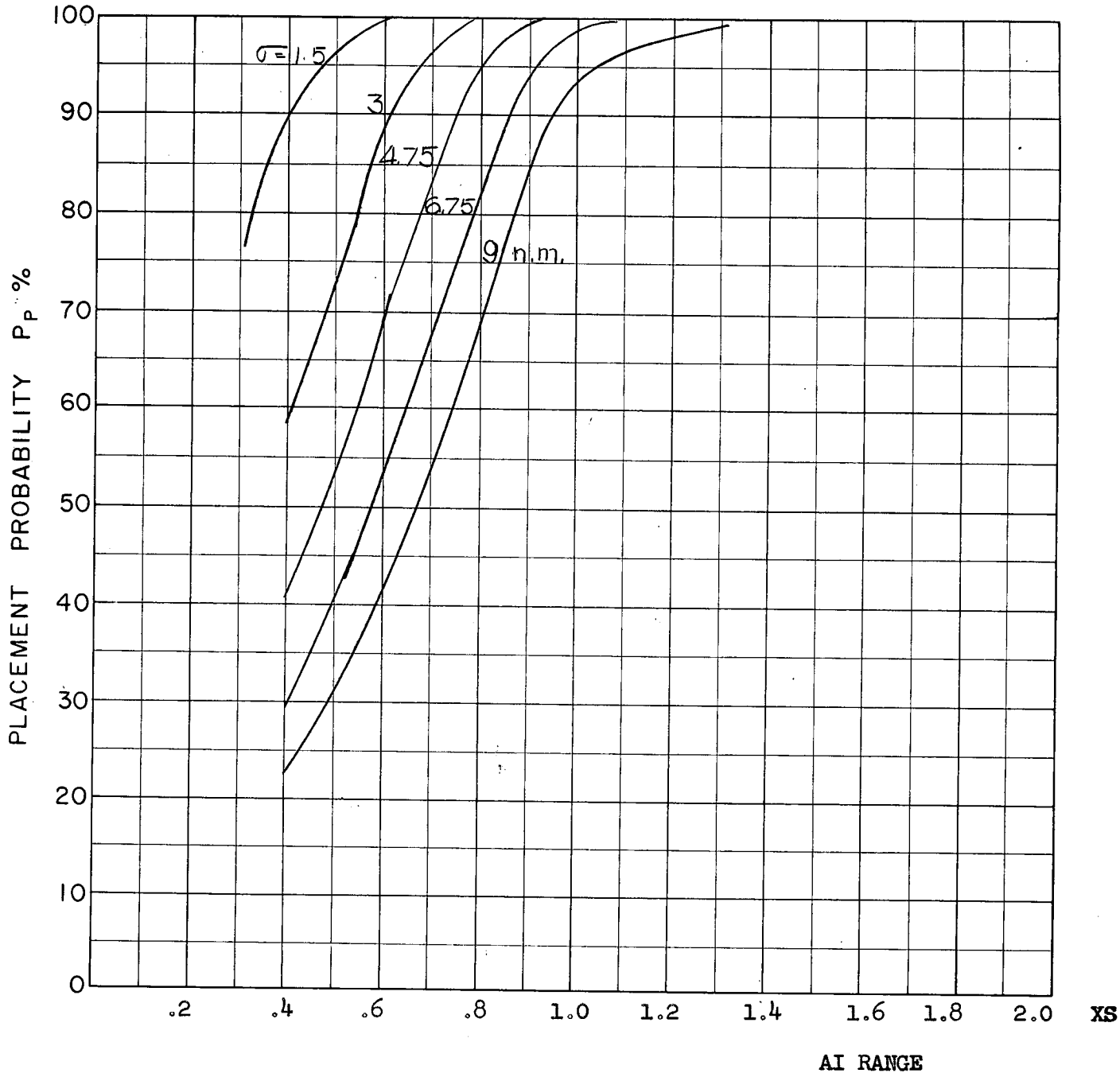

COURSE DIFFERENCE: 180°
TARGET EVASION: 0.5
TARGET MACH NO.: 2.0
INTERCEPTOR LATERAL G's: 2 1/4 Load Factor Limit
INTERCEPTOR MACH NO.: 2.0 Initial
σ OF G.C.I. ACCURACY: 5 Values
A.I. DETECTION RANGE AS FRACTION OF SPECIFICATION RANGE, S: ABSCISSA
A.I. DETECTION RANGE CONTOUR: Delta
ALTITUDE: 50 K
AVRO 2.2 Aerodynamics

D216
F

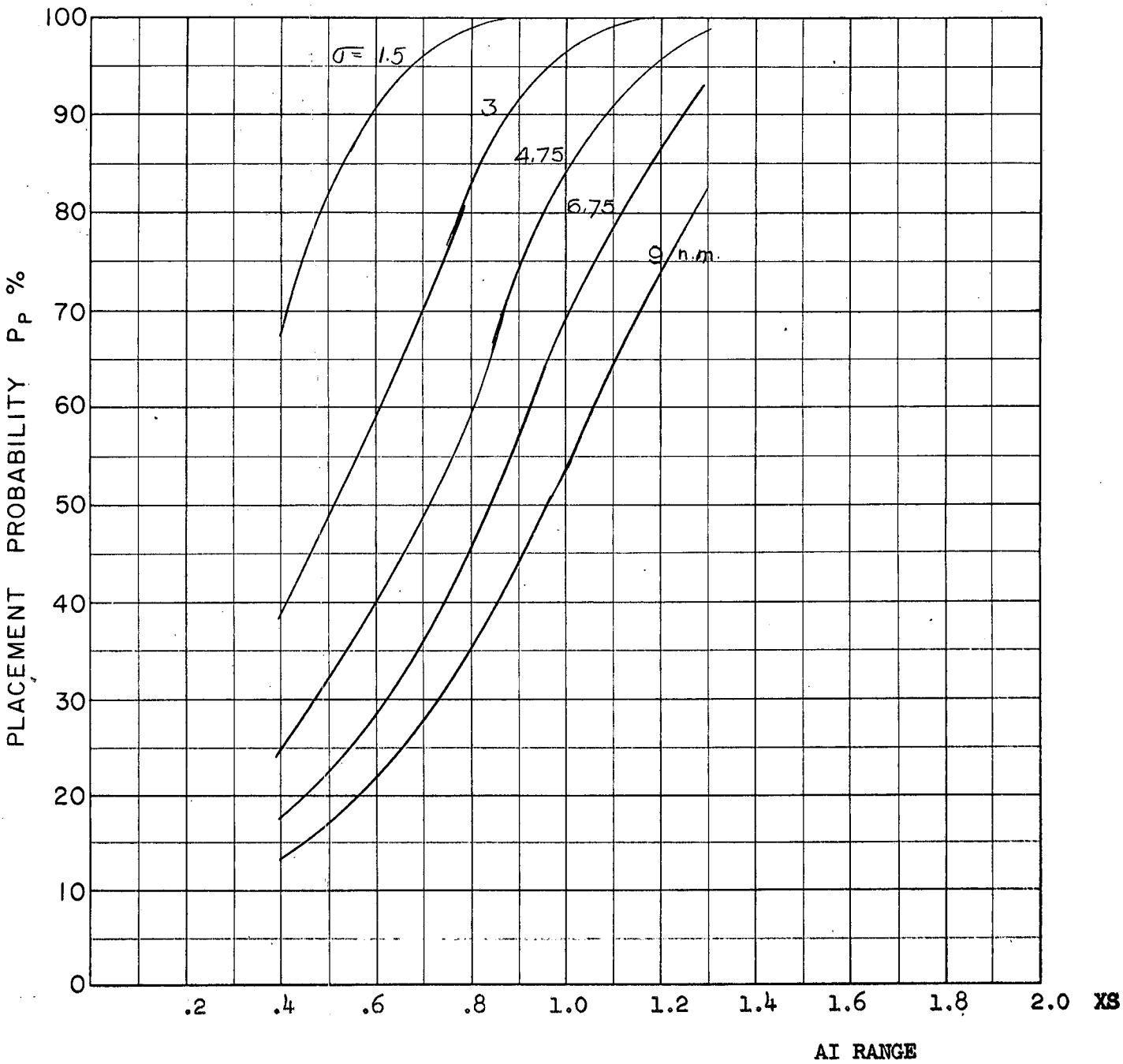

COURSE DIFFERENCE: 180°
TARGET EVASION: 0.5
TARGET MACH NO.: 2.0
INTERCEPTOR LATERAL G's: 1.414 Load Factor Limit
INTERCEPTOR MACH NO.: 2.0 Initial
σ OF G.C.I. ACCURACY: 5 Values
A.I. DETECTION RANGE AS FRACTION OF SPECIFICATION RANGE, S: ABSCISSA
A.I. DETECTION RANGE CONTOUR: Delta
ALTITUDE: 50 K
AVRO 2.2 Aerodynamics

D21c
F

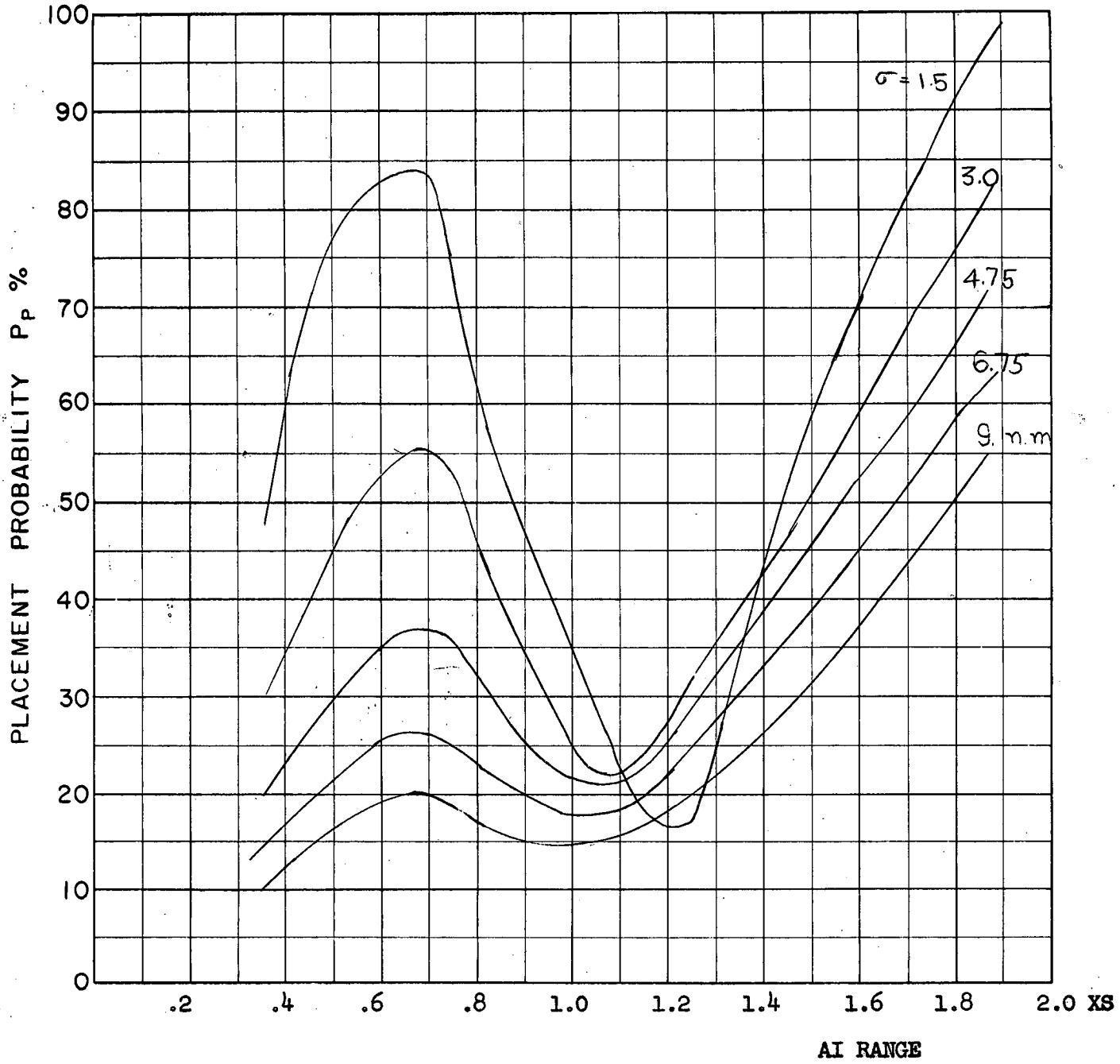

COURSE DIFFERENCE: 90°
TARGET EVASION: 0.5
TARGET MACH NO.: 2.0
INTERCEPTOR LATERAL G's: 1.414 Load Factor Limit
INTERCEPTOR MACH NO.: 1.5 Initial
σ OF G.C.I. ACCURACY: 5 Values
A.I. DETECTION RANGE AS FRACTION OF SPECIFICATION RANGE, S: ABSCISSA
A.I. DETECTION RANGE CONTOUR: Straight
ALTITUDE: 50 K
AVRO 2.2 Aerodynamics

S-1
F

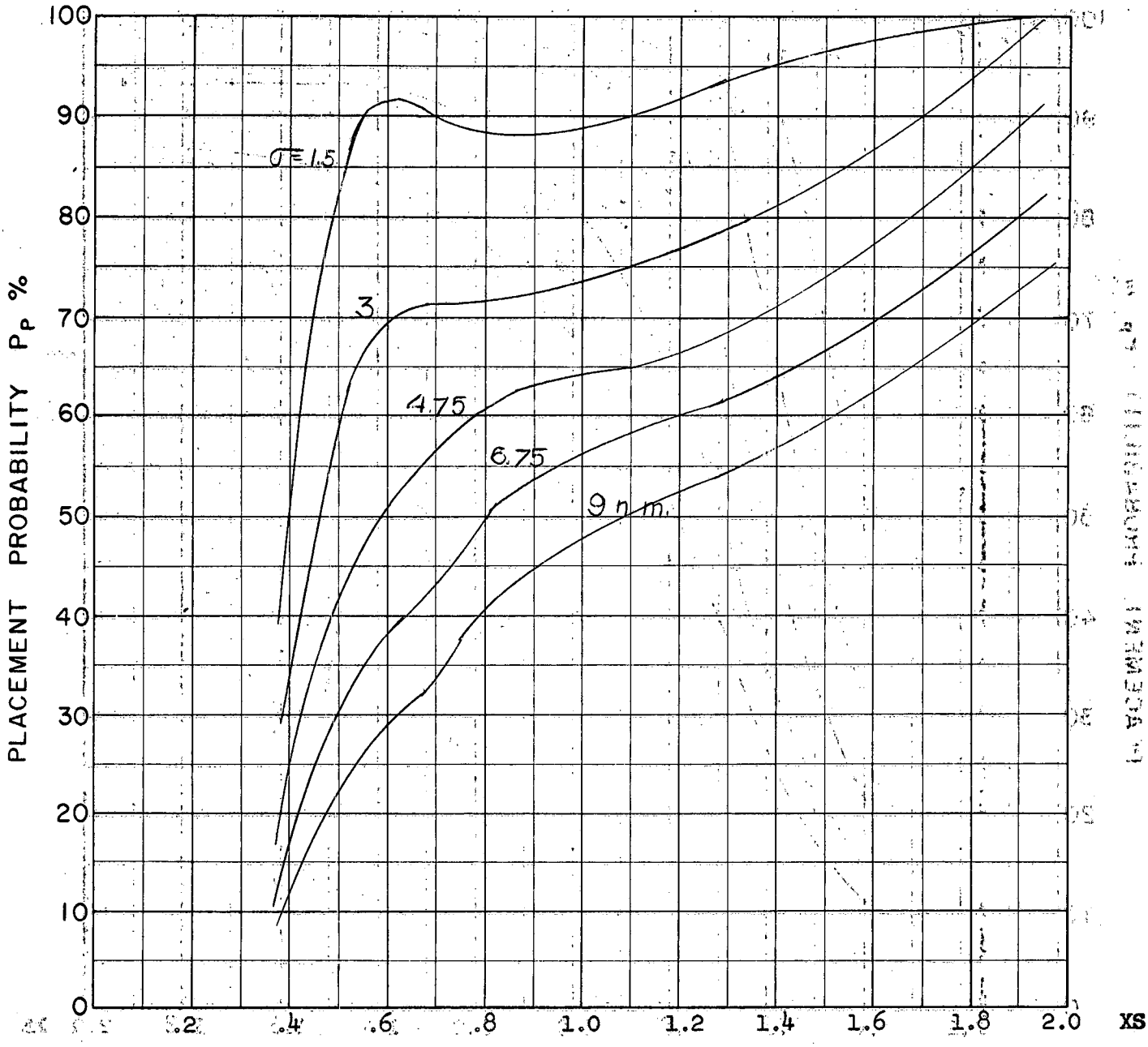

COURSE DIFFERENCE: 110°
TARGET EVASION: 0.5
TARGET MACH NO.: 2.0
INTERCEPTOR LATERAL G's: 4 Load Factor Limit
INTERCEPTOR MACH NO.: 1.5 Initial
σ OF G.C.I. ACCURACY: 5 Values
A.I. DETECTION RANGE AS FRACTION OF SPECIFICATION RANGE, S: ABSCISSA
A.I. DETECTION RANGE CONTOUR: Straight
ALTITUDE: 50 K
AVRO 2.2 Aerodynamics

S2a

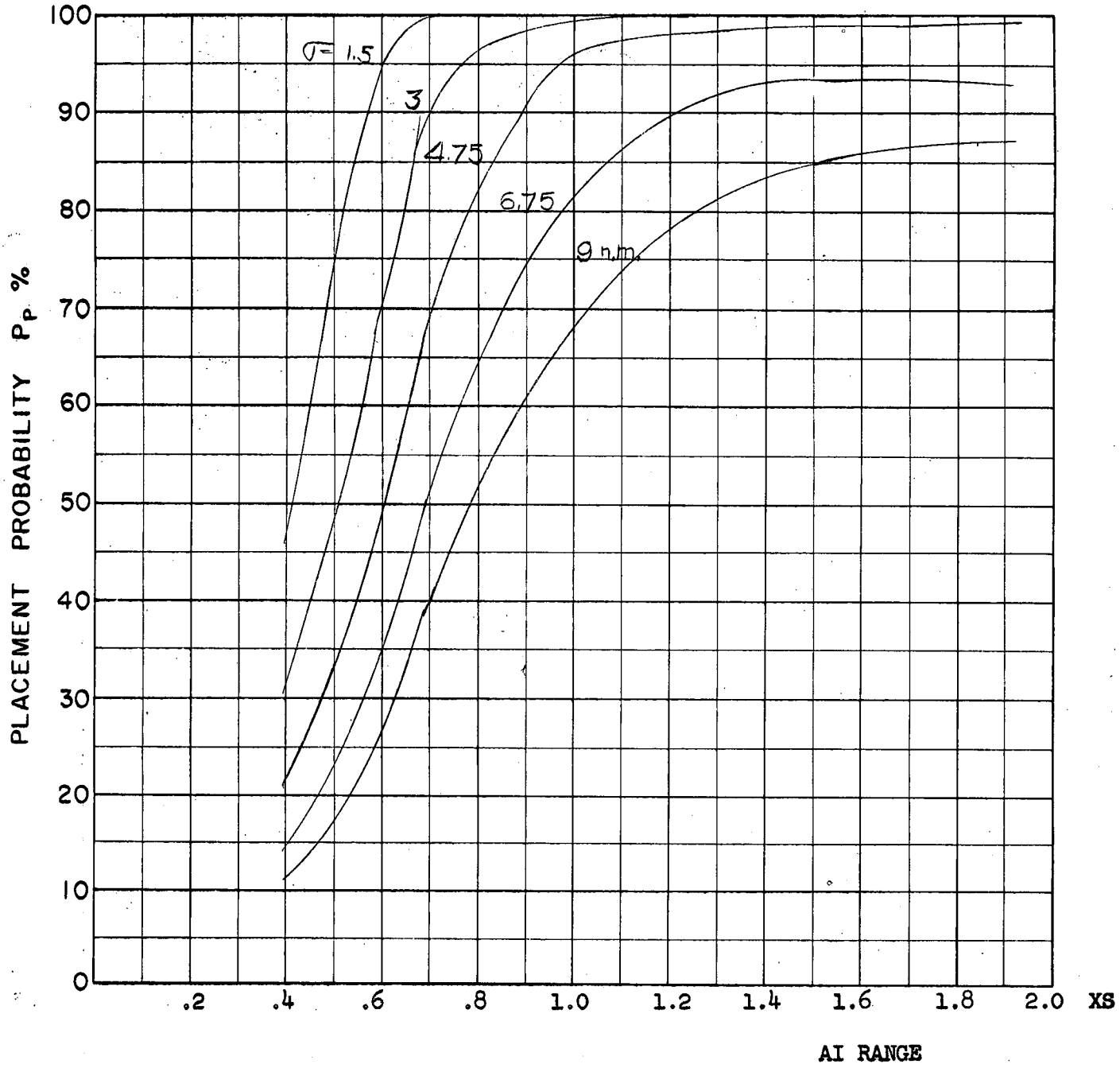

COURSE DIFFERENCE: 110°
TARGET EVASION: 0.5
TARGET MACH NO.: 2.0
INTERCEPTOR LATERAL G's: 2 1/4 Load Factor Limit
INTERCEPTOR MACH NO.: 1.5 Initial
σ OF G.C.I. ACCURACY: 5 Values
A.I. DETECTION RANGE AS FRACTION OF SPECIFICATION RANGE, S: ABSCISSA
A.I. DETECTION RANGE CONTOUR: Straight
ALTITUDE: 50 K
AVRO 2.2 Aerodynamics

S 2b
F

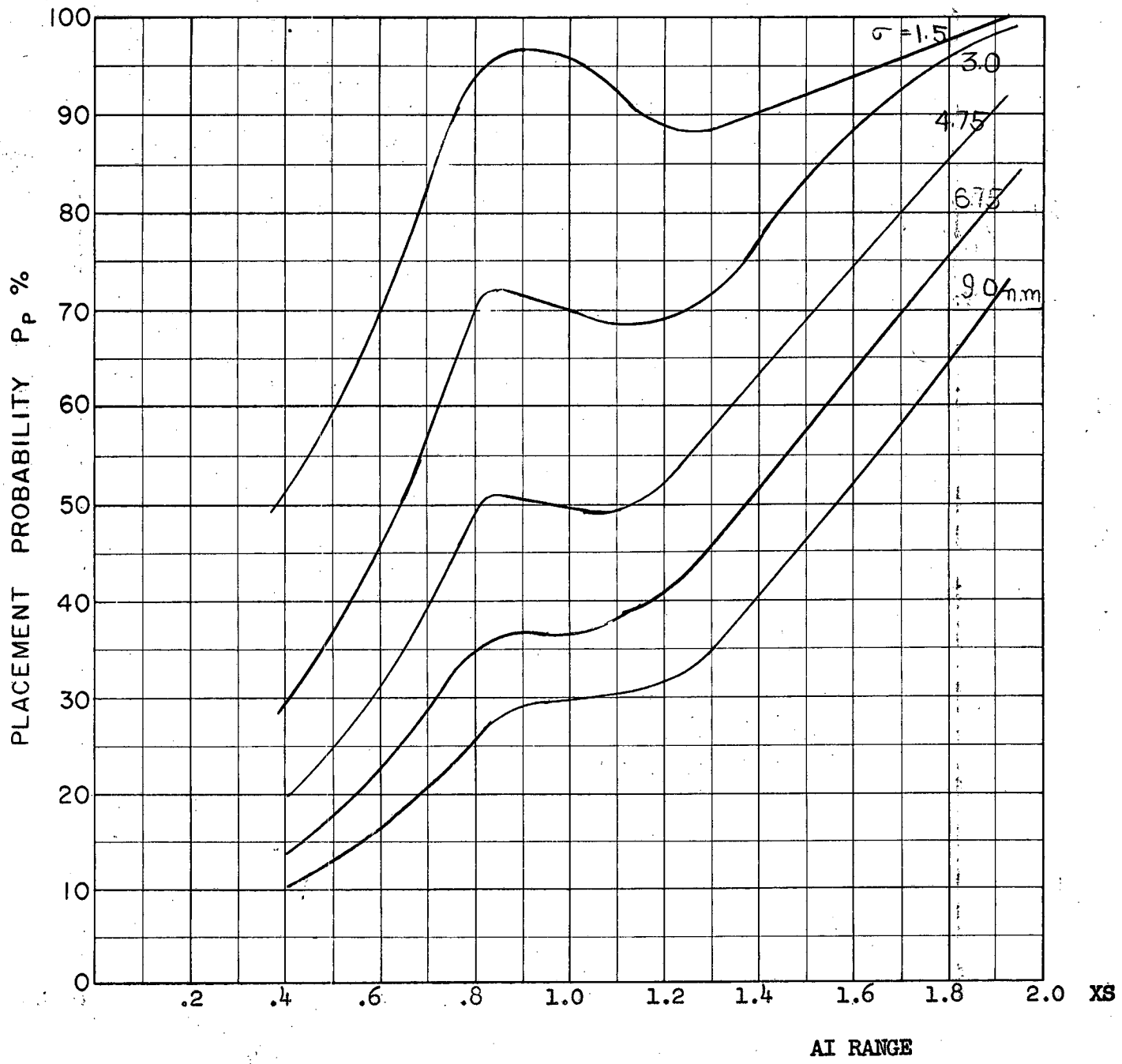

COURSE DIFFERENCE: 110°
TARGET EVASION: 0.5
TARGET MACH NO.: 2.0
INTERCEPTOR LATERAL G's: 1.414 Load Factor Limit
INTERCEPTOR MACH NO.: 1.5 Initial
σ OF G.C.I. ACCURACY: 5 Values
A.I. DETECTION RANGE AS FRACTION OF SPECIFICATION RANGE, S: ABSCISSA
A.I. DETECTION RANGE CONTOUR: Straight
ALTITUDE: 50 K
AVRO 2.2 Aerodynamics

S-2c
F

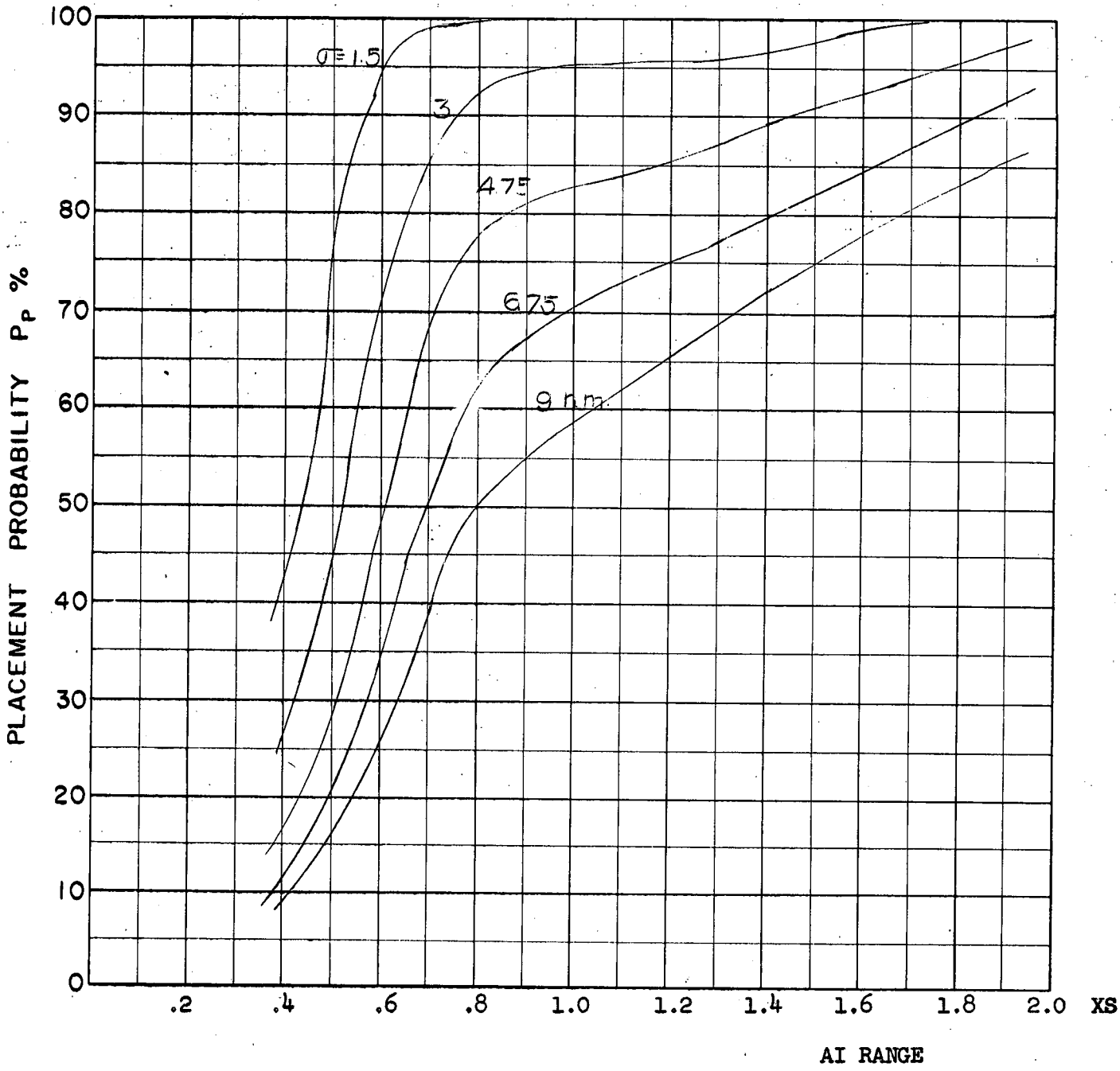

COURSE DIFFERENCE: 135°
TARGET EVASION: 0.5
TARGET MACH NO.: 2.0
INTERCEPTOR LATERAL G's: 4 Load Factor Limit
INTERCEPTOR MACH NO.: 1.5 Initial
σ OF G.C.I. ACCURACY: 5 Values
A.I. DETECTION RANGE AS FRACTION OF SPECIFICATION RANGE, S: ABSCISSA
A.I. DETECTION RANGE CONTOUR: Straight
ALTITUDE: 50 K
AVRO 2.2 Aerodynamics

S3a
F

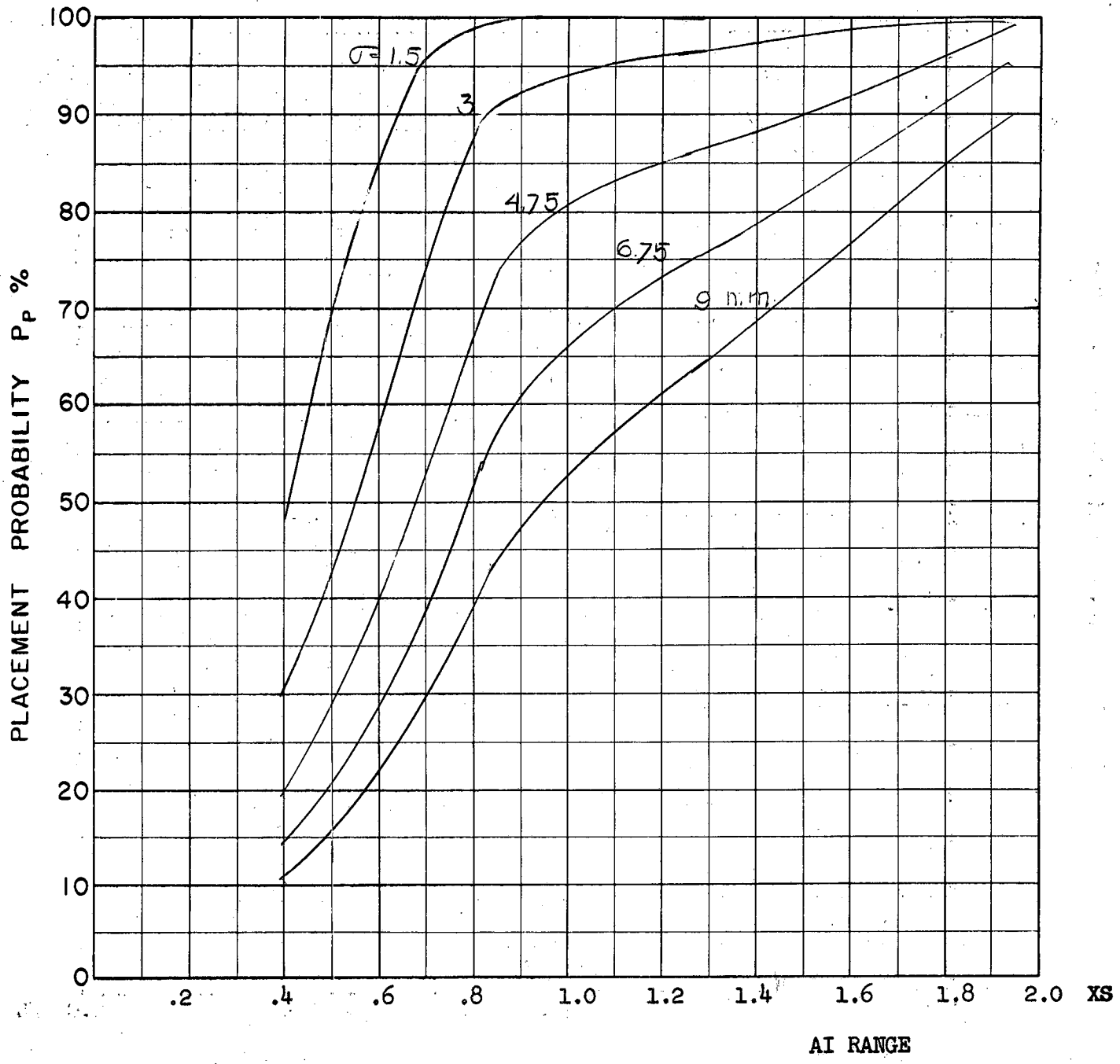

COURSE DIFFERENCE: 135°
TARGET EVASION: 0.5
TARGET MACH NO.: 2.0
INTERCEPTOR LATERAL G's: 2 1/4 Load Factor Limit
INTERCEPTOR MACH NO.: 1.5 Initial
σ OF G.C.I. ACCURACY: 5 Values
A.I. DETECTION RANGE AS FRACTION OF SPECIFICATION RANGE, S: ABSCISSA
A.I. DETECTION RANGE CONTOUR: Straight
ALTITUDE: 50 K
AVRO 2.2 Aerodynamics

S36
F

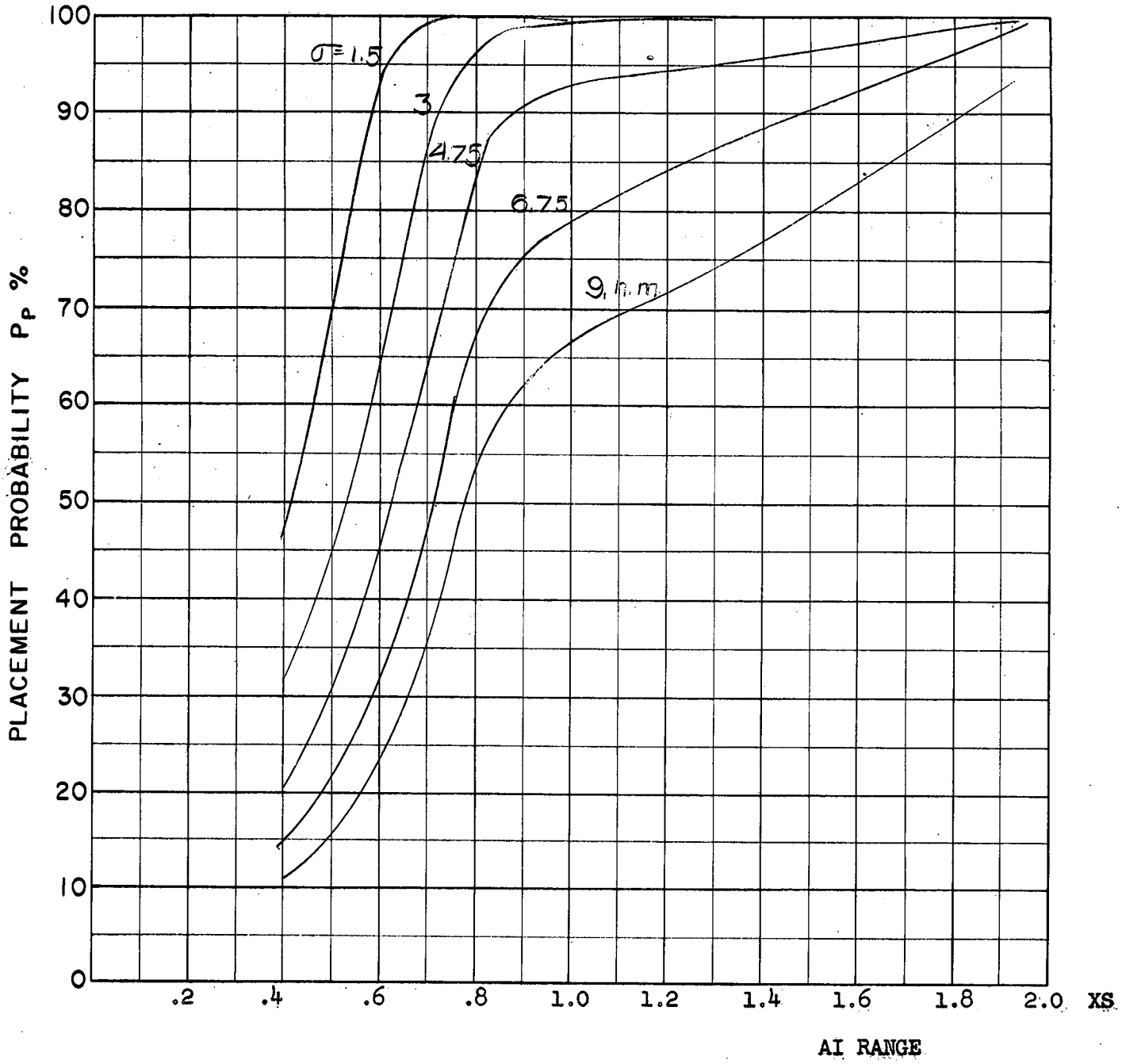

COURSE DIFFERENCE: 160°
TARGET EVASION: 0.5
TARGET MACH NO.: 2.0
INTERCEPTOR LATERAL G's: 4 Load Factor Limit
INTERCEPTOR MACH NO.: 1.5 Initial
σ OF G.C.I. ACCURACY: 5 Values
A.I. DETECTION RANGE AS FRACTION OF SPECIFICATION RANGE, S: ABSCISSA
A.I. DETECTION RANGE CONTOUR: Straight
ALTITUDE: 50 K
AVRO 2.2 Aerodynamics

S4a
F

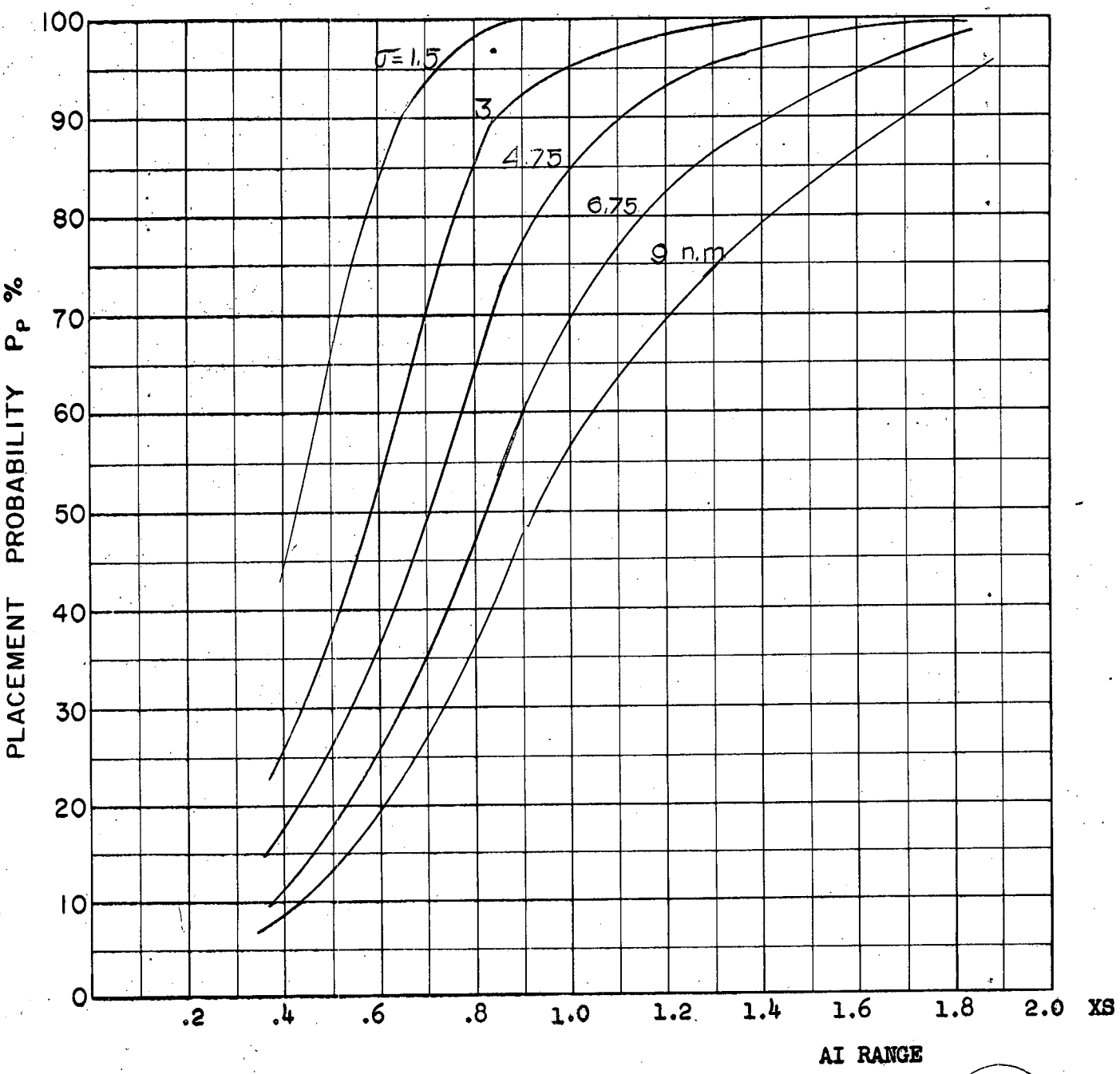

S46
F

COURSE DIFFERENCE: 160°
TARGET EVASION: 0.5
TARGET MACH NO.: 2.0
INTERCEPTOR LATERAL G's: 2 1/4 Load Factor Limit
INTERCEPTOR MACH NO.: 1.5 Initial
σ OF G.C.I. ACCURACY: 5 Values
A.I. DETECTION RANGE AS FRACTION OF SPECIFICATION RANGE, S: ABSCISSA
A.I. DETECTION RANGE CONTOUR: Straight
ALTITUDE: 50 K
AVRO 2.2 Aerodynamics

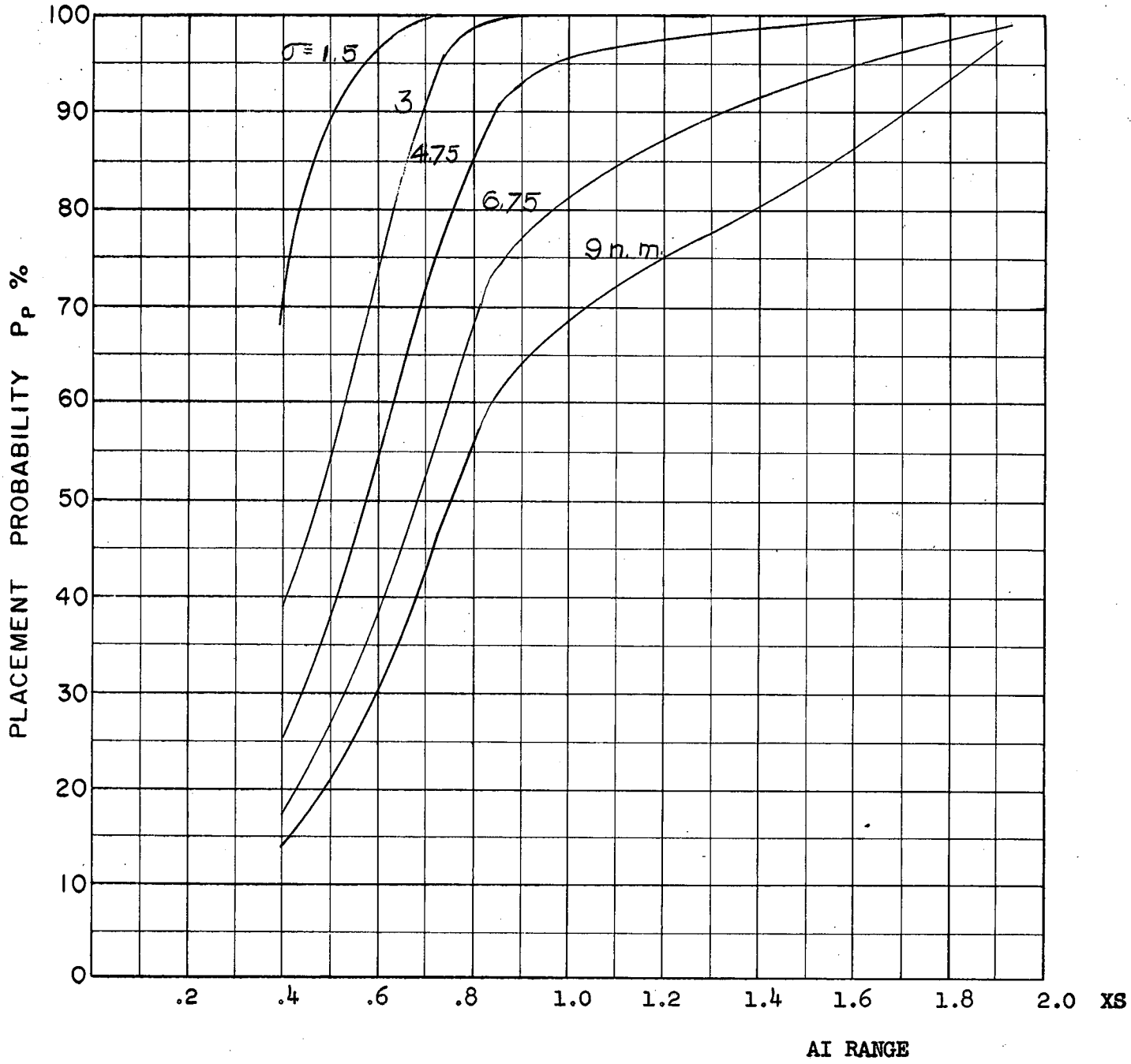

COURSE DIFFERENCE: 180°
TARGET EVASION: 0.5
TARGET MACH NO.: 2.0
INTERCEPTOR LATERAL G's: 4 Load Factor Limit
INTERCEPTOR MACH NO.: 1.5 Initial
σ OF G.C.I. ACCURACY: 5 Values
A.I. DETECTION RANGE AS FRACTION OF SPECIFICATION RANGE, S: ABSCISSA
A.I. DETECTION RANGE CONTOUR: Straight
ALTITUDE: 50 K
AVRO 2.2 Aerodynamics

S5a
F

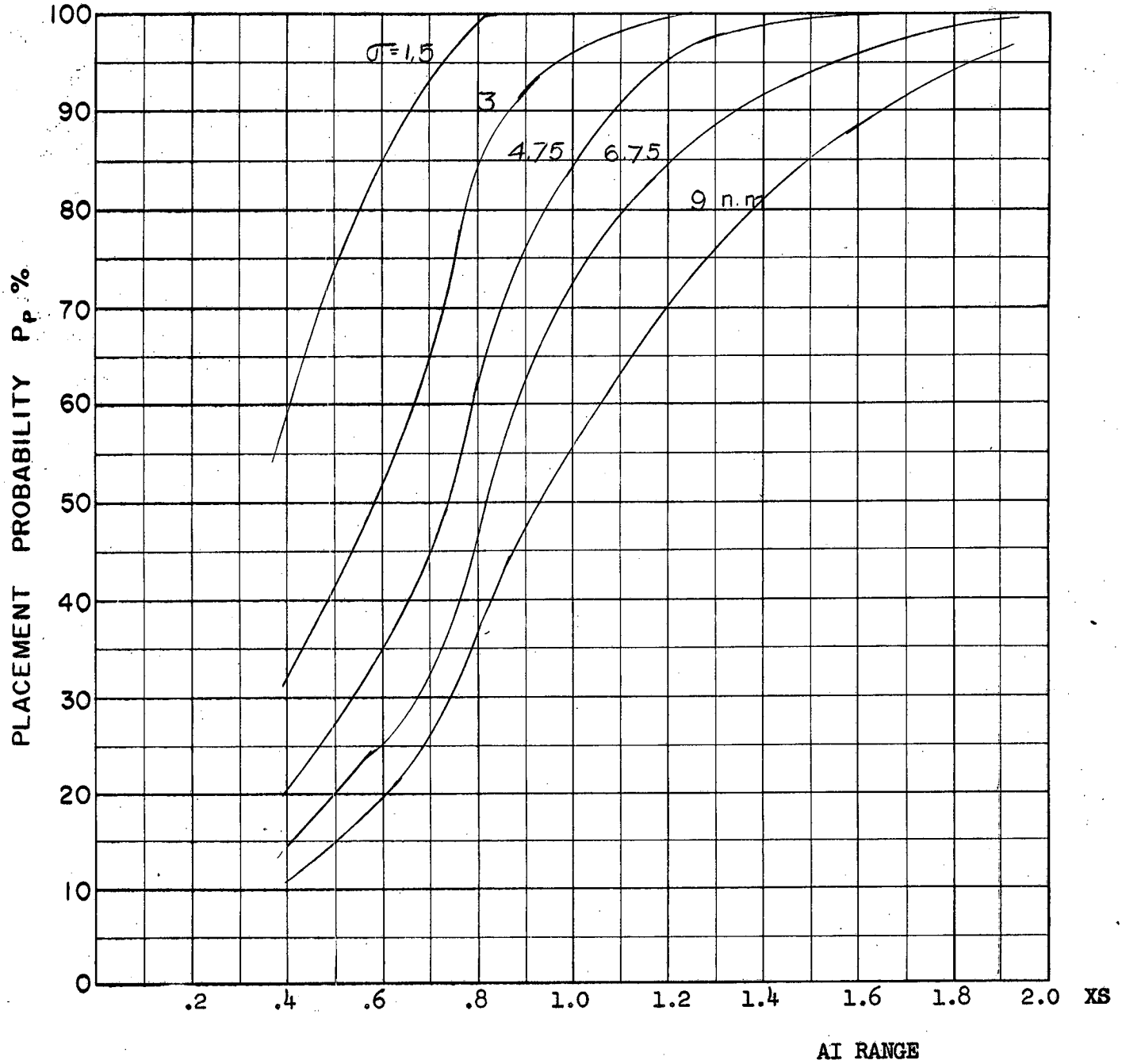

COURSE DIFFERENCE: 180°
TARGET EVASION: 0.5
TARGET MACH NO.: 2.0
INTERCEPTOR LATERAL G's: 2 1/4 Load Factor Limit
INTERCEPTOR MACH NO.: 1.5 Initial
σ OF G.C.I. ACCURACY: 5 Values
A.I. DETECTION RANGE AS FRACTION OF SPECIFICATION RANGE, S: ABSCISSA
A.I. DETECTION RANGE CONTOUR: Straight
ALTITUDE: 50 K
AVRO 2.2 Aerodynamics

S5b
F

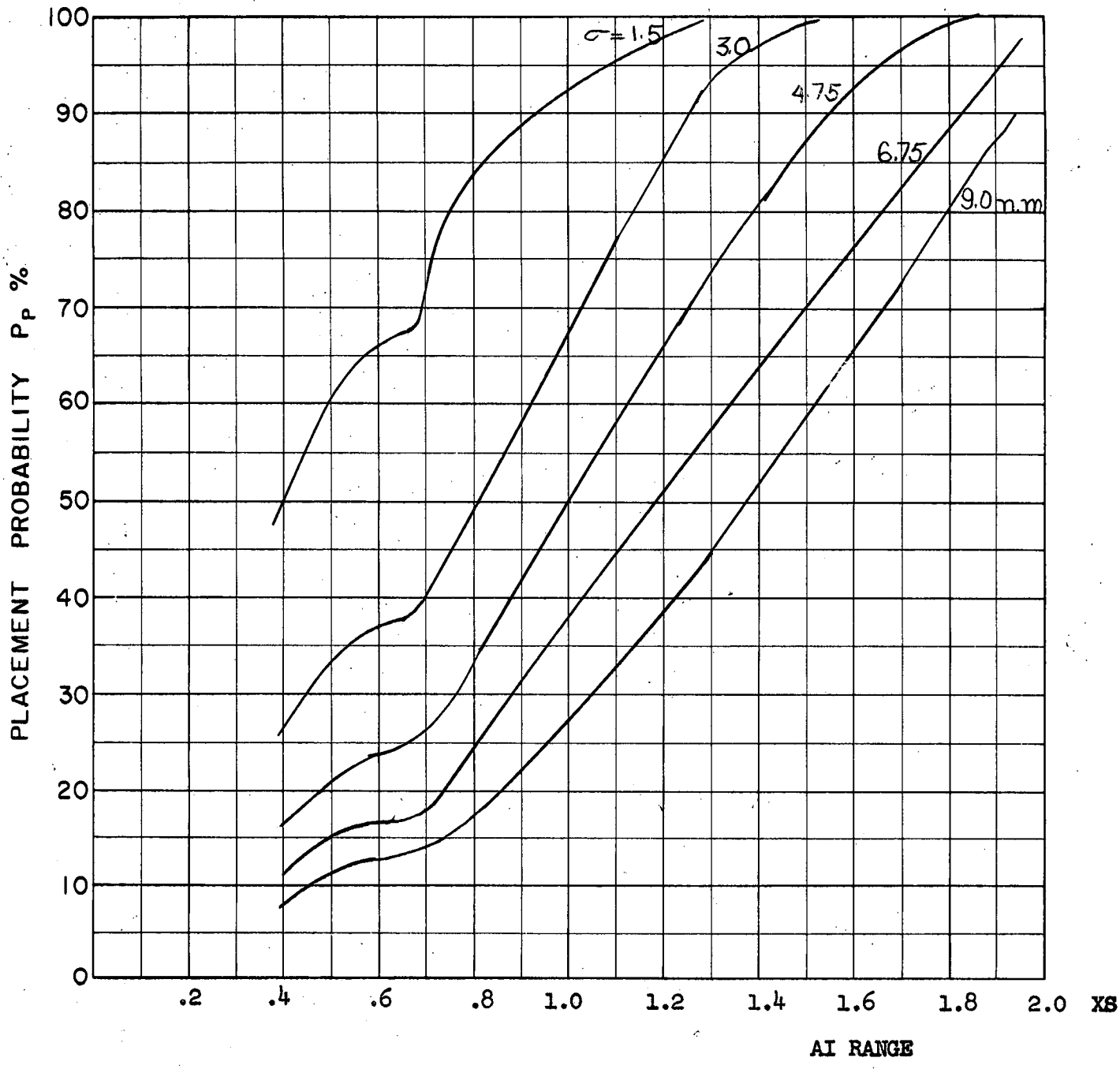

COURSE DIFFERENCE: 180°
TARGET EVASION: 0.5
TARGET MACH NO.: 2.0
INTERCEPTOR LATERAL G's: 1.414 Load Factor Limit
INTERCEPTOR MACH NO.: 1.5 Initial
σ OF G.C.I. ACCURACY: 5 Values
A.I. DETECTION RANGE AS FRACTION OF SPECIFICATION RANGE, S: ABSCISSA
A.I. DETECTION RANGE CONTOUR: Straight
ALTITUDE: 50 K
AVRO 2.2 Aerodynamics

S 5c
F

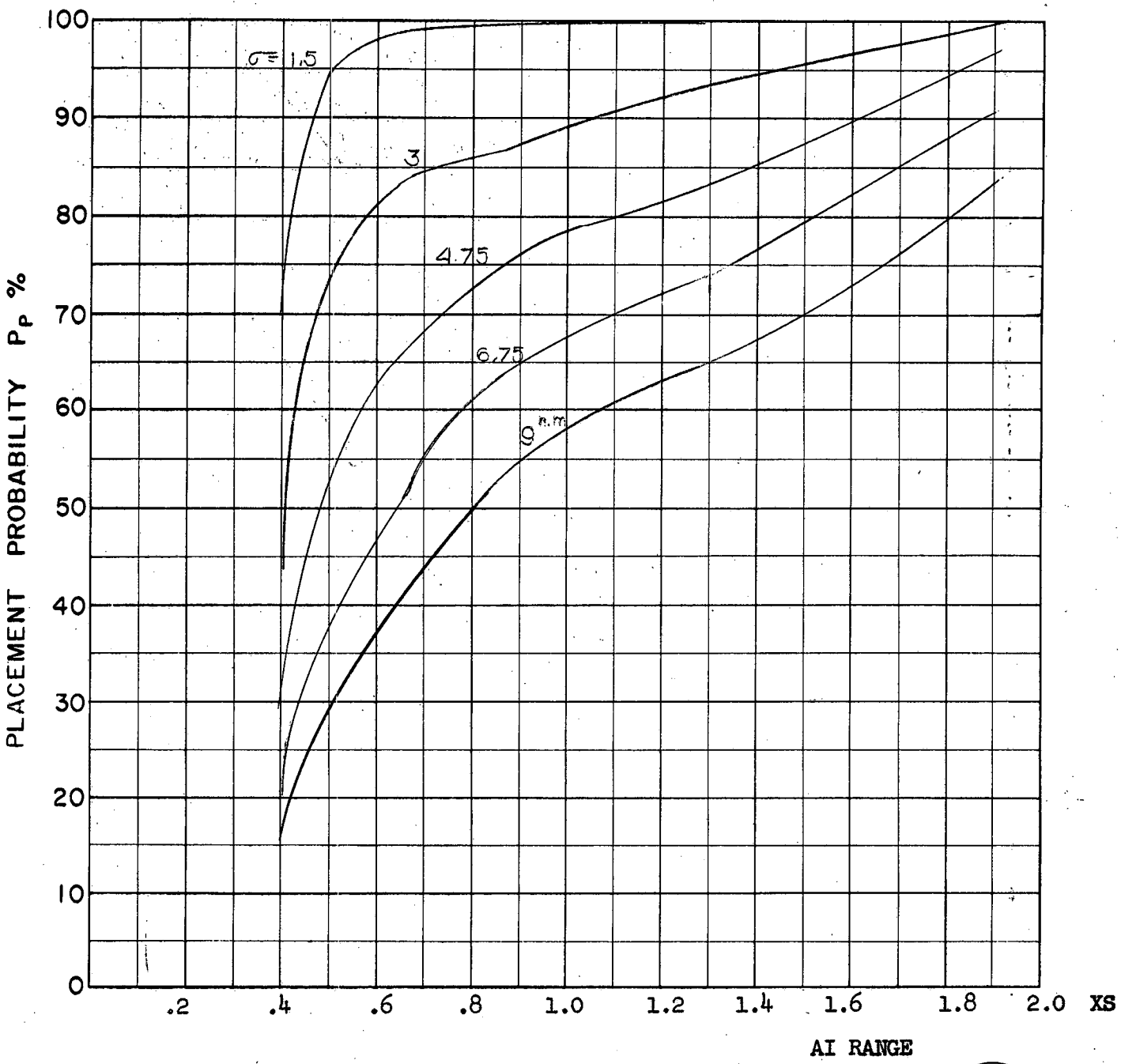

COURSE DIFFERENCE: 110°
TARGET EVASION: 0.5
TARGET MACH NO.: 2.0
INTERCEPTOR LATERAL G's: 4 Load Factor Limit
INTERCEPTOR MACH NO.: 1.8 Initial
σ OF G.C.I. ACCURACY: 5 Values
A.I. DETECTION RANGE AS FRACTION OF SPECIFICATION RANGE, S: ABSCISSA
A.I. DETECTION RANGE CONTOUR: Straight
ALTITUDE: 50 K
AVRO 2.2 Aerodynamics

S 6a
F.

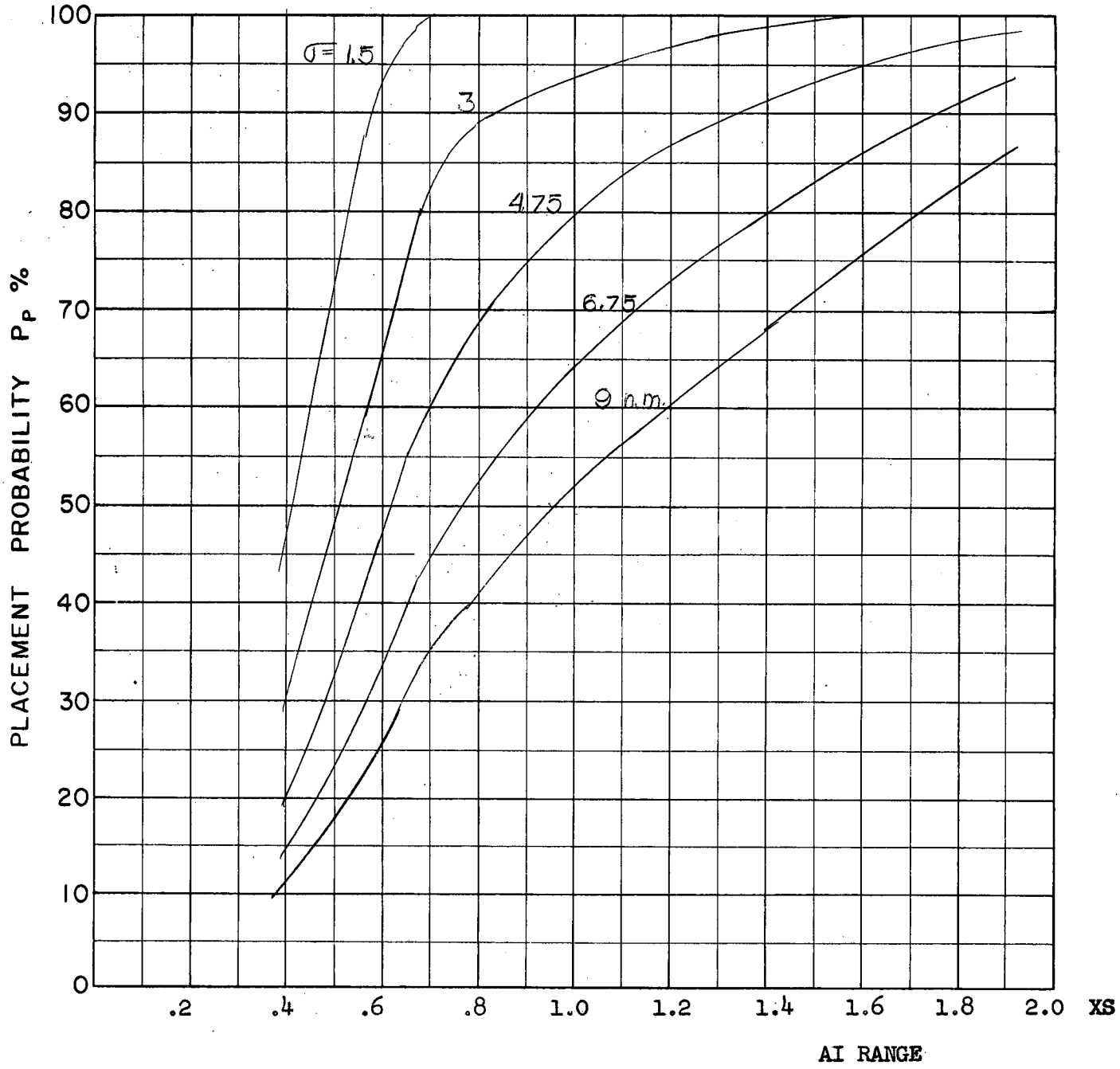

COURSE DIFFERENCE: 110°
TARGET EVASION: 0.5
TARGET MACH NO.: 2.0
INTERCEPTOR LATERAL G's: 2 1/4 Load Factor Limit
INTERCEPTOR MACH NO.: 1.8 Initial
σ OF G.C.I. ACCURACY: 5 Values
A.I. DETECTION RANGE AS FRACTION OF SPECIFICATION RANGE, S: ABSCISSA
A.I. DETECTION RANGE CONTOUR: Straight
ALTITUDE: 50 K
AVRO 2.2 Aerodynamics

S6b
F

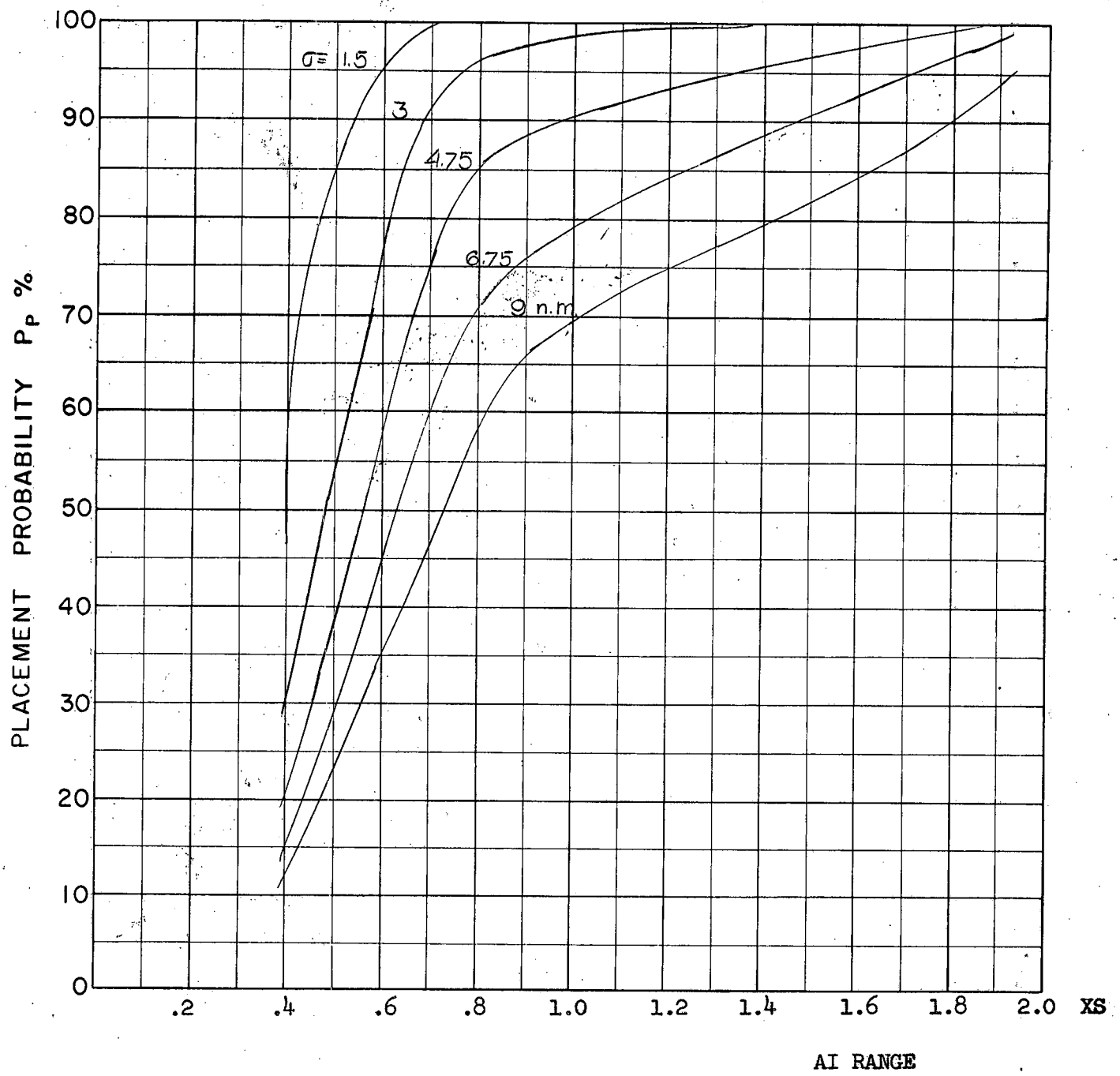

COURSE DIFFERENCE: 135°
TARGET EVASION: 0.5
TARGET MACH NO.: 2.0
INTERCEPTOR LATERAL G's: 4 Load Factor Limit
INTERCEPTOR MACH NO.: 1.8 Initial
σ OF G.C.I. ACCURACY: 5 Values
A.I. DETECTION RANGE AS FRACTION OF SPECIFICATION RANGE, S: ABSCISSA
A.I. DETECTION RANGE CONTOUR: Straight
ALTITUDE: 50 K
AVRO 2.2 Aerodynamics

57a
F

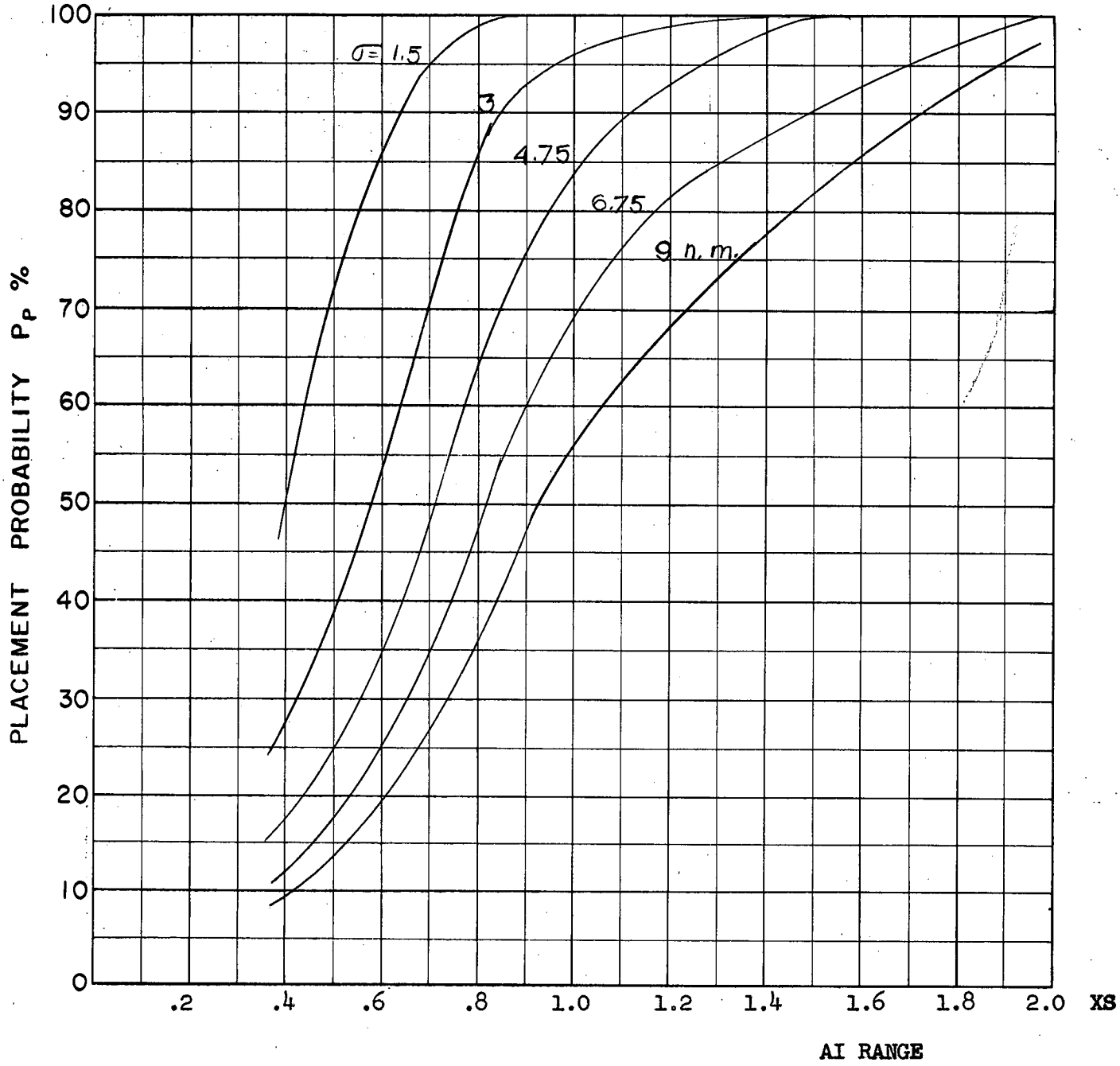

COURSE DIFFERENCE: 135°
TARGET EVASION: 0.5
TARGET MACH NO.: 2.0
INTERCEPTOR LATERAL G's: 2 1/4 Load Factor Limit
INTERCEPTOR MACH NO.: 1.8 Initial
σ OF G.C.I. ACCURACY: 5 Values
A.I. DETECTION RANGE AS FRACTION OF SPECIFICATION RANGE, S: ABSCISSA
A.I. DETECTION RANGE CONTOUR: Straight
ALTITUDE: 50 K
AVRO 2.2 Aerodynamics

S7b
F

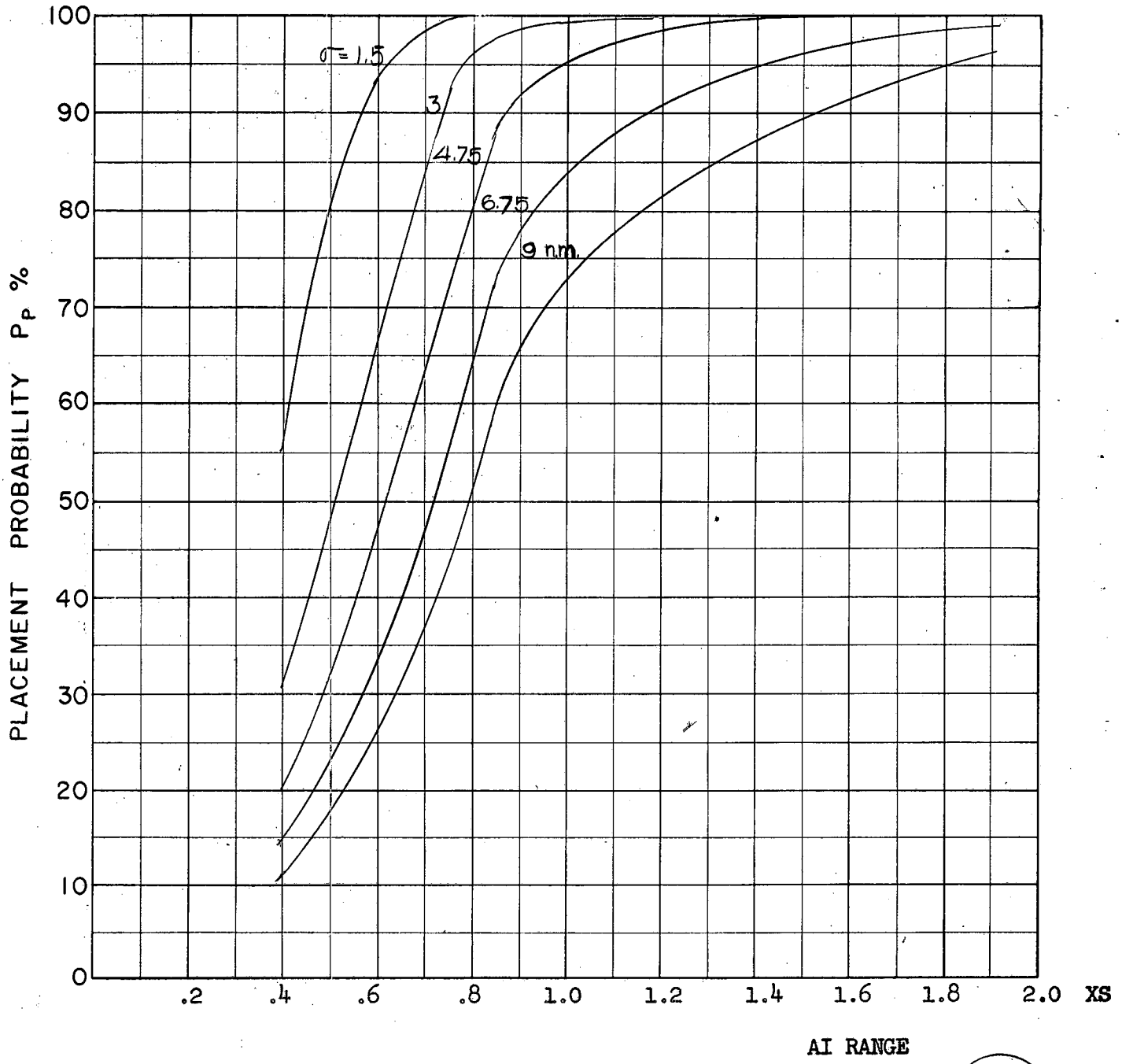

COURSE DIFFERENCE: 160°
TARGET EVASION: 0.5
TARGET MACH NO.: 2.0
INTERCEPTOR LATERAL G's: 4 Load Factor Limit
INTERCEPTOR MACH NO.: 1.8 Initial
σ OF G.C.I. ACCURACY: 5 Values
A.I. DETECTION RANGE AS FRACTION OF SPECIFICATION RANGE, S: ABSCISSA
A.I. DETECTION RANGE CONTOUR: Straight
ALTITUDE: 50 K
AVRO 2.2 Aerodynamics

S8a
F

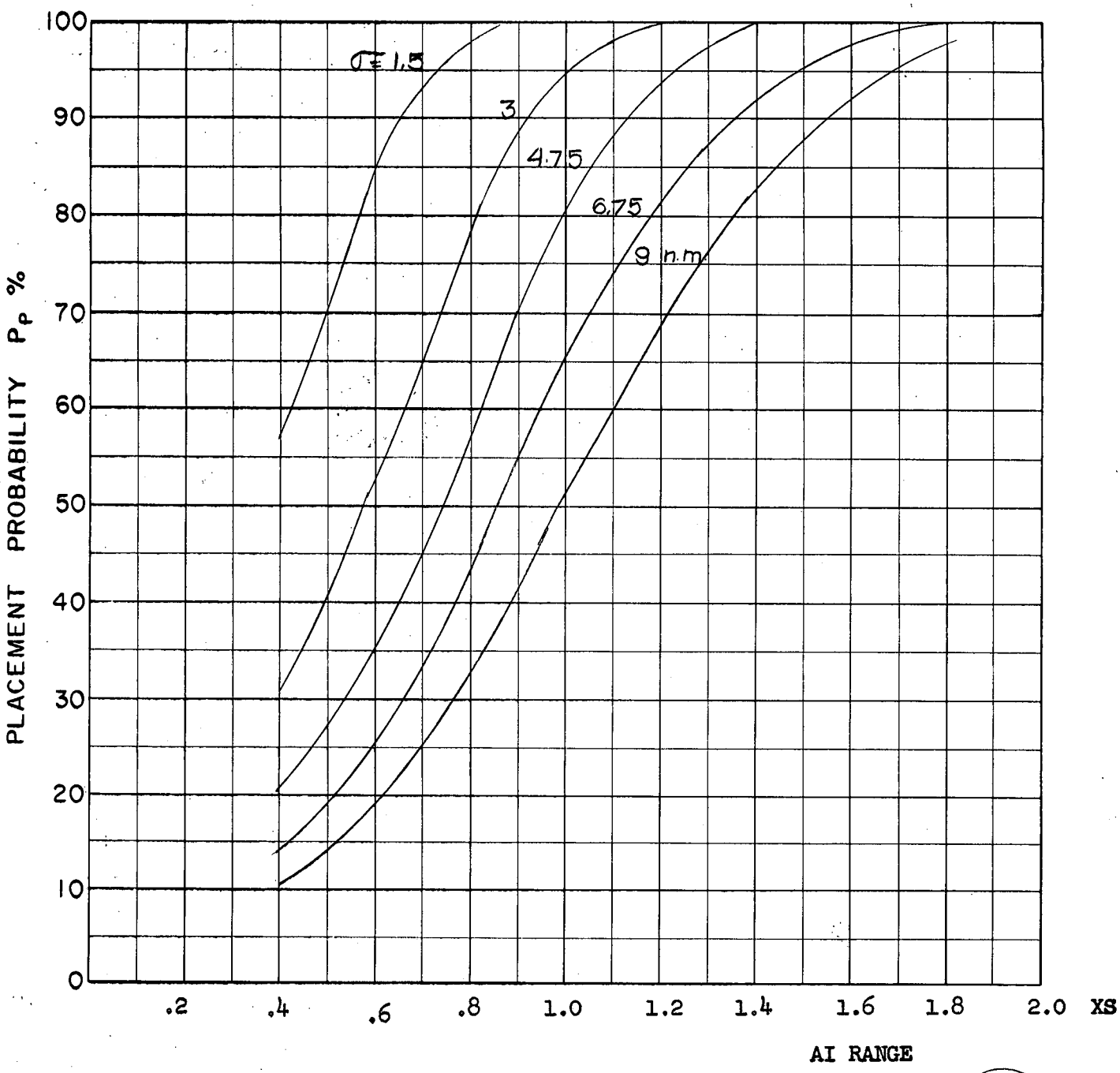

COURSE DIFFERENCE: 160°
TARGET EVASION: 0.5
TARGET MACH NO.: 2.0
INTERCEPTOR LATERAL G's: 2 1/4 Load Factor Limit
INTERCEPTOR MACH NO.: 1.8 Initial
σ OF G.C.I. ACCURACY: 5 Values
A.I. DETECTION RANGE AS FRACTION OF SPECIFICATION RANGE, S: ABSCISSA
A.I. DETECTION RANGE CONTOUR: Straight
ALTITUDE: 50 K
AVRO 2.2 Aerodynamics

S-81 F

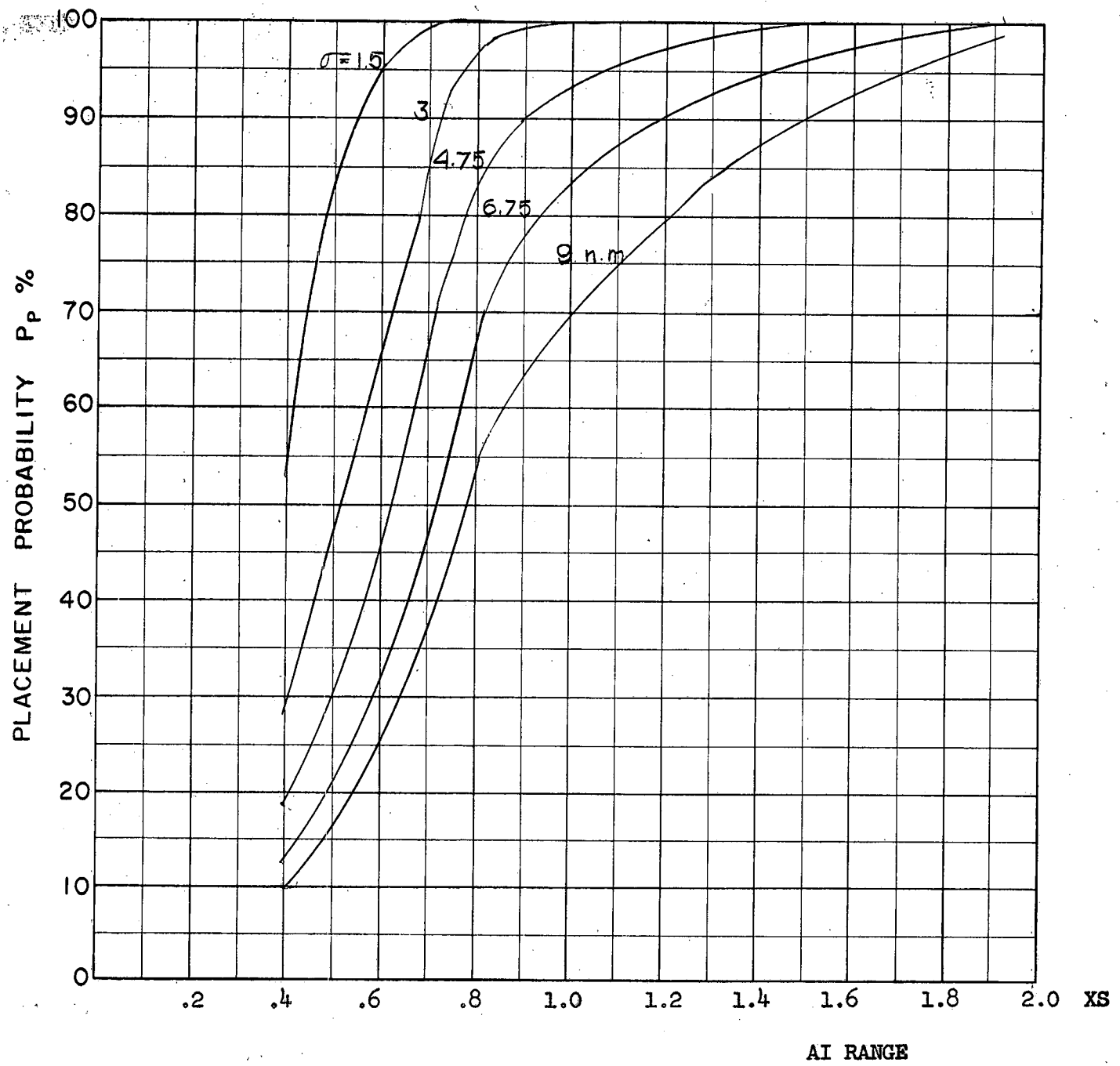

COURSE DIFFERENCE: 180°
TARGET EVASION: 0.5
TARGET MACH NO.: 2.0
INTERCEPTOR LATERAL G's: 4 Load Factor Limit
INTERCEPTOR MACH NO.: 1.8 Initial
σ OF G.C.I. ACCURACY: 5 Values
A.I. DETECTION RANGE AS FRACTION OF SPECIFICATION RANGE, S: ABSCISSA
A.I. DETECTION RANGE CONTOUR: Straight
ALTITUDE: 50 K
AVRO 2.2 Aerodynamics

58a
F

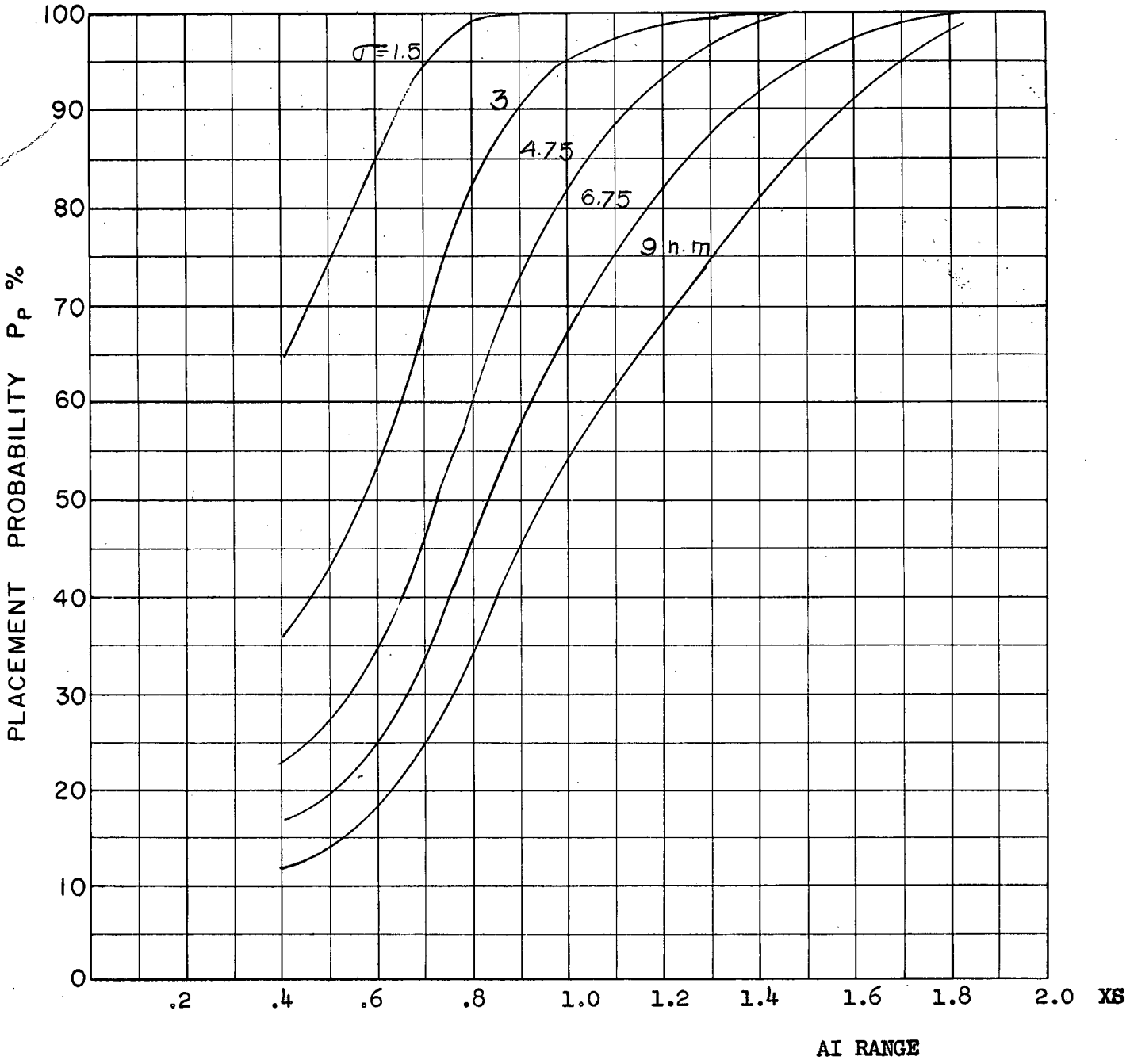

COURSE DIFFERENCE: 180°
TARGET EVASION: 0.5
TARGET MACH NO.: 2.0
INTERCEPTOR LATERAL G's: 2 1/4 Load Factor Limit
INTERCEPTOR MACH NO.: 1.8 Initial
σ OF G.C.I. ACCURACY: 5 Values
A.I. DETECTION RANGE AS FRACTION OF SPECIFICATION RANGE, S: ABSCISSA
A.I. DETECTION RANGE CONTOUR: Straight
ALTITUDE: 50 K
AVRO 2.2. Aerodynamics

S8b
F

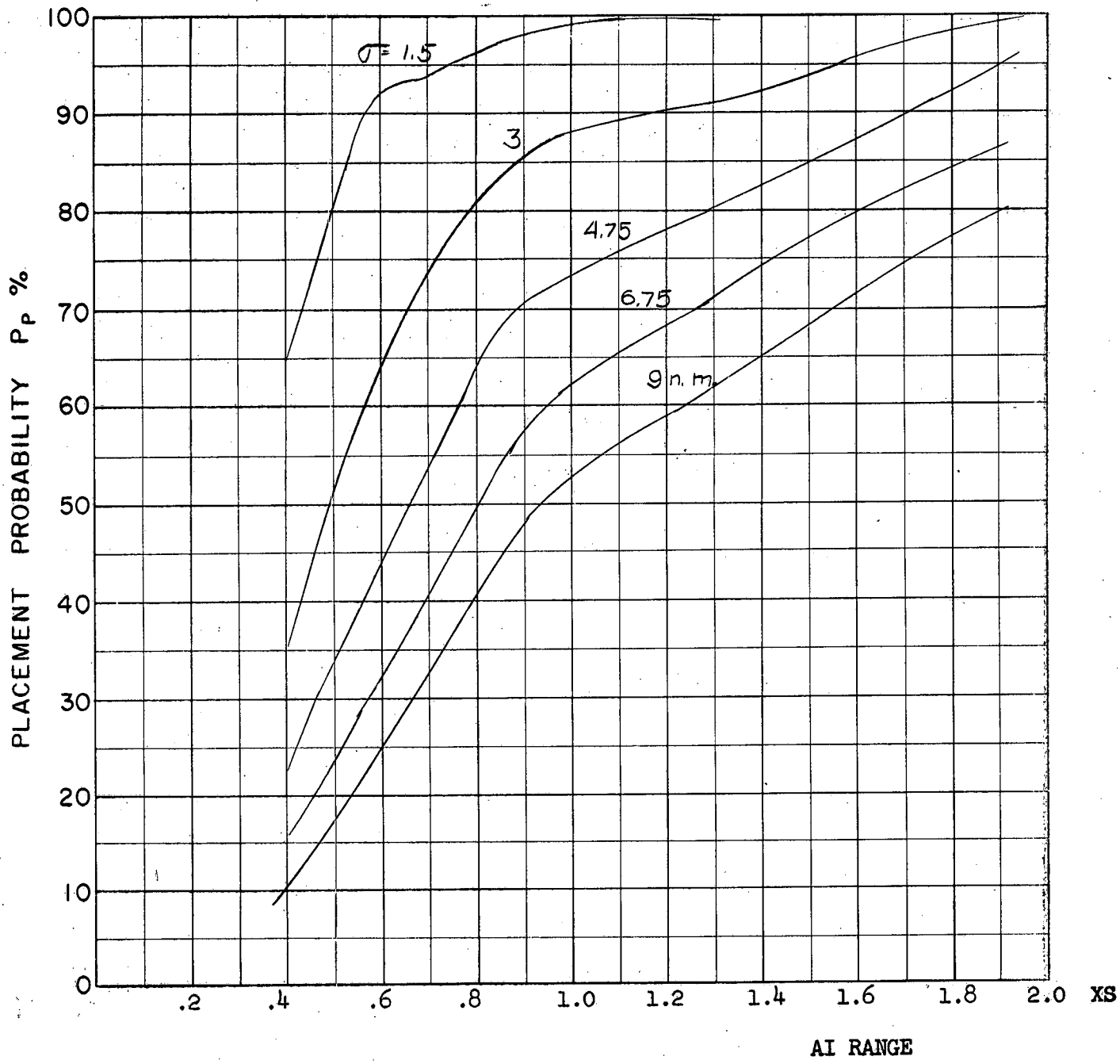

COURSE DIFFERENCE: 110°
TARGET EVASION: 0.5
TARGET MACH NO.: 2.0
INTERCEPTOR LATERAL G's: 4 Load Factor Limit
INTERCEPTOR MACH NO.: 1.8 Initial
σ OF G.C.I. ACCURACY: 5 Values
A.I. DETECTION RANGE AS FRACTION OF SPECIFICATION RANGE, S: ABSCISSA
A.I. DETECTION RANGE CONTOUR: Straight
ALTITUDE: 50 K
AVRO 2.2 Aerodynamics
LAUNCH ZONE 1

S.9 F

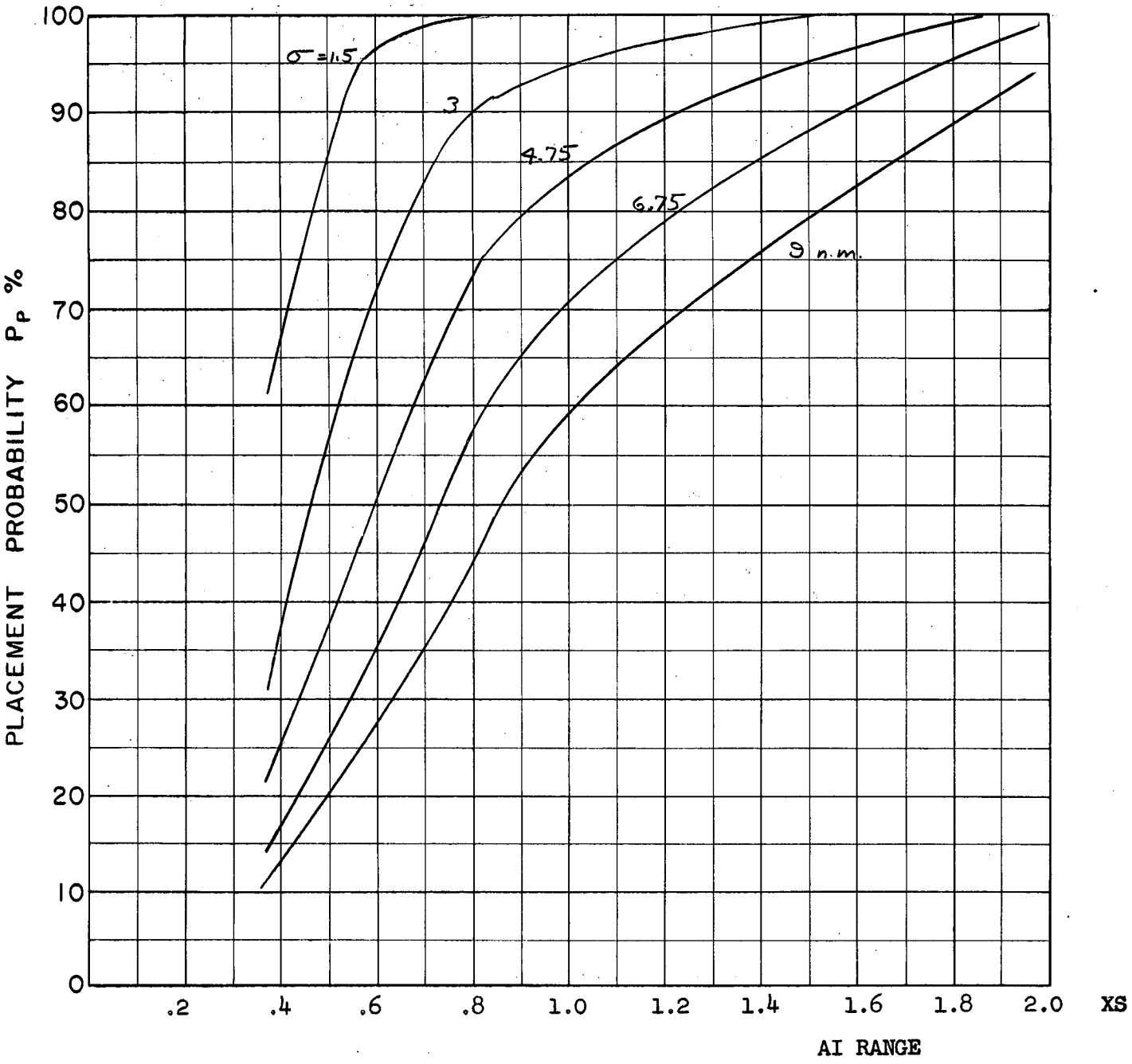

COURSE DIFFERENCE: 135°
TARGET EVASION: 0.5
TARGET MACH NO.: 2.0
INTERCEPTOR LATERAL G's: 4 Load Factor Limit
INTERCEPTOR MACH NO.: 1.8 Initial
σ OF G.C.I. ACCURACY: 5 Values
A.I. DETECTION RANGE AS FRACTION OF SPECIFICATION RANGE, S: ABSCISSA
A.I. DETECTION RANGE CONTOUR: Straight
ALTITUDE: 50 K
AVRO 2.2 Aerodynamics
LAUNCH ZONE 1

S.10 F

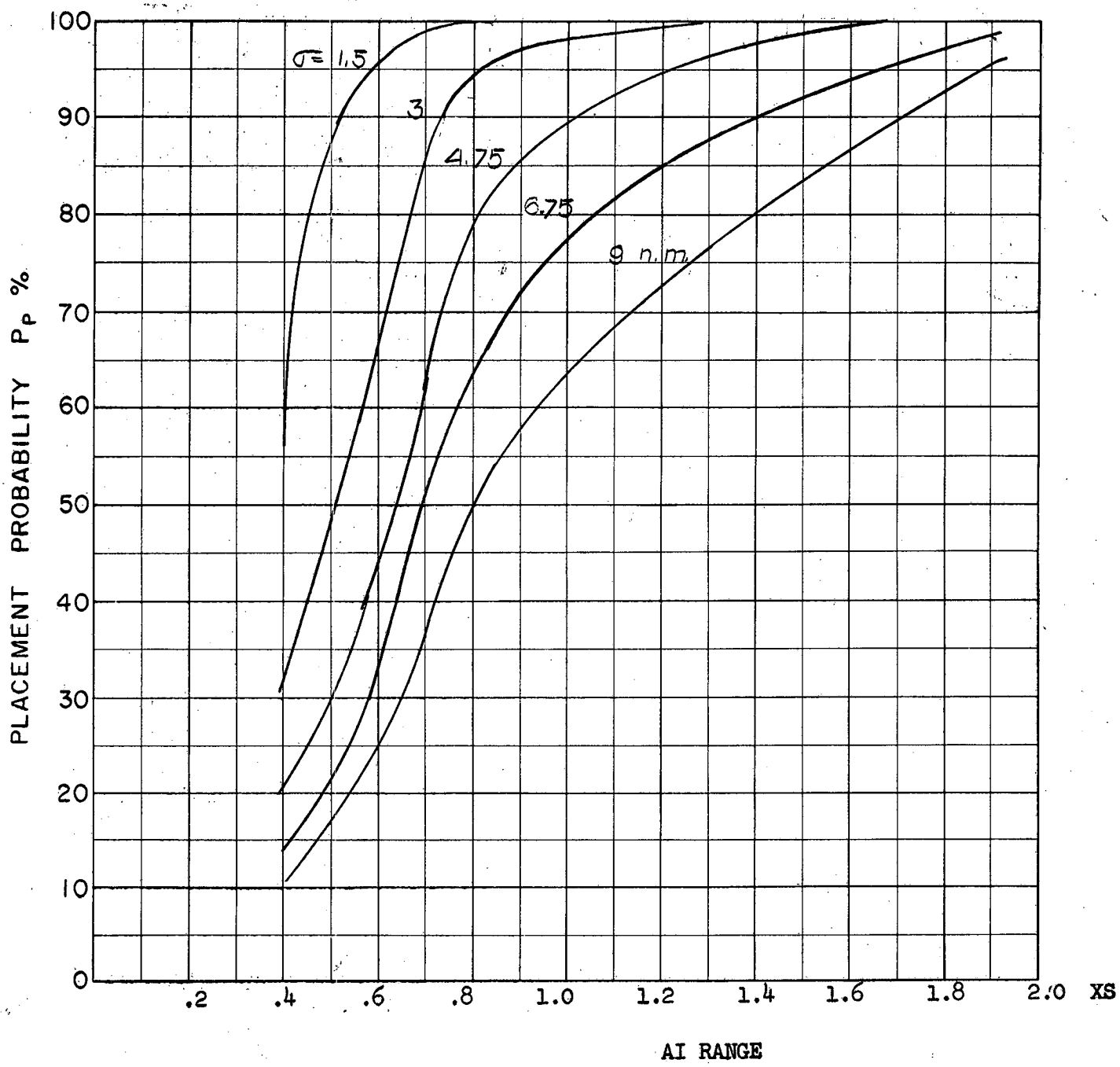

COURSE DIFFERENCE: 160°
TARGET EVASION: 0.5
TARGET MACH NO.: 2.0
INTERCEPTOR LATERAL G's: 4 Load Factor Limit
INTERCEPTOR MACH NO.: 1.8 Initial
σ OF G.C.I. ACCURACY: 5 Values
A.I. DETECTION RANGE AS FRACTION OF SPECIFICATION RANGE, S: ABSCISSA
A.I. DETECTION RANGE CONTOUR: Straight
ALTITUDE: 50 K
AVRO 2.2 Aerodynamics
LAUNCH ZONE 1

S 11
F

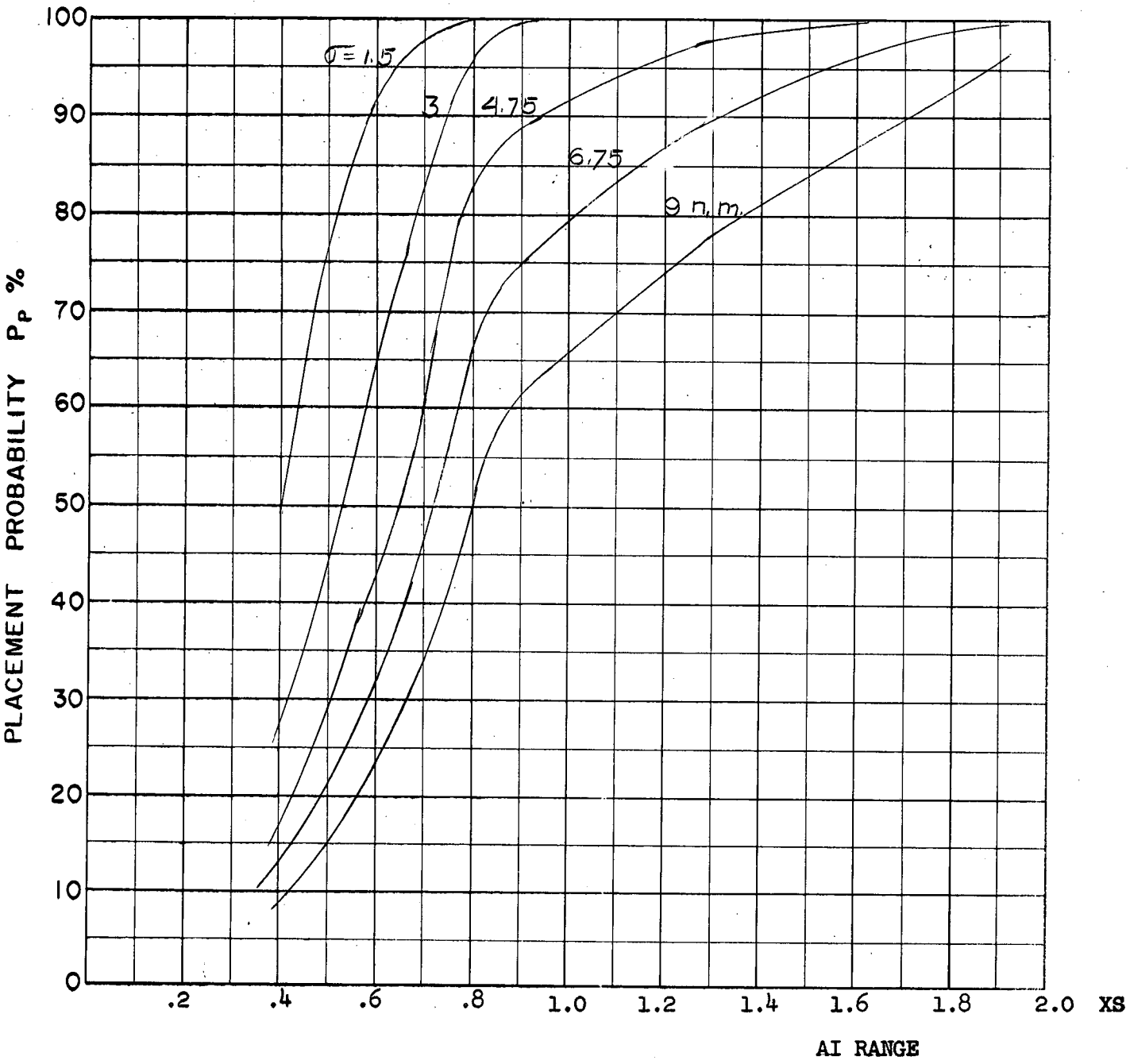

COURSE DIFFERENCE: 180°
TARGET EVASION: 0.5
TARGET MACH NO.: 2.0
INTERCEPTOR LATERAL G's: 4 Load Factor Limit
INTERCEPTOR MACH NO.: 1.8 Initial
σ OF G.C.I. ACCURACY: 5 Values
A.I. DETECTION RANGE AS FRACTION OF SPECIFICATION RANGE, S: ABSCISSA
A.I. DETECTION RANGE CONTOUR: Straight
ALTITUDE: 50 K
AVRO 2.2 Aerodynamics
LAUNCH ZONE 1

S12
F

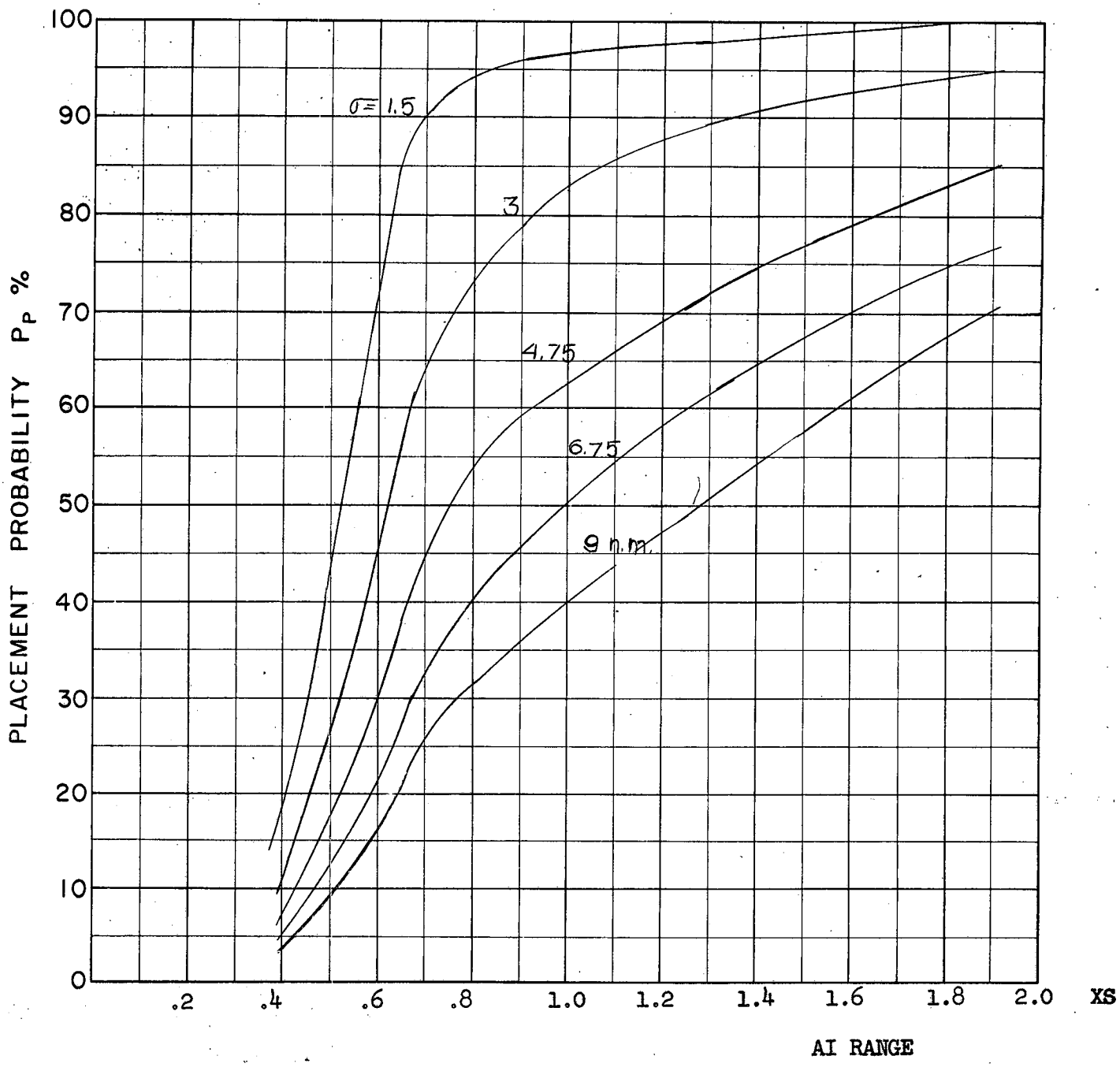

COURSE DIFFERENCE: 110°
TARGET EVASION: 0.5
TARGET MACH NO.: 2.0
INTERCEPTOR LATERAL G's: 4 Load Factor Limit
INTERCEPTOR MACH NO.: 1.8 Initial
σ OF G.C.I. ACCURACY: 5 Values
A.I. DETECTION RANGE AS FRACTION OF SPECIFICATION RANGE, S: ABSCISSA
A.I. DETECTION RANGE CONTOUR: Straight
ALTITUDE: 60 K
AVRO 2.2 Aerodynamics

S13
F

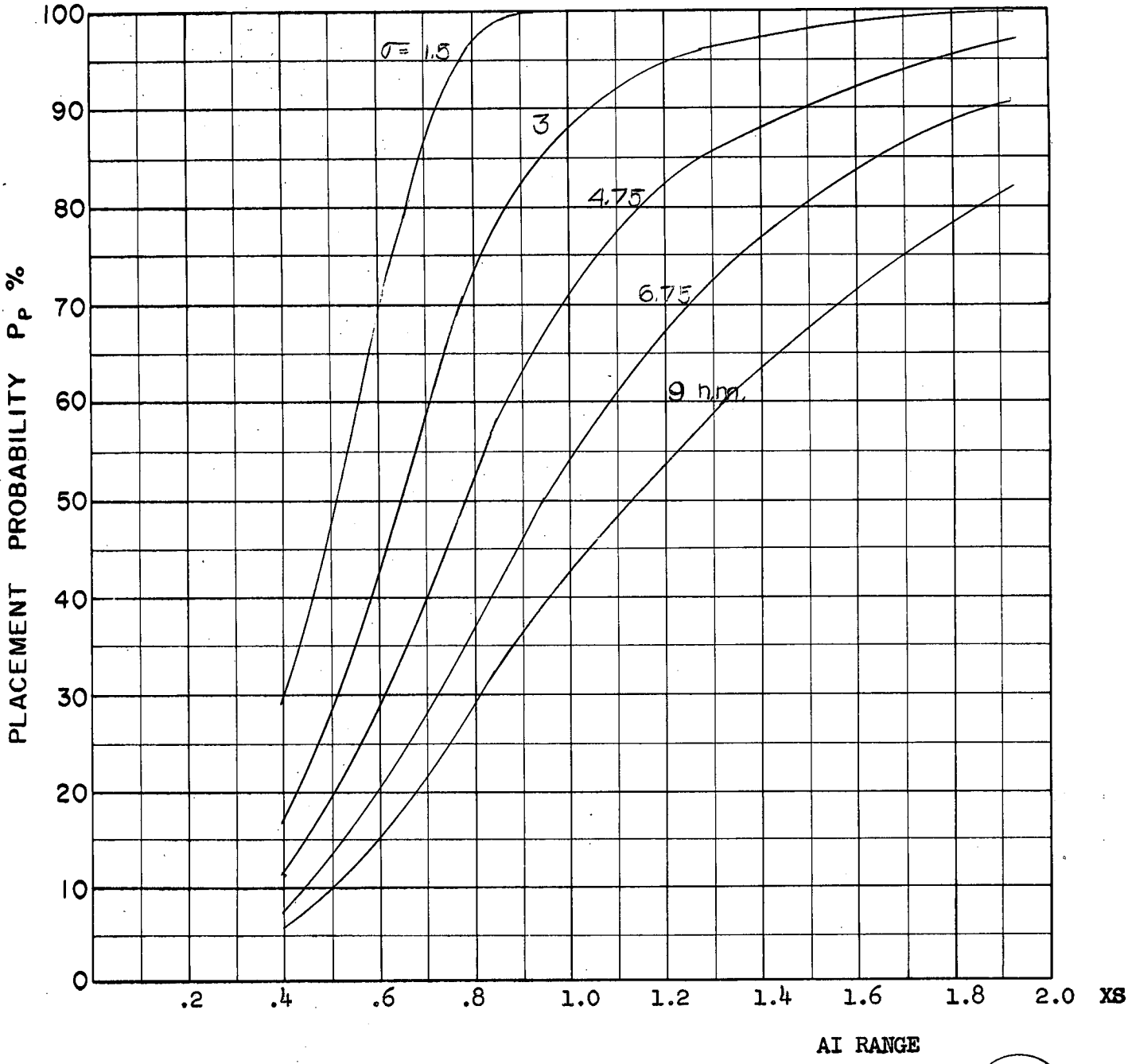

COURSE DIFFERENCE: 135°
TARGET EVASION: 0.5
TARGET MACH NO.: 2.0
INTERCEPTOR LATERAL G's: 4 Load Factor Limit
INTERCEPTOR MACH NO.: 1.8 Initial
σ OF G.C.I. ACCURACY: 5 Values
A.I. DETECTION RANGE AS FRACTION OF SPECIFICATION RANGE, S: ABSCISSA
A.I. DETECTION RANGE CONTOUR: Straight
ALTITUDE: 60 K
AVRO 2.2 Aerodynamics

S-13
F

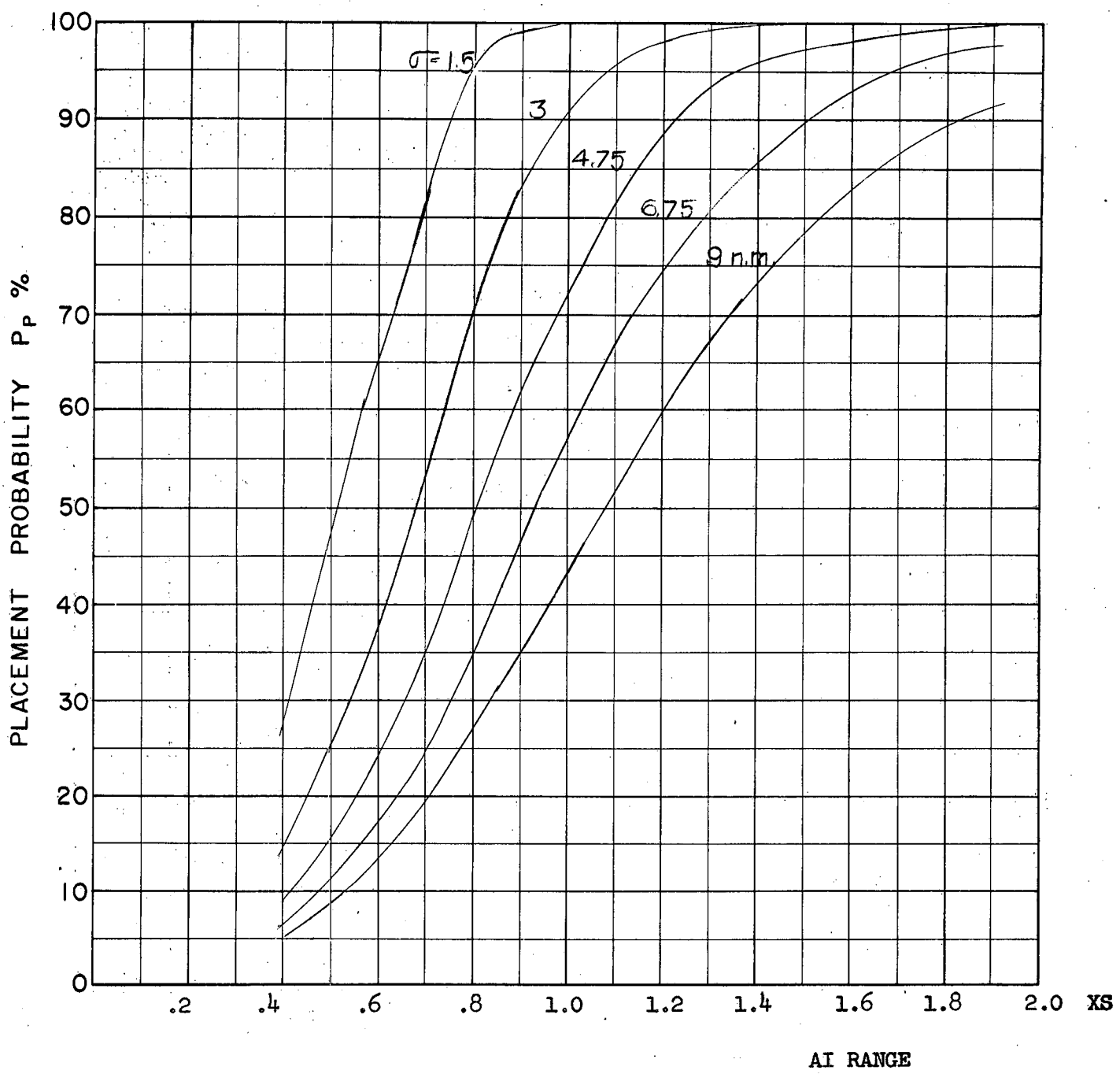

COURSE DIFFERENCE: 160°
TARGET EVASION: 0.5
TARGET MACH NO.: 2.0
INTERCEPTOR LATERAL G's: 4 Load Factor Limit
INTERCEPTOR MACH NO.: 1.8 Initial
σ OF G.C.I. ACCURACY: 5 Values
A.I. DETECTION RANGE AS FRACTION OF SPECIFICATION RANGE, S: ABSCISSA
A.I. DETECTION RANGE CONTOUR: Straight
ALTITUDE: 60 K

S.15
F

AVRO 2.2 Aerodynamics

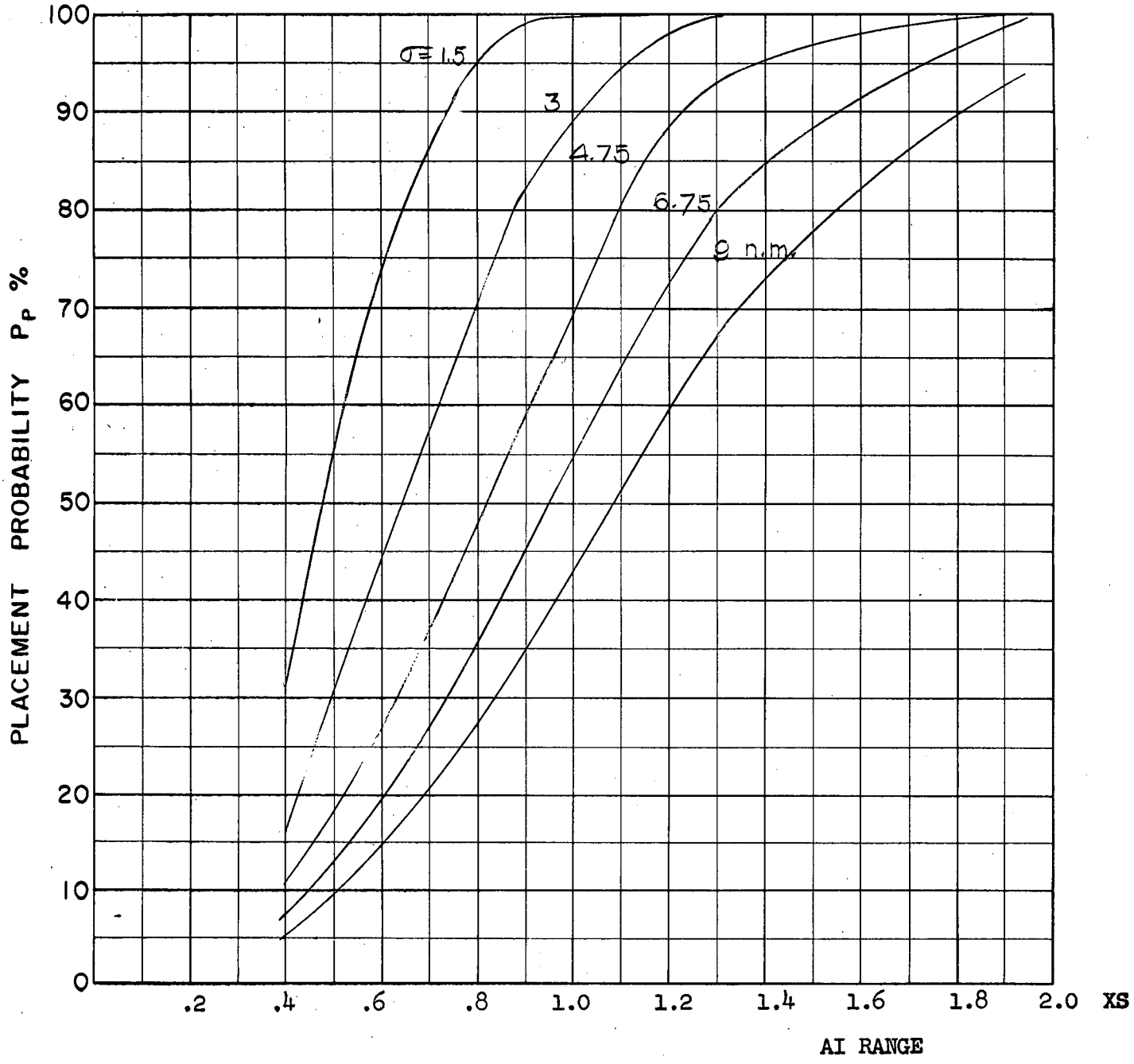

COURSE DIFFERENCE: 180°
TARGET EVASION: 0.5
TARGET MACH NO.: 2.0
INTERCEPTOR LATERAL G's: 4 Load Factor Limit
INTERCEPTOR MACH NO.: 1.8 Initial
σ OF G.C.I. ACCURACY: 5 Values
A.I. DETECTION RANGE AS FRACTION OF SPECIFICATION RANGE, S: ABSCISSA
A.I. DETECTION RANGE CONTOUR: Straight
ALTITUDE: 60 K
AVRO 2.2 Aerodynamics

S 16
F

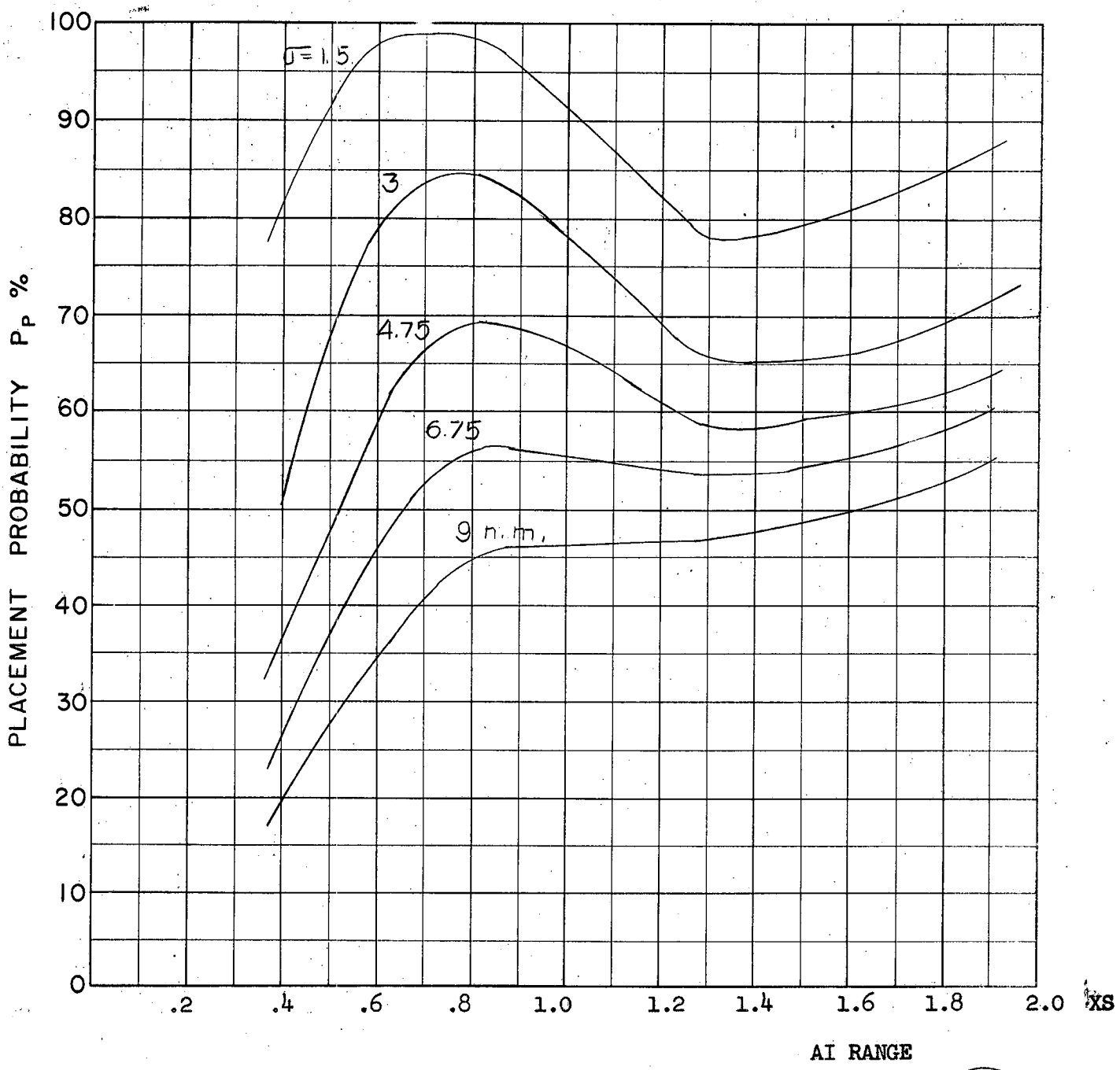

COURSE DIFFERENCE: 90°
TARGET EVASION: 0.5
TARGET MACH NO.: 2.0
INTERCEPTOR LATERAL G's: 4 Load Factor Limit
INTERCEPTOR MACH NO.: 2.0 Initial
σ OF G.C.I. ACCURACY: 5 Values
A.I. DETECTION RANGE AS FRACTION OF SPECIFICATION RANGE, S: ABSCISSA
A.I. DETECTION RANGE CONTOUR: Straight
ALTITUDE: 50 K
AVRO 2.2 Aerodynamics

S17a
F

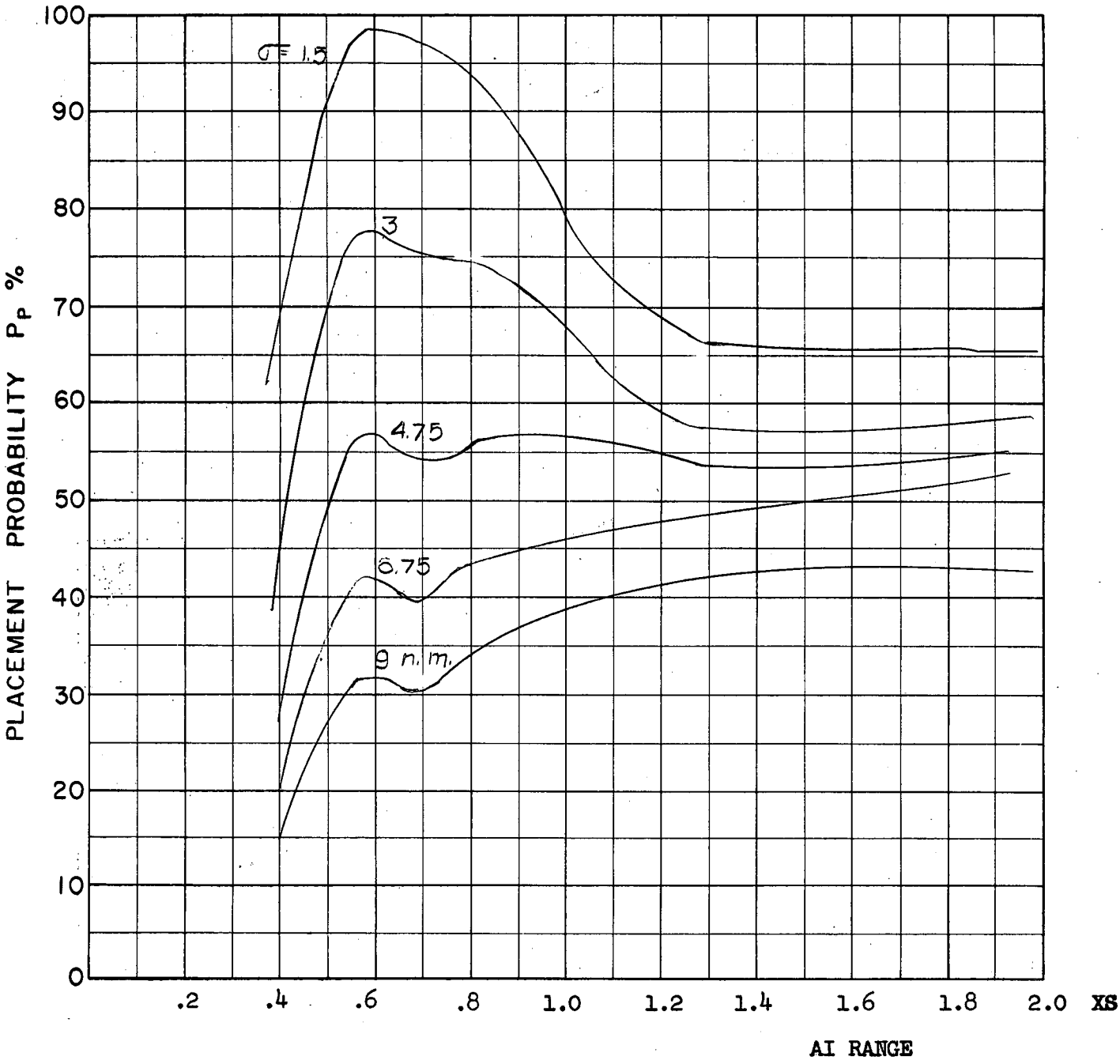

COURSE DIFFERENCE: 90°
TARGET EVASION: 0.5
TARGET MACH NO.: 2.0
INTERCEPTOR LATERAL G's: 2 1/4 Load Factor Limit
INTERCEPTOR MACH NO.: 2.0 Initial
σ OF G.C.I. ACCURACY: 5 Values
A.I. DETECTION RANGE AS FRACTION OF SPECIFICATION RANGE, S: ABSCISSA
A.I. DETECTION RANGE CONTOUR: Straight
ALTITUDE: 50 K
AVRO 2.2 Aerodynamics

S17b
F

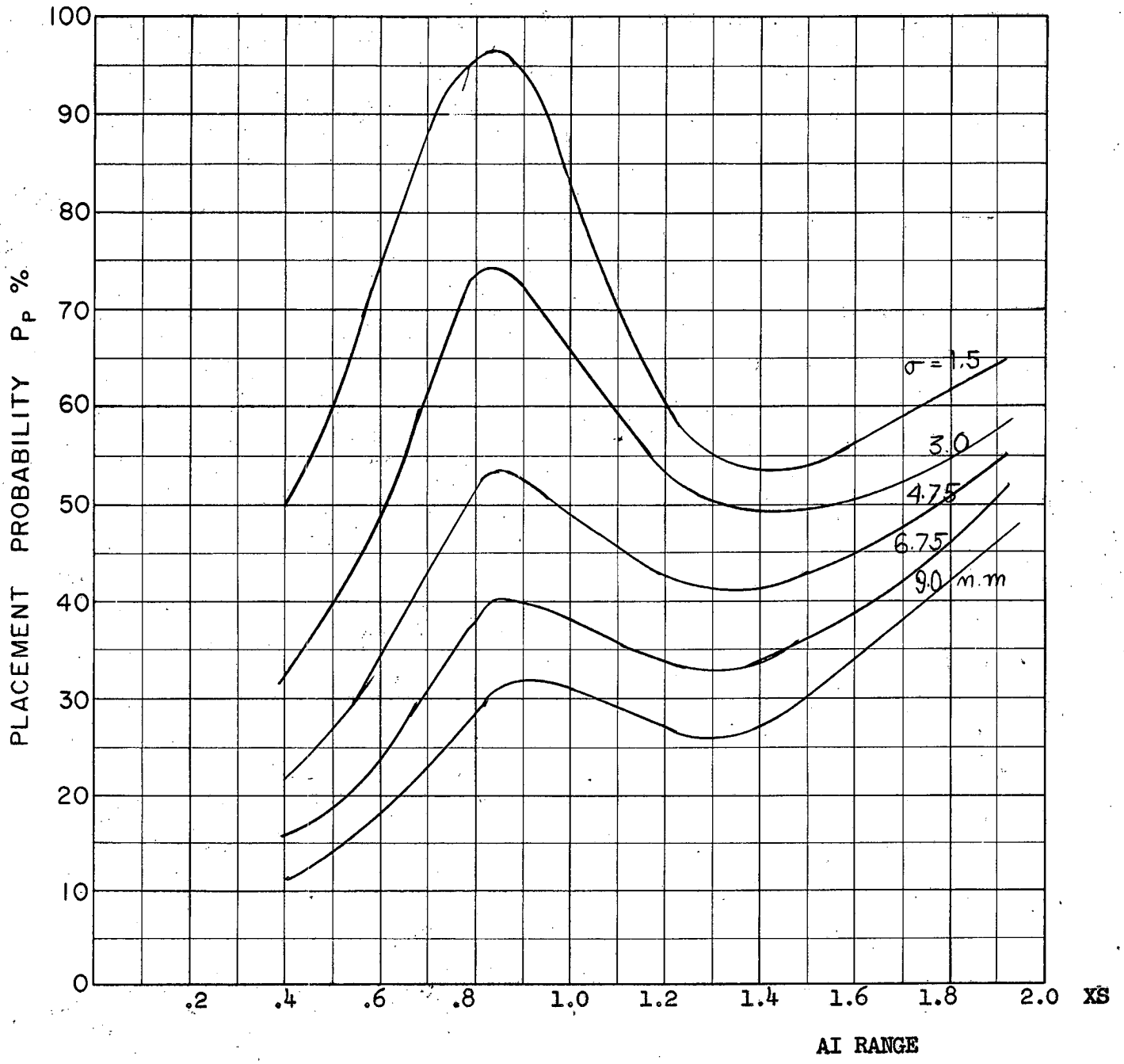

COURSE DIFFERENCE: 90°
TARGET EVASION: 0.5
TARGET MACH NO.: 2.0
INTERCEPTOR LATERAL G's: 1.414 Load Factor Limit
INTERCEPTOR MACH NO.: 2.0 Initial
σ OF G.C.I. ACCURACY: -5 Values
A.I. DETECTION RANGE AS FRACTION OF SPECIFICATION RANGE, S: ABSCISSA
A.I. DETECTION RANGE CONTOUR: Straight
ALTITUDE: 50 K
. AVRO 2.2 Aerodynamics

S17c
F

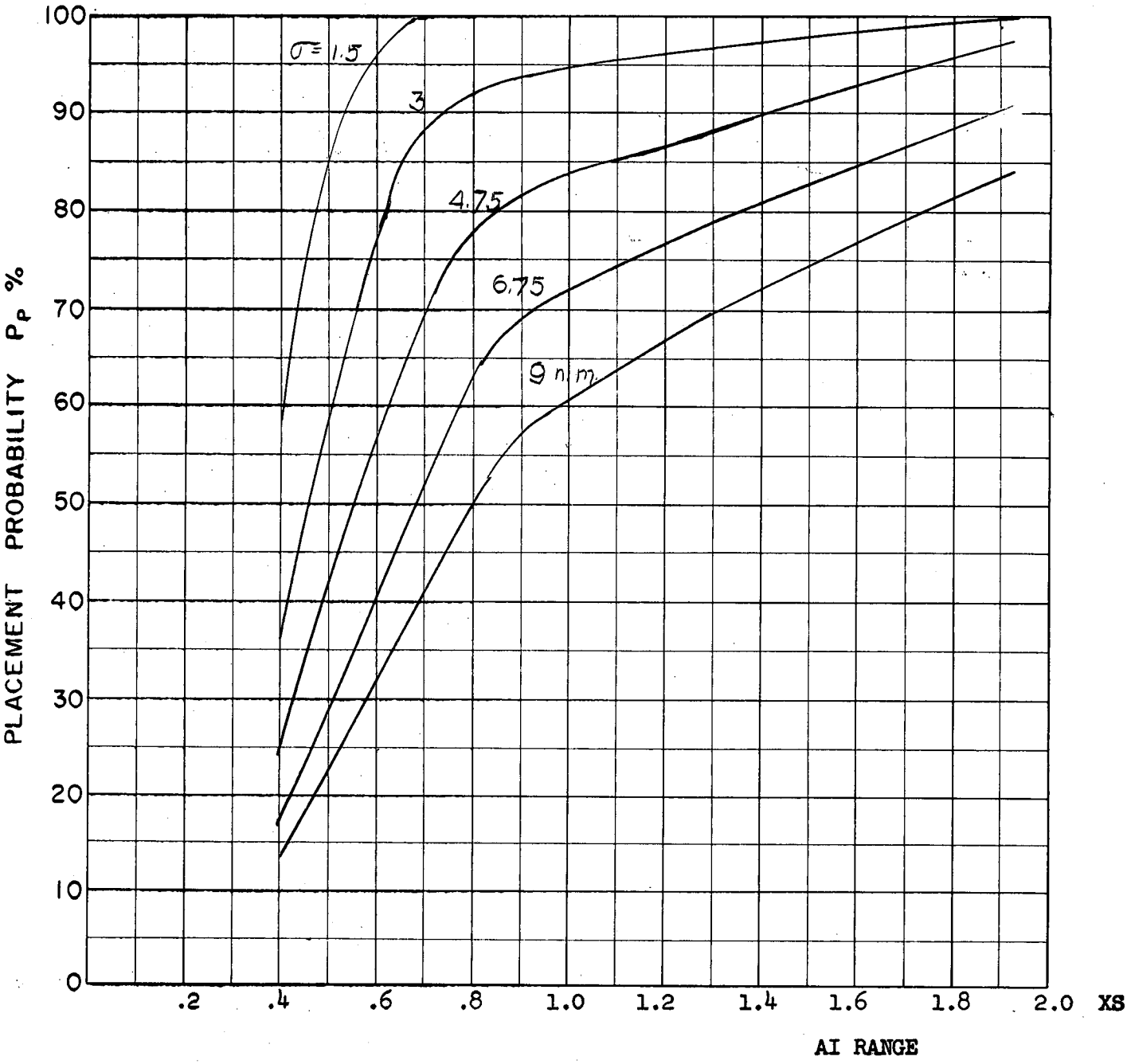

COURSE DIFFERENCE: 110°
TARGET EVASION: 0.5
TARGET MACH NO.: 2.0
INTERCEPTOR LATERAL G's: 4 Load Factor Limit
INTERCEPTOR MACH NO.: 2.0 Initial
σ OF G.C.I. ACCURACY: 5 Values
A.I. DETECTION RANGE AS FRACTION OF SPECIFICATION RANGE, S: ABSCISSA
A.I. DETECTION RANGE CONTOUR: Straight
ALTITUDE: 50 K
AVRO 2.2 Aerodynamics

S18a
F

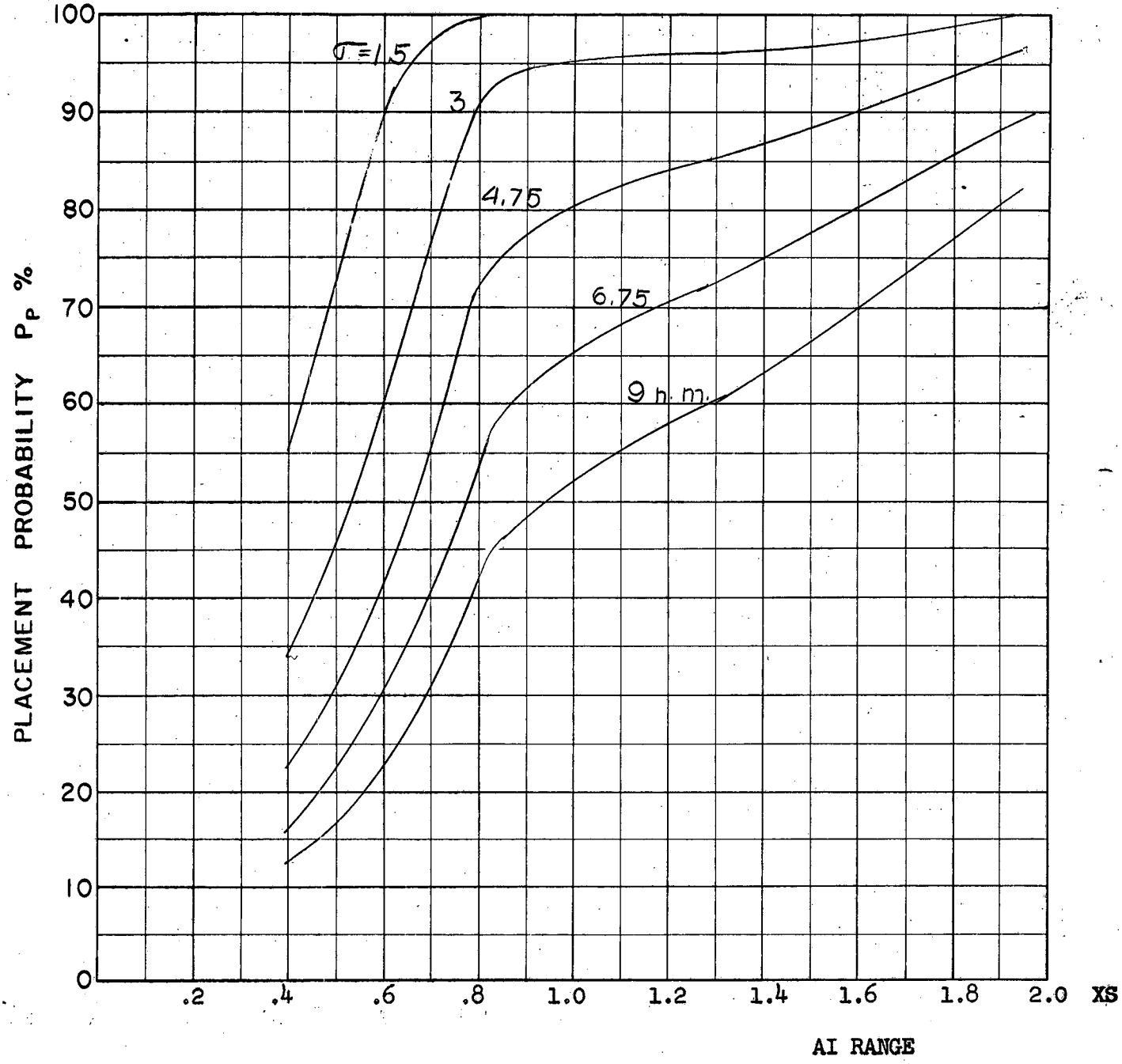

COURSE DIFFERENCE: 110°
TARGET EVASION: 0.5
TARGET MACH NO.: 2.0
INTERCEPTOR LATERAL G's: 2 1/4 Load Factor Limit
INTERCEPTOR MACH NO.: 2.0 Initial
σ OF G.C.I. ACCURACY: 5 Values
A.I. DETECTION RANGE AS FRACTION OF SPECIFICATION RANGE, S: ABSCISSA
A.I. DETECTION RANGE CONTOUR: Straight
ALTITUDE: 50 K
AVRO 2.2 Aerodynamics

S18b
F

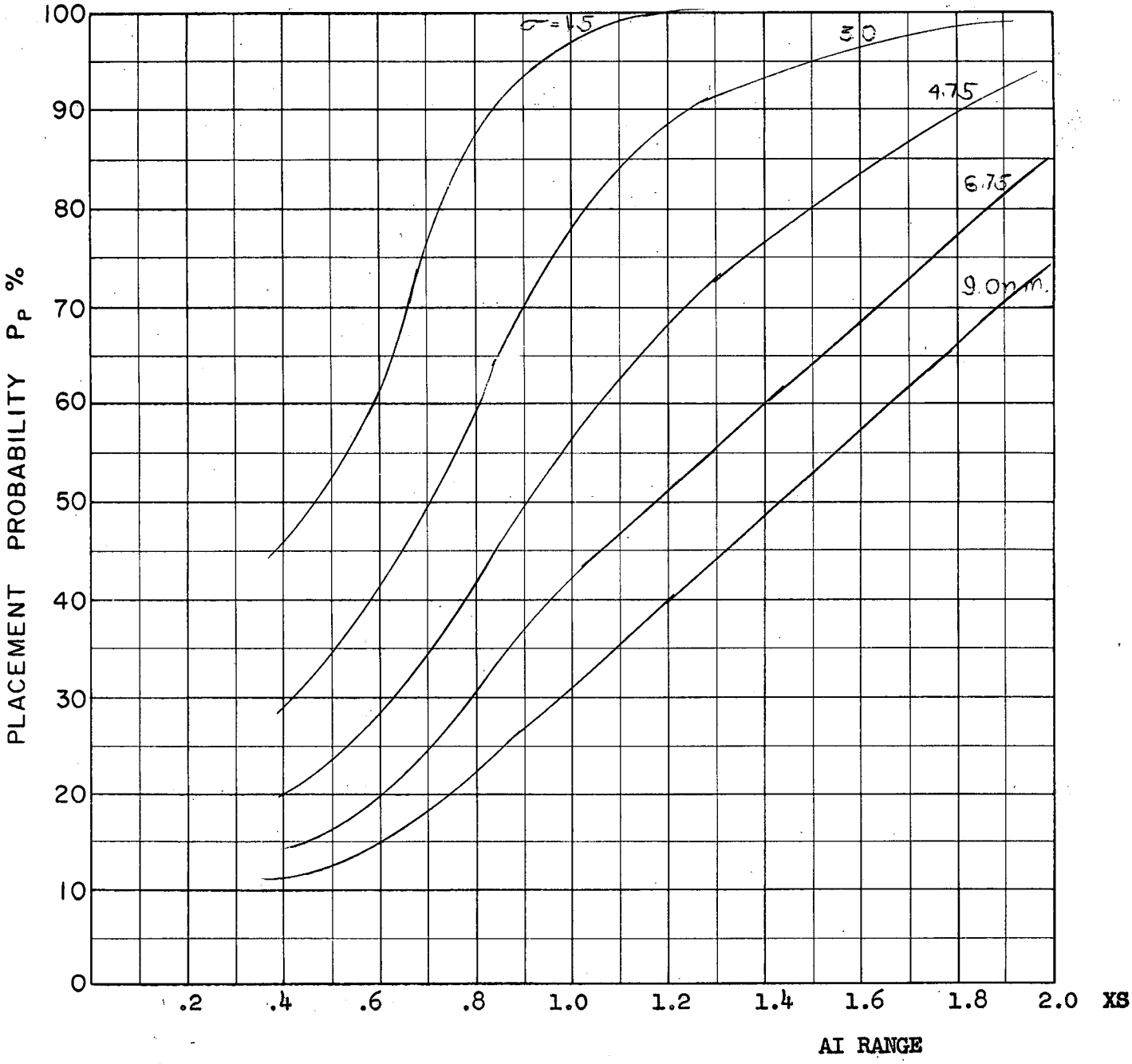

COURSE DIFFERENCE: 110°
TARGET EVASION: 0.5
TARGET MACH NO.: 2.0
INTERCEPTOR LATERAL G's: 1.414 Load Factor Limit
INTERCEPTOR MACH NO.: 2.0 Initial
σ OF G.C.I. ACCURACY: 5 Values
A.I. DETECTION RANGE AS FRACTION OF SPECIFICATION RANGE, S: ABSCISSA
A.I. DETECTION RANGE CONTOUR: Straight
ALTITUDE: 50 K
AVRO 2.2 Aerodynamics

S18c
F

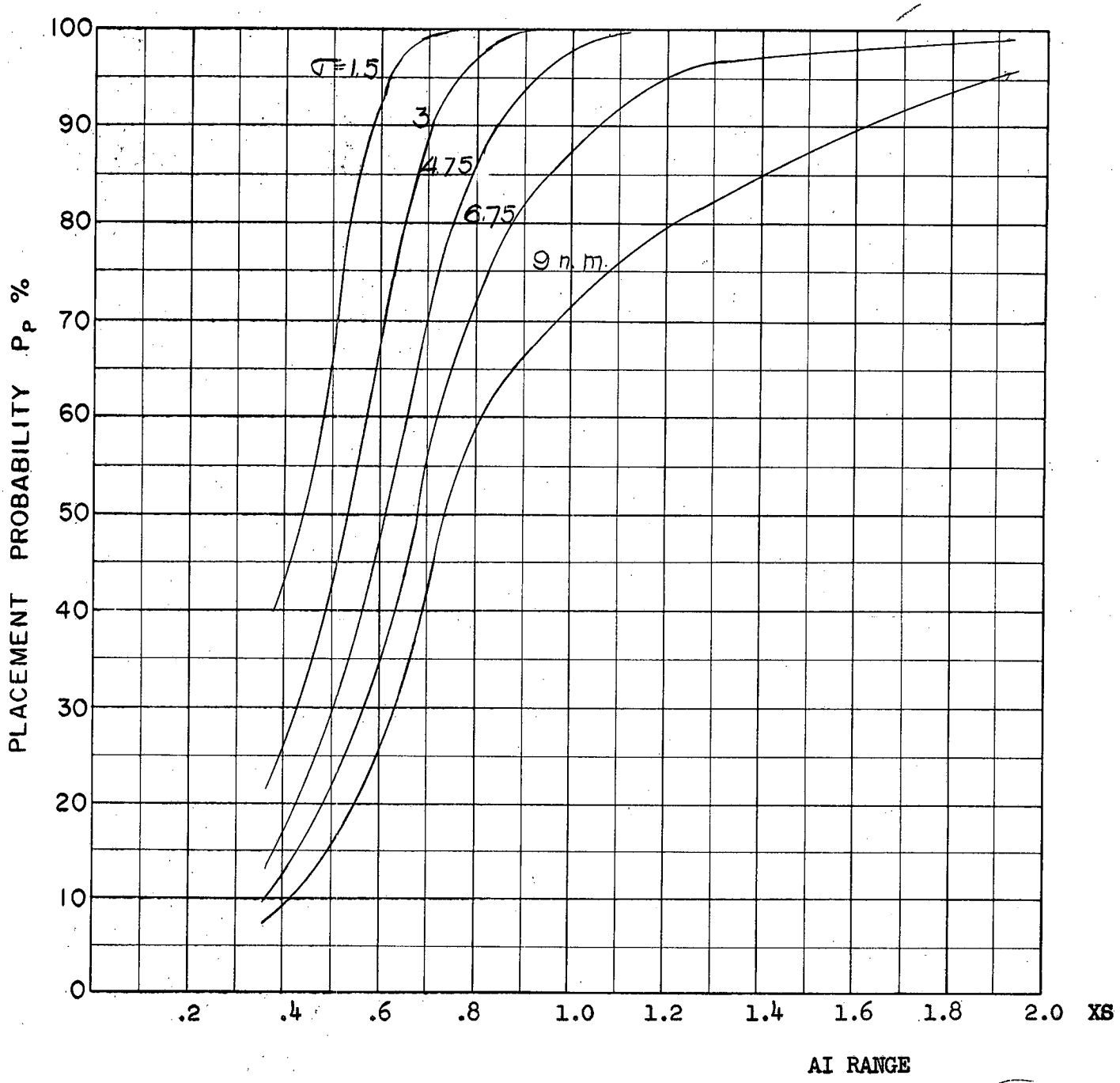

COURSE DIFFERENCE: 135°
TARGET EVASION: 0.5
TARGET MACH NO.: 2.0
INTERCEPTOR LATERAL G's: 4 Load Factor Limit
INTERCEPTOR MACH NO.: 2.0 Initial
σ OF G.C.I. ACCURACY: 5 Values
A.I. DETECTION RANGE AS FRACTION OF SPECIFICATION RANGE, S: ABSCISSA
A.I. DETECTION RANGE CONTOUR: Straight
ALTITUDE: 50 K
AVRO 2.2 Aerodynamics

S19a
F

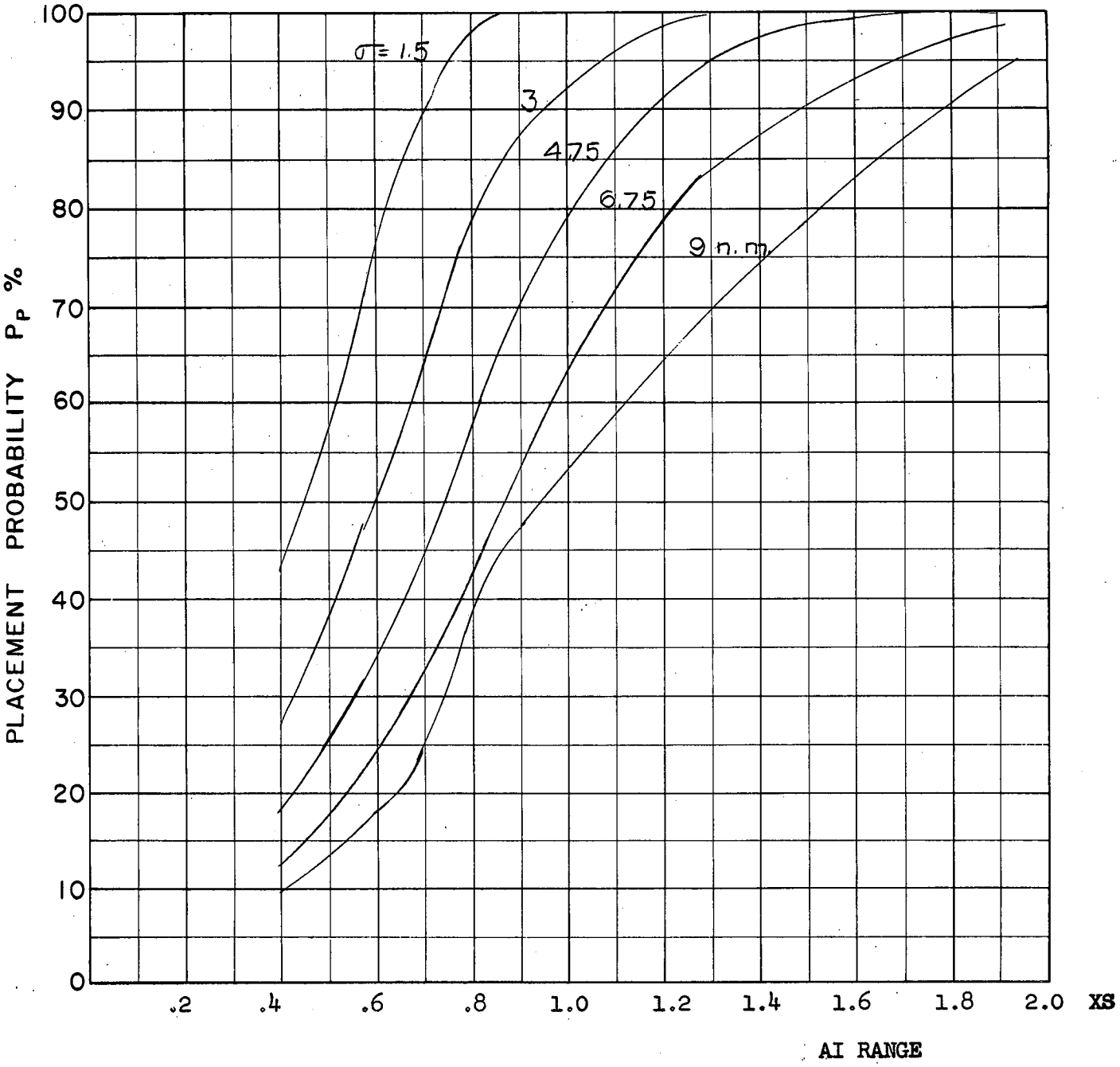

COURSE DIFFERENCE: 135°
TARGET EVASION: 0.5
TARGET MACH NO.: 2.0
INTERCEPTOR LATERAL G's: 2 1/4 Load Factor Limit
INTERCEPTOR MACH NO.: 2.0 Initial
σ OF G.C.I. ACCURACY: 5 Values
A.I. DETECTION RANGE AS FRACTION OF SPECIFICATION RANGE, S: ABSCISSA
A.I. DETECTION RANGE CONTOUR: Straight
ALTITUDE: 50 K
AVRO 2.2 Aerodynamics

S191 F

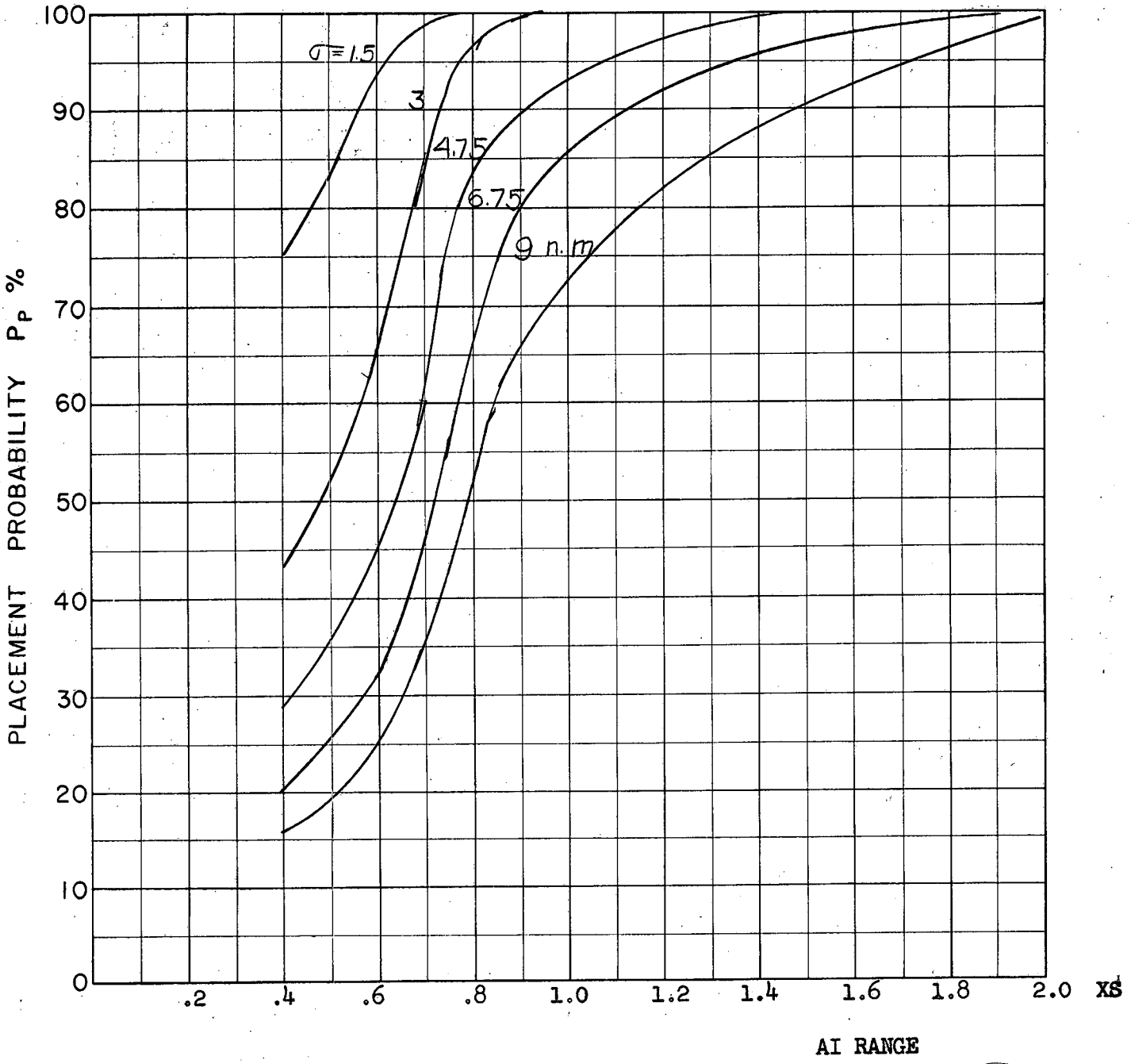

COURSE DIFFERENCE: 160°
TARGET EVASION: 0.5
TARGET MACH NO.: 2.0
INTERCEPTOR LATERAL G's: 4 Load Factor Limit
INTERCEPTOR MACH NO.: 2.0 Initial
σ OF G.C.I. ACCURACY: 5 Values
A.I. DETECTION RANGE AS FRACTION OF SPECIFICATION RANGE, S: ABSCISSA
A.I. DETECTION RANGE CONTOUR: Straight
ALTITUDE: 50 K
AVRO 2.2 Aerodynamics

$ 20a
F

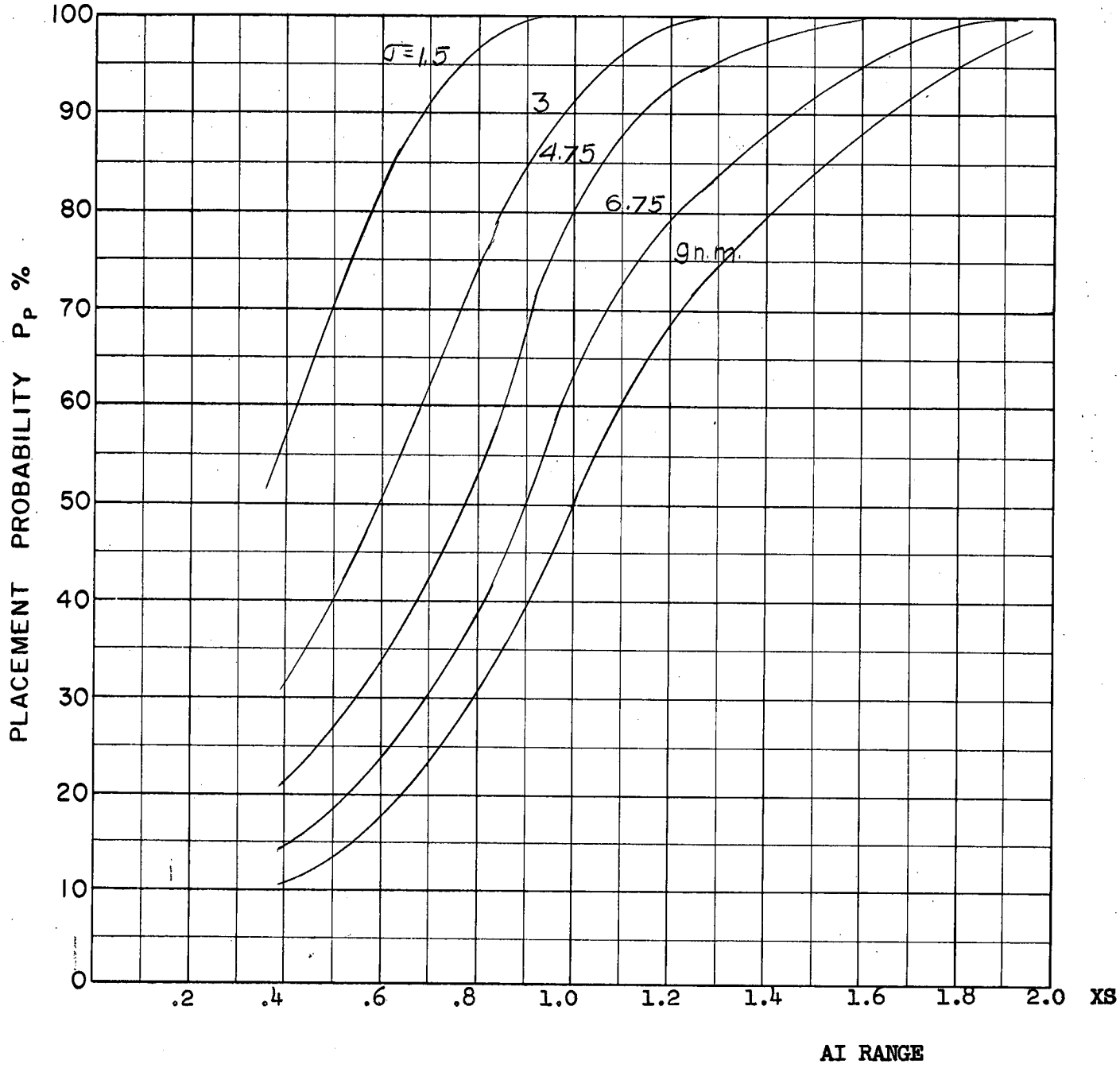

COURSE DIFFERENCE: 160°
TARGET EVASION: 0.5
TARGET MACH NO.: 2.0
INTERCEPTOR LATERAL G's: 2 1/4 Load Factor Limit
INTERCEPTOR MACH NO.: 2.0 Initial
σ OF G.C.I. ACCURACY: 5 Values
A.I. DETECTION RANGE AS FRACTION OF SPECIFICATION RANGE, S: ABSCISSA
A.I. DETECTION RANGE CONTOUR: Straight
ALTITUDE: 50 K
AVRO 2.2. Aerodynamics

S 20b
F

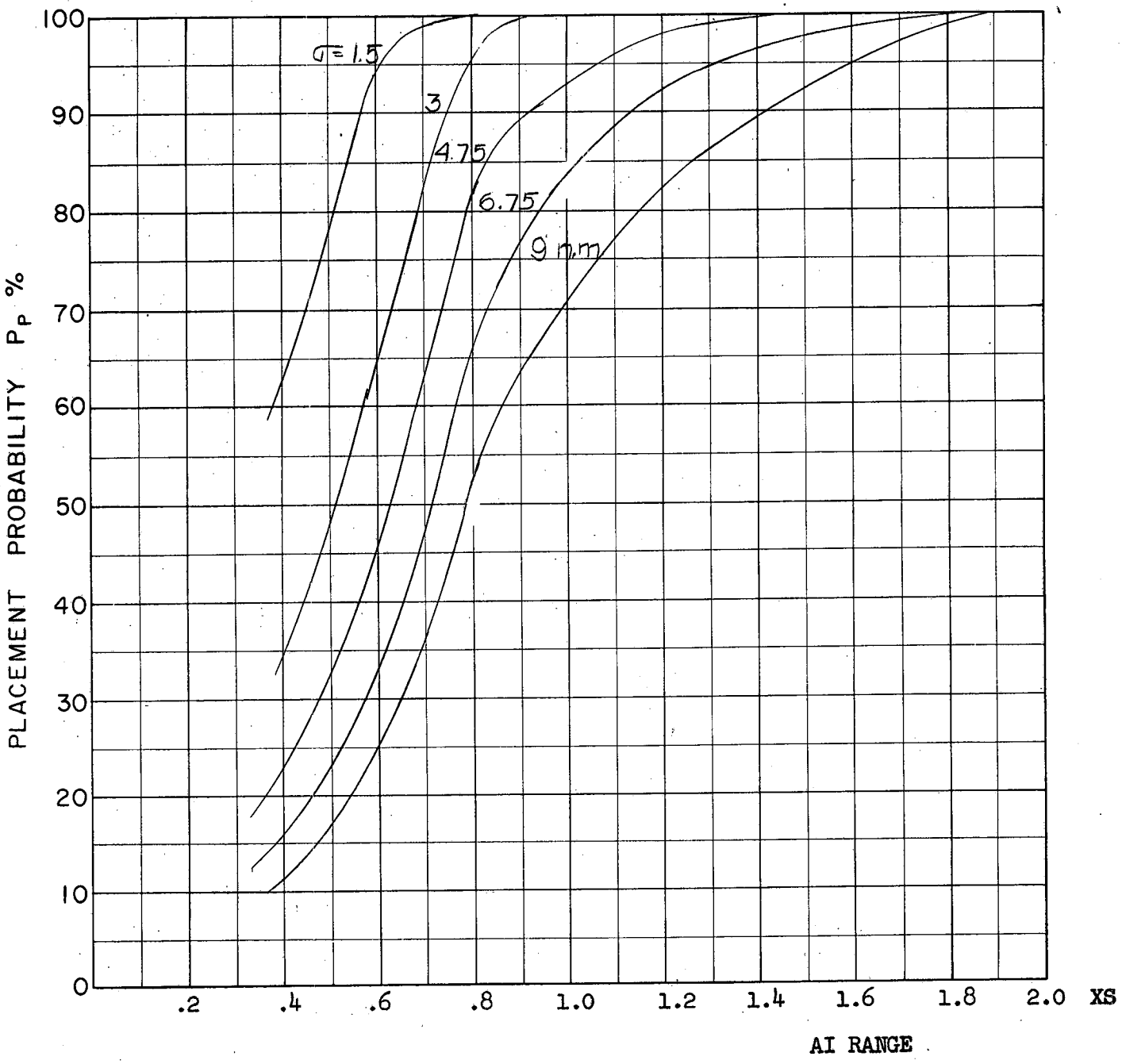

COURSE DIFFERENCE: 180°
TARGET EVASION: 0.5
TARGET MACH NO.: 2.0,
INTERCEPTOR LATERAL G's: 4 Load Factor Limit
INTERCEPTOR MACH NO.: 2.0 Initial
σ OF G.C.I. ACCURACY: 5 Values
A.I. DETECTION RANGE AS FRACTION OF SPECIFICATION RANGE, S: ABSCISSA
A.I. DETECTION RANGE CONTOUR: Straight
ALTITUDE: 50 K
AVRO 2.2 Aerodynamics

S21a
F

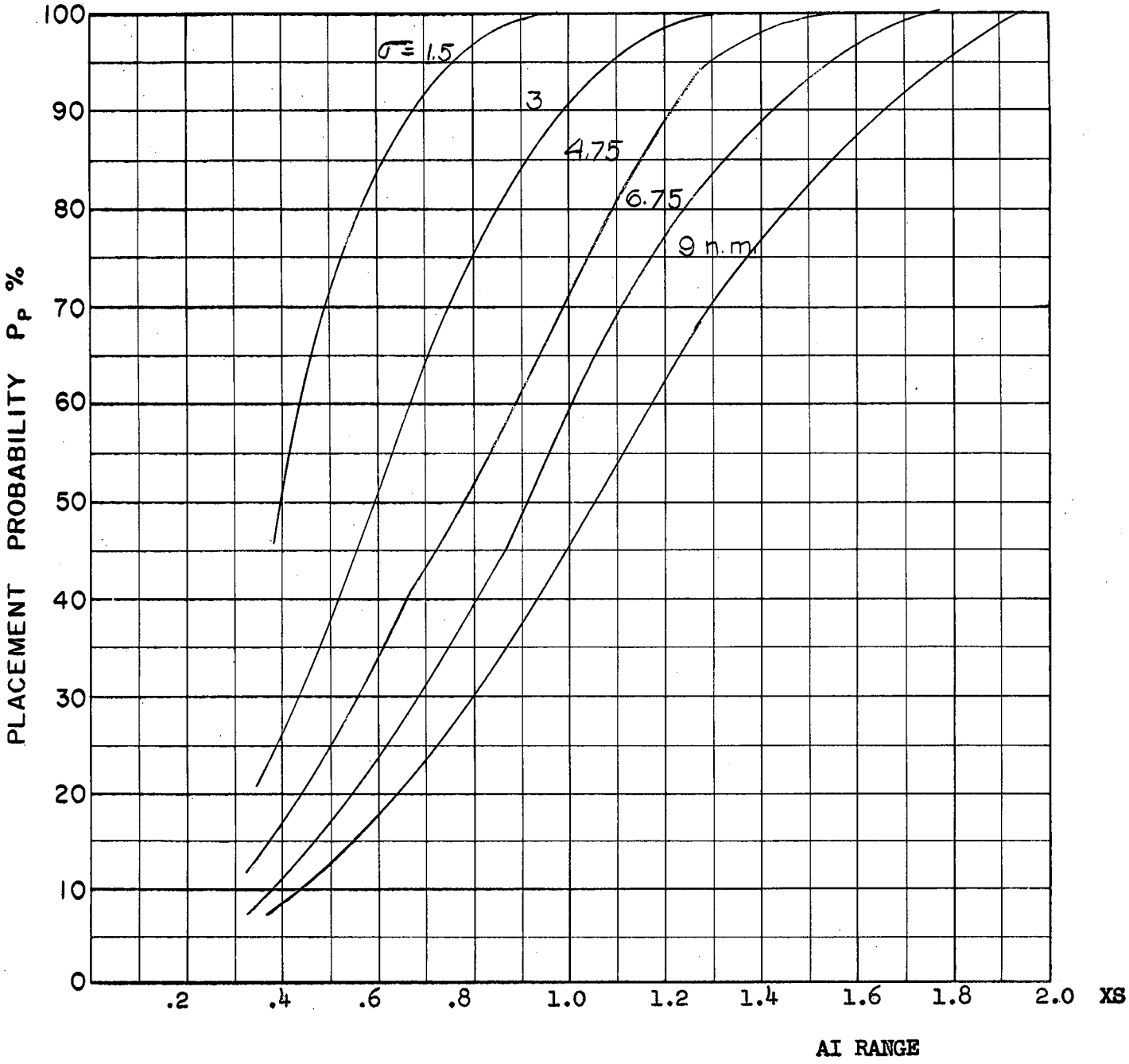

COURSE DIFFERENCE: 180°
TARGET EVASION: 0.5
TARGET MACH NO.: 2.0
INTERCEPTOR LATERAL G's: 2 1/4 Load Factor Limit
INTERCEPTOR MACH NO.: 2.0 Initial
σ OF G.C.I. ACCURACY: 5 Values
A.I. DETECTION RANGE AS FRACTION OF SPECIFICATION RANGE, S: ABSCISSA
A.I. DETECTION RANGE CONTOUR: Straight
ALTITUDE: 50 K
AVRO 2.2 Aerodynamics

S 21b
F

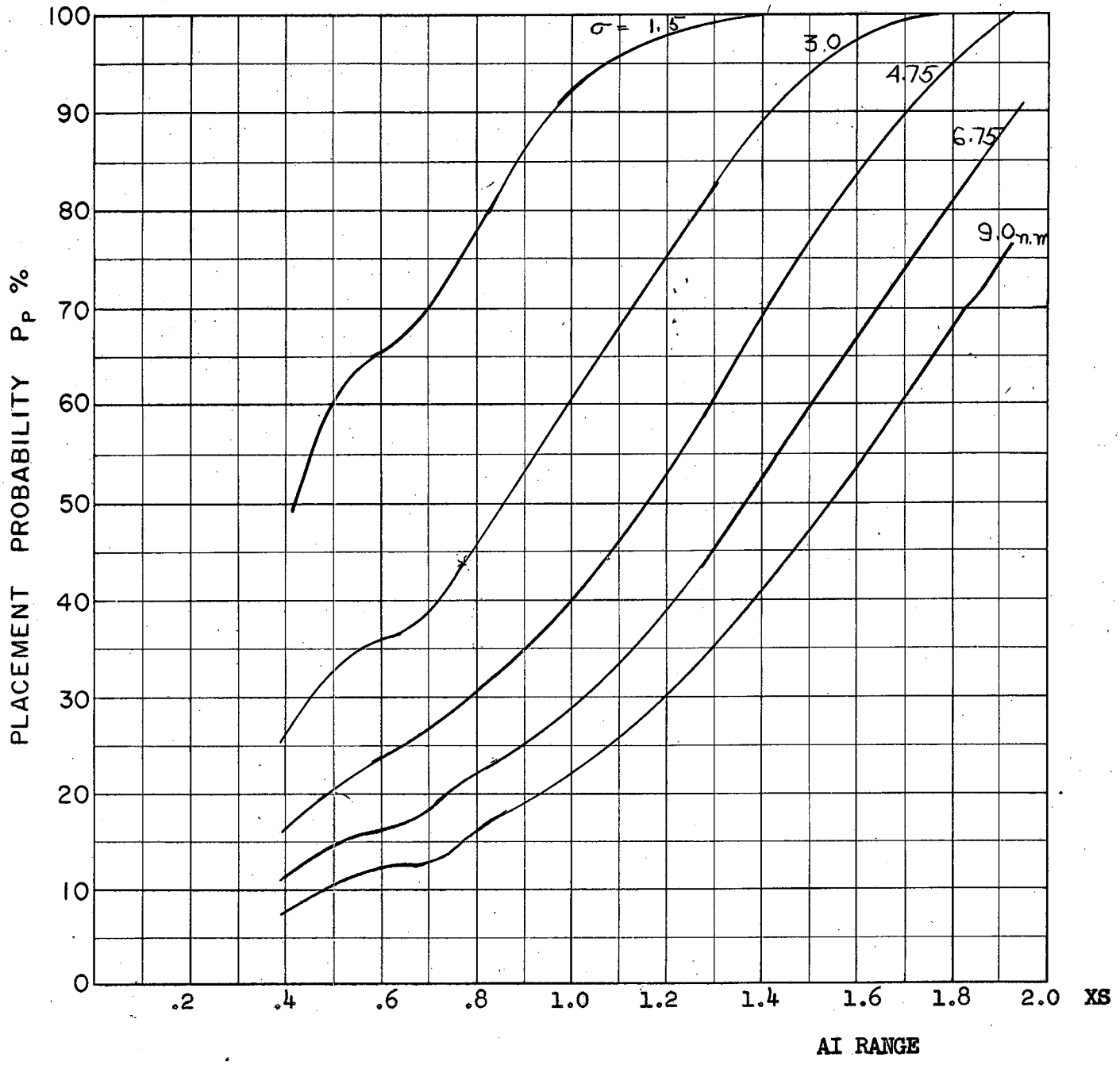

COURSE DIFFERENCE: 180°
TARGET EVASION: 0.5
TARGET MACH NO.: 2.0
INTERCEPTOR LATERAL G's: 1.414 Load Factor Limit
INTERCEPTOR MACH NO.: 2.0 Initial
σ OF G.C.I. ACCURACY: 5 Values
A.I. DETECTION RANGE AS FRACTION OF SPECIFICATION RANGE, S: ABSCISSA
A.I. DETECTION RANGE CONTOUR: Straight
ALTITUDE: 50 K
AVRO 2.2 Aerodynamics

S 21c
F

APPENDIX 'G'

The Three-Dimensional Placement Study

by C.J. Wilson

1. Introduction

A three-dimensional simulation of the aerodynamics of the CF-105 interceptor and of an attack situation has been set up on the CARDE REAC. A proposal for this study was first published in Appendix G of Reference 1, and a discussion of the method of simulating aircraft performance was given in Appendix D of Reference 2.

The period from December to February was spent in setting up the circuit and verifying the results it produces. Useful results are now being obtained. This appendix gives a brief review of the problem and some of the early results.

2. Method

2.1 Launch Zone

The interceptor steers a lead-collision course in three dimensions whenever this is allowed by the constraints in the system, and flies this course to missile launch. The missile is assumed to fly for a time t_f equal to 12.88 seconds with a mean velocity relative to the interceptor of 1165 ft/sec. Thus the launch zone of the missile is represented as a launch sphere centred about a point a distance $V_t t_f$ ahead of the target. The values of t_f and relative velocity were chosen to give a close approximation to the known launch zones for Sparrow missiles. The launch zone was represented in this way in order to make the overall representation of fire control system and launch zone compatible.

2.2 Aerodynamics

The aerodynamic performance estimates which are used are the N.A.E. "28% MAC C. of G. pessimistic" estimates (Reference 3). These data predict that the CF 105 will make a 1.29 g load factor power limited turn at Mach 1.5 at 50,000 ft. altitude. The latest AVRO estimates predict 1.63 g's under the same conditions. The newer estimates will be incorporated into the study at a later date.

2.3 Look Angle

In the two-dimensional placement work it has been assumed that the maximum permissible look angle (angle between the aircraft datum and line of sight) is independent of bank angle and target direction. To allow for over-optimism the limit was taken as 66° whereas the physical limitation is 70° in azimuth. In the three-dimensional model the true geometrical look angle is measured and resolved into azimuth and elevation gimbal deflections of the AI radar antenna. These angles are then compared with the limits quoted by RCA: ± 70° in azimuth, + 75° and -45° in elevation. No information is available as to the exact shape of the general azimuth/elevation limit graph. The field of view that has been assumed in the study to date is shown in figure 1.

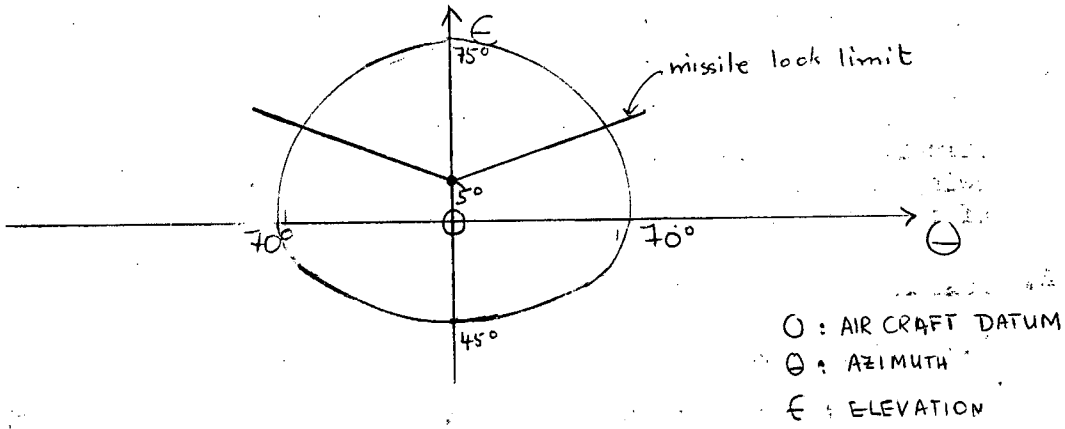

FIG 1

The look angle at launch when Sparrow II missiles are considered is subject to an additional restriction because of the under fuselage position and the necessity for lock-on before launch. The effect this has on the field of view is also shown in figure 1; the limit is of the form

$$\epsilon^{\circ}_{L} = 5.0^{\circ} + 0.241 \ \theta^{\circ}$$

which is an approximation to the limits given on page 33 of Reference 1. If the simultaneous blinding of two missiles is to be considered the limit could extend to

$$\epsilon^{\circ}_{L} = 8.0^{\circ} + 0.495 \ \theta^{\circ}$$

3. Results

A non-evading target flying at Mach 2.0 at 60,000 feet has been considered so far in the study. Attack runs have been made against this target by a CF-105 interceptor flying initially straight at Mach 2.0. Initial interceptor

altitudes between 40,000 and 60,000 feet, and course differences of 75°, 90°, 110°, 135°, 160° and 180° have been considered. Limits of the allowable placement zone have been determined for each case.

The placement charts are reproduced as figures 2 to 7 of this appendix; each figure is drawn for a particular course difference. The chart as drawn is a horizontal projection of the three dimensional placement zone. The boundaries are the limits to the zone within which the interceptor, originally flying straight and level, must start manoeuvring to correct errors in position. "Ideal" approach lines have been drawn on these charts defined as the line along which an interceptor at the target altitude could close to the missile launch point at Mach 2.0 without making a corrective turn.

In this case the results show that variation in interceptor approach altitude does not change appreciably the horizontal limits of the placement zone except at very short AI acquisition ranges where the time available for manoeuvre is short. It also appears that the "ideal" approach line is no longer ideal; that it would be preferable to vector the interceptor ahead of the target when attempting a beam attack. The interceptor loses speed rapidly during high load factor manoeuvres, so that it is easier to turn into a lead-collision course from ahead of the (constant-speed) "ideal" approach line, where the deceleration helps obtain the correct heading, than from the rear, where acceleration would really be required. Further discussion of this effect is given in Appendix 'K'.

4. References

1. CARDE Technical Letter N-47-8, "First Quarterly Progress Report on CF 105 Assessment", Aug 1956. SECRET.

2. CARDE Technical Letter N-47-12, "Second Quarterly Progress Report on CF 105 Assessment", Nov 1956. SECRET.

3. N.A.E. Lab. Memo. No. AE 46g "High Altitude Performance Data for the CF 105 Aircraft". SECRET.

ΔH = 0
ΔH = 10kft
ΔH = 20kft
Ideal Approach
0 10 20 30 40 50 kft

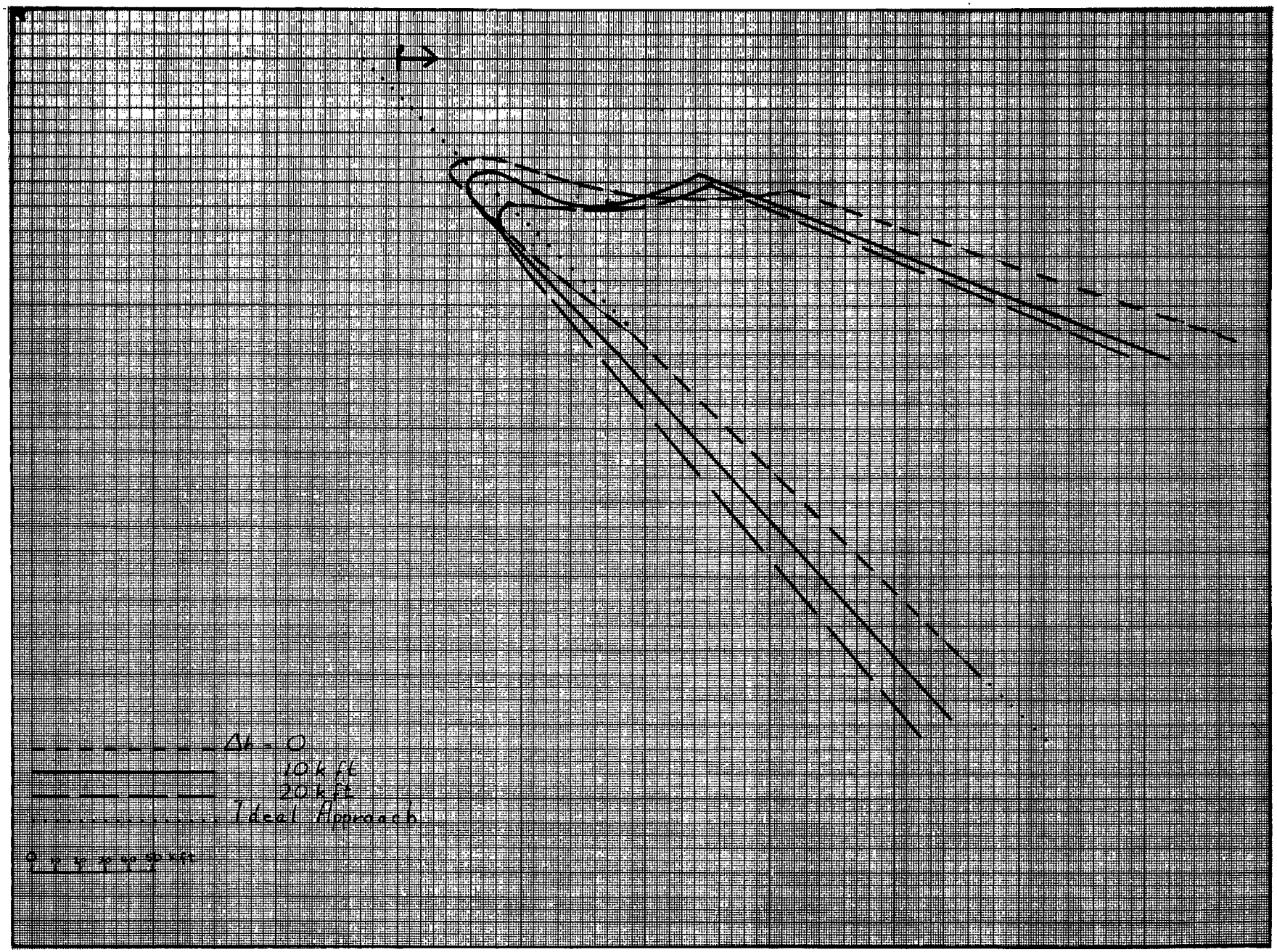
Δh = 0
10 k ft
20 k ft
Ideal Approach

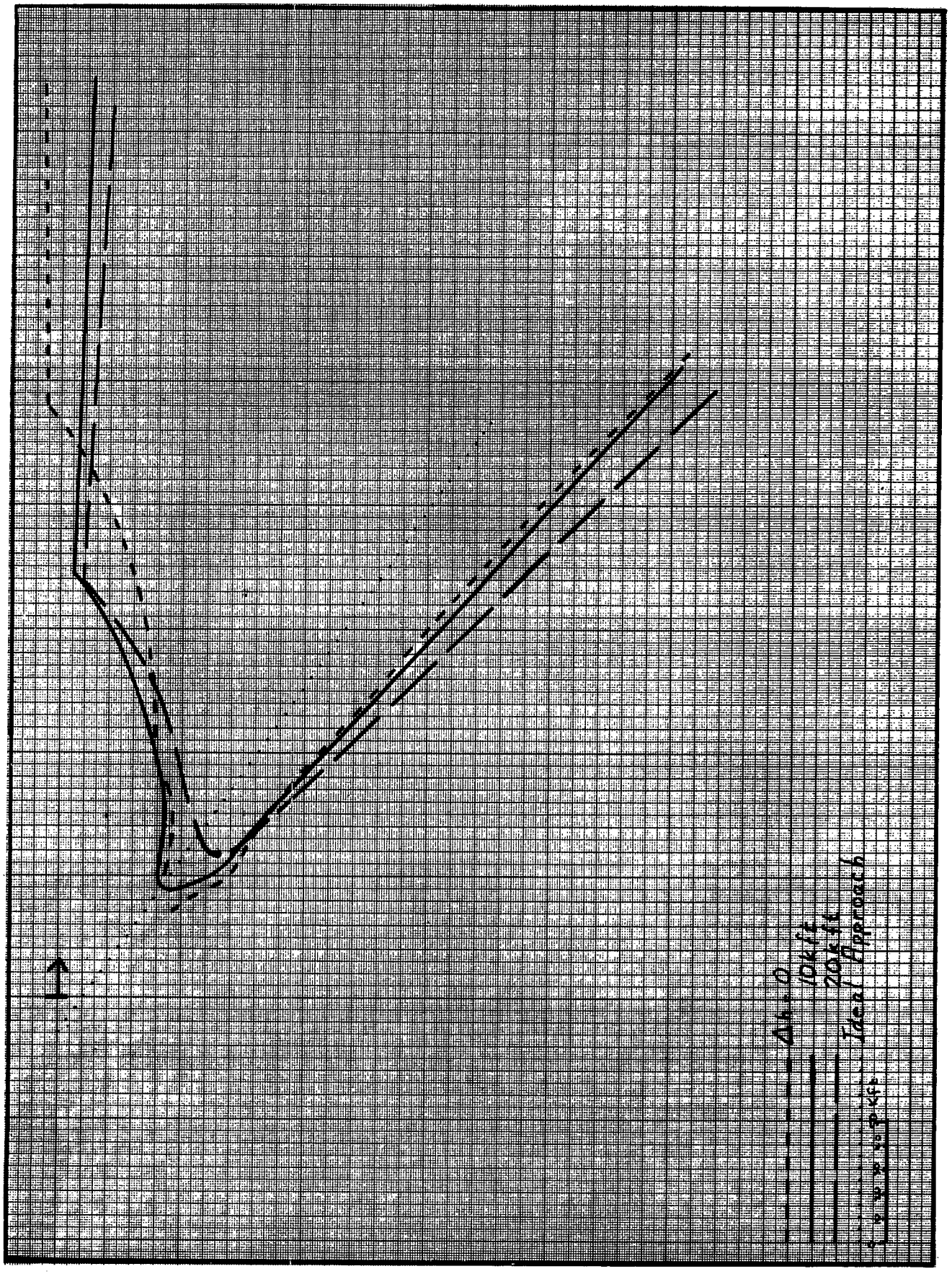
Δh = 0
10kft
20kft
Ideal Approach
H

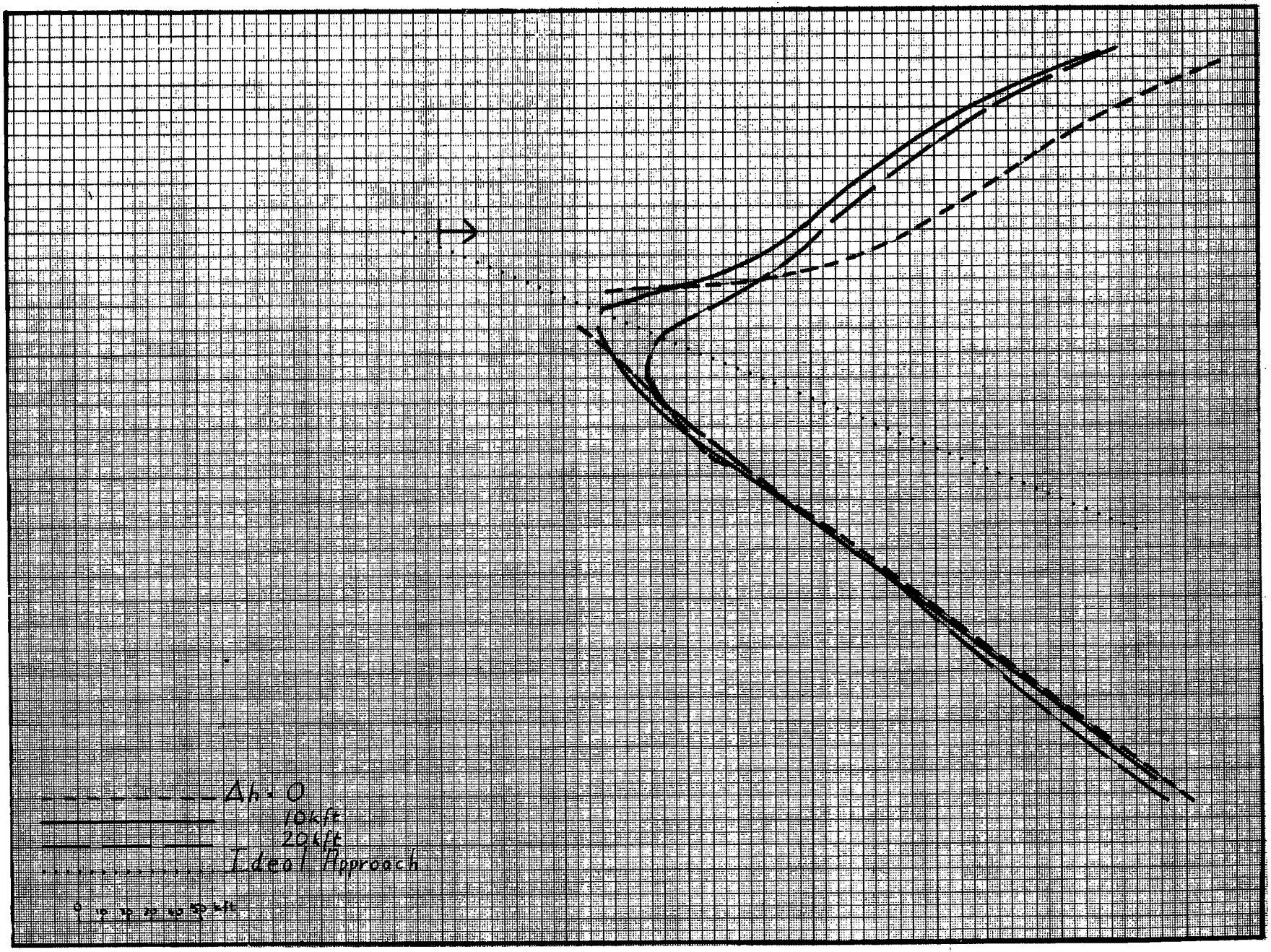
Δh = 0
10kft
20kft
Ideal Approach

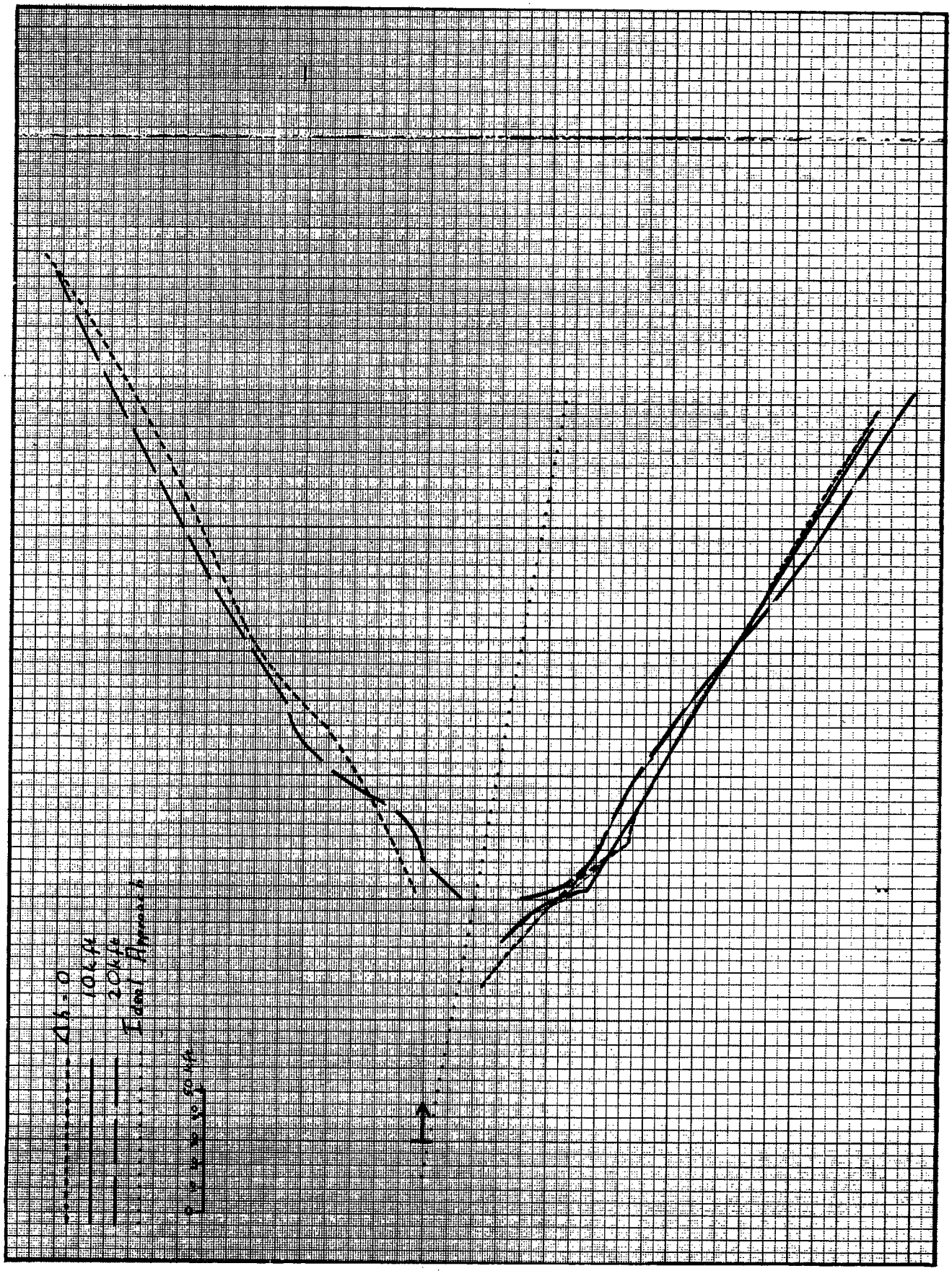
Δh = 0
10 ft
20 ft
Equal Amounts
Equal Amounts

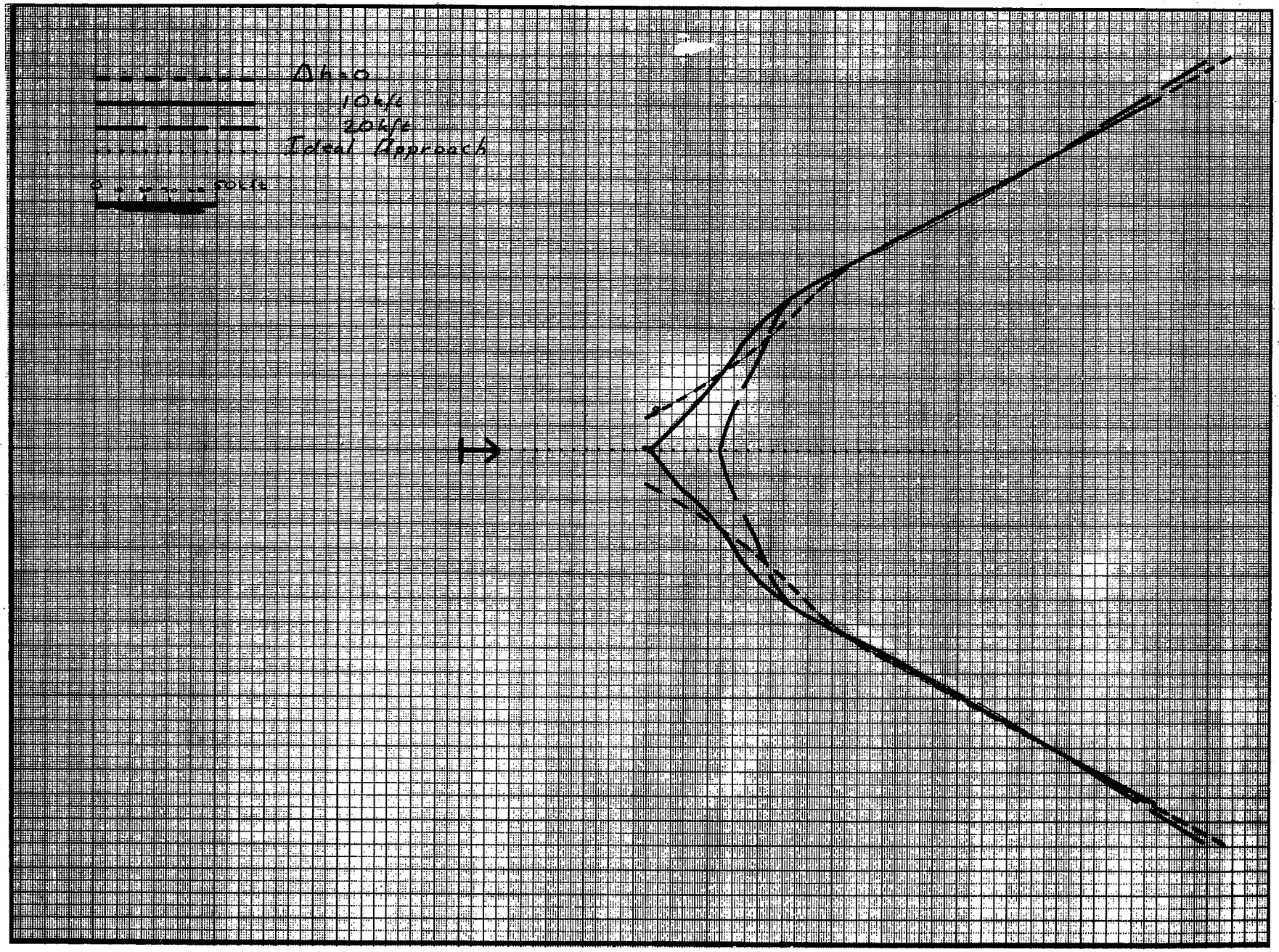
Δh=0
10kfc
20kfc
Ideal Approach
South

APPENDIX 'H'

Study of Engagement Time (Supersonic Targets)

by M.A. Meldrum

1. Introduction

In cases of frontal or near frontal attacks, the time from detection of target to missile firing becomes important from the point of view of time available for pilot or navigator to perform duties in manually firing the missile. Consideration of such a problem will determine which functions must be performed automatically to fire the missile.

2. General Conditions

(a) Engagement time was computed on the ideal approach line for various A.I. radar detection ranges, target and fighter speeds and course differences near 180°, with both evading and non-evading targets.

(b) Missile launch range was assumed to be 50,000 ft. at aspects near 180°. This is a somewhat pessimistic range since in practice the missile would probably be launched at shorter ranges.

3. Constant Speed Fighter

(a) $$T_e = \frac{R_s - 50{,}000}{971\sqrt{M_f^2 + M_t^2 - 2M_fM_t \cos \gamma_o}}$$

where

T_e = engagement time in seconds

R_s = initial range of fighter when target detection takes place

γ_o = initial course difference

M_t = target Mach no.

M_f = fighter Mach no.

(b) Cases Examined

1) $\gamma_o = 180^\circ$ $M_f = 1.8$ $M_t = 2$

2) $\gamma_o = 180^\circ$ $M_f = 1.5$ $M_t = 2$

3) $\gamma_o = 180^\circ$ $M_f = 0.9$ $M_t = 2$

Results are shown in Figure 1.

4. Variable Speed Fighter

(a) Assumed conditions

$M_t = 2.0$ M_f initial = 1.8 Height = 50,000 ft.

Target evasion is unlimited

(b) Cases examined

1) $g_t = 0.5$ $\gamma_o = 180^\circ$ 3) $g_t = 0.75$ $\gamma_o = 180^\circ$

2) $g_t = 0.5$ $\gamma_o = 135^\circ$ 4) $g_t = 0.75$ $\gamma_o = 135^\circ$

Results are shown in Figure 2.

5. Conclusions

(a) The worst case possible of $M_t = 2.0$, $M_f = 1.8$ and $\gamma_o = 180^\circ$ showed engagement time to be 13.5 seconds at 100,000 ft. acquisition range. If the minimum engagement time is considered to be 10 seconds, then placement of the fighter at a range less than 100,000 ft. from the target, for this case, will produce an "engagement time barrier".

(b) Decreased fighter or target speed would allow the fighter further engagement time.

(c) Since the variable speed fighter decelerates in turning, the relative closing rate between target and fighter is less than that as compared to the constant speed case. Figure 2 shows that for the cases examined, there is some increase in available engagement time, although it is not too significant.

(d) Since the time of missile firing was considered to occur at the outer launch contour, an additional 2 to 3 seconds is still available for launching at the minimum launch contour.

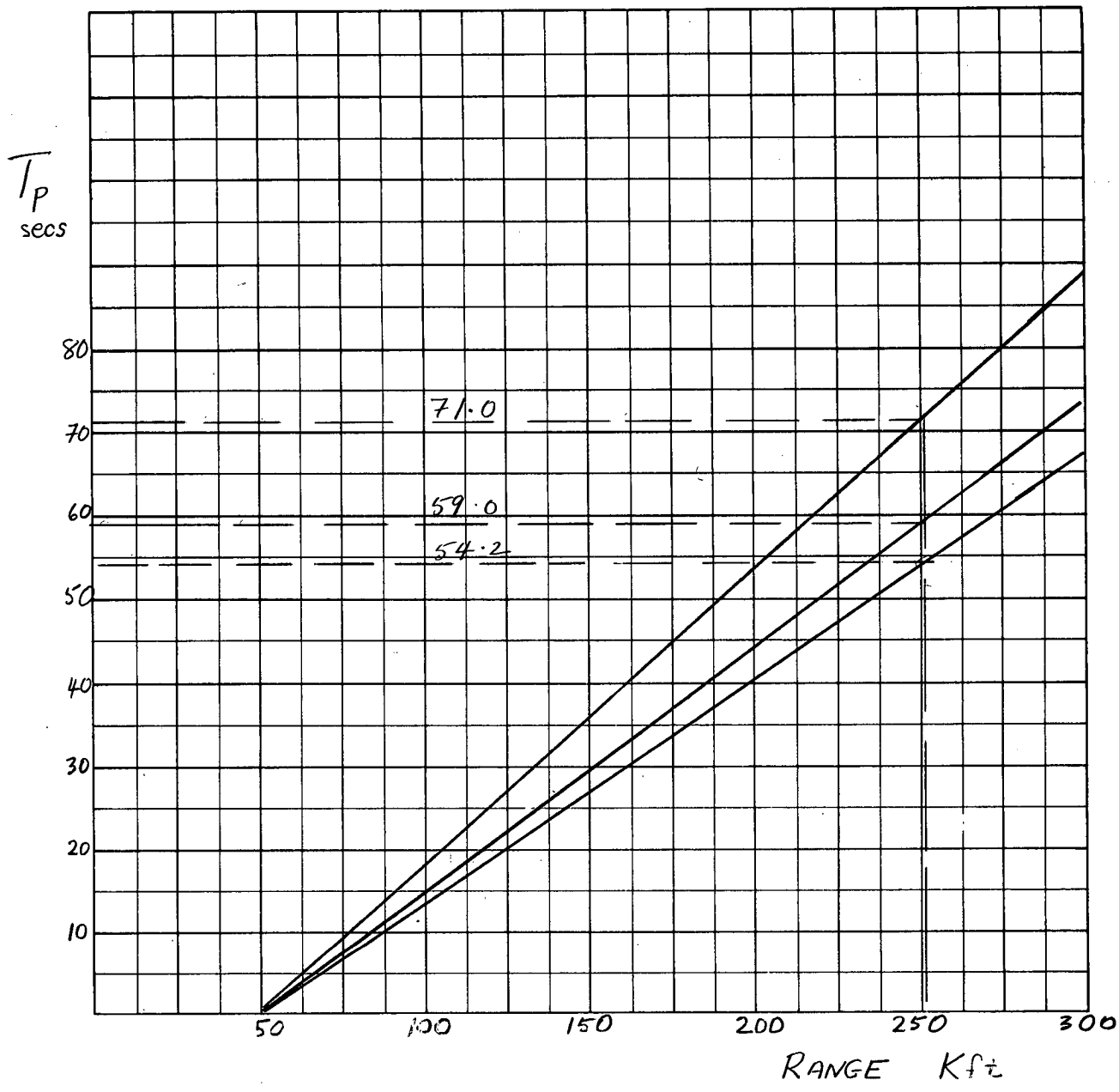
T_P
secs
80
70
60
50
40
30
20
10
71·0
59·0
54·2
50
100
150
200
250
300
RANGE Kft

FIG 1

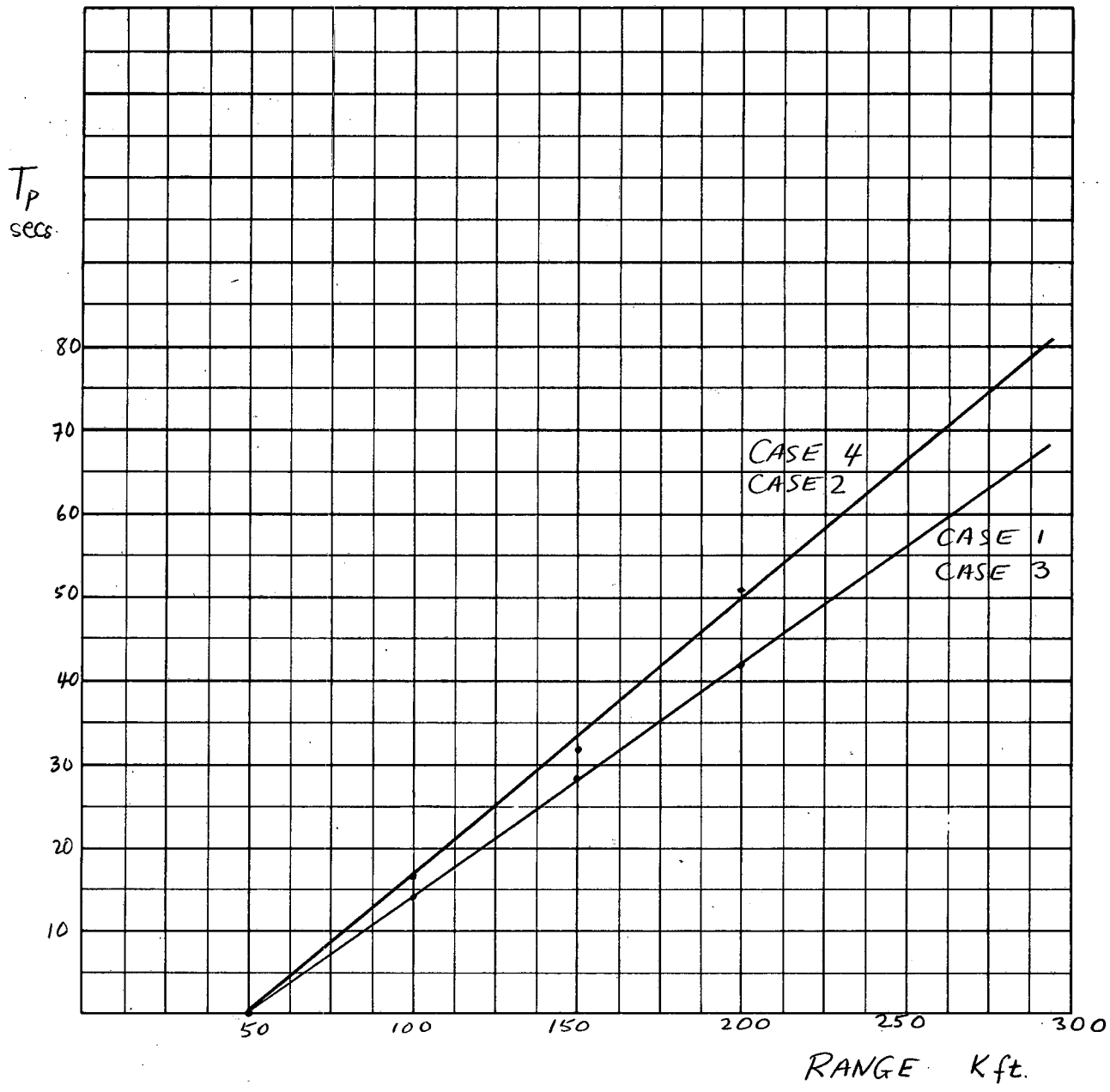
T_P
secs
80
70
60
50
40
30
20
10
50
100
150
200
250
300
CASE 4
CASE 2
CASE 1
CASE 3
RANGE Kft.

FIG. 2

APPENDIX 'J'

A Study of the Attack after Missile Launch

by Lloyd Shepherd

1. Introduction

An investigation has been made into the phase of the attack after missile launch. There was concern about the safety of the interceptor after launching the missile and about illuminating the target until the kill is achieved if a semi-active missile is used. The three questions involved then are:

i) danger of collision with the target,

ii) danger of being shot down by the target if a K kill is not achieved,

iii) possibility that the radar in the fighter will not illuminate the target for the duration of the missile flight, in the case of a semi-active missile.

2. Method of Solution

A graphical method of solution was adopted for this problem. Fighter trajectories in target coordinates based on N.A.E. performance estimates were available in Appendix C of CARDE Tech. Letter N-47-12, (Second Quarterly Report on CF-105 Weapon System Assessment). The data used was for a fighter with initial velocity of Mach 1.5 and target velocities of Mach 2.0, 1.5 and 0.85, flying at initial course differences of 180°, 160°, 135°, 110°, 90°, and 75°.

The launch zones were constructed for a hypothetical missile similar to Sparrow II. The maximum range contour was drawn for a missile having an incremental missile velocity of 1000 ft./sec., a time of flight of 20 sec. and an F-pole of 20,000 ft. The maximum range contour was modified by a seeker range of 50,000 ft. which is consistent with other work done in this report. The minimum range contour for the Mach 2 target was taken as a circle representing a flight time of 10 seconds. Some recent information on minimum launching range of Sparrow II obtained on a visit to the U.S.A. (CARDE Tech. Letter N-47-16) showed missile flight distances somewhat shorter than was originally assumed. The minimum flight distance against a Mach 0.85 target was given as approximately 15,000 ft. A minimum range launch contour was drawn for the Mach 0.85 target using this 15,000 ft. radius, and the effects of launching missiles at this range was investigated.

The trajectories for maximum rate of turn were traced on the launch zones for the six course differences. A measurement could then be made to determine the minimum closing range. The total interceptor turn could be calculated using the trajectory data and the time of flight of the missile. From this the value of look angle at the time of missile impact was determined.

3. Results

Curves representative of the results are included. Some of the expected trends were verified.

i) The time of missile flight determines to a large extent the angle through which the fighter turns and the distance it can move from its initial path.

ii) At head-on aspects the approach distance and the final look angle are both smaller than at beam aspects. Especially at beam aspects there is a danger of exceeding the look angle before a kill is achieved. Depending on the speeds, however, this could occur at any aspect.

iii) The decreased manoeuvrability at increased altitudes will decrease the approach distance and also the final look angle.

iv) If the missile is launched with a heading error, both the approach distance and the look angle are affected in an almost linear way. The effect is not extensive.

v) Evasion by the target toward the fighter path will decrease the approach distance and decrease the look angle. Evasion away from the interceptor will have the opposite effect on both quantities. With the rates of evasion considered in the placement studies, evasion is not a serious consideration.

The cases studied were not extensive; however, with the present knowledge of the interceptor and possible targets, the study has given some information on the phase of the attack after missile launch.

The minimum approach range which was encountered in the study was 3000 ft. in the case of launch at minimum range, 180° aspect and against the Mach 0.85 target. The maximum effective range of enemy cannon is believed to be 3000 ft. It is further believed that the tracking rate of cannon is about 15°/sec. whereas at these velocities and at close ranges, the angular change in aspect is of the order of 30°/sec.

4. Conclusions

Conclusions from this study can then be stated:

i) If the interceptor manoeuvres after launching the missile it is capable of avoiding collision with the target.

ii) It can be concluded that unless there is a considerable improvement in bomber armament, there is little danger of being shot down in this phase of the attack. At head-on aspects it is necessary to begin the manoeuvre immediately after missile launch and to turn away from the target's path rather than across it.

iii) Under the conditions of beam aspects and slow flying targets, the interceptor will not be able to turn away indiscriminately after launching its missiles if the missiles are semi-active. With proper instructions it would be possible to illuminate the target for the entire time of flight of the missile and still not approach dangerously close to the target.

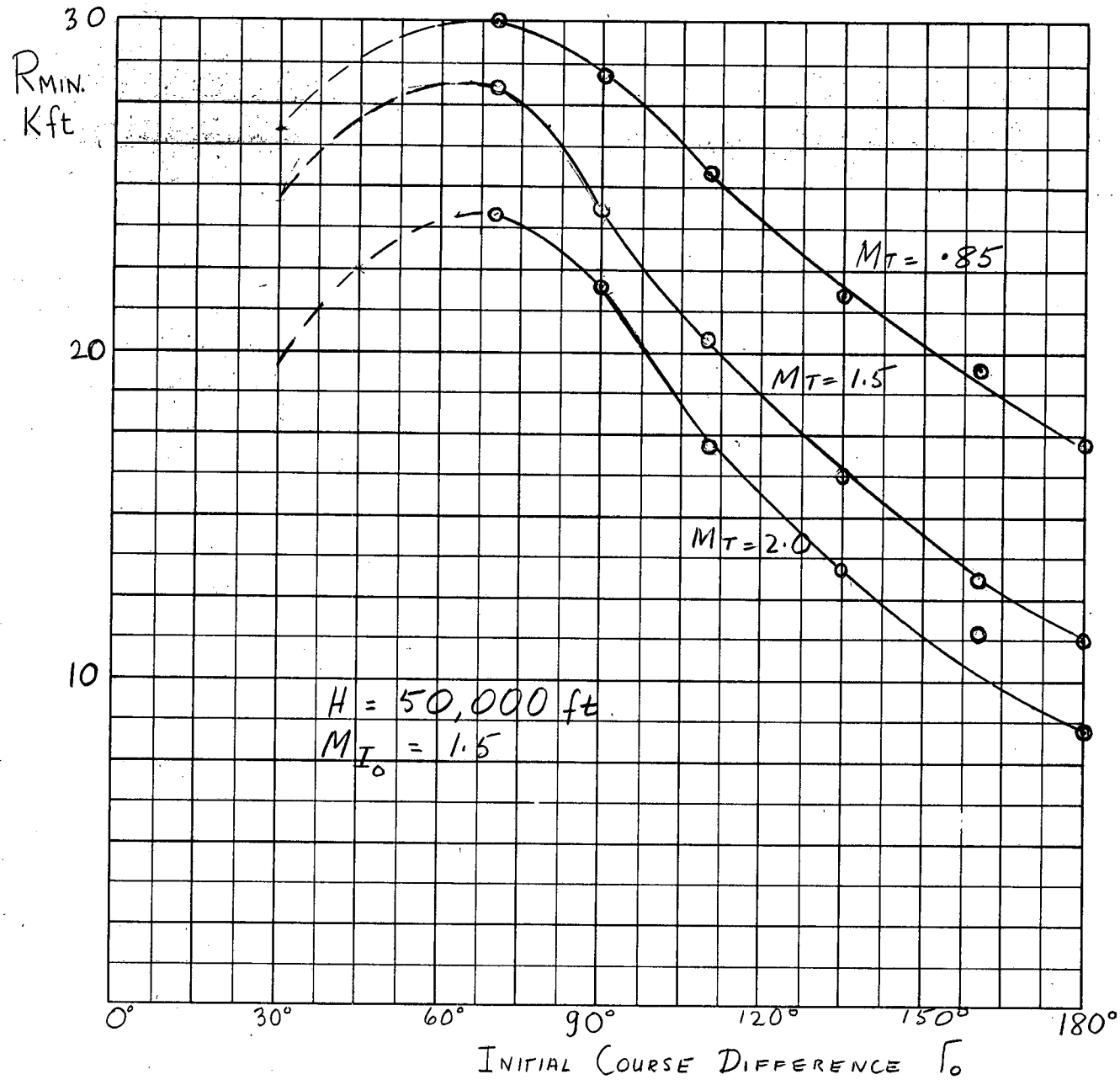
30
RMIN.
Kft
20
10
M_T = .85
M_T = 1.5
M_T = 2.0
H = 50,000 ft
M_{I_0} = 1.5
0°
30°
60°
90°
120°
150°
180°
INITIAL COURSE DIFFERENCE Γ_0

FIG 1A
J

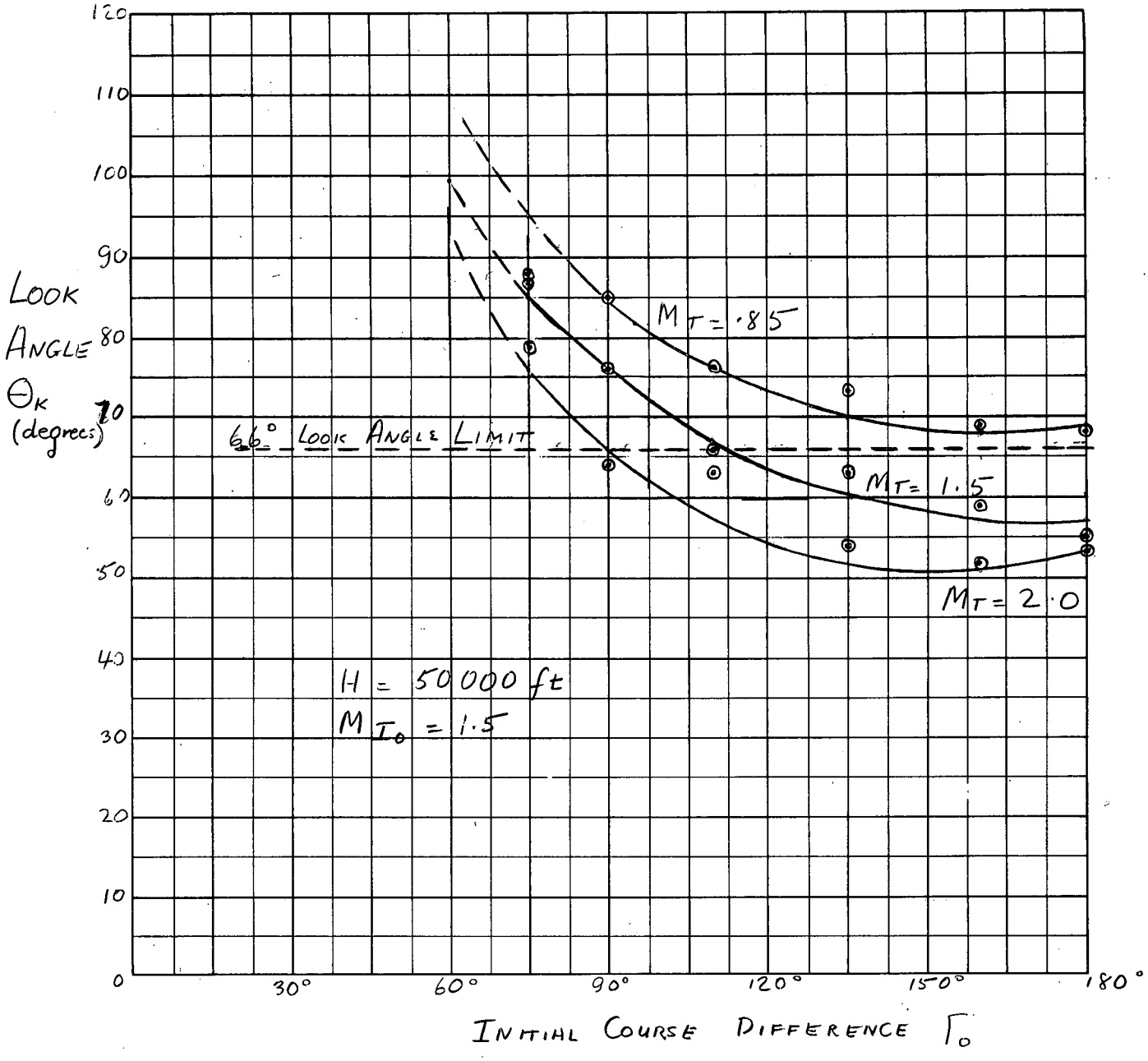
120
110
100
90
80
70
60
50
40
30
20
10
0
LOOK ANGLE Θ_K (degrees)
66° LOOK ANGLE LIMIT
$M_T = .85$
$M_T = 1.5$
$M_T = 2.0$
H = 50 000 ft
$M_{I_0} = 1.5$
30°
60°
90°
120°
150°
180°
INITIAL COURSE DIFFERENCE Γ_0

FIG 1B
J

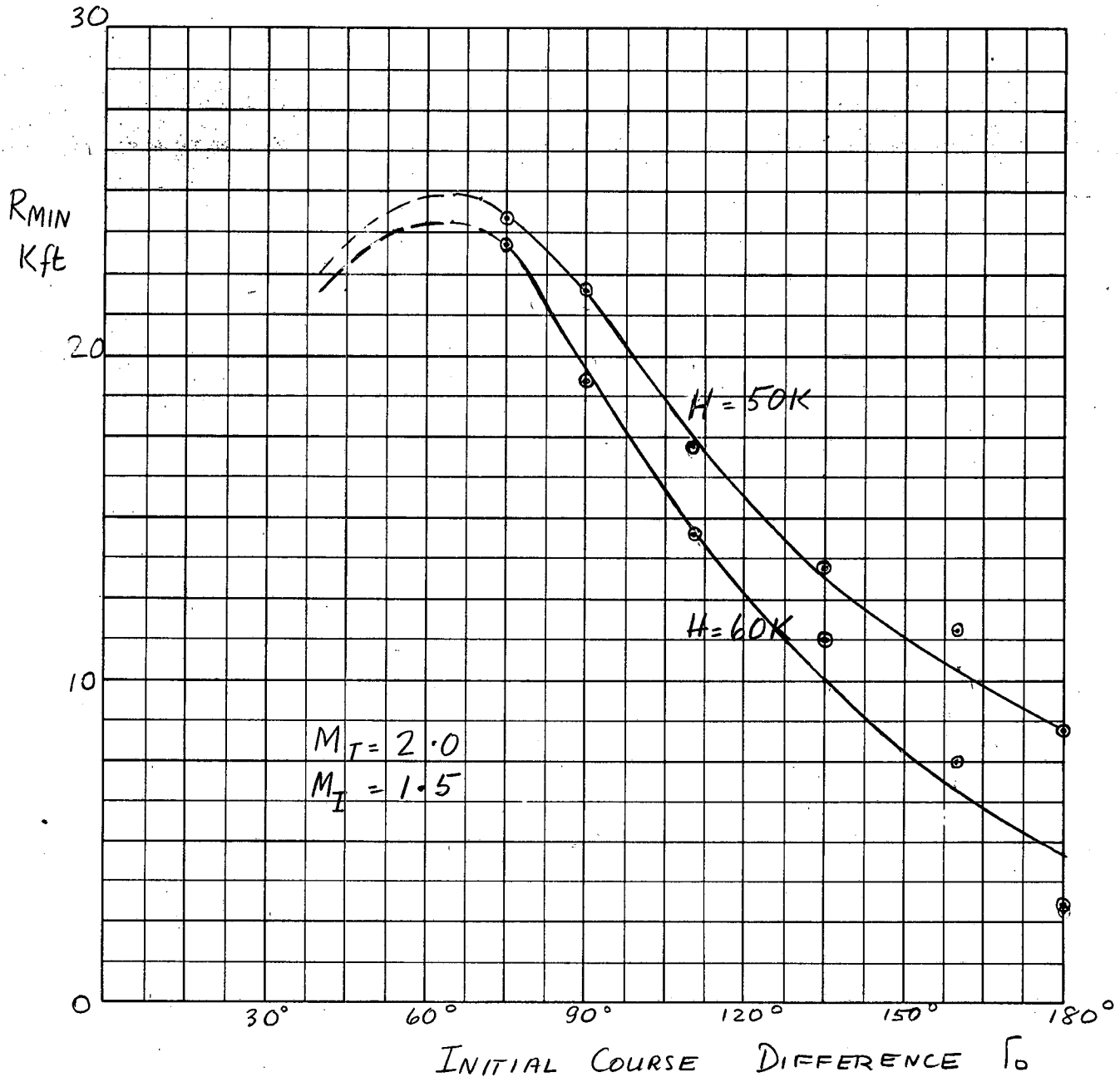
30
20
10
0
R_{MIN} Kft
H = 50K
H = 60K
$M_T = 2.0$
$M_I = 1.5$
30°
60°
90°
120°
150°
180°
INITIAL COURSE DIFFERENCE Γ_0

FIG 2A
J

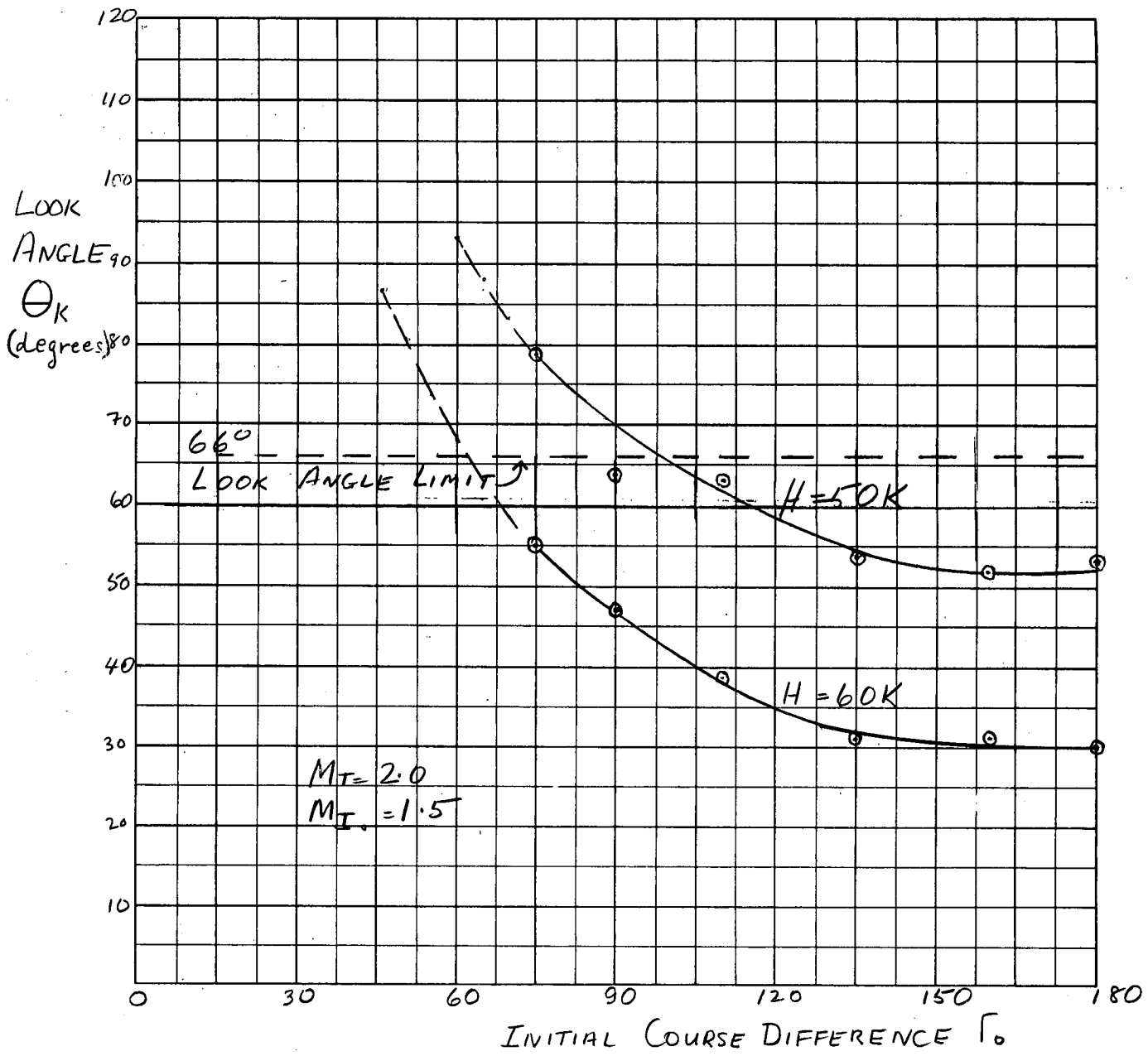
LOOK ANGLE θ_K (degrees)
120
110
100
90
80
70
60
50
40
30
20
10
0
30
60
90
120
150
180
66°
LOOK ANGLE LIMIT
H = 50K
H = 60K
M_T = 2.0
M_{T_0} = 1.5
INITIAL COURSE DIFFERENCE Γ_0

FIG 2B
J

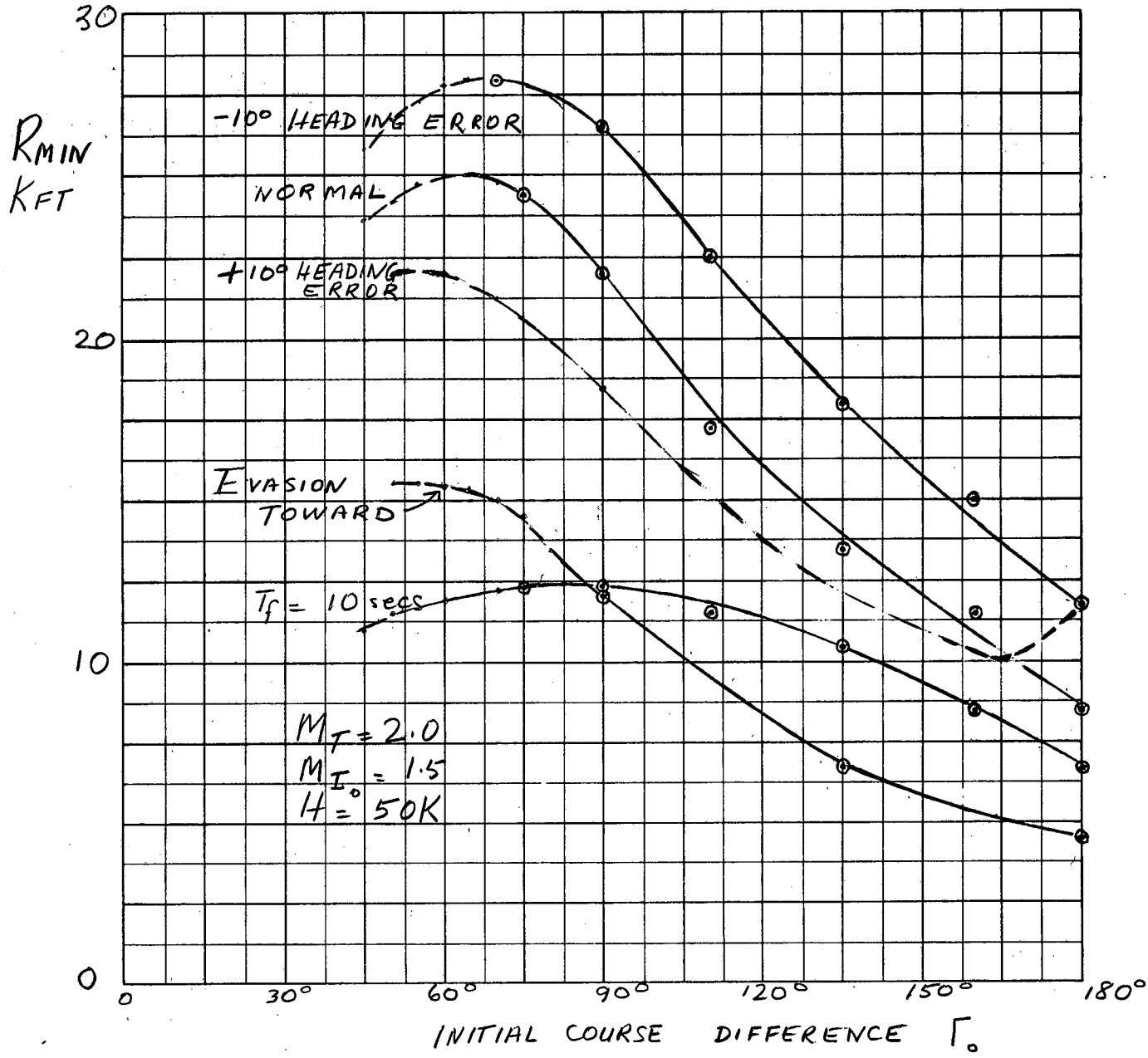
30
20
10
0
R_{MIN} KFT
-10° HEADING ERROR
NORMAL
+10° HEADING ERROR
EVASION TOWARD
T_f = 10 secs
M_T = 2.0
M_{T_0} = 1.5
H = 50K
0
30°
60°
90°
120°
150°
180°
INITIAL COURSE DIFFERENCE Γ_0

FIG 3A
J

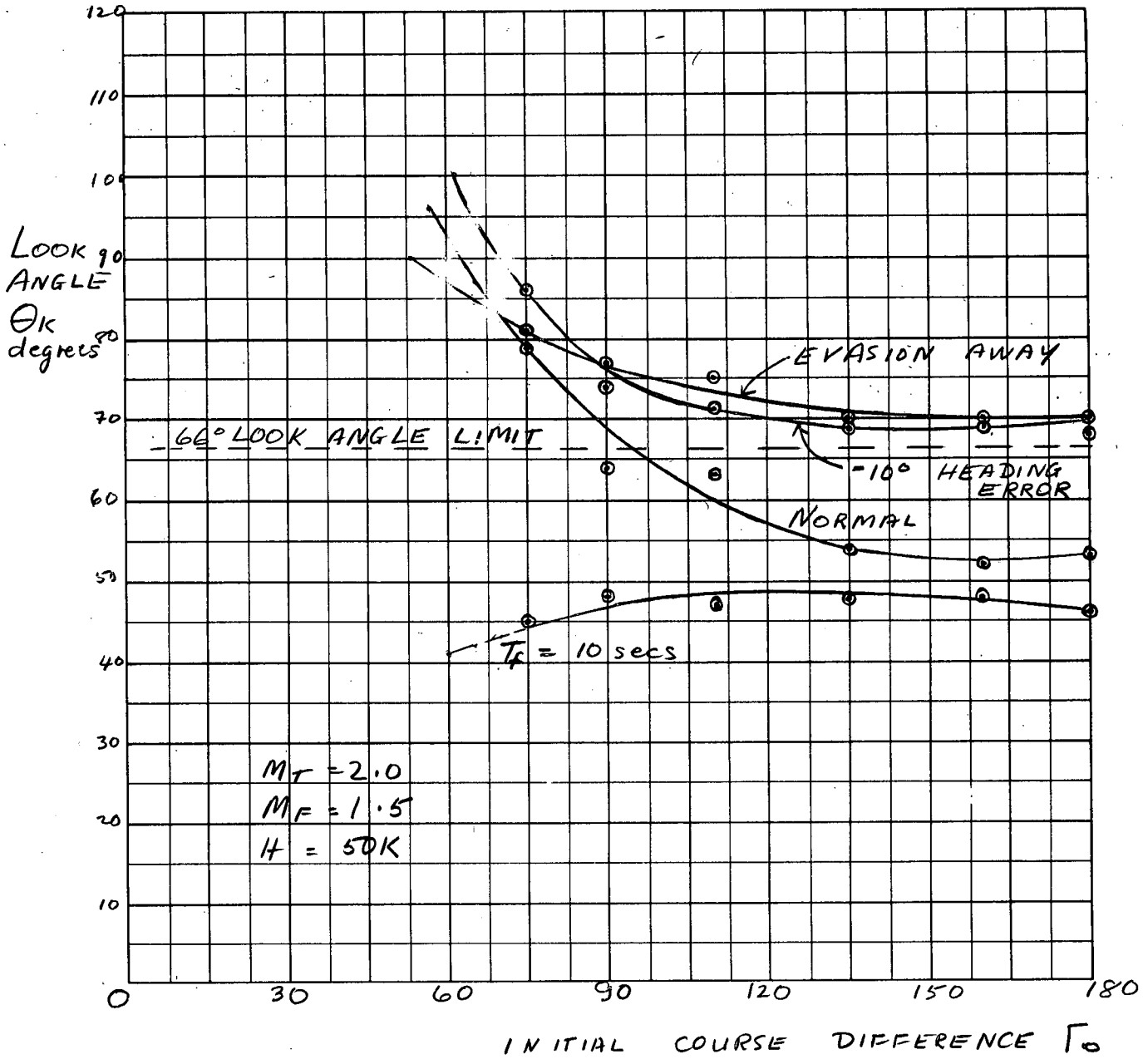
LOOK ANGLE θK degrees
120
110
100
90
80
70
60
50
40
30
20
10
0
30
60
90
120
150
180
INITIAL COURSE DIFFERENCE Γo
66° LOOK ANGLE LIMIT
EVASION AWAY
-10° HEADING ERROR
NORMAL
Tc = 10 secs
MT = 2.0
MF = 1.5
H = 50K

FIG 3B

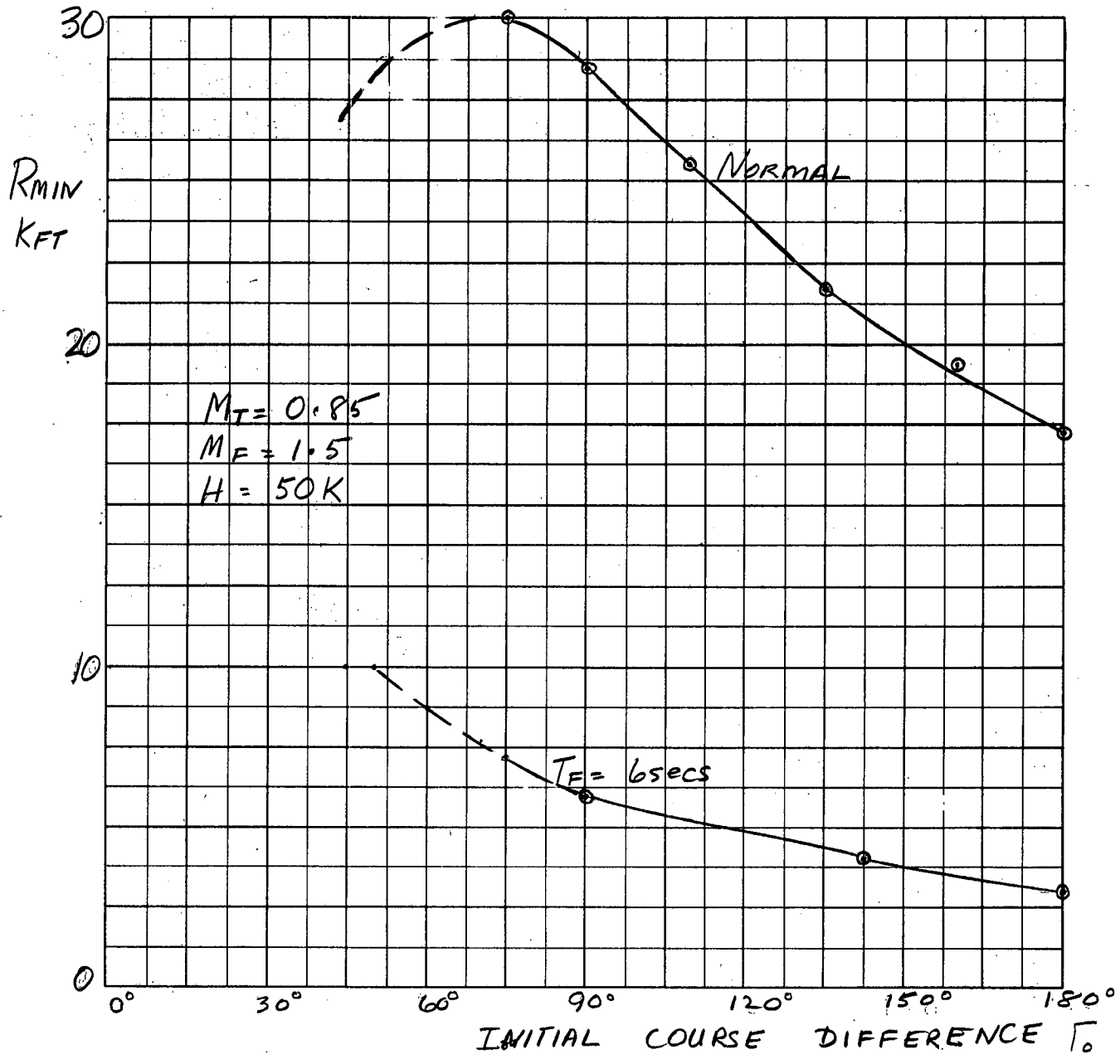
30
20
10
0
RMIN
KFT
NORMAL
MI = 0.85
MF = 1.5
H = 50K
TF = 65ecs
0°
30°
60°
90°
120°
150°
180°
INITIAL COURSE DIFFERENCE Γo

FIG 4A
J

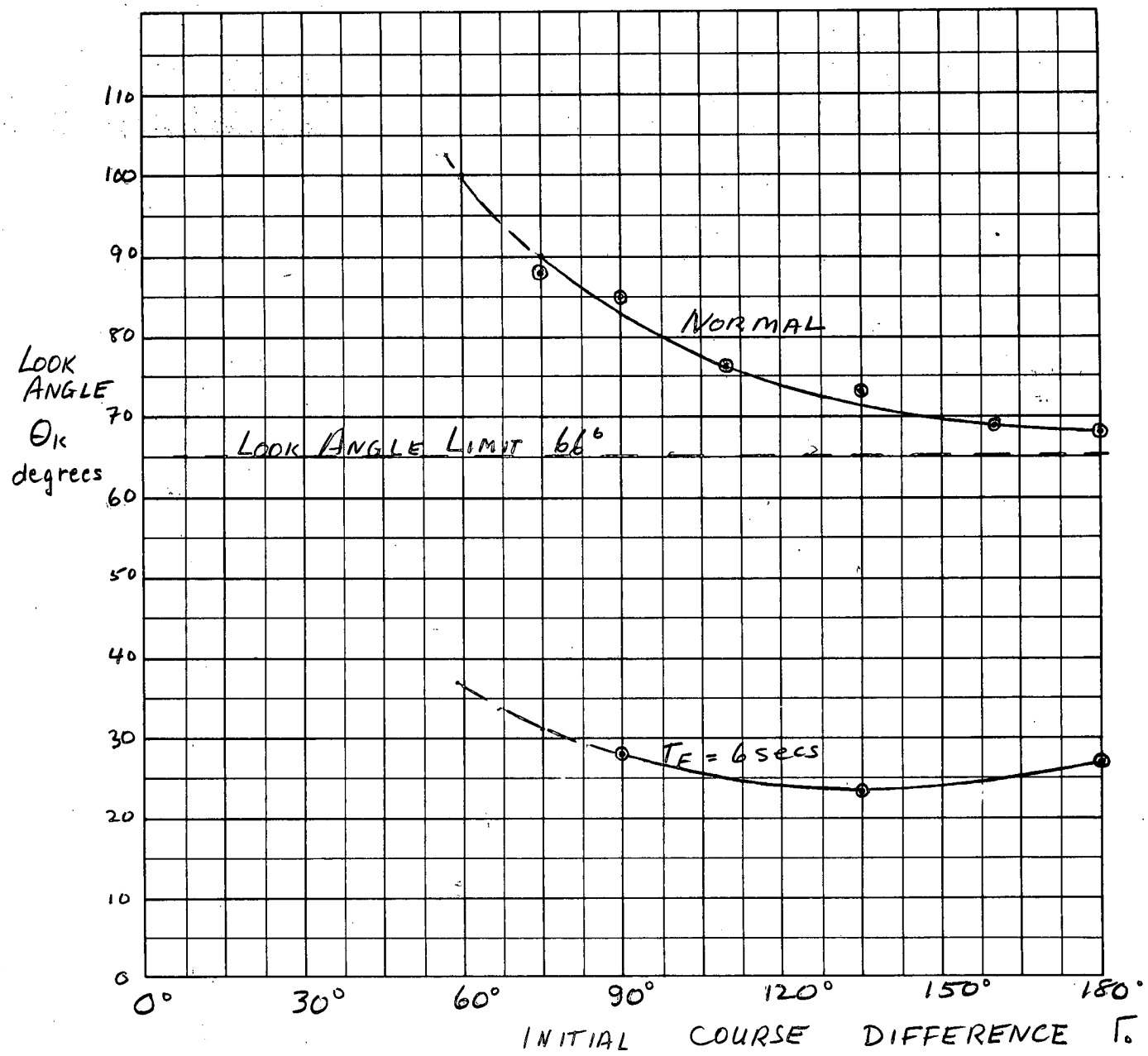
110
100
90
80
70
60
50
40
30
20
10
0
LOOK ANGLE θ_k degrees
NORMAL
LOOK ANGLE LIMIT 66°
T_E = 6 secs
0°
30°
60°
90°
120°
150°
180°
INITIAL COURSE DIFFERENCE Γ_0

FIG 4B

J

APPENDIX 'K'

The Restrictive Effects of the AI Radar Look Angle Limits

by J. Cummins & C.J. Wilson

1. Introduction

The required value of the angle between the direction of the interceptor track and the line of sight to the target, called the lead angle, is a function of the interceptor and target speeds, their instantaneous position, and the attack mode. If the interceptor has a considerable speed advantage the lead angle need never be very large. For example, for speed ratio 3:2 it will never exceed 45°. For equal speed interceptions, or where the interceptor has a speed disadvantage, the required lead angle may exceed the look angle limits of the AI radar. Some possible methods of avoiding failures produced by this cause are considered in this appendix.

2. Descriptive Example

Consider a co-altitude equal speed interception, steered on a true collision course, with initial course difference between interceptor and target of 135°. Look-angle limit is assumed to be 70°.

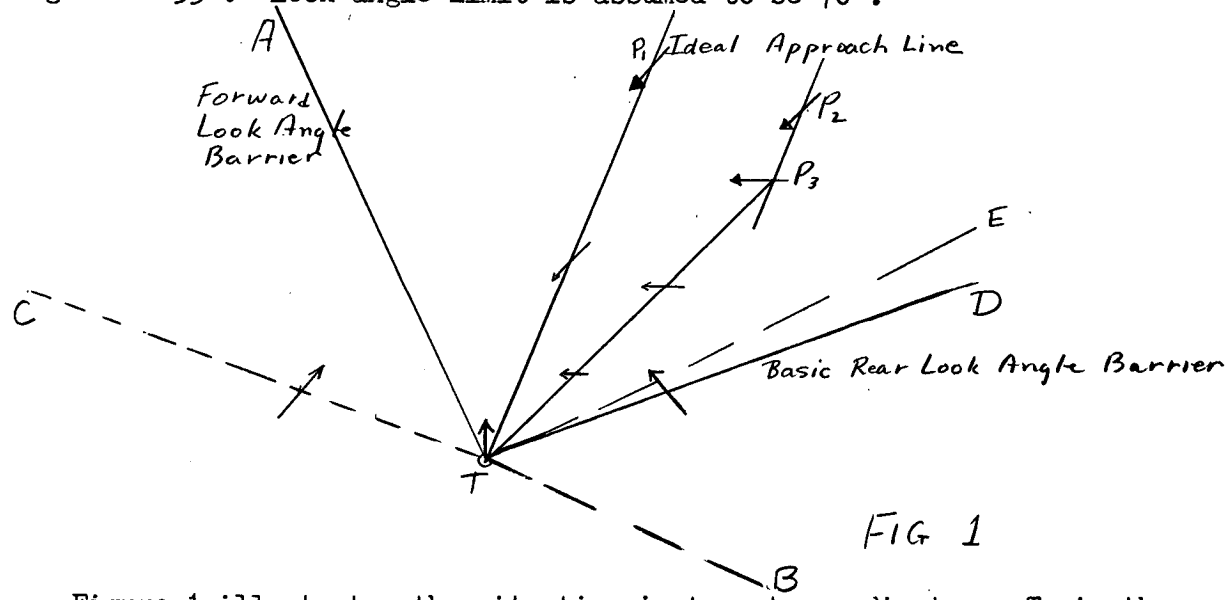

FIG 1

Figure 1 illustrates the situation in target coordinates. T is the target, and P_1 an interceptor on the ideal approach line for the attack conditions assumed. An interceptor approaching along any other line must make a corrective turn in order to complete a successful attack.

In effect the interceptor must position itself on a new ideal approach line corresponding to a new relative heading. For instance a fighter P_2 can turn through 45° at P_3 and approach on the ideal line for 90° course difference.

2.1 Rear Look Angle Barrier

The limiting approach line behind the original ideal line is TD which is that along which the interceptor's lead angle is equal to the look angle limit, 70° in this case; the course difference for equal speeds being 40°. An interceptor which is behind the original ideal line must have made AI contact and its corrective turn before reaching this line TD. Since the interceptor requires a finite time to make its turn and the line TD is the line by which turn must be completed, the effective look angle barrier is therefore in front of this line, and is in general curved, as TE.

If the interceptor is allowed to decelerate while turning, the effective look angle barrier tends to move still farther forward since the approach line on which the lead angle is 70° is farther forward for a slower interceptor.

The line TB in the figure, is drawn to represent the limit behind which the interceptor on its original course difference will no longer see the target. The sector DTB is however of no use to an interceptor which must fly a collision course.

2.2 Forward Look Angle Barrier

On the other side of the original ideal line, a line AT is the limit at which the interceptor's AI can view the target on its original course. The corrective turn must take place on or before this line is reached, unless it is to be made blind.

Thus the lines ATD include the segment of target space within which the interceptor must make its corrective turn, for the given initial course difference.

Symmetrical with the line TD, the line CT is drawn, to indicate the line by which the corrective turn to a collision course must be complete for approach ahead of the ideal line. CT is the approach line for course difference -40° (320°).

It is thus seen that the effective look angle barriers are AT and TE. The sectors of target space ATC and DTB can in some cases be used, and it is the object of this note to discuss this.

3. Suggested Tactics

3.1 Fixed Lead Angle Attack

Conversion of the mode of attack from Lead collision when the look angle reaches its limit, to a course with the look angle fixed near its limit, allows the interceptor to turn less quickly and thus to accelerate. The interceptor will tend to fall back into a tail chase, thus overcoming the look angle limit, and eventually a lead collision course may be re-established if the interceptor has a potential speed advantage over the target. Since look angle is a function of bank angle it would be difficult in practice to fly a fixed lead course for an accelerating interceptor.

3.2 Constant Speed Turns

Limiting the interceptor's load factor to a value such that no deceleration occurs during turns. This means that the bank angle remains small and the 45° depression limit proposed for the CF 105's radar will not become restrictive. Also, since the interceptor speed would be maintained the look angle barrier would be farther back.

3.3 Lead Pursuit Mode

A lead pursuit mode of attack for a given speed ratio requires a smaller value of lead angle. The possibility that this may be the best attack mode in view of this fact has not been fully analysed as yet at CARDE.

3.4 Choice of Ideal Line for Vectoring

Vectoring along an ideal line which is ahead of the interceptor produces the largest probability of successful placement since it permits more room for non decelerating manoeuvre behind the line; deceleration on manoeuvre ahead of the ideal line is not objectionable.

4. Simulation Results

To illustrate the look angle problem, a placement zone has been drawn using the REAC interception simulation, with the NAE assumed CF 105 performance. Parameter values chosen were

Target Mach No. 1.5
Initial Interceptor Mach No. 1.8
Altitude 50,000 feet
Initial course difference 135°
No target manoeuvre

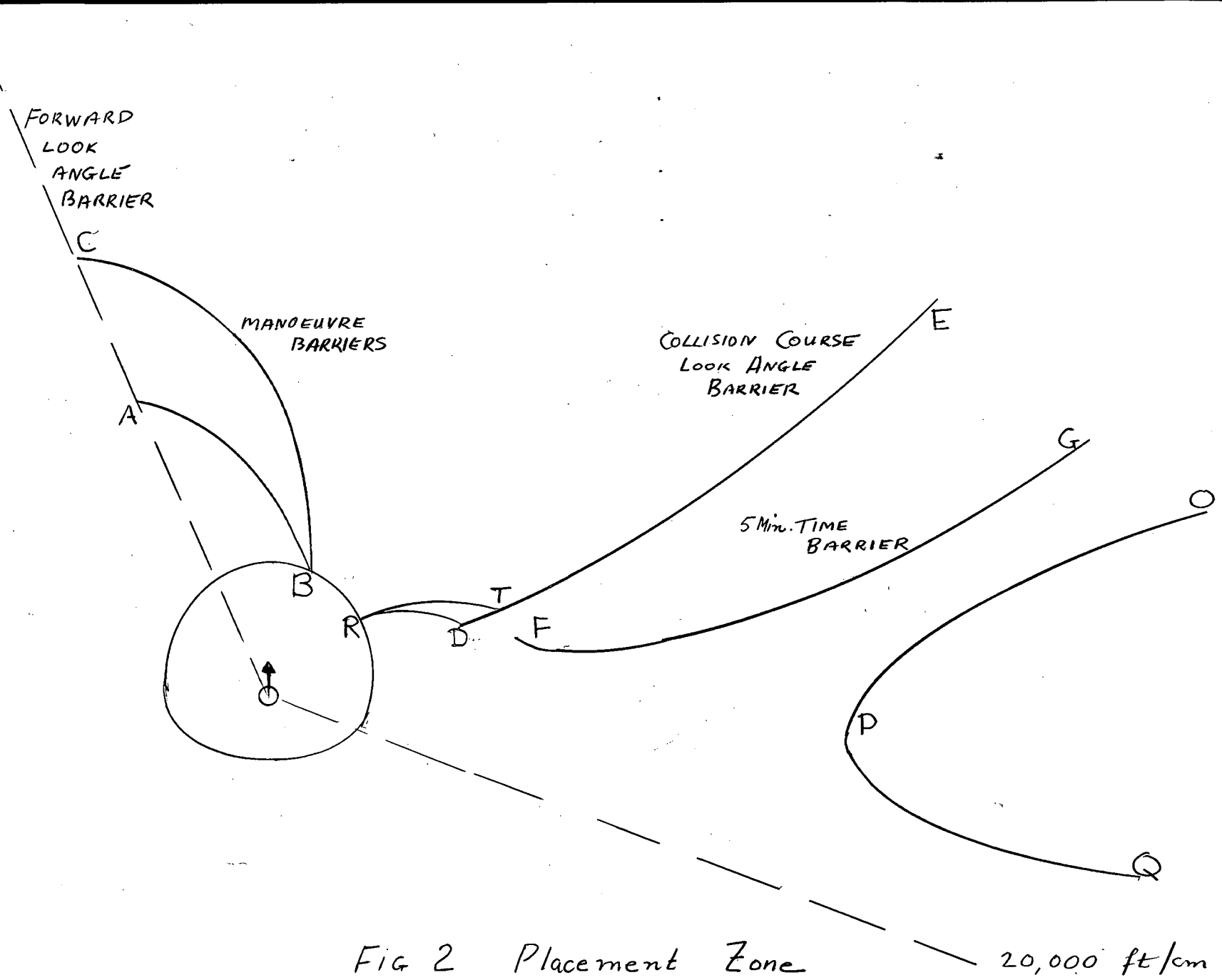

Fig 2 Placement Zone

4.1 The Placement Zone

The system of barriers obtained is shown in figure 2.

ED is the rear look angle barrier obtained for the usual lead collision navigation.

AB and RD are the manoeuvre barriers obtained when the interceptor is allowed to manoeuvre to the buffet limit.

If the interceptor lateral acceleration is limited to 1.5 g (load factor 1.8) the speed loss is reduced, but the manoeuvre barriers are moved to BC and RT . The look angle barrier is then OPQ.

If the lead-collision navigation equations are replaced by a fixed look angle steering mode when the look angle approaches its limit, the look angle barrier disappears. It may be replaced by a time limit barrier, FG is the barrier for interception within five minutes.

4.3 Trajectories

A few sample interceptor trajectories in target corrdinates are drawn in figures 3 and 4 to illustrate the modes of attack described.

The trajectories of figure 3 are for the case of an interceptor using buffet limit load factor turns on a lead collision course, with conversion to fixed lead angle steering at the points marked C on the curves.

For trajectory numbered 2 on figure 3, the simulator records show that interceptor speed drops from Mach 1.8 to Mach 1.25 in 35 seconds. The lead angle is then 70° and would increase beyond the permissible limit if the lead collision course were maintained. The aspect angle is about 90° at that instant, and the interceptor is behind the fall back barrier for its present speed, and a tail chase would be difficult unless speed is regained.

After the interceptor converts to the fixed lead angle steering mode the lateral acceleration reduces almost to zero and the speed increases. Two minutes later the interceptor speed has increased to Mach 1.5, the aspect angle is then 70°, and the lead collision error has become zero. The lead collision mode is then resumed and the launch zone contour reached after a total flight time from assumed AI acquisition point of 4.5 minutes. The error at launch is almost zero so that the attack is judged a success.

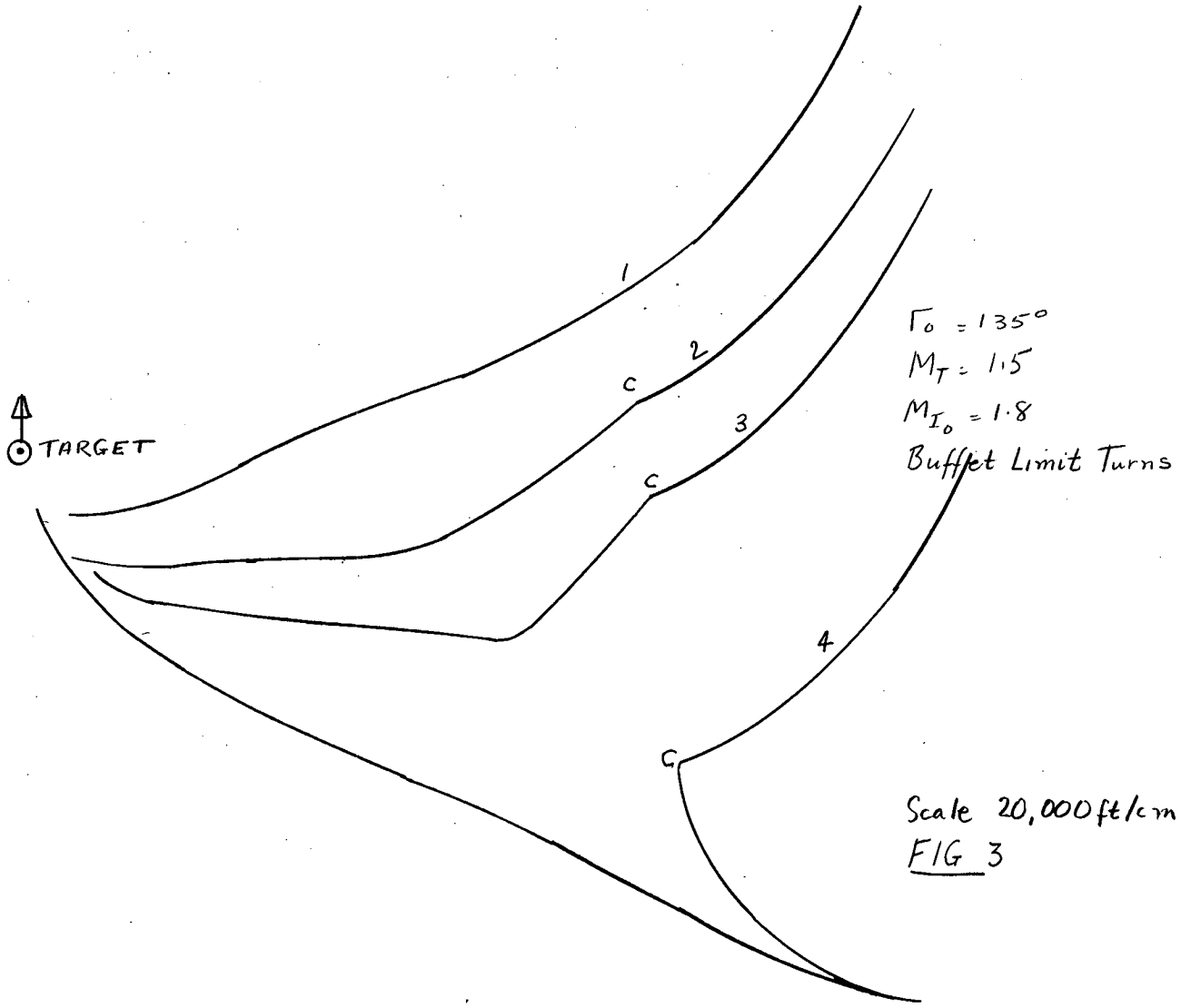

FIG 3

Trajectories in Target Coordinates in which the interceptor converts to fixed lead angle steering at the point C. Trajectory 1 is successful with lead collision steering, trajectories 2, 3 and 4 would not normally be successful but are with the conversion.

The trajectories of figure 4 are for the case of an interceptor using a lateral acceleration limit of 1.5 g's (approximately fixed bank angle turn), obeying lead-collision navigation all the way.

For the trajectory number 7, the interceptor speed drops from Mach 1.8 to 1.5 in 70 seconds. The look angle was not exceeded although the starting point for the trajectory is in a region from which interception would have been impossible using buffet limit manoeuvre. The total flight time is 5 minutes to interception.

5. Conclusions

Some interesting conclusions may be drawn from this work.

During attacks against high-speed targets the CF-105 interceptor must maintain its speed whenever it falls behind the ideal approach line. It should fly constant speed turns to profit by the increased horizontal field of view of the radar antenna. If the required lead angle for a collision course exceeds the look angle limit the CF-105 must fall into a tail chase. This may be achieved by fixed lead angle steering. The area of allowable placement may be considerably extended by these procedures.

Whenever the interceptor is ahead of the ideal approach line it is preferable to make high load factor turns, since the deceleration during turn is an advantage in this case.

The placement zones which are drawn indicate that the greatest probability of successful placement will be achieved if the ground control vectors the interceptor along the middle of the allowable placement zone. The "ideal" approach line so obtained in many cases is ahead of that for a pure collision course.

Further consideration of these tactical means of increasing placement probability is planned for the future.

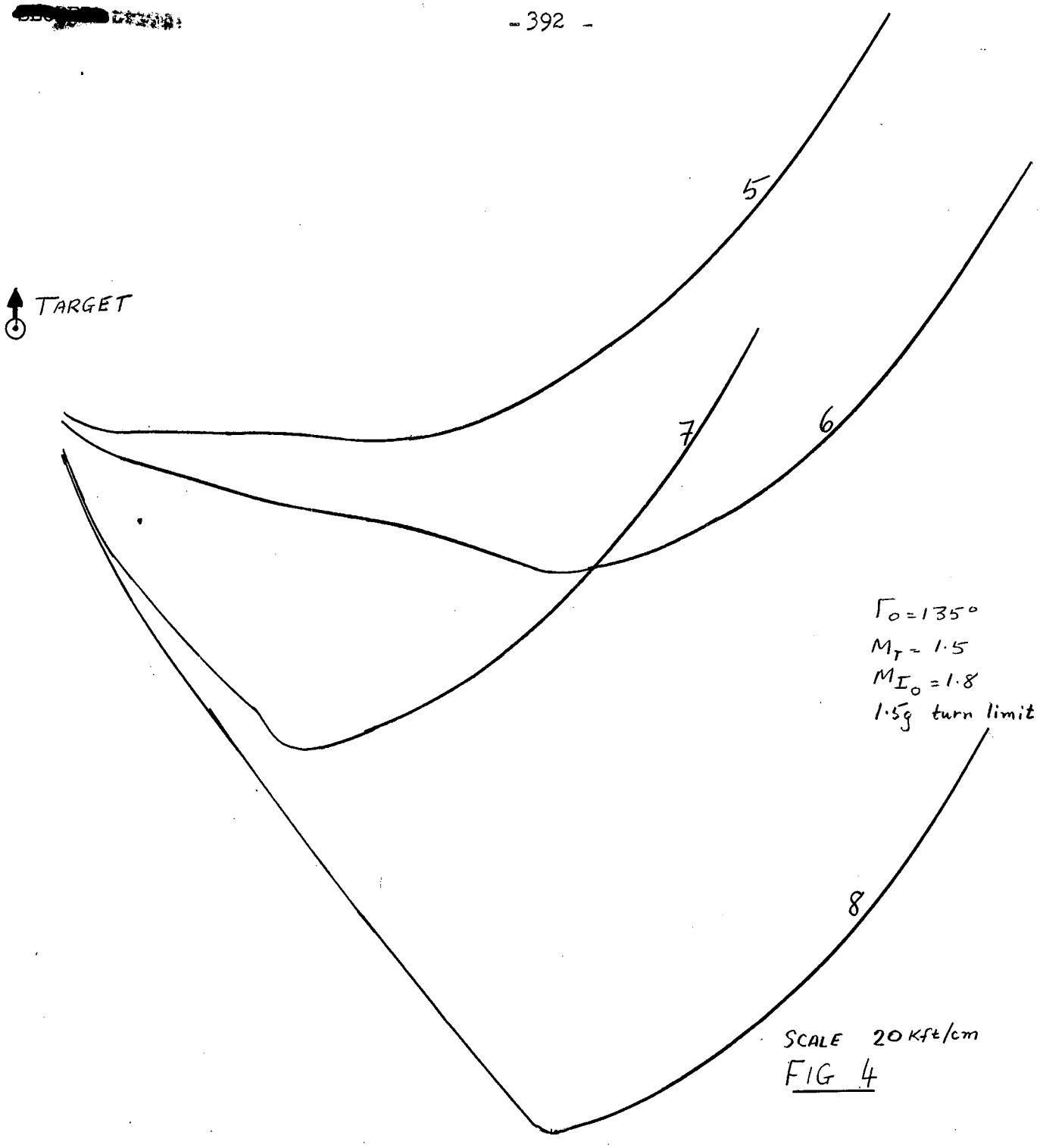

FIG 4

Trajectories in target coordinates in which the interceptor flies a lead collision course, its manoeuvre being limited to 1.5 load factor g's.

APPENDIX 'L'

Dog-Leg Manoeuvre of a Subsonic Target

by J. Cummins

1. Description of Problem

In the constant speed phase of the two-dimensional placement problem, a study was made using the REAC of the case of an evading subsonic target (Mach No. 0.85) attacked by a subsonic fighter with speed advantage (Mach No. 0.92). The maximum lateral accelerations assumed were 2 g's for the target and 1.8 g's for the fighter. These correspond to load factors of $2\frac{1}{4}$ g's for the target and 2.1 g's for the fighter.

Because of the interceptor speed advantage the placement zone will be limited only by the initial look-angle and the time allowed for making the interception. The time chosen for the maximum permissible duration of an attack was five minutes.

It was estimated that the most successful type of evasion for a target having a speed disadvantage was the dog-leg manoeuvre. Fig.1 shows the type of evasion adopted for this study.

The time barriers given by the REAC can be approximated by a circle of mean radius: $V_F \times 300 \times 0.93$, the center of the circle being the position of the target after five minutes.

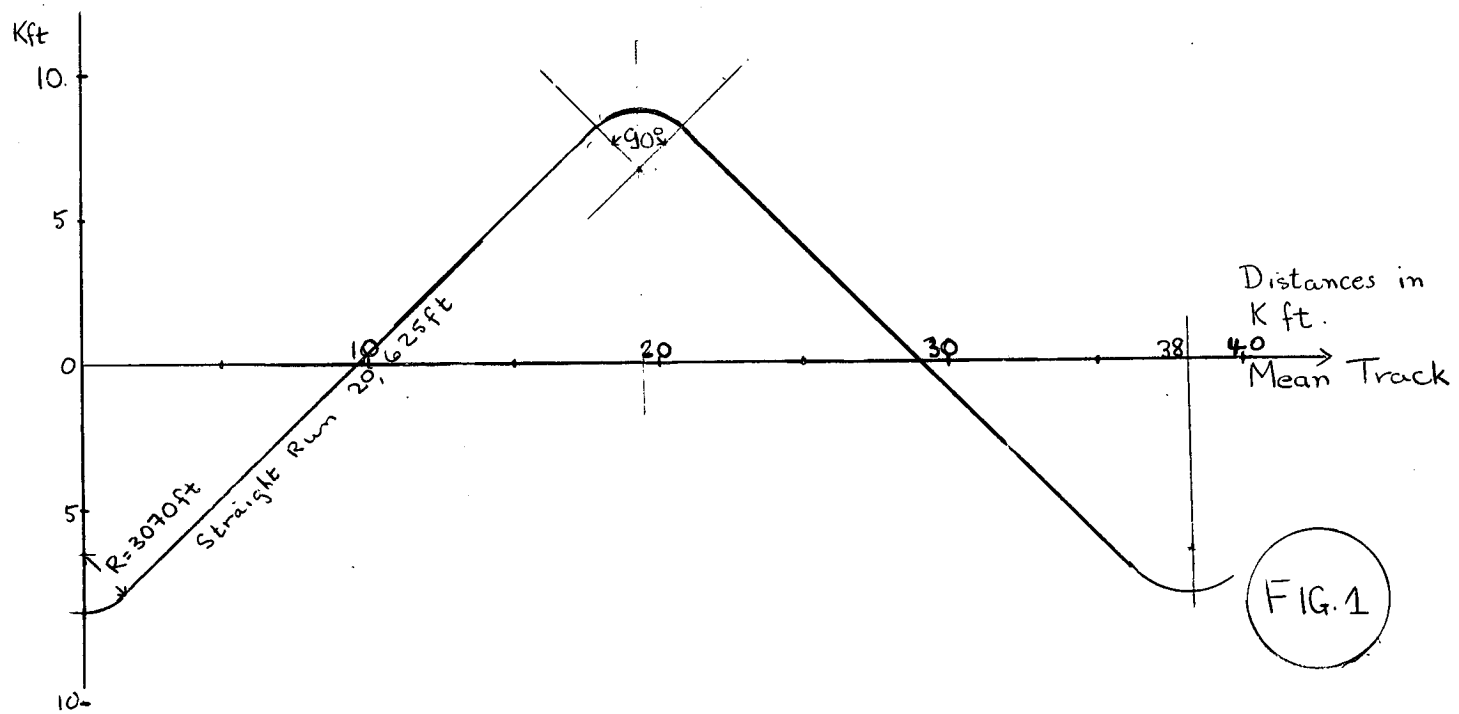

FIG. 1

2. Results

A list of the REAC results is given in the table below. The following quantities are tabulated:

Column 1: The initial course difference Γ_o between the target and the fighter.

Column 2: The distance R between the points computed by the REAC and the center of the circle used for the approximation.

Column 3: The error ϵ made by using the approximation.

Column 4: The percentage error.

TABLE 1

Approximation made for the Radius: $R_n = V_F \times 300 \times .93$
$= 0.92 \times 971 \times 300 \times .93 = 250000$ ft.

1	2 R(ft)	3 Error	4 %
0°	261 K	11 K	4.4
	249 K	1 K	0.4
	256 K	6 K	2.4
60°	266 K	16 K	6.4
	280 K	30 K	12
	280 K	30 K	12
	252 K	2 K	0.8
120°	231 K	19 K	7.6
	252 K	2 K	0.8
	247 K	3 K	1.2
	272 K	22 K	8.8
	245 K	5 K	2
180°	242 K	8 K	3.2
	239 K	11 K	4.4
	250 K	0	0
	249 K	1 K	0.4
	239 K	11 K	4.4
	242 K	8 K	3.2

1	2 R(ft.)	3 Error	4 %
240°	235 K	15 K	6
	217 K	33 K	13.2
	242 K	8 K	3.2
	257 K	7 K	2.8
	248 K	2 K	0.8
	232 K	18 K	7.2
300°	236 K	14 K	5.6
	247 K	3 K	1.2
	256 K	6 K	2.4
	248 K	2 K	0.8

3. Conclusions

For the type of dog-leg evasion considered and under the assumed condition of a fighter having a speed advantage, these computations show that the error made by taking the time barrier as being a circle of radius $V_F \times 300 \times .93$ with the target final position as the center, will be in general less than 5%.

APPENDIX 'M'

Effect of Reduced Magnetron Power on Placement Probability, Using Ding Dong Rockets

by J.A. Ockenden

1. Recent information from R.C.A. reveals that the expected CF-105 magnetron power is now 650 kilowatts, compared with the 1000 kilowatts previously stated. Since A.I. radar range is proportional to the fourth root of magnetron power, the expected acquisition range must be multiplied by a factor of 0.89 to account for the 0.65 power reduction.

2. A limited placement study has been carried out for the CF-105 Ding Dong system to find placement probability as a function of acquisition range. To enable a direct probability comparison of the two magnetron powers the resulting probabilities are shown as a function of the ratio of A.I. range to expected range. Ratios greater or less than unity represent improvement or degradation of any factor affecting A.I. range other than magnetron power.

3. One speed combination only is considered, a target (non-evading) of Mach 2.0 and a fighter of initial speed Mach 2.0, at a coaltitude of 50,000 feet. AVRO 2.2 aerodynamic estimates* are used to determine fighter turns and decelerations. It is assumed that the fighter turns at maximum g's if there is a steering error, or flies straight at constant speed if there is no steering error. Four initial course differences, 180°, 135°, 110° and 75° are used. The placement probabilities are determined using three G.C.I. standard deviations, 1.5, 4.75 and 9 nautical miles, for A.I. contours corresponding to a straight wing target.

4. The fighter navigates according to lead collision equations with F = 20,000 feet and fires when time-to-go is 7.6 seconds. Ding Dong performance curves show that the time to travel a distance ($F + V_f t_f$) is 7.1 secs. if F is 20,000 feet, V_f is 1500 feet/sec. and t_f is 7.6 secs. Thus the rocket will reach the centre of the F - circle 0.5 sec. before the target, and if the target speed is Mach 2.0, the separation at explosion (set for 7.1 secs. after launch) will be 970 feet, compared with a required value of 1000 feet. For launch speeds of Mach 2.0 and Mach 1.0 the separations will be 870 feet and 1070 feet. It should be remembered that the separation distance is directly proportional to target speed.

5. The allowable heading error at launch is zero, and five seconds of straight flight are required before launch.

---

* Aerodynamic data as in AVRO Periodic Performance Report No. 9
Thrust data as in AVRO Periodic Performance Report No. 10
C.G. position 29.5% M.A.C., combat weight 51,600 lbs.

The "expected range" for each magnetron is the range for 80% detection probability which will occur if RCAF Specification Air 7-6 is met. (80% detection probability of 25 n.m. on a 5 sq.m. target). If this can just be obtained with the 1 megawatt magnetron, the expected 80% range on a target of echoing area A using a P megawatt magnetron is taken as:

$$R_E = 25\left[\frac{AP}{5}\right]^{\frac{1}{4}}$$

Values of A used are the revised values for the Straight Wing Bomber listed in Table I page 104 of CARDE Tech. Letter N-47-12.

In using the 80% detection range for computing placement probabilities it is implicitly assumed that this range represents the average or 50% range at which the interceptor will commence corrective turns.

6. Probability curves for the four initial course differences are in Figures 1 - 4. Six A.I. contours are available for the straight wing target, corresponding to 0.27, 0.4, 0.57, 0.86 and 1.28 multiplied by expected range. For the reduced magnetron power these factors become 0.3, 0.45, 0.63, 0.75, 0.95 and 1.43.

7. A noticeable feature of the results for frontal attacks is the zero probability up to 0.5 or 0.6 expected range. The effect is due to the five seconds settling time, which prevents manoeuvre at ranges less than some 70,000 feet, so that no error is allowable inside this range. Above 0.6 expected range, probability rises sharply. Since the probability deterioration with magnetron power reduction depends on the slope of the probability curve, large deteriorations accompany the sharp rise. Above the expected A.I. range the slope is small, particularly with low values which give high probabilities, so that the deterioration is not serious.

8. In general, it is seen that the probability deterioration decreases with decreasing course difference. However, probability also decreases with decreasing course difference, so that the foregoing result is not a reason for favouring beam attacks with the lower powered magnetron. A secondary result of the investigation is that with extreme A.I. range degradation, frontal attacks against a straight wing target are useless at the fighter and target speeds considered.

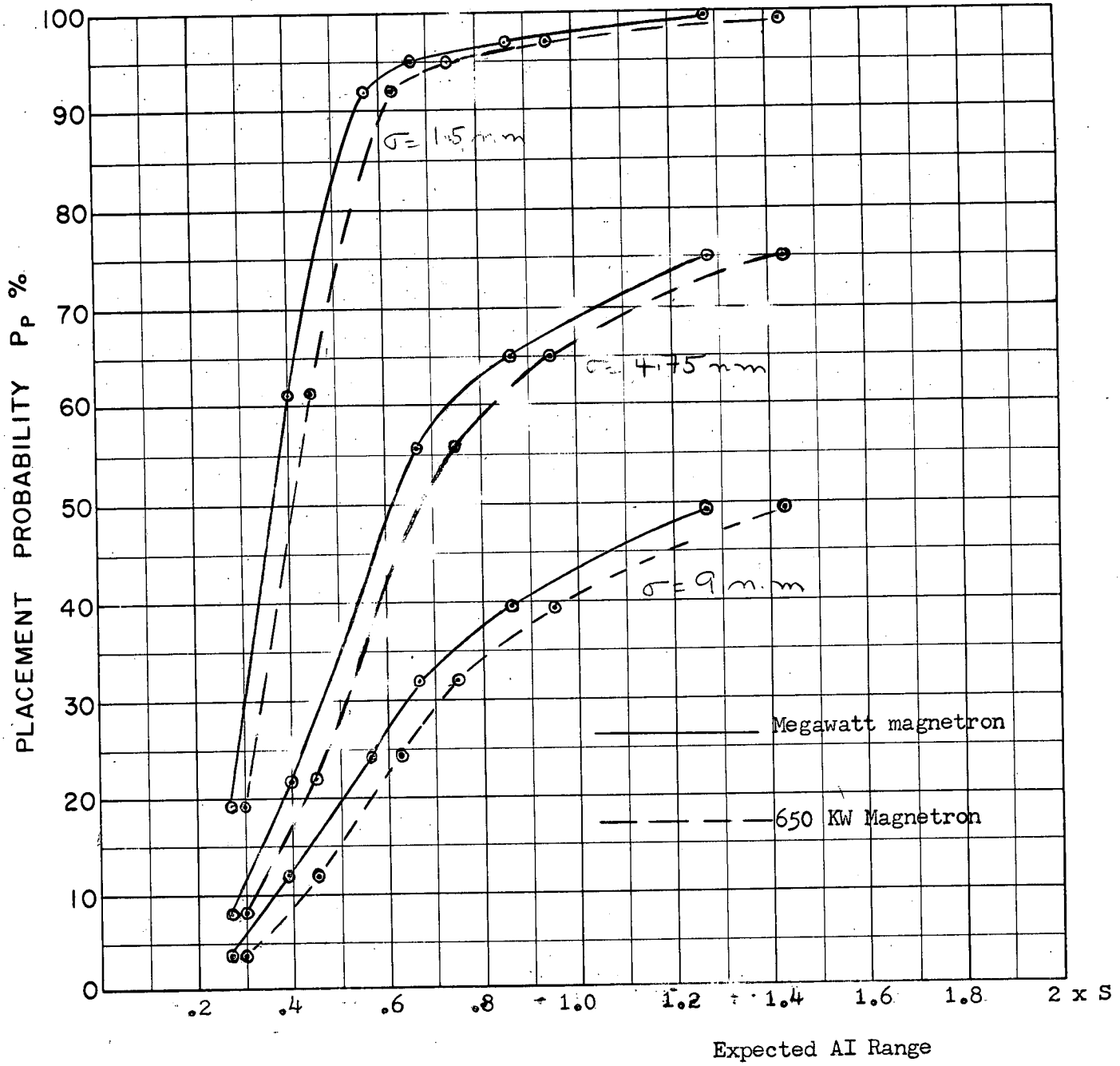

COURSE DIFFERENCE: 75°
TARGET EVASION: None
TARGET MACH NO.: 2.0
INTERCEPTOR LATERAL G's: Maximum g's, Avro 2.2 performance
INTERCEPTOR MACH NO.: 2.0 initially
σ OF G.C.I. ACCURACY: Three values
A.I. DETECTION RANGE AS FRACTION OF SPECIFICATION RANGE, S: Abscissa
A.I. DETECTION RANGE CONTOUR: Straight wing
ALTITUDE: 50,000 feet

FIG. 1 M

Lead Collision Course with F = 20,000 ft; t_F = 7.6 sec.

Zero heading error allowance (Long Range Unguided Rocket)

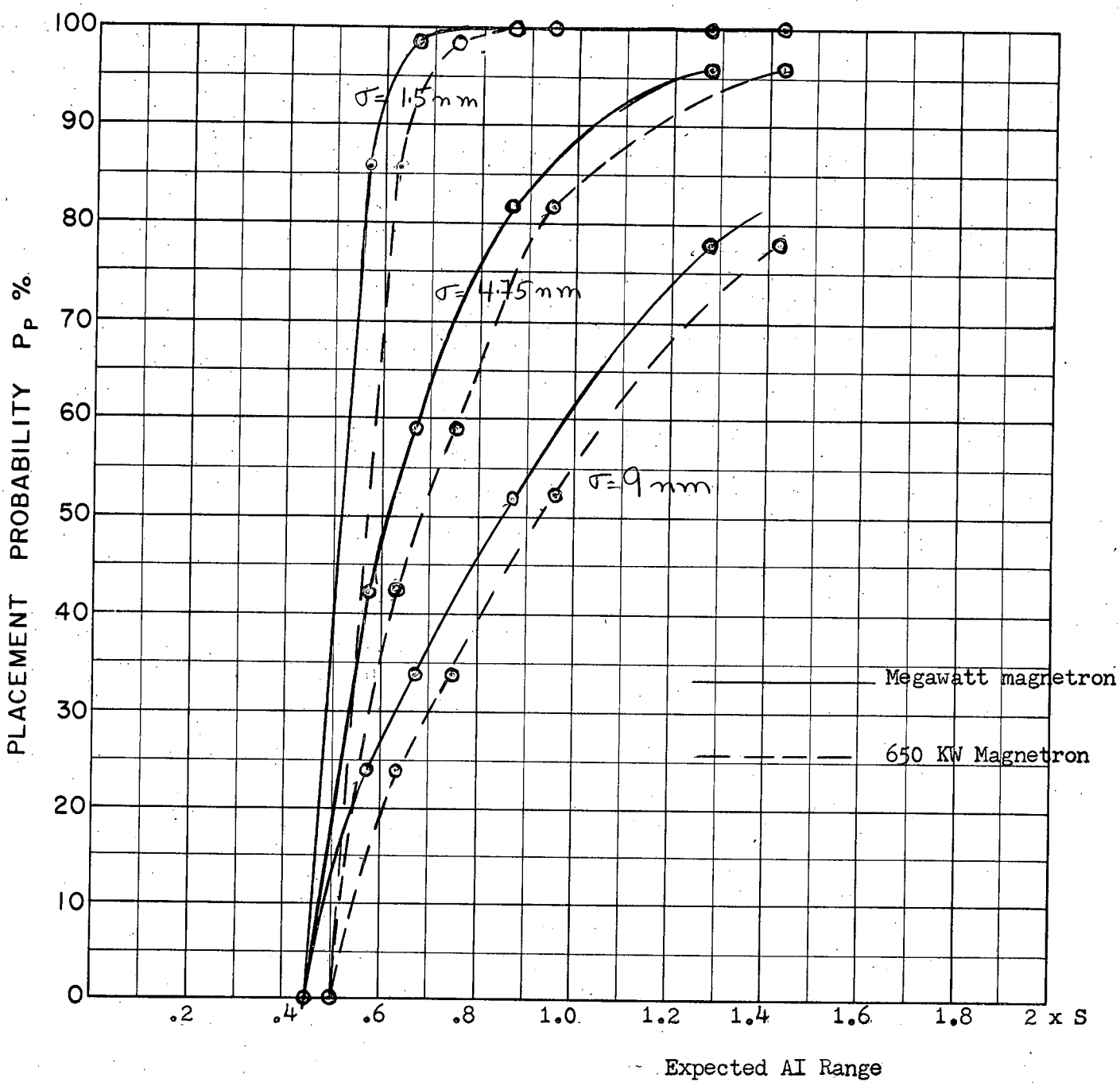

COURSE DIFFERENCE: 110°
TARGET EVASION: None
TARGET MACH NO.: 2.0
INTERCEPTOR LATERAL G's: Maximum g's, Avro 2.2 performance
INTERCEPTOR MACH NO.: 2.0 initially
σ OF G.C.I. ACCURACY: Three values
A.I. DETECTION RANGE AS FRACTION OF SPECIFICATION RANGE, S: Abscissa
A.I. DETECTION RANGE CONTOUR: Straight wing
ALTITUDE: 50,000 feet

FIG. 2

Lead Collision Course with F = 20,000 ft; t_F = 7.6 sec.

Zero heading error allowance (Long Range Unguided Rocket)

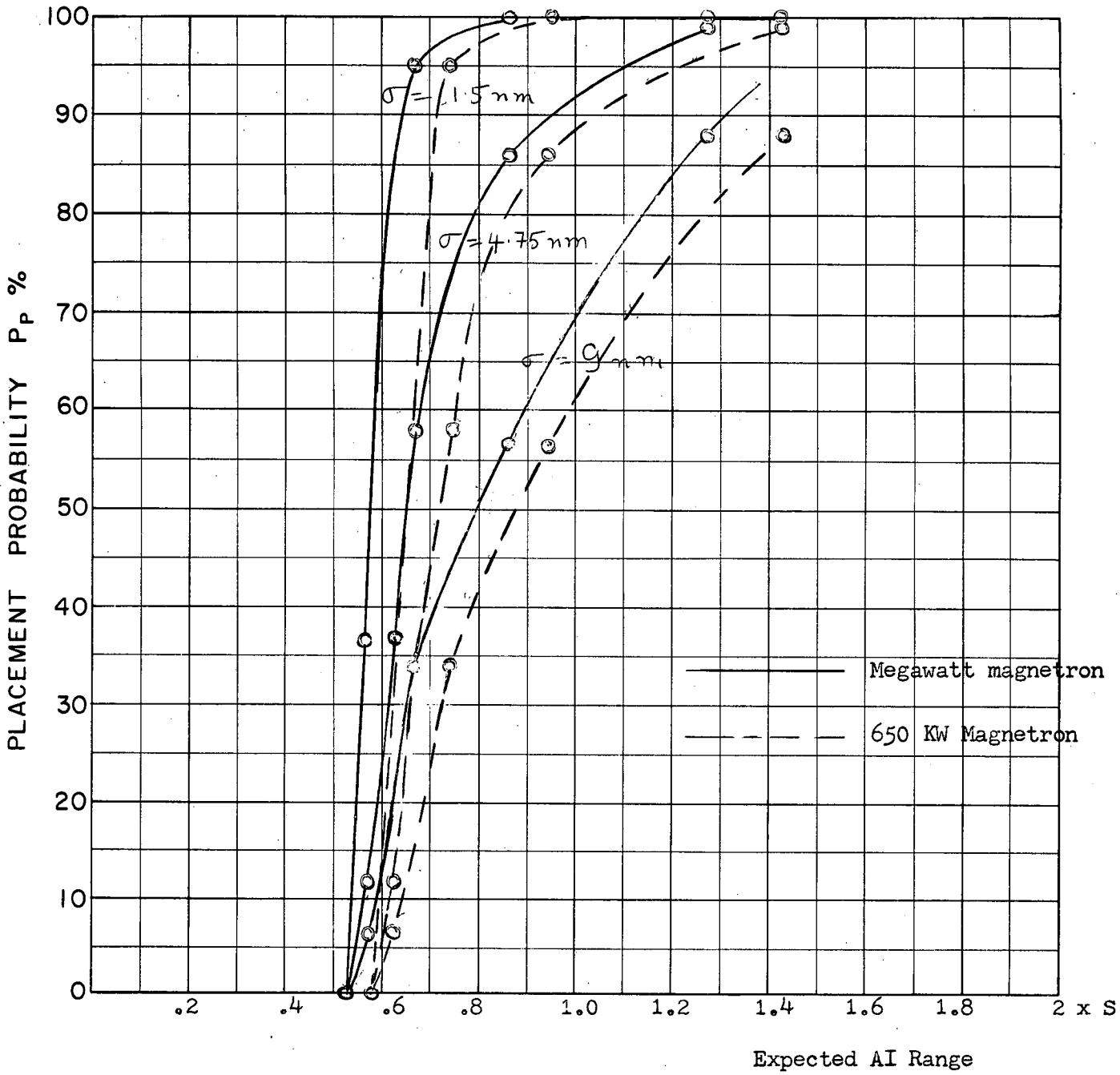

COURSE DIFFERENCE: 135°
TARGET EVASION: None
TARGET MACH NO.: 2.0
INTERCEPTOR LATERAL G's: Maximum g's, Avro 2.2 performance
INTERCEPTOR MACH NO.: 2.0 initially
σ OF G.C.I. ACCURACY: Three values
A.I. DETECTION RANGE AS FRACTION OF SPECIFICATION RANGE, S: Abscissa
A.I. DETECTION RANGE CONTOUR: Straight wing
ALTITUDE: 50,000 feet

FIG. 3
M

Lead Collision Course with F = 20,000 ft; t_F = 7.6 sec.

Zero heading error allowance (Long Range Unguided Rocket)

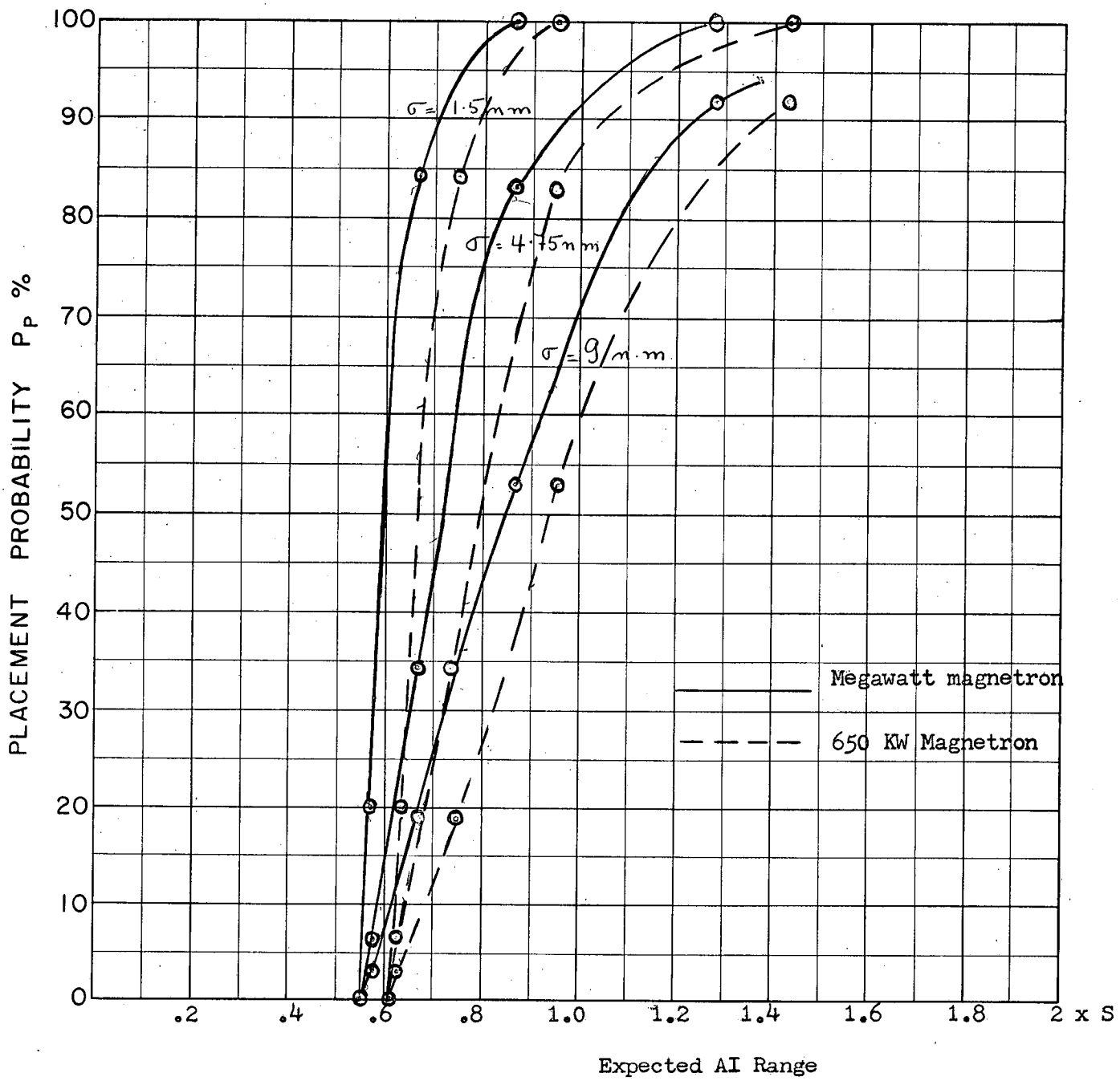

COURSE DIFFERENCE: 180°
TARGET EVASION: None
TARGET MACH NO.: 2.0
INTERCEPTOR LATERAL G's: Maximum g's, Avro 2.2 performance
INTERCEPTOR MACH NO.: 2.0 initially
σ OF G.C.I. ACCURACY: Three values
A.I. DETECTION RANGE AS FRACTION OF SPECIFICATION RANGE, S Abscissa
A.I. DETECTION RANGE CONTOUR: Straight wing
ALTITUDE: 50,000 feet.

FIG. 4
M

Lead Collision Course with F = 20,000 ft; t_F = 7.6 sec.

Zero heading error allowance (Long Range Unguided Rocket)

APPENDIX 'N'

Lethality Studies

by J.T. Baker

1. Review of Lethality Computations

1.1 Division of the Problem

A comprehensive study of air-to-air missile lethality which is to be successful in providing a quantitative Kill probability value must involve the use of many assumptions relating to missile trajectories, fuzing, and warhead. The necessary input data are:

i) Frequency distribution of missile heading error at launch. This is a fire-control problem; the answer is dependent on kinematic attack parameters such as speed ratio, altitude and altitude differential, course difference of interception; there may also be a dependence on ground environment accuracy σ and the AI range performance which has been taken as a parameter in this study.

ii) Relationship of Miss distance distribution of the missile to the launch heading error. This distribution is presumably a function of missile launch range, target aspect at launch, target velocity, missile launch velocity, altitude and target type.

iii) Distribution of hit "points" - points at which the line of approach passes through the plane of the target. This goes further than (ii) above which implies miss distance measurements for a point target; what is really required is the distribution of missile end-course trajectories.

iv) Distribution of warhead burst point along the missile approach line. This may very well be combined with (iii) so that what is provided is a space distribution of burst points around the target. The inputs which affect this are fuzing, missile blind range behaviour, and effect of target scintillation on the missile guidance.

v) Warhead characteristics.

vi) For each burst point, the distance and direction of vulnerable components from the burst point.

vii) The absolute vulnerability of each vulnerable component for the type of projectile considered.

1.2 Working Plan

To date CARDE work has been concentrated on the final item (vii) of the list of section 1.1. Some tentative decisions as to what components will be assumed vulnerable, and to what degree, for two targets to be studied, have been made. These are described in section 3 of this appendix.

The engagement simulator has been constructed in order to make the analysis implied by item (vi) of section 1.1. For a large number of burst points it will be possible to derive values of hit probability for fragmenting and rod warheads, and using vulnerability assumptions, compute corresponding values of Kill probability.

The distributions outlined in items (i) to (iv) above are in doubt for the Sparrow type missiles which are considered as possible weapons for the CF-105.

Since a V.T. fuze point can be varied by altering the computing circuit, it has been decided not to use a distribution of burst points determined by a definite fuzing system, but rather to direct the lethality study towards determining optimum burst points and from this optimum fuze delay. This involves a greater amount of engagement simulation but the advantage of this approach in aiding the RCAF to fix the parameters of the CF-105 Weapon System is evident.

The knowledge of distributions of missile trajectories would be of great use, since the value of optimum burst point may well depend on the trajectory assumptions that are made. It is hoped that missile studies can be made to determine approximate distributions for representative missiles. In the meantime it is proposed to use in the engagement simulations a uniform distribution of burst points throughout target space, keeping the burst point always within lethal distance. To obtain a final value of Kill probability it is apparent however that some missile trajectory assumptions must be inserted in the analysis.

2. Warhead Assumptions

Two types of warhead are being assumed in the engagement simulations being undertaken. These are both warheads which are of such size and dimension that they could be the payload of a Sparrow type missile. Pertinent characteristics are given here.

2.1 Continuous Rod Warhead

Rod material - Mild steel

Rod Cross Section - 3/16 x 3/16 in.

Length of Segments - about 11 in.

Initial velocity - 5000 ft/sec.

Velocity at 32 feet - 4200 ft/sec.

Maximum Opening radius - 32 feet.

Assumed maximum useful opening radius before break up - 24 feet.

2.2 Fragmenting Warhead

Number of fragments - 1200

Fragment weight - 140 grain

Total fragmenting material - 24 lbs.

Change to metal ratio - .8 (needed for computation of blast effect)

Fragment velocity - 5000 ft/sec.

Beam width - 10° (centre of static beam perpendicular to the missile axis)

The fragment velocity assumed is somewhat low, but permits use of the same warhead simulator for both types of warhead.

3. Vulnerabilty Assumptions

Accurate assessment of target vulnerability implies an intimate knowledge of the structural design, aerodynamic performance, and equipment of the target aircraft being studied. Intelligence information is able to provide basic data on target aircraft configuration and performance; these combined with a knowledge of usual practice in the aircraft industry permit reasonable decisions to be made concerning construction details. The vulnerability of typical aircraft components to various types of projectile is the subject of continuing experimental work in both the U.S. and U.K. Thus the probable vulnerability of target aircraft can be deduced.

3.1 Controversial Subjects

Two types of damage which may contribute to aircraft kill are damage to the pressure cabin, and fuel fires. Many lethality assessments which are done discount both of these factors since little is

known of the kill chance for a high altitude target due to these causes*.

3.1.1 Fuel Fires

Experimental work is being undertaken at present in the U.S. and the U.K. to determine the feasibility of setting and maintaining fuel fires at altitude. CARDE has access to the results of this work through representation on the regular Tripartite Anti-Aircraft Lethality conferences (Ref. 2,3,4). Most recent reports indicate that fuel fires can be caused by fragments. In the work to be done at CARDE two values of kill probability will be given, one for the case where fuel fires are considered possible, and one where they are not. In any case fuel fires do not contribute to KK or K kills, since several minutes are required for loss of control; thus they affect only the assessment of A or five-minute kills. In assessing possibility of fuel fires, assumptions must be made regarding the scheduling of fuel between fuselage and wing tanks on a long range mission. It will be generally assumed that over the target fuel will be in the fuselage.

3.1.2 Pressure Cabin Vulnerability

When considering subsonic targets cruising at about 42,000 feet altitude, decisions regarding K or A kills due to cabin depressurization are difficult to make. At this altitude the crew can possibly maintain reasonable operating efficiency by breathing pure oxygen if their flying suits are of the most advanced design. Only damage to the oxygen system (which is certainly duplicated and of very small effective vulnerable area) and to other vital controls can be considered as lethal damage to the cabin.

For the supersonic target which is treated in the CARDE assessment operation at 60,000 feet or at least 50,000 feet altitude is postulated. Maintenance of cabin pressure is essential at these altitudes and any damage which destroys the structural integrity of the cabin may be considered as producing at least 'A' kill.

---

* See report on a recent visit by a CARDE group to U.S. establishments, Ref.1, Part I-C, describing work being done at N.A.D.C. in Johnsville.

[redacted]

3.2 Vulnerable Components of the Bear

Figure 1 gives an outline plan view of the subsonic turbo-prop bomber Bear which is being considered as a typical subsonic target in the CARDE lethality assessment. The main vulnerable components and their degree of vulnerability are summarised in the legend attached to the figure. Derivations of vulnerable area to fragments and single fragment kill probability are at present being made and will be reported later.

3.3 Vulnerable Components of Supersonic Target

Figure 2 gives an outline plan sketch of a hypothetical supersonic bomber. The main vulnerable components are summarised in the legend attached to the figure. Values of vulnerable area and of single fragment or rod component kill probabilities will be greatly different from those for the subsonic case. Structure is assumed to be of integral honeycomb steel throughout. The particular configuration suggested effectively separates the more vulnerable components so that kills made up of composite damage to many parts of the structure will not often occur.

Blast damage at the extreme altitude considered will be carefully assessed for realism before being admitted as a contributing factor to kill.

4. References

1. CARDE Technical Letter N-47-16, "Report on a Visit to U.S. Establishments", December 2-17, 1956, J.Y. Caron & J.T. Macfarlane.

2. CARDE Technical Letter N-50.2,"Report on a Visit to U.S.A. in connection with the A.A. Lethality Mission", Oct/No. 1956, G. Mc Laughlin.

3. CARDE Technical Letter N-50.3,"Report of a Visit to the USA as a Member of the Joint British and Canadian A.A. Lethality Mission 8-17 Oct 56",T.Sterling.

4. Report on the Tripartite Symposium on A.A. Lethality, June 1955. (OB/AALC 44).

Vulnerability of Bear

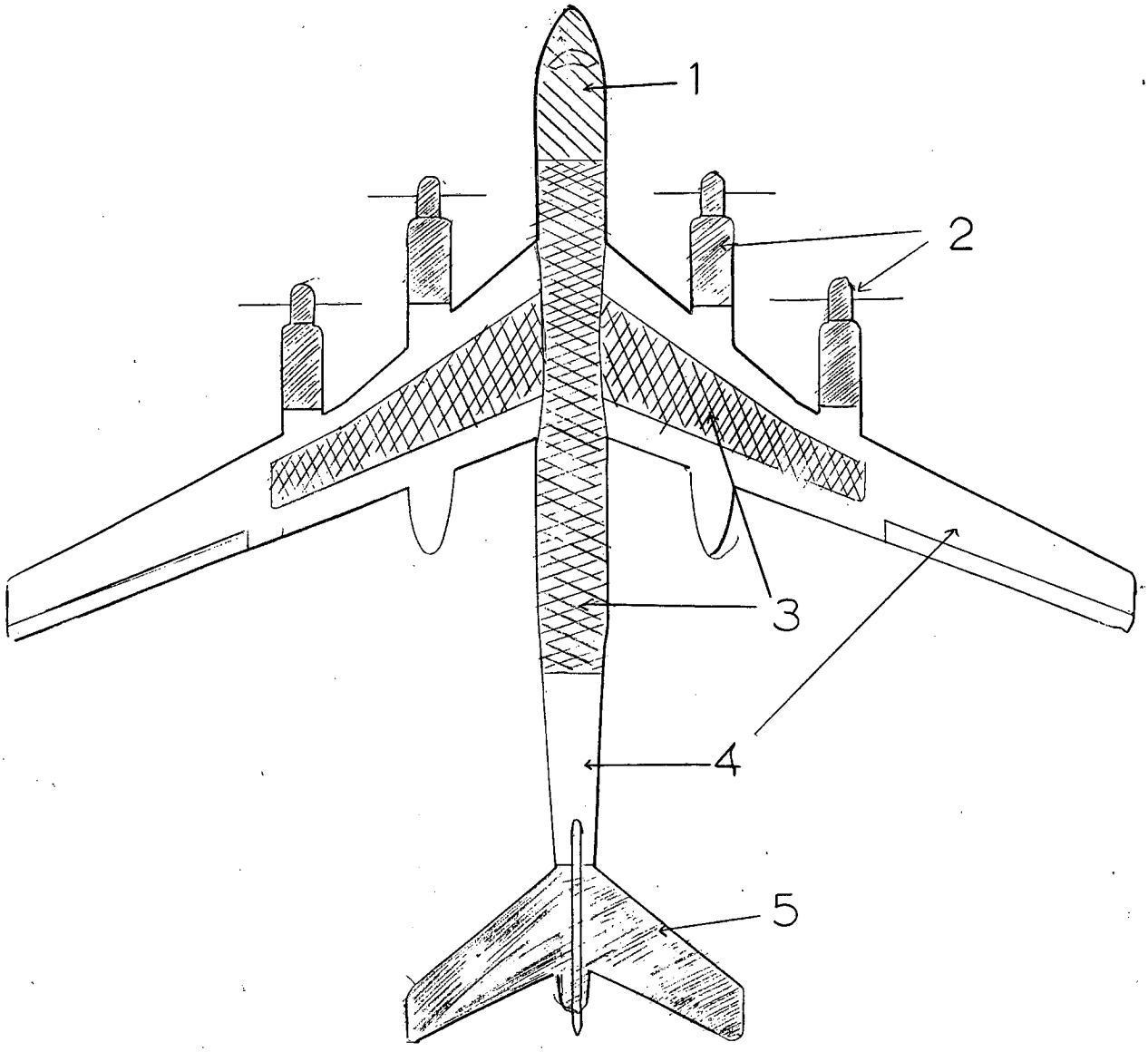

1. Cabin. Rod, blast. Personnel and vital services vulnerable to fragments.

2. Engines. Fragments; less vulnerable to rod. Partly shielded control lines in wing trailing edge.

3. Fuel; fuselage structure vulnerable to rod.

4. Vulnerable structure whose kill would not produce K-Kill of aircraft. Exception is large transverse rod cut on fuselage.

5. Tail surface and fin. Large amount of damage required for kill.

FIG 1

VULNERABILITY OF HYPOTHETICAL
SUPERSONIC TARGET -

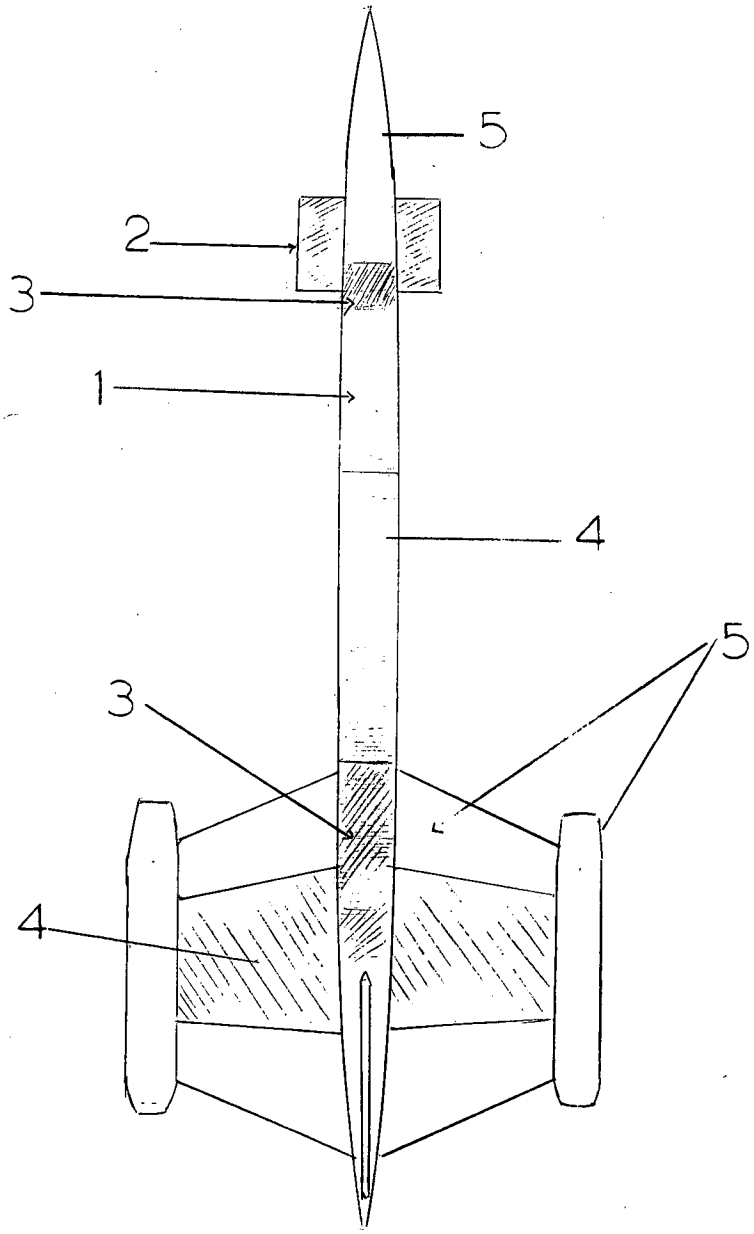

1. Cabin. Vulnerable to rod, blast. Personnel and vital services vulnerable to fragments. Depressurization by large cut is fatal.

2. Control Surfaces. Vulnerable to rod, blast.

3. Control (and fuel?) lines; rod, blast fragments.

4. Structure vulnerable only.

5. Invulnerable components, or those which may be killed without K-Killing aircraft.

FIG. 2

[redacted]

APPENDIX 'P'

Evaluation of the RCAF Specification for the CF-105 Electronic System, and of the RCA Proposal

by A. Matheson

I - R.C.A.F. Air 7-6 Evaluation

Introduction

This evaluation or criticism of the Air 7-6 specification has been prepared as part of the CARDE CF-105 study programme. It was originally intended to be made available at the end of December 1956, but as there were no serious faults in the specification which would have then necessitated immediate action to revise the specification, it was decided to wait and see whether or not later developments or information would give cause for revision of the specification. Generally speaking such has not been the case.

General

The specification as a whole is satisfactory. It specifies an aircraft electronic control system which is as futuristic as the present state of the art would seem to permit now or in the very near future. It specifies an aircraft electronic control system which from presently available information, seems to be very similar to modern or future U.S. aircraft electronic control systems. This in itself may make the system very desirable and the aircraft a very useful one in the North American ground environment. It may also make it possible for the suppliers of the control system to incorporate in the aircraft relatively new U.S. developments in this type of control. Two general points which should have more stress placed upon them in the specification are the following. First it should be made clear that the specification is a minimum specification and that any improvements in equipment or operational methods appearing in the development period of the aircraft, are highly desirable and if feasible and approved should be included in the electronic system if delivery dates are not affected adversely. This statement is made in section 2.1.6 but should be made more positively and definitely.

Another desirable inclusion in the Specification would be a section emphasizing the importance and need for the weapons system approach to the electronic control system. The contractor (RCA) may take the weapon system approach for granted but nevertheless the specification should include a section demanding the utmost liaison and co-operation between electronic control system and airframe suppliers.

A more important revision should be made in sections 3.1.5 and 3.1.6 which are concerned with operational stability and operational life. Section 3.1.5 states that "the equipment shall operate continuously or intermittently for 24 hours without failure". Section 3.1.6.1 states that "the equipment shall have a reliable operating life ...". Although it is admittedly very difficult to define the degree of stability or reliability required, sections 3.1.5 and sections 3.1.6 could and should be improved upon. Section 4.4.1 raises a similar type of question when it mentions a "major malfunction". The simplest improvement would be to say that the equipment shall operate continuously or intermittently for 24 hours within the limits outlined for the Air 7-6 specification. Another way would be to say that the equipment or system shall operate continuously or intermittently for 24 hours with a degradation of no more than 10% on the probability factor assigned to the function and performance of the electronic control sub-system in the computing of total kill probability.

Another factor to be considered is that operating stability priorities should be assigned to each of the sub-systems. Some sub-systems are much more important than others and the most important sub-system such as the power supply sub-system should have the highest operating stability priority assigned to them. A suggested listing is:

1. Power Supply Sub-System
2. Auto-Flight Control Sub-System
3. Cockpit Controls and Presentation
4. Flight Data Sub-System
5. Fire Control Sub-System
6. Navigation Sub-System
7. Telecommunication Sub-System

The term design objective should be very clearly defined and used carefully. Its use in Air 7-6 tends to indicate that a requirement described as being a design objective is a desirable objective which is not necessary but is desirable if it does not interfere with or degrade radar performance. If this is the case, a design objective appears to be of even lower priority than "shall" with "major design objective or criterion" having the top-most priority. The use of "design objective" is most objectionable in sections 3.2.1.3.1 and 3.2.2.4.1 where maximum antenna look angles are described as being only design objectives the attainment of which should not interfere with radar acquisition range. If "design objective" is used here in the intended sense, minimum values should be set for the maximum radar look angles.

The remainder of this note lists criticisms of individual specification sections.

Section 2 General

It is suggested that all major design criteria of a general nature be included in this section. At present the only one listed is reliability. Elsewhere listed is accessibility. To these should be added, maintainability, which could be called self-test ability, avoidance of duplication, and a weapon system approach.

Major design criteria would then be:

1. Reliability
2. Maintainability
3. Accessibility
4. Self-test ability
5. Avoidance of duplication
6. Weapon system approach

Section 2.2.1.1 Intercept Functions

This general description would be clearer if reworded as follows from sentence 3 onwards. "In the close control mode the aircraft shall be controlled automatically or manually by the pilot, in accordance with steering information received from the ground via data link. In the broadcast control mode, the aircraft shall be controlled automatically or manually in accordance with aircraft position information computed in the aircraft and target position information received from the ground either automatically via data link, or by voice and set into the computer by the NAV/AI".

This rewording would make the mode description conform more closely to the usual interpretation of close and broadcast control modes.

2.2.1.2 Attack Functions

It is suggested that this section be rewritten to include the right of the pilot to fire his armament manually if he so desires or if the automatic firing function is inoperative.

3.1.4 Total Weight

Since the weight of mounting bases and cables can be relatively large, as high as 30% of the equipment weight, it is desirable to specify total weight. It is also advisable to specify that the weight and volume distribution of the equipment conform to a pattern arranged at a later date between control system and airframe suppliers.

Sections 3.1.5 and 3.1.6

See General Comments.

3.1.7 Interconnecting Cabling

It is very unlikely that a system of the specified complexity will ever become static from the design viewpoint and hence the specification for this section should be revised to make it necessary to include spare pins in each connector.

3.2.1 Fire Control System - General

Although it is questionable where the information should most suitably be included, it is suggested that reference be made in this general section to the C.W. transmitter required for Sparrow III.

In a detailed section, the C.W. transmitter requirements should be listed in more detail.

3.2.2.4.1 Attack, Blind

It is suggested that this section be reworded as follows.."The aircraft shall be automatically directed to the optimum firing point relative to the target for the specific type of ordnance selected so as to insure maximum probability of kill. The sub-system shall in co-operation with other sub-systems, automatically direct the interceptor in a selectable navigation mode to the selected target and shall give a signal for automatic firing of the armament at such time as to give maximum probability of kill. Notwithstanding the above automatic mode of operation the sub-system shall provide information to enable the pilot if he so desires to direct the interceptor manually in a selectable navigation mode to the optimum firing point, etc, etc".

The reason for eliminating "offset point" is that usually the term refers to a point to which the interceptor may be steered for A.I. interception and is not used in referring to the variable position point from which the armament is fired.

Reference to particular modes of navigation i.e. lead collision and lead pursuit has been eliminated because of the possibility of including snap-up and the excluding one or other of lead collision and lead pursuit in favour of a compromise form of navigation. Reference to a manual firing mode should also be made.

3.2.2.5 Airborne Moving Target Indicator

This section should be reworded to include the need for a low altitude track phase if studies show such a phase to be feasible.

3.2.2.6 I.F.F.

It is advisable to specify that I.F.F. be possible in both search and track modes. This capacity will facilitate identification amid multiple targets in the search phase and is obviously needed in the track phase.

3.2.4 Airborne Interceptor Radar

Reference should be made in this section or in the Fire Control Section to the need for the C.W. magnetron.

3.2.4.2 Automatic Search Requirements

Since search detection probability will vary in auto search with the volume scanned, this section should specify that the 80% detection probability be realized when the volume being scanned is a maximum.

3.2.4.2.5 NAV/AI's Presentation

It is suggested that an elevation marker corresponding to the elevation of the target marker be specified in this phase to permit the NAV/AI to position his antenna main axis most accurately in the lock-on phase.

3.2.4.3.1 Antenna Positioning

Although a 180° included angle cone is specified in this section, the foot note indicates that the included angle may be decreased if its attainment degrades the radar acquisition range. If this is the case, minimum limits should be set upon the azimuth and elevation limits. It is suggested that these be ± 70° on both azimuth and elevation.

3.2.4.3.4 Attack Presentation

Rather than have the attack scope blank, it could be used in the intercept phases to indicate to the pilot the required steering even though the aircraft is under automatic control. If the pilot were to override manually he could follow this steering dot information.

3.2.4.4.1 Angular Tracking Limits

The same comment applies to this section as did to section 3.2.4.3. If the 180° included angle cone is to be degraded, minimum limits should be set. These should be no less than ± 70° for azimuth and elevation.

3.2.5.7.1 Attack Phase - Blind Mode

In the present state of the art, the IR detection unit will be able to provide angle information only and hence by itself the IR detection unit will not be able to supply sufficient information to the Fire Control Computor for steering error calculation.

II - The R.C.A. Proposal

Introduction

This note is a summary of comments on the CF-105 electronic control system as proposed by the Radio Corporation of America in their proposal DSG-105-1-5405 to meet the requirements laid down by the R.C.A.F in its Air 7-6 specification. The comments are concerned mainly with the AI radar and Fire Control aspects of the control system and are not intended to constitute a proposal evaluation, since insufficient information is available at the present time on which to base a proper evaluation. It should be noted too, that these comments pertain only to the Astra I electronic control system as it is understood that there are no definite plans at the present time for the Astra II version of the system.

General

The sections of proposal DSG-105-1-5405 which deal with the Astra I version of the electronic control system are generally realistic in concept, although several goals are set which may prove troublesome if they are to be realized in the given time schedule. Otherwise the system should present no unforeseen problems in development. The basis for this statement is that the Astra I system resembles,in its essentials, electronic control systems which may now be in or near the operational stage in U.S. aircraft. A specific example is the Convair F-102-A and its electronic control system. Assuming that access is possible to the results of studies entailed in the development of these and other U.S. control systems, it is to be hoped that sufficient information is available to permit the development on schedule as the electronic control system for the CF 105.

The following are the comments on the A.I. radar and Fire control sections.

A.I. Radar

Antenna - The proposed antenna is an improvement over A.I. antennas now in operational use and if developed in the proposed time schedule should be satisfactory, provided that

(a) Maintainability is not a problem. Some hydraulic-drives for antennas have been troubled with hydraulic fluid leakage.

(b) The question of antenna look angles is resolved. The Air 7-6 specification specifies positioning of the antenna in manual search and track within a 180° included angle cone as a design objective. The R.C.A. proposal states that azimuth look-angle limits will be $\pm 70^{\circ}$ and that elevation look-angle limits will be $\pm 75^{\circ}$. However the last quarterly report states that the

elevation limits are now +75° and -45° and if it should be shown that these limits are unacceptable, it may be necessary to redesign the antenna.

(c) The antenna search mechanisation satisfies the major design goal of section 3.2.2.1.1 of the Air 7-6 specification. The proposal states that the scanning sector will be capable of being directed by data link computer information but does not say whether or not any of the search and radar parameters will be varied automatically as required in flight. The proposal effectively states that they will not. If there are no data available to back up this decision, it would be advisable to conduct studies on this aspect of search and track.

(d) Careful study is made of the use of the selectable polarization feature. For instance it should be kept in mind that in the Sparrow III attack phase of operation, it will be necessary to ensure that vertical polarization is used when target illumination is required of the interceptor.

Microwave Plumbing - It should be noted that the microwave plumbing can be a troublesome item if the 1 megawatt peak pulse power magentron is achieved. Corona and/or arcing may occur.

1 Megawatt-peak-pulse-power magnetron - This magnetron may present a serious development problem if it is to be ready for 1959 delivery. However since it is impossible to say definitely that this will be the case and since R.C.A. has made considerable progress toward the tunable magnetron, it perhaps may be best to accept their judgment, apparently optimistic though it may be. Nevertheless it is to be hoped that R.C.A. has available or is developing a suitable magnetron to substitute for the proposed 1 megawatt tunable magnetron should the need arise.

Difficult though it be to design this 1 megawatt magnetron for operation in the conventional search and track modes, the problems are considerably less severe than those encountered in the A.M.T.I. mode of operation. The proposal describes on pages 24 and 25 some of the problems which must be overcome before operation can be achieved in the A.M.T.I. mode. For a magnetron of this power to operate successfully at P.R.F.'s as high as 6000/sec., jitter and missing pulses must be very closely controlled. The necessarily high duty ratio will also probably limit "on" times to the order of 5 minutes. Tracking in the AMTI mode presents a severe problem and may not be feasible.

Fire Control Sub-System

The section on fire control is general and preliminary in nature and so can only be evaluated in a general way. The proposed Fire Control system is conventional and similar to the E and MG series and so should be straightforward in its design and mechanisation. The basis for the system will be the stabilized antenna system.

The modes of operation are those specified in Air 7-6. It is possible that the proposal modes are not the modes which will be provided in the aircraft. Considerable attention is being given to a modified attack mode combining lead collision with lead pursuit and it may be that this "switchover" mode may replace either lead collision, or lead pursuit, or both for the missiles. Studies on the snap-up attack (R.C.A. Quarterly #1) have shown that there is a possibility that the snap-up mode may not be necessary because of the climbing characteristics of the CF 105. So it is seen that nothing much can be said about the proposed Fire Control Modes. Those listed simply follow the specification.

The sections discussing lead pursuit and lead collision for the armament are brief summaries of the theory of these modes of attack.

Similarly the remainder of the Fire Control Section is devoted to a straightforward description of a conventional system. The information relative to the Sparrow II and Sparrow III is a summary of known information.

Displays

The displays are conventional displays with a few additions. The addition of the local target designator during search is worthwhile, in that it will permit a form of manual tracking during the search phase. This will be done by giving to the NAV/AI range and azimuth control of the circle. During search he will be able to place the designator on the target and if the closing rate permits, he will be able to manually track the target from scan to scan, while continuing to survey or search the selected volume of space in front of the interceptor. Lock-on will also be easier than in the MG-2, since upon the initiation of lock-on by closing the lock-on trigger, the antenna will rotate to the position indicated by the designator, the range strobe will replace the target designator circle, and will automatically sweep a one-mile range increment until lock-on is achieved. This modification is a definite improvement.

R.C.A. suggests in their proposal that the pilot's scope be used in the intercept phase for display of steering and attitude information. This suggestion has merit as it will provide a ready means of monitoring the performance of the system.

E.C.M. Evasion and Homing

The electronic control system for CF 105 will have adequate E.C.M. evasion and homing facilities if equipped as described in the proposal and judged by the present state of the art.

APPENDIX 'Q'

Infra Red A.I.

by
J. Hampson
G. T. Pullan
J. Merner

1. Introduction

The discussion below is a criticism of the infra-red sub-system as described in the first Quarterly Report issued by HCA on the ASTRA I Advanced Electronic System. In the main the discussion is based on the premises that have been taken by the contractor; accepting these premises it appears to us that the contractor is somewhat optimistic about the system performance. This optimism arises mainly from the facts that:

a) the assumed target emissivity of 0.2 is omitted in the calculations giving an overestimate of target radiation.

b) the estimate of atmospheric transmittance is based on inadequate and out-of-date data and is probably considerably too high.

c) the variation of detector sensitivity with wavelength is ignored -- such data as is available to us on this point indicates that the sensitivity for wavelengths around 10 microns will be so low that radiation in the 7.5 to 10 micron region will be of considerably less value than the report indicates.

On the other hand it seems to us that the initial premises that are taken are unduly conservative. In particular we feel that:

a) the assumption that the target can be taken as a 2.0 m^2 body of emissivity 0.2 is very pessimistic; targets can be expected to have a frontal area considerably more than 2 m^2 and in addition large parts of the target, such as the engine intakes, the radomes and the cockpit, can be expected to have emissivities approaching unity;

b) the calculations in the report are all based on an altitude of 28,000 ft; operational altitudes are likely to be considerably greater than this figure and the performance to be expected of any given I.R. system should improve markedly with increasing altitude.

It is felt that a more careful study of the problem should be undertaken and that such a study is likely to lead to the conclusion that an infra-red sub-system will be a most valuable adjunct to the ASTRA I system.

A detailed criticism of the report now follows.

2. Target Radiation (p. 164)

The basic assumptions of this part of the report appear to be that the target will be equivalent to a body of area 2.0 m^2. (We are assuming that the statement "Frontal Area -- 2/0 m^2" is a misprint and should read 2.0m^2), temperature 120°C and emissivity 0.2 and that only radiation in the wavelength intervals $7.5\,\mu < \lambda < 10\,\mu$ and $3.0\,\mu < \lambda < 5.8\,\mu$ will be transmitted through the atmosphere. From these assumptions it is concluded that the target will emit 868 watts in the atmospheric windows.

However the figure (1.4×10^3 w./m^2.) quoted for the total radiation is that appropriate to a black body at 120°C: the correct figure for a target of emissivity 0.2 is only 237 w./m^2.

The statement that the spectral radiation peak is at 7.5 microns and is in an atmospheric window is not true -- the peak wavelength is 7.35 microns, which is inside a water vapour absorption band.

The assumptions made about the target seem at variance with the probable facts of the situation.

The relevant emissivity to consider in the problem is the emissivity for the aircraft surfaces at 120°C and in the wavelength range considered; for the wavelengths with which we are concerned this will be close to the total emissivity at 120°C. Typical total emissivity values quoted in the "Handbook of Physics and Chemistry" are:

Aluminum, unoxidized 0.03	Steel, unoxidized .. 0.08
Aluminum, highly polished .. 0.08	Steel, oxidized .... 0.70 to 0.80
Aluminum, oxidized 0.11	Aluminum paint 0.55
Monel, polished 0.09	Non-metallic paints and
Monel, oxidized ..... 0.37 to 0.43	typical dielectrics. 0.80 to 0.95

Cavities in the structure, such as jet engine intakes, will have emissivities near unity irrespective of the material of construction. In fact, then, the target aircaft will be a complex structure with the emissivity varying from point to point over the structure. Even in direct head-on aspect it is likely to present an area considerably in excess of 2.0m^2 --- the wings alone of a target of 80 ft. span and 6 inches mean chord will present an area of about 4m^2. The emissivity of the wing surface under operational conditions may be around 0.2 (or still higher if steel construction is used) and so it is not unreasonable to suppose that the wings of the target alone may emit twice the amount of radiation estimated above. Every jet intake may easily emit as much

radiation as the wings, so that the total radiation available may be several times greater than the 868 watts quoted in the report. At angles off the nose of the target the apparent target area will increase and the total radiation emitted will probably be considerably larger than for direct nose-on aspect.

Two further points which seem to deserve some attention are the facts that the target will be viewed against a background which is itself radiating and that it will reflect radiation from its surroundings. Both of these factors will influence the detection range. A crude estimate of the magnitudes of these effects suggests that they will largely compensate each other, except in exceptional circumstances such as strong reflection of sunlight. However a more careful examination may be worth-while.

The problem of estimating the effective radiation from the target against its background is hampered by lack of:

a) some definite assumptions about the size, shape and structural materials of likely targets and some experimental measurements of emission from the skin of aircraft at velocities of Mach 1.5 and above.

b) experimental observations of atmospheric backgrounds at high altitudes and of the general flux of radiation within the atmosphere. It is hoped that some useful information on this point may be obtained from the present CARDE programme of high-altitude measurements.

3. Hot Gas Radiation (p. 164)

The effective intensity of the CO_2 radiation at 4.3 microns for a single jet engine will be around 1000 watts broadside on aspect. Hand-on aspect, when the structure of the target aircraft prevents a direct line of sight from the interceptor to the radiating gas, the effective intensity of the gas radiation source may be only a watt or two. In any case atmospheric absorption in the 4.3 region over a 25n. mi. path will be so strong, only a small amount of the emitted radiation will reach the interceptor. The "safety factor" provided by the gas radiation may thus be quite small at ranges of the order of 25n. mi. There is a need for much more information on the CO_2 radiation from pure jets, by-pass jets and ramjets in actual flight conditions as a function of target altitude, range and aspect, before more specific amount can be given.

4. Atmospheric Transmittance Coefficient (p. 165)

The assumptions here are that there is a "mean" (wavelength-independent) transmittance coefficient, that this can be deduced from the measurements of Adel and Lampland and there is an exponential decay of intensity with distance. This lends to the conclusion that 60% of the radiation emitted by the target in the 3 - 5.8 μ and 7.5 - 10 μ windows will reach an interceptor 25 n. mi. away.

We would disagree with all three of the basic assumptions. The data of Adel and Lampland are are from being the best available. The report does not discuss absorption by zone which should be marked at 28,000 ft and still more important at higher altitudes. Absorption by N_2O should also enter the future.

However even the most pertinent available experimental data do not enable one to make more than a very crude estimate of the likely transmittance coefficient. There is an urgent need for more data on atmospheric transmission at high altitudes.

Such crude estimates as we have been able to make suggest that over 25 n.mi. paths the fraction of target radiation reaching the interceptor will probably be nearer 25% than 60% at an altitude of 28,000 ft.

However at higher altitudes more and more radiation should be received so that the effectiveness of the I.R. system will increase as the intercept altitude increases.

We feel that a more careful study of the probable atmospheric transmittance should be made and that this quantity should be evaluated as a function of altitude.

5. Detector Sensitivity (p. 165)

The information given here is inadequate to perform an intelligent evaluation of the system. One figure ($2.\times10^{-9}$ w/cm^2) only is quoted for the "detector sensitivity" (presumably this means noise equivalent power) of a typical detector at an unspecified wavelength and using an unspecified bandwidth. Ideally the data required to evaluate the detector performance are a noise frequency spectrum over all relevant frequencies, measurements of noise equivalent power for monochromatic radiation and a specified bandwidth over all wavelengths of interest and full details of detector geometry. Alternatively a curve of the Jones "S" figure as a function of wavelength for a typical detector is required. More detailed data on the time constants of the cell are also desirable. Data available to us on gold-arsenic-doped germanium cells suggests the following performance may be achieved.

a) The figure of n.e. p. = $2.\times10^{-9}$ w/cm^2 for a 15 mm^2 cell appears reasonable for 8 μ radiation and a bandwidth Δf equal to the chopping frequency, f.

b) The sensitivity may fall by a factor of 15 in going from 8 to 10 μ and rise by a factor of 3 in going from 8 to 3 μ.

c) The sensitivity at 8 μ is many times less than the sensitivity at the intrinsic peak --- not half the sensitivity as stated in the report. This discrepancy however is irrelevant to the problem as we are not concerned with wavelengths as short at 1.8 μ .

Assuming that the R.C.A. cells behave as we have suggested it is apparent that radiation in the 3 - 5.8 μ region will be more useful from the detection point of view than the report leads one to believe, while the 7.5 - 10 μ region will be less valuable.

6. Irdome (pp.165-6)

Usually optical silicon has a pronounced absorption band at 9.1 μ and therefore a high emissivity in this region. The 9.1 μ band is due to the presence of oxygen in the silicon. Have R.C.A. succeeded in obtaining silicon windows of this size free from oxygen? The performance of silicon will probably be satisfactory up to 300°C or more.

We do not understand the statement that "the transmittance peaks at 70° for this high index material."

7. Optical Configuration (p. 166)

This calculation appears to be based on the unstated assumptions that:

a) the optical system will have a square field of view of $\pm$ 2°.

b) the detector used, of area $A_1 = S^2$, will have the same Jones "S" figure as the detector, of area A_2 = 15 mm^2, discussed on p. 165.

c) the Jones "S" will be independent of wavelength.

d) the bandwidth to be used will be the same as the (unspecified) bandwidth used in making the noise equivalent power measurements on detector A_2.

e) absorption of radiation in the optical system can be neglected.

f) the intensity of the target as a source will be $868/\pi$ watts per stradian.

g) the atmospheric transmittance will be 0.6.

With these assumptions the equation given for S/N follows. However the solution of this equation is D = 3.5", S = 6.2mm; not D = 3.85", S = 6.7 mm. The value of D given is that required for the target to give a signal equal to the detector noise at a range of 25 n.mi.

As we have discussed above we are inclined to disagree with assumptions (c), (f) and (g) and possibly (d).

8. Seeker Position (pp 166-7)

The contractor appears to be aware of the disadvantages of the position he has chosen, particularly from the point of view of restricted field of view.It should be pointed out that the advantages listed on p. 167 are not by any means peculiar to the selected position of the seeker head.

9. PP. 168-170

Comment on this section of the report is difficult without further information on the requirements for compatibility with the radar system. The bandwidths quoted however seem very wide. It is important to know if these bandwidths are the same as those used in the measurement of detector performance mentioned in p. 165. It should be borne in mind that the detection range decreases as the inverse square root of the bandwidth.

10. Enemy Countermeasures Considerations (pp 46-51)

It is noticed that for most modes of ECM, switching to I.R. homing is recommended as either preferred or alternate action on the part of NAV/AI. However no consideration is given to the possibility of infra-red ECMs. Such ECM's might consist of the ejection of flares simultaneously with the radar ECM -- a flare weighing about a pound could give about 5,000 watts for 60 seconds in the wavelength regions considered. An alternative ECM could be the use of modulated I.R. source in the target operating at one of the frequencies of the A.I. system.

It is felt that some consideration of these possibilities may be worthwhile.

Another possible countermeasure is the use by the enemy of a non-radar reflecting coating in the aircraft skin,--if this becomes possible at the target speeds envisaged. It may be pointed out that such a procedure would probably result in a high emissivity over the entire aircraft structure and would greatly enhance the range of the I.R. search and tracking system.

11. Conclusions

The report makes a number of gross over-simplifications of the problems of an infra-red A.I. system. We feel that more careful consideration should be given to the following points.

a) probable infra-red emission from the target,

b) transmission of the radiation through the atmosphere as a function of altitude,

c) background radiation from the atmosphere and reflection of radiation from the target,

d) variation of detector characteristics with wavelength,

e) variation of detector noise with the bandwidth used.

The general problem of infra-red A.I. systems is hampered by lack of adequate data on the following points:

a) probable target characteristics, including the radiation reflected from the surroundings of the target,

b) atmospheric transmission at high altitudes,

c) atmospheric backgrounds at high altitude,

d) intensity of infra-red emission from jet exhausts under operational conditions, and the absorption of this radiation over long path lengths.

Further experimental investigation on these points is needed.

It is felt that the choice of gold-doped germanium detectors is a happy one, especially as substantial improvements in the performance of these cells may be expected as a result of current research and development work, in which R.C.A. is playing a major role.

It is thought that although the discussion in the report leaves much to be desired, a more careful study will very possibly indicate that an I.R. subsystem will be a most valuable adjunct to the ASTRA I system and that it will be particularly effective under high altitude conditions.

Corrections to CARDE Technical Letter N-47-12.

"Second Quarterly Report on CF-105 Weapon System Assessment" 15 November 56.

(a) Pages 74 and 75. The captions on the curves were inadvertently confused in preparation of the report. The correct legends, reading from left to right, should be:

page 74

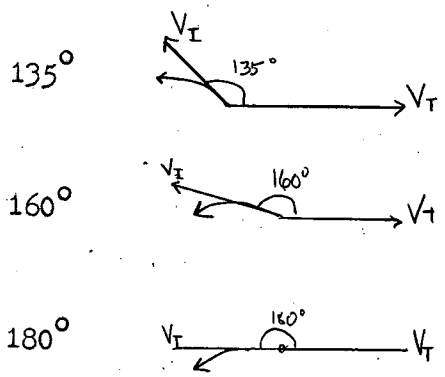

page 75

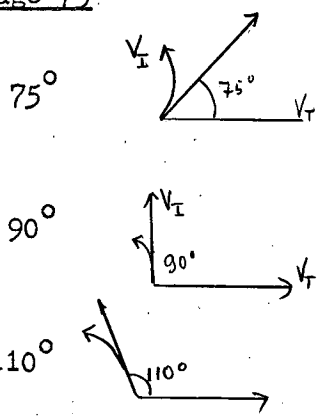

(b) Errors have been discovered in the work for decelerating turns of the CF-105 for weights other than the standard value of combat weight. The following figures and tables are therefore incorrect:

Figure	Page	Table	Page
1	82	1	83
3	86	3	87
4	88	4	89
6	92	6	93
7	94	7	95
9	98	9	99

APPENDIX 'R'

Susceptibility of the ASTRA I AI to ECM *

B.A. Walker
R.M. Dohoo
(D.R.T.E. EL)

1. Introduction

1.1 This estimate is required as part of an overall effectiveness study which is being carried out by CARDE. To be useful for their purposes it must take the form of expressing system performance by a number. The selection of the particular cases considered and the assessment of their probability of occurrence must inevitably be arbitrary, and the limitations of attempting to allot actual numbers to a subject of such diverse possibilities must be well understood by the reader. There is a limited time available to complete the CARDE study, and the arbitrary nature of many of our assumptions arises either from lack of information or of time for more detailed analysis.

We are concerned with the AI radar, weapon seeker and fuze sub-systems, but this report covers only the Astra I AI proposed by RCA.

1.2 The overall CARDE assessment is restricted, initially at least, to the case of one fighter vs. one bomber.

Bomber tactics in fact are based almost invariably upon the use of formations of varying sizes, and both the main study and this ECM evaluation to some extent form the foundation for the analysis of more realistic tactical situations employing a number of aircraft. These formations will exploit, in particular, a wider range of ECM than is admissible here. Our assumptions about the bomber's ECM load are restricted to that which he may carry for his own defence against a fighter weapon system on a mission involving the crossing of a ground-to-air missile belt as well as an average of 10 fighter attacks. We make no attempt to examine the many possibilities which arise when, as part of a formation, a much larger part of his payload may be given over to ECM equipment to be used against targets other than fighter weapon systems, but we make some attempt to estimate how the effectiveness of active jamming and chaff against the AI radar changes with the transition from one bomber to a group.

1.3 The complete weapon system proposed includes an infrared detector coupled to the AI radar. This represents a most desirable diversity in detection and tracking data sources, of particular value when we consider ECM techniques which may deny both radar range and passive radar tracking.

---

* This appendix reproduces the essential content of EL Report 5086-1, published by the Defence Research Telecommunications Establishment. This is a preliminary draft only, and is subject to revision.

However, the effectiveness of infra-red under various atmospheric conditions, over the range of altitudes encountered in bomber interceptions, and in the face of enemy countermeasures, is not known, and we are not prepared to assume complete dependence upon it. The radar system should be designed to meet unaided, so far as is possible, all feasible ECM conditions, and our study will judge its performance from this standpoint. Our conclusions will, therefore, be subject to re-consideration when a study of similar scope has been made of the operation of an infra-red airborne tracker.

1.4 In assessing the payoff to the enemy of the use of various ECM techniques, we start with the performance of the sub-system in the absence of ECM. We assume that the Specification requirement of a detection range of 25 nm on a 5 sq. metre target will be met and so derive performance on any target from its echoing area. Three classes of aircraft target are being considered in this study as follows:-

(a) A B52 subsonic type bomber (swept wing).

(b) A delta wing bomber capable of supersonic flight.

(c) A conjectured straight wing supersonic aircraft.

The values of echoing area adopted for various angles in the horizontal plane are given in Table I. ($\theta = 0^\circ$ is head on).

TABLE I

Echoing Areas Adopted for Various Targets (Sq.M.)

θ	B52	Delta	Supersonic Straight Wing
0°	4	17.5	2.5
30°	4	16.5	2.25
60°	10	18.5	2.75
70°	10	18.5	2.75
80°	100	18.5	2.75
90°		200	600
100°	140	22.5	4
110°	4.5	22.5	4
120°	4.5	22.5	4
150°	4	6	1
180°	4	8	1

1.5 Two of our basic assumptions in assessing the probability of various forms of ECM being adopted by the enemy should be stated.

(1) The basic design of the Astra I radar is the same as that employed in virtually all centimetric AI systems during and since the last war, and it will be assumed that the enemy is familiar with its principles.

(2) We are concerned in the overall study with the personal defensive armoury of the individual bomber, including active ECM, chaff, manoeuvre and decoy targets. The importance to him, in deciding when to apply his countermeasures, of detecting the transmissions from a typical tracking radar locked onto him is obvious and a listening receiver which, to be effective, need not be complex, will be assumed to be freely used for this purpose.

2. Protective Coatings and Artificial Glint

For the purpose of the overall study to which this ECM paper contributes, it is important to assess probability of occurrence of various ECM techniques. Where this probability appears very low we shall not attempt a detailed analysis, and we dismiss protective coatings and artificial glint with the following brief discussion.

2.1 The use of materials which reduce the power re-radiated by a radar target is well established. They can be classified as either absorbers of the incident energy or materials relying upon destructive interference between reflections from outer and inner surfaces. These latter are essentially resonant and their effectiveness is dependent upon angle of incidence, so that the absorbing materials are the more attractive for the protection of aircraft but are generally bulkier.

To be acceptable to the aircraft designer we would expect the material to have at least the following properties:-

(1) To be effective at all radar frequencies likely to be encountered in the operational role of the aircraft, since some penalty -- at least of weight -- will attach to their use.

(2) They must be suitable as skin material from an aerodynamic point of view. We are considering supersonic aircraft and this means at least a high degree of surface smoothness, reasonable thickness and the ability to withstand high temperatures.

The absorbent materials are suggested by (1) above, but existing samples of which we are aware are rough and thick and most unlikely to meet requirement (2). They do not appear to have been tried as aircraft coatings.

The ideal material would be an absorbing paint, and claims have been made for such materials, which, however, do not appear to have been substantiated. Trials of a resonant type of material on a low performance aircraft have been made at RAE, and although no detailed report has been received, we understand that performance is as would be expected from the known properties of the material. The trials are apparently being extended to include a higher performance (subsonic) aircraft.

2.2 The phenomenon of glint is a well known property of aircraft radar targers, particularly at wavelengths very short compared to the principal dimensions of the aircraft. The contribution made by various parts of the target structure to the total power re-radiated towards the radar is highly aspect sensitive. The main centre of re-radiation therefore appears to move within the physical boundary of the target and provides a noise-like modulation of the signal to the radar tracking circuits.

This effect can be enhanced by the use of passive or active devices such as corner reflectors or transponders. However, the dimensions of the target set a limit to what is achievable, and while we may later find this significant when we come to study missile homing and fuzing, we neglect its effect upon the AI when used with guided weapons.

3. Active Jamming

3.1 Two basic types of electronic tubes make a considerable contribution to the art of jamming, the travelling wave wide-band amplifier and the carcinotron oscillator. This latter may be readily modulated over a wide band by a variety of waveforms. A noise waveform modulation giving effectively a 'continuous' jamming spectrum is possible and widely used. It compels the radar designer to regard the jamming signal as fundamental in the sense that receiver noise is fundamental, and no more susceptible to countering by circuit techniques. We shall assume this latter type of modulation by the jammer. Modulation by a repetitive waveform at a frequency related to the AI radar antenna scan rate is dealt with under repeater jamming.

3.2 We first consider the effect of a barrage noise jammer in which the available jamming power is distributed uniformly across any desired band up to the maximum proposed for the AI system. It is useful to compute the crossover range, which is the range at which the received radar power bears some fixed relation to the received jamming power within the radar bandwidth. For the Astra I system, in which the transmitted peak power is 1 megawatt and the antenna gain about 3,000, this corssover range is given by

$$8.34 \times \sqrt{\frac{\sigma}{P_{TJ} \times G_J \times K}} \quad \text{nautical miles,}$$

where K is the ratio specified between received radar and jamming powers for reliable radar detection, σ is the echoing area of the target in sq. metres, P_{TJ} is the jamming power in watts radiated within the radar bandwidth, and G_J is the gain of the jamming antenna.

Table II shows the crossover ranges computed for the three standard aircraft targets. The ratio K for effective radar detection is assumed = 4, σ is the echoing area taken from Table I, $G_J = 1$ and $P_{TJ} = 2.0$ watts. This figure is based upon a single jammer delivering a total power of 300 watts simultaneously to two orthogonally polarized antennas and covering a bandwidth of 600 Mc/s (the range covered by the Astra I transmitter). The radar bandwidth is 4 Mc/s but, except at the ends of the jammed band, the image channel also admits jamming power so that the effective bandwidth is 8 Mc/s. (The basis for claiming to jam any polarization employed by the AI with about 4 db loss of jamming power is briefly as follows. We consider an omni-directional horizontally polarized system consisting of two crossed dipoles fed in quadrature with half the jammer power. We feed the other half of the power to a vertical dipole a short distance away. Then, at the radar, the phase of the vertically polarized component relative to the horizontally polarized is very aspect sensitive, due to path difference. If the two transmitting antennas are separated by 50 λ (about 6 feet), this phase difference changes $\pm 90^\circ$ for $\pm$ 20 minutes of arc change in aspect. We therefore claim that any circular or elliptical polarization in the radar will be jammed due to unstable fluctuations in aspect. Note that with circular polarization there is also a degradation in radar performance of the order of 6 db compared to that with linear polarization.)

TABLE II

Crossover Ranges for Barrage Jamming (Nautical Miles)

Q	B52	Delta	Supersonic Straight Wing
0°	5.9	12.3	4.7
30°	5.9	11.9	4.4
60°	9.3	12.7	4.9
70°	9.3	12.7	4.9
80°	29.5	12.7	4.9
90°		41.7	72
100°	34.8	13.9	5.9
110°	6.5	13.9	5.9
120°	6.5	13.9	5.9
150°	5.9	7.2	2.9
180°	5.9	8.3	2.9

3.3 The Astra I system is to be designed with passive tracking of a jamming transmitter, the radar transmitter being held in a standby condition permitting frequent testing of the situation to see whether radar range can be obtained. Comments on this are made later but it may be assumed, if any passive tracking system is used, that for jamming to deny useful range measurement, the corssover range should be not greater than about 2 nm. A significant improvement over the figures of Table II is therefore required from the jammer's point of view and this must be achieved by an increase in either transmitting power or jammer antenna gain. The latter implies a highly directional antenna with problems of training it upon the fighter and is not considered.

(It is, of course, possible to design a practicable jammer having a significant antenna gain, but its use implies tracking of the fighter, probably by a radar carried for the purpose. Such equipments have been used in bombers, including scanning microwave systems, and omni-directional coverage could be achieved with two or more such systems (as fighter type AI systems) with subsequent rotation of the jamming antenna beam into the required direction. Such complexity is more appropriate to a defensive system than to the mere increase of the jammer power level, and the ECM implications of a situation in which fighter and bomber employ similar radar equipments suggest a separate study.)

An effective increase of jamming transmitter power by concentration in a narrow band (effectively, spot jamming) may be possible. If all the jammer power can be concentrated in the radar bandwidth, the crossover ranges of Table II are reduced by a factor of 8.65 and jamming becomes effective if we neglect a small range of angles around the beam.

It is considered that this condition is unlikely to be achieved, considering the known limited stability of magnetron transmitters and the difficulty of performing the operation of frequency measurement and jammer tuning automatically. We conclude somewhat arbitrarily that a practicable spot jammer of this type will use a receiver to measure the radar transmitter frequency, time sharing the antenna system with the jamming transmitter sufficiently frequently to cope with a relatively slow frequency change in the AI system, and stay within 10 Mc of the radar frequency. This jammer would then radiate 300 watts in a band 20 Mc/s wide in the region of the measured radar frequency.

With the spot jammer as defined above, the crossover ranges are those shown in Table III, and represent our final conclusions as to the performance of this type of jamming practised by a single bomber aircraft.

TABLE III

Crossover Ranges. Spot Jamming of Astra I

θ	B52	Delta	Supersonic Straight Wing
0°	1.52	3.18	1.2
30°	1.52	3.1	1.15
60°	2.42	3.27	1.26
70°	2.42	3.27	1.26
80°	7.6	3.27	1.26
90°		10.8	18.6
100°	9.0	3.6	1.52
110°	1.69	3.6	1.52
120°	1.69	3.6	1.52
150°	1.52	1.86	0.76
180°	1.52	2.16	0.76

3.4 The important assumption made in postulating the spot jammer of Section 3.2 is that of a low rate of frequency change by the radar. We have in mind a magnetron transmitter and a conventional klystron local oscillator, tunable electronically over a limited range, a combination not considered capable of optimum rapid frequency change while maintaining the flow of radar data required for tracking. We will assume that if radar frequency can be changed at a rate not more than 50 Mc/s, the spot jammer forming the basis of Table III is possible. If, however, the radar frequency can be changed continuously at a rate exceeding 200 Mc/s not necessarily, though desirably, at random, we assume the jammer look-through and tuning problem is made sufficiently difficult to compel the enemy to resort to barrage jamming.

It may be interesting to examine the results of achieving this. We are informed that it is not unrealistic to consider a magnetron ring tuned with a ring mounted on a vibrating diaphragm, and that a 3% band might be covered with a tube giving 400 KW peak output. It would appear necessary to use a completely electronically tuned local oscillator (e.g. carcinotron); even so, synchronization with the magnetron tuning is a major problem.

Table IV has been prepared to show the effect on crossover range of a system such as Astra I but with peak power of 400 KW, rapidly tunable over a band of 300 Mc/s, against a barrage jammer as in Table II, but jamming only the 300 Mc/s band.

TABLE IV

Crossover Ranges. Astra I System with Peak Power 400 KW Against Barrage Jamming in a Band of 300 Mc/s. (Radar Image Channel also Jammed)

Θ	B52	Delta	Supersonic Straight Wing
0°	3.34	7.0	2.64
30°	3.34	6.8	2.53
60°	5.33	7.2	2.77
70°	5.33	7.2	2.77
80°	16.7	7.2	2.77
90°	.	23.8	41.0
100°	20.0	7.9	3.34
110°	3.72	7.9	3.34
120°	3.72	7.9	3.34
150°	3.34	4.1	1.67
180°	3.34	4.75	1.67

These figures are, of course, obtained at the cost of a reduction of 20% in maximum detection range in the absence of jamming, compared to the 1 MW case. In the presence of jamming this is irrelevant, however, and Table IV can be compared with Table III to assess the improvement in performance obtained by rapid tuning of the AI transmitter at the expense of a 60% reduction in peak power.

If barrage or spot jamming can be expected to determine system performance under operational conditions, it appears that rapid tuning of the AI transmitter is a more important design objective than high peak power.

3.5 We have discussed the spot jammer performance from the point of view of crossover range, assuming that operationally passive homing is possible at ranges greater than the crossover range. The spot jammer has been made effective by the assumed introduction of a listening receiver and so the possibility of responsive jamming arises, i.e., the jammer is switched on only when radar illumination is detected. Therefore, to guarantee passive homing against a noise jammer, it is necessary to keep the AI radar transmitter switched on.

3.6 We now ask whether repeater jamming may not be more effective than spot jamming with no greater complexity.

A simple repeater consisting of a wide band pulse amplifier is mentioned under decoys later in this paper. To be effective as bomber protection, a variable time delay may be added which would capture the AI range gate. This

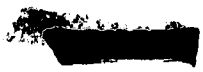

is not a highly effective form of jamming, particularly if a monitor display is available in the fighter aircraft. In any case, a variable delay technique at microwave frequencies is not available.

An alternative method of capturing the range gate, and one less easily countered by the AI operator using a monitor display, would be to re-radiate pulses, preferably at a rate several times the radar p.r.f., almost, but not quite, locked to the p.r.f. However, the drift rate must be held very low in order to overcome the tracking velocity memory. If the radar can change frequency, even at a low rate, jammer design now becomes difficult, and if (as is the case with Astra I) the p.r.f. can be continuously varied as well, we conclude that such a repeater jammer is unlikely to capture the range gate.

Proposals have been made for a more effective type of repeater jamming in which false bearing information is given to a sequential lobing amplitude-comparison type of tracker. The nutation frequency is readily determined from the AI transmission when locked, and it is only necessary to interfere with the phase of the amplitude modulation before re-radiating. This can be done according to the Inverse Gain Proposal which has been analyzed in a Stanford University report.

The peak power scattered by a target illuminated by Astra I is given by

$$\frac{66.4\sigma}{r^2} \text{ watts}$$

where σ is in sq. meters and r is in nautical miles, so that a 5 sq. m. target scatters 3.3 watts peak at 10 nm range and 82.5 watts at 2 nm. A travelling wave tube capable of delivering about 100 watts peak appears to be adequate for this type of repeater jammer.

Considering the split beam system representing either azimuth or elevation, the radar information cannot be misleading when one of the beams does not illuminate the target. However, integration of the received signal is necessary, covering some cycles of nutation, and if the antenna, under the impetus of the false bearing information, is moving at near its maximum rate, it moves through one beam width in the order of one nutation cycle. Thus, under automatic tracking conditions, one expects this form of repeater jamming to unlock the tracker. This is confirmed by the only field tests of which we are aware.

A duplexing problem arises in the design of such a jammer. Viewed as an installation involving two separate antennas, the coupling between them needs to be comfortably below the gain of the repeater. From the figures quoted above at 10 miles range, this is some 60 db and, while difficult to achieve for omni-directional antennas, we feel it safe to assume that a solution can be found, possibly by the use of more than one pair of antennas, or by time sharing between transmitter and receiver with a period much shorter than the pulse width in use. Ideally, the receiver period should be equal to the delays in the repeater.

3.7 Some possible counters to this form of jamming appear to be:-

(1) Adoption of simultaneous lobing in the track mode.

(2) Coding of the AI transmission so that on lock it resembles the search mode to the listening receiver.

(3) Use of very short pulses.

(4) Manual tracking.

(5) Simultaneous transmission and sequential switching only on 'receive'.

(1) The first of these appears to be a complete answer to this type of repeater jammer and is therefore a very desirable feature for a tracking system.

(2) This is only achieved at considerable sacrifice of target information. To simulate the search mode exactly, only one cycle of the nutation frequency would be received every two seconds. The objections to it are:

(a) The loss of continuous target information will render the system susceptible to fluctuations in signal amplitude due to glint and noise.

(b) A rapid response and long memory are required. (These open the way to unlocking by chaff dropped at the correct time).

(c) If the bomber chooses to use his repeater jammer without definitely identifying the AI tracking mode, the AI is still defeated.

(3) With a repeater jammer of which we have seen reports, the time delay in the jammer-video circuits is of the order of 0.1 microseconds. Thus, range discrimination against the jamming pulses could be achieved with a very short pulse system, say of the order of 0.05 microseconds.

(4) Manual tracking is possible directly from the B-scope display, and failure to lock compels the adoption of this manual mode of operation.

(5) Deals with the Inverse Gain Jammer, but see Section 3.8 below.

3.8 There are other possibilities than this inverse gain jammer which may unlock the angle tracking circuits of a sequential lobing system. Amplitude modulation of the re-radiated pulses at a frequency in the region of the nutation frequency (if this is known - or slowly varying between 30 and 100 cps if not) would probably be effective. Suggestions have been made by E. Heaton-Jones of the Royal Aircraft Establishment (private communication) for exploiting the versatility of the carcinotron by using various combinations of noise modulation together with amplitude modulation (which may be pulse) at almost the nutation frequency.

There are attractive possibilities (to the jammer designer) in this proposal, and our conclusion that the sequential lobing of the Astra I system renders it dangerously susceptible to active jamming is notably strengthened by it.

4. Chaff

4.1 Summary

4.1.1 It is possible to differentiate between two uses for chaff, one in which a quantity of chaff forms an extensive background of high radar signal level within which the true target echo cannot be distinguished, and the other in which controlled sowing of smaller quantities breaks lock in either the range or angle tracking channel during a fighter interception. The development of extensive areas of chaff presupposes the use of a formation of aircraft. This case is considered later. Here we are concerned with the single aircraft which is capable of protecting itself only by breaking lock during a fighter interception.

4.1.2 We distinguish also between two methods of launching. In the first of these, sometimes called gravity launching, the chaff is released through a chute on the aircraft and blossoms in the turbulent air. We regard this as representative of the existing state of the art in releasing chaff. From an analysis of the effect of chaff launched by this method against a tracking radar, it will be seen that the delay from first launching to the development of a significant radar echo is a serious disability, and it is known that considerable work is being done to eliminate this by forward firing of the chaff bundle from the aircraft, with subsequent dispersion by explosive means. This is the second method of launching.

4.1.3 We proceed to analyse the use of gravity launched chaff against the range and angle tracking circuits of the tracking radar, and shall see the significance of the delays which occur with gravity launching before the chaff echo develops. We shall suggest that attention should be given to some aspects of the radar design to minimize chaff effectiveness.

4.1.4 From this point we proceed to consider what may be achieved with further development of chaff techniques. It is known that development is proceeding along the lines of forward firing of chaff to eliminate the delays. It seems that further development along these lines may well succeed in permitting a single aircraft to evade the tracking radar by projecting ahead sufficient chaff to form a cloud within which he will evade the tracking system by the use of manoeuvre or by projecting the chaff to form a cloud at a suitable angle to the aircraft track. We have little knowledge of work proceeding along these lines, but can deduce the requirements for this power launching of chaff such that tracking systems of the AstraI type can be successfully unlocked.

4.1.5 We therefore foresee that chaff techniques will evolve capable of defeating tracking radars operating basically on signal amplitude. There remains to the radar designer another approach based upon the fact that when chaff blossoms its velocity is substantially that of the air. Thus, a system based upon Doppler shift should prove capable of tracking a target through chaff. There will be tactical implications in the use of such a system since in order to keep the line of sight component of target velocity high, useful target aspects will be restricted to the region around the nose and tail.

4.2 Significant Parameters of the AI Radar

4.2.1 Effective Gate Width - It is necessary to know the effective gate width (α) of the tracking system, which we define as the distance a target echo has to travel from the balanced gate condition (whether symmetrical, leading or trailing edge tracking be in use) to get clear of the gate. For a normal balanced gate system using half-microsecond pulses we adopt a value of α = 375 ft. We are aware of two methods of achieving edge tracking. In the first, the two halves of the split gate are given different gains so that at balance the target sits to one side of centre. We assume a value of (α) = 200 ft. for the Astra I system in this case. Alternatively, the target echo can be differentiated and the appropriate edge selected on the basis of polarity. This differentiated signal can then be held in a narrow gate system, and for our purposes, can be regarded as the equivalent of using a very short radar pulse. To cover these cases we assume a value of (α) of 75 ft.

4.2.2 Target Velocity - In calculations involving specific cases we shall adopt a target speed of 500 knots for the subsonic bomber and 1000 knots for the two supersonic bombers.

4.2.3 Range Servo Characteristics - The response characteristic of the servo circuit which positions the range gate, working from position error signals, can give a large measure of protection to the auto tracking circuits against chaff echoes. We do not know what tracking circuits will be proposed for the Astra I system, and so state some general considerations.

The typical response curves of a servo with various degrees of damping are well known. This response is analogous to that of a low-pass filter, and it can be shaped by the error integrating circuits to approach an ideal low-pass characteristic. Thus, it is not too unrealistic to think of a control system which has little effect upon strobe position until an error signal has been present for some period of time, after which it rapidly corrects both position and velocity. This 'waiting time' is evidently important in preventing capture of the gate by a large transient echo.

The ideal operation for the circuits to perform is evidently to recognize the presence of chaff and then to ignore the signal inputs while the chaff echo persists, proceeding with remembered velocity. We cannot assume this to happen and, in fact, our idealized circuit has merely delayed its response to its input signals. The characteristic difference between chaff and target echoes therefore upon which we hope to capitalize, is their time duration within the gate. This means that if our analysis shows a given delay or memory time to be required under given circumstances, the actual time designed into the circuit will need to be longer than this, say, 2 times.

We will use initially a time of 0.1 sec. to represent typical gating circuits not designed specifically with a view to defeating chaff by use of heavy damping.

In order to get a feel for the order of memory time which the tactical situation permits, we note that the specification for the fighter aircraft flight control system quotes a maximum fore and aft acceleration of 1.5g. Assuming both fighter and target to be capable of this, and taking the extreme case of a relative acceleration of 3 g, we find that our three values of effective gate width permit maximum velocity memory times of 2.5, 2 and 1 second respectively for the 375 ft., 200 ft., and 75 ft. effective gate widths.

The use of heavily damped range tracking circuits complicates the acquisition phase of AI operation. However, rate-aided manual setting of the range strobe is certainly possible, and automatic circuits having different maximum accelerationswhen on acquisition and on lock appear to be so. We will therefore assume that waiting times approaching the values quoted above can be employed.

4.2.4 Angle Servo Characteristics - It is necessary to define a similar parameter for the azimuth and elevation servoes. From the equipment specification we note that these servoes must be capable of angular rates up to 1 radian/sec. and accelerations up to $4500^{\circ}/sec.^{2}$. If we assume that the angular distance from the centre of the split beam system to its edge is 2° this means that the maximum permitted delay in response of these servoes is of the order of 1/30 sec. It is therefore evident that damping of these servoes cannot be used as a protective means against chaff as is the case with the range servo.

4.3 The Use of Gravity Launched Chaff

4.3.1 In Appendix A we examine from the experimental evidence available to us the way in which chaff echoes develop from the time of launch for different sized bundles, and we use two bases for these computations which lead to the curves of Figs. 1 and 2. Figure 1 represents a somewhat

pessimistic assumption about chaff echo development, and we add to it an initial time delay of 0.1 sec., which has been observed to occur between release of the chaff package and the commencement of blossoming. Figure 2 on the other hand represents a more optimistic estimate of the rate of chaff development and is used without any initial delay. It is known that the initial delay and the blossoming time are markedly dependent on the position of the launcher on the aircraft and on the aircraft's speed.

In Appendix B we also derive quantities of chaff (which are related to aircraft echoing area) for our three standard targets. The weight of chaff bundles is also obtained from Figs. 1 and 2 so that we are able to ensure that overall weight of chaff proposed does not exceed some rational limit.

4.3.2 Because of the initial delays and the finite blossoming time assumed with this launching technique, there will be some combinations of target aspect and velocity for which the chaff echo will not blossom within the AI range gate tracking the target. Figs. 3, 4 and 5 show these regions for our three target aircraft and various combinations of relevant parameters discussed in 4.2.

For the regions in which the chaff does blossom within the range gate with an echoing area assumed in the appendix to give at least 3 times the target signal amplitude, we can proceed to examine the effect of chaff upon the range and angle tracking circuits.

4.4 Results for Chaff Dispersed from the Bomber

4.4.1 This section is intended to cover the use of chaff launched by gravity, as is current practice, and also the possible use of some technique of explosive launching and dispersal which may be used to eliminate the delays in chaff echo development which are a disadvantage of gravity launching. We examine this latter case first and then introduce a modification which takes account of the delays with gravity launching.

4.4.2 In Appendix C we derive a method of presenting the results when chaff is launched directly from the bomber aircraft against the range and angle tracking components of the AI system. Following the procedure of Appendix C, we can draw the curves of Fig. 6 and from these we can draw polar plots, typical samples of which are reproduced as Figs. 7-12. The method of interpretation of these plots is also found in Appendix C.

In preparing Fig. 6 allowance has been made for the overall length of the bomber aircraft, which clearly enters into the argument which is based upon the separation with time between target and chaff echoes. A value of 100 ft. is being assumed for bomber length.

4.4.3 To take account of the delays with the current technique of gravity launching we must take account of Figs. 3-5. For the appropriate aircraft, speed, effective gate width, and launching technique (derived from Fig. 1 or Fig. 2) these pictures show bearings where the delayed chaff will be ineffective because it blossoms outside the range superimposed upon a polar plot such as Figs. 7-12.

The main practical result is to prevent unlocking of the azimuth servo at short ranges, particularly at bearings near the nose or tail. The chaff delay also adds to the servo response delay, but this is generally a secondary effect if servo delays of the order of 0.5 sec. are assumed.

4.4.4 Before discussing the results, it will be useful to recapitulate the bases of the information in Figs. 6-12.

(a) We have assumed the chaff echo to be greater than the target echo so that the tracking circuits tend to follow the chaff rather than the target.

(b) In order to present our conclusions in numerical form, we have assumed an idealized servo response delayed by a known time. The actual response time designed into the system must be longer than this.

(c) The assumption about relative size of chaff and target echo does not hold for some region close to the target beam. In Table I we have shown echoing areas of the order of 100 sq. metres, and if these figures in fact obtain we must assume chaff will be virtually ineffective. We lack any detailed knowledge of the echoing area in this region and so can only point out that over a small range of angles close to the beam our analysis breaks down and the chaff is ineffective.

(d) Figs. 7 to 12 represent the forward starboard sector of the horizontal plane around the bomber. The complete picture can be drawn from symmetry.

4.4.5 Figures 7 to 12 are reproduced principally to show the effect of varying the two parameters at the disposal of the radar designer.

Considering range servo response or velocity memory, the advantage of increasing this is apparent at a glance. Large areas around the bomber become tenable by the fighter without unlocking occurring. All the values of memory time shown on these plots are practicable without affecting the ability of the range tracker to follow target manoeuvre.

The regions below the full curves within which azimuth unlocking occurs are principally of interest because they extend round almost to the nose and tail of the target, though at short range. The real value of the very short range gate is that it protects the azimuth tracker in these regions. Otherwise, the only other factor which affords relief is the existence of chaff

echo development delays which occur with conventional gravity launching. The effectiveness of this is also increased markedly by the use of a very narrow gate (see Figs. 3-5).

4.5 Effect of Video Limiting

Up to this point it has been assumed that the chaff echo in the range gates can be large compared with the target echo; indeed, it has been assumed that it was necessary, to unlock the AI radar, to make the average chaff echo three times as great as the target echo. It has been suggested in a General Electric report that video limiting is very desirable, but no discussion is given as to how such limiting can be effected. Since the angle tracking and AGC circuits require signal amplitude information, it is necessary to remove the angle tracking and AGC information before the signal is passed through the range gates. An arrangement such as that shown in Figure 6 appears to be possible. If signal limiting can be used in the range tracker our conclusions about unlocking the azimuth circuits are not affected. In the ideal condition of no fading of the target echo and perfect limiting it appears that the effect of chaff will be only to lengthen the target echo and thus to contribute a small unbalance signal to the rear gate. The chance of stealing the gate is thus very considerably reduced. The narrow gate is still a desirable feature.

Fading is however a characteristic of the target echo, and so even with limiting some servo delay is desirable. The combination seems capable of giving almost complete protection to the range gate, and the concept of signal limiting deserves serious experimental investigation.

4.6 Continuously Launched Chaff

Before proceeding to consider the possible effects of chaff when projected ahead of the bomber, we should look at the possible use of chaff launched continuously or at intervals short enough to achieve a virtually continuous chaff trail. This may occur when the bomber is sowing chaff principally for the protection of following aircraft. We are aware of a proposal for continuous launching by allowing chaff to be sucked out from a negative pressure area on the wing.

From Fig. 6 we can deduce that, if the individual chaff package is to unlock the tracker, it will achieve this in practically all cases within 2 secs. at a speed of 500 knots or 1 sec. at 1000 knots. This suggests 1 to 2 seconds, depending upon bomber speed, as the optimum interval between successive launchings and represents the best tactic for the bomber using gravity launched chaff against the AI tracker.

If the interval is much shorter than this or if launching is continuous, it can be predicted that both range and azimuth circuits will track a point some distance astern of the target. Figures 1 and 2 can be used to obtain a picture of the chaff trail in this case. The chaff echo takes up to 3 seconds to develop fully so that the aircraft echo will be followed by a chaff echo increasing in amplitude to a maximum which may be one mile astern. In general, it will be much closer to the bomber and for unlocking a tracker this represents a wasteful and inefficient use of chaff.

4.7 Forward Firing

We now consider the possible use of forward firing of chaff. If the aim is to fire only a short distance forward so as to overcome the effects of delayed development of the chaff echo we have the situation indicated in Figs. 7 to 12. However if, say, s small projectile were used which dispensed chaff continuously (or individual bundles at very short intervals) a useful deceptive trail could be set up. We have considered the use of such a trail set up ahead of the bomber, with deceleration of the aircraft while concealed by the chaff, and concluded that some 100 bundles of chaff would be needed with dispersion at 1/10 sec. intervals. During a discussion at WRDC, however, we learned of a proposal to fire such a chaff projectile forward and downwards so that a drooping trail of chaff is created over which the bomber flies. Now, there will be chaff signal within the range gate at an increasing distance below the target, which can be expected to unlock the elevation tracker. This is effective at all bearings in or near to the bomber's horizontal plane, and to depress the elevation tracker sufficiently to insure its removal from the target appears to require only some dozen launches at about 200 ft. intervals. With such techniques under active development, it is difficult to escape the conclusion that radar trackers, such as Astra I, are seriously limited by their ability to use only the amplitude characteristic of the received signal. Chaff has one inherent weakness in that deceleration is rapid when it blossoms, so that Doppler frequency represents a useful basis for discrimination between target and chaff echoes in a suitably designed system. Restriction of angles of approach to the nose and tail regions around the bomber will probably result, due to the necessity to maintain a large line of sight component of target velocity.

It should also be borne in mind that the bomber is unlikely to have capacity for sufficient chaff projectiles to permit continuous launching while in a defended area, and there is therefore complete dependence upon a listening receiver to give warning of lock. Infrared tracking may have considerable significance in permitting tracking with only intermittent use of the AI radar, but our attitude to infrared at this stage has been stated in the introduction to this paper.

5. The Effect of Possible Group Tactics

5.1 The fighter weapon system is a logical target for ECM. Active ECM by a bomber is considered most likely to be employed in case of imminent attack by a fighter or missile weapon system, since some added risk of detection attaches to its use. On the other hand, a group of aircraft is less likely to go undetected and may logically plan its operations with considerable emphasis upon ECM of all kinds working continuously. In such conditions, ground data gathering systems seem likely to be attacked, and the ground-to-air data link would appear to be a particular ECM target. These things, however, are beyond the scope of our investigation, and we will consider briefly how group tactics may affect the arguments so far presented in this paper.

5.2 Active Jamming

We must eliminate spot jamming with "look through" since, in a formation of aircraft all carrying jammers, listening receivers are unlikely to be useful. We also reject the possibility that the jamming power density will be increased by each aircraft jamming a narrow band since a fighter close to the formation could avoid jamming on his particular frequency. We therefore consider a situation in which each aircraft carries a barrage jammer as discussed when deriving Table II.

The critical factor in jamming effectiveness appears to be the bomber aircraft spacing. We consider a formation arranged as in Fig. 14, which is selected to minimize so far as possible the chance that an aircraft on the outside of the formation can be selected by a fighter with a 3° beam homing into his jammer. If the separation of aircraft within the formation is of the order of 3 miles due to defensive weapon capability, then a fighter approaching along the line indicated in Fig. 14 has adequate azimuth discrimination to pick off a winger at a range of 30 miles.

Another advantage which may be expected to arise from the formation is the increased jamming power level due to a number of aircraft along any sight line. For instance, when the nearest bomber is at 5 miles there may be contributions from other bombers at 8 and 11 miles. However, in this case, the jammer power level is increased by only 75%, and when the nearer bomber is at 2 miles, the increase is only 20%.

We must, therefore, conclude that little additional effectiveness in barrage jamming of the AI system is achieved due to the use of a formation of bombers. The crossover ranges of Fig. 2 are not significantly altered, and passive homing onto one aircraft on the edge of the formation can readily be achieved. This latter conclusion holds unless the bomber spacing can be kept to about $\frac{1}{4}$ mile.

5.3 Chaff

We no longer examine the use of chaff to unlock a tracking system, but consider it as a means of providing false targets or a general high "noise" background.

A significant fact arising from study of Figs. 1 and 2 is that if only the fully developed echoing area of a chaff cloud is of importance, then very little chaff is required. A 20 sq. m. echo can be generated with 4 oz. of chaff within 1 second of launch. If each of the leading aircraft in the formation releases one bundle per second, chaff echoes will be spaced at 1700 ft. intervals at 1000 knots. If, further, the leading aircraft can fire forward some 500 ft. and explosive dispersal enables us to use the development times of Fig.2, they will achieve some measure of protection for themselves.

Thus, at the expense of a trivial chaff load (some 15 lbs. of chaff per minute per lead aircraft) the formation appears able to gain an appreciable measure of protection against AI radars not readily able to discriminate in velocity. For aircraft separations of the order of 3 miles, there will be, within the area occupied by the formation, some 10 times as many chaff clouds as aircraft echoes.

The chaff returns immediately on blossoming are omnipolarized, but there is a tendency for horizontally polarized echoes to predominate with time. This is less at X-band than at lower frequencies, and the only measurement of which we are aware shows 1 db ratio of horizontal to vertical polarization after 1 minute. This can be overcome for larger formations by having aircraft other than the lead aircraft dispense chaff.

6. Decoys

The possible use of small unmanned aircraft, which may be carried by members of the bomber force to the defended area, has been mentioned by several writers. By fitting them with pulse repeaters and/or corner reflectors, and possibly with IR radiators, they can be made to simulate bombers with a degree of exactness sufficient to deceive systems of the type under discussion. We consider these decoys to be powered and capable of some hundreds of miles of flight, at bomber speed and altitude. The main function would be to dilute the bomber stream with false targets, which may perhaps be more difficult to destroy than the bomber because of their smaller size and smaller number of vulnerable features.

The bare possibility exists that, in an unpowered form, it may be possible for the individual bomber to carry one of these devices for release at a critical point in a fighter interception, combined perhaps with a maximum manoeuver by the bomber itself. It seems probable, however, that

penalties of weight and drag would make this considerably less attractive than alternative forms of defence, particularly considering its essentially 'one-shot' nature.

Decoys therefore enter into our study only when considering formation tactics, and we need to estimate the extent to which the defence is diluted. Presumably special carrier aircraft will be required and it may conservatively be estimated that each carrier releases two decoys. It is conceivable that sufficient may be carried to achieve equal numbers of bombers and decoys in the formation.

The decoys may be employed more usefully than as mere dummy aircraft, e.g., as lead aircraft dispensing chaff as discussed in Section 5.

7. Conclusions

7.1 Summary

7.1.1 Repeater Jamming - AM jamming aimed at unlocking the angle tracker appears to be a serious threat to trackers of the Astra I type. The Inverse Gain jammer is the sophisticated version of repeater jammer for this purpose, but AM at about the nutation frequency (which may be an additional feature of a carcinotron noise jammer) is a real possibility having advantages of jammer simplicity and of countering the use of lobe switching in the tracker receiver only.

7.1.2 Barrage Jamming - With barrage jamming from a single 300 watt source we find operationally useful crossover ranges for all targets at all aspects with the high gain antenna and one MW transmitter.

7.1.3 Spot Jamming - The defence against spot jamming depends upon the rate at which AI radar frequency can be changed while maintaining the flow of radar data. We consider the critical tuning rate to lie in the region 50 to 200 Mc/s/s. Above 200 Mc/s/s the jammer is compelled to resort to barrage jamming.

7.1.4 Responsive Jamming - Spot or barrage jamming can be made responsive where a listening erceiver is employed. It thus becomes necessary to operate the radar transmitter while homing onto jamming.

7.1.5 Chaff - We have been mainly concerned with the use of chaff to break lock. Initially we have relied upon data relating to current practice in gravity launching, which is characterised by a delay which occurs before a significant chaff echo develops. The treatment also covers the possible development of techniques which will eliminate this delay. There are advantages in the use of short pulses (or equivalent techniques) and delayed servo response which can be quantitatively assessed. Signal amplitude limiting in the range tracking circuits should also be evaluated experimentally.

Techniques of forward firing of chaff are being evolved which are relevant to our case of one bomber vs. one fighter, and it can be anticipated that the effectiveness of chaff will increase against trackers not based on Doppler frequency measurement.

7.1.6 Other Forms of ECM - The use of unmanned aircraft is considered mainly as a means of diluting the bomber force. Such dècoys can be made indistinguishable from bomber aircraft to radar.

On the evidence available we assign a low probability to the successful use of non-reflecting materials on high performance bombers, and consider the enhancement of target glint not to be significant for an AI used with guided weapons.

7.1.7 Influence of Formation Tactics on the Above Conclusions - The wide range of possibilities arising when large scale use of ECM is planned for a bomber formation is a subject for a special study, and we have restricted discussion to the possible influence of formation tactics on our conclusions as to the effect of active jamming of the AI system and the use of chaff.

Based on the assumption that defensive weapon capability will enforce aircraft spacing of the order of 3 miles, we find our active jamming conclusions not significantly modified.

It seems probable that very large chaff clouds can be sown at small expense in bomber payload. Target acquisition under these circumstances becomes difficult, and reinforces our opinion that Doppler frequency discrimination should be exploited in AI radar design.

7.2 Design Recommendations Arising from the Study

7.2.1 Passive Homing - Arising from our assumption of free use of a listening receiver in the bomber, responsive jamming is possible. Probably the best (and simplest) homing system is to retain the normal radar mode, probably with a wide receiver range gate.

7.2.2 Spot Jamming - We consider rapid tuning of the AI transmitter to be required to counter spot jamming. This could be justified even at the expense of some loss in peak transmitter power.

We have not had the benefit of discussion with the Design Contractor and do not know his detailed proposal on tuning. However, there appears to be some reliance upon infrared homing in the presence of radar jamming, and we feel that such systems cannot yet be adequately assessed. The radar should be designed to be self-sufficient in this respect.

7.2.3 Repeater Jamming - We find this serious cause for concern to sequential lobing trackers and strongly recommend a system based on simultaneous lobing on both transmit and receive.

7.2.4 Chaff - With established techniques in launching, chaff remains a serious threat to systems not designed to discriminate targets on a Doppler frequency basis. Considerable protection can be achieved by adoption of:

(a) very narrow gates, either with short pulses or differentiation as used in some edge tracking techniques.

(b) long integration or velocity memory times in range tracking circuits.

(c) signal amplitude limiting.

Present trends in the development of forward firing of chaff indicate that such modifications will have limited success, and that AI radars based on Doppler technique will be found essential.

7.3 Notes on ECCM Aspects of the Contractor's Proposal

These comments refer to the Proposal for an Advanced Electronic Weapon System for the A.V. Roe CF-105 Aircraft, dated 21 February 1956.

7.3.1 High Power Transmitter - We confirm the value of this feature in ensuring high crossover ranges.

7.3.2 Tunable Magnetron and Fast AFC - Transmitter tuning is really useful only when the rate and the range of frequency shift make following by a spot jammer impossible. The data rate of the radar should remain unchanged during tuning which should be a continuous process.

7.3.3 Jittered PRF - We expect this feature to eliminate the possibility that a repeater jammer using an almost locked train of pulses will unlock the range tracking circuits. Its use, however, is not compatible with delay line AMTI.

7.3.4 High Gain Antenna - This is another element contributing to the advantages of high power operation. Note, however, that where receiver noise controls, maximum range varies directly as dish diameter but, if jamming noise controls, maximum range varies as the square root of dish diameter.

7.3.5 Polarization Diversity - This is in the category of design features more easily achieved by the jammer than by the radar. Justification for its use rests rather on other claims, e.g. its use against rain clutter. Otherwise the complexity is scarcely justified against ECM.

When chaff is used to unlock we are concerned only with cloud durations of a few seconds, and for this time the experimental evidence shows it is omni-polarized.

7.3.6 Infrared Detection - This appears to be an excellent example of diversity in data sources, but a separate study of its effectiveness is required.

7.3.7 Passive Homing - Radar operation in the face of active jamming is completely dependent upon this, and we have been at pains to establish whether practical jammers can deny it to the fighter. There are disadvantages to the fighter. There are disadvantages to the proposed passive mode for Astra I in that a responsive jammer can deny both range and passive homing, and it is not clear why the transmitter dummy load and a special wide band homing receiver are proposed.

7.3.8 The increased dynamic range by use of a microwave AGC does not derive from jamming considerations. We find the crossover point is always achievable with a 1 megawatt transmitter.

Appendix C - Derivation of Polar Plots. Figures 7 - 12.

In Fig. 13 we show the geometry with the fighter sight line at an angle Θ to the bomber track. $\frac{\phi}{2}$ is one-half the total azimuth coverage of the tracking system and α, as before, is the effective gate width, R is the range.

We are concerned with the projection of the target track along and normal to the line of sight. The first of these represents the limit of resolution of the AI azimuth system and the latter that of the range gate. These are respectively $\frac{R\phi}{2}$ cosec Θ and α sec Θ.

In Fig. 6 we have plotted curves of these quantities for various values of R and α, assuming 2° for $\frac{\phi}{2}$.

If we consider the vertical scale of Fig. 6 to represent the separation between target echo and chaff echo the significance of the intersection between a secant and a co-secant curve is that for that value of α and R, intersecting at a given value of Θ, the azimuth system

cannot follow both chaff and target. If the chaff echo is appreciably bigger than the target echo it can be expected that the tracker will be unlocked.

We can also use Figure 6 to show the effect of delays in range servo response. The product of bomber speed and servo delay represents a distance which can be marked off as a horizontal line on Fig.6. The significance of the intersection of this horizontal reference with any secant curve is that for values of θ below that at which the curves intersect, the servo delay prevents the range gate from being unlocked. There is an important exception, however, to be noted. A co-secant curve will also intersect the secant curve at the same point. At this range and target bearing the azimuth system will be unlocked, and as we follow the secant curve to the left successive intersection with co-secant curves show combinations of range and target bearing at which the azimuth system is unlocked in spite of the range servo delay.

We will illustrate the above by deriving the polar plot of Figure 7. This represents the case of a bomber speed of 500 knots with an effective gate width of 375 ft. The full curve is taken from Fig. 6 and reproduces the intersections of various co-secant curves with the secant curve for α = 375 ft. In the area below this full curve the azimuth servo is unlocked.

We can now show the effect of servo delay be selecting the appropriate product of the delay time and 500 knots and finding the point at which this line cuts the secant curve for = 375 ft. This angle can be marked on the polar plot as a dotted radial line. Now, the significance of servo delay is readily seen. We have seen already that servo delay does not affect the significance of the full curve. However, in the regions above the full curve the range servo is only unlocked for values of θ greater than the limit shown by the dotted radial line. In Figure 7, for example, the effect of increasing the servo delay from .5 sec. to 1 sec. gains for the AI the area lying between 28° and 63° at all ranges above the full curve.

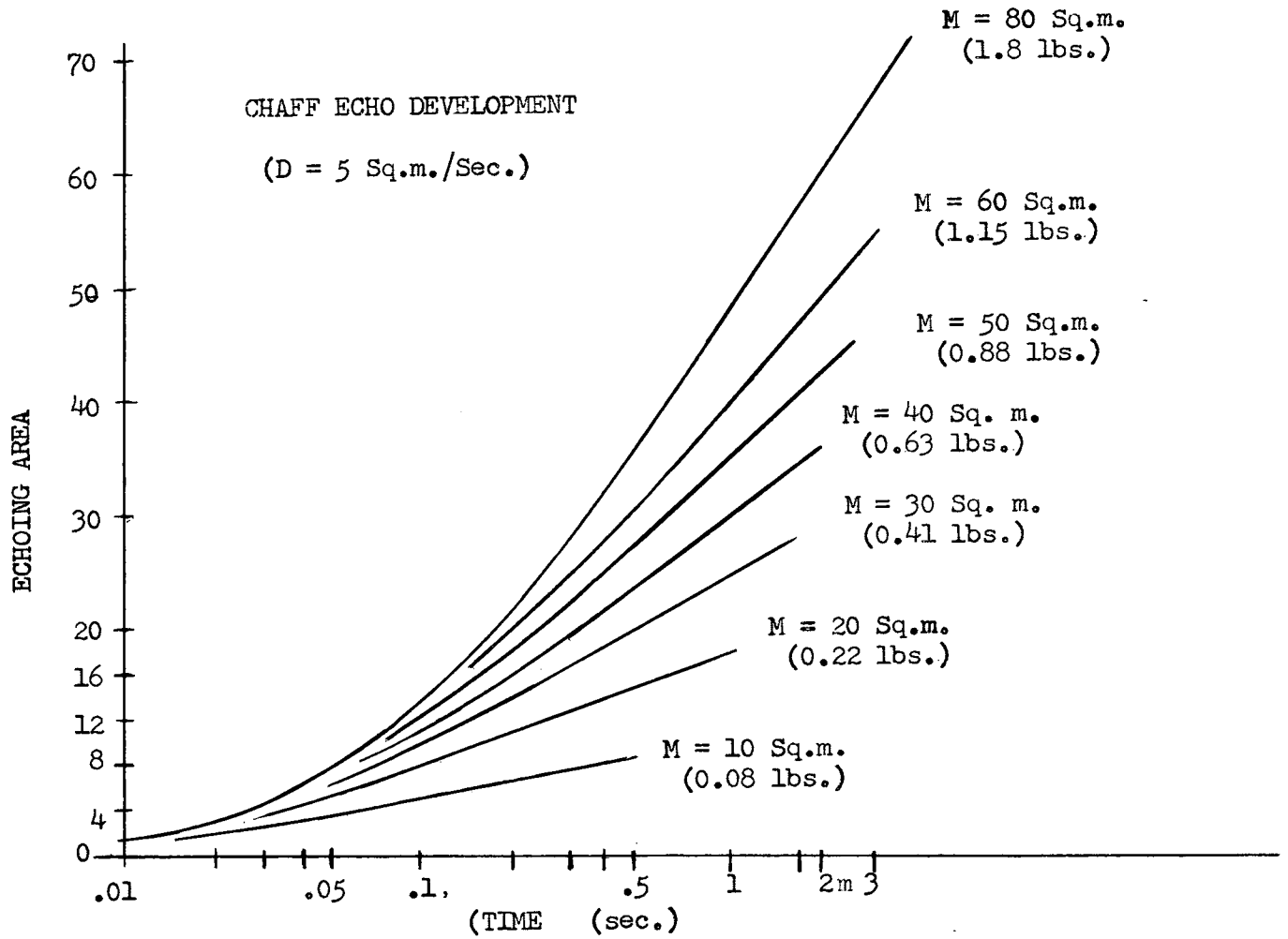
CHAFF ECHO DEVELOPMENT
(D = 5 Sq.m./Sec.)
M = 80 Sq.m.
(1.8 lbs.)
M = 60 Sq.m.
(1.15 lbs.)
M = 50 Sq.m.
(0.88 lbs.)
M = 40 Sq. m.
(0.63 lbs.)
M = 30 Sq. m.
(0.41 lbs.)
M = 20 Sq.m.
(0.22 lbs.)
M = 10 Sq.m.
(0.08 lbs.)
ECHOING AREA
70
60
50
40
30
20
16
12
8
4
0
.01
.05
.1,
.5
1
2m 3
(TIME (sec.)

FIGURE 1

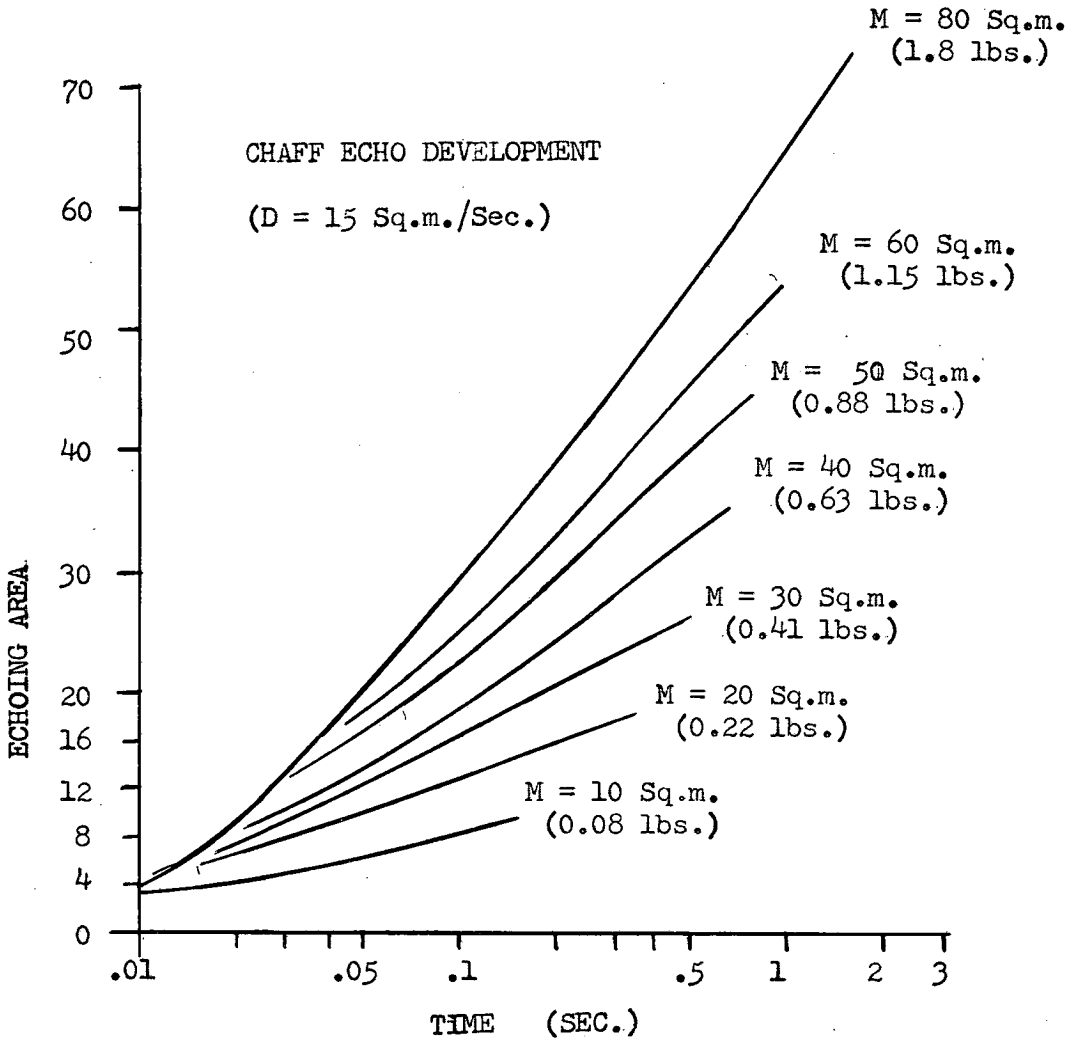
CHAFF ECHO DEVELOPMENT
(D = 15 Sq.m./Sec.)
M = 80 Sq.m.
(1.8 lbs.)
M = 60 Sq.m.
(1.15 lbs.)
M = 50 Sq.m.
(0.88 lbs.)
M = 40 Sq.m.
(0.63 lbs.)
M = 30 Sq.m.
(0.41 lbs.)
M = 20 Sq.m.
(0.22 lbs.)
M = 10 Sq.m.
(0.08 lbs.)
ECHOING AREA
70
60
50
40
30
20
16
12
8
4
0
.01
.05
.1
.5
1
2
3
TIME (SEC.)

FIG. 2

TARGET - SWEPT WING
SPEED - 500 KNOTS

CHAFF BLOSSOMS OUTSIDE RANGE GATE	
APPROXIMATE REGOIN IN WHICH CHAFF ECHO $\ll \sigma$	

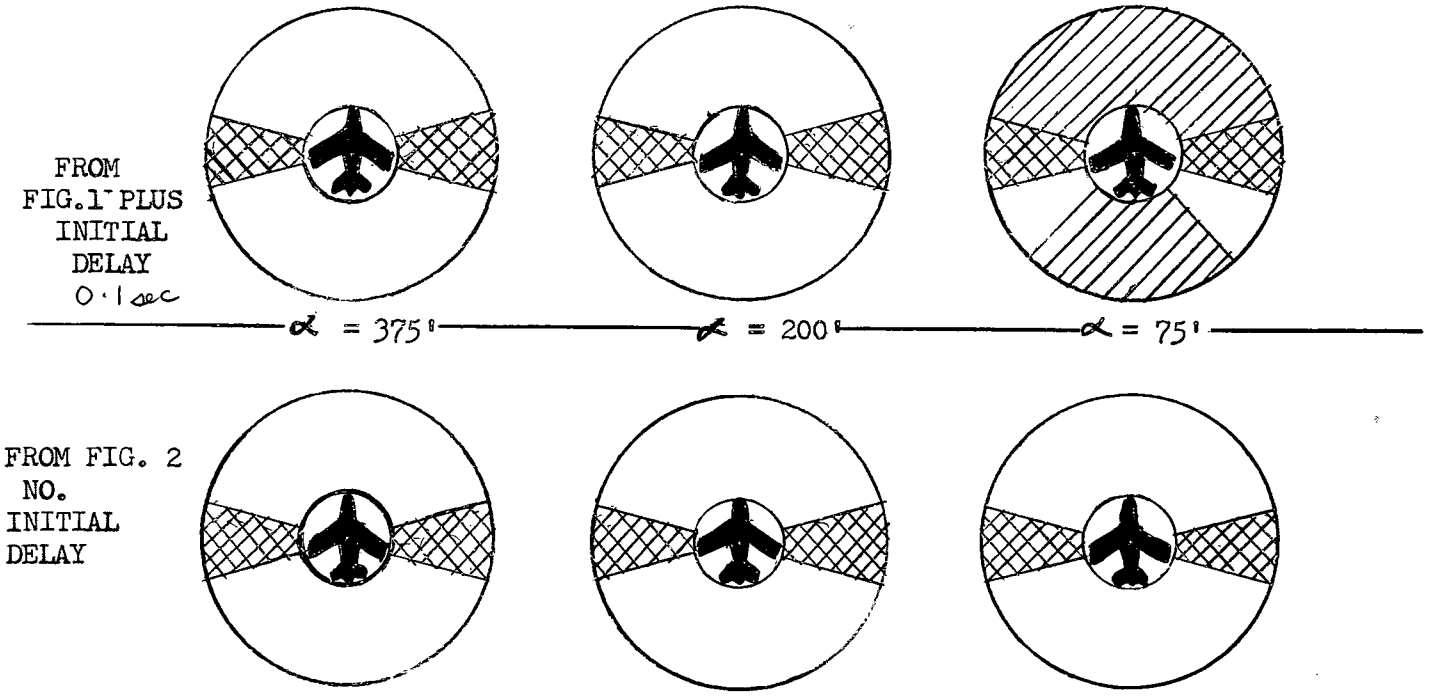

EFFECT OF DELAY IN CHAFF ECHO DEVELOPMENT WITH GRAVITY LAUNCHING

FIG. 3

TARGET DELTA

SPEED 1000 Knots

CHAFF BLOSSOMS OUTSIDE RANGE GATE	
APPROXIMATE REGION IN WHICH CHAFF ECHO $<<\sigma$	

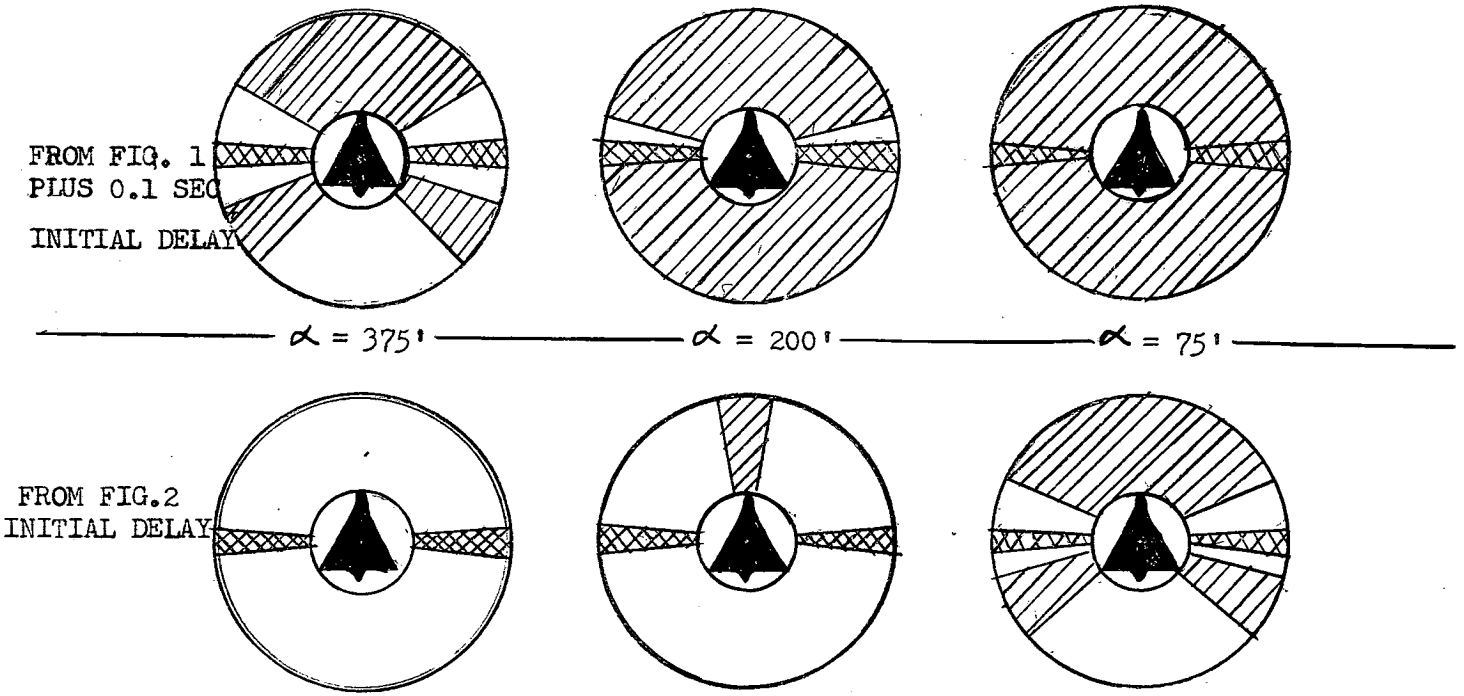

EFFECT OF DELAY IN CHAFF ECHO DEVELOPMENT WITH GRAVITY LAUNCHING

FIG. 4

TARGET STRAIGHT WING

SPEED 1000 KNOTS

CHAFF BLOSSOMS OUTSIDE RANGE GATE	
APPROXIMATE REGION IN WHICH CHAFF ECHO $<< \sigma$	

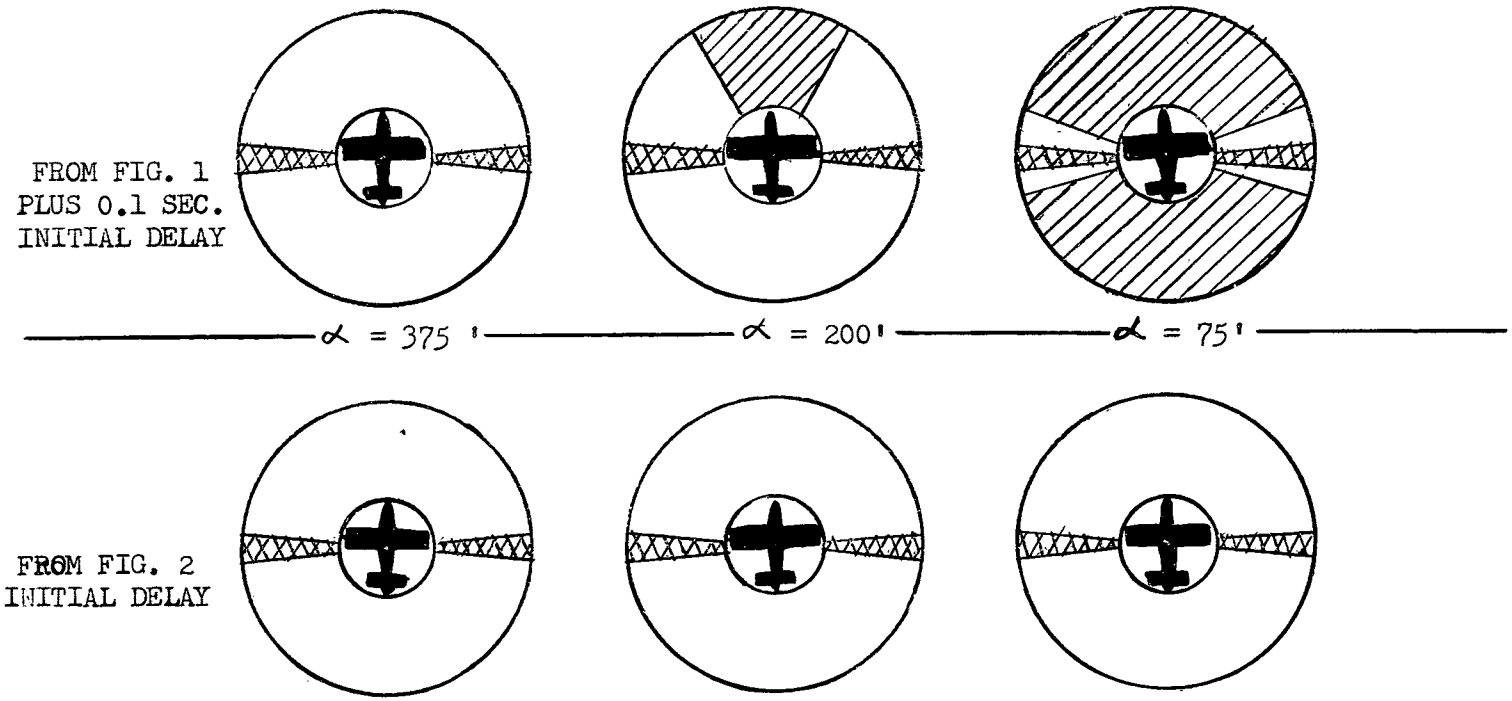

EFFECT OF DELAY IN CHAFF ECHO DEVELOPMENT WITH GRAVITY LAUNCHING

FIG. 5

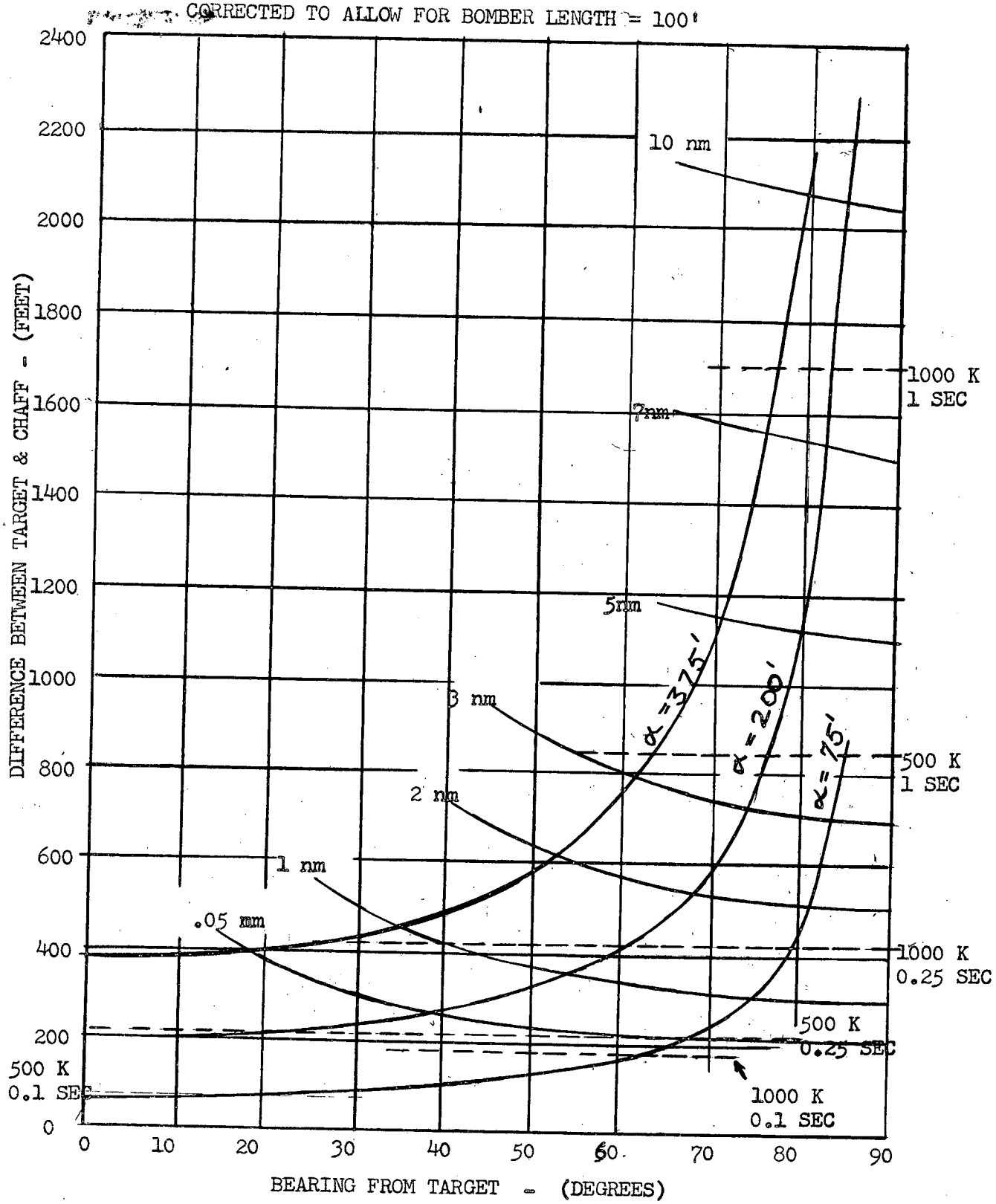
CORRECTED TO ALLOW FOR BOMBER LENGTH = 100'
DIFFERENCE BETWEEN TARGET & CHAFF - (FEET)
2400
2200
2000
1800
1600
1400
1200
1000
800
600
400
200
0
0
10
20
30
40
50
60
70
80
90
BEARING FROM TARGET - (DEGREES)
10 nm
7nm
5nm
3 nm
2 nm
1 nm
.05 mm
1000 K
1 SEC
500 K
1 SEC
1000 K
0.25 SEC
500 K
0.25 SEC
500 K
0.1 SEC
1000 K
0.1 SEC
α = 375'
α = 200'
α = 75'

FIGURE 6

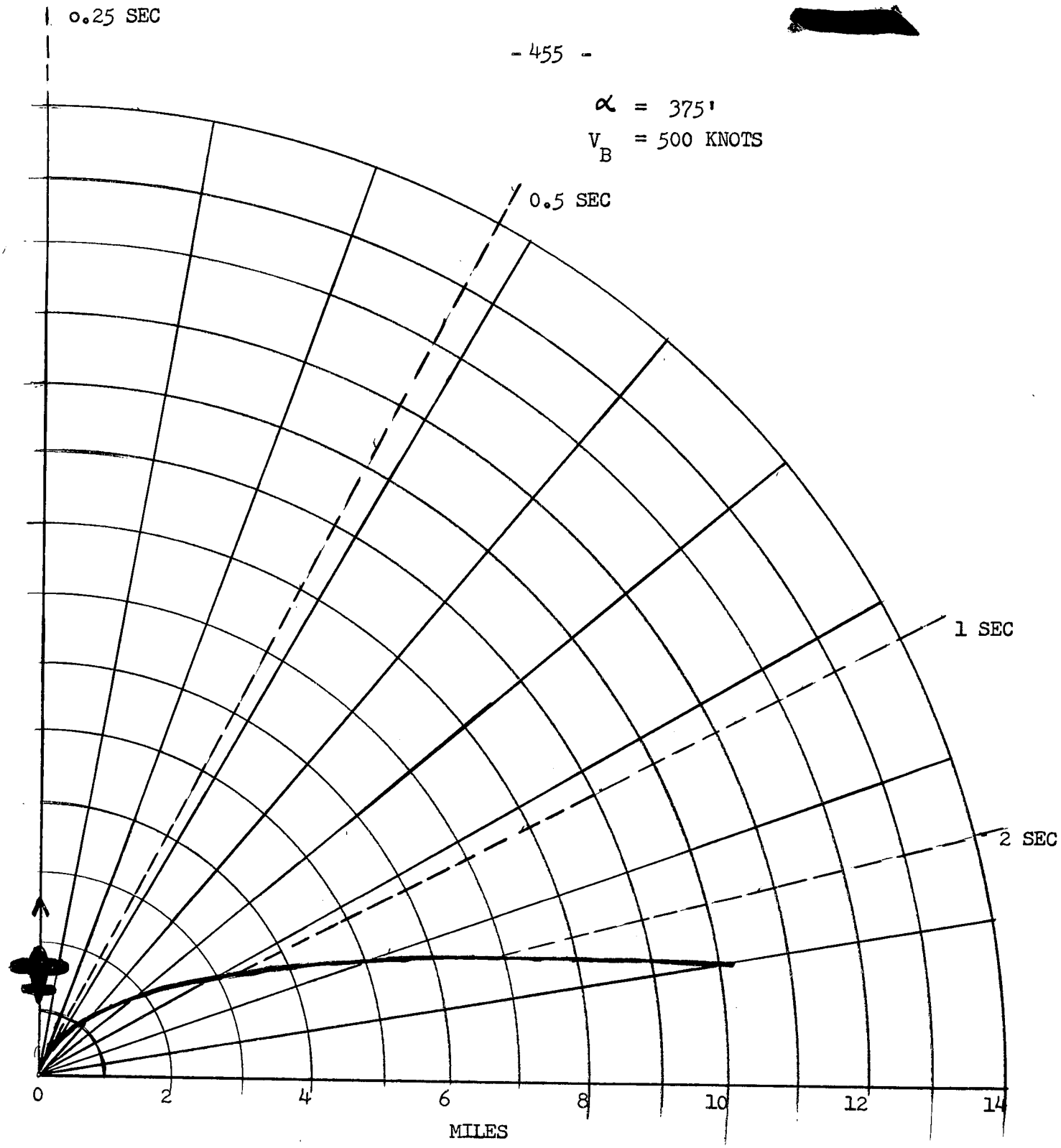

FIG. 7

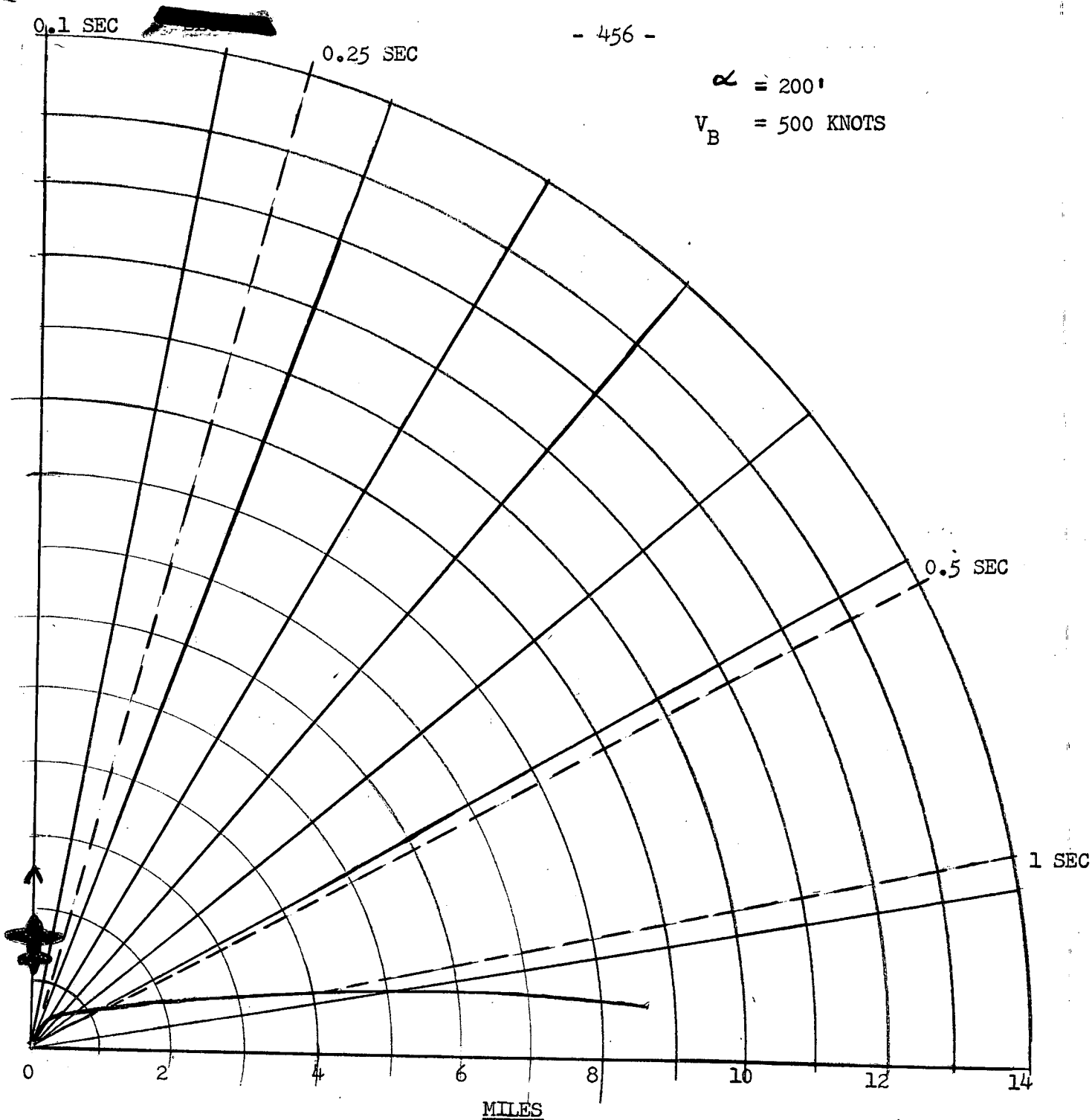
0.1 SEC
0.25 SEC
0.5 SEC
1 SEC
α = 200'
V_B = 500 KNOTS
0
2
4
6
8
10
12
14
MILES

FIGURE 8

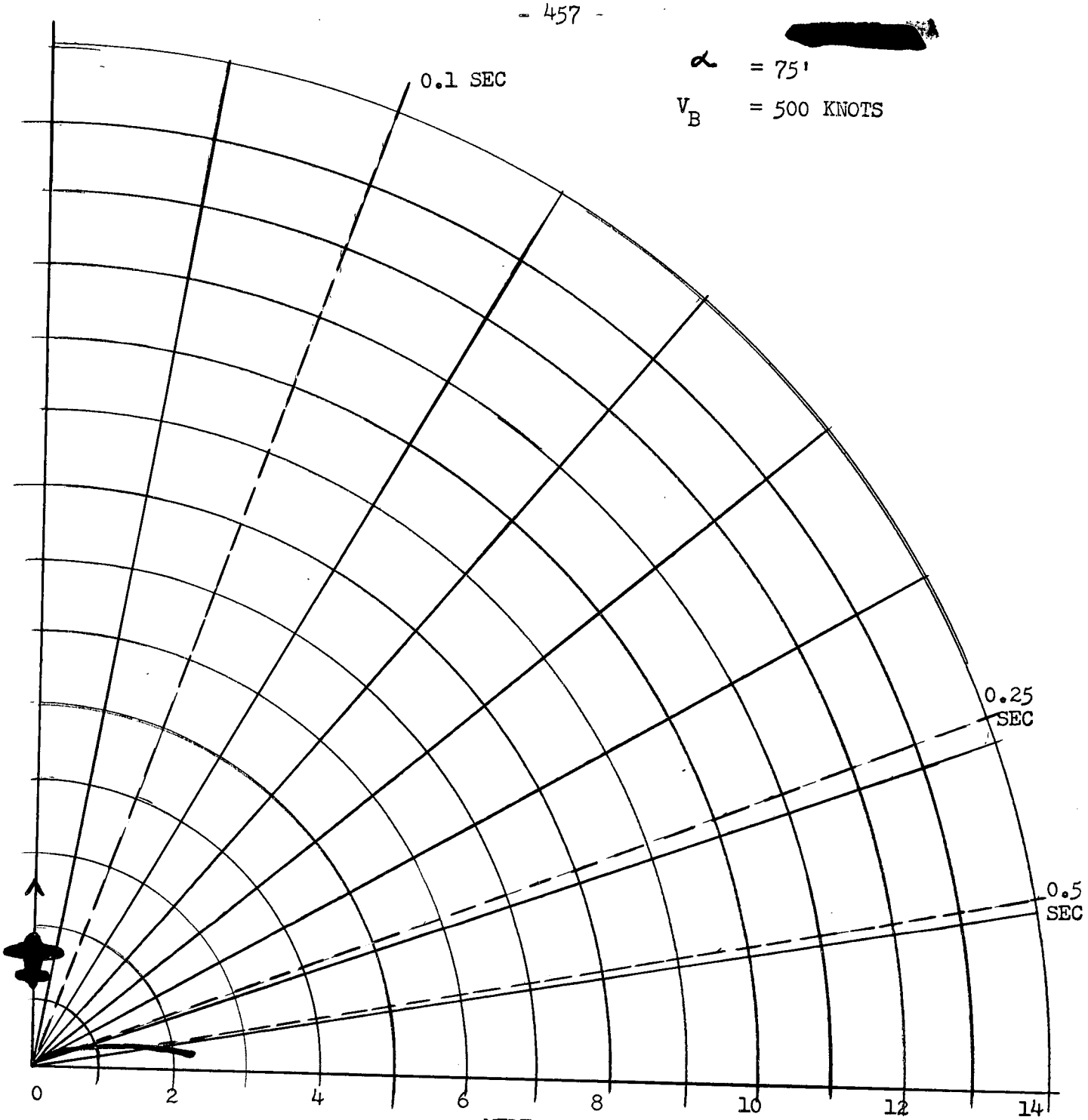

FIGURE 9

α = 375'

V_B = 1000 KNOTS

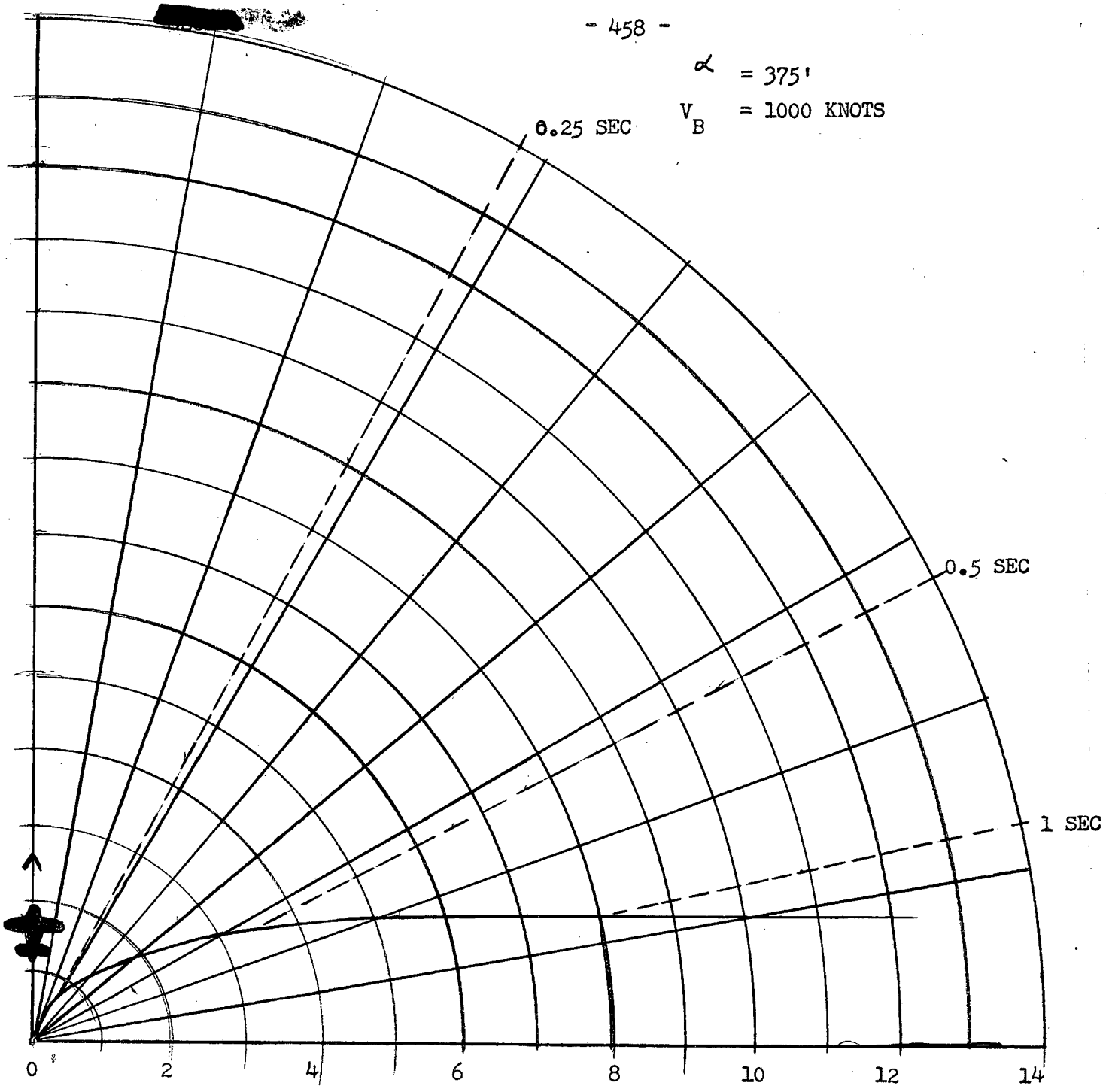

FIGURE 10

α = 200'

V_B = 1000 KNOTS

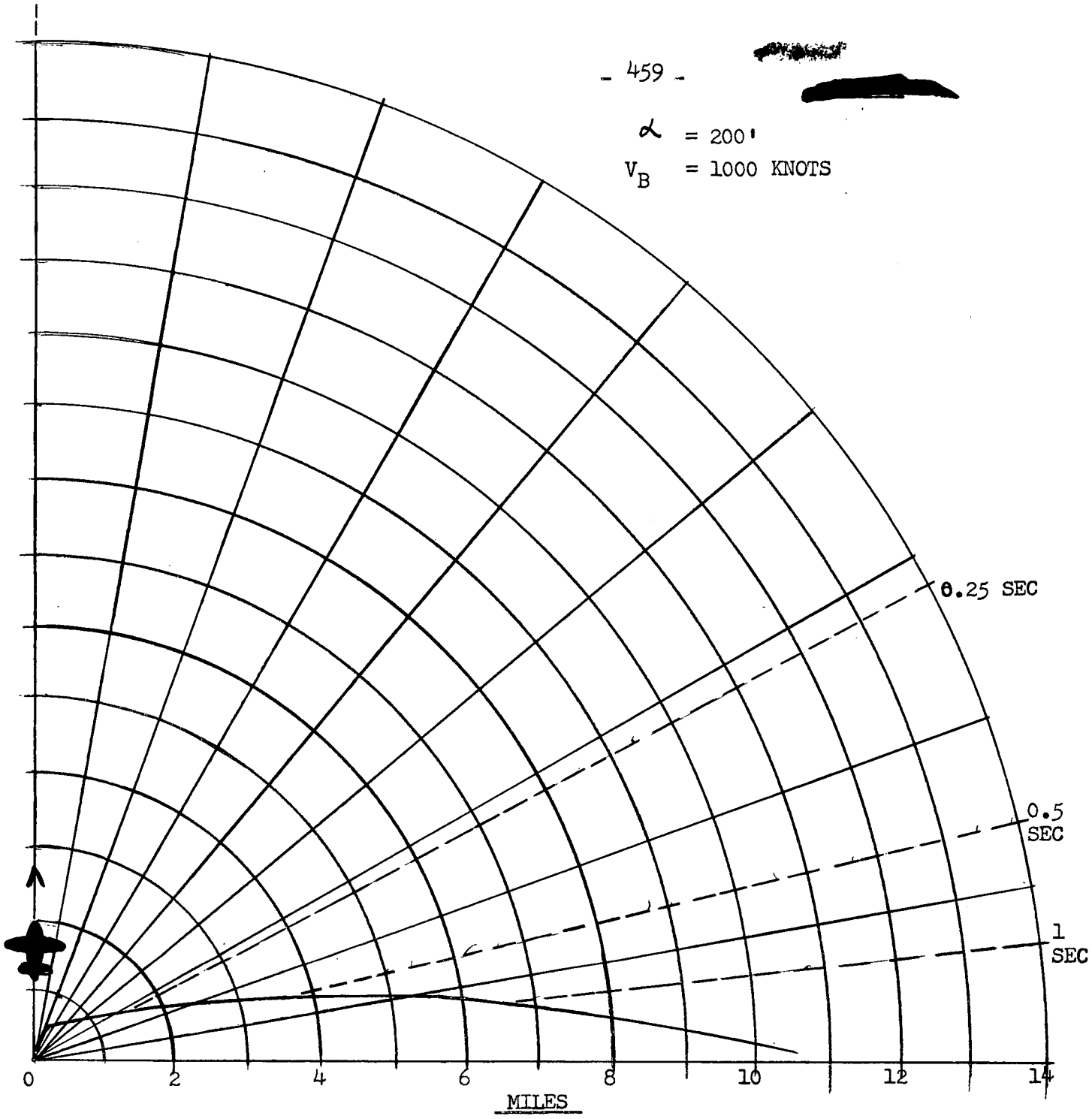

FIGURE 11

α = 75°

V_B = 1000 KNOTS

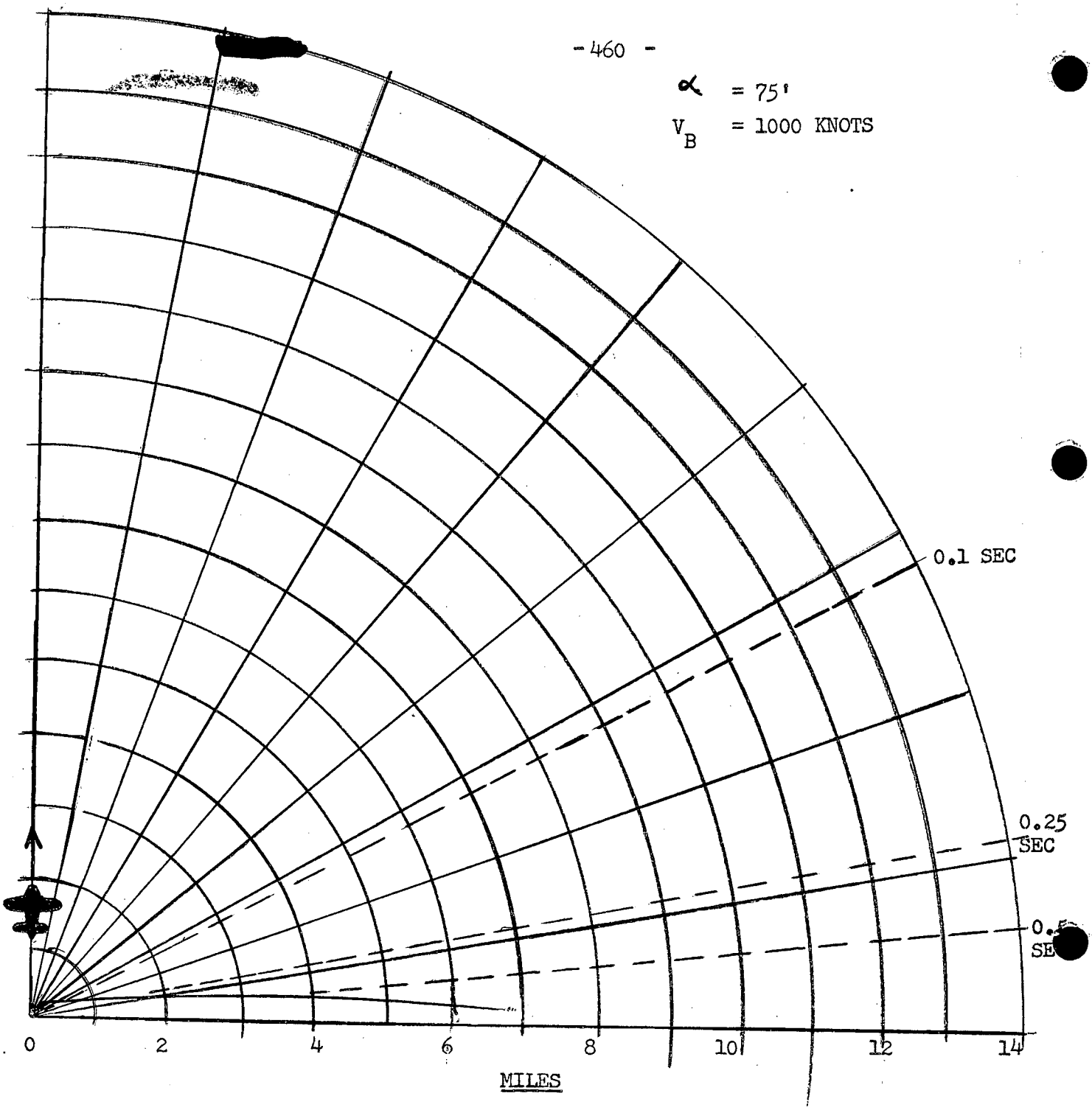

FIGURE 12

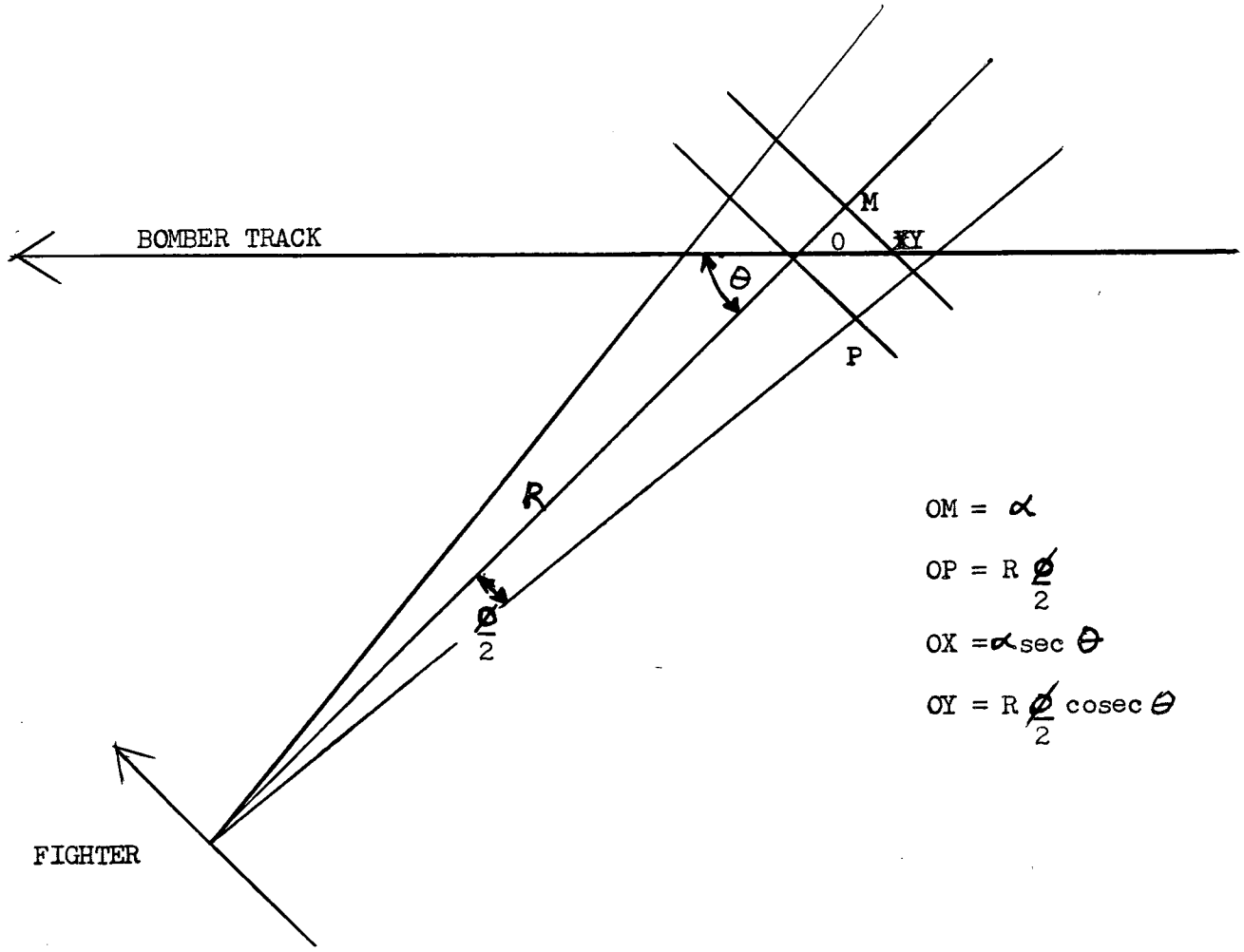

$OM = \alpha$

$OP = R \frac{\phi}{2}$

$OX = \alpha \sec \theta$

$OY = R \frac{\phi}{2} \operatorname{cosec} \theta$

GEOMETRY FOR FIG. 6

FIGURE 13

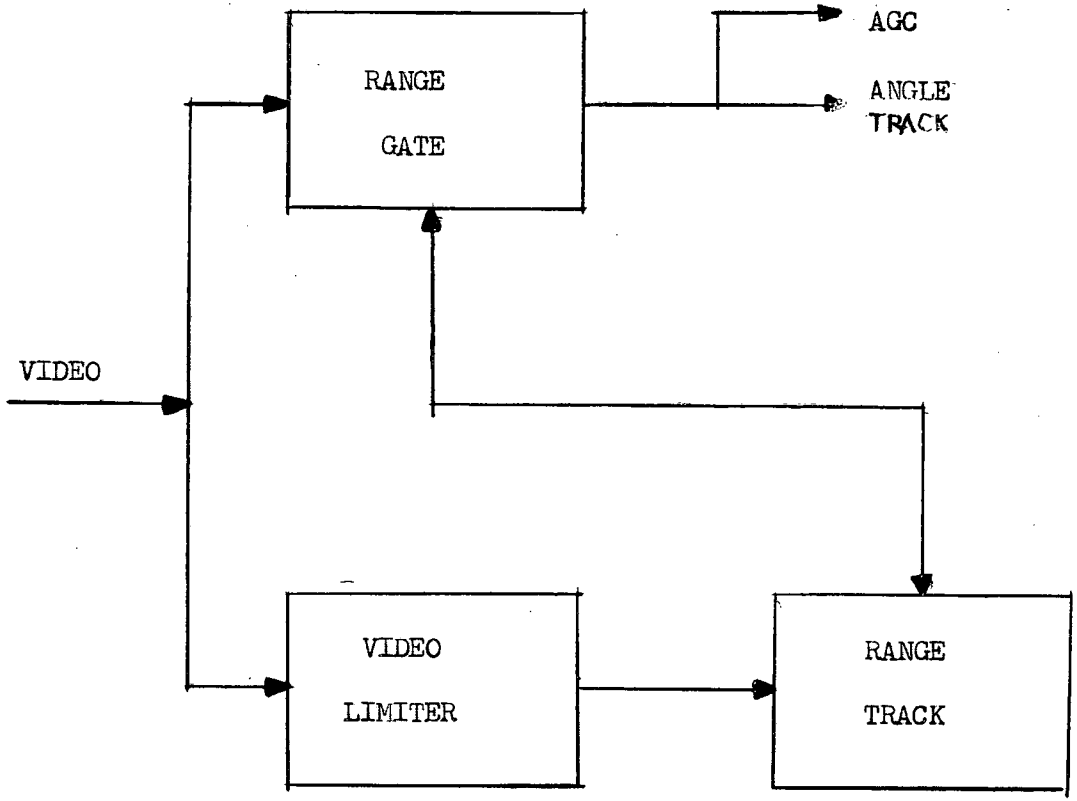

SIGNAL LIMITING PROPOSAL

FIGURE 14

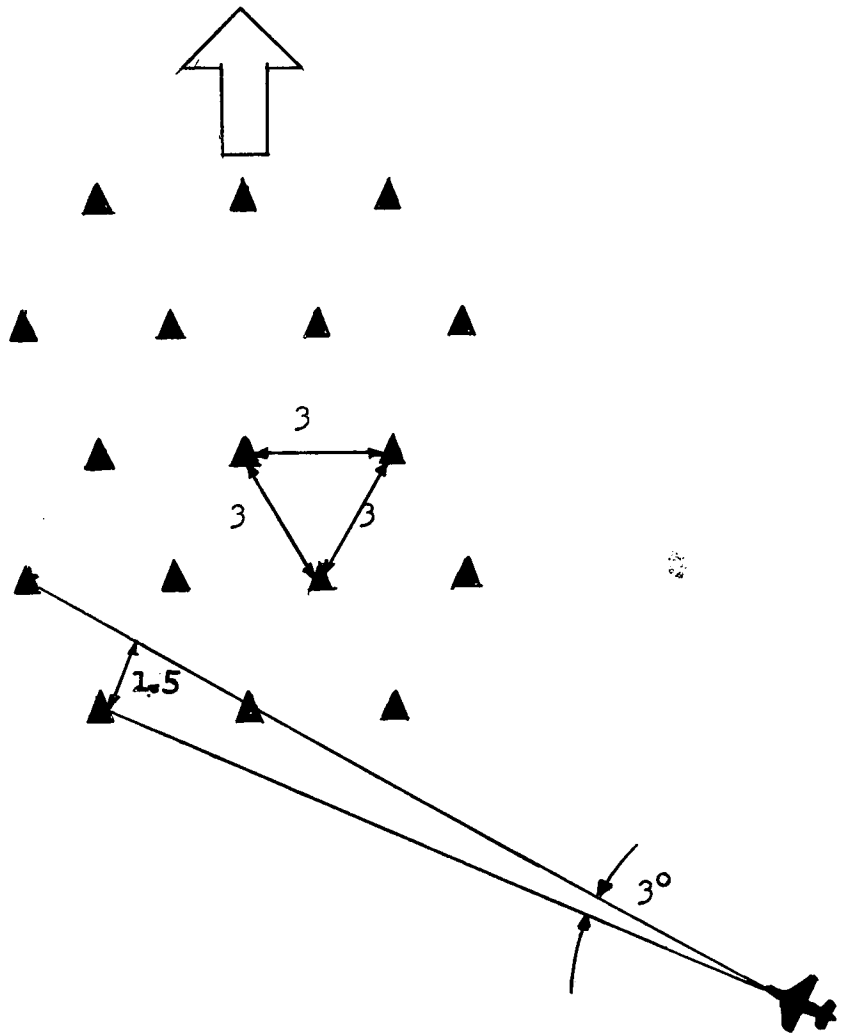

PASSIVE HOMING ONTO ONE
BOMBER IN A FORMATION

FIGURE 15

APPENDIX 'S'

Plan for Phase II of the CF 105 Study

by J. Macfarlane

Continuation of the CF 105 Assessment Study for the ensuing year has been recently approved. The areas which it is intended to study include:

(1) Three Dimensional Attack Simulation - The work in the study of non-co-altitude attacks will continue, for several targets and different fighter approach tactics.

(2) Fire Control Studies - The proposed ASTRA I fire control system will be evaluated, and possible improvements to it investigated.

(3) Missile Studies - It is planned to extend the present knowledge of permissible launch conditions for Sparrow type missiles for supersonic targets and interceptors. In connection with the lethality studies, it will be necessary to determine the distribution of miss distance and of missile end-course trajectories.

(4) Lethality - Lethality assessments for at least two targets, the subsonic Bear and a hypothetical straight-wing supersonic bomber are to be conducted.

(5) E.C.M. - DRTE is making a study of the effects of ECM on the Sparrow missile seeker and fuze. The results of this study will become available within the year. Investigations of anti-ECM tactics will be continued.

(6) Long Range Rockets - The use of long range unguided rockets as a weapon to be carried by the CF 105 will be considered. This includes launch zone, placement, and fire control studies, and should include both subsonic and supersonic targets.

(7) Low Altitude Targets - A short study of the effectiveness of the CF 105 system against subsonic targets at 2000 ft. altitude is planned.

(8) I.R. Work - It is planned to make a brief investigation of the tactical effectiveness of the CF 105 interceptor system using infra-red AI and missiles.

APPENDIX 'T'

Summary of U.S. Visit*

by J. Macfarlane

In December 1956 a party from CARDE visited several U.S. establishments to obtain information which would be of use in the CF-105 Assessment Study. The CARDE group were particularly interested in obtaining details of methods used in evaluation of interceptor/missile systems, and in seeing results of any studies which may have been done for systems to operate in the post-1960 era.

Personnel

The composition of the party was as follows:

W/C E.A. Smith	C/O CEPE Detachment at CARDE, and Assistant Chief Superintendent at CARDE.
R.S. Mitchell	Systems Group
J.T. Macfarlane	" "
F.W. Slingerland	" "
B. Cheers	Aerodynamics Section, B-Wing.
C. Wilson	System Analysis Section, G-Wing
Y. Caron	" " " "
J.P. Regniere	Missile Electronics Section, G-Wing.

Itinerary

The organizations which were visited, the chief aim, and the main results of each visit, are as follows.

1. Naval Air Development Center, Johnsville, Pa.

To discuss methods and results of a general interception study for interceptor missile systems for the post 1960 era. This study was based on requirements for Naval Task Force Defence and so emphasis on various parameters appears to be different than for area defence. The chief result of the studies here is that the optimum interceptor system combines a low performance, high endurance subsonic interceptor with a long-range high performance missile and extremely high performance A.I. radar.

* The visit has been fully reported in CARDE Technical Letter N-47-16.

2. Bell Telephone Laboratories, Whippany, N.J.

To discuss methods used and results obtained in the recently concluded Naval Intercept Project, an interception study considering the missile carrying interceptors for the post 1960 period. The methods used at Bell are different from those used by Rand, Hughes, and CARDE, and would not appear to be superior, in that it is difficult to see how missile Kill probability can be included in an evaluation by this method.

3. Raytheon Manufacturing Company, Missiles Engineering Division, Bedford, Mass.

Information was sought on Sparrow III launch zones, and performance in supersonic launch. The characteristics of the F4H fire control system were also of interest.

4. R.C.A., Waltham, Mass.

One member of the CARDE party only visited the CF-105 group at R.C.A. to compare work being done there on interceptor missile system studies with that being done at CARDE. Further visits to R.C.A. both at Waltham and Camden, are planned for March 1957.

5. Bendix Aviation Corporation, Detroit and Los Angeles.

The group visited Bendix Research Laboratories in Detroit and Bendix Pacific Division in Los Angeles, to obtain a complete picture of the present status and performance of the Sparrow II guidance head.

6. Rand Corporation, Santa Monica, Cal.

The group discussed Rand methods and results for interception studies. Rand has set up a digital computer program for rapid calculation of placement probability, under certain simplifying assumptions such as non-evading targets and constant speed fighters.

7. Hughes Aircraft Company, Los Angeles.

The group visited the Tactical Analysis Section at Hughes, and discussed methods and results of interceptor/missile tactical studies.

8. Douglas Aircraft Company, Los Angeles.

The CARDE party visited both the El Segundo and Santa Monica divisions of Douglas, and was able to obtain the latest results of Sparrow II launch zone simulation. A description of the work on the fire control system for the F5D airplane was also useful.

9. Mc Donnel Aircraft Corporation, St. Louis, Mo.

At Mc Donnel, the group was able to obtain some information on the F4H airplane and its fire control system. In this respect this visit complemented that to Raytheon.

General Observations

1. Evaluations

In general, interception studies as being done at CARDE are at least as comprehensive as those done elsewhere. In most other establishments target evasion is not considered, or if it is, in a very elementary manner. Fighter speed disadvantage which is a very possible case, is analysed almost nowhere. Lethality considerations are universally left out of evaluations of missile/interceptor systems. It is generally assumed that missile manufacturers produce launch zones for equivalent kill probabilities. It can be concluded from these visits that the Bell Laboratories' method for interception analysis is inferior to Rand and Rand-like methods. The most interesting and advanced interception studies are those being done by Hughes Aircraft Company, and it is felt that continued liaison between the CARDE group and the group at Hughes would be mutually beneficial.

It was suggested at several of the establishments that the CARDE group should also visit Cornell Aeronautical Laboratories, where advanced interception studies are also being carried out.

Methods for considering E.C.M. quantitatively in interceptor system studies have not been developed at any of the establishments visited.

2. Missiles

It is apparent that missiles, both Sparrow II and Sparrow III, as they exist to-day, are not capable of being launched above Mach numbers of about 1.4. Modifications to the radomes, and cooling provisions will have to be made for both missiles.

Launch zones for Sparrow III, launched at supersonic speeds, are not known. Those published in the brochure are merely extrapolations from subsonic data, guided by previous work done on generalized missiles, and should not be used with confidence.

Test firings for both missiles have all been at low altitude and low speeds, and for rear aspects. This imposes limitations on tactical evaluations based on these flight tests.

The information obtained on the missiles during this visit, even when combined with that already at CARDE, will not support a detailed comparison of the performance characteristics of the Sparrow II and Sparrow III missiles.

It would appear that the Sparrow X program is further advanced than is generally admitted by BuAer or the contractors. Possibility of using a second generation missile of about 800 lbs weight as armament for the CF-105 should be kept in mind.

3. Criticisms of the CF-105 Study

Several criticisms of the CARDE study were advanced by the groups visited, during comparison of methods used. It was generally felt that restriction to a one fighter vs. one target analysis was unrealistic, and that results obtained may be of lesser value than those which would be obtained if multiple aircraft were considered. Most groups felt that ground environment considerations, and map studies, were essential to proper evaluation of an interceptor system. A large number of groups are doubtful about proposals for instrumenting the aircraft for several different missile types.
